Synthesis of Diazaphospholenes for Improved Catalysis

by

Erin Norah Welsh

Submitted in partial fulfilment of the requirements
for the degree of Doctor of Philosophy

at

Dalhousie University
Halifax, Nova Scotia
August 2023

Dalhousie University is located in Mi'kma'ki, the
ancestral and unceded territory of the Mi'kmaq.
We are all Treaty people.

What I love about science is that as you learn, you don't really get answers. You just get better questions.

John Green

Table of Contents

List of Tables

List of Figures

List of Schemes

Abstract

Diazaphospholene (DAP) synthesis and reactivity has been emerging over the last two decades. Recently, DAPs have been employed as catalysts for asymmetric reduction transformations. Specifically in the Speed group we use DAP catalysts for asymmetric reduction of imines. This thesis provides a comprehensive overview of the synthetic procedures employed to manipulate the substituents surrounding the DAP scaffold. The subsequent investigation involved testing each isolated DAP compound to assess its enhanced reactivity and selectivity in imine reduction.

Initially, the objective was to produce DAP variants with different substituents around the stereogenic centre, specifically larger aryl or alkyl groups that offer increased steric hindrance. We hypothesized that these bulkier substituents would establish a more restrictive stereochemical environment around the phosphorus centre, thereby improving enantioselectivity. However, this led to only one DAP variant that had comparable reactivity and selectivity to the current best DAP.

The synthesis of DAPs containing larger aryl or alkyl groups around the stereogenic centre led to more efficient syntheses of 1-dibenzothiophene derivatives and 3-bromonaphthothiophene as starting materials for additional DAP derivatives. However, neither DAPs were fruitful for improved reactivity or selectivity for imine reduction.

Considering the limited success achieved when modifying the substituents around the stereogenic centre, it became apparent that exploring alternative strategies was necessary. Consequently, attention was shifted towards alternating the backbone of the DAP scaffold. This led to a more rigid DAP that has shown improved enantioselectivity for imine reduction to make acyclic and exocyclic amines.

List of Abbreviations Used

Ad = adamantyl
Aq = aqueous
BAr^F = tetrakis(3,5- bis(trifluromethyl)phenyl)borate
BT = benzothiophene
Boc = *tert*-butoxycarbonyl
COD = 1,5-cyclooctadiene
δ = chemical shift (ppm)
d = doublet
DAP = 1,3,2-diazaphospholene
DAP-OTf = diazaphospholene triflate
DAP-H = diazaphospholene hydride
DAP-Br = diazaphospholene bromide
DAP-Cl = diazaphospholene chloride
DBT = dibenzothiophene
$DBTO_2$ = dibenzothiophene sulfone
DMF = *N*-dimethylformamide
eqn = equation
equiv. = equivalents
e.r. = enantiomeric ratio
ESI = electron spray ionization
Fc = ferrocene
h = hour
HBpin = 4,4,5,5-tetramethyl-1,3,2-dioxaborolane
HMPT = hexamethylphosphorus triamide
HPLC = high pressure liquid chromatography
HRMS = high resolution mass spectrometry
Hz = hertz
$^nJ_{xx'}$ = n bond coupling constant between atoms X and X'
m = multiplet
Mes = Mesityl
NTT = naphthothiophene
ppm = parts per million
NMR = nuclear magnetic resonance
Red-Al = sodium bis(2-methoxyethoxy)aluminum hydride
RT = room temperature
s = singlet
SPO = secondary phosphine oxide
t = triplet
TBSOTf = *tert*-Butyldimethylsilyl trifluoromethanesulfonate
TH = thianthrene
TMSOTf = Trimethylsilyl trifluoromethanesulfonate
TFA = trifluoroacetic acid

Acknowledgements

First, I would like to start off by thanking my supervisor Dr. Alex Speed, for all of the mentorship, guidance, history lessons, and story times over the years. Alex has provided me with the space to grow not only as a chemist but as an individual as well and I will be forever grateful to him. I would also like to extend a thank you to all the past and present Speed group members and the 4th floor crew. The continuous support and friendship helped tremendously through the journey of graduate school. Special thanks go to Prof. Kate Marcenzko, Drs. Dylan Hale, Blake Huchenski, and Helia Hollenhorst, as well as future Drs. Tyler Saunders and Joe Bedard.

I would like to thank my supervisory committee Drs. Laura Turculet, Mark Stradiotto and Norman Schepp for their continuous guidance and feedback throughout my degree. I would also like to express my appreciation to my external examiner, Dr. Michel Gravel, for taking the time to evaluate my work. In addition, I would like to acknowledge Dr. Katherine Robertson from Saint Mary's University for X-ray data collection and solution refinement, Dr. Mike Lumsden for his help with the NMR and maintaining the magnets, as well as Mr. Xiao Feng for obtaining MS of all my compounds.

I would like to extend a thank you to the Nunatsiavut Government, specifically the Post-Secondary Student Support Program, for the financial support that has enabled me to pursue my education. I would like to acknowledge the additional funding agencies, NSERC, NSGS and BioActives, for their contributions.

In addition, I am immensely grateful to my family who are all over the world but have always made me feel unconditionally loved and supported. A special recognition goes to my mom, Debbie Shiwak, my dad and stepmom, Nigel Welsh and Alyson Thompson and my sister, Kelly Welsh. Regardless of the time and distance that separate us, their unwavering pride in my achievements never fails to uplift me. I would not be where I am without them. I would also like to express my appreciation to my chosen family here in Nova Scotia, the Manette/Firth families, who have embraced me as one of their own and have been a constant source of support and encouragement since I met them.

Lastly, but certainly not least, I want to extend a heartfelt thank you to my life partner, Benjamin Firth. Words cannot adequately convey my gratitude for your unwavering encouragement, love and support throughout this journey.

This thesis is dedicated to the memory of my nan, Delphine Shiwak.

Chapter 1 Introduction

1,3,2-Diazaphospholenes (DAPs) are unsaturated five-membered heterocycles that contain a phosphorus centre, connected to two nitrogens that are tied together with an unsaturated carbon-carbon backbone (Figure 1-1, Generic Structure). DAPs are a subset of *N*-heterocyclic phosphines (NHPs) which are a larger class of compounds that contain varying ring sizes and degrees of saturation. Several synthetic routes varying in terms of mildness and practicality have been reported to access DAPs.[1] These routes will be further discussed in the following sections of this Chapter. DAPs have emerged as an important main group-based catalyst due to the unusual hydridic character of the P-H bond in DAP hydrides.[2]

The reductive ability of a P-H bond may be counterintuitive, as a typical compound containing this bond would be thought of as containing a partial negative charge on the phosphorus leading to a protic reactivity of the hydrogen.[3] The hydridic behaviour of the P-H bond in DAPs, is a result of inversed polarity modulated by the surrounding atoms (Figure 1-1, Reactivity). This umpolung reactivity of hydride bound to phosphorus can occur due to the closely matched electronegativities of phosphorus and hydrogen. Experimental and computational studies revealed a high degree of polarization of the P-X bond in DAP-halides and hydrides is due to the interactions between the lone pair on each nitrogen atom, the unsaturated carbon backbone, and the antibonding σ*-orbital on phosphorus.[2] This is the basis of DAP reactivity and specific reductive examples will be explained later in this Chapter. The reactivity of DAPs has garnered a lot of attention recently with three independent reviews being published in 2020.[1][4][5]

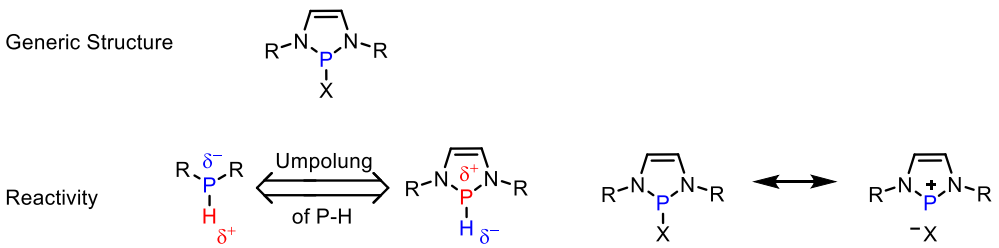

Figure 1-1. Generic DAP structure and relative reactivity.

The DAP-hydride (DAP-H) is the active species in catalyzing reductive transformations. The isolation of various DAP-H compounds revealed the physical properties to be an undesired air and moisture sensitive liquid at room temperature. These physical properties increase difficulty for direct use of this reagent in exploratory organic synthesis. Accordingly, most reports of DAP catalysts have involved the synthesis of a neutral DAP-alkoxide pre-catalyst or a diazaphosphenium catalyst that are converted to the DAP-H *in situ*. While the DAP-alkoxide and diazaphosphenium are also air and moisture sensitive, they are solids which are relatively convenient to handle in the glovebox. More recently, a way to synthesize an air and moisture stable pre-catalyst has been reported. The secondary phosphine oxide (SPO) analogues of DAPs are air and moisture stable, and can be converted to the DAP-H using pinacolborane (HBpin).[6] The syntheses and use in catalysis of these pre-catalysts and catalysts have been emerging over the last ten years mainly reported by the Speed, Cramer, and Kinjo groups (Figure 1-2).[6][7][8][9][10][11][12]

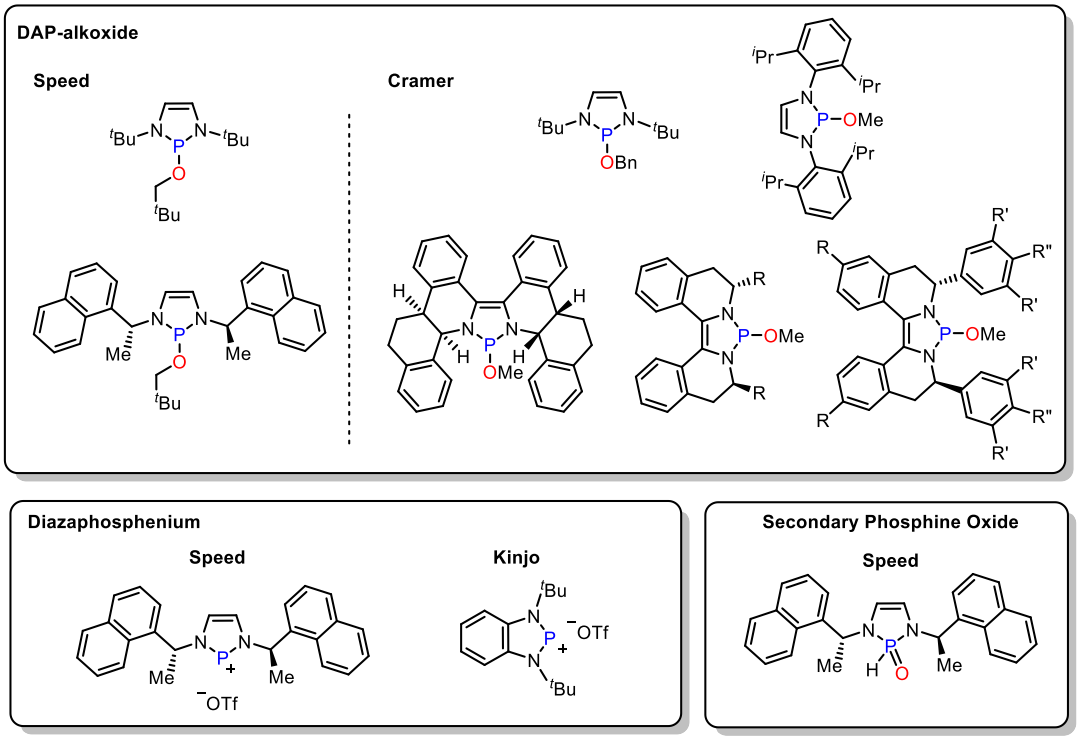

Figure 1-2. Various DAPs that have been used to catalyze reductive transformations.

1.1 Synthesis of Diazaphospholene Halides

Diazaphospholenes exhibit resemblance to familiar *N*-heterocyclic carbenes (NHC) with the caveat that the central atom is a phosphorus rather than a carbon (Figure 1-3).[13][14] This structural relationship means the synthetic routes towards DAPs contain similarities to the synthesis of NHCs, especially routes that begin with diimines. The key difference being the introduction of the phosphorus central atom, which has required multiple strategies depending on the diimine structural features. The most commonly used DAP contains an unsubstituted backbone, **1-1**, with a wide variety of substituents on each nitrogen, but other variants contain a benzo-fused backbone as shown by generic structure, **1-2**, with aryl or alkyl substituents on each nitrogen. Additionally, there have been reports of backbone substituted variants with alkyl groups combined with only aryl substituents on

each nitrogen, **1-3a**, or a single halogenated backbone with aryl or alkyl groups on each nitrogen, **1-3b**.

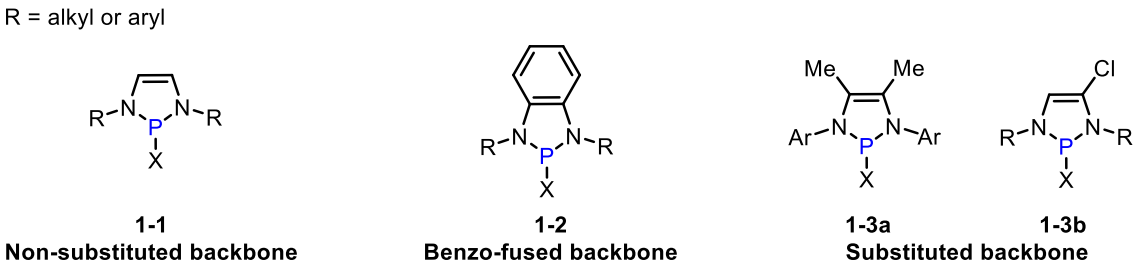

Figure 1-3. Representative structural classes of DAPs.

The synthesis of benzo-fused DAPs has been derived from *N*,*N*′-disubstituted *ortho*-phenylenediamines via treatment with hexamethylphosphorus triamide (HMPT) or a phosphorus halide and a base.[15] A diazaphospholene-chloride (DAP-Cl) containing a benzo-fused backbone, **1-4**, is typically synthesized through cyclization of *N*,*N*′-disubstituted *ortho*-phenylenediamines with phosphorus trichloride (PCl_3) and triethylamine (Scheme 1-1, eqn 1).[10][16] The use of these benzo-fused DAPs in catalysis has been quite limited. Preparation of the other typical classes of DAPs begins from 1,2-diimines, **1-5**, which requires the reduction of the diimine to introduce the phosphorus (III) centre. Diaryl and dialkyl diimines **1-5** are readily formed from a condensation reaction between glyoxal or 2,3-butadione with anilines or aliphatic primary amines under mild dehydrating conditions or a drying reagent such as sodium sulfate, molecular sieves, or a Dean-Stark trap (Scheme 1-1, eqn 2).[17] An acid catalyst can be used to accelerate the formation of the diimine and often diimine formations are cleaner with more sterically encumbered amines and anilines.

Early reports of DAP synthesis reduced the diimine **1-5** with lithium metal which formed a diazine dianion **1-6** that is a mixture of *Z* and *E* isomers. Only the *Z* isomer can

cyclize so the dianion was treated with triethylammonium chloride to converge both isomers to an aminoaldimine **1-7**. This intermediate could undergo a cyclization to the DAP-Cl **1-8** with the addition of PCl_3 in the presence of a base (Scheme 1-1, eqn 3).[18][19] It does require harsh conditions of a strong reducing agent, which could limit the functional group tolerance for more multifaceted DAPs. Specifically, it is not tolerant of aromatic rings since the ring could undergo a Birch reduction under these conditions. Additionally, the purification of the DAP requires the use of a long Soxhlet extraction in specialized apparatus to extract the product air sensitive diazaphospholene from the residual salts.

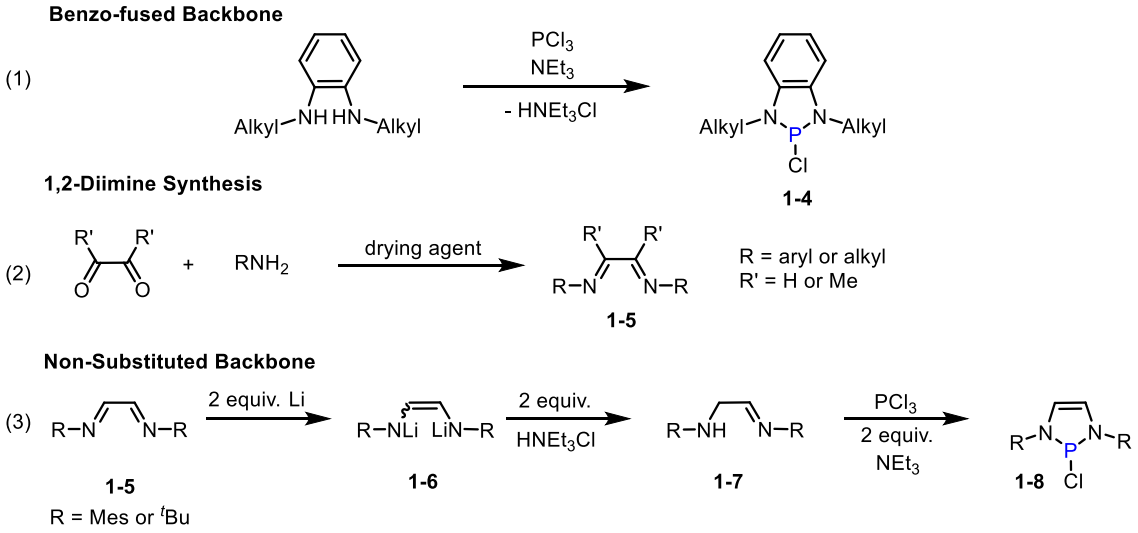

Scheme 1-1. Synthesis of DAP-Cls through salt metathesis. (1) Generation of DAP-Cl **1-4** containing a benzo-fused backbone. (2) Generic synthesis of 1,2-diimines **1-5** as precursors for DAP-halides. (3) Generation of DAP-Cl **1-8** with a non-substituted backbone.

A more efficient and milder route to access DAPs involves a redox reaction between phosphorus tribromide (PBr_3) and a diimine, which was first reported by Macdonald and co-workers.[20] Aryl or alkyl diimines derived from glyoxal react with PBr_3 in the presence of cyclohexene to form the DAP-bromide (DAP-Br) **1-9** and dibromocyclohexane (Scheme 1-2, eqn 1). The DAP-Br can be isolated and purified from the mixture based on the

insolubility of the DAP-halide in pentane or diethyl ether. This method has also been proven to be successful for aryl diimines derived from 2,3-butadione but the cyclization of alkyl diimines derived from 2,3-butadione does not work with this method, leading to side-reactions and decomposition, as will be described later in this thesis. The PBr_3 cyclization method is the most convenient and inexpensive way to introduce the phosphorus centre and directly accesses the DAP-halide in one step without an intermediate reduction step. The Speed group has found the order of addition to be important for the cleanliness and yield of the cyclization with some diimines (Scheme 1-2, eqn 2). Taking a solution of the diimine and adding it to a solution of PBr_3 and cyclohexene is the preferred order to generate DAP-Br **1-10** cleanly but this is not generalizable to all diimines, since many examples do work well with the addition of PBr_3 last.[1]

Combined computational and experimental work reported by Gudat and co-workers indicated the first step in the mechanism of this reaction is the cycloaddition of the phosphorus tribromide with the diimine to form a P(V) phosphorane intermediate. This is followed by an elimination of molecular bromine which brominates the cyclohexene and returns the phosphorus centre to the P(III) oxidation state. In some cases, it has been shown PBr_3 can brominate the backbone (effectively a disubstituted alkene formed when a non-substituted backbone diimine is used) to varying extents during the cyclization. Running the reaction at higher temperatures or the use of trialkylamine base increases the amount of backbone bromination. This occurs by a ring opening of the phosphorane, followed by a halide attack then a hydrogen halide elimination. This backbone halogenation is the exclusive pathway with the use of PCl_3 for cyclizations of 1,2-diimines, so non-substituted backbone DAPs are not accessible with PCl_3. [21]

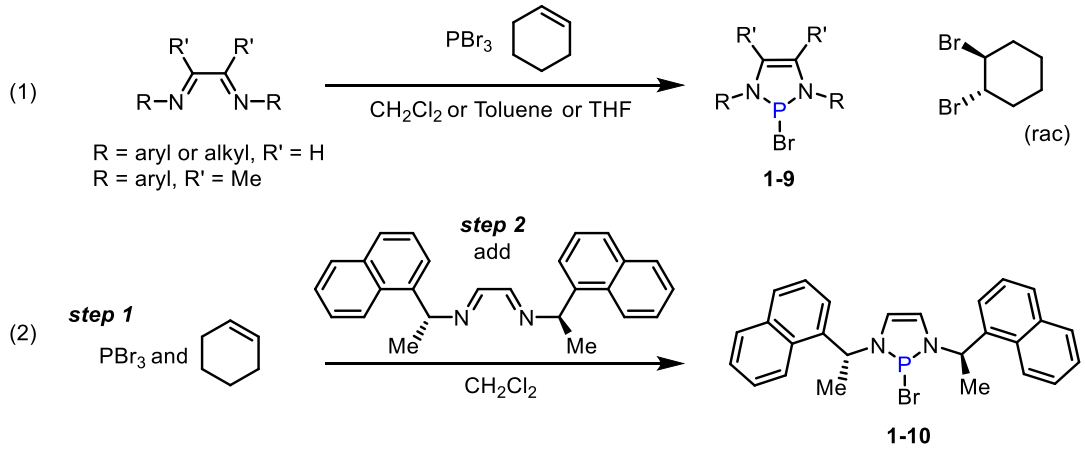

Scheme 1-2. Cyclization of diimines to DAP-Brs through a redox reaction with PBr_3 and cyclohexene. (1) Addition of PBr_3 and cyclohexene to the diimine to generate DAP-Br **1-9**. (2) Addition of diimine to the PBr_3 and cyclohexene to generate DAP-Br **1-10**.

Cyclization of unsubstituted backbone diimines with PCl_3 was first reported by Pudovik and co-workers, where the dominant product was a DAP-halide that resulted in backbone monochlorination.[22] Diimines in the presence of PCl_3 and base form the asymmetrical DAP-Cl **1-3b** with a chlorinated backbone (Scheme 1-3, eqn 1).

The Cowley and Macdonald groups reported alternate conditions for the cyclization of diimines, using phosphorus triiodide (PI_3) which produced phosphenium triiodide (DAP-I_3) **1-11**.[20][23] The triiodide counterion can be exchanged for tetraphenyl borate anion to generate **1-12** (Scheme 1-3, eqn 2) or hexafluorophosphate anions via salt metathesis. Reduction of the triiodide has also been reported with the use of harsh reducing agents, such as potassium metal[24] or lithium hydride[8] to generate the DAP-iodide, a neutral DAP containing a covalent P-I bond from DAP-I_3. One case reported by the Speed group was a failed PBr_3 and cyclohexene cyclization, with a diimine with bulky *tert*-butyl groups, but no decomposition of diimine was observed. The use of PI_3 for this cyclization resulted in a clean cyclization to DAP-I_3 **1-13** (Scheme 1-3, eqn 3).[8] This shows the potential value of exploring more than one route to cyclization. The PI_3 cyclization method tends to

generate very clean DAPs and encompasses a broader scope of diimines. However, disadvantages include the high expense of PI_3, and the limitation of converting triiodides to other species.

Gudat and co-workers also suggested the mechanism of the cyclization using PI_3 was distinct to the PBr_3 and PCl_3 cyclization, based off combined experimental and computational data. The loss of molecular iodine from a charge transfer complex between PI_3 and diimine results directly in the formation of the DAP without forming the phosphorane P(V) intermediate. The molecular iodine that was released abstracts the iodide from the phosphorus resulting in the DAP phosphenium cation. [21]

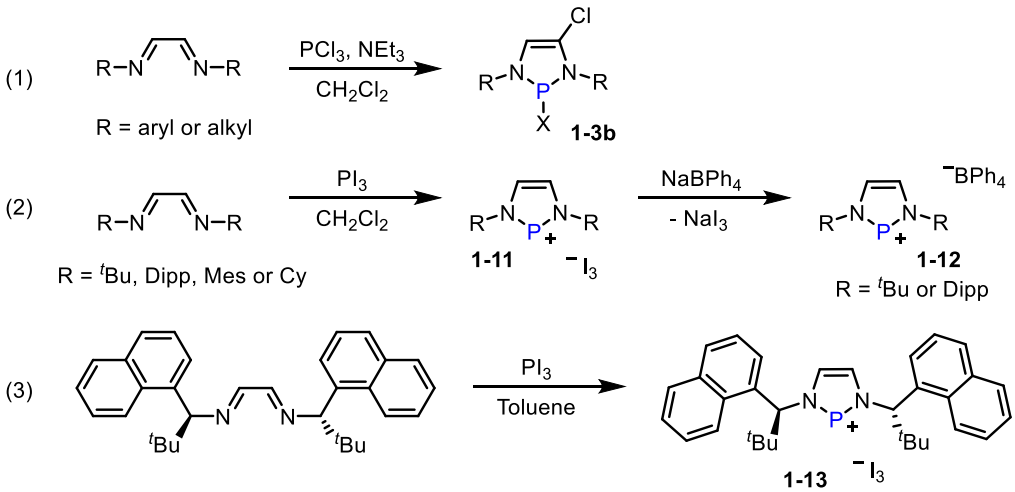

Scheme 1-3. Cyclizations of non-substituted backbone diimines with (1) PCl_3 and triethylamine in dichloromethane to generate DAP-Cl **1-3b**. (2) PI_3 in dichloromethane to generate DAP-I_3 **1-11** and subsequently formed diazaphosphenium **1-12**. (3) PI_3 in toluene to generate DAP-I_3 **1-13**.

1.2 Synthesis and Stoichiometric Reactions of Diazaphospholene Hydrides

Diimine cyclizations to DAP-halides are the foundation of synthesizing DAPs that can be used directly in catalysis for reductive transformations. Gudat and co-workers directly accessed the diazaphospholene-hydride (DAP-H) **1-14** from the DAP-Br by reducing the DAP-Br with $LiAlH_4$,[2] then later optimized the reduction with the use of Red-Al instead

(Scheme 1-4).[19] In addition to the improved reductant, they reported the first DAP-alkoxides **1-15a** and **1-15b** through stoichiometric hydrophosphination reactions between the DAP-H **14** and a ketone or aldehyde, respectively, that resulted in covalent P-O bond products. It is interesting to note that cinnamaldehyde exclusively gave the product from a 1,4 reduction rather than a 1,2 reduction, with a 3:1 mixture of *E*:*Z* enol phosphine isomers. Gudat's report of the stoichiometric hydrophosphination of aldehydes or ketones with a DAP-H was the last report of DAP-alkoxide synthesis for several years until Kinjo and co-workers reported the use of HBpin as a terminal reductant to regenerate the DAP-H **1-14** from the DAP-alkoxide **1-16** in 2015 (Scheme 1-5, eqn 1).

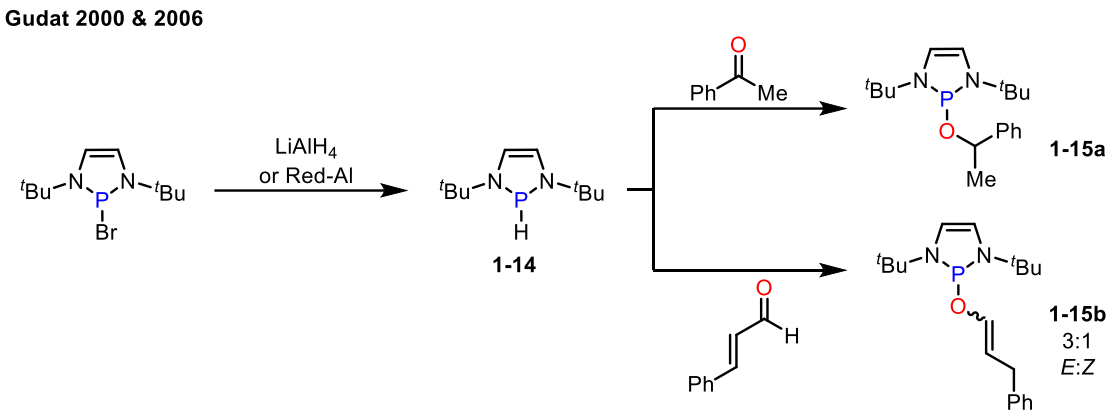

Scheme 1-4. DAP-Br converted to DAP-H **1-14** then subsequently to DAP-alkoxides **1-15a** and **1-15b** through hydrophosphination of a ketone and aldehyde, respectively.

The work reported by Kinjo and co-workers made Gudat's work catalytic, the DAP-H **1-14** initially reacts with an aldehyde to generate the DAP-alkoxide **1-16**, then Kinjo showed the DAP-alkoxide could undergo a σ-bond metathesis with boranes (such as HBpin, pinacolborane) to regenerate the DAP-H **1-14** and produce a borylated alcohol, such reactivity was exploited for the catalytic hydroboration of aldehydes and ketones with DAPs (Scheme 1-5, eqn 2). Additionally, they proposed a catalytic cycle for the hydroboration of aldehydes and ketones starting from the DAP-H **1-14** (Scheme 1-5, eqn

3).[25] Initially DAP-H **1-14** reacts with the carbonyl containing substrate to generate DAP **1-16** followed by the addition of HBpin which goes through a four-membered ring, σ-bond metathesis, transition state to regenerate DAP-H **1-14** and form a borylated alcohol. An aqueous work-up can be used to remove the Bpin and obtain the alcohol if desired. This was just the beginning of DAP catalytic reactivity and demonstrated its potential as a main group-based catalyst for reductive transformations. The Speed, Cramer, and Kinjo groups went on to further exploit this reactivity to catalyze other reductive transformations.[7][8][11][12]

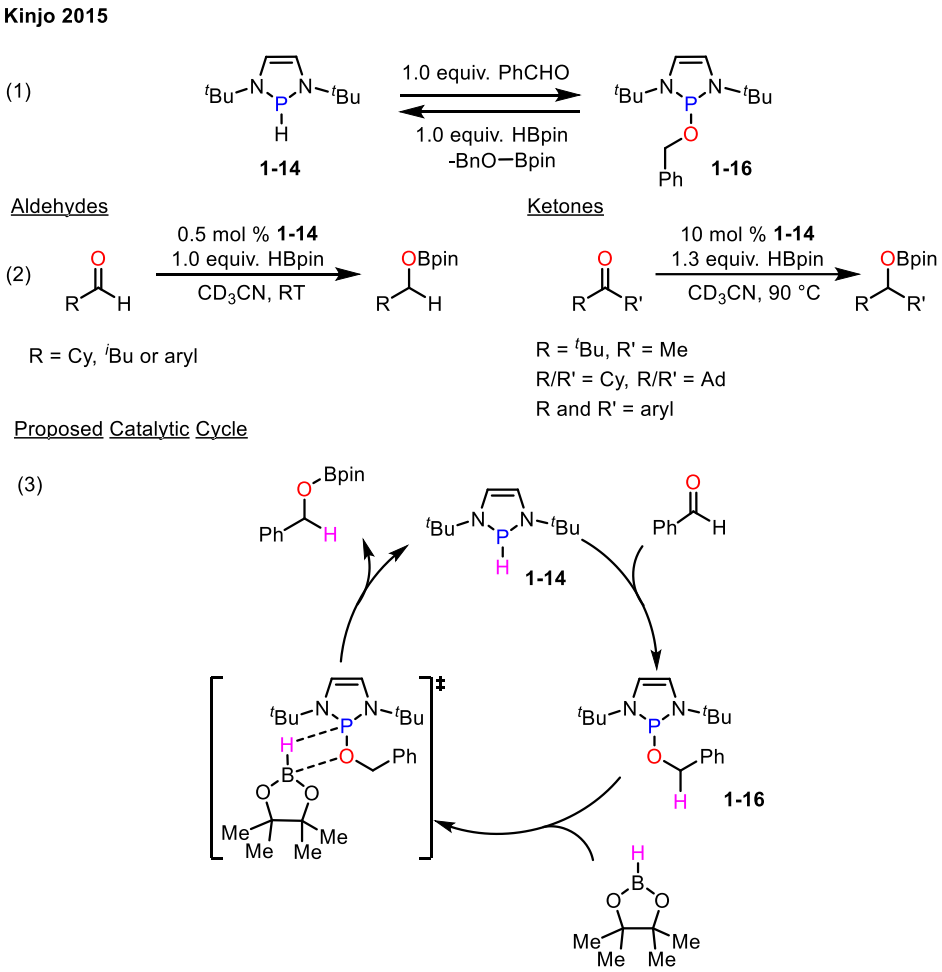

Scheme 1-5. (1) DAP-H **1-14** reversible reactivity with HBpin. (2) Hydroboration of carbonyl compounds catalyzed by DAP-H **1-14**. (3) Proposed catalytic cycle of the reduction of aldehydes and ketones by DAP-H **1-14**.

1.3 Synthesis and Reactivity of Achiral Neutral Diazaphospholene Pre-Catalysts

Kinjo's development of DAP-H **1-14** as a catalyst for the reduction of carbonyl compounds led the Speed and Cramer groups to independently report the synthesis of a DAP-alkoxide as a pre-catalyst. Based off Kinjo's proposed catalytic cycle, the Speed group rationalized the DAP-alkoxide would be a suitable point of entry for catalysis. The Speed group reported the synthesis of achiral DAP-alkoxide **1-17** (Scheme 1-6, eqn 1) and its ability to catalytically reduce two distinct substrate scopes, imines and conjugate reduction of ketones and esters (Scheme 1-6, eqn 2).[7] Later the Speed group showed DAP **1-17** can also be used to catalyze the hydroboration of pyridines (Scheme 1-6, eqn 3).[26] The Cramer group reported the use of achiral DAP-alkoxides to catalyze a Claisen rearrangement, described later.[11] Additionally, the alkoxide pre-catalyst was found to be a powder leading to easy user handling properties and can be stored in the absence of water and moisture for an extended period of time (years). Both groups have reported distinct syntheses to generate DAP-alkoxides. The Speed group, starting from the DAP-Br, reported the use of neopentyl alcohol as a nucleophile which displaces the bromide to form the DAP-alkoxide **1-17**. Additionally, HBr is generated so the presence of triethylamine is imperative to quench the acid (Scheme 1-6, eqn 1).

The achiral DAP-alkoxide, **1-17**, was used as a pre-catalyst to reduce imines and α,β-unsaturated ketones and esters (Scheme 1-6, eqn 2) with HBpin as the terminal reductant. Shortly after, the Speed group reported the use of achiral DAP-alkoxide **1-17** as a pre-catalyst to hydroborate 3-substituted pyridines with HBpin (Scheme 1-6, eqn 3). The substrates specifically required electron-withdrawing substituents. The majority of the substrates exclusively produced a 1,4-reduced product with a select few producing both the

1,2- and 1,4-reduction products. Substrates required a specific substitution pattern to be reduced, only pyridines containing an electron-withdrawing substituent in the 3-position could be reduced. Electron-donating substituents in the 3-position or electron-withdrawing substituents in the 2- or 4-position were not reduced. This work was published in rapid succession to Kinjo's work that also reduces pyridines, with less stringent substitution pattern requirements using a diazaphosphenium-based catalyst which shows distinctly different reactivity to the neutral phosphine and will be explained in detail later.[10]

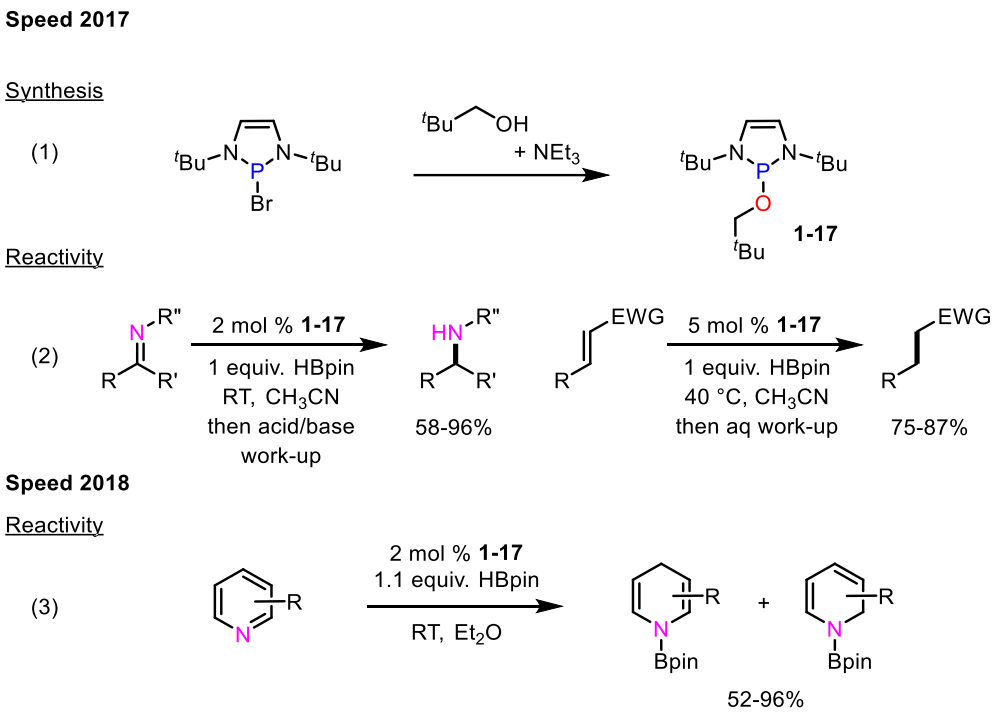

Scheme 1-6. (1) Synthesis of achiral DAP-alkoxide by the Speed group. (2) DAP catalyzed imine and conjugate reduction. (3) DAP catalyzed pyridine reduction.

The Cramer group reported the synthesis of DAP-alkoxides for another type of reductive transformation, namely a Claisen rearrangement.[11] They used the same synthesis reported by the Speed group to generate **1-18** but instead of neopentyl alcohol they used benzyl alcohol (Scheme 1-7, eqn 1). They reported an additional synthesis with a slight variation to generate DAP-alkoxides **1-19**, **1-20a**, **1-20b**, and **1-21**. Instead of an

alcohol and a base, they used a strong oxygen containing base, sodium methoxide, to displace the bromine and form the DAP-alkoxide, in this case the by-product of this method is sodium bromide (Scheme 1-7, eqn 2).

The DAP-alkoxide **1-18** with HBpin as the reductant was found to be optimal to catalyze the reductive Claisen rearrangement of allyl-ester enoates (Scheme 1-7, eqn 3). A wide variety of substrates were tolerated. The diastereoselectivity was modulated with the use of different catalysts, such as **1-19**, and solvents (Scheme 1-7, eqn 4).[5] This was the first report of DAPs catalyzing C-C bond formation. Mechanistic studies revealed two different pathways to achieve this transformation. Certain substrates underwent the Claisen rearrangement spontaneously from the formation of a P-O enolate. Alternatively, other substrates initially generated a C-P enolate which reacts with HBpin to form an O-Bpin enolate then undergoes a spontaneous Claisen rearrangement. A chiral DAP **1-21** was synthesized and demonstrated proof of principle that enantioinduction can be achieved in the Claisen. This is limited to substrates that favour the P-O enolate intermediate.[11] The synthesis of chiral diimine precursor for **1-21** is relatively complex and requires five steps, then an additional two steps to generate the DAP-OMe.[12]

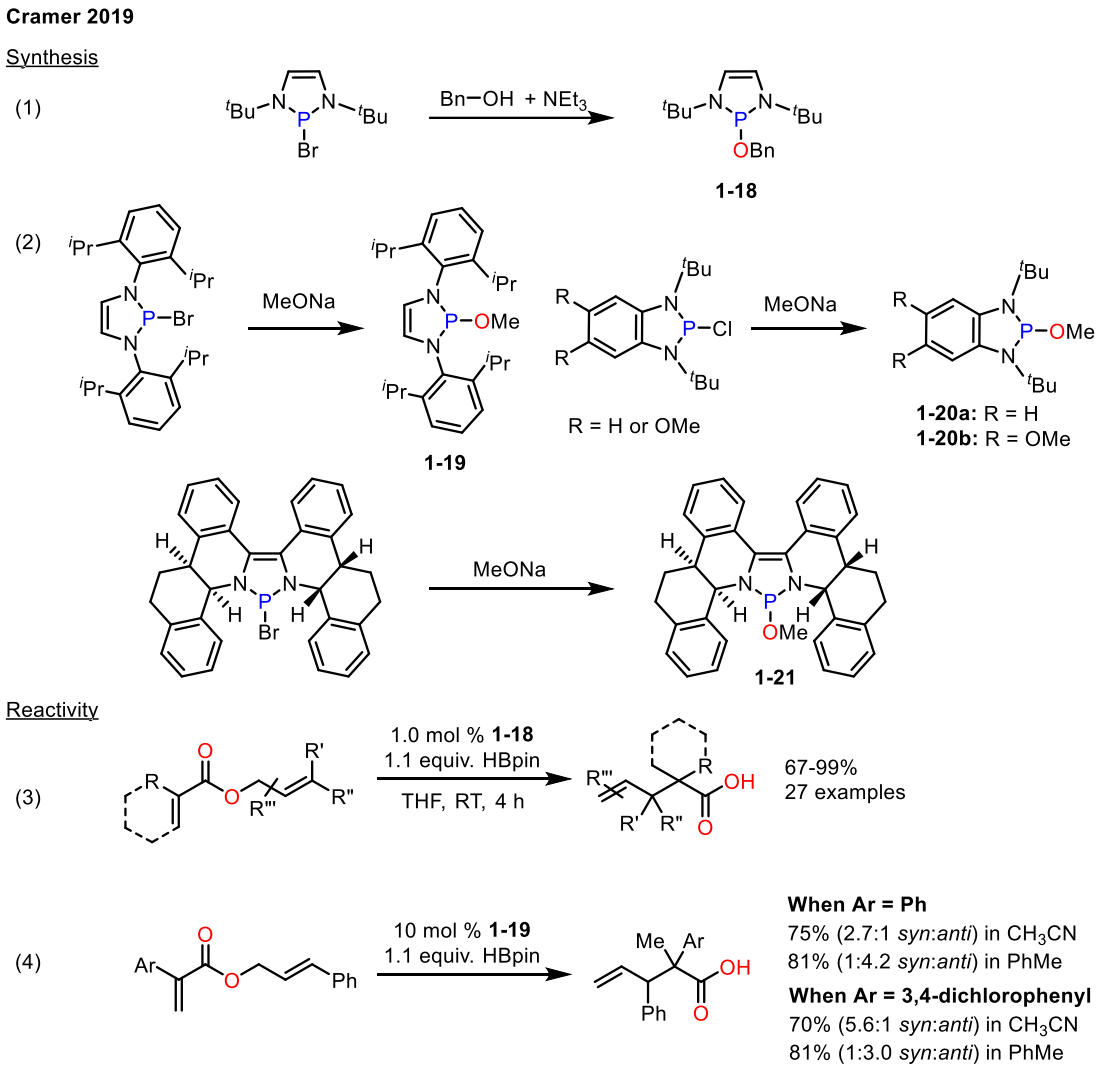

Scheme 1-7. (1) Synthesis of DAP-alkoxide **1-18** with benzyl alcohol and triethylamine. (2) Synthesis of DAP-alkoxides **1-19** to **1-21** with sodium methoxide. (3) Catalyzed Claisen rearrangement by DAP **1-18**. (4) Catalyzed Claisen rearrangement by DAP **1-19**.

1.4 Synthesis and Reactivity of Chiral Diazaphospholenes

1.4.1 Synthesis and Reactivity of Chiral Neutral Diazaphospholenes

The first reported synthesis of chiral DAP-alkoxides was by the Speed group in 2017. The synthesis is identical to the achiral variants where the DAP-Br is treated with neopentyl alcohol and triethylamine to generate the DAP-alkoxide. The more important aspect to note about the synthesis of the chiral variant, is the formation of the diimine. The diimine was derived from a commercially available enantiopure amine which requires just a one-step

condensation reaction to generate the diimine. The increased complexity with the addition of chiral moieties to DAP structure maintains a simple three step synthesis to isolate the DAP-alkoxide **1-22** (Scheme 1-8, eqn 1).[8] The enantiopure chiral amine is a relatively inexpensive starting material, and when coupled with the ease of synthesis demonstrates the practicality of this pre-catalyst.

In addition, the Speed group reported **1-22** as the first main group-based catalyst to catalyze the asymmetric hydroboration of imines with good to high yields and modest to good enantioselectivities (Scheme 1-8, eqn 2). The reaction proceeds under mild conditions but depended on sufficient steric differentiation on either side of the imine to obtain high enantioinduction. The highest enantiomeric ratio reported for this system was 88:12.[8] One way to achieve higher enantioselectivity would be to cool the reaction. Cooling the reduction reaction revealed no conversion of imine to amine, meaning there was a reactivity limitation of the neutral DAP pre-catalyst. However, this provided a good starting point for DAP asymmetric reactivity with room for improvement.

The proposed catalytic cycle (Scheme 1-8, eqn 3) begins with the initiation of DAP-alkoxide **1-22** through a σ-bond metathesis reaction with HBpin to generate the catalytically active DAP-H **1-23**. The hydride is delivered to an imine-borane adduct, forming a diazaphosphenium intermediate **1-24** and an amido-borane adduct which transfers the hydride to the diazaphosphenium to regenerate **1-23** and generate the borylated amine. No conversion upon cooling implies **1-22** is not initiated to the DAP-H **1-23** at colder temperatures, or the hydride transfer from the DAP to the imine is sluggish, limiting the enantioselectivity (or reactivity) observed.

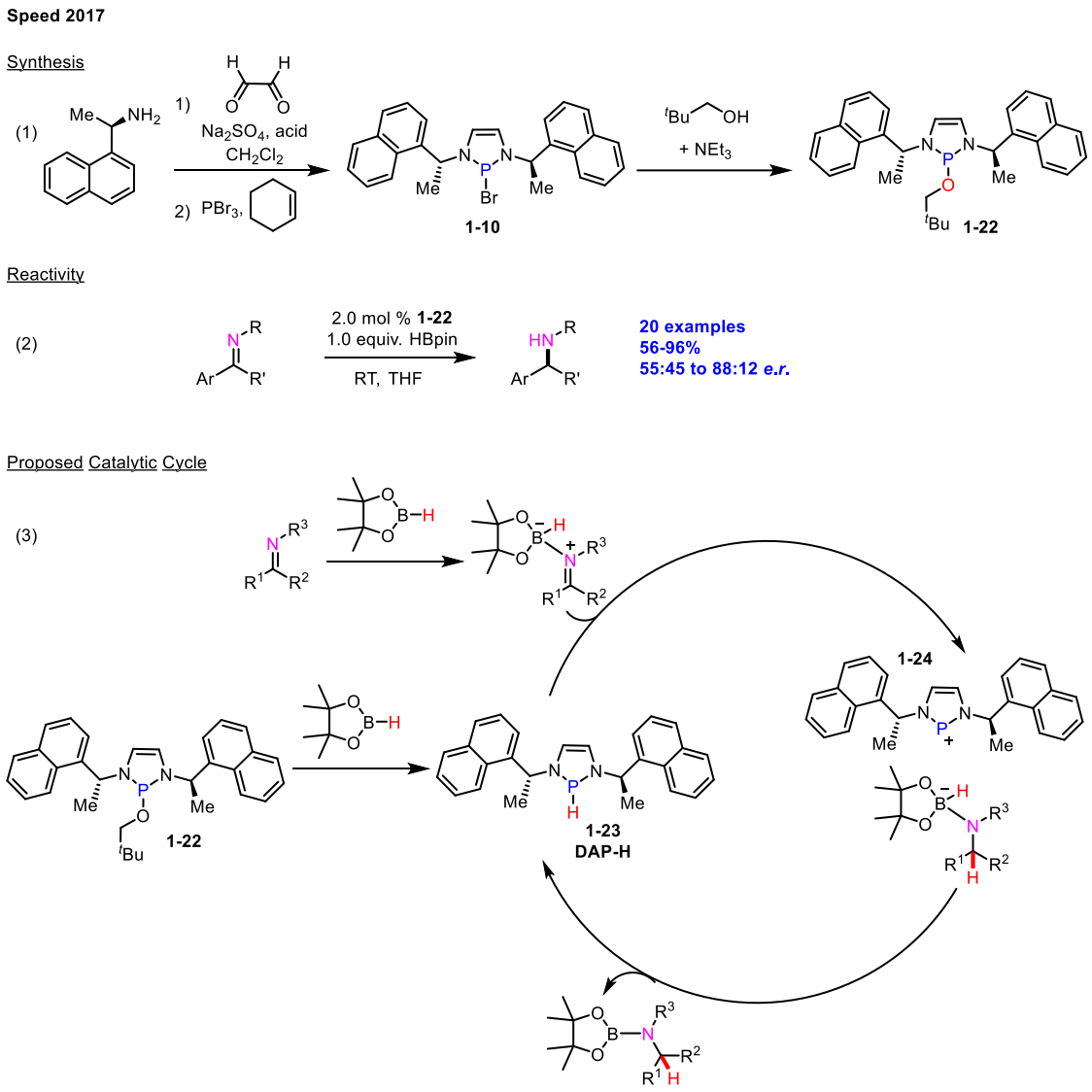

Scheme 1-8. (1) A three-step synthesis to DAP-alkoxide **1-22** from a commercially available amine. (2) Asymmetric reduction of imines catalyzed by DAP **1-22**. (3) Proposed catalytic cycle of imine reduction by DAP **1-22** and HBpin.

The Cramer group also reported the synthesis of chiral DAP-alkoxide **1-25** in 2018 for asymmetric conjugate reductions. As mentioned previously, the synthesis requires multiple steps to obtain the diimine. Specifically for **1-25**, the synthesis of the diimine precursor involved a rhodium-based catalyst that would also need to be synthesized (albeit using methodology developed within the Cramer group). Once the diimine is cyclized to the

DAP-Br, they reported the use of sodium methoxide to generate the DAP-alkoxide **1-25** (Scheme 1-9, eqn 1).[12]

The elaborate chiral DAP **1-25** was used to catalyze the asymmetric conjugate reductions (Scheme 1-9 eqn 2). A wide variety of substrates were tolerated with good to high yields and good to high enantioselectivities. Chiral DAPs synthesized from simple commercially available starting material were tested in addition to the elaborate version and DAP-alkoxide **1-25** was found to be the optimal catalyst. The authors hypothesized the free rotation around the exocyclic N-C bond in DAPs synthesized from commercially available chiral amines had an insufficient defined stereochemical environment around the phosphorus centre.[5] My project described in Chapter 4, details a way to increase the rigidity of the stereochemical environment by limiting the rotation of the exocyclic N-C bond by adding alkyl substituents in the backbone.

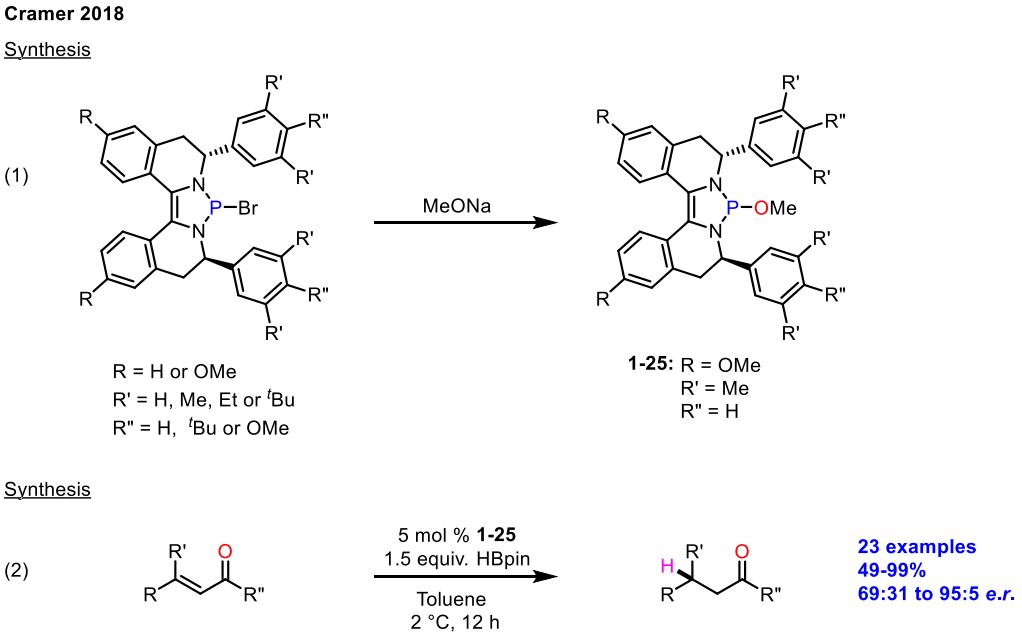

Scheme 1-9. (1) Synthesis of chiral DAP-alkoxide **1-25**. (2) Asymmetric conjugate reduction catalyzed by DAP **1-25**.

1.4.2 Synthesis and Reactivity of Chiral Cationic Diazaphospholenes

The synthesis and use of diazaphosphenium catalysts have been prevalent in recent literature, independently reported by Kinjo and Speed groups. In Gudat's initial study in 2000, they reported the synthesis of a diazaphosphenium-triflate from the mono chloro-substituted backbone DAP upon treating the DAP-H with triflic acid which released hydrogen gas (Scheme 1-10, eqn 1).[2] This resulted in a cationic DAP **1-26** with a triflate counterion (DAP-OTf) and further proved the point the hydrogen attached to the phosphorus centre was hydridic rather than protic.

After the initial reports of the neutral DAP-alkoxide variants in 2017, the Kinjo group reasoned that enhanced Lewis acidity at the phosphorus centre meant the phosphenium could be used as a hydride transfer reagent for hydroboration reduction of pyridines.[10] This work was done simultaneously to the report of DAP-alkoxide **1-17** for this same transformation from the Speed group.[26] Kinjo reported the synthesis of an achiral benzo-fused backbone diazaphosphenium with a triflate counterion **1-27** by treating the DAP-Cl with silver triflate (Scheme 1-10, eqn 2).

The cationic DAP **1-27** proved to have superior reactivity for pyridine hydroboration compared to the neutral DAP reported by the Speed group (Scheme 1-10, eqn 3). A broad scope of substrates, with electron-withdrawing and electron-donating substituents in the 2- and 3-position, were tolerated. Results heavily favoured the 1,4-reduced products in good to high yields. Limitations of this system were electron-donating groups in the 3-position produced mixtures of 1,2- and 1,4-reduced products, and pyridines with substituents in the 4-position were not reduced.

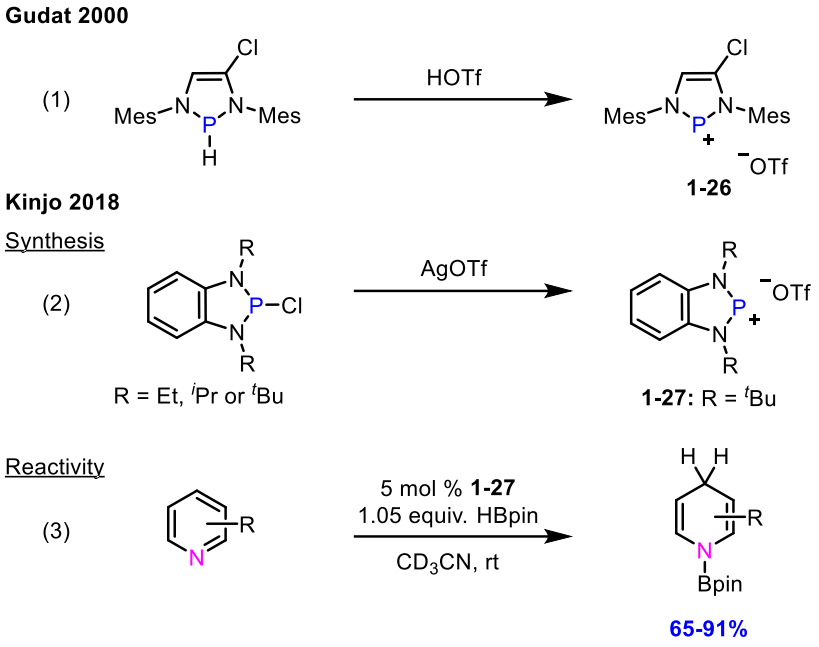

Scheme 1-10. (1) Synthesis of diazaphosphenium **1-26**. (2) Synthesis of achiral diazaphosphenium with triflate counterion **1-27**. (3) 1,4-Pyridine reduction catalyzed by achiral diazaphosphenium **1-27**.

The enhanced Lewis acidic phosphorus centre was adopted by the Speed group to improve the reactivity and enantioselectivity of imine hydroboration reactions catalyzed by chiral DAPs. The Speed group reported the synthesis of DAP-OTf **1-28** by treating the DAP-Br **1-10** with TMSOTf (Scheme 1-11, eqn 1).[9] DAP-OTf **1-28** had improved reactivity relative to the chiral neutral DAP-alkoxide **1-22**, variant and because of the increased reactivity the reduction reaction of imines could be cooled and maintain conversion of imines to amines (Scheme 1-11, eqn 2). More importantly to note, enantioselectivity was overall improved and some substrates achieved enantiomeric ratios as high as 97:3. A broad scope of cyclic imine substrates were tolerated with good to high yields and good to high enantioselectivities. One class of substrates not well tolerated for the system was acyclic imines. The enantioselectivity of acyclic imine substrates remained below a 90:10 enantiomeric ratio, meaning there was still substantial improvement

available for this class of substrates, prompting further development of DAP reduction catalysts.

The improved reactivity can be explained by the proposed catalytic cycle (Scheme 1-11, eqn 3). The catalytic cycle begins with **1-28**, and the formation of the imine-borane adduct, this means the first step is the delivery of the hydride to the phosphenium, generating the DAP-H **1-23** and an imine supported borenium adduct. The DAP-H **1-23** delivers the hydride to the adduct, generating the borylated amine and regenerating the DAP-OTf **1-28**. One hypothesis for improved reactivity is that the diazaphosphenium **1-28** is an on-cycle catalyst, as it is regenerated through the reduction process, and does not require initiation like the neutral DAP-alkoxide **1-22**. Another hypothesis is that the hydride delivery from the DAP-H **1-23** to the imine supported borenium adduct process has an overall positive charge associated with it. This can be thought of as the catalyst reacting with a more activated electrophilic substrate, compared with the neutral reduction, which is a faster process and requires less energy (can happen at cooler temperatures) to proceed. This improved reactivity allows for the reaction temperature to be colder, helping increase enantioselectivity. Additionally, we hypothesize the improved selectivity is also aided by the cyclic imine structure as it is a more rigid class of substrates. This could give reason as to why the acyclic substrates did not give as high enantioselectivity for this system.

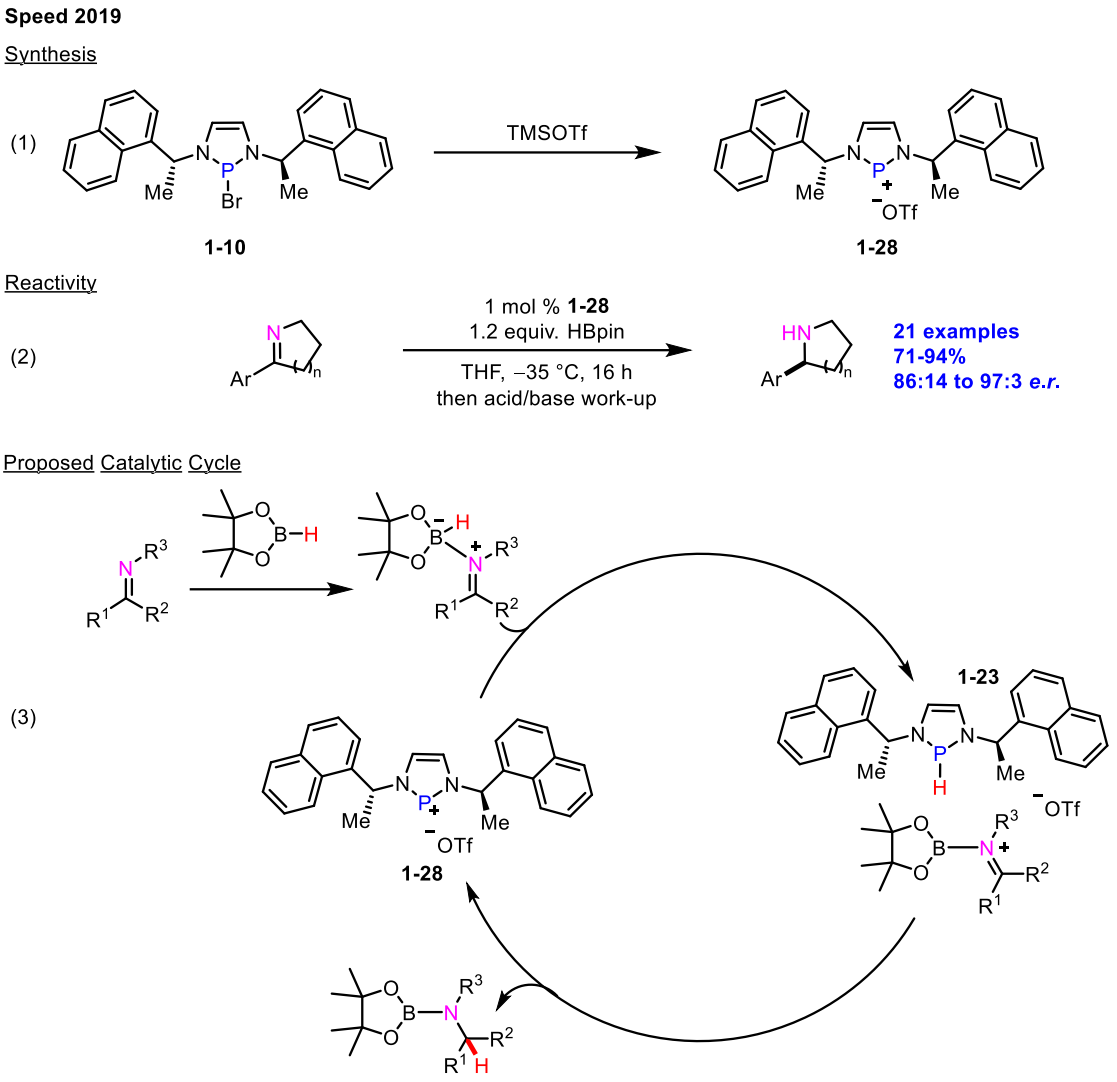

Scheme 1-11. (1) Synthesis of DAP-OTf **1-28**. (2) Asymmetric reduction of cyclic imines catalyzed by **1-28**. (3) Proposed catalytic cycle of asymmetric reductions of cyclic imines by **1-28**.

In the last ten years, there has been substantial improvement in the ease of DAP-halide synthesis which have been useful precursors to access DAPs that can be used in catalysis for many reductive transformations. The isolation of DAP-alkoxides and diazaphospheniums has superior user properties relative to the DAP-H and can be easy to access from inexpensive starting materials. One drawback to these DAP-alkoxide and diazaphosphenium variants is that they remain air and moisture sensitive. Recently the

Speed group has published the secondary phosphine oxide (SPO) **1-29** variant.[6] Treating the DAP-Br **1-10** with water and triethylamine generates the air and moisture stable SPO **1-29** (Scheme 1-12). This maintains three step synthesis starting from the commercially available amine and the SPO is purifiable by column chromatography under non-inert conditions. This is useful for users that may not have access to a glovebox. The SPO has shown promise to be a pre-catalyst directly in reductions or it can be easily transformed to the DAP-OTf *in situ*, with silyl triflates.

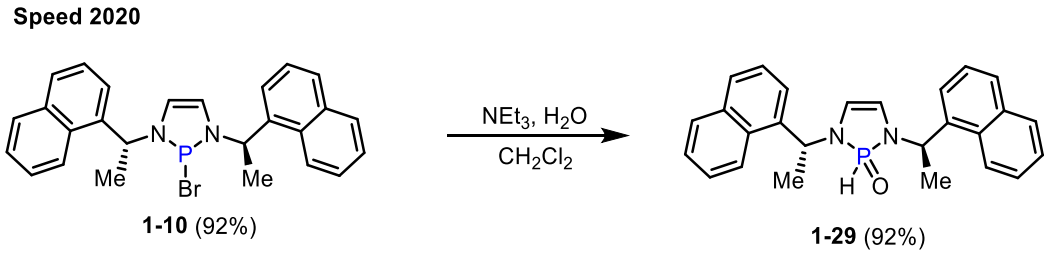

Scheme 1-12. Synthesis of SPO variant **1-29**.

There have been a few imine hydroboration reactions reported with the use of SPO **1-29**. In one case, a catalytic amount of SPO can catalyze the imine hydroboration at cool temperatures and maintain high yield and enantioselectivity (Scheme 1-13, eqn 1). For a heterocyclic containing cyclic imine, there was no selectivity and poor yield when catalyzed by the SPO **1-29** (Scheme 1-13, eqn 2) even at room temperature. However, when a catalytic amount of SPO **1-29** was mixed with a catalytic amount of *tert*-butyldimethylsilyl trifluoromethanesulfonate (TBSOTf) to generate the diazaphosphenium *in situ*, the reduction of the heterocyclic containing cyclic imine substrate at room temperature had high yield and enantioselectivity, showing the improved reactivity of the cationic catalyst (Scheme 1-13, eqn 3).[6]

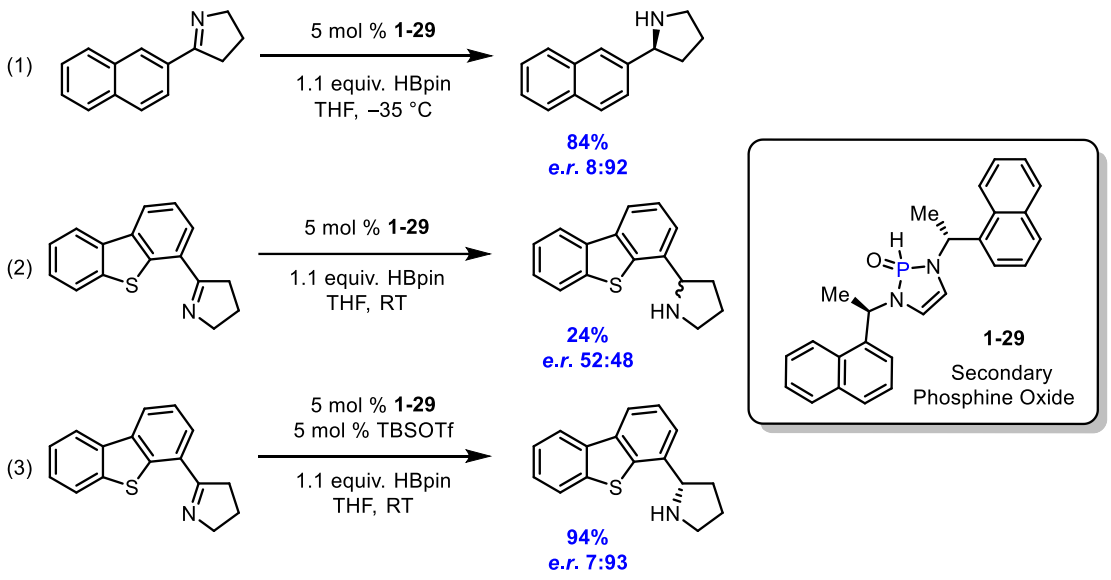

Scheme 1-13. (1) Reduction of cyclic imine catalyzed by SPO **1-29** at −35 °C with high enantioselectivity. (2) Reduction of cyclic imine catalyzed by SPO **1-29** at room temperature with poor enantioselectivity. (3) Reduction of cyclic imine catalyzed by SPO **1-29** initiated with TBSOTf at room temperature with high enantioselectivity.

The proposed catalytic cycle (Scheme 1-14) of the SPO is similar to the neutral DAP-alkoxide. We hypothesize the SPO **1-29** is in equilibrium with the tautomer **1-29a** which can undergo a σ-bond metathesis with HBpin to generate the DAP-H **1-23**, which enters the rest of the catalytic cycle. This is analogues to the DAP-alkoxide version. The DAP-H **1-23** delivers a hydride to the imine-borane adduct which forms the diazaphosphenium **1-24** and amino-boronate adduct. The hydride on the Bpin is transferred to the diazaphosphenium to regenerate the DAP-H **1-23** and produce the borylated amine product.

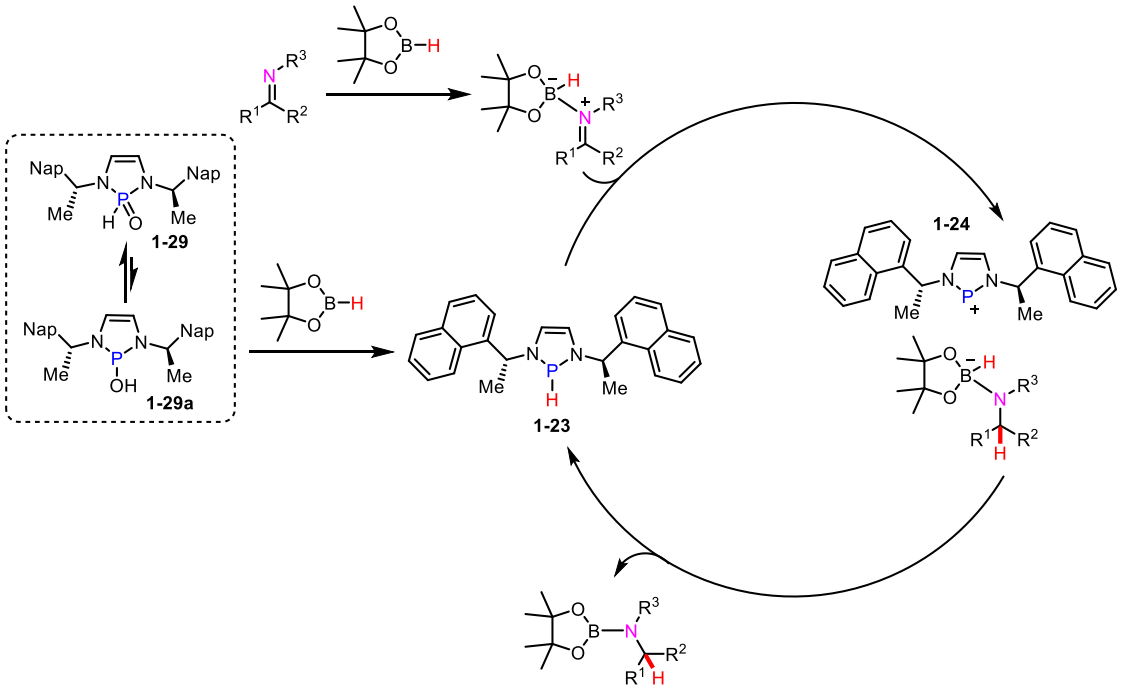

Scheme 1-14. Proposed catalytic cycle of imine reduction by SPO **1-29**.

The work described in my thesis uses these foundational concepts of diazaphospholenes in catalysis with the hopes of generating a library of diazaphospholenes with structural modifications to overcome the enantioselectivty limitations within DAP catalysis, specifically in imine reduction. As will be explained in the next section, development of highly enantioselective catalysts for imine reduction remains an active research area, to which DAPs can continue to make a strong contribution.

1.5 Asymmetric Reduction of Imines

Asymmetric catalysis has been an important field for many years. In 2001 Noyori and Knowles were awarded the Nobel prize for their contribution to asymmetric hydrogenation of enamines and alkenes.[27][28] In 2021, MacMillan and List were awarded the Nobel prize for asymmetric organocatalysis, highlighting the impact this field has for pharmaceutical research and green chemistry.[29] The selective preparation of one enantiomer of the chiral

product is important for pharmaceutical research because usually only one enantiomer is biologically active. The other enantiomer may be harmful or at best inactive, some examples include thalidomide, and methorphan (Figure 1-4). Thalidomide (Figure 1-4A) was prescribed to pregnant women to treat morning sickness back in the 1950's, which is true for (*R*)-thalidomide but it was later determined that (*S*)-thalidomide caused birth defects. In this case, enantioselective synthesis would not have helped as it was later determined at the natural pH of the body, (*R*)-thalidomide racemizes generating (*S*)-thalidomide which cause severe side effects and has been since removed from the market (though it remains in use as a cancer drug).[30] Another example is methorphan (Figure 1-4B), where dextromethorphan is used to relieve common cold symptoms and levomethorphan is a stronger opioid than morphine.[31] These examples highlight the importance of synthesizing each enantiomer independently and testing the toxicology properties.

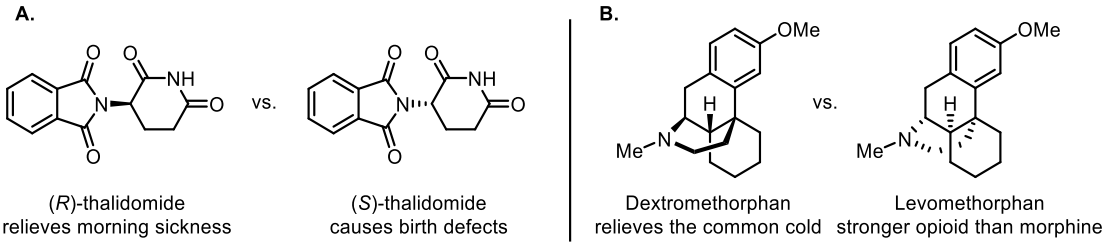

Figure 1-4. Biological difference of enantiomers for (A) thalidomide and (B) methorphan.

A common moiety found in drug molecules is the chiral amine. In addition to the methorphan (Figure 1-4b), some other notable pharmaceutical drugs that contain chiral amines are rasagiline,[32] used to treat Parkinson's disease, fendiline,[33] a calcium channel blocker, and sertraline,[34] used to treat depression (Figure 1-5). The most direct way to access chiral amines would be catalyzed asymmetric hydrogenation of imine precursors.

This method has been well developed with the use of precious transition metal-based catalysts containing chiral ligands.

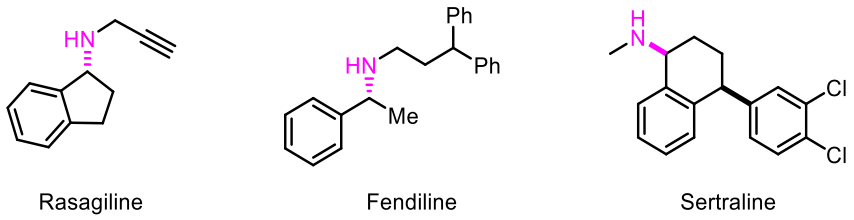

Figure 1-5. Examples of pharmaceutical drugs that contain a chiral amine.

The most commonly employed metal based-catalysts found in the literature for this transformation are iridium (Ir) and rhodium (Rh)-based catalysts with chiral bis-phosphines (P,P) or similarly, mixed phosphorus, nitrogen (P,N) chelating ligands. A notable example in recent literature was the synthesis of cationic [IrH(THF)(P,N)(imine)] [BAr^F] **1-30** for the asymmetric hydrogenation of *N*-alkyl imines (Scheme 1-15).[35] This is a remarkable catalytic system with low pressure, and low catalyst loading providing high selectivity in the reduction of *N*-alkyl imines substrates which are notoriously hard to reduce with such high selectivity. There were a handful of substrates reduced and the system was shown to tolerate electron poor and electron rich substituents in the *meta*- or *para*-position of the aryl rings and multiple alkyl side chains. A class of functional groups not presented or discussed were heterocyclic containing imines or *ortho*-substituted aryl rings.

Analyzing a transition metal-based system, it is always important to consider the synthesis of the ligand. For **1-30** the chiral P,N ligand comprises of three fragments, an amino alcohol, an amino acid and a P-stereogenic phosphinous acid.[36] An advantage of this ligand is the ability to easily modulate the substituents to tune the ligand for a desired reaction. However, it requires three synthetic steps starting from the boc-protected amino

acid including the step containing the chiral phosphinous acid, which requires four synthetic steps to isolate.[37] Once the ligand was synthesized, to isolate **1-30**, Ir[COD]Cl_2 was the metal source and the additive acetophenone *N*-phenyl imine was required which was two more synthetic steps. Each time a new variation is required for optimal performance it would be nine total synthetic steps to isolate the desired catalyst. Additionally, second and third row late-transition metal salts, especially Pt-group based are scarce, expensive, and toxic.[38] The limitations of precious metal supply and cost, coupled with relatively complex ligands, mean there is considerable interest in developing alternative methods, such as base metal, or main group catalysts, to complement or even replace these complexes.

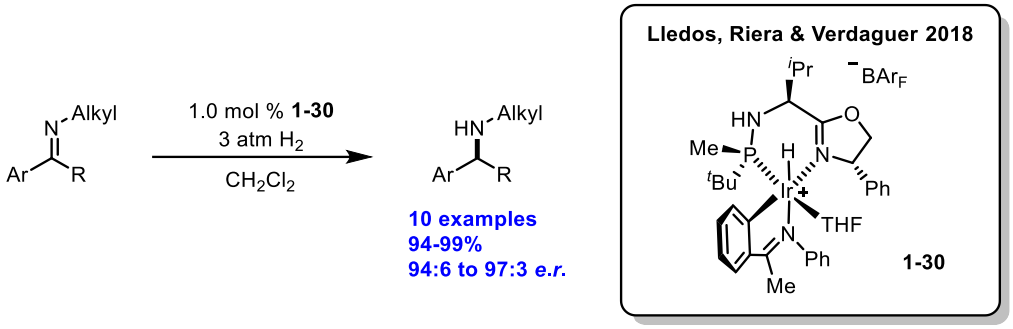

Scheme 1-15. Asymmetric hydrogenation of imines with chiral Ir-based catalyst.

While hydrogenation of imines is the most direct and atom economical method of accessing amines and the most developed reductive transformation for transition metal-based catalyst. It does require specialized equipment and increase of safety concerns when high pressures are required to perform adequate catalysis. Hydroboration, while not as atom economical, does not pose such safety concerns and pinacolborane (HBpin) is an easy reagent to handle as it is a liquid at room temperature and therefore has its advantages in exploratory reactivity, conducted at small to medium scales. Asymmetric hydroboration of imines with the use of transition metal-based catalysts is a much less developed field than

asymmetric hydrogenation yet is most pertinent as a competitor to the asymmetric hydroboration of imines catalyzed by DAPs. Recently, in 2020, Gade and co-workers reported the use of an iron (Fe) based-catalyst supported with a bis(oxazolinylmethylidene)isoindoline ("boxmi") pincer ligand **1-31** for the asymmetric hydroboration of imines (Scheme 1-16).[39] This is state-of-the-art asymmetric reduction of imines with a base metal catalyst for *N*-methyl imine substrates with a broad functional group tolerance, high yields and high enantioselectivities. The limitations of this system include heteroatom and ortho-substituted aryl groups, as well as exocyclic imines. The catalyst was reported to be isolated in a relatively short five step synthesis. Notably, the enantioselectivities obtained with acyclic imines in this system are superior to the those obtained by the Speed group's published DAP catalysts.

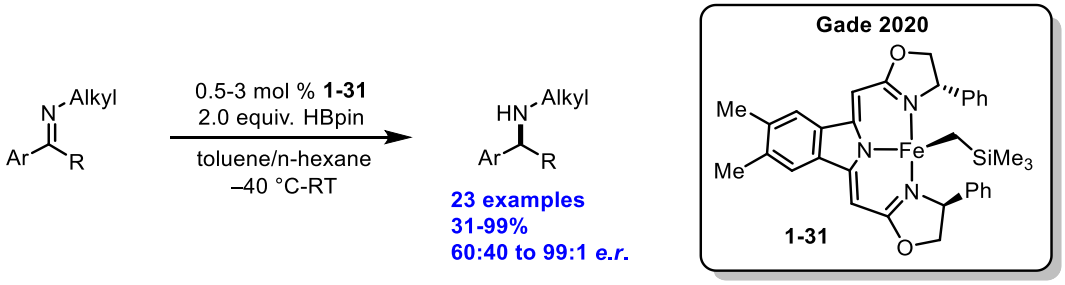

Scheme 1-16. Asymmetric hydroboration of imines with chiral Fe-based catalyst.

While developing main group-based catalysts, such as DAPs, there is already the advantage of it being phosphorus based, where phosphorus is a relatively highly abundant element relative to noble metals, a similar advantage as base metals hold. Like all catalysts it is important to be cognizant of the number of synthetic steps, the ease of synthesis, and ease of use properties. Main group-based catalysts have yet to show comparable reactivity to transition metal-based catalysts, but there does seem to be considerable potential in developing systems with complementary reactivity.

1.6 Thesis Overview

There have been remarkable developments of DAP synthesis and catalysis over the last decade. Overall, my thesis describes in detail the synthetic processes for modulating the substituents around the DAP scaffold, then testing each successfully isolated DAP for improved reactivity and selectivity in imine reduction. Initially, the goal was to generate DAP-OTfs with alternative substituents around the stereogenic centre with more sterically encumbered aryl or alkyl groups. The hypothesis was that the bigger substituents would create a better defined stereochemical environment around the phosphorus centre and enhance enantioselectivity.

To alter the substituents around the stereogenic centre requires different chiral amines, which required the synthesis of enantiopure chiral amines. Originally focusing on biaryl derivatives, this required an eight-step synthesis just to isolate the amine, then encountered purification issues with the resulting DAP-Brs and so the project was quickly abandoned. Due to ease of synthesis, my goal switched to generating heterocyclic containing amine derivatives. This was interesting because I was altering the steric and electronic environments around the DAP which could potentially teach us about the effects of these changes on DAP reactivity. The amine synthesis required only three-steps using Ellman methodology and an additional three steps to generate the DAP-OTfs. I successfully isolated six non-commercially available enantiopure amines and converted three of them to the corresponding DAP-OTf. Only one variant was comparable in terms of reactivity and enantioselectivity of amines to the current best DAP-OTf **1-28**. The heterocyclic variant that worked the best resembled naphthalene the most, but did not have enhanced reactivity relative to the naphthyl environment. This taught us that altering the electronics

and sterics around the stereogenic centre to improve reactivity and selectivity may prove challenging.

While I was synthesizing the heterocyclic containing derivatives, this led to a hypothesis of accessing an alternative substitution pattern on the heterocycles could lead to geometrical differences around the phosphorus centre. This difference could lead to a better substituent-differentiated stereochemical environment around the phosphorus than the original heterocyclic containing derivatives. This required the development of a one-pot synthesis to access a non-commercially available aldehyde, namely dibenzothiophene-1-carboxaldehyde, as precursor to the desired chiral amines. The key was two benzyne intermediates that were rapidly trapped by a nucleophile within the reaction. Ultimately, it led to a more efficient synthesis with safer reagents than previously reported literate to generate this compound. This was extended to a few other variants and published on its own. Additionally, there was a need for *N*-phenylphenothiazine in the laboratory for exploratory purposes. While this reagent can be purchased, it is relatively expensive. Instead, I started from phenothiazine and used the benzyne intermediate chemistry to generate 7.0 g of *N*-phenylphenothiazine. These projects steered away from synthesizing DAPs directly, and provided a good lesson to reiterate that just because there is already a published viable way to synthesize a reagent or even purchase it, does not mean it is necessarily the best choice.

After the side projects, it was evident from the prior results that altering the substituents around the stereogenic centre required a lot of work, yet yielded minimal success. I went back to the DAP scaffold and looked at an alternative position to modulate, the backbone. Replacing the protons in the backbone with an alkyl substituent, such as methyl, was

hypothesized to increase the rigidity of the DAP. This increased rigidity could lead to enhanced reactivity and enantioselectivity. To synthesize a DAP with a methyl substituent in the backbone required the use of an alternative phosphorus reagent to PBr_3, in the past the PBr_3 cyclization was attempted and led to complete decomposition. I found an alternative reagent that cyclized the diimine with methyl substituents in the backbone, diisopropylaminodichlorophosphine. This generated a DAP with a P(V) centre that was ultimately turned into the secondary phosphine oxide variant. The SPO with methyl substituents in the backbone was found to have improved enantioselectivity for acyclic imines.

Chapter 2 Heterocyclic Containing Chiral Diazaphospholenes

2.1 Research Overview and Contribution Report

The author wishes to clarify her contributions to the research described in Chapter 2 of this Thesis document. This Chapter describes the successful and unsuccessful syntheses of a library of chiral DAP derivatives containing different bulky aryl substituents. This required the synthesis of non-commercially available chiral amines as precursors to DAPs then converting the enantiopure amines to the corresponding DAP-OTf with precedented methods. The initial goal was to synthesize biaryl derivatives, but this quickly revealed some difficulties and these targets were discarded. For ease of synthesis and maintaining increased steric bulk, heterocyclic containing derivatives were the next targets. Successfully synthesized were three out of six DAP-OTf variants, **2-24a**, **2-24c**, and **2-24e**. The reactivity and enantioselectivity was tested and one variant, **2-24e**, had comparable results to the current best DAP-OTf **1-28**.

My contributions to the study included the initial synthesis of all compounds and intermediates leading to the DAP-OTf derivatives except for amine **2-9**, which was synthesized by Dr. Alex Speed. I obtained, processed and compiled the characterization data including ^{1}H, ^{13}C, ^{31}P, and ^{19}F NMR spectra and optical rotations as required, for the majority of the compounds. Some compounds have incomplete characterization as the preliminary results showed the complexes could not be prepared cleanly or had poor reactivity. Xiao Feng carried out mass spectroscopy analysis for all compounds described in this Chapter.

Reference (for synthesis and characterization of intermediates leading to 2-24e):

T. Lundrigan, **E. N. Welsh**, T. Hynes, C. H. Tien, M. R. Adams, K. R. Roy, K. N. Robertson, A. W. H. Speed, *J. Am. Chem. Soc*. **2019**, *141*, 14083–14088.

2.2 Introduction

A robust synthetic platform for diazaphospholenes is essential to generate structural variants to examine their selectivity. The generic structure of a diazaphospholene (Figure 2-1) details four positions, described as R^1–R^4, that can be altered to generate different analogues. Obstacles encountered during the synthesis of these modified DAPs are important for understanding the limitations of the catalyst synthesis and present potential opportunities for developing new methodology. The variation of the backbone position R^1 will be discussed in Chapter 4. The simplest point of variation is the counterion to the cationic phosphorus centre, defined as R^4. The effect of changing the counterion to enhance activity was first reported by the Kinjo group.[10] In the context of the Speed group's enantioselective chemistry, the use of a triflate counterion gave increased reactivity. The increased reactivity of the cationic DAP with a triflate counterion (DAP-OTf) enabled cooling of the catalytic reduction of imines to amines, and this cooling resulted in greater reaction enantioselectivity.[9] The last two positions defined as R^2 and R^3 are on the chiral side chains, and will be distinguished as the aryl and alkyl position respectively. This Chapter focuses on the synthesis of DAPs containing varying substituents in the aryl and alkyl positions, with the goal of increasing the imine reduction enantioselectivity. As described in Chapter 1, the DAP that produced the best amine enantioselectivity was when R^1 = H, R^2 = naphthyl, R^3 = methyl and R^4 = triflate. The first series of modifications

involved exchanging the naphthyl group with biphenyl derivatives and the second series of modifications involved exchanging the naphthyl with bulky heterocyclic derivatives.

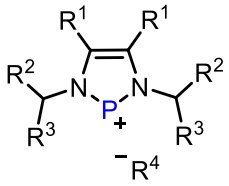

Figure 2-1. General structure of a cationic diazaphospholene.

The relatively limited number of commercially available enantiopure primary amines bearing different R^2 and R^3 groups limits the architectures available for catalyst synthesis. To address this limitation, the synthesis of non-commercially available enantiopure primary amines is required. Amine synthesis is relatively straightforward starting from an aldehyde or ketone via reductive amination, the challenging part is obtaining the enantiopure form.

One method to obtain a primary chiral amine is a chiral resolution of a racemic amine via diastereomeric salt pairs or covalent amides.[40] This process involves a reaction between a racemic compound (e.g. amine) and an enantiopure compound (e.g. acid, or acid chloride) resulting in diastereomeric products. These can be either ionic salts, or covalent compounds such as carbamates or amides. Diastereomers have the potential to be separated as they can have differing physical properties such as solubility or polarity and may be separated with purification techniques such as column chromatography or preferential recrystallization of one diastereomer. A classic example of this is the resolution of 1-phenylethylamine, **2-1**, with enantiopure tartaric acid, **2-2**, (Scheme 2-1).[41] The racemic amine reacts with enantiopure (2*R*, 3*R*)-tartaric acid forming diastereomeric products **2-3a** and **2-3b**. One diastereomer, **2-3a** (the salt pair containing (*R*)-1-phenylethylamine), is more soluble and remains in solution while the other diastereomer, **2-3b**, crystallizes out

of solution. The advantages of the resolution method are that it can be inexpensive and relatively easy to scale up. However, a major disadvantage of this method is that the separation of the diastereomeric products may be challenging if their properties do not differ substantially. Additionally, there is a 50% yield limitation on the desired enantiomer, though both enantiomers can potentially be accessed, which may be a favourable feature, if both enantiomers of the subsequent catalyst are desired.

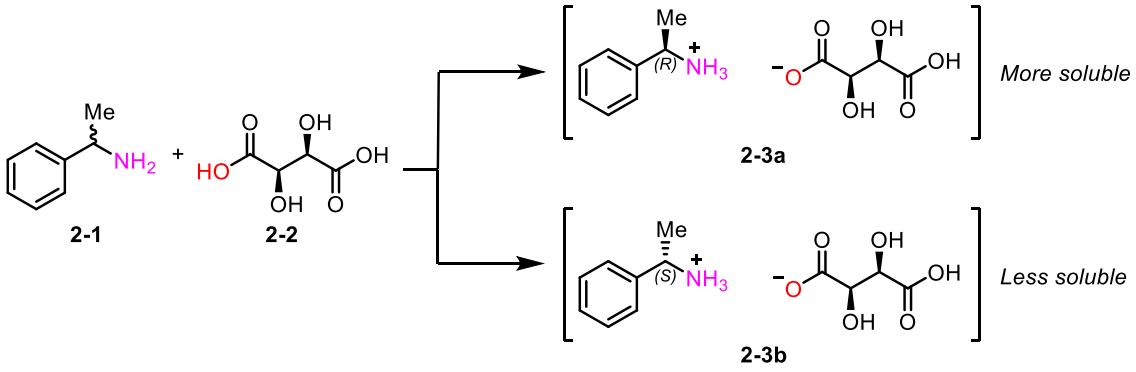

Scheme 2-1. Resolution of racemic phenylethylamine with enantiopure tartaric acid**.**

Another method to obtain enantiopure amines is through a kinetic resolution of the racemic amine with an acylating agent and a catalyst, typically an enzyme.[42] Kinetic resolution relies on a chiral catalyst to facilitate a reaction, e.g. acylation, that occurs faster with one enantiomer than the other. An example of this, is the use of an enzyme, CAL-B, to catalyze the acylation of one amine enantiomer (Scheme 2-2).[43] This results in two different products, the enantiomerically enriched unreacted primary amine **2-4a** and an amide enantiomerically enriched in the opposite enantiomer **2-4b**. These products now have substantially different polarities and could be separated and purified via column chromatography, acid-base extraction, or recrystallization. The advantages of using a kinetic resolution are that many enzymes are inexpensive, racemic amines are readily available, and the reaction is relatively easy to scale up. The major disadvantage is that

enzymes are extremely specific to particular substrates or structural features and may not tolerate variation, resulting in no reaction, or no selectivity. There is a limitation of a 50% yield for the desired enantiomer, though both enantiomers can be potentially accessed, via recovery of either the unreacted amine, or the amide.

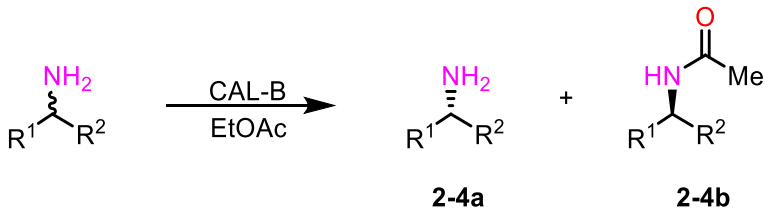

Scheme 2-2. Enzymatic resolution of racemic amines.

An alternative method to resolution to obtain an enantiopure amine is enantioselective catalytic reduction of imines. There have been many examples of different chiral catalysts for this transformation.[8][35][39][44][45] The advantages of reduction methods over resolution methods are that sub-stoichiometric amounts of catalyst are used, and there is potential for greater than 50% yield of the desired enantiomer, in contrast to resolutions. Disadvantages of catalytic methods are that the catalyst may not be completely selective for one enantiomer, and if the enantiomer ratio is poor, the separation of enantiomers rather than diastereomers is required. Often the catalyst must also be synthesized. It should be noted that DAPs have not yet been used to prepare primary amines, partially because of the instability of primary imines.

A different approach to synthesizing enantiopure amines involves chiral auxiliaries. There are many types of auxiliary reagents, however Ellman auxiliaries are best suited for chiral amine synthesis.[46] A general example of this approach begins with an aldehyde or ketone **2-5**, which reacts with enantiopure Ellman reagent **2-6**, to form a chiral sulfinimine intermediate **2-7** (Scheme 2-3). Intermediate **2-7** is treated with a Grignard reagent to

generate generic diastereomers, **2-8a** and **2-8b**. The absolute configuration of the sulfur atom on the Ellman auxiliary remains intact during the addition and a new stereocentre is formed during the addition which results in diastereomers. This method allows for the separation of the diastereomers through column chromatography or sometimes recrystallization or trituration to purify one diastereomer. Once purified, the auxiliary can then be removed from each diastereomer to give the respective enantiomeric amines. Advantages of this method are that it is generally robust, reliable and ultimate enantioselectivity relies on diastereomeric separation. Disadvantages of this method is that diastereoselectivity is often low, separation of diastereomers is often difficult and the scalability is limited as chromatography is often required for the separation.

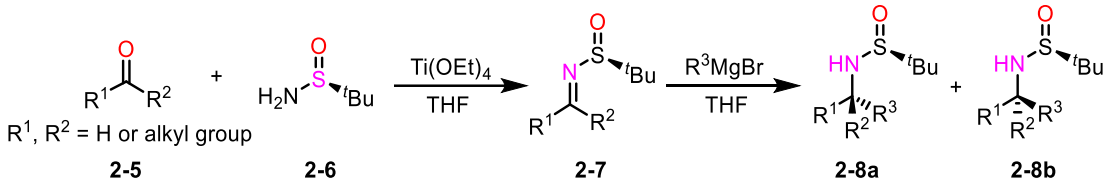

Scheme 2-3. Synthesis of enantiopure amines via Ellman chemistry.

This Chapter describes the synthesis of non-commercially available enantiopure primary amines, where each of the methods just described have been attempted or used to obtain the enantiopure amine. If the enantiopure amine was successfully generated, the end goal was to convert the enantiopure amine to a chiral diazaphospholene with the goal of discovering catalysts with higher enantioselectivity or potentially complementarity selectivity compared to the previously synthesized diazaphospholene catalysts. Enantiopure amines containing biphenyl derivates were the original goal followed by heterocyclic containing derivatives (Figure 2-2).

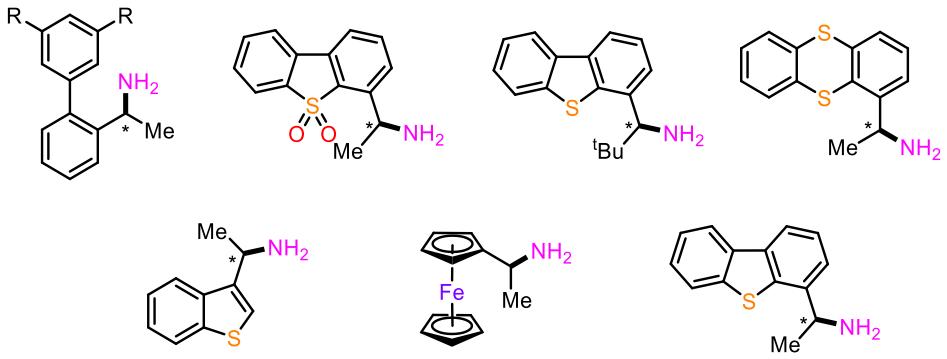

Figure 2-2. Chiral amines targeted in this Chapter.

2.3 Results and Discussion

2.3.1 Attempted Synthesis of Biaryl-Containing DAP Derivatives

The intention was to design a DAP with increased steric demand relative to the current best DAP catalyst **1-28** in the Speed group with the hypothesis that bulkier substituents would lead to increased enantioselectivity for imine reduction. The approach to attain this was to replace the biggest substituent, naphthyl, with an even larger aryl group. The initial attempt was to replace the naphthyl group with a biaryl derivative. The biaryl group was chosen because it would occupy a larger spatial volume than the naphthyl group, which was hoped to increase steric differentiation between the aryl and alkyl positions. In addition, biaryl groups could be easily modified by varying the substituents on the aryl groups by cross-coupling, and consequently it would be straightforward to synthesize a library of biaryl diazaphospholene derivatives. Although bulky biaryl amines were commercially unavailable, they were previously reported for NHC scaffolds prepared by the Gung group (Figure 2-3).[47] The following section describes a similar synthesis reported by the Gung group to isolate the desired chiral amines, and the efforts to convert them to the corresponding DAPs.

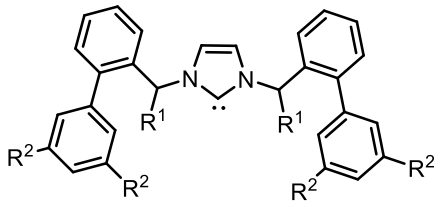

R^1= methyl, ethyl or isopropyl
R^2 = methyl or tert-butyl

Figure 2-3. Carbenes derived from biphenyl amines synthesized by Gung and co-workers.

To isolate enantiopure biaryl amines **2-13a** and **2-13b** required six synthetic steps (Scheme 2-4).[47] Dr. Alex Speed generated racemic amine **2-9** from commercially available 2′-bromoacetophenone through a Leuckart-Wallach reaction. The racemic amine was resolved[48] by the formation of a salt with enantiopure mandelic acid and the resulting diastereomers were separated on the basis of solubility. It should be noted that a relatively exotic solvent combination (ethanol and isopropyl acetate) was required for success of this literature-known resolution, which indicates the challenges associated with the development of new resolution methods. Automated screening was used in the original discovery of these conditions, a resource not readily accessible to us. The diastereomerically pure salt was treated with base to isolate enantiopure amine, **2-10**. The enantiopure amine, **2-10**, was boc-protected to generate amide **2-11** (boc = *tert*-butyloxycarbonyl). The boc-protection was imperative to ensure the Suzuki coupling with a boronic acid formed the desired C-C coupled products, **2-12a** and **2-12b** instead of an undesired intermolecular C-N cross-coupling. The final step was a boc-deprotection with trifluoroacetic acid to obtain the enantiopure biaryl amines, **2-13a** and **2-13b**. Despite the lengthy synthesis, an advantage of this method was that the biphenyl derivates would be tunable by using boronic acids that have alternative substitution patterns in the cross-coupling reactions.

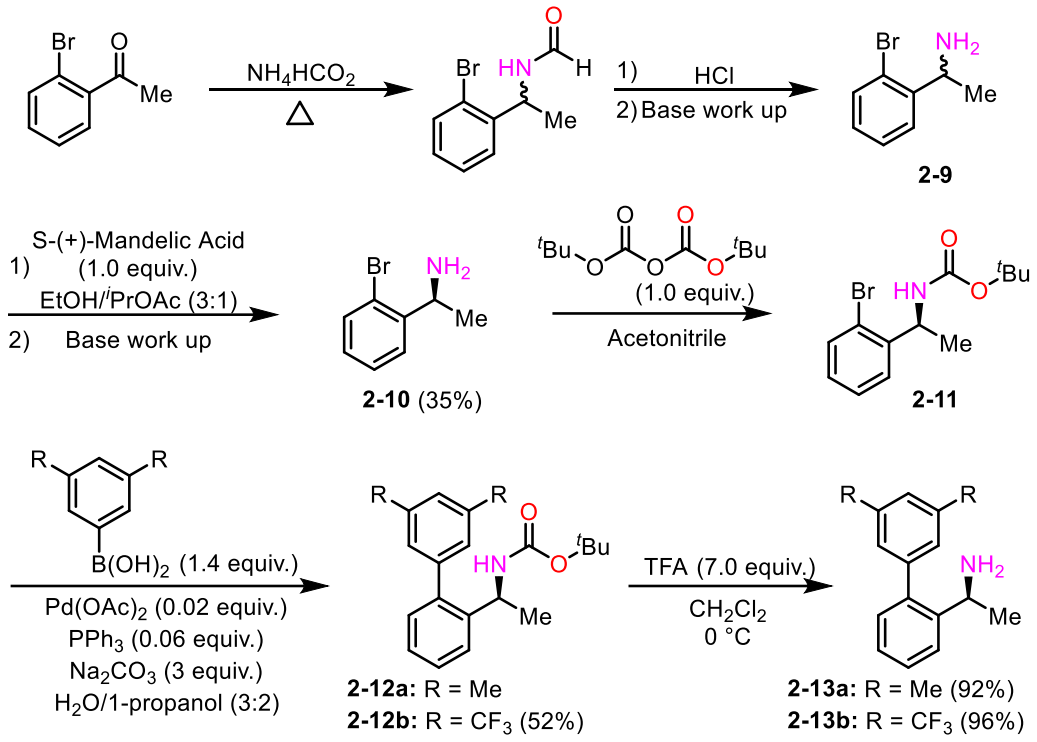

Scheme 2-4. Synthesis of chiral biaryl amines.

With the enantiopure amines **2-13a** and **2-13b** in hand, the subsequent steps to generate the corresponding cationic DAPs were anticipated to be uncomplicated, as the steps were well-known in the Speed group. This was proved to be untrue (Scheme 2-5). The enantiopure amines underwent an acid catalyzed condensation reaction with glyoxal to generate diimines **2-14a** and **2-14b**. The diimines **2-14a** and **2-14b** were treated with PBr_3 and cyclohexene to form DAP-Br **2-15a** and **2-15b** respectively, where the unforeseen issue arose. The desired products, DAP-Br **2-15a** and **2-15b**, were found to be partially pentane-soluble, unlike previous DAPs, along with the pentane-soluble impurities. This caused the purification and isolation step to be difficult as substantial amounts of the products were being extracted with the impurities of the cyclization, which resulted in low yields. Given the relative length and low throughput of this synthesis, this added complication severely limited quantities of material that could be prepared for testing. The

cationic DAPs or DAP triflates (DAP-OTfs), **2-16a** and **2-16b**, were not successfully isolated, as attempts to abstract the bromide to form the phosphenium triflate led to oils that were not readily purified.

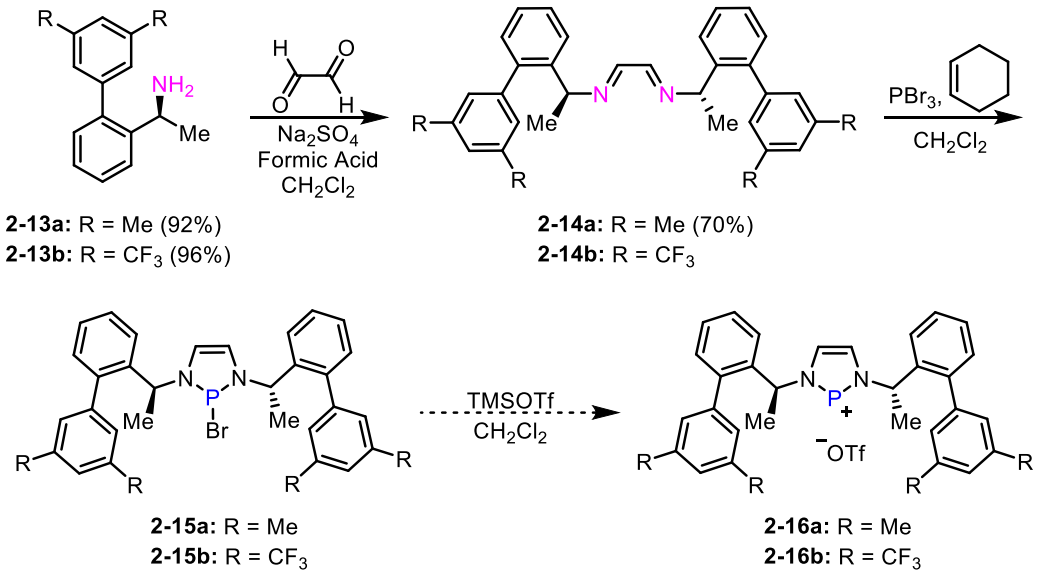

Scheme 2-5. Synthesis of chiral biaryl DAP-Br.

The DAP-Brs **2-15a** and **2-15b**, were used as pre-catalysts for the reduction of the benchmark substrate **2-17a**, a 2-naphthyl-bearing cyclic imine (Scheme 2-6) to determine if it would be worth the effort to optimize the purification of the DAP-Brs. This substrate is commonly used for initial screening tests within the Speed group. Imine **2-17a** is the benchmark substrate because it was found to be a good substrate for the best DAP catalyst, but not the best, meaning there is room for improvement. Additionally, and more importantly, the separation times of the enantiomers of amine **2-17b** on the HPLC are significantly different and the starting imine **2-17a** and does not overlap with either enantiomer. This means if the reduction does not have complete conversion, no further purification is required to determine enantioselectivity. This substrate will appear multiple times as the test substrate in each Chapter. For DAP-Brs, **2-15a** and **2-15b**, the results were

not promising, with an *e.r.* for amine **2-17b** below 80:20. For comparison, for the DAP-Br where the aryl group was the naphthyl as the pre-catalyst, the *e.r.* for **2-17b** was 90:10. These results suggest that the biaryls were not promising leads for a better catalyst. Given the low initial performance, combined with a lengthy synthesis and difficult purification, we decided to target other non-commercially available sterically encumbered chiral amines that bore closer resemblance to the most successful naphthyl groups. We assumed the high pentane solubility of these compounds was in part due to the presence of the methyl and trifluoromethyl groups on the biaryl motif. Dr. Speed separately investigated the parent unsubstituted biaryl and found it was also not promising, delivering poor enantioselectivity. Accordingly, the focus turned to the synthesis of heterocyclic chiral amines, which would be expected to have increased polarity, and lower solubility in non-polar solvents, leading to easier work-up/purification procedures.

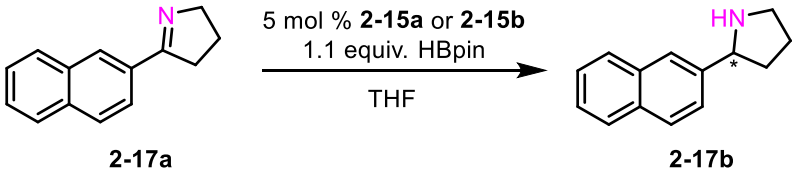

Scheme 2-6. Reduction of test substrate with biaryl DAP-Br analogues.

2.3.2 Synthesis of Heterocyclic Containing DAP Derivatives

A logical extension to increase the steric bulk of naphthalene would be to consider anthracene. Previously, Dr. Alex Speed and Matt Adams synthesized enantiopure 1-anthracen-9-yl ethylamine and generated the corresponding cationic DAP **2-18** (Figure 2-4). The amine was converted to the diimine then cyclized to the corresponding DAP-Br. The cyclization resulted in a substantially less clean DAP-Br than the naphthyl derivative. While the anthracene containing DAP-Br was not partially soluble in pentane, in contrast to DAP-Br **2-15a** and **2-15b**, the washing resulted in a partially purified DAP-Br due to

other unknown impurities remaining insoluble. Despite the impurities the bromine abstraction was successful which generated **2-18**. DAP-OTf **2-18** was used as a catalyst for some imine reductions that resulted in much lower enantioselectivity than the current best DAP-OTf **1-28** (on the order of 70:30). The inadequate cyclization, and inferior enantioselectivity relative to the naphthyl derivate proved it was not a good catalyst.

The decreased enantioselectivity could indicate a limitation of the catalyst design but upon further analysis it was hypothesized the additional ring could be too far from the chiral pocket to aid in selectivity (Figure 2-4). It is noticeable the additional ring is towards the back of the DAP in the comparison of **1-28** and **2-18** 2D structures. Comparison of the 3D structures, **1-28** and **2-18**, indicate the additional ring is away from where the substrate would be approaching and not aiding the selectivity. Furthermore, this modification could potentially result in conformations of the catalyst that result in lower selectivity. A more desirable derivative would be 1-anthracen-1-yl ethylamine, so the increased steric bulk would be added to one side. Unfortunately, there is no trivial synthesis to obtain this compound, or the required 1-halo anthracene starting materials.

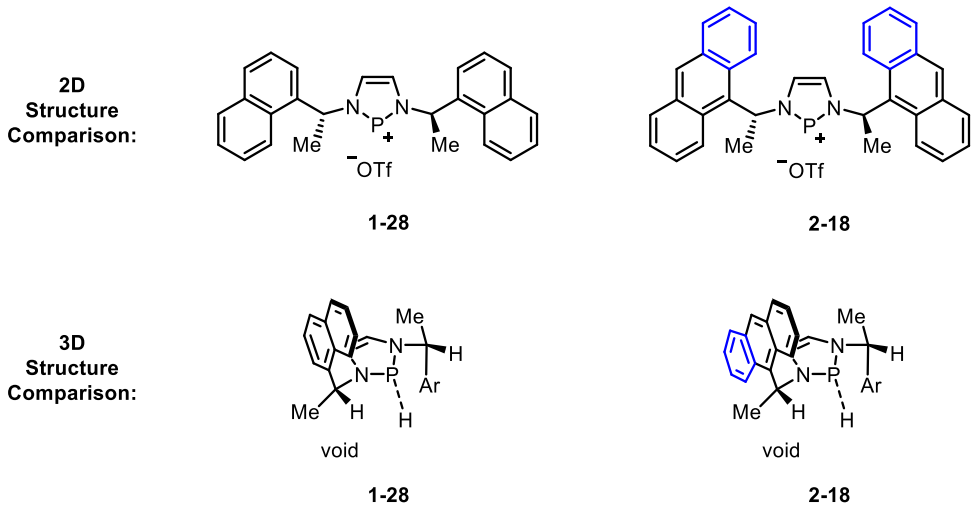

Figure 2-4. Structure comparison of the naphthyl derived diazaphospholene to the anthracene derived diazaphospholene.

In addition to the synthetic challenges that come with substituting anthracene in alternative positions, anthracene is a relatively symmetrical structure allowing for only a few variations. Parent naphthalene also only has two derivatives that are different, either 1-substituted or 2-substituted naphthalenes. Heterocyclic analogues with two or more aryl rings would allow for a relatively short synthesis and selective functionalization with more positions to functionalize as there is typically less symmetry within the heterocycle molecule. In addition, this would provide information about electronic tolerance of DAPs as all other aryl derivatives have been hydrocarbons. As Dr. Speed was synthesizing 1-anthracen-9-yl ethylamine (as opposed to the illustrated 9-anthracenyl compound), a colleague, Dr. Travis Lundrigan, discovered that a dibenzothiophene (DBT)-based imine was one of the best substrates screened (i.e. the naphthyl cationic catalyst obtained a high *e.r.* in reduction of this substrate) (Scheme 2-7).[9]

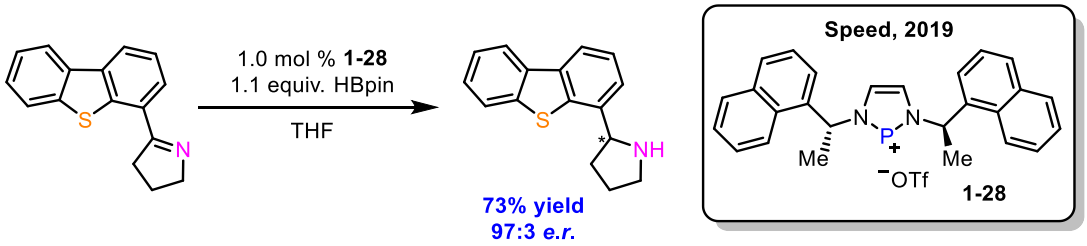

Scheme 2-7. Reduction of the dibenzothiophene derived cyclic imine.

The combination of attempting to synthesize a DAP that contain an aryl group bulkier than naphthyl, the challenging and limiting anthracene chiral amine synthesis, and the high enantioselectivity of the DBT-derived substrate led to the proposition that a DBT could be a new suitable motif in catalyst design. In essence, DBT could serve as a surrogate for 1-substituted anthracene. Presumably, the beneficial effect as a substrate stemmed from high steric demand, so we hypothesized the aryl component of a good substrate could make a good catalyst component. Additionally, DBT is easier to functionalize at certain positions

via lithiation, relative to anthracene, due to the presence and directing effects of the sulfur heteroatom. The numbering position of DBT is displayed in Figure 2-5 for consistent interpretation. Functionalizing DBT in the 4-position was the primary target, as it is the most accessible position to functionalize via lithiation.

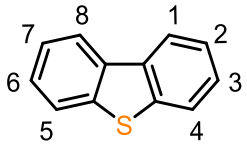

Figure 2-5. Numbering scheme for dibenzothiophene (DBT).

The synthesis of the chiral amine derived from the lithiation at the 4-position of DBT was successful (details to follow in the next section). This led to the synthesis of multiple chiral amines that contained heterocycles such as dibenzothiophene sulfone ($DBTO_2$), thianthrene (TH), benzothiophene (BT), and ferrocene (Fc). To limit the variations, most heterocycles were combined with a methyl group in the alkyl position except for one combination of aryl = DBT and alkyl = ^{t}Bu. Depending on the heterocycle, two synthetic approaches were used which I have categorized into lithiation or Grignard addition. The lithiation method begins with the heterocycle of interest while the Grignard addition begins with the heteroaryl aldehyde.

2.3.3 Synthesis of Heterocyclic Amines

Similar to the Grignard route as outlined in Section 2.2 (Scheme 2-3) the conversion of lithiated heterocycles to chiral amines is best accomplished through the Ellman auxiliary technique. The commercially available heterocycles DBT, $DBTO_2$ and TH, underwent a two-step synthesis to generate amines **2-21a** to **2-21d** (Scheme 2-8). Initially, the heterocycle, DBT, $DBTO_2$ or TH, was lithiated with *n*-butyllithium (*n*BuLi) at −78 °C or 0 °C for 0.5 h followed by the addition of a solution of a previously derived (from

condensation of acetaldehyde and (*S*)-*tert*-butanesulfinamide) Ellman imine **2-19a**, in THF to generate intermediates **2-20a**, **2-20b**, and **2-20c** respectively. Intermediate **2-20d** was generated by the addition of Ellman imine **2-19b** (derived from condensation of pivaldehyde and (*S*)-*tert*-butanesulfinamide) in THF to lithiated DBT. Each reaction resulted in the formation of two diastereomers that were cleanly separated via column chromatography. Each diastereomerically pure Ellman–protected amine, **2-20a** to **2-20d**, was separately treated with dilute anhydrous HCl to cleave the Ellman auxiliary directly resulting in the corresponding amine salt. Enantiopure amines, **2-21a**, **2-21b**, **2-21c**, and **2-21d**, were isolated by treating the acid salt with dilute $NaOH_{(aq)}$ then extracting into an organic solvent and removing the solvent via rotary evaporation.

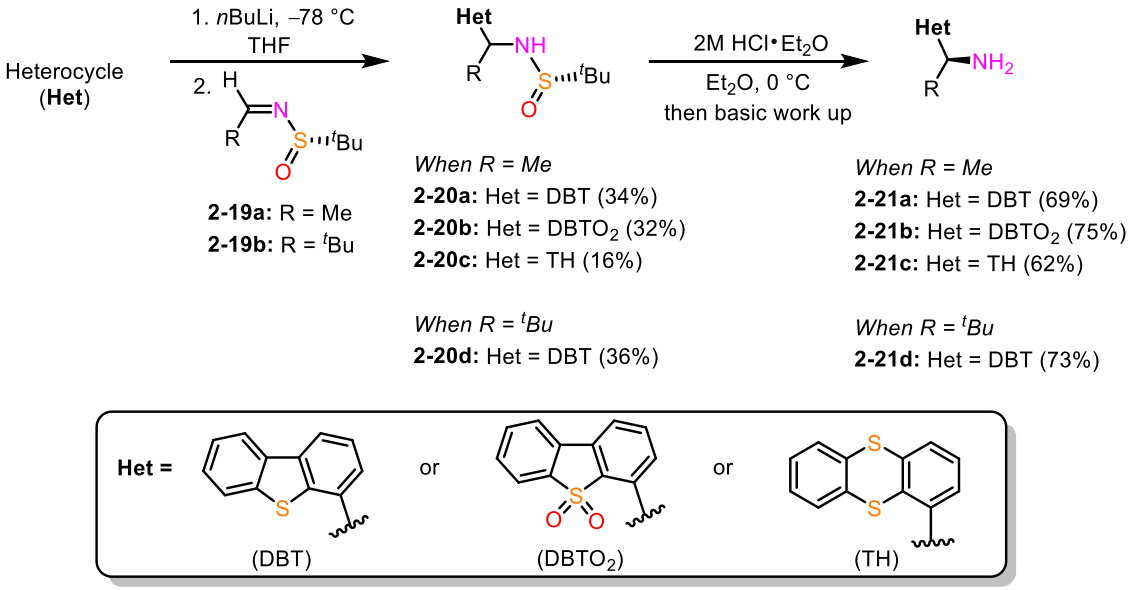

Scheme 2-8. General synthesis of heterocyclic containing chiral amines via lithiation.

The $DBTO_2$ chiral amine, **2-21b**, was an attractive variant to synthesize because the presence of the two oxygens would present an even greater steric demand than DBT. This modification could also potentially provide more information on the effects of electronic modification as a role in selectivity of chiral diazaphospholenes. The 1,4-thianthrene (TH)

containing chiral amine **2-21c** was synthesized as a comparison to geometrically distinct "hetero-anthracene". Thianthrene would also serve to compare the reactivity and potentially determine some limits of heterocyclic catalyst design. The chiral amine **2-21d**, where the aryl position contains a DBT group and the alkyl position contains a *tert*-butyl (^{t}Bu) group, was synthesized to compare if altering the position of the steric demand of the alkyl group would be tolerated and if it would influence selectivity. It should be noted that previous attempts to use a *tert*-butyl substituent with a naphthyl aryl group led to a decrease in enantioselectivity for the neutral chiral catalyst.[8] This modification was still imperative for learning and understanding potential trends within the heterocyclic variants.

The BT and Fc heterocyclic containing amines **2-21e** and **2-21f** (Scheme 2-9) were synthesized from the respective commercially available aldehydes which is analogues to the generic route described in Section 2.2 (Scheme 2-3). The first step generated Ellman imines **2-19c** and **2-19d** through a titanium mediated condensation reaction with the heterocyclic containing aldehyde and (*S*)-*tert*-butanesulfinamide (Ellman auxiliary). Each intermediate was separately treated with methyl Grignard to generate diastereomers of **2-20e** and **2-20f**. The diastereomers were separated via column chromatography to ensure one enantiomer is formed in the following step. The final step, identical to the lithiation synthesis, was to cleave the Ellman auxiliary from the purified diastereomer of **2-20e** and **2-20f** by treating with dilute HCl in ether, generating the enantiopure amine salts. The enantiopure amines **2-21e** and **2-21f** were isolated by treating the respective acid salt with dilute $NaOH_{(aq)}$ then extracting into an organic solvent and removing the solvent via rotary evaporation. This route was used because selective lithiation of the desired position is challenging for these two heterocycles specifically. BT would selectively lithiate in the 2-

position rather than the 3-position, and the monolithiation of ferrocene is notoriously challenging, while in contrast, the ferrocene carbaldehyde is relatively inexpensive.[49]

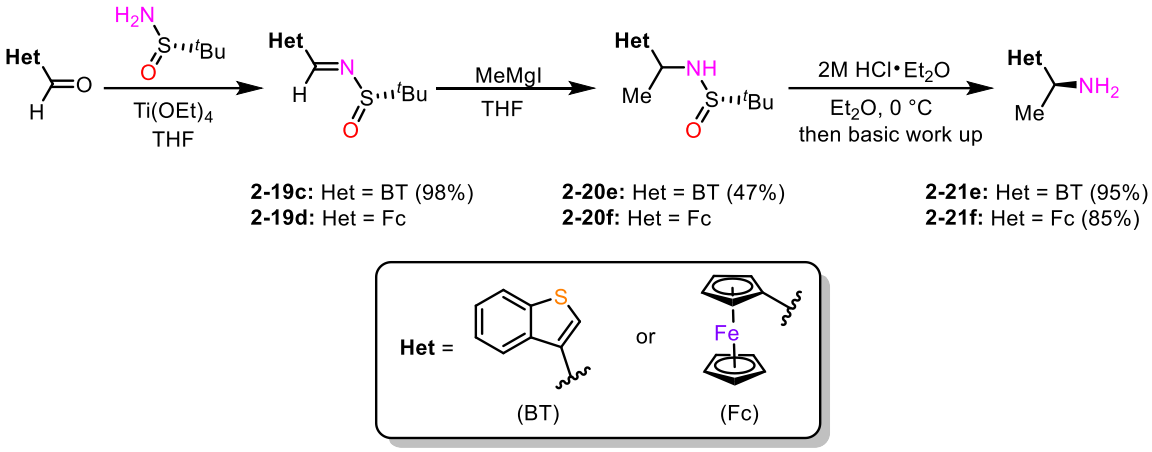

Scheme 2-9. Synthesis of enantiopure amines containing a benzothiophene or a ferrocene motif via Grignard addition.

The BT analogue was chosen because it had the closest resemblance to the 1-naphthyl analogue, and the Fc derivative was desirable as ferrocene is a component in privileged ligands; the planar chiral ferrocene ligands are known for high selectivity in hydrogenation reactions.[50] While the mono-substituted ferrocene does not exhibit planar chirality, is has a distinct geometric profile to the other heterocycles, being more three dimensional (barrel-shaped) than the planar aromatic rings which could lead to interesting results. Incorporation of such an electron-rich fragment could also potentially provide information on catalyst design limits. With a library of enantiopure heterocyclic containing amines, the following steps were to convert them to the corresponding cationic DAPs.

2.3.4 Synthesis of Heterocyclic Containing DAPs

The synthesis of the cationic DAPs from the enantiopure heterocyclic chiral amines were consistent with the synthesis of the cationic DAPs described in Chapter 1 and Section 2.3.1. The chiral amines, **2-21a** to **2-21f**, underwent an acid catalyzed condensation

reaction with glyoxal in the presence of sodium sulfate which successfully generated the desired diimines, **2-22a** to **2-22f** (Scheme 2-10). The diimines were used without further purification as diimines are hydrolytically sensitive which make column chromatography an infeasible choice, and crystallization of diimines has generally not been successful. In some cases, impurities can be decreased by washing the diimine with small quantities of cold ether. It should be noted in most cases the relative configuration of the Ellman adducts was not determined, so the absolute configuration of the amines was not certain. We anticipated a more in-depth investigation of stereochemistry could be done with the most selective DAPs.

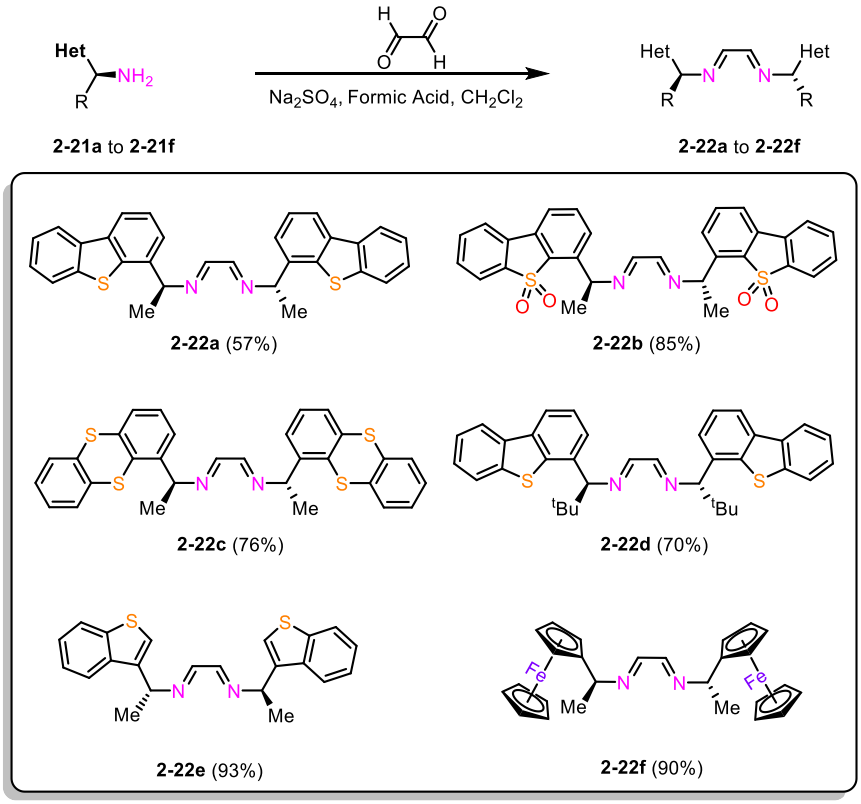

Scheme 2-10. Diimine synthesis of heterocyclic containing amines.

The subsequent steps were to cyclize the diimines into the corresponding DAP-Br compounds, followed by a bromide abstraction with TMSOTf to generate the desired DAP-

OTfs (Scheme 2-11). The diimines, **2-22a** to **2-22f**, were subjected to the usual PBr_3 and cyclohexene reaction to generate DAP-Brs **2-23a** to **2-23f**. This was only successful for three derivatives, **2-23a**, **2-23c**, **2-23e**, which were treated with TMSOTf to generate DAP-OTfs, **2-24a**, **2-24c**, and **2-24e** (Scheme 2-11A) Unfortunately the cyclization to DAP-Brs, **2-23b**, **2-23d**, and **2-23f** were unsuccessful (Scheme 2-11B). Based on speculation from the proton (^{1}H) NMR spectra, it was believed diimines **2-23b** and **2-23f** have undesired reactions that compete with the cyclization. Diimine **2-23b** contains a Lewis-basic sulfone that could interfere with the PBr_3 reaction, as there appeared to be extensive decomposition. The ^{1}H NMR spectrum of the crude reaction mixture with the hopes of generating **2-23f** also revealed decomposition, as well as trace amounts of vinyl ferrocene. This is indicative of an elimination reaction occurring. The ^{1}H NMR spectrum for DAP-Br **2-23d** showed unconsumed diimine **2-22d** leading to conclude the increased steric bulk in the alkyl position, the ^{t}Bu group, prevented the cyclization.

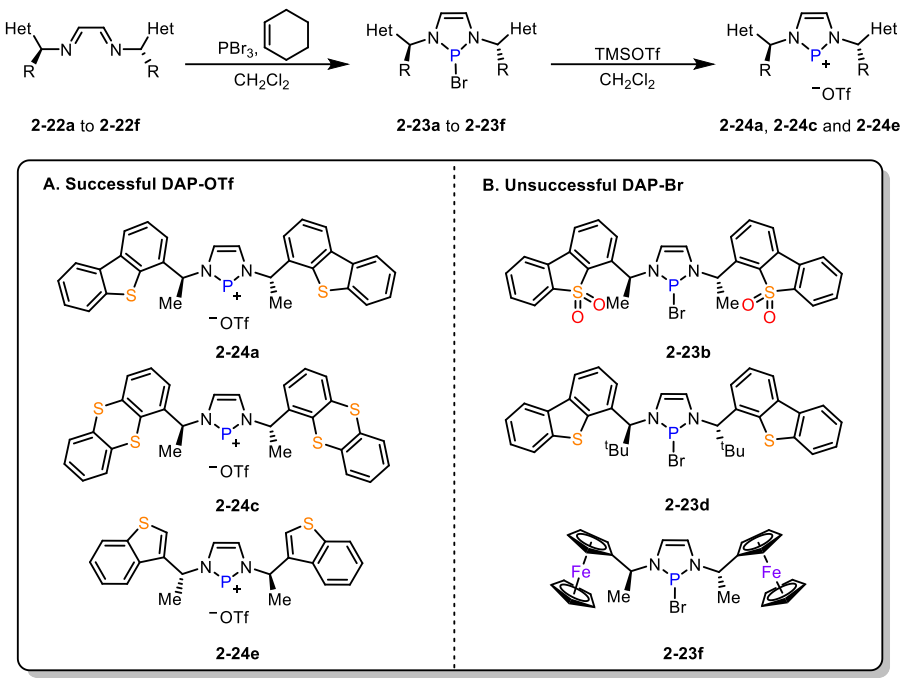

Scheme 2-11. General synthesis of heterocyclic DAP-OTfs. (A) The successfully isolated DAP-OTfs (B) The unsuccessfully cyclized DAP-Brs.

There is an alternative cyclization method using PI_3 to generate DAPs with a positive charge on the phosphorus and an I_3 counterion (DAP-I_3), as mentioned in Chapter 1. In previous work reported by the Speed group, the use of PI_3 in place of PBr_3 has proven to be successful in cyclizing diimines that contain a *tert*-butyl group in the alkyl position.[8] Disadvantages associated with the use of PI_3 is the conversion of the cyclized DAP-I_3 to the DAP-OTf with TMSOTf is not feasible, and in the past the DAP-I_3 have shown to occasionally exhibit limited stability by releasing iodine. In addition, PI_3 is far more expensive and less stable than PBr_3. Despite the disadvantages, the unsuccessfully cyclized diimines **2-22b**, **2-22d** and **2-22f** were separately exposed to PI_3 as an attempt to generate the respective DAP-I_3 **2-25b**, **2-25d**, and **2-25f** (Scheme 2-12). This method was also unsuccessful in cyclizing these diimines and similar hypothesis were made about each

individual diimine as to why they did not cyclize. These results hint at current DAP synthesis limitations with extremely bulky or reactive heterocycles.

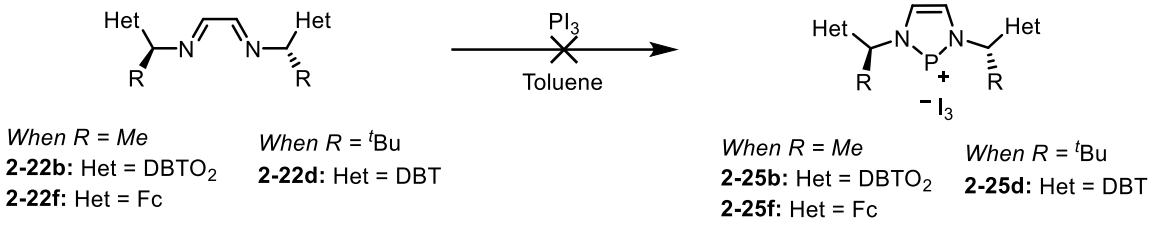

Scheme 2-12. Attempted cyclization of heterocyclic diimines with PI_3.

2.3.5 Reduction Results

To assess the selectivity of the successfully synthesized chiral heterocyclic diazaphospheniums, **2-24a**, **2-24c** and **2-24e**, the standard test reaction was conducted (Scheme 2-13). The standard reaction conditions for screening DAP-OTfs consists of combining the cyclic imine benchmark substrate **2-17a** and a catalyst in THF, and cooling the solution to −35 °C, followed by the addition of 1.1 equivalents of HBpin and keeping it cool for 16–18 h. The reaction is quenched with dilute acid resulting in the amine salt that is in the aqueous layer. The aqueous layer is then treated with dilute base until the solution is basic to generate the desired amine. This is followed by the addition of an organic solvent to extract the amine and the solvent is removed to isolate the desired amine. The results of the reduction reactions are summarized in Table 2-1.

The enantioselectivity of each new catalyst for amine **2-17b** was compared to the enantioselectivity of the current best DAP-OTf, with an *e.r.* 96:4 for amine **2-17b** (Entry 1). The DBT-containing DAP-OTf, **2-24a**, had a mediocre *e.r.* of 80:20 for amine **2-17b** (Entry 2). The TH-containing DAP-OTf, **2-24c**, had an inferior *e.r.* of 73:27 for amine **2-17b** (Entry 3). The BT-containing DAP-OTf, **2-24e**, presented the most promising result with an *e.r.* of 90:10 for amine **2-17b** (Entry 4). This result led to the publication of the

synthesis of DAP-OTf **2-24e** along side of the synthesis and reactivity of DAP-OTf **1-28** by Dr. Travis Lundrigan in the *Journal of American Chemical Society* in 2019.[9]

Table 2-1. Summary of test reaction results with heterocyclic DAP analogues.

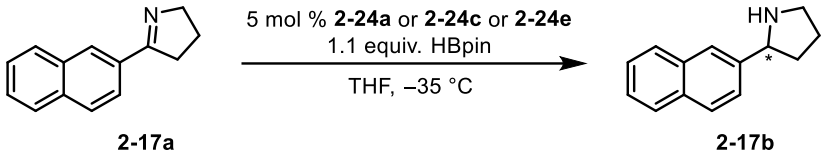

2-17a **2-17b**

Entry	Catalyst Number	Catalyst Structure	Selectivity (*e.r.*)
1	**1-28**	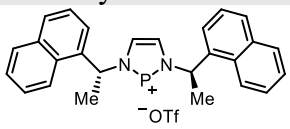	96:4
2	**2-24a**	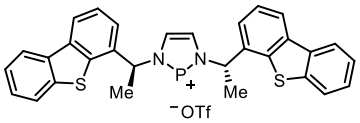	80:20
3	**2-24c**	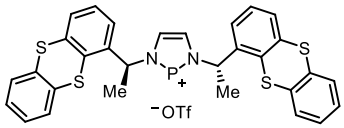	73:27
4	**2-24e**	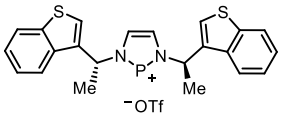	90:10

The results of DAP-OTfs, **2-24a**, **2-24c**, and **2-24e**, were used as a guide for the next steps in the project for new catalyst design. Synthesis of further TH derivatives would not be pursued as the results were not indicative of higher amine enantioselectivity, coupled by lack of cleanliness of the cyclization reaction. A possible explanation for the particularly poor selectivity of the TH-containing DAP-OTf, **2-24c**, is that TH is a bent structure, rather than planar, and may have a smaller steric profile than the two-dimensional drawings suggest. The DBT-containing analogue, **2-24a**, gave a mediocre enantioselectivity result while the BT-containing analogue, **2-24e**, gave the most promising result. The BT-containing derivative resembles the naphthyl group the most in terms of steric bulk, indicating the change in electronic profile (presence of the sulfur) has minimal impact on

enantioselectivity. Comparing only the BT- and DBT- containing derivative, the obvious difference is the additional ring, while potentially less obvious difference that may have a huge impact on the selectivity is the point of attachment relative to the sulfur. These considerations were the beginning of the design of a second generation of heterocyclic cationic DAPs, described in the next Chapter.

2.4 Summary

The synthesis and isolation of non-commercially available chiral amines was successful for both biaryl and heterocyclic derivatives. For the biaryl derivatives, the cyclization of the corresponding diimines to DAP-Br were successful, but the purification was difficult as the desired products were soluble in pentane and washed away with the impurities. This significantly impacted the yield and could not be carried forward to the DAP-OTf. To determine if it would be worth scaling up and optimizing the purification, the minimal amount of DAP-Br collected was used as a pre-catalyst in a test reduction to assess the enantioselectivity of the benchmark substrate. The enantioselectivity of the DAP-Brs were less than desirable and further efforts were concentrated on synthesizing the heterocyclic containing DAP-OTf derivatives.

The generation of heterocyclic containing DAP-OTfs were semi successful. Specifically, the DBT, TH and BT combined with a methyl in the alkyl position were successfully synthesized. Unfortunately, diimines derived from the $DBTO_2$, the DBT with a *tert*-butyl in the alkyl position, the Fc containing analogues did not successfully cyclize. The DBT with a *tert*-butyl group in the alkyl position was too bulky whereas the $DBTO_2$ and Fc analogues had competing decomposition. The reactivity and enantioselectivity of the successfully synthesized DAP-OTf were assessed with a cooled reduction reaction with

the benchmark substrate. The results varied, the DAP-OTf containing TH had the poorest enantioselectivity. This is thought to be because the steric profile is smaller in three-dimensional space. The DBT containing derivative was mediocre and the BT derivative was the best and was published in 2019 with the naphthyl containing DAP-OTf derivative.

2.5 Experimental

2.5.1 General Considerations

Unless stated otherwise all reactions were carried out in a fumehood using oven dried Schlenk glassware under a nitrogen, inert atmosphere. Filtration and purification of diazaphospholene derivatives were carried out in a nitrogen filled, inert atmosphere of a 2001 issue IT Glovebox. Hydroboration reductions were carried out in 4 dram oven dried scintillation vials in the IT Glovebox. ^{1}H, ^{13}C, ^{11}B, ^{31}P, and ^{19}F NMR spectra were acquired at 300K on Bruker AV-500 MHz and AV-300 MHz NMR spectrometers. Standard NMR tubes and caps were used. Caps on sensitive samples were overwrapped with PTFE tape. Chemical shifts are reported in parts per million (ppm). ^{1}H NMR spectra are referenced to residual non-deuterated NMR solvent ($CHCl_3$ = 7.26 ppm or CD_2HCN = 1.94 ppm) or to the TMS standard in the deuterated chloroform (Me_4Si = 0.00 ppm). ^{13}C NMR spectra are referenced to the central $CDCl_3$ peak (77.16 ppm) or CD_3CN peak (1.32 ppm). Mass spectrometric data were acquired by Mr. Xiao Feng (Mass Spectrometry Laboratory, Dalhousie University). X-Ray data collection, solution and refinement were carried out by Dr. Katherine Robertson at St. Mary's University. High Performance Liquid Chromatography (HPLC) data was acquired on a Varian Prostar instrument, equipped with detection at λ = 254 nm, using either Astec Cellulose DMP, or Chiralpak ADH columns. A 99:1 hexanes/isopropanol solvent mixture was used as the eluent, with a flow rate of 0.5 mL/min.

Solvents

Pentane for reactions was deoxygenated and dried by sparging with nitrogen gas, followed by passage through a double-column solvent purification system from mBraun Inc. The solvents were stored over activated 3 Å molecular sieves in the glovebox.

Diethyl ether for work-ups (ACS grade) was purchased from Fisher and used as received. Diethyl ether for reactions was distilled from a purple solution of benzophenone/sodium ketyl and stored over activated 3 Å molecular sieves in the glovebox.

Tetrahydrofuran (Anhydrous >99%, inhibitor free) was purchased in a Sure/Seal™ container from Aldrich and used as received for lithiation reactions. For reaction screenings in the glovebox, the bottle was brought into the glovebox through the antechamber with nitrogen purge, the septum was removed from the bottle, and activated 3 Å molecular sieves were added for long term storage.

Dichloromethane (ACS grade) was purchased from Fisher and distilled from calcium hydride immediately before use if required.

Deuterochloroform (Cambridge Isotopes) was stored over activated 3 Å molecular sieves but otherwise was used as received.

Reagents

Ellman Sulfinamide Auxiliaries were purchased from Oakwood Chemical and configuration was verified by measurement of optical rotation.

Glyoxal solution was purchased from Aldrich as 40 wt. % in water solution.

Thiophenes for direct lithiation were purchased from Oakwood Chemical and used as received.

Titanium ethoxide was purchased from Oakwood Chemical and used as received.

Triethylamine was purchased from Aldrich in a Sure/Seal® bottle and used as received.

Trimethylsilyl triflate was purchased from Oakwood Chemical and distilled at 10 torr before use.

Pinacolborane was purchased from Oakwood Chemical stored at ambient temperature in the glovebox, and otherwise used as received. Distillation of pinacolborane gave no improvement on enantioselectivity.

Phosphorus (III) Bromide was purchased as the 99% purity grade from Aldrich in a Sure/Seal® bottle and used as received. The 97% purity grade can also be used with no detriment to yield or purity, however products may be darker in colour.

2.5.2 Procedure for the Removal of an Ellman Auxiliary

Anhydrous 2M HCl in diethyl ether (4.0 equiv.) was added dropwise to a non-anhydrous solution of diethyl ether containing the appropriate sulfinimide (*Ellman protected amine*, 1.0 equiv.). After 1–5 min (depending on the amine) some white precipitate formed, and the suspension was stirred overnight (16–18 h). The precipitate was isolated by filtration, then transferred to a separatory funnel. An aqueous solution of 2M $NaOH_{(aq)}$ was added to the separatory funnel to basify the amine. The amine was extracted into dichloromethane (3 × 50 mL) and the combined organic layers were dried over Na_2SO_4 then filtered and concentrated to give the desired amine, which was used without further purification.

2.5.3 Procedure for the Synthesis of Diimines

In a round bottom flask equipped with a magnetic stir bar, the appropriate enantiopure amine (2.0 equiv.) was dissolved in dichloromethane in open air. The rest of the reagents were added in the following order: Na_2SO_4 (4.0 equiv.), glyoxal solution (40 wt. % in H_2O, 1.0 equiv.) and a drop of formic acid. The solution was enclosed with a rubber septum and stirred for 2–4 h as required. The reaction was monitored by ^1H NMR spectra of aliquots (no work-up of the aliquots were conducted, the withdrawn sample was diluted with $CDCl_3$ and assessed). When the reaction was complete, the Na_2SO_4 was removed by filtration and rinsed with dichloromethane. The filtrate was concentrated to give the desired diimine and used without further purification.

2.5.4 Procedure for the Synthesis of Diazaphospholene Bromides (DAP-Br)

As stated in the literature procedure,[9] cyclohexene (5.0 equiv.) and PBr_3 (1.0 equiv.) were sequentially added to dichloromethane in a Schlenk flask with a stir bar. A solution of the appropriate diimine (1.0 equiv.) in dichloromethane was added. The solution was stirred for 2 h. At lower ambient temperatures, a solid may form during this reaction, which has no detrimental impact on subsequent steps. After 2 h, the dichloromethane was removed in vacuo, the tube was backfilled with nitrogen, sealed and brought into the glovebox. The resulting foam was triturated with pentane and a metal spatula to form a powder. The suspension was transferred to a filter frit, filtered, and washed with further pentane. NMR spectra of the powder were obtained during the wash to ensure the removal of the dibromocyclohexane byproduct. If this material was still present, the washing was continued until pure.

2.5.5 Procedure for the Synthesis of Diazaphospholene Triflates (DAP-OTf)

As stated in the literature procedure,[9] the appropriate DAP-Br (1.0 equiv.) was weighed into a Schlenk flask equipped with a stir bar inside the glovebox. The flask was removed from the glovebox then placed on the Schlenk line in the fumehood. The DAP-Br was dissolved in dichloromethane followed by the addition of trimethylsilyl triflate (1.1 equiv.) over 2 min. The solution was stirred for 1 h, then the dichloromethane was removed in vacuo. The flask was backfilled with nitrogen, sealed and brought back into the glovebox. The resulting foam was triturated with diethyl ether and a metal spatula to form a powder. The suspension was transferred to a Schlenk filter, filtered, and washed with further diethyl ether. The compound was then held under vacuum until a constant weight was achieved.

*2.5.6 Synthesis and Characterization of **2-10** to **2-24e***

Compound 2-10:[47] This compound was resolved from 1-(2-bromophenyl)ethylamine following a literature procedure in a 35% yield.

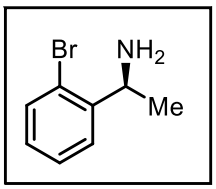

^{1}H NMR (500 MHz, $CDCl_3$): δ 7.49–7.47 (m, 2H), 7.29–7.26 (m, 1H), 7.06–7.03 (m, 1H), 4.47 (q, *J* = 6.6 Hz, 1H), 1.34 (d, *J* = 6.6 Hz, 3H).

The enantiomeric excess was determined by HPLC on an Astec Cellulose DMP column, t_{major}= 23.287 min, t_{min}= 26.699 min. Enantiomeric ratio > 99:1.

Compound 2-11:[47] Compound **2-10** (2.17 g, 10.86 mmol, 1.0 equiv.) was dissolved in acetonitrile (30 mL). Di-*tert*-butyl dicarbonate (2.5 mL, 10.86 mmol, 1.0 equiv.) was added which generated a colourless solution that was stirred for 24 h. The majority of acetonitrile was removed *in vacuo*. The residue was purified through column chromatography (10% EtOAc/hexanes). The solvent was removed in vacuo that resulted in a colourless powder. The initial NMR spectrum showed excess EtOAc remained, compound was left under high vacuum for multiple days before proceeding to the following step. For a fully detailed characterization, VT NMR would be helpful due to the presence of rotamers but was not obtained because the subsequent results leading to the abandonment of this project.

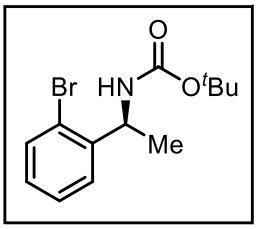

^{1}H NMR (300 MHz, $CDCl_3$): δ 7.53 (m, 1H), 7.32–7.29 (m, 2H), 7.12–7.07 (m, 1H), 5.07 (br. s, 1H), 4.94 (br. s, 1H), 1.41 (br. s, 12H).

Compound 2-12a:[47] Compound **2-12a** was isolated as a colourless foam in a quantitative yield following a literature procedure.

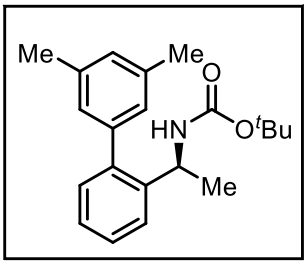

^{1}H NMR (500 MHz, $CDCl_3$): δ 7.40 (ap. d *J* = 7.6 Hz, 1H), 7.36 (t, *J* = 7.4 Hz, 1H), 7.27 (ap. t, *J* = 7.5 Hz, 1H), 7.28–7.25 (m, 1H), 7.18 (ap. d, *J* = 7.2 Hz, 1H) , 6.99–6.96 (m, 3H), 4.89 (br. s, 1H), 4.72 (br. s, 1H), 2.35 (s, 6H), 1.39 (br. s, 9H), 1.27 (ap. d, *J* = 6.4 Hz, 3H).

HRMS(ESI): calculated $(M+Na)^+$ $[C_{21}H_{27}NNaO_2]$: 348.1934; found: 348.1922.

$[\alpha]^{21}_D$= −46° (c= 0.36, CH_2Cl_2).

Compound 2-12b: Compound **2-12b** was isolated as a colourless oil in a 52% yield following a literature procedure.[47]

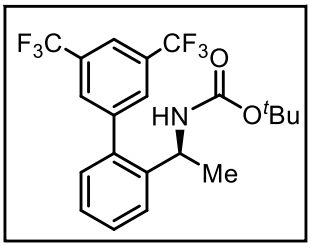

^{1}H NMR (500 MHz, $CDCl_3$): δ 7.89 (br. s, 3H), 7.49–7.43 (m, 2H), 7.34 (ap. t, *J* = 7.3 Hz, 1H), 7.18 (ap. d, *J* = 7.6 Hz, 1H), 4.66 (br. s, 2H), 1.37 (br. s, 9H), 1.29 (ap. d, *J* = 6.0 Hz, 3H).

HRMS(ESI): calculated $(M+Na)^+$ [$C_{21}H_{21}F_6NNaO_2$]: 456.1369; found: 456.1368.

$[\alpha]^{21}_D$= −32° (c= 1.36, CH_2Cl_2).

Amine 2-13a: In a round bottom flask that contained a stir bar, compound **2-12a** (1.40 g, 4.30 mmol, 1.0 equiv.) was dissolved in dichloromethane (2 mL) and cooled to 0 °C. Trifluoroacetic acid (2.3 mL, 30.1 mmol, 7.0 equiv.) was added dropwise and created a clear pink solution. After 19 h of stirring the solution colour changed to orange and the reaction was quenched with 2 M $NaOH_{(aq)}$. The product was extracted with 2 × 50 mL of dichloromethane. The organic layers were combined, dried over Na_2SO_4, filtered, and concentrated which gave compound **2-13a** as an orange oil (0.89 g, 3.88 mmol, 92% yield). Spectrum values match literature values.[47]

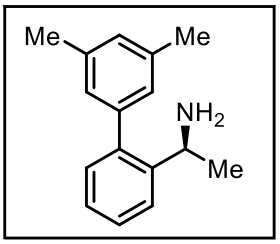

^{1}H NMR (500 MHz, $CDCl_3$): δ 7.58 (ap. d, *J* = 7.8 Hz, 1H), 7.36 (ap. t, *J* = 7.6 Hz, 1H), 7.25–7.23 (m, 1H), 7.16 (ap. d, *J* = 7.6 Hz, 1H), 6.99 (br. s, 1H), 6.90 (br. s, 2H), 4.23 (q, *J* = 6.6 Hz, 1H), 2.35 (s, 6H), 1.42 (br. s, 2H), 1.29 (d, *J* = 6.6 Hz, 3H).

HRMS(ESI): calculated $(M+H)^+$ [$C_{16}H_{20}N$]: 226.1590; found: 226.1596.

$[\alpha]^{21}_D$= +33° (c= 3.40, CH_2Cl_2).

Amine 2-13b: In a round bottom flask that contained a stir bar, compound **2-12b** (2.61 g, 6.01 mmol, 1.0 equiv.) was dissolved in dichloromethane (3 mL) and cooled to 0 °C. Trifluoroacetic acid (3.2 mL, 42 mmol, 7.0 equiv.) was added dropwise which created a clear orange solution. After 19 h of stirring the solution colour changed to yellow and the reaction was quenched with 2M $NaOH_{(aq)}$. The product was extracted with 2 × 50 mL of dichloromethane. The organic layers were combined, dried over Na_2SO_4, filtered, and concentrated to give compound **2-13b** as a yellow oil (1.92 g, 5.76 mmol, 96% yield).

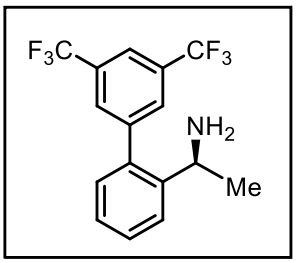

^{1}H NMR (500 MHz, $CDCl_3$): 7.89 (br. s, 1H), 7.81 (br. s, 2H), 7.68 (ap. d, *J* = 7.9 Hz, 1H), 7.47 (ap. t, *J* = 7.0 Hz, 1H), 7.32 (ap. t, *J* = 7.5 Hz, 1H), 7.17 (ap. d, *J* = 7.6 Hz, 1H), 4.06 (q, *J* = 6.5 Hz, 1H), 1.41 (br. s, 2H), 1.32 (d, *J* = 6.5 Hz, 3H).

^{19}F NMR (470 MHz, $CDCl_3$): δ −62.8.

$[\alpha]^{21}_D$= +18° (c= 2.83, CH_2Cl_2).

HRMS(ESI): calculated $(M+H)^+$ [$C_{16}H_{14}F_6N$]: 334.1025; found: 334.1017.

Diimine 2-14a: Amine **2-13a** (0.45 g, 2.00 mmol) was treated as described in S*ection 2.5.3* in 5 mL of dichloromethane (0.40 M) for 2 h to generate diimine **2-14a** as a bright yellow powder in a 70% yield.

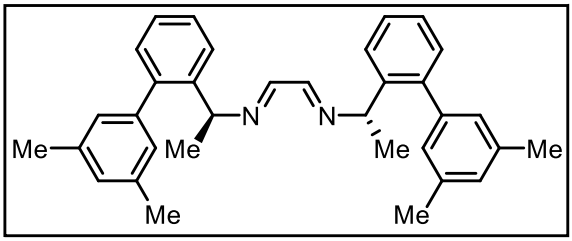

^{1}H NMR (500 MHz, $CDCl_3$): 7.67 (s, 2H), 7.59 (m, 2H), 7.34 (m, 2H), 7.23 (m, 2H), 7.16 (m, 2H), 6.97 (s, 2H), 6.82 (s, 4H), 4.66 (q, J = 6.6 Hz, 2H), 2.31 (s, 12H), 1.44 (d, J = 6.7 Hz, 6H).

^{13}C NMR (125 MHz, $CDCl_3$): δ 161.1, 141.5, 141.3, 141.0, 137.7, 130.1, 128.8, 127.8, 127.3, 127.0, 126.7, 65.1, 24.4, 21.5.

HRMS(ESI): calculated $(M+H)^+$ [$C_{34}H_{37}N_2$]: 473.2951; found: 473.2955.

Diimine 2-14b: Amine **2-13b** (1.00 g, 2.31 mmol) was treated as described in S*ection 2.5.3* to generate diimine **2-14b**.

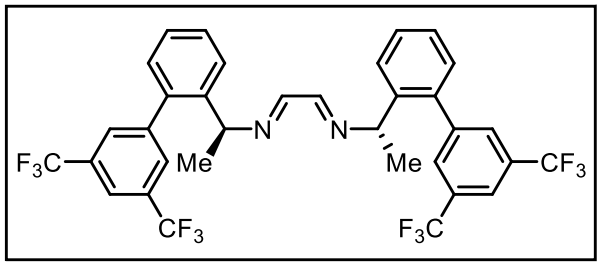

^{1}H NMR (500 MHz, $CDCl_3$): 7.88 (s, 2H), 7.72 (s, 4H), 7.66 (m, 4H), 7.47 (m, 2H), 7.34 (m, 2H), 7.19 (m, 2H), 4.49 (q, J = 6.6 Hz ,2H), 1.46 (d, J = 6.6 Hz, 6H).

^{13}C NMR (125 MHz, $CDCl_3$): δ 160.8, 143.3, 141.0, 138.1, 131.7 ($^2J_{CF}$ = 34 Hz), 130.1, 129.7, 129.4, 127.7, 127.5, 124.5, 122.3, 121.3, 65.1, 24.0.

^{19}F NMR (470 MHz, $CDCl_3$): δ −62.8

HRMS(ESI): calculated $(M+Na)^+$ [$C_{34}H_{24}F_{12}N_2Na$]: 711.1640; found: 711.1667.

Compound 2-20a: In a round bottom flask equipped with a stir bar, dibenzothiophene (1.93 g, 10.5 mmol, 1.0 equiv.) was dissolved in tetrahydrofuran (10 mL). The solution was cooled to 0 °C followed by the addition of *n*BuLi (4.2 mL, 2.5 M in hexanes, 10.5 mmol, 1.0 equiv.). As the reaction stirred for 2 h it was gradually warmed to room temperature then cooled to −78 °C. Once cooled, the Ellman imine (derived from acetaldehyde and (*S*)-tertbutanesulfinamide) solution (2.00 g, 13.6 mmol, 1.3 equiv.) in tetrahydrofuran (10 mL) was added. An additional 5 mL of tetrahydrofuran was used to rinse the flask and complete the transfer. The solution stirred for 1 h then quenched with $NH_4Cl_{(aq)}$ and extracted with dichloromethane (2 × 75 mL). The organic layers were combined, dried over Na_2SO_4, filtered, and concentrated. The resulting yellow oil was purified via column chromatography (60% EtOAc/Hexanes). Product **2-20a** was obtained as a yellow oil (1.18 g, 7.15 mmol, 34% yield).

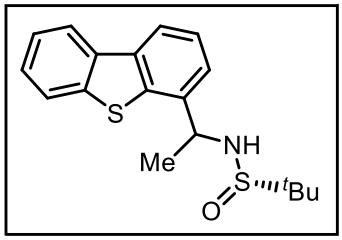

^{1}H NMR (400 MHz, $CDCl_3$): δ 8.17–8.15 (m, 1H), 8.11–8.09 (m, 1H), 7.88–7.86 (m, 1H), 7.48–7.45 (m, 4H), 4.91 (qd, *J* = 6.8 Hz, 3.0 Hz, 1H), 3.70 (ap. d, *J* = 3.6 Hz, 1H), 1.74 (d, *J* = 6.7 Hz, 3H) 1.22 (s, 9H).

^{13}C{^{1}H} NMR (100 MHz, $CDCl_3$): δ 139.5, 137.7, 137.6, 136.6, 135.6, 127.0, 124.9, 124.5, 122.8, 121.7, 121.0, 56.0, 54.6, 22.9, 22.8.

HRMS(ESI): calculated $(M+Na)^+$ $[C_{18}H_{21}NNaOS_2]$: 354.0957; found: 354.0966.

Compound 2-20b: In a round bottom flask equipped with a stir bar, dibenzothiophene sulfone (2.60 g, 12.0 mmol, 1.0 equiv.) was suspended in tetrahydrofuran (20 mL). The solution was cooled to −78 °C followed by the addition of *n*BuLi (4.8 mL, 2.5 M in hexanes, 12.0 mmol, 1.0 equiv.). The reaction stirred for 2 h at −78 °C. The Ellman imine (derived from acetaldehyde and (*S*)-*tert*-butanesulfinamide) solution (2.12 g, 14.4 mmol, 1.2 equiv.) in tetrahydrofuran (15 mL) was added. The solution stirred for 0.5 h at −78 °C then warmed to room temperature and stirred for 0.5 h. The reaction was quenched with $NH_4Cl_{(aq)}$ and extracted with diethyl ether (2 × 75 mL). The organic layers were combined, dried over Na_2SO_4, filtered, and concentrated. The crude product was purified via column chromatography (75% EtOAc/Hex). Product **2-20b** was obtained as a beige powder (1.40 g, 3.85 mmol, 32% yield).

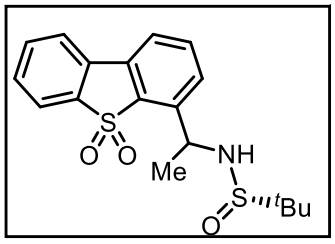

^{1}H NMR (400 MHz, $CDCl_3$): δ 7.79 (m, 2H), 7.70–7.68 (m, 1H), 7.65–7.60 (m, 3H), 7.53–7.49 (m, 1H), 5.35–5.29 (m, 1H), 1.75 (d, *J* = 6.8 Hz, 3H) 1.21 (s, 9H).
^{13}C{^{1}H} NMR (100 MHz, $CDCl_3$): δ 142.5, 137.6, 134.8, 134.3, 134.0, 132.0, 131.5, 130.5, 128.6, 122.0, 121.7, 120.7, 56.1, 51.1, 23.3, 22.6.

HRMS(ESI): calculated $(M+Na)^+$ $[C_{18}H_{21}NNaO_3S_2]$: 386.0855; found: 386.0864.

$[\alpha]^{21}_D$= –58° (c= 0.7, CH_2Cl_2).

Compound 2-20c: In a round bottom flask equipped with a stir bar, thianthrene (5.34 g, 24. 7 mmol, 1.0 equiv.) was dissolved in tetrahydrofuran (50 mL). The solution was cooled to −84 °C followed by the addition of *n*BuLi (9.9 mL, 2.5 M in hexanes, 1.0 equiv.). The reaction stirred for 10 min then allowed to warm to room temperature and stirred for 1 h. The reaction was cooled back to −84 °C and the Ellman imine (derived from acetaldehyde and (*S*)-*tert*-butanesulfinamide) solution (4.36 g, 29.6 mmol, 1.2 equiv.) in tetrahydrofuran was added. The solution stirred for 10 mins then allowed to gradually warm to room temperature and stirred for an additional 40 min. The reaction was then quenched with $NH_4Cl_{(aq)}$ and extracted with dichloromethane (2 × 75 mL). The organic layers were combined, dried over Na_2SO_4, filtered, and

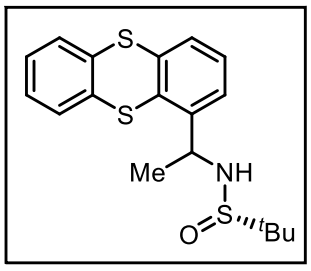

concentrated. The crude product was purified via column chromatography (75% EtOAc/Hex). Product **2-20c** was obtained as a white foam (1.46 g, 4.02 mmol, 16% yield).

^{1}H NMR (400 MHz, $CDCl_3$): δ 7.53–7.51 (m, 1H), 7.49–7.47 (m, 1H), 7.45–7.43 (m, 1H), 7.40–7.38 (m, 1H), 7.25–7.22 (m, 3H), 5.20 (qd, *J* = 6.5 Hz, 3.0 Hz, 1H), 3.65 (ap. d, *J* = 3.4 Hz, 1H), 1.57 (d, *J* = 6.7 Hz, 3H) 1.22 (s, 9H).

^{13}C{^{1}H} NMR (100 MHz, $CDCl_3$): δ 143.6, 136.7, 136.6, 135.1, 134.6, 129.3, 128.7, 128.3, 128.1, 127.9, 127.7, 125.4, 55.8, 51.4, 22.7, 22.3.

$[\alpha]^{21}_D$= +88° (c= 1.13, CH_2Cl_2).

HRMS(ESI): calculated $(M+H)^+$ $[C_{14}H_{14}NS_2]$: 260.0562; found: 228.0572.

Compound 2-20d: In a round bottom flask equipped with a stir bar, dibenzothiophene

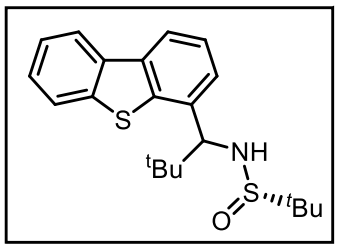

(1.50 g, 8.13 mmol, 1.0 equiv.) was dissolved in tetrahydrofuran (6 mL). The solution was cooled to 0 °C followed by the addition of *n*BuLi (3.3 mL, 2.5 M, 8.1 mmol, 1.0 equiv.). As the reaction stirred for 2 h it was gradually warmed to room temperature then cooled to −78 °C. Once cooled, the Ellman imine (derived from pivaldehyde and (*S*)-*tert*-butanesulfinamide) solution (2.00 g, 10.6 mmol, 1.3 equiv.) in tetrahydrofuran (5 mL) was added. An additional 5 mL of tetrahydrofuran was used to rinse the flask and complete the transfer. The solution stirred for 1 h then quenched with $NH_4Cl_{(aq)}$ and extracted with dichloromethane (2 × 75 mL). The organic layers were combined, dried over Na_2SO_4, filtered, and concentrated. The resulting yellow oil was purified via column chromatography (60% EtOAc/Hex). Product **2-20d** was obtained as a white powder (1.1 g, 2.9 mmol, 36% yield).

^{1}H NMR (500 MHz, $CDCl_3$): δ 8.15–8.13 (m, 1H), 8.09–8.08 (m, 1H), 7.84–7.83 (m, 1H), 7.45–7.43 (m, 4H), 4.57 (s, 1H), 3.68 (s, 1H), 1.16 (s, 9H), 1.08 (s, 9H).

^{13}C{^{1}H} NMR (125 MHz, $CDCl_3$): δ 141.4, 139.2, 136.0, 135.8, 135.0, 126.9, 126.8, 124.5, 124.2, 122.8, 121.7, 120.8, 66.0, 55.8, 37.0, 27.0, 22.6.

HRMS(ESI): calculated $(M+Na)^+$ $[C_{21}H_{27}NNaOS_2]$: 396.1426; found: 396.1431.

$[\alpha]^{21}_D$= +95° (c= 1.14, CH_2Cl_2).

Amine 2-21a: Compound **2-20a** (2.37 g, 7.16 mmol, 1.0 equiv.) was treated as described

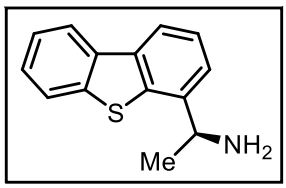

in *Section 2.5.2* which resulted in a 69% yield of compound **2-21a** as an off-white powder.

^{1}H NMR (500 MHz, $CDCl_3$): δ 8.16–8.14 (m, 1H), 8.06–8.04 (m, 1H), 7.88–7.86 (m, 1H), 7.54–7.53 (m, 1H) 7.49–7.45 (m, 3H), 4.50 (q, *J* = 6.6 Hz, 1H), 1.68 (s, 2H), 1.56 (d, *J* = 6.6 Hz, 3H).

^{13}C NMR (125 MHz, $CDCl_3$): δ 142.0, 139.5, 137.2, 136.2, 135.9, 126.8, 125.1, 124.4, 122.9, 122.8, 121.7, 120.2, 51.0, 23.8.

HRMS(ESI): calculated $(M+H)^+$ [$C_{14}H_{14}NS$]: 228.0841; found: 228.0849.

$[\alpha]^{21}_D$= −51° (c= 1.18, CH_2Cl_2).

Amine 2-21b: Compound **2-20b** (1.4 g, 3.9 mmol, 1.0 equiv.) was treated as described in *Section 2.5.2* with a solvent modification of toluene instead of ether. This resulted compound **2-21b** as a white powder in a 75% yield.

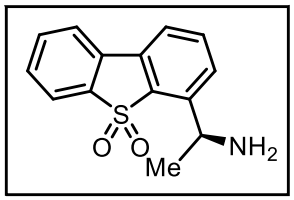

^{1}H NMR (400 MHz, $CDCl_3$): δ 7.82–7.76 (m, 2H), 7.72–7.70 (m, 1H), 7.67–7.59 (m, 3H), 7.53–7.50 (m, 1H), 4.95 (q, *J* = 6.6 Hz, 1H), 1.83 (br. s, 2H), 1.53 (d, *J* = 6.6 Hz, 3H).

^{13}C NMR (100 MHz, $CDCl_3$): δ 146.1, 137.9, 134.6, 134.3, 133.9, 131.7, 131.6, 130.4, 127.8, 122.1, 121.6, 120.1, 46.5, 24.6.

HRMS(ESI): calculated $(M+H)^+$ [$C_{14}H_{14}NO_2S$]: 260.0740; found: 260.0734.

$[\alpha]^{21}_D$= −109° (c= 0.34, CH_2Cl_2).

Amine 2-21c: Compound **2-20c** (1.3 g, 4.0 mmol, 1.0 equiv.) was treated as described in *Section 2.5.2* with a solvent modification of dichloromethane instead of ether. This resulted in compound **2-21c** as a yellow oil in a 66% yield.

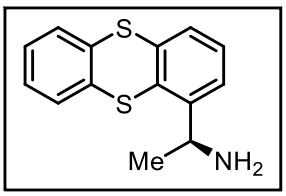

^{1}H NMR (500 MHz, $CDCl_3$): δ 7.55–7.47 (m, 3H), 7.41 (ap. d, *J* = 7.6 Hz, 1H), 7.27–7.24 (m, 3H), 4.76 (ap. sextet, *J* = 6.2 Hz, 1H), 1.52 (br. s, 2H), 1.43 (d, *J* = 6.6 Hz, 3H).

^{13}C NMR (125 MHz, $CDCl_3$): δ 147.3, 136.9, 136.1, 135.6, 134.2, 129.2, 128.8, 128.0, 127.8, 127.6, 124.3, 48.6, 24.6.

HRMS(ESI): calculated $(M+H)^+$ [$C_{14}H_{14}NS_2$]: 260.0562; found: 260.0572.

$[\alpha]^{21}_D$= +88° (c= 1.13, CH_2Cl_2).

Amine 2-21d: Compound **2-20d** (1.1 g, 2.9 mmol, 1.0 equiv.) was treated as described in *Section 2.5.2* which resulted in compound **2-21d** as a light-yellow powder in a 73% yield.

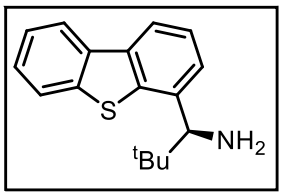

^{1}H NMR (500 MHz, $CDCl_3$): δ 8.15–8.14 (m, 1H), 8.06 (ap. d, *J* = 7.7 Hz, 1H), 7.85–7.84 (m, 1H), 7.55–7.54 (m, 1H), 7.48–7.44 (m, 3H), 4.15 (s, 1H), 1.58 (s, 2H), 1.04 (s, 9H).

^{13}C NMR (125 MHz, $CDCl_3$): δ 140.0, 139.4, 139.2, 136.0, 135.7, 126.8, 126.0, 124.4, 122.6, 121.7, 120.3, 64.5, 37.0, 27.0.

HRMS(ESI): calculated $(M+H)^+$ [$C_{17}H_{20}NS$]: 270.1311; found: 270.1322.

$[\alpha]^{21}_D$= +45° (c= 0.89, CH_2Cl_2).

Compound 2-19c: In a 250 mL round bottom flask, 3-formyl benzothiophene (4.86 g, 30.0 mmol, 1.0 equiv.) and (*S*)-*tert*-butylsulfinamide (3.68 g, 30.0 mmol, 1.0 equiv.) were dissolved in 50 mL of tetrahydrofuran. Titanium ethoxide (12.6 mL, 60.0 mmol, 2.0 equiv.) was added, and the reaction was stirred for 21 h. The reaction was quenched with 100 mL of brine, diluted with 100 mL of dichloromethane, and pressed through a fine frit, washing with another 100 mL of dichloromethane. The organic layer was isolated, dried over Na_2SO_4, filtered, and concentrated to give compound **2-19c** (7.80 g, 29.3 mmol, 98% yield). The compound was a white waxy solid and used directly in the next step without further purification.

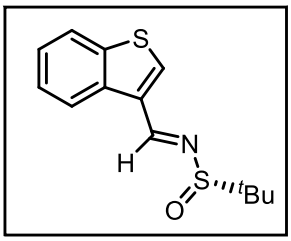

^{1}H NMR (500 MHz $CDCl_3$): δ 8.80 (s, 1H), 8.71 (ap. d, *J* = 8.4 Hz, 1H), 8.07 (s, 1H), 7.89 (ap. d, *J* = 8.4 Hz, 1H), 7.50 (ap. t, *J* = 7.7 Hz, 1H), 7.45 (ap. t, *J* = 7.7 Hz, 1H), 1.31 (s, 9H).

^{13}C NMR (125 MHz, $CDCl_3$): δ 156.9, 140.8, 138.2, 136.0, 132.5, 125.9, 125.8, 125.0, 122.8, 57.6, 22.7.

HRMS(ESI): calculated $(M+Na)^+$ [$C_{13}H_{15}NNaOS_2$]: 288.0487; found: 288.0494.

Compound 2-19d: In a round bottom flask, ferrocenecarboxaldehyde (2.53 g, 11.8 mmol, 1.0 equiv.) and (*S*)-*tert*-butylsulfinamide (1.43 g, 11.8 mmol, 1.0 equiv.) were dissolved in 30 mL of tetrahydrofuran. Titanium ethoxide (4.9 mL, 23.6 mmol, 2.0 equiv.) was added, and the reaction was stirred for 24 h. The reaction was quenched with brine, diluted with dichloromethane, and pressed through a fine frit and washed with excess dichloromethane. The organic layer was isolated, dried over Na_2SO_4, filtered, and concentrated to give compound **2-19d**.

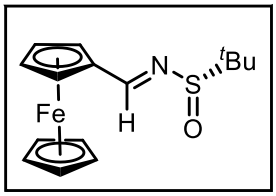

^{1}H NMR (400 MHz $CDCl_3$): δ 8.51 (s, 1H), 4.75–4.73 (m, 2H), 4.52–4.51 (m, 2H), 4.22 (s, 4H), 1.25 (s, 9H).

^{13}C NMR (100 MHz, $CDCl_3$): δ 164.2, 78.7, 72.0, 69.9, 69.6, 69.2, 56.8, 22.7, 22.2.

HRMS(ESI): calculated $(M+Na)^+$ [$C_{15}H_{19}FeNNaOS$]: 340.0429; found: 340.0436.

Compound 2-20e: In a round bottom flask, compound **2-19c**, (7.50 g, 28.2 mmol, 1.0 equiv.) was dissolved in 50 mL toluene, and cooled to –78 °C. A solution of MeMgBr in diethyl ether (18.8 mL, 3.0 M in THF, 3.0 equiv.) was added, and the cooling bath was allowed to decay naturally. The brownish solution was stirred for 16 h, then quenched with $NH_4Cl_{(aq)}$ and extracted with 2 × 150 mL diethyl ether. The organic layers were combined dried over Na_2SO_4, filtered, and concentrated. This resulted in the isolation of a crude product as a yellow oil that was purified by column chromatography (80% EtOAc/hexanes). Compound **2-20e** was obtained as a pale yellow oil (3.73 g, 13.2 mmol, 47% yield).

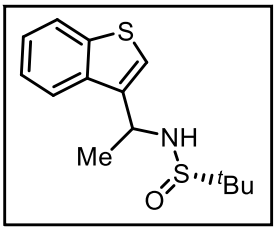

^{1}H NMR (500 MHz, $CDCl_3$): δ 7.86–7.85 (m, 2H), 7.39–7.33 (m, 3H), 4.96 (ap. p, *J* = 6.5 Hz, 1H), 3.33 (ap. d, *J* = 5.4 Hz, 1H), 1.75 (d, *J* = 6.7 Hz, 3H), 1.21 (s, 9H).

^{13}C NMR (125 MHz, $CDCl_3$): δ 141.1, 138.3, 137.5, 124.6, 124.0, 123.1, 123.1, 122.7, 56.0, 50.6, 23.4, 22.8.

HRMS(ESI): calculated $(M+Na)^+$ [$C_{14}H_{19}NNaOS_2$]: 304.0800; found: 304.0800.

$[\alpha]^{21}_D$= +23° (c= 0.97, $CHCl_3$).

Compound 2-20f: In a round bottom flask, compound **2-19d**, (3.7 g, 11.7 mmol, 1.0 equiv.) was dissolved in 50 mL toluene, and cooled to –84 °C. A solution of MeMgI in diethyl ether (7.8 mL, 3.0 M in THF, 3.0 equiv.) was added dropwise, and the cooling bath was allowed to decay naturally and the reaction stirred for 18 h. The reaction was quenched with $NH_4Cl_{(aq)}$ and extracted with diethyl ether (2 × 150 mL). The organic layers were combined dried over Na_2SO_4, filtered, and concentrated. This resulted in the isolation of a red/brown oil that was purified by column chromatography (60% EtOAc/hexanes). Compound **2-20f** was obtained as a deep red liquid.

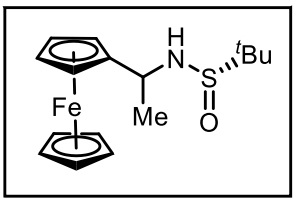

^{1}H NMR (500 MHz, $CDCl_3$): δ 4.25 (ap. p, *J* = 6.8 Hz, 1H), 4.18–4.15 (m, 9H), 3.31 (ap. d, *J* = 8.3 Hz, 1H), 1.63 (d, *J* = 6.8 Hz, 3H), 1.24 (s, 9H).

^{13}C NMR (125 MHz, $CDCl_3$): δ 92.6, 68.6, 68.0, 67.8, 65.9, 56.0, 51.6, 23.7, 22.9.

HRMS(ESI): calculated $(M+Na)^+$ [$C_{16}H_{23}FeNNaOS$]: 356.0742; found: 356.0730.

$[\alpha]^{21}_D$= +23° (c= 0.97, $CHCl_3$).

Amine 2-21e: Compound **2-20e** (2.5 g, 8.9 mmol, 1.0 equiv.) was treated as described in *Section 2.5.2* which generated amine **2-21e** as a clear yellow oil in a 95% yield.

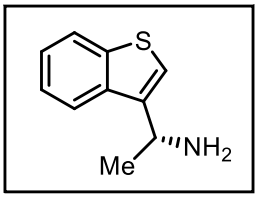

^{1}H NMR (500 MHz, $CDCl_3$): δ 7.86 (ap. t, *J* = 8.1 Hz, 2H), 7.41–7.35 (m, 2H), 7.33 (s, 1H), 4.54 (q, *J* = 6.6 Hz, 1H), 1.55 (d, *J* = 6.6 Hz, 3H).

^{13}C NMR (125 MHz, $CDCl_3$): δ 143.0, 141.2, 137.9, 124.4, 124.1, 123.2, 122.0, 120.3, 46.1, 24.3.

HRMS(ESI): calculated $(M+H)^+$ $[C_{10}H_{12}NS]$: 178.0685; found: 178.0682.

$[\alpha]^{21}_D$= +39.7° (c= 1.09, CH_2Cl_2).

Amine 2-21f: Compound **2-20f** (1.0 g, 3.0 mmol, 1.0 equiv.) was treated as described in *Section 2.5.2* and resulted in amine **2-21f** as an orange oil in an 85% yield.

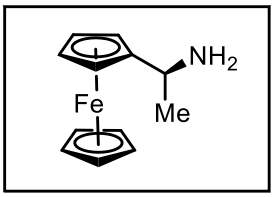

^{1}H NMR (500 MHz, $CDCl_3$): δ 4.15–4.11 (m, 9H), 3.80 (q, *J* = 6.6 Hz, 1H), 1.34 (d, *J* = 6.6 Hz, 3H).

$[\alpha]^{21}_D$= −21° (c= 0.87, CH_2Cl_2).

Diimine 2-22a: Amine **2-21a** (1.14 g, 5.01 mmol, 2.0 equiv.) was treated as described in *Section 2.5.3* which resulted in diimine **2-22a** as a beige powder in a 57% yield.

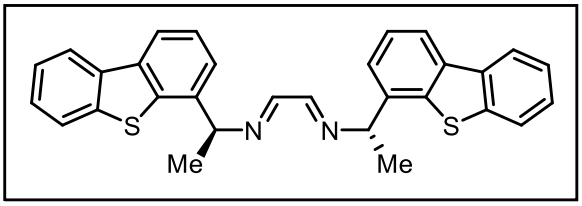

^{1}H NMR (500 MHz $CDCl_3$): δ 8.23 (s, 2H), 8.13–8.11 (m, 2H), 8.05 (ap. d, *J* = 7.7 Hz, 2H), 7.84–7.82 (m, 2H), 7.56 (ap. d, *J* = 7.4 Hz, 2H), 7.47–7.42 (m, 6H), 4.88 (q, *J* = 6.6 Hz, 2H), 1.74 (d, *J* = 6.6 Hz, 6H).

^{13}C NMR (125 MHz, $CDCl_3$): δ 161.4, 139.5, 138.2, 137.7, 136.4, 135.9, 126.9, 125.1, 124.5, 124.4, 122.8, 121.7, 120.6, 68.9, 22.9.

HRMS(ESI): calculated $(M+H)^+$ $[C_{30}H_{25}N_2S_2]$: 477.1454; found: 477.1447.

$[\alpha]^{21}_D$= +67° (c= 0.36, CH_2Cl_2).

Diimine 2-22b: Amine **2-21b** (0.75 g, 2.90 mmol, 2.0 equiv.) was treated as described in *Section 2.5.3* which resulted in diimine **2-22b** as an orange powder in an 85% yield. Significant amounts of baseline material were observed, however attempts to remove this by washing with diethyl ether were unsuccessful due to the high solubility of the diimine.

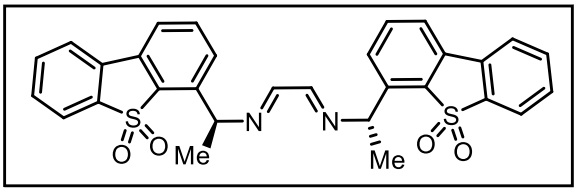

^{1}H NMR (500 MHz $CDCl_3$): δ 8.22 (s, 2H), 7.81–7.76 (m, 5H), 7.72 (m, 2H), 7.61–7.54 (m, 7H), 7.47 (m, 2H), 5.31 (q, *J* = 6.6 Hz, 2H), 1.70 (d, *J* = 6.6 Hz, 6H).

^{13}C NMR (125 MHz, $CDCl_3$): δ 162.4, 142.9, 137.8, 134.3, 133.9, 131.7, 130.3, 129.3, 122.0, 121.6, 120.2, 64.3, 25.3.

HRMS(ESI): calculated $(M+Na)^+$ $[C_{30}H_{24}N_2NaO_4S_2]$: 563.1070; found: 563.1094.

Diimine 2-22c: Amine **2-21c** (0.65 g, 2.5 mmol, 2.0 equiv.) was treated as described in *Section 2.5.3* which resulted in diimine **2-22c** as a white powder in a 76% yield.

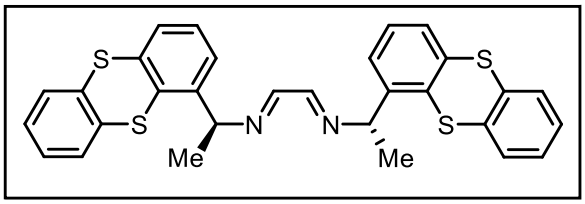

^{1}H NMR (500 MHz $CDCl_3$): δ 8.14 (s, 2H), 7.52–7.47 (m, 6H), 7.42 (ap. d, *J* = 7.7 Hz, 2H), 7.25–7.17 (m, 6H), 5.24 (q, *J* = 6.6 Hz, 2H), 1.59 (d, *J* = 6.6 Hz, 6H).

^{13}C NMR (125 MHz, $CDCl_3$): δ 161.8, 143.4, 136.8, 136.3, 135.3, 134.5, 129.3, 128.7, 128.1, 128.0, 127.8, 126.1, 66.0, 23.6.

HRMS(ESI): calculated $(M+H)^+$ $[C_{30}H_{25}N_2S_4]$: 541.0895; found: 541.0897.

Diimine 2-22d: Amine **2-21d** (0.57 g, 2.1 mmol. 2.0 equiv.) was treated as described in *Section 2.5.3* which resulted in diimine **2-22d** as a solid yellow powder in a 70% yield.

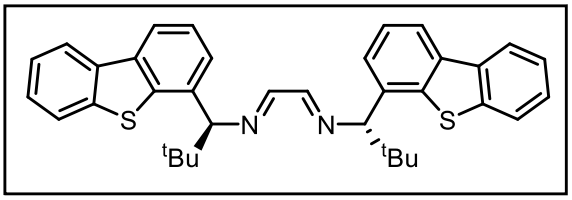

^{1}H NMR (500 MHz $CDCl_3$): δ 8.13 (s, 2H), 8.09–8.07 (m, 2H), 7.98 (ap. d, *J* = 7.6 Hz, 2H), 7.83–7.81 (m, 2H), 7.52 (ap. d, *J* = 7.4 Hz, 2H), 7.41–7.34 (m, 6H), 4.35 (s, 2H), 1.05 (s, 18H).

^{13}C NMR (125 MHz, $CDCl_3$): δ 161.5, 139.5, 139.4, 136.3, 136.0, 135.9, 127.3, 126.7, 124.4, 124.2, 122.5, 121.6, 120.3, 84.1, 37.6, 27.4.

HRMS(APCI): calculated $(M+H)^+$ $[C_{36}H_{37}N_2S_2]^+$ 561.2392, found 561.2418.

Diimine 2-22e: Amine **2-21e** (1.5 g, 8.5 mmol, 2.0 equiv.) was treated as described in S*ection 2.5.3* which resulted in diimine **2-22e** as a flaky orange foam in a 93% yield.

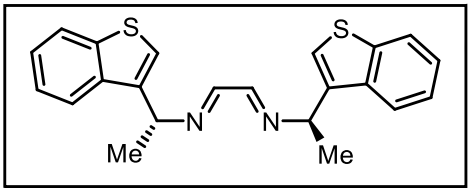

^{1}H NMR (500 MHz, $CDCl_3$): δ 8.09 (s, 2H), 7.85–7.77 (m, 4H), 7.37–7.33 (m, 6H), 5.00 (ap. q, *J* = 6.6 Hz, 2H), 1.69 (d, *J* = 6.7 Hz, 6H).

^{13}C NMR (125 MHz, $CDCl_3$): δ 161.3, 141.0, 138.2, 137.7, 124.5, 124.2, 123.1, 122.6, 122.2, 63.6, 22.7.

HRMS(ESI): calculated $(M+Na)^+$ $[C_{22}H_{20}N_2NaS_2]$: 399.0960; found: 399.0946

$[\alpha]^{21}_D$= +18° (c= 0.96, CH_2Cl_2).

Diimine 2-22f: Amine **2-21f** (0.58 g, 2.5 mmol, 2.0 equiv.) was treated as described in *Section 2.5.3* which resulted in diimine **2-22f** as a deep red tacky oil in a 90% yield.

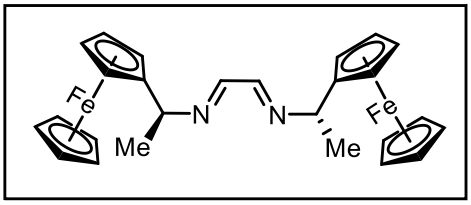

^{1}H NMR (500 MHz $CDCl_3$): δ 7.96 (s, 2H), 4.33 (q, *J* = 6.6 Hz, 2H), 4.13 (s, 18H), 1.54 (d, *J* = 6.6 Hz, 6H).

^{13}C NMR (125 MHz, $CDCl_3$): δ 160.3, 91.5, 68.7, 68.1, 67.8, 67.5, 66.1, 64.9, 22.7.

HRMS(ESI): calculated $(M+Na)^+$ $[C_{26}H_{28}Fe_2N_2Na]$: 503.0844; found: 503.0844.

DAP-Br 2-23a: Diimine **2-22a** (0.68 g, 1.4 mmol, 1.0 equiv.) was treated as described in S*ection 2.5.4* which resulted in DAP-Br **2-23a** in a 91% yield, as a brown powder. Despite extensive washing some dibromocyclohexane remained.

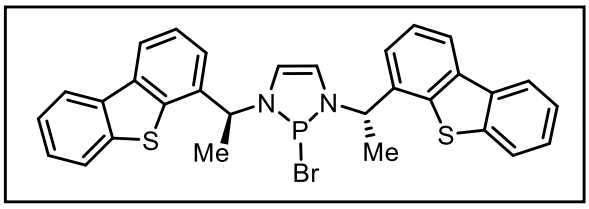

^{1}H NMR (500 MHz, $CDCl_3$): δ 8.15–8.12 (m, 4H), 7.66–7.61 (m, 4H), 7.52–7.43 (m, 6H), 6.60 (s, 2H), 5.55–5.49 (m, 2H), 2.23 (d, *J* = 6.6 Hz, 6H).

^{13}C NMR (125 MHz, $CDCl_3$): δ 139.1, 137.9, 137.0, 135.5, 135.0 (d, *J* = 5.8 Hz), 127.3, 125.5 (d, *J* = 8.8 Hz), 124.9, 123.7 (d, *J* = 7.7 Hz), 122.8, 122.1, 121.9, 58.4 (d, *J* = 12.6 Hz), 20.0 (d, *J* = 11.9 Hz).

^{31}P NMR (202 MHz, $CDCl_3$): δ 184.6.

DAP-Br 2-23c: Diimine **2-22c** (0.30 g, 0.55 mmol, 1.0 equiv.) was treated as described in *Section 2.5.4* which generated DAP-Br **2-23c** as a green powder in a 49% yield.

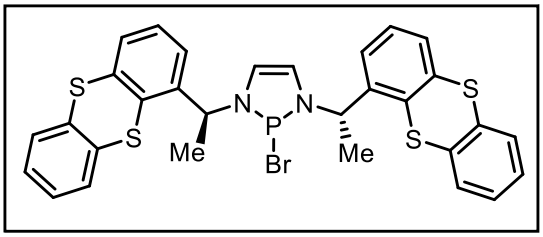

^{1}H NMR (500 MHz, $CDCl_3$): δ 7.52–7.47 (m, 7H), 6.59 (s, 2H), 5.93–5.90 (m, 2H), 2.13 (d, *J* = 6.6 Hz, 6H).

^{31}P NMR (202 MHz, $CDCl_3$): δ 185.5.

DAP-Br 2-23e: Diimine **2-22e** (0.69 g, 1.84 mmol, 1.0 equiv.) was treated as described in *Section 2.5.4* which generated DAP-Br **2-23e** as an orange powder in a 96% yield.

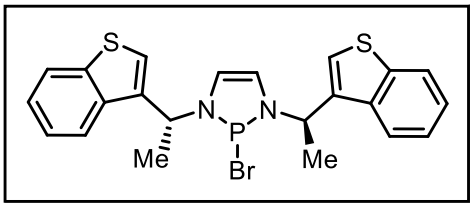

^{1}H NMR (500 MHz, $CDCl_3$): δ 7.89 (ap. d, *J* = 8.0 Hz, 2H), 7.72 (s, 2H), 7.60 (ap. d, *J* = 8.0 Hz, 2H), 7.40–7.36 (m, 2H), 7.34–7.31 (m, 2H), 6.80 (s, 2H), 5.64–5.58 (m, 2H), 2.15 (d, *J*= 6.8 Hz, 6H).

^{13}C NMR (125 MHz, $CDCl_3$): δ 141.0, 136.8, 134.6 (d, *J* = 6.4 Hz), 126.7, 125.1, 124.7, 124.2 (d, *J* = 7.7 Hz), 123.4, 121.4, 53.4 (d, *J* = 13.8 Hz), 20.9 (d, *J* = 8.7 Hz).

^{31}P NMR (202 MHz, $CDCl_3$): δ 184.6.

DAP-Br 2-24a: DAP-Br **2-23a** (0.51 g, 0.87 mmol, 1.0 equiv.) was treated as described in S*ection 2.5.5* to generate DAP-OTf **2-24a** as a pale-yellow powder. This was poorly soluble in $CDCl_3$, so was characterized in CD_3CN.

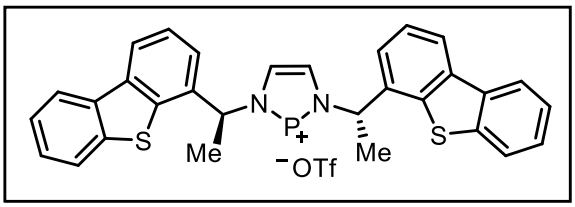

^{1}H NMR (500 MHz, CD_3CN): δ 8.28, (d, *J* = 7.8 Hz, 2H), 8.23 (d, *J* = 7.6 Hz, 2H), 7.96 (s, 2H), 7.69 (d, *J* = 7.4 Hz, 2H), 7.65 (d, *J* = 7.7 Hz, 2H), 7.58 (t, *J* = 7.7 Hz, 2H), 7.52–7.45 (m, 4H), 5.95 (p, *J* = 6.8 Hz, 2H), 2.10 (d, *J* = 6.7 Hz, 6H).

^{13}C NMR (125 MHz, CD_3CN): δ 139.3, 139.2, 138.0, 136.1 134.8 (d, *J* = 3.2 Hz), 133.7 (d, *J* = 4.7 Hz), 128.8, 126.7, 126.3, 124.4, 123.8, 123.2, 118.3, 61.5 (d, *J* = 12.2 Hz), 21.8 (d, *J* = 7.0 Hz).

^{31}P NMR (202 MHz, CD_3CN): δ 210.3.

^{19}F (282 MHz, CD_3CN): δ –79.2.

DAP-OTf 2-24c: DAP-Br **2-23c** (0.18 g, 0.27, mmol, 1.0 equiv.) was treated as described in S*ection 2.5.5* to generate DAP-OTf **2-24c** as a green powder. The spectra were unclean however based off of the complete consumption of DAP-Br **2-23c** and a chemical shift change in the phosphorus NMR, we assumed DAP-OTf **2-24c** was present.

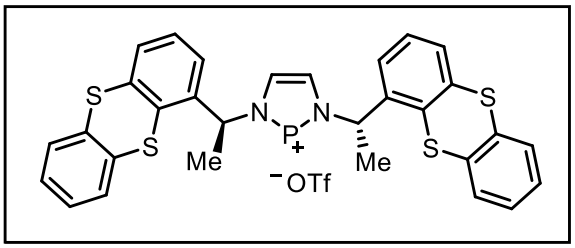

^{31}P NMR (162 MHz, $CDCl_3$): δ 207.1.

^{19}F (377 MHz, $CDCl_3$): δ −78.3.

DAP-OTf 2-24e: DAP-Br **2-23e** (0.86 g, 1.76 mmol, 1.0 equiv.) was treated as described in *Section 2.5.5* to generate DAP-OTf **2-36** as a brown powder in a 65% yield.

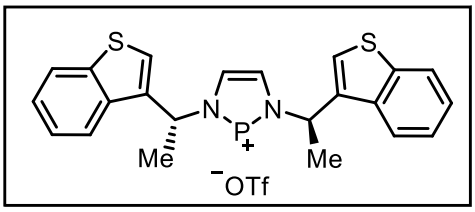

^{1}H NMR (500 MHz, $CDCl_3$): δ 8.27 (s, 2H), 7.87 (ap. d, *J* = 8.1 Hz, 2H), 7.72 (s, 2H), 7.57 (ap. d, *J* = 7.9 Hz, 2H), 7.41–7.38 (m, 2H), 7.34 (ddd, *J* = 8.1, 7.1, 1.1 Hz, 2H), 6.08 (p, *J* = 6.9 Hz, 2H), 2.08 (d, *J* = 6.9 Hz, 6H).

^{13}C NMR (125 MHz, $CDCl_3$): δ 141.0, 136.2, 134.6, 132.9 (d, *J*= 6.6Hz), 128.3, 125.7, 125.5, 123.5, 121.3, 55.7 (d, *J*= 13.0Hz), 23.1 (d, *J*= 5.1Hz).

^{31}P NMR (202 MHz, $CDCl_3$): δ 207.5.

^{19}F (282 MHz, $CDCl_3$): δ –78.2.

Chapter 3 More Efficient Syntheses of Heterocyclic Compounds

3.1 Research Overview and Contribution Report

The author wishes to clarify her contributions to the research described in Chapter 3 of this Thesis document. This Chapter describes shorter and more efficient syntheses of substituted heterocyclic derivatives **3-6**, **3-8**, **3-9**, and **3-31** that have been previously disclosed in the literature and are not commercially available. Derivatives **3-6** and **3-31** were precursors for synthesizing the enantiopure amines that was converted to corresponding DAP-OTfs. Additionally disclosed is a one-step synthesis and isolation of 7.0 g of *N*-phenylphenothiazine **3-20a** which is less expensive than if it was purchased.

I performed all the synthetic steps, along with the collection and processing of the appropriate characterization data for all compounds disclosed in Chapter 3 except for the work by my colleague, Emily Burke. She synthesized and characterized 3-bromonaphthothiophene and the intermediates leading to this product (**3-26** to **3-31**). Xiao Feng carried out mass spectroscopy analysis of all compounds. The sections that contained published work were adapted directly from the respective papers: 1) © 2021 The Royal Society of Chemistry, 2) © 2023 Canadian Science Publishing and 3) © 2022 Thieme.

References: 1. **E. N. Welsh**, K. N. Robertson, A. W. H. Speed, *Org. Biomol. Chem*. **2021**, *19*, 2000– 2007.

2. **E. N. Welsh**, K. N. Robertson, A. W. H. Speed, *Can. J. Chem*. **2022**, *100*, 809–8133.

3. E. K. Burke, **E. N. Welsh**, K. N. Robertson, A. W. H. Speed, *Synthesis* **2023**, *55*, A–I.

3.2 Introduction

The simple heterocyclic derivatives described in Chapter 2 proved to have relatively general syntheses using Ellman chemistry, and gave promising leads, the benzothiophene

(BT) containing DAP-OTf, was the most selective of the heterocycle-containing DAPs and was successfully published.[9] The next best heterocyclic analogue was the 4-dibenzothiophene (DBT) containing DAP-OTf. This result inspired us to target a 1-dibenzothiophene containing DAP-OTf. As mentioned previously, one of the advantages of using heterocyclic derivatives is the possibility of accessing multiple substitution patterns. Considering the size and shape of 4-DBT and 1-DBT relative to 1-naphthyl (Figure 3-1), indicates the position of catalyst attachment on the DBT motif may have an impact on the DBT's steric profile. The blue coloured molecule represents the 1-substituted naphthalene and R represents the DAP in all structures. On the left side, the 4-substituted DBT is represented as the black coloured molecule. It is evident that the DBT curves away from the DAP in this substitution pattern. On the right side, the black coloured molecule represents 1-substitued DBT. This illustrates the DBT portion curves towards the DAP. Accordingly, the hypothesis was that catalysts containing a 1-substituted DBT would present a larger steric profile than the 4-substituted DBT and potentially be more selective.

4-Dibenzothiophene (black)
1-Naphthlene (blue)
R = DAP

1-Dibenzothiophene (black)
1-Naphthlene (blue)
R = DAP

Figure 3-1. Geometry comparison of 4-dibenzothiophene vs. 1-naphthalene (left) and 1-dibenzothiophene vs. 1-naphthalene (right).

1-substituted DBT analogues are not available for purchase and the current literature reported a four-step synthesis for the desired 1-dibenzothiophenecarboxaldehyde. This means using this route would result in a ten-step synthesis to generate the desired DAP, four steps to generate the 1-DBT aldehyde, three steps to obtain the amine with Ellman

methodology, then three steps to generate the DAP catalyst. This high synthetic step count for a catalyst would decrease its desirability substantially. To simplify the synthesis of the 1-substituted dibenzothiophene, a one-pot cascade reaction to access 1-lithiodibenzothiophene involving benzyne intermediates was developed, inspired by the existing literature route (Scheme 3-1A). This is currently the most efficient way of accessing 1-substitued DBT derivatives reported, and successfully generated the desired 1-dibenzothiophenecarboxaldehyde required for the synthesis of the chiral amine. Given the efficiency of this reaction, the project was expanded and other potentially useful 1-substituted DBT motifs were isolated by quenching the one-pot reaction with different electrophiles. The one-pot cascade synthesis and the products isolated from the reaction were successfully published in *Organic & Biomolecular Chemistry*.[51]

As this project was underway, the Speed group was also conducting research in the photocatalysis field[52][53] and wanted to use *N*-phenylphenothiazine as a photocatalyst, however *N*-phenylphenothiazine is expensive to purchase, $102 per 100 mg from Aldrich. We recognized the benzyne chemistry used in the one-pot cascade reaction could be employed to react with lithiated phenothiazine to synthesize *N*-phenylphenothiazine (Scheme 3-1B). I developed a viable route to *N*-phenylphenothiazine using this route, and this synthesis was separately published in *Canadian Journal of Chemistry*.[54]

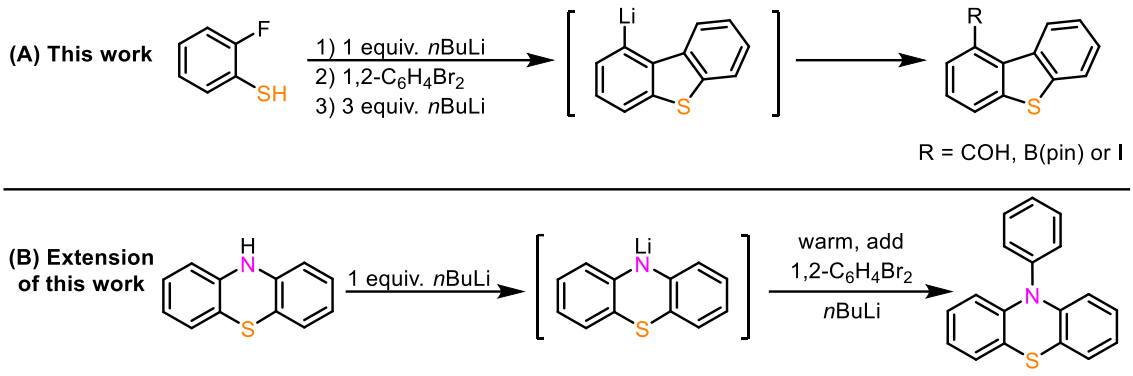

Scheme 3-1. (A) One pot cascade synthesis of 1-dibenzothiophene substituted derivates described in this Chapter. (B) The synthesis of *N*-phenylphenothiazine described in this Chapter.

An isomer of dibenzothiophene that is not commercially available is the naphthothiophene (NTT) derivative. This involved a separate synthesis that did not involve benzyne intermediates but is included here since NTT is an isomer of DBT and has a distinct steric profile (Scheme 3-2). The NTT project was a joint effort between me and Emily Burke, a summer student at the time and now an MSc candidate in the Speed group. Emily devised an efficient four-step synthesis to generate 3-bromonaphthothiophene from 4-bromo-2-thiophenecarboxaldehyde. From 3-bromonaphthothiophene, I employed the Ellman chemistry via the lithiation route to generate the desired chiral amine, and the amine was converted to the corresponding DAP. The reactivity and selectivity of the DAP for imine reduction was tested. The initial synthesis of 3-bromonaphthothiophene and the chiral amine synthesis was recently published in *Synthesis*.[55]

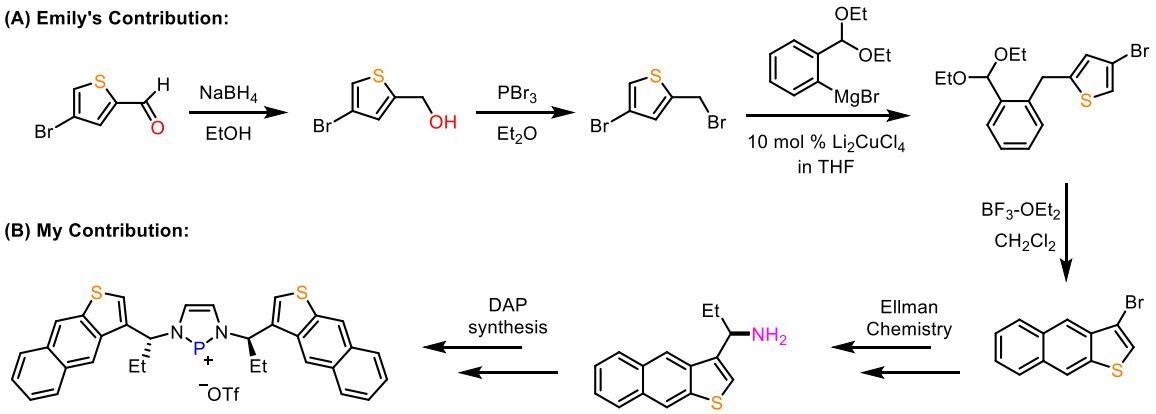

Scheme 3-2. (A) Synthesis of 3-bromonaphthothiophene developed by Emily Burke. (B) Generic synthesis of DAP-OTf containing naphthothiophene motif by Erin Welsh.

While this Chapter describes progress made towards efficient sulfur heterocyclic synthesis itself, it was determined that none of the heterocyclic containing DAPs were superior to the current best DAP **1-28**. The best DAP, containing naphthyl combined with methyl side chains, requires a short three-step synthesis starting from relatively inexpensive commercially available materials, can be synthesized on a 100 g scale and has been highly enantioselective for cyclic amines. Everything described within this Chapter, and the previous Chapter requires a minimum of three steps for the synthesis of non-commercially available chiral amines then an additional three steps to the DAP catalyst and provides at best comparable reactivity and selectivity for imine reduction. Despite this, valuable lessons were learned about heterocycle synthesis. This Chapter concludes the heterocyclic series for this thesis and the following Chapter will explore alternative backbone substitution patterns.

3.3 Results and Discussion

3.3.1 Synthesis of 1-Dibenzothiophene Derivatives in a One-Pot Cascade Reaction

Sanz and co-workers reported a four-step synthesis to access 1-substituted DBT derivatives (Scheme 3-3).[56] The first step was a cross coupling reaction between 2-

fluorothiophenol **3-1** and 2-nitro-1-chlorobenzene to generate **3-2**, followed by a reduction of the nitro group to generate aniline sulfide **3-3**. The amine was converted to an iodide through a Sandmeyer reaction to generate **3-4**. Sulfide **3-4** was cyclized to the desired DBT motif through a reactive benzyne intermediate **3-5**. The benzyne intermediate was generated by the addition of 3.3 equiv. of *tert*-butyllithium (*t*BuLi) which causes this sequence of steps to occur: lithium-halogen exchange, ortho-lithiation next to the fluoride, and lithium fluoride elimination. Benzyne **3-5**, generated via Li-F elimination cyclized with the pendant aryllithium to form 1-lithiodibenzothiophene, this second aryllithium was quenched with the desired electrophile (E). One example used *N*-dimethylformamide (DMF) as the electrophile (E^+) to obtain the DBT 1-carboxaldehyde **3-6** where E = COH. This is the desired starting material to generate the chiral amine using Ellman methodology. As mentioned previously, Sanz' lengthy synthesis to get to the aldehyde decreases the desirability of the DAP even if it was found to have better reactivity and enantioselectivity. The last step of this reaction, the cyclization of **3-4** to **3-6** via benzyne intermediate **3-5**, prompted the idea if benzyne could be used once potentially benzyne could be used twice in a cascade to form the same product in fewer steps.

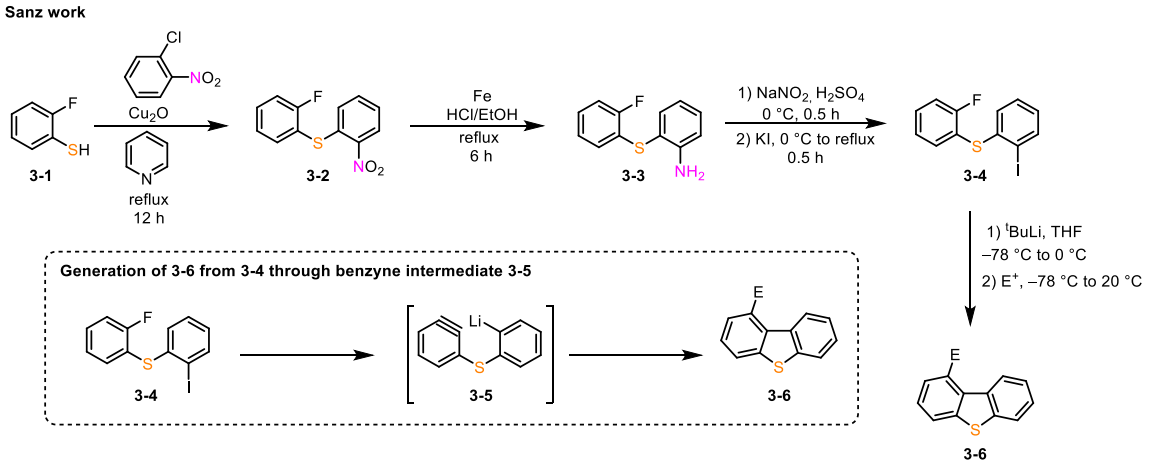

Scheme 3-3. Synthesis of 1-substituted dibenzothiophene derivatives by Sanz group.

Prior to the one-pot cascade reaction, a shorter step-by-step synthesis was performed to generate 1-substituted DBT derivatives to verify the potential of a one-pot reaction to be successful (Scheme 3-4). The first step was to determine if it was possible to go from 2-fluorothiophenol **3-1** to dibenzothiophene 1-carboxaldehyde **3-6**, via addition of a thiophenolate **3-1MgCl** to benzyne derived from 1-bromo-2-fluorobenzene **3-7a**. This still required the formation and isolation of the sulfide intermediate **3-4** but remains more efficient than the Sanz synthesis since **3-4** is accessed in one step rather than three. From intermediate **3-4**, the important factor to test was the replacement of *tert*-butyllithium, used in the Sanz synthesis, with *n*-butyllithium to determine if the byproduct would interfere with the cyclization step and form the desired product **3-6**, because if not, *n*-butyllithium would be a safer alternative than *tert*-butyllithium especially on the multigram scale required for throughput in the DAP synthesis.

In the first reaction, compound **3-1** was deprotonated with isopropylmagnesium chloride (^{i}PrMgCl) in THF, with 1 equivalent of magnesium (Mg^0) turnings already in the reaction flask. Benzyne precursor, 1-bromo-2-fluorobenzene **3-7a**, was cautiously added in portions while the mixture was heated at reflux. Compound **3-7a** reacted with the magnesium turnings to form benzyne which was immediately trapped as it formed by deprotonated **3-4MgX**. Upon complete reaction of the magnesium turnings, the reaction was allowed to cool, then transferred into a suspension of iodine in THF. This order of addition was satisfactory to control the exotherm from the reaction of the magnesiated intermediate with the iodine. Aqueous work-up, followed by crystallization from hexanes afforded dihalothioether **3-4** in 60–65% yield depending on scale. 1,2-Dibromobenzene **3-7b** could be used as the benzyne precursor instead of **3-7a**, however a reduction in yield to

36% was observed. This one-step preparation of **3-4** compares favourably to the previously reported three step route and could readily provide up to 18 grams of compound **3-4** in one step from the same starting material (**3-1**) originally used in Sanz's three-step sequence.

With an abundant supply of **3-4** in hand, the cyclization of **3-4** without the use of *tert*-butyllithium was tested. The *n*-butyllithium was anticipated to be effective for both lithium–halogen exchange on **3-4**, and deprotonation ortho to the aryl fluoride, however it was unclear if the 1-iodobutane resulting from the initial lithium halogen exchange would interfere with the subsequent cyclization steps. Three equivalents of *n*-butyllithium at −78 °C were added and stirred for 30 minutes, then the reaction was warmed to 0 °C for 30 minutes. The reaction mixture was re-cooled to −78 °C and DMF was added as an electrophile. The reaction was allowed to re-warm. After completion of the reaction and work-up, 1-dibenzothiophene carbaldehyde **3-6** was obtained in 78% yield, showing that *n*-butyllithium could conveniently replace *tert*-butyllithium in the cascade reaction.

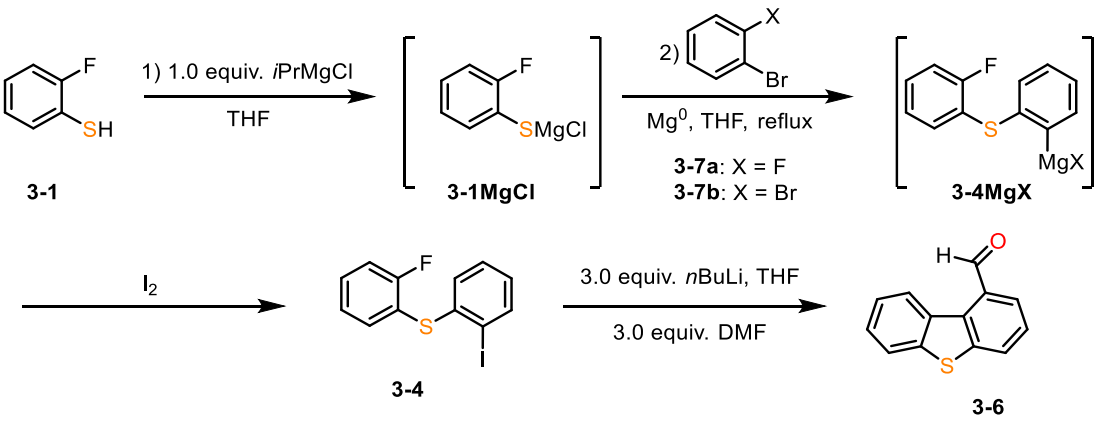

Scheme 3-4. Two step synthesis of 1-dibenzothiophenecarboxaldehyde from 2-fluorothiophenol.

The positive conclusion was that *tert*-butyllithium could be replaced with *n*-butyllithium in a lithiation-initiated cascade. Having success with initial more efficient synthesis of **3-4**, the goal was to further streamline the process by eliminating the formation

and isolation of iodinated intermediate **3-4**. The next investigation was the use of *n*-butyllithium for both thiolate anion formation and initial benzyne formation, rather than magnesium (Scheme 3-5). This would directly intercept the lithiated intermediates and allow access to **3-1Li** and subsequent derivatives in one pot from thiol **3-1**. Avoiding the use of iodine and magnesium, the redox and step-efficiency of this cascade reaction is further increased. Thiol **3-1** was deprotonated with *n*-butyllithium at −78 °C, followed by addition of either benzyne precursor **3-7a** or **3-7b**. Subsequent addition of three equivalents of *n*-butyllithium was followed by aging at −78 °C for 30 minutes.[57] The reaction mixture was then warmed to 0 °C for 30 minutes, re-cooled, and quenched with excess DMF. Benzyne precursor **3-7a** gave a complex mixture, and while DBT was present, it was a minor component. The benzyne precursor **3-7a** requires the elimination of LiF in both benzyne formations for this cascade. This could result in the two benzyne formations occurring out of the desired sequence, making the required intramolecular benzyne trapping impossible. Fortunately, substitution of **3-7a** with 1,2-dibromobenzene **3-7b** allowed production of aldehyde **3-6** in 40% isolated yield after purification by column chromatography (Scheme 3-5A). Benzyne formation from **3-7b** and *n*-butyllithium is known to be complete at −78 °C, meaning the thiolate addition to the first benzyne would be complete prior to warming the reaction to generate the second benzyne on the other ring by elimination of LiF, which occurs at a higher temperature.[57][58] The success of this reaction also depends on the thiolate rather than butyllithium preferentially adding to the benzyne. Use of THF as the solvent was critical. Substitution of diethyl ether or toluene for THF using the same procedure provided more complicated mixtures than the THF reaction, with only traces of **3-6**. Bailey has reported heptane/THF mixtures can provide

cleaner lithium halogen exchanges than pure THF.[59] Replacing THF with a 10:1 mixture of heptane and THF in the cascade resulted in a complex mixture of products. The deprotonation of thiophenol **3-1** in the 10:1 mixture of heptane/THF at either −78 °C or 0 °C resulted in the formation of a white precipitate. The lack of solubility of the thiophenoxide in this solvent system presumably prevented rapid addition of the thiophenoxide anion to benzyne, allowing side reactions.

With a convenient one-pot synthesis of 1-lithiodibenzothiophene (**3-1Li**), the scope was expanded with the use of other quenching agents. The potential cross-coupling partners were targeted as the products would be of value to researchers desiring to access diverse 1-dibenzothiophene derivatives by cross-coupling. Boronic acids of 1-DBT are frequently reported in the patent literature and have been prepared from 1-bromodibenzothiophene by lithiation and quenched with borate esters followed by hydrolysis. The 1-bromodibenzothiophene was accessed via a multi-step sequence, meaning a direct route to 1-DBT boronic esters is yet unrealized.[60] Quenching the aryllithium with iodine afforded iodide **3-8** in 33% yield from **3-1Li** (Scheme 3-5B). Quenching the aryllithium with isopropoxy Bpin allowed isolation of pinacolborate **3-9** in 33% yield from **3-1Li** (Scheme 3-6C). This compound was crystallized, and single crystal X-ray diffraction allowed confirmation of the regioselectivity. While the final yields of these reactions were modest, the single-pot protocol from commercial materials means these 1-substituted DBT synthons are now more rapidly available than prior protocols which require isolation and purification of multiple intermediates. Each product was made in >500 mg scale in one step on the first attempt, and several were made on gram scale. Given the high value of time and effort, this fast route to 1-substituted DBTs means they now become more

attractive motifs for synthetic investigation. It is worth noting that this one-pot procedure takes a comparable amount of time as the lithiation of DBT to produce 4-lithiodibenzothiophene, so now it could be argued the 1-lithiodibenzothiophene isomer is now as easily accessed as the 4-lithiodibenzothiophene isomer.[61]

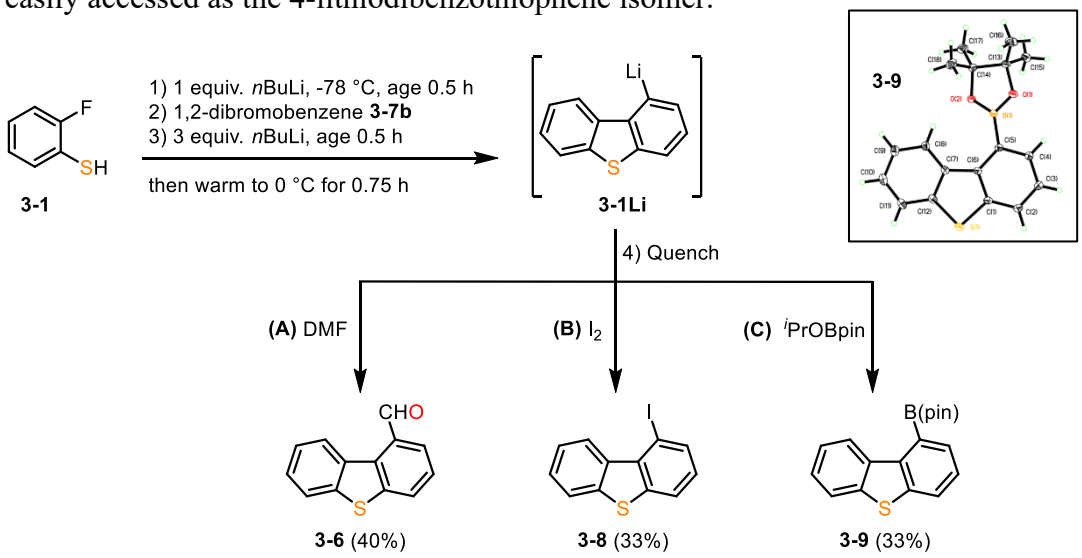

Scheme 3-5. Synthesis of 1-substituted dibenzothiophene derivates with different quenching reagents. (A) Quenched with DMF. (B) Quenched with I_2. (C) Quenched with Isopropxy Bpin.

The scope was attempted to be broadened further by the variation of the fluorothiophenol nucleophile. Other fluorothiophenols that could act as benzyne precursors have limited commercial availability. Accordingly, the replacement of the thiol with a fluorophenol (Scheme 3-6A) or a fluoroaniline (Scheme 3-6B) were attempted. These reactions were unsuccessful and revealed the high nucleophilicity of the thiophenoxide appeared crucial to the reaction's success. Attempts to prepare the dibenzofuran analogue with the optimized cascade starting with 2-fluorophenol **3-10** yielded complex mixtures of products with nothing that could be attributed to dibenzofuran **3-11**. Sanz and co-workers reported the preparation of 1-substituted *N*-methylcarbazoles such as **3-13** by a comparable route to that used with the dibenzothiophenes. Attempted use of aniline **3-12** in the one-pot

sequence resulted in an intractable mixture. The hypothesis was that the addition of either the lithiated aniline or phenol to benzyne were slower than the corresponding lithium thiophenoxide, allowing undesirable side reactions such as benzyne oligomerization to predominate.

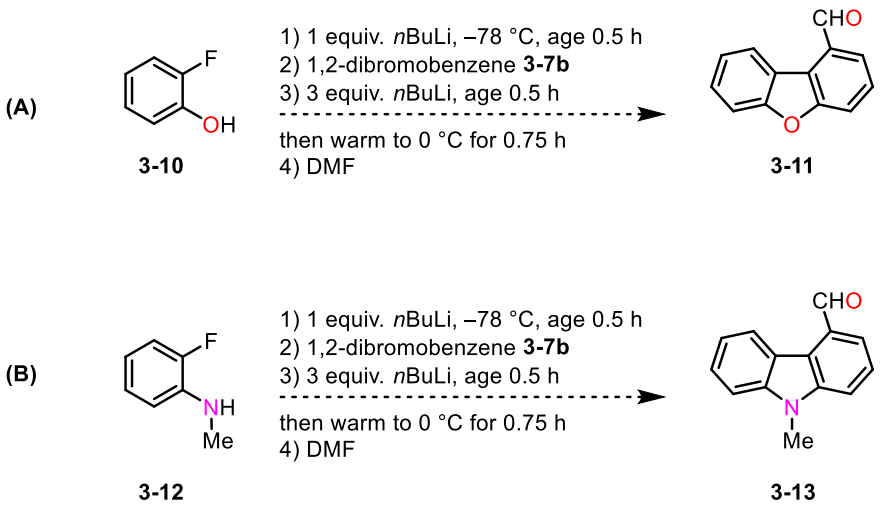

Scheme 3-6. One pot cascade reactions attempted with alternative starting materials. (A) 2-fluorophenol. (B) 2-fluoro-*N*-methylaniline.

3.3.1.1 Attempted Synthesis of DAP Catalyst Containing 1-Substituted DBT

With exploration of the 1-DBT synthesis complete, we turned the focus back to the original purpose of accessing a DAP-OTf with a 1-substituted DBT motif. With a successful one-pot preparation of aldehyde **3-6**, the following steps were taken to synthesize the enantiopure chiral amine containing the 1-DBT motif. Using the Grignard route described in Chapter 2, aldehyde **3-6** was first condensed with (*S*)-*tert*-butanesulfinamide in the presence of titanium ethoxide to generate imine **3-14**. This was followed by the addition of methylmagnesium bromide to a solution of **3-14** in toluene, unfortunately this resulted in poor diastereoselectivity and a mixture of isomers **3-15a** and **3-15b** (Scheme 3-7A). The separation of **3-15a** and **3-15b** by silica gel chromatography was not possible with the readily available resources within the lab. Addition of

ethylmagnesium bromide afforded isomers **3-16**, the major diastereomer along with the minor isomer, with an improved diastereoselectivity of 81:19, however most importantly, the separation of these isomers by column chromatography was relatively straightforward in comparison to the methyl-containing compounds (Scheme 3-7B). The relative configuration of the major isomer of **3-16a** was confirmed by single crystal X-ray crystallography. Deprotection of major isomer **3-16a** with ethereal HCl and freebasing afforded new bulky amine **3-17**, demonstrating that synthesis of chiral amines containing the 1-dibenzothiophene group is feasible.

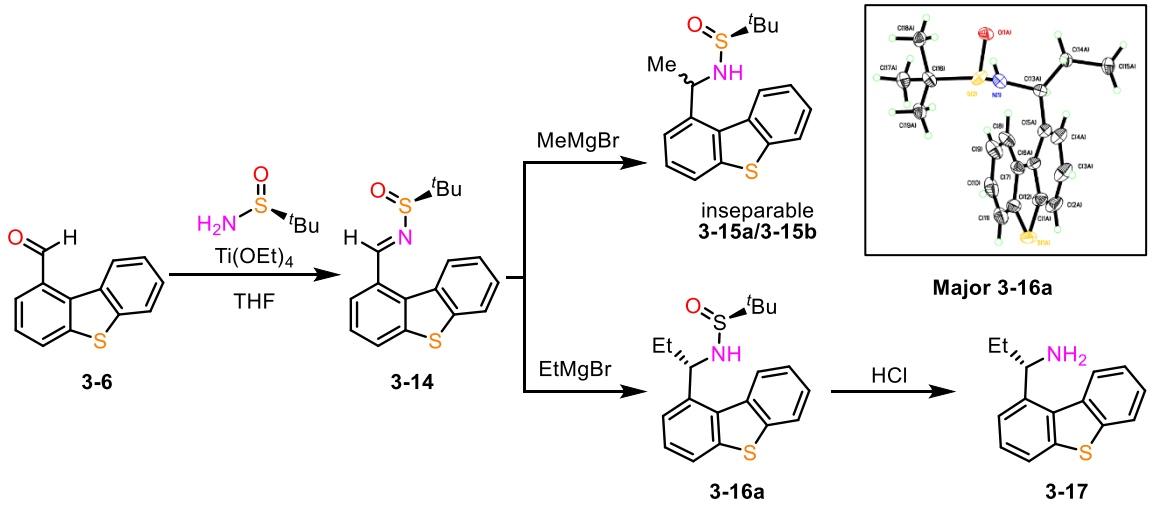

Scheme 3-7. Synthesis of 1-substituted DBT chiral amine. (A) Using MeMgBr resulting in inseparable diastereomers. (B) Using EtMgBr and successfully isolating the major enantiomer.

The typical synthesis to access the DAP-Br **3-19** from amine **3-17** was attempted (Scheme 3-8). Diimine **3-18** was successfully generated from an acid catalyzed condensation reaction between amine **3-17** and glyoxal in the presence of excess sodium sulfate. Accordingly, the diimine **3-18** was exposed to PBr_3 and cyclohexene in dichloromethane to generate the DAP-Br **3-19**. After purification with diethyl ether, the results did not appear promising as there were only broad illegible signals within the ^1H

NMR spectrum and two minimal signals in the phosphorus (^{31}P) NMR spectrum. With these disappointing results from using 1-DBT derivatives as side chains for DAPs, this concluded our attempts to use them within the catalyst manifold.

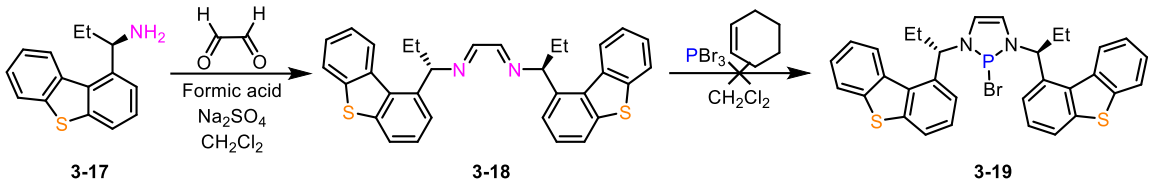

Scheme 3-8. Attempted synthesis of 1-substituted DBT containing DAP-Br **3-19** from amine **3-17**.

3.3.2 Gram-Scale Synthesis of N-Phenylphenothiazine

We recognized one further application of the benzyne chemistry for exploratory purposes within the Speed group. Recently the group developed interest in photoredox catalysis, more specifically in the reactivity of sulfur hexafluoride (SF_6), which is known for being relatively unreactive with most reductants under thermal conditions. SF_6 is used as an industrial gas because of its relative inertness, but the unfortunate side effect of this relative inertness is the lifetime of SF_6 released into the atmosphere is thousands of years. Because of the high global warming potential of SF_6, and its common use, chemistry to decompose surplus SF_6 is a sought-after goal.[62]

One of the only photoredox catalysts that has been shown to add SF_5 across an alkene via reduction of SF_6 is *N*-phenylphenothiazine.[63] While the Speed group research focuses on exploiting the photoredox properties of DAPs to expand this area of the field, there was interest in obtaining *N*-phenylphenothiazine within the lab for exploratory/comparison purposes and potential test reactions. The cost of *N*-phenylphenothiazine guided the idea of using my expertise in benzyne chemistry to synthesize the photocatalyst. A common way to synthesize *N*-phenylphenothiazine would be to arylate the nitrogen from

phenothiazine via cross coupling reaction (Scheme 3-9).[64] However, if *N*-phenylphenothiazine was synthesized without the use of a precious metal catalyst that would be attractive for sustainability reasons and more cost effective. We envisioned adding deprotonated phenothiazine to benzyne could provide an alternate approach to this motif. There would be a close analogy to the thiolate addition to benzyne described previously in this Chapter.

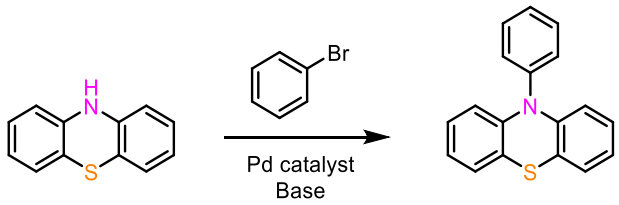

Scheme 3-9. Synthesis of *N*-phenylphenothiazine via cross coupling reaction.

Initially phenothiazine **3-20a** or 2-chlorophenothiazine **3-20b** were attempted to be deprotonated by *n*-butyllithium but this resulted in the formation of precipitates at –78 °C (Scheme 3-10). This indicates majority of the phenothiazide anion **3-20Li** was not in solution and would not rapidly quench the benzyne formed from the addition of *n*-butyllithium to 1,2-dibromobenzene. The following attempt allowed the reaction mixture to warm, by removing the flask from the dry-ice bath, until the lithiated phenothiazine dissolved. Followed by the addition of 1,2-dibromobenzene **3-7b** then *n*BuLi was successful in the formation of aryl phenothiazines **3-21a** and **3-21b**, as detected by NMR spectroscopy of the crude reaction products. Despite the observed product formation, a scale up of the organolithium procedure at these intermediate temperatures could result in a runaway exotherm during the benzyne formation. Due to the difficulty of balancing the correct temperature for the solubility of lithiated precursors versus reaction temperature control with the equipment available within the lab, we did not continue this line of

investigation.[65] By either flow chemistry, or a temperature-controlled chiller capable of sustaining a low temperature high enough for the anion to dissolve, the lithium route could likely be made viable but we do not have ready access to either and therefore attempts to optimize this procedure were not performed.

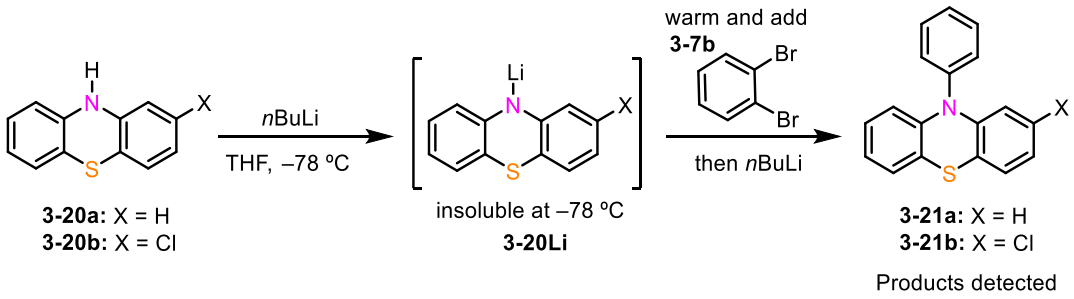

Scheme 3-10. Attempted synthesis of *N*-phenylphenothiazine and 2-chloro-*N*-phenylphenothiazine via benzyne generated from lithium-halogen exchange.

The next route investigated was the use of a Grignard reagent to generate an organomagnesium intermediate that would add to the benzyne. This reaction is done at high temperatures and the rate of benzyne formation is controlled by the addition of the benzyne precursor. This contrasts to the organolithium procedure where the rate of benzyne formation is based off the rate of heat released from the reaction mixture, which could build up quantities of reactive intermediates. The work described in Section 3.3.1, showed 1-bromo-2-fluorobenzene **3-7a** was found to be a higher-yielding benzyne precursor than 1,2-dibromobenzene under magnesiation conditions. Phenothiazine **3-20a** was treated with isopropylmagnesium chloride in the presence of magnesium turnings to generate the organomaganesium **3-20aMgCl**, followed by the slow addition of 1-bromo-2-fluorobenzene. This led to the formation of **3-21a** in 29% yield after purification on a 3 g scale of phenothiazine **3-20a**. Despite the low yield, 1.2 g of **3-21a** was prepared on the first attempt (Scheme 3-11) and there was limited substitution tolerated. The 2-

chlorophenothazine substrate **3-20b** generated the corresponding arylated phenothiazine **3-21b** in 23% yield.[66] No dechlorination to form **3-21a** was observed in the isolated product. An electron-withdrawing CF_3 group was tolerated, with 2-trifluoromethylphenothiazine **3-20c** giving a 32% yield of the arylated phenothiazine **3-21c**. An electron-donating methoxy group was also tolerated, with arylated phenothiazine **3-21d** arising from 2-methoxyphenothiazine **3-20d** in 27% yield.

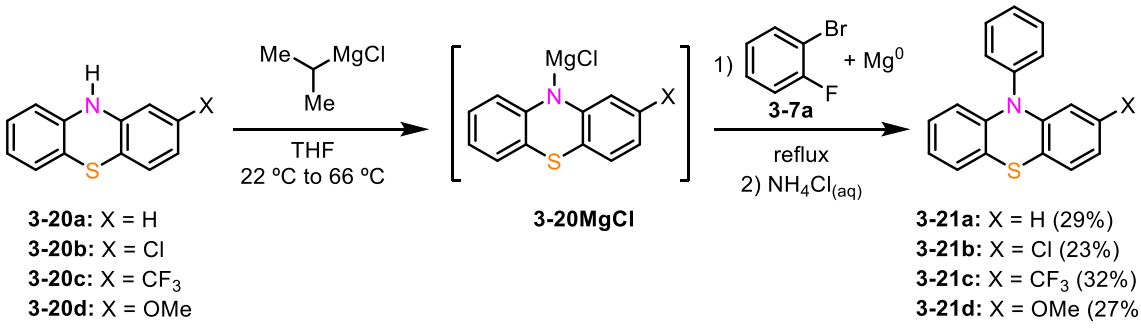

Scheme 3-11. Syntheses of *N*-phenylphenothiazine and 2-substituted-*N*-phenylphenothiazine derivatives via benzyne generated from Grignard formation.

A 2-cyanophenothiazine **3-20e** (Scheme 3-12A) was found to be unreactive, we hypothesized this could be due to the reduced nucleophilicity of the resulting phenothiazide anion. Phenothiazine thioethers **3-20f** and **3-20g** were reactive but gave an unexpected product. Dealkylation followed by arylation of the thio group to form **3-21f** was observed, based on signals observed in the proton NMR spectrum. Furthermore, crystals of **3-21f** grew from ethyl acetate and hexanes fractions during chromatographic purification. Analysis by X-ray crystallography identified two sets of similar polymorphs and confirmed the identity of the product. Specifically, dealkylation of methyl thioether **3-20f** transformed the phenothiazine to phenylthioether **3-21f** in 40% yield, while the nitrogen remained unarylated (Scheme 3-12B). The addition of the benzyne to the thioether, followed by reductive removal of the methyl group, presumably occurred; however, reaction products

containing the methyl group could not be identified.[67] Notably, the methyl group was not transferred to either the nitrogen or to the introduced phenyl ring, shown by both NMR and X-ray analysis. Reactions of aryl methyl thioethers,[68] and other thioethers with benzyne to give either ylides or phenyl thioethers have been reported previously.[69][70] Ethyl thioether **3-20g** gave the same product, **3-21f**, showing the reaction was not limited to the small methyl group. This unexpected outcome revealed an undesirable reaction mode that was not initially anticipated as it was not observed. There were no products arising from benzyne attack on the phenothiazine sulfur noted in any of the reactions.

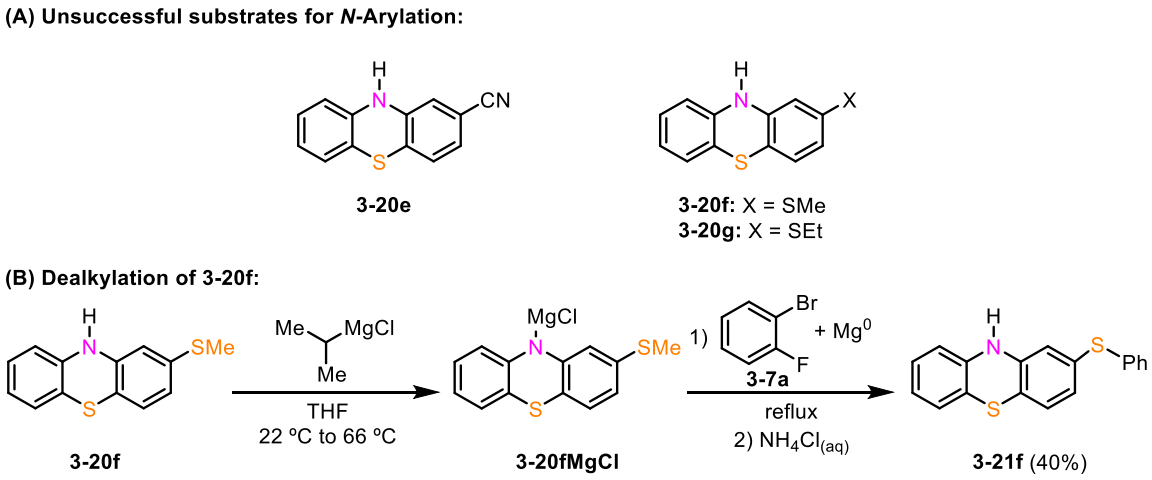

Scheme 3-12. Scope limitations of 2-substituted-*N*-phenylphenothiazine derivatives (A) the substrates that resulted in failed *N*-arylation. (B) Unexpected dealkylation of **3-20f**.

Attempts to synthesize other variants containing cross-coupling partners by quenching with an electrophile other than a proton revealed this was not readily feasible. Attempting to quench the organomagnesium intermediate **3-20aMgX** formed after the addition of the phenothiazide to the benzyne (Scheme 3-13), with Weinreb amide **3-22a**, diphenylchlorophosphine **3-22b**, or iodine **3-22c** did not result in productive formation of compounds **3-23a**, **3-23b**, or **3-23c** (Scheme 3-13A).

We decided to try a deuterium quench to try and verify an anion was present. Quenching the reaction with methanol-*d4* **3-22d** did result in formation of the monodeuterated version of **3-21a** (Scheme 3-13B), as identified by mass spectrometry and ^{1}H and ^{2}D NMR spectroscopy, in comparable yield to the non-deuterated protocol. This provides strong evidence for the intermediacy of **3-20aMgX**, and for the quenching reagent (either NH_4Cl or CD_3OD) being the proton or deuteron source. We hypothesized the lack of productive reactivity with the other quenching reagents could be due to the high steric demand at the ortho position of the phenylphenothiazine.

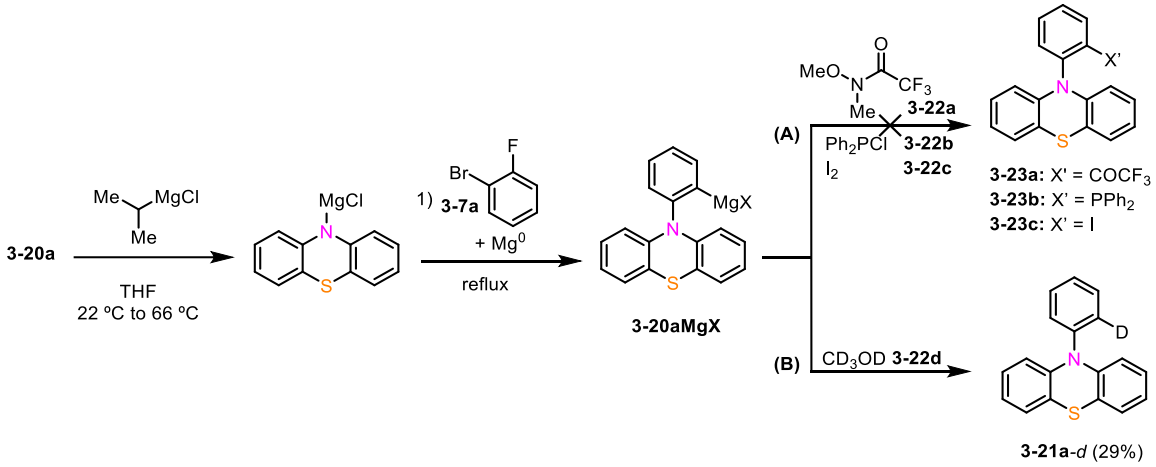

Scheme 3-13. (A) Attempts to trap magnesiated intermediate **3-20aMgX** with alternative quenching reagents. (B) Trapped **3-20aMg** with CD_3OD to generate deuterated *N*-phenylphenothiazine **3-21a-*d***.

Investigation of alternative dibromobenzenes as benzyne precursors was not fruitful. Neither 1,2-dibromo-4,5-difluorobenzene **3-24a** nor 1,2-dibromo-4,5-dimethylbenzene **3-24b** resulted in **3-25a** or **3-25b** respectively under the same conditions (Scheme 3-14). Modified conditions where dibromoethane was mixed with either **3-24a** or **3-24b** in THF solution resulted in more rapid magnesium consumption, but still did not lead to products **3-25a** and **3-25b**. In both cases, consumption of magnesium was observed, but unreacted phenothiazine was recovered from the reaction mixture.

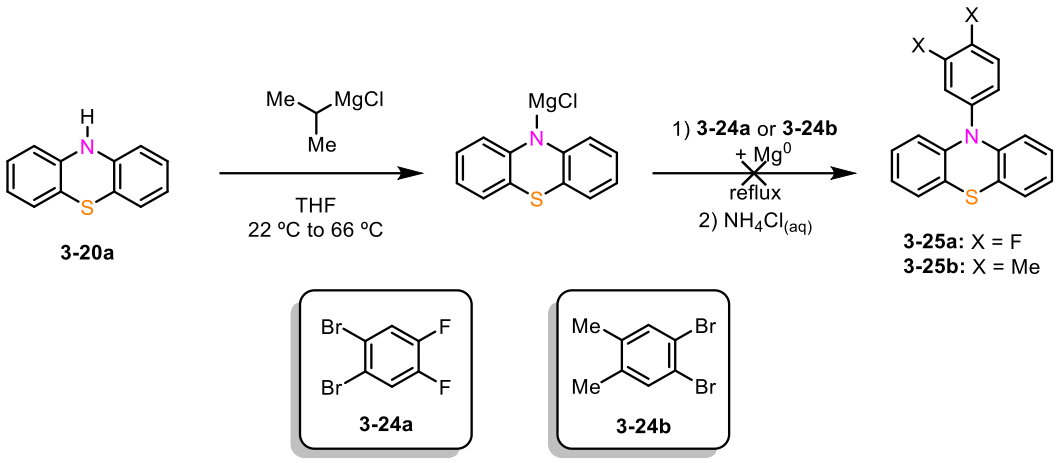

Scheme 3-14. Alternative dibromobenzene benzyne precursor attempts to generate substituted arylated phenothiazines.

In a final reaction, the synthesis of **3-21a** was scaled up. A reaction on a 15 g scale of starting material **3-20a** was conducted. Here, the yield of purified product **3-21a** (Scheme 3-15) increased to 37%, providing 7.6 g of material.

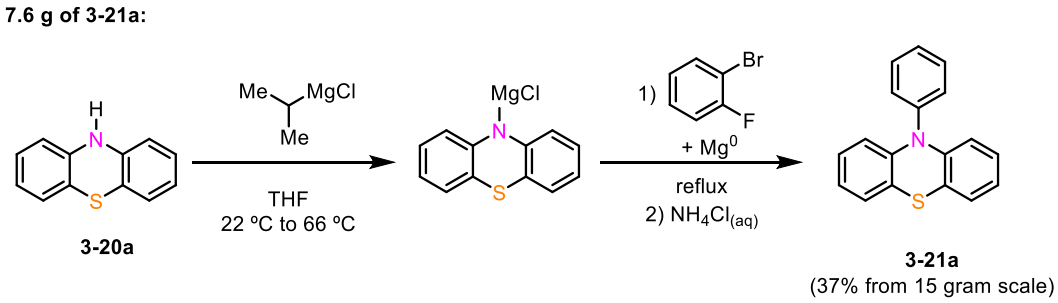

Scheme 3-15. Multigram scale synthesis of *N*-phenylphenothiazine.

While the yield of the reaction from starting material **3-20a** is not comparable with some previously reported Buchwald Hartwig couplings, this synthesis uses economical reagents, and no precious metal catalysts, so it is cost-effective given the very inexpensive starting materials. It is likely that the increased cost of the more expensive substituted phenothiazines **3-20b** to **3-20d** would justify the use of higher yielding cross-coupling protocols with more expensive catalysts to conduct the arylation. Such catalytic protocols would also likely be successful with substrates **3-20e** and **3-20f**, which did not successfully

react with benzyne. However, to the best of our knowledge, this is the largest scale preparation of **3-21a** that has been reported in the literature.

3.3.3 Synthesis of 3-Substituted Naphthothiophene

As the DBT and *N*-phenylphenothiazine projects were underway, a summer student at the time, Emily Burke (currently an MSc student), developed an efficient synthesis to access 3-bromonaphthothiophene. Naphthothiophene (NTT) is another heterocyclic derivative that is not commercially available and is an isomer of DBT. More interestingly NTT can be thought of as a 1-anthracene analogue, in analogy to how benzothiophene (BT) could be thought of as a naphthalene analogue. The original goal of accessing substituted NTT derivatives originated during the synthesis of 1-substituted BT, as NTT is easier to substitute on one end of the steric bulk relative to anthracene (Figure 3-2). The 9-substituted analogue accessible for anthracene (originally mentioned in Section 2.4) relative to naphthalene increases the steric bulk in a way that resulted in lower enantioselectivity. The hypothesis was the substitution on the thiophene ring of NTT, would be comparable to benzothiophene, increasing the steric bulk in one direction. Therefore, if NTT derivatives could be converted to the DAP there may be increased enantioselectivity in imine reduction.

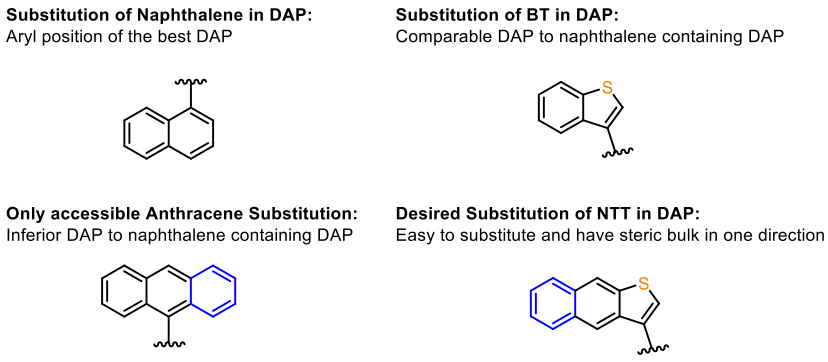

Figure 3-2. Comparing substitution patterns between naphthalene and anthracene vs. benzothiophene and naphthothiophene.

3.3.3.1 Synthesis of 3-Bromonaphthothiophene

The successful synthesis of 3-bromonaphthothiophene **3-31** from commercially available **3-26** was developed by Emily Burke but is shown for completeness (Scheme 3-16).[55] Alcohol **3-27** prepared by sodium borohydride reduction of **3-26**, was brominated with PBr_3 in diethyl ether. Thienyl bromide **3-28** was coupled with Grignard reagent **3-29MgBr**, mediated by lithium tetrachlorocuprate to give **3-30**. Unpurified **3-30** underwent Bradsher cyclization with $BF_3{\cdot}OEt_2$ to form **3-31** in 48% yield over two steps. Only one positional isomer of bromide **3-31** was observed after the Bradsher cyclization, which is the analogue of a 1-haloanthracene. 3-Bromonaphthothiophene **3-31** was prepared on a 2.5-gram scale by Emily Burke over four steps from aldehyde **3-26** by this route.[71]

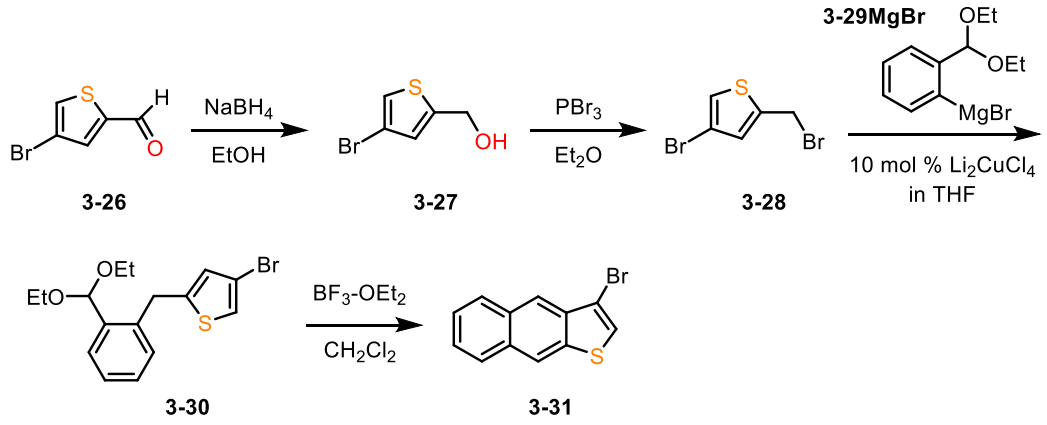

Scheme 3-16. Synthesis of 3-bromonaphthothiophene.

3.3.3.2 Synthesis and Reactivity of DAP Derivative Containing NTT

3-Lithionaphthothiophene **3-31Li** intermediate was derived from a solution of **3-31** was added to a cooled solution of *n*BuLi in tetrahydrofuran. (*S*)-Imine[72][73] derived from propionaldehyde and Ellman auxiliary **3-32**, was added to 3-lithionaphthothiophene **3-31Li** (Scheme 3-17).[74] This protocol gave **3-33a** and **3-33b** as a mixture of diastereomers, separable by chromatography. X-Ray quality crystal structures of both diastereomers **3-**

33a and **3-33b** were grown from cooled saturated diethyl ether solutions of the isolated diastereomers. X-Ray crystallography analysis confirmed the products from the Ellman addition were epimers at the newly created stereocentre, rather than regioisomers from proton migration on the lithated heterocycles. Deprotection of the major diastereomer **3-33a** with ethereal HCl followed by free-basing afforded chiral amine **3-34**. An attempt to perform the Ellman chemistry with an Ellman imine **2-19a**, derived from acetaldehyde rather than propionaldehyde, resulted in inseparable diastereomers. This issue was encountered earlier in this Chapter with the dibenzothiophene-containing chiral amine, where ethyl side chains allowed chromatographic separation, while methyl side chains did not (Scheme 3-7).[51] As is a common theme in these past two Chapters, use of Ellman auxiliary for the synthesis of bulky amines such as **3-34** has often resulted in poor diastereoselectivity in the imine addition step, with both organolithium and Grignard reagents, despite the generally good performance of this method with simpler substrates. This means choosing systems with separable diastereomers is important to obtain enantiomerically enriched material for DAP synthesis.

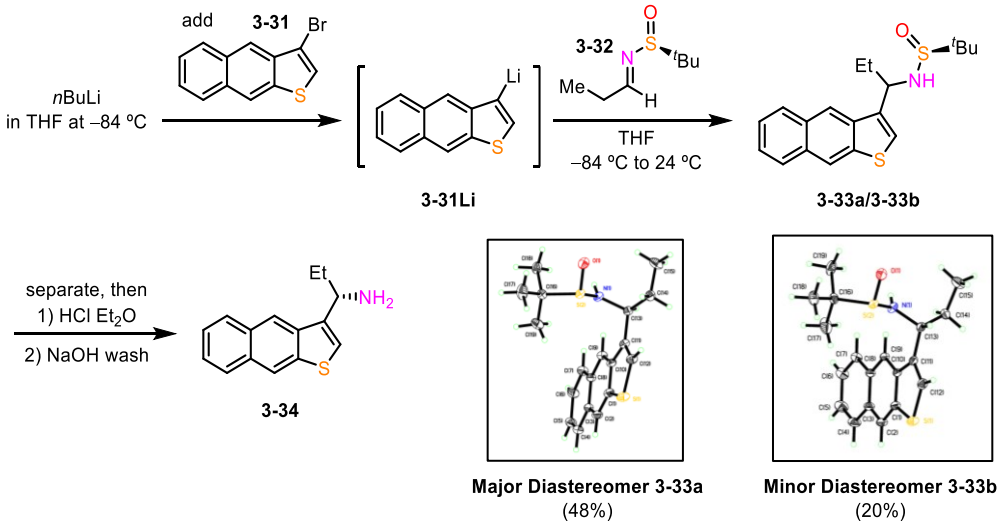

Scheme 3-17. Synthesis of NTT derived chiral amine via Ellman chemistry.

After the successful isolation and purification of the enantiopure amine, the salt form **3-34•HCl** was used directly and successfully converted to the DAP-OTf **3-37** through a similar synthetic route to previously reported DAP-OTfs (Scheme 3-18). The choice of starting with the salt removes the basification work-up when isolating the enantiopure amine and reduces the risk of decreasing yield. Amine salts also have a much longer shelf life, as they are more stable to air oxidation. The use of **3-34•HCl** required slight modifications to the usual synthesis of the DAP-OTf. First, the amine salt **3-34•HCl** required a deprotonation, therefore excess triethylamine (NEt_3) was added, to form the amine in-situ. Presumably the conjugate acid triethylamine hydrochloride catalyzed the condensation reaction with glyoxal in the presence of Na_2SO_4 to generate diimine **3-35**. Another modification was the use of toluene as the solvent over the typical dichloromethane as the amine salt **3-34•HCl** has increased solubility in toluene, while the triethylammonium chloride has reduced solubility.

Once the diimine **3-35** was successfully isolated and purified with toluene washes, the cyclization to the DAP-Br **3-36** was successful with PBr_3 and cyclohexene in dichloromethane at 0 °C. This contrasts with **3-18**, which did not cyclize. The lower temperature for the cyclization was another slight modification to the usual method. Other students working on similar projects at the time had found the cyclization at the cooler temperature resulted in a cleaner DAP-Br as it decreased the potential for background reactions. Analysis of the ^{31}P NMR spectrum of the cyclization to DAP-Br **3-36** revealed one major peak with minor PBr_3 remaining, even after excess washing with diethyl ether. Without fully removing the excess starting material, the DAP-Br **3-36** was treated with TMSOTf in dichloromethane to successfully generate the DAP-OTf **3-37**, again according

to the ^{31}P NMR spectrum results. The DAP-OTf **3-37** was used as is from the reaction in test reduction reactions to determine how this catalyst compared to the best DAP OTf.

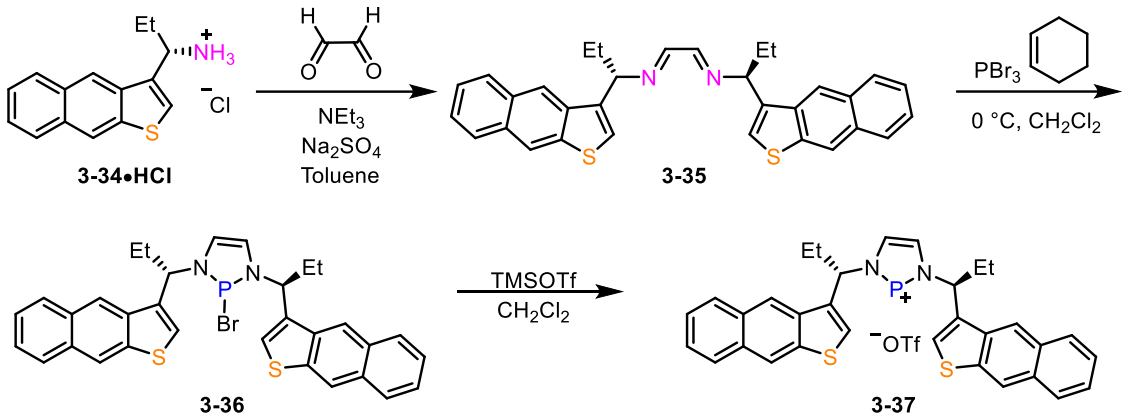

Scheme 3-18. Synthesis of DAP-OTf containing NTT for the aryl side chain.

Preliminary reduction results using the NTT-derived DAP-OTf **3-37** are summarized in Table 3-1. Three different substrates were tested at two different temperatures and directly compared to the current best DAP. The first substrate **2-17b** was the usual benchmark, for comparison the *e.r.* of **2-17b** using the best DAP-OTf **1-28** was reported to be 95:5. The NTT containing DAP-OTf **3-37** gave inferior selectivity with *e.r.* of 88:12 for **2-17b** (Entry 1). We considered this catalyst may have complementary reactivity, therefore other substrates that had lower selectivity for the current best DAP-OTf **1-28** was tested. Substrate **3-38**, at −35 °C had slightly inferior selectivity of a reported *e.r.* 93:7 with catalyst **1-28**. Unfortunately, the DAP-OTf **3-37** at room temperature showed a significant decrease in selectivity for **3-38**, giving an enantiomer ratio of only 21:79 (Entry 2). There is the argument that the reduction was run at room temperature rather than cooled, however the difference is so large that cooling would still be inferior to the current best DAP. One more substrate, **3-39** was tested and has a reported *e.r.* of 88:12 for the current best DAP at −35 °C. As shown, the selectivity with the new catalyst **3-37** is again inferior to the

current best DAP with an *e.r.* of 19:81 at room temperature. If the reaction was cooled, the selectivity would likely increase and be comparable to the best DAP **1-28** or slightly more selective. However, the increased number of synthetic steps to obtain the catalyst would decrease the impact of comparable enantioselectivity.

Table 3-1. Preliminary reduction results with catalyst **3-37** for a few substrates**.**

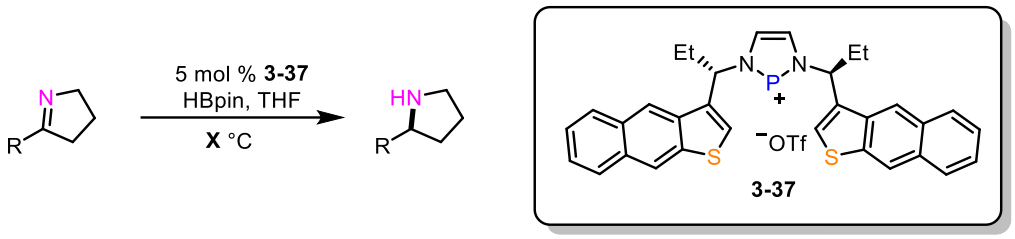

Entry	Product	Product Number	Temperature **X** (°C)	*e.r.*
1	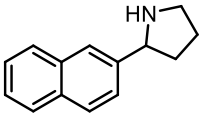	**2-17b**	−35	88:12
2	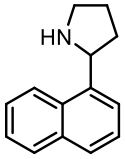	**3-38**	+24	21:79
3	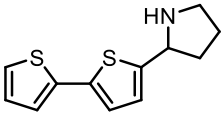	**3-39**	+24	19:81

This work concluded the attempts at replacing the naphthyl aryl group in the current best DAP with a heterocyclic containing analogue. While this chemistry gave success in developing efficient syntheses for accessing substituted heterocyclic analogues, unfortunately there was no improvement towards the goal in developing DAP-OTf with superior reactivity and selectivity than the current best DAP-OTf.

3.4 Summary

There were significant impacts made in developing efficient synthesis of substituted heterocyclic analogues, specifically for 1-substituted DBT and 3-substituted NTT analogues. A one-pot cascade reaction starting with 2-fluorothiophenol that goes through two benzyne intermediates to generate **3-1Li** was successfully quenched with three different electrophiles, DMF to form 1-dibenzothiophenecarboxaldehyde **3-6**, iodide to generate **3-8** containing an iodide substituent, and isoproxy pinacol borane to form **3-9** containing a Bpin substituent. The aldehyde **3-6** was successfully converted to enantiopure chiral amine **3-17** via Ellman chemistry and subsequently converted to the diimine **3-18**. Unfortunately, the cyclization step to the DAP-Br **3-19** was not fruitful and put a halt to this motif as a part of the catalyst manifold.

As the one pot reaction to generate 1-substituted DBT derivatives was being developed, the Speed group was exploring the use of DAPs for photocatalysis and radical chemistry. This led to the desire of obtaining *N*-phenylphenothiazine **3-21a** for exploratory purposes. The cost of purchasing **3-21a** inspired the use of a benzyne intermediate to arylate a lithiated phenothiazine. This route was successful and expanded to a limited number of derivatives, 2-chloro-*N*-phenylphenothiazine substrate **3-21b**, 2-trifluoromethyl *N*-phenylphenothiazine **3-21c**, and 2-methoxy *N*-phenylphenothiazine **3-21d**. It should be noted that these derivatives were low yielding. Alternative quenching reagents were attempted to quench **3-20MgX** such as a Weinreb amide, diphenylchlorophosphine, and iodine but these did not result in productive formation of the respective compounds. Alternative dibromobenzene reagents as benzyne precursors were unsuccessful as well. For the purposes of the lab, the only desire was *N*-phenylphenothiazine and despite the low

yield, it was scaled to 15 g and produced 7.5 g which is still much cheaper than purchasing it from a vendor.

While this project was underway, a colleague Emily Burke, was developing an efficient synthesis for 3-bromonaphthothiophene **3-31**. I converted **3-31** to the corresponding DAP-OTf **3-37**. The successfully synthesized 3-bromoNTT was successfully converted to the enantiopure chiral amine **3-34** via Ellman chemistry. Amine **3-34** was subsequently converted to the diimine **3-35** and successfully cyclized to the DAP-Br **3-36**. The DAP-OTf **3-37** was successfully generated from the DAP-Br. The DAP-OTf **3-37** was used in a few catalytic reductions to test its reactivity and selectivity for imines. These results determined the NTT containing DAP was inferior to the best DAP catalyst for all substrates tested. This concluded the use of heterocyclic containing analogues for the DAP catalyst manifold.

3.5 Experimental

3.5.1 General Considerations for 1-Dibenzothiophene Derivatives

Reactions were run under nitrogen, using oven-dried glassware unless otherwise specified. ^{1}H, ^{13}C, and ^{11}B NMR data were collected at 300K on a Bruker AV-500 NMR spectrometer. ^{1}H NMR spectra are referenced to residual non-deuterated NMR solvent ($CHCl_3$ = 7.26 ppm). ^{13}C NMR spectra are referenced to the central $CDCl_3$ peak (77.16 ppm). Mass spectrometric data were acquired by Mr. Xiao Feng (Mass Spectrometry Laboratory, Dalhousie University). Optical rotations were obtained in the solvents stated, using a DigiPol 781 Automatic Polarimeter from Rudolph Instruments. Concentrations for optical rotation are given in g/100 mL.

Solvents

Diethyl ether was purchased as anhydrous ACS reagent grade, >99.0% stabilized by BHT in 1 L metal cans from Aldrich.

Dichloromethane (ACS grade) was purchased from Fisher. Dichloromethane for reactions was distilled from calcium hydride immediately before use, while no purification was carried out on dichloromethane used for extractive work-ups.

Methanol was purchased from Fisher and used as received.

Tetrahydrofuran was purchased from Aldrich in a Sure/seal® bottle (anhydrous, >99.9%, inhibitor free, catalogue number 401757). Tetrahydrofuran was used directly from this bottle for Grignard reactions and lithiations.

Reagents

Benzaldeyhde, *n*-Butyllithium, dimethyl formamide, ethylmagnesium bromide in diethyl ether, hydrochloric acid in diethyl ether, magnesium turnings, dimethyl malonitrile, priopionaldehyde, and trifluoroacetic acid were purchased from Aldrich and used directly as received. The *n*-butyllithium was periodically titrated in tetrahydrofuran using 1,10-phenanthroline as an indicator, and 2-butanol as the titrant and concentration varied from 2.5 to 2.6 M.

Sodium borohydride was purchased in a 250 g container from Aldrich and was stored in a solvent-free glovebox to maintain high activity.

***N*-methoxy-*N*-methytrifluoroacetamide, 2-fluorothiophenol, 2-fluoro-*N*-methylaniline, 1,2-dibromobenzene, 1-bromo-2-fluorobenzene, isopropoxy B(pin), pinacolborane, and titanium ethoxide** were purchased from Oakwood Chemical and used directly as received.

4,5-dibromo-o-xylene, 1,2-dibromo-4,5-(methylenedioxy)benzene, 1,2-dibromo-4,5-difluorobenzene, 2,3-dibromopyridine, and *N*-boc-pyrrolidinone were purchased from CombiBlocks and used directly as received.

Ellman Sulfinamide Auxiliary was purchased from Oakwood Chemical and configuration was verified by measurement of optical rotation.

3.5.2 Experimental Procedures and Tabulated Data for 1-Dibenzothiophene Derivatives

2-fluorophenyl-2-iodophenyl thioether 3-4 (1-bromo-2-fluorobenzene procedure):

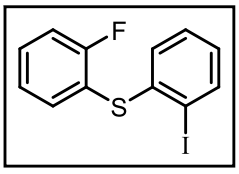

Magnesium turnings (683 mg, 28.1 mmol, 1 equiv.) were placed in a 100 mL three neck flask equipped with a condenser under a nitrogen atmosphere. tetrahydrofuran (28 mL) was added. Thiophenol **3-1** (3.0 mL, 28.1 mmol, 1 equiv.) was added. Isopropylmagnesium chloride (16.8 mL, 1.67 M in THF, 28.1 mmol, 1 equiv.) was carefully added, which resulted in heating of the reaction to reflux. After bubbling subsided, the reaction was placed in an oil bath at 80 °C. When reflux resumed, halide **3-7a** (3.07 mL, 28.1 mmol, 1 equiv.) was cautiously added in 5 portions with 10 minutes between each portion. The reaction was heated for a further hour, at which time negligible magnesium remained and the solution was clear and light brown. The reaction was removed from heat, allowed to cool to ambient temperature, and solid iodine was cautiously added with stirring. The reaction self-heated to a gentle reflux, which abated as the reaction was stirred for a further hour. The resulting cloudy brown mixture was poured

into 50 mL of saturated aqueous $Na_2S_2O_3$ and stirred for 10 minutes. The mixture was extracted with 2 × 100 mL portions of diethyl ether, and the combined organic layers were washed with brine, dried over Na_2SO_4, and concentrated to give a yellow oil, which slowly solidified. This was dissolved in 100 mL hexanes with heating and placed in a –15 °C freezer. Colourless crystals formed, which were collected by filtration to afford 3.34 g of **3-4**. The mother liquor was purified by column chromatography (1% EtOAc/hexanes) to afford a further 2.70 g of **3-4** (6.04 g total, 18.2 mmol, 65% yield from **3-1**). Spectral data agreed with literature values.[6]

1,2-dibromobenzene procedure: The procedure with 3.0 mL of **3-1** (28.1 mmol) was carried out in the same manner as the top procedure, except 1,2-dibromobenzene **3-7b** (3.38 mL, 28.1 mmol) was used instead of 1-bromo-2-fluorobenzene **3-7a**. The crude product was an orange oil, which did not solidify. Chromatography (1% EtOAc/hexanes) afforded 3.39 g of product as a colourless solid (10.3 mmol, 37% yield).

Spectral data from 6.04 gram procedure:

^{1}H NMR (500 MHz, $CDCl_3$): δ 7.85 (dd, *J* = 7.9, 1.4 Hz, 1H), 7.40–7.36 (m, 2H), 7.23–7.14 (m, 3H), 6.96 (ap. d, *J* = 7.9 Hz, 1H), 6.89 (td, *J* = 7.6, 1.6 Hz, 1H).

^{13}C{^{1}H} NMR (125 MHz, $CDCl_3$): δ 162.0 (d, *J* = 248.4 Hz), 140.5, 139.9, 135.2, 130.9 (d, *J* = 8.1 Hz), 129.3, 128.9, 127.9, 125.2 (ap. d, *J* = 3.44 Hz), 121.2 (d, *J* = 18.3 Hz), 116.5 (d, *J* = 22.3 Hz), 99.3.

^{19}F NMR (470 MHz, $CDCl_3$): δ −107.0 – −107.1 (m)

1-dibenzothiophenecarboxaldehyde 3-6 prepared from 3-4: Compound **3-4** (6.86 g, 20.8 mmol) was dissolved 30 mL tetrahydrofuran in a 100 mL Schlenk flask. The mixture was cooled to –78 °C in dry ice/acetone. *N*-Butyllithium (25 mL, 2.5 M in hexanes, 62.5 mmol, 3 equiv.) was added dropwise over 5 minutes. The reaction was stirred for 30 minutes at –78 °C, then moved from the dry ice/acetone bath to an ice bath and stirred for 30 minutes. The reaction was then returned to the dry ice/acetone bath, allowed to cool for 5 minutes, then DMF (4.83 mL, 62.3 mmol, 3 equiv.) was added. The reaction was warmed to room temperature, stirred for 2 hours, then quenched pouring into 100 mL 1 N HCl. The mixture was extracted with 3 × 150 mL portions of diethyl ether, and the combined organic layers were washed with brine, dried over Na_2SO_4, and concentrated. The residue was purified by column chromatography (7.5% EtOAc/hexanes) to afford **3-6** (3.43 g, 16.2 mmol, 78% yield) as a yellow solid. Spectral data were in accordance with literature values.[7]

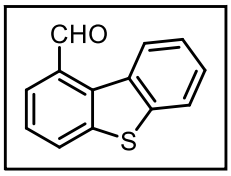

^{1}H NMR (500 MHz, $CDCl_3$): δ 10.72 (s, 1H), 8.98 (ap. d, *J* = 7.6 Hz, 1H), 8.11 (ap. d, *J* = 7.9 Hz, 1H), 7.99 (ap. d, *J* = 7.5 Hz, 1H), 7.92 (ap. d, *J* = 7.2 Hz, 1H), 7.61 (ap. t, *J* = 7.7 Hz, 1H), 7.56–7.50 (m, 2H).

$^{13}C\{^1H\}$ NMR (125 MHz, $CDCl_3$): δ 192.0, 141.6, 140.4, 134.7, 134.6, 134.1, 130.6, 128.6, 127.7, 127.4, 125.9, 125.0, 122.9.

HRMS (ESI): *m/z* $[M+Na]^+$ calculated for $C_{13}H_8NaOS$: 235.0188 found: 235.0184.

Single-pot Cascade Reactions:

1-lithiodibenzothiophene (3-1Li): Compound **3-1Li** (0.84 mL, 7.86 mmol, 1 equiv.) was dissolved in 10 mL tetrahydrofuran in a 100 mL Schlenk flask. The mixture was cooled to –78 °C in dry ice/acetone. *N*-Butyllithium (3.12 mL, 2.6 M in hexanes, 8.1 mmol, 1 equiv.) was added dropwise over 1 minute. The reaction was stirred for 30 minutes, then 1,2-dibromobenzene (0.96 mL, 7.95 mmol, 1 equiv.) was added. *N*-butyllithium (9.36 mL, 2.6 M in hexanes, 24 mmol, 3 equiv.) was added dropwise over 5 minutes, and the reaction was stirred for 30 minutes. The reaction was moved from the dry ice/acetone bath to an ice bath and stirred for 45 minutes. The reaction was then returned to the dry ice/acetone bath, allowed to cool for 5 minutes, the appropriate quenching agents was added. A tan precipitate usually formed during the warming and second cooling cycle.

1-dibenzothiophenecarboxaldehyde 3-6: To the above prepared solution of 1-lithiodibenzothiophene was added DMF (1.81 mL, 23.2 mmol, 3 equiv.). A thick precipitate immediately formed. The reaction was removed from the dry ice/acetone bath, stirred for 2 hours, and then quenched by the addition of 25 mL 1 N HCl. The mixture was extracted with 2 × 100 mL portions of diethyl ether, and the combined organic layers were washed with brine, dried over Na_2SO_4, and concentrated. The residue was purified by column chromatography (7.5% EtOAc/hexanes) to afford **3-6** (667 mg, 3.14 mmol, 40% yield) as a yellow solid. Spectral data were in accordance with literature values.[7] Spectral data were in agreement with **3-6** prepared from **3-4**, according to the procedure on page 102**.**

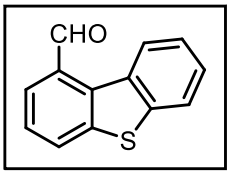

1-iododibenzothiophene 3-8: To the above prepared solution of 1- lithiodibenzothiophene **3-1Li** was added solid iodine (3.96 g, 15.6 mmol, 2 equiv.) was added through the top of the flask with a strong countercurrent of nitrogen. The reaction was then moved from the dry ice/acetone bath to the ice bath, stirred for 30 minutes, and then quenched by the addition of 25 mL saturated $Na_2S_2O_3$. The mixture was extracted with 2 × 100 mL portions of diethyl ether, and the combined organic layers were washed with brine, dried over Na_2SO_4, and concentrated. The waxy residue was purified by chromatography with pure hexanes, to give an inseparable mixture of 1-iododibenzothiophene and dibenzothiophene. This mixture was placed in a sublimation chamber with a dry-ice finger and evacuated to approximately 5 torr. The residue was heated with a heat gun until it became liquid, and a white sublimate was observed on the cold finger. The chamber was disassembled, the finger cleaned, and the process was repeated twice more, until a negligible amount of sublimation was observed. The remaining material in the bottom of the sublimation chamber (803 mg, 2.59 mmol, 33% yield), was found to be approximately 95% 1-iododibenzothiophene **3-8** with the balance being dibenzothiophene. No 1-iododibenzothiophene sublimed under these conditions.

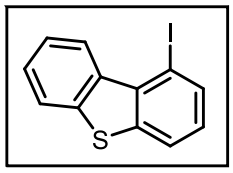

^{1}H NMR (500 MHz, $CDCl_3$): δ 9.41–9.39 (m, 1H), 8.03 (ap. d, J = 7.6 Hz, 1H), 7.88–7.86 (m, 2H), 7.57–7.52 (m, 2H), 7.12–7.09 (m, 1H).

^{13}C{^{1}H} NMR (125 MHz, $CDCl_3$): δ 141.7, 140.5, 137.7, 135.7, 134.9, 127.4, 127.2, 124.9, 123.4, 122.9, 122.8, 88.9.

HRMS (APCI): *m/z* [M radical cation]$^+$ calculated for $C_{12}H_7IS$: 309.9308 found: 309.9298.

1-(4,4,5,5-tetramethyl-1,3,2-dioxaborolan2-yl)-dibenzothiophene 3-9: To the above prepared solution of 1-lithiodibenzothiophene was added *i*PrOBpin (3.2 mL, 15.7 mmol, 2 equiv.) was added. The cooling bath was removed, and the reaction was stirred for 1 hour, and then quenched by the addition of 15 mL 1 N HCl. The mixture was extracted with 2 × 100 mL portions of diethyl ether, and the combined organic layers were washed with brine, dried over Na_2SO_4, and concentrated. The grey waxy residue was purified by column chromatography with 2.5% EtOAc/hexanes, then further recrystallized by cooling a solution in hexanes with a few drops of ethyl acetate to give boronate **3-9** (804 mg, 2.59 mmol, 33% yield) as white colourless crystals, which were suitable for X-ray analysis.

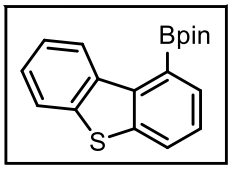

^{1}H NMR (500 MHz, $CDCl_3$): δ 9.03–9.02 (m, 1H), 7.96–7.94 (m, 1H), 7.89–7.84 (m, 2H), 7.45–7.43 (m, 3H), 1.50 (s, 12H).

^{13}C{^{1}H} NMR (125 MHz, $CDCl_3$): δ 139.8, 139.7, 138.9, 136.8, 132.7, 126.5, 125.6, 125.5, 125.2, 124.0, 122.7, 122.6, 84.5, 25.1.

^{11}B NMR (160 MHz, $CDCl_3$): δ 32.1 (br. s).

HRMS (ESI): *m/z* [M+Na]$^+$ calculated for $C_{18}H_{19}BNaO_2S$: 333.1091 found: 333.1100.

Compound 3-14: Compound **3-6** (3.5 g, 16.6 mmol, 1 equiv.) and (*S*)-*tert*-butanesulfinamide (2.0 g, 16.6 mmol, 1 equiv.) were placed in a 100 mL Schlenk flask and dissolved in tetrahydrofuran (20 mL) followed by the addition of $Ti(OEt)_4$ (3.8 mL, 20.1 mmol, 1.1 equiv.) and stirred overnight. The resulting orange solution was quenched with water, filtered then extracted with EtOAc (2 × 100mL). The combined organic layers were dried over Na_2SO_4 and concentrated. The crude orange oil was purified with column chromatography (60% EtOAc/hexanes) to yield compound **3-7** as a yellow solid (2.1 g, 6.65 mmol, 40% yield). Attempts to acquire an optical rotation for this compound were unsuccessful, as has been common in our experience for yellow-coloured compounds.

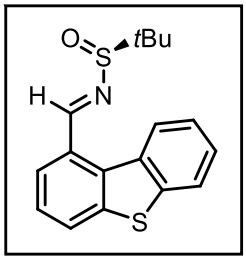

^{1}H NMR (500 MHz, $CDCl_3$): δ 9.75 (s, 1H), 8.41–8.39 (m, 1H), 8.05 (ap. d, J = 7.6 Hz, 1H), 8.00 (ap. d, J = 7.8 Hz, 1H), 7.92–7.90 (m, 1H), 7.55–7.50 (m, 3H), 1.35 (s, 9H).

$^{13}C\{^1H\}$ NMR (125 MHz, $CDCl_3$): δ 161.6, 140.7, 140.2, 134.8, 134.5, 131.7, 127.2, 126.3, 126.2, 126.1, 125.4, 123.2, 58.2, 22.8.

HRMS(ESI): *m/z* $[M+Na]^+$ calculated for $C_{17}H_{17}NNaOS_2$: 338.0644 found: 338.0652.

Compound 3-16a: Compound **3-14** (500 mg, 1.58 mmol, 1 equiv.) was placed in 250 mL flask and dissolved in 15 mL of toluene and cooled to −78 °C followed by the addition of ethyl magnesium bromide in diethyl ether (1.6 mL, 3.0 M, 4.75 mmol, 3 equiv.) that stirred overnight. The resulting solution was poured into an Erlenmeyer flask containing $NH_4Cl_{(aq)}$ and extracted with ether (2 × 50 mL). The organic layers were combined and dried over Na_2SO_4 then concentrated. The crude yellow solid (81:19 *d.r.*) was purified with column chromatography (40% EtOAc/hexanes) resulting in compound **3-16a** as a white powder (300 mg, 0.87 mmol, 55% yield). The minor diastereomer was not obtained as a pure substance. Attempts to acquire an optical rotation for this compound were unsuccessful, potentially due to low intrinsic rotation at the sodium D line. A crystal suitable for X-ray analysis was grown by evaporation of a $CDCl_3$ solution over 4 months during the COVID pandemic, which was used to establish the relative configuration, and confirmed the absolute configuration.

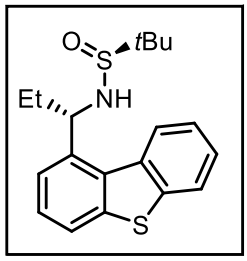

^1H NMR (500 MHz, $CDCl_3$): δ 8.39 (ap. d, *J* = 6.7 Hz, 1H), 7.88 (ap. d, *J* = 7.3 Hz, 1H), 7.81 (ap. d, *J* = 7.9 Hz, 1H), 7.60 (ap. d, *J* = 6.8 Hz, 1H), 7.49–7.45 (m, 3H), 5.60 (br. s, 1H), 3.76 (ap. d, *J* = 3.4 Hz, 1H), 2.25–2.22 (m, 1H), 2.14–2.11 (m, 1H), 1.23 (s, 9H), 0.96 (ap. t, *J* = 6.6 Hz, 3H).

$^{13}C\{^1H\}$ NMR (125 MHz, $CDCl_3$): δ 140.5, 139.9, 139.5, 135.1, 132.7, 126.3, 126.2, 125.8, 124.8, 123.1, 122.3, 56.1, 55.2, 28.3, 22.8, 9.6.

HRMS(ESI): *m/z* $[M+Na]^+$ calculated for $C_{18}H_{21}ONNaS_2$: 354.0957 found: 354.0951.

(*S*)-(–)-1-amino-1-(1-dibenzothienyl)propane 3-17: In 20 mL of dichloromethane was dissolved 1.30 g of major diastereomer **3-16a** (3.76 mmol, 1 equiv.). To the solution was added 7.5 mL of 2 M HCl in diethyl ether (15 mmol, 4 equiv.). A white solid formed within 1 minute. The suspension was stirred for 2 hours, then 40 mL diethyl ether was added. The reaction was filtered, and the white precipitate was collected, washed with diethyl ether, and then suspended in 50 mL of dichloromethane in a separatory funnel. The dichloromethane suspension was treated with 2 M aqueous NaOH and shaken until both layers were clear. The organic layer was dried over Na_2SO_4 and concentrated in vacuo to give 875 mg of amine **3-17** as an off-yellow solid (3.62 mmol, 97% yield). The configuration of this compound was known because the absolute and relative configuration of precursor **3-14** was known. Furthermore, the negative sign of the optical rotation obtained for this

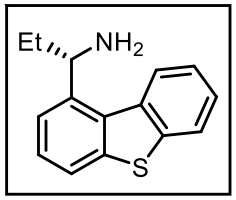

compound is consistent with other (*S*) configured aryl-alkylamines which also have negative optical rotations.

^{1}H NMR (500 MHz, $CDCl_3$): δ 8.34 (ap. d, *J* = 7.6 Hz, 1H), 7.90–7.89 (m, 1H), 7.77 (ap. d, *J* = 7.9 Hz, 1H), 7.65 (ap. d, *J* = 7.4 Hz, 1H), 7.50–7.44 (m, 3H), 5.02–5.00 (m, 1H), 2.12–2.07 (m, 1H), 1.85–1.75 (m, 1H) 1.69 (br. s, 2H), 1.13 (t, *J* = 7.4 Hz, 3H).

^{13}C{^{1}H} NMR (125 MHz, $CDCl_3$): δ 144.2, 140.3, 140.0, 135.5, 132.5, 126.5, 126.0, 125.6, 124.6, 123.1, 121.4, 121.3, 53.1, 30.7, 11.1.

HRMS(ESI): *m/z* $[M+H]^+$ calculated for $C_{15}H_{16}NS$: 242.0998 found: 242.0990.

Optical Rotation: $[\alpha]^{21}_D = -34°$ (c = 1.38, CH_2Cl_2).

Diimine 3-18: In 20 mL of dichloromethane was dissolved 0.89 g of amine **3-17** (3.63 mmol, 2 equiv.). To the solution was added, in order, 1.0 g of sodium sulfate (7.25 mmol, 4 equiv.), 0.21 mL of glyoxal (1.81 mmol, 1 equiv.) followed by 1 drop of formic acid. The suspension was stirred for 3 hours. The reaction was filtered, washed with excess dichloromethane (50 mL) and concentrated. An orange solid was recovered and used without further purification or characterization.

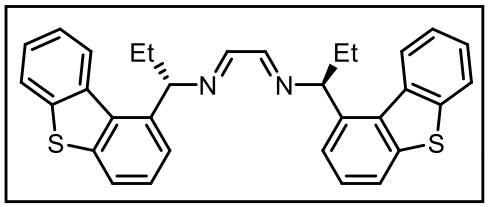

^{1}H NMR (500 MHz, $CDCl_3$): δ 8.20 (s, 2H), 7.91–7.89 (m, 2H), 7.76 (ap. dd, *J* = 7.9, 1.1 Hz, 2H), 7.69 (ap. d, *J* = 7.4 Hz, 2H), 7.50–7.45 (m, 4H), 7.40 (t, *J* = 7.7 Hz, 2H), 5.37 (br. s, 2H), 2.22–2.19 (m, 2H), 2.11–2.05 (m, 2H), 1.06 (t, *J* = 7.4 Hz, 3H).

^{13}C{^{1}H} NMR (125 MHz, $CDCl_3$): δ 161.8, 141.0, 140.4, 140.0, 135.3, 132.0, 126.4, 126.1, 125.4, 124.5, 123.4, 123.2, 121.7, 72.3 (br), 30.1, 11.4.

HRMS(ESI): calculated $(M+Na)^+$ $[C_{32}H_{28}NNaS_2]$: 527.1586; found: 527.1600.

3.5.3 General Considerations for N-Phenylphenothiazine and Derivatives

Reactions were run under nitrogen, using oven-dried glassware unless otherwise specified. ^{1}H, ^{13}C, and ^{19}F NMR data were collected at 300K on a Bruker AV-500 NMR spectrometer. NMR spectra were reported in DMSO. While the aryl phenothiazine products were highly soluble in chloroform, in some cases the proton and especially carbon spectra yielded extreme line broadening in $CDCl_3$, while the spectra in DMSO were well-defined. ^{1}H NMR spectra are referenced to trace DMSO-*d5* solvent (DMSO = 2.50 ppm). ^{13}C NMR spectra are referenced to the central DMSO peak (39.5 ppm). Mass spectrometric data were acquired by Mr. Xiao Feng (Mass Spectrometry Laboratory, Dalhousie University).

Solvents

Tetrahydrofuran was purchased from Aldrich in a Sure/seal® bottle (anhydrous, >99.9%, inhibitor free, catalogue number 401757). Tetrahydrofuran was used directly from this bottle for Grignard reactions and lithiations.

Reagents

4,5-Dibromo-o-xylene and **1,2-dibromo-4,5-difluorobenzene** were purchased from CombiBlocks and used as received.

Isopropylmagnesium Chloride was purchased from Aldrich as a 2.0 M solution in tetrahydrofuran in a Sure-Sealed Container, and the concentration was verified by titration against 1-butanol in tetrahydrofuran with 1,10 phenanthroline as the indicator before use.

***N*-methoxy-*N*-methytrifluoroacetamide**, **1,2-dibromobenzene** and **1-bromo-2-fluorobenzene** were purchased from Oakwood Chemical and used as received.

Phenothiazine was purchased from both Oakwood and Fisher Scientific and used as received.

Substituted Phenothiazines were purchased from Aldrich (**3-20b**), Oakwood (**3-20c**), and Combi-Blocks (**3-20d** to **3-20g**) and used as received.

3.5.4 Experimental Procedures and Tabulated Data for N-Phenylphenothiazine and Derivatives

General procedure: The appropriate phenothiazine derivative (1 equiv.) and magnesium turnings (1 equiv.) were placed in a dry 100 mL three neck round bottom flask equipped with a magnetic stir bar and condenser under a nitrogen atmosphere. Tetrahydrofuran was added which form a 1.0 M solution of the phenothiazine, followed by the addition of 2.0 M isopropylmagnesium chloride (1 equiv.), which resulted in heating of the reaction to reflux. After bubbling subsided, the reaction was placed in an oil bath at 70 °C. When reflux resumed, 1-bromo-2-fluorobenzene (1 equiv.) was cautiously added in 0.1 mL portions with 4 minutes between each portion. The reaction was heated for a further hour, at which time negligible magnesium remained. The reaction was removed from heat, allowed to cool to ambient temperature, then poured into an Erlenmeyer flask containing saturated ammonium chloride solution. The mixture was extracted with two appropriate portions of ethyl acetate, and the combined organic layers were dried over Na_2SO_4, and concentrated. The resulting crude sample was purified via column chromatography with the appropriate eluent system specified for each product.

Compound 3-21a: Prepared according to the general procedure on a 3.0 g scale of phenothiazine **3-20a**. Purification by flash chromatography (100% hexanes) provided **3-21a** (1.2 g, 29% yield) as a white solid.

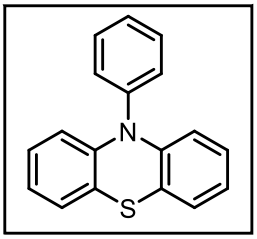

^{1}H (500 MHz, DMSO-d$_6$): δ 7.66 (t, *J* = 7.8 Hz, 2H), 7.53 (ap. t, *J* = 7.5 Hz, 1H), 7.41 (ap. d, *J* = 8.1 Hz, 2H), 7.07 (dd, *J* = 7.5, 1.6 Hz, 2H), 6.92 (ap. t, *J* = 8.3 Hz, 2H), 6.85 (td, *J* = 7.4, 1.2 Hz, 2H), 6.16 (ap. d, *J* = 8.2 Hz, 2H).

^{13}C{^{1}H} (125 MHz, DMSO-d$_6$): δ 143.5, 140.3, 131.0, 130.2, 128.3, 127.2, 126.6, 122.7, 119.4, 116.0.

HRMS (ESI): calculated for $C_{18}H_{13}NS$ [$M^{\cdot+}$] 275.0763 found: 275.0761.

SCALE UP of 3-21a: 15.0 g of phenothiazine **3-20a** (75.3 mmol, 1 equiv.) followed by 1.83 g of Mg^0 turnings (75.3 mmol, 1 equiv.) was placed in a dry 250 mL three neck round bottom flask equipped with a magnetic stir bar and a dry condenser that was placed under a nitrogen atmosphere. Dry tetrahydrofuran (75 mL) was added which dissolved the phenothiazine and suspended the Mg^0 turnings. A 2 M solution of isopropylmagnesium chloride (37.6 mL, 75.3 mmol, 1 equiv.) was cautiously added. Once the bubbling subsided, the reaction flask was placed in an oil bath of 70 °C and when reflux resumed 8.2 mL of 1-bromo-2-fluorobenzene (75.3 mmol, 1 equiv.) was added in approximately 2 mL portions every 4–6 minutes until the entire liquid was dispensed. The reaction stirred at reflux for 18 hours. The deep dark red solution was cooled to room temperature then slowly poured into an Erlenmeyer flask containing 100 mL of sat. $NH_4Cl_{(aq)}$ which created an extremely exothermic reaction and produced two layers. One cloudy aqueous layer and one clear bright orange organic layer. The organic layer was extracted three times with an appropriate amount of ethyl acetate. The organic layers were combined, dried over Na_2SO_4 then filtered and concentrated to produce a crude yellow solid. This crude product was purified via column chromatography (100% hexanes) to obtain **3-21a** as an off-white powder in 37% yield (7.6 g).

^{1}H (500 MHz, DMSO-d$_6$): δ 7.67 (t, *J* = 7.7 Hz, 2H), 7.54 (ap. t, *J* = 7.5 Hz, 1H), 7.41 (ap. d, *J* = 8.2 Hz, 2H), 7.07 (dd, *J* = 7.5, 1.5 Hz, 2H), 6.93 (ap. t, *J* = 8.0 Hz, 2H), 6.85 (td, *J* = 7.4, 1.2 Hz, 2H), 6.17 (ap. d, *J* = 8.2 Hz, 2H).

^{13}C{^{1}H} (125 MHz, DMSO-d$_6$): δ 143.6, 140.3, 131.0, 130.2, 128.3, 127.2, 126.6, 122.7, 119.4, 116.0.

Figure S3-1: Image of 7.6 gram batch of 3-21a:

Deuterium Quench: Prepared according to the general procedure on a 1.0 g scale of phenothiazine with one modification. Once the reaction cooled, a vial of methanol-d_4 was added to the mixture and allowed to stir for one hour remaining under $N_{2(g)}$ atmosphere. After one hour the reaction was worked up as stated in the general procedure. Purification by flash chromatography (100% hexanes) provided **3-21a**-*d* (40 mg, 29% yield) as a white solid.

^{1}H (500 MHz, DMSO-d_6): δ 7.67−7.65 (m, 2H), 7.53 (ap. t, *J* = 7.4 Hz, 1H), 7.41 (ap. d, *J* = 7.9 Hz, 1H), 7.07 (ap. dd, *J* = 7.5, 1.5 Hz, 2H), 6.92 (ap. t, *J* = 8.5 Hz, 2H), 6.85 (ap. td, *J* = 7.4, 1.0 Hz, 2H), 6.16 (ap. d, *J* = 8.2 Hz, 2H).

^{2}H (77 MHz, DMSO): δ 7.39 (br. s).

^{13}C{^{1}H} (125 MHz, DMSO-d_6): δ 143.6, 140.3, 140.3, 131.0, 130.9, 130.2, 130.2, 128.3, 127.2, 126.6, 122.7, 119.4, 116.1.

HRMS (ESI): calculated for $C_{18}H_{13}NNaDS$ $[M+Na]^+$ 299.0724 found: 299.0732.

Compound 3-21b: Prepared according to the general procedure on a 3.0 g scale of 2-chlorophenothiazine **3-20b**. Purification by flash chromatography (100% hexanes then 2% EtOAc/hexanes) provided **3-21b** (92 mg, 23% yield) as a beige solid.

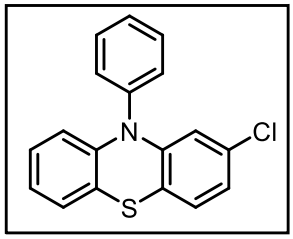

^{1}H (500 MHz, DMSO-d_6): δ 7.70 (t, *J* = 7.7 Hz, 2H), 7.59 (ap. t, *J* = 7.4 Hz, 1H), 7.45 (d, *J* = 8.1 Hz, 2H), 7.09−7.06 (m, 2H), 6.94−6.86 (m, 3H), 6.11 (ap. d, *J* = 8.1 Hz, 1H), 6.01 (ap. d, *J* = 2.1 Hz, 1H).

^{13}C{^{1}H} (125 MHz, DMSO-d_6): δ 144.9, 142.8, 139.6, 131.6, 131.3, 130.4, 129.0, 127.8, 127.4, 126.6, 123.1, 122.1, 118.6, 118.1, 116.0, 115.1.

HRMS (ESI): calculated for $C_{18}H_{12}ClNS$ [$M^{\cdot+}$] 309.0373 found: 309.0376.

Compound 3-21c: Prepared according to the general procedure on a 1.0 g scale of the 2-(trifluoromethyl)phenothiazine **3-20c**. Purification by flash chromatography (2% EtOAc/hexanes) provided **3-21c** (41 mg, 32% yield) as a brown solid.

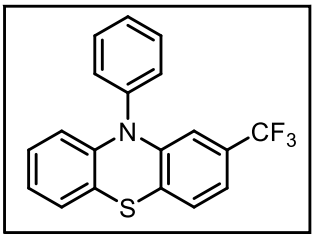

^{1}H (500 MHz, DMSO-d$_6$): δ 7.72 (t, *J* = 7.7 Hz, 2H), 7.60 (ap. t, *J* = 7.3 Hz, 1H), 7.48 (d, *J* = 7.9 Hz, 2H), 7.26 (d, *J* = 8.0 Hz, 1H), 7.15 (d, *J* = 8.0 Hz, 1H), 7.07 (dd, *J* = 7.5, 1.5 Hz, 1H), 6.94 (ap. td, *J* = 7.3, 1.6 Hz, 1H), 6.88 (ap. td, *J* = 7.4, 1.1 Hz, 1H), 6.20 (s, 1H), 6.10 (ap. d, *J* = 8.2 Hz, 1H).

^{13}C{^{1}H} (125 MHz, DMSO-d$_6$): δ 144.1, 142.6, 139.4, 131.4, 130.5, 129.1, 127.7, 127.6 (q, $J_{C\text{-}F}$ = 32 Hz), 127.3, 126.7, 124.6, 123.7 (q, $^1J_{C\text{-}F}$ = 272.2 Hz), 119.0 (d, $J_{C\text{-}F}$ = 3.5 Hz), 117.8, 116.0, 110.9 (d, $J_{C\text{-}F}$ = 3.9 Hz).

^{19}F (470 MHz, DMSO-d$_6$): δ −61.8.

HRMS (ESI): calculated for $C_{19}H_{12}F_3NS$ [$M^{\cdot+}$] 343.0637 found: 343.0643.

Compound 3-21d: Prepared according to the general procedure on a 1.0 g scale of the 2-methoxyphenothiazine **3-20d**. Purification by flash chromatography (100% hexanes then 2% EtOAc/hexanes) provided **3-21d** (36 mg, 27% yield) as a yellow oil.

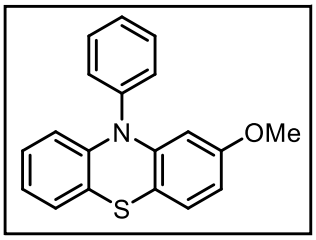

^{1}H (500 MHz, DMSO-d$_6$): δ 7.67 (t, *J* = 8.0 Hz, 2H), 7.55 (ap. t, *J* = 7.5 Hz, 1H), 7.41 (ap. d, *J* = 7.2 Hz, 2H), 7.07 (ap. dd, *J* = 7.5, 1.6 Hz, 1H), 6.99 (d, *J* = 8.4 Hz, 1H), 6.92 (ap. td, *J* = 8.2, 1.6 Hz, 1H), 6.85 (td, *J* = 7.4, 1.2 Hz, 1H), 6.50 (dd, *J* = 8.4, 2.5 Hz, 1H), 6.16 (dd, *J* = 8.2, 1.1 Hz, 1H), 5.69 (d, *J* = 2.6 Hz, 1H), 3.54 (s, 3H).

^{13}C{^{1}H} (125 MHz, DMSO-d$_6$): δ 158.8, 144.8, 143.3, 140.3, 131.0, 130.2, 128.5, 127.2, 127.0, 126.6, 122.7, 119.9, 116.0, 110.1, 106.9, 103.9, 55.0.

HRMS (ESI): calculated for $C_{19}H_{15}NOS$ [$M^{\cdot+}$] 305.0869 found: 305.0867.

Compound 3-21f: Prepared according to the general procedure on 1.0 g scale of the 2-methylthiophenothiazine **3-20f**. Purification by flash chromatography (2% EtOAc/hexanes then 5% EtOAc/hexanes) provided **3-21f** (50 mg, 40% yield) as a yellow powder.

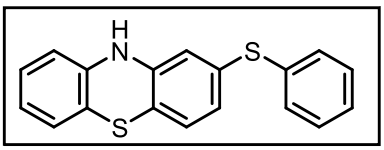

^{1}H (500 MHz, DMSO-d$_6$): δ 8.63 (s, 1H), 7.40−7.31 (m, 5H), 6.98 (ap. t, *J* = 7.6 Hz, 1H), 6.91 (d, *J* = 7.8 Hz, 2H), 6.78−6.72 (m, 2H), 8.63−6.62 (m, 2H).

^{13}C{^{1}H} (125 MHz, DMSO-d$_6$): δ 142.9, 141.4, 134.7, 133.7, 130.5, 129.5, 127.6, 127.3, 126.9, 126.2, 124.0, 122.0, 116.1, 116.0, 116.0, 114.5.

HRMS (ESI): calculated for $C_{18}H_{13}NS_2$ [M$^{\cdot+}$] 307.0484 found: 307.0483.

3.5.5 General Considerations for the Synthesis of Naphthothiophene Derivatives

Reactions were run under nitrogen using oven-dried glassware, unless otherwise specified. ^{1}H, ^{13}C, and ^{11}B NMR data were collected at 300 K on a Bruker AV-500 NMR spectrometer. ^{1}H NMR spectra are referenced to residual non-deuterated NMR solvent ($CHCl_3$: 7.26 ppm). ^{13}C NMR spectra are referenced to the central $CDCl_3$ peak (77.16 ppm). Mass spectrometric data were acquired by Mr. Xiao Feng (Mass Spectrometry Laboratory, Dalhousie University). Optical rotations were obtained on an Anton Paar MCP 150 Modular Compact Polarimeter. Concentrations are given in g/100 mL for polarimetry measurements, and were measured in dichloromethane. Chemicals were obtained as the best grades available from Aldrich or Oakwood, and otherwise used as received.

3.5.6 Experimental and Tabulated Data for Naphthothiophene Derivatives

Ellman Imine 3-32: Propanal (4.15 mL, 61.9 mmol, 1.5 equiv) was added to a stirring mixture of (*S*)-*tert*-butanesulfinamide (5.00 g, 41.2 mmol, 1 equiv), pyridinium *p*-toluenesulfonate (0.52 g, 2.1 mmol, 0.05 equiv), and anhydrous $MgSO_4$ (24.8 g, 206 mmol, 5 equiv) in anhydrous CH_2Cl_2 (50 mL). The mixture was stirred under a static nitrogen atmosphere for 18 h, and was worked up via filtration through Celite and rotary evaporation. The product was briefly stirred under a 5 torr vacuum for 1 h to remove excess aldehyde. Product **3-32** was obtained as a yellow oil (5.76 g, 35.7 mmol, 87% yield). This was used without further purification, as the product is somewhat volatile. Attention during exposure to vacuum to avoid undue material loss should be taken. Small amounts of CH_2Cl_2 were noted but did not prove detrimental to the next reaction. Spectral data were in accordance with literature values.[29]

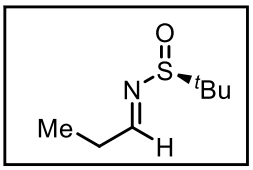

^{1}H NMR (500 MHz, CDCl$_3$): δ 8.10 (t, *J* = 4.3 Hz, 1H), 2.58–2.50 (m, 2H), 1.20–1.18 (m, 12H).

^{13}C{^{1}H} NMR (125 MHz, CDCl$_3$): δ 170.2, 56.3, 29.4, 22.2, 9.5.

$[\alpha]_D^{25}$ +277 (*c* 1.0, CH_2Cl_2); as determined on the unpurified product obtained above.

Sulfinamides 3-33a and 3-33b: In a recovery flask, 3-bromonaphthothiophene (**3-31**; 1.00 g, 3.80 mmol, 1 equiv) was dissolved in THF (5 mL). Separately THF (7 mL) was placed in a Schlenk flask and cooled to –84 °C (liquid nitrogen/EtOAc). *N*BuLi (1.98 mL, 2.5 M in hexanes, 4.94 mmol, 1.3 equiv) was added to the Schlenk flask, and the solution was allowed to stir at –84 °C for another 10 min. The solution of **3-31** was added over 1 min, running the solution down the inside of the flask to facilitate precooling, with further THF (2 mL) used to quantitate the transfer. The solution became inky blue in colour. The reaction was stirred at –84 °C for 5 min, then a solution of imine **3-32** (0.88 g, 5.5 mmol, 1.4 equiv) in THF (3 mL) was added. The resulting clear orange reaction mixture was stirred for 2 h, then allowed to warm to room temperature. The mixture was then quenched with $NH_4Cl_{(aq)}$ (10 mL). The reaction was extracted with Et_2O. The combined organic layers were dried over Na_2SO_4, and concentrated. The resulting residue was purified by flash chromatography (40% EtOAc/hexanes moving to 50% EtOAc/hexanes when the first diastereomer eluted). The less polar diastereomer **3-33a** was the major one. Compound **3-33a** was obtained as a yellow tacky solid (631 mg, 1.83 mmol, 48% yield). Minor diastereomer **3-33b** was obtained as a colourless tacky solid (263 mg, 0.761 mmol, 20% yield). X-ray quality crystals of both diastereomers were obtained by slow evaporation of Et_2O solutions of the products.

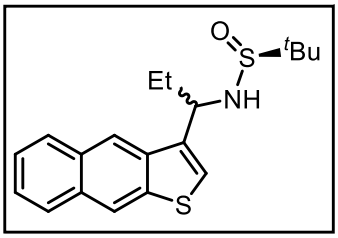

Major Diastereomer 3-33a

$[\alpha]_D^{25}$ +86.8 (*c* 1.0, CH_2Cl_2).

R_f = 0.15 (50% EtOAc/hexanes); R_f = 0.50 (80% EtOAc/hexanes).

^{1}H NMR (500 MHz, $CDCl_3$): δ 8.43 (s, 1H), 8.35 (s, 1H), 8.02–7.96 (m, 1H), 7.92–7.87 (m, 1H), 7.51–7.43 (m, 3H), 4.90–4.83 (m, 1 H), 3.64 (br. s, 1H), 2.25–2.12 (m, 2H), 1.24 (s, 9H), 0.94 (ap. t, *J* = 7.4 Hz, 3H).

^{13}C{^{1}H} NMR (125 MHz, $CDCl_3$): δ 139.2, 136.7, 136.0, 131.1, 130.7, 128.7, 127.2, 125.8, 125.7, 125.2, 121.3, 120.9, 55.9, 55.0, 27.9, 22.7, 10.4.

HRMS (ESI): m/z $[M+Na]^+$ calculated for $C_{19}H_{23}NOS_2$: 368.1113 found: 368.1104.

Minor Diastereomer 3-33b

$[\alpha]_D^{25}$ +58.5 (*c* 1.0, CH_2Cl_2).

R_f = 0.10 (50% EtOAc/hexanes); R_f = 0.40 (80% EtOAc/hexanes).

^{1}H NMR (500 MHz, $CDCl_3$): δ 8.38 (s, 1H), 8.35 (s, 1H), 7.98–7.87 (m, 2H), 7.49–7.44 (m, 2H), 7.43 (s, 1H), 4.83 (ap. t, *J* = 7.0 Hz, 1H), 3.53 (br. s, 1H), 2.30–2.14 (m, 1H), 2.14–2.09 (m, 1H), 1.17 (s, 9H), 0.96 (t, *J* = 7.6 Hz, 3H).

$^{13}C\{^1H\}$ NMR (125 MHz, $CDCl_3$): δ 139.5, 136.7, 135.6, 131.1, 130.6, 128.6, 127.3, 126.4, 125.6, 125.2, 121.4, 121.3, 56.6, 55.8, 29.7, 22.8, 10.9.

HRMS (ESI): m/z $[M+Na]^+$ calculated for $C_{19}H_{23}NNaOS_2$: 368.1113 found: 368.1113.

Chiral Amine 3-34: In a 30-mL round-bottom flask, compound **3-33a** (500 mg, 1.45 mmol, 1 equiv) was dissolved in Et_2O/CH_2Cl_2 (1:1, 10 mL). To the mixture was added 2 M HCl in Et_2O (2.89 mL, 5.8 mmol, 4 equiv). The resulting tan suspension was stirred for 12 h. The product was collected by filtration, and washed with additional Et_2O. The HCl salt, **3-34•HCl**, was collected as a beige solid (362 mg, 1.30 mmol, 90% yield). Due to low solubility, the HCl salt was characterized as the free base. A portion was suspended in CH_2Cl_2, and washed with 1 M $NaOH_{(aq)}$. The organic layer was dried over Na_2SO_4, and concentrated to give the free base as a beige oil. NMR, MS, and optical rotation were acquired on this sample. The negative optical rotation is consistent with (*S*)-configured arylalkylamines.

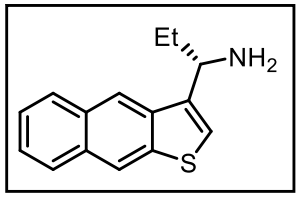

^1H NMR (500 MHz, $CDCl_3$): δ 8.36 (s, 1H), 8.34 (s, 1H), 8.00–7.98 (m, 1H), 7.91–7.90 (m, 1H), 7.49–7.45 (m, 2H), 7.38 (s, 1H), 4.42 (ap. t, J = 6.6 Hz, 1H), 2.10–2.02 (m, 1H), 1.91–1.82 (m, 1H), 1.81 (br. s, 2H), 1.03 (ap. t, J = 7.4 Hz, 3H).

$^{13}C\{^1H\}$ NMR (125 MHz, $CDCl_3$): δ 139.6, 137.5, 131.1, 130.7, 128.6, 127.3, 125.5, 125.1, 122.9, 121.2, 120.4, 52.3, 30.8, 11.0.

HRMS (ESI): m/z $[M+Na]^+$ calculated for $C_{15}H_{15}NNaS$: 264.0817 found: 264.0822.

$[\alpha]_D^{25}$ –21.7 (*c* 1.0, CH_2Cl_2).

Diimine 3-35: In 10 mL of toluene, 0.36 g of **3-34•HCl** (1.31 mmol, 2 equiv.) was dissolved. Then the following reagents were added, in order, 0.07 mL of glyoxal (0.65 mmol, 1 equiv.), 1.3 g of sodium sulfate (2.61 mmol, 4 equiv.), and 0.18 mL of triethylamine (1.31 mmol, 2 equiv.). The reaction stirred for 2 h then the sodium sulfate was filtered and washed with excess toluene (20 mL). The filtrate was concentrated resulting in diimine **3-35** as an orange powder (0.31 g, 97% yield).

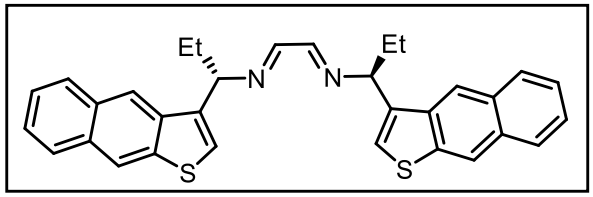

^1H NMR (500 MHz, $CDCl_3$): δ 8.32 (s, 4H), 8.18 (s, 2H), 7.96–7.94 (m, 2H), 7.88–7.86 (m, 2H), 7.47–7.43 (m, 4H), 7.42 (s, 2H), 4.77–4.75 (m, 2H), 2.27–2.18 (m, 2H), 2.17–2.10 (m, 2H), 1.01 (t, J = 7.6 Hz, 3 H).

$^{13}C\{^{1}H\}$ NMR (125 MHz, $CDCl_3$): δ 161.7, 139.3, 137.0, 136.8, 131.1, 130.7, 128.6, 127.3, 125.5, 125.1, 124.7, 121.2, 120.6, 71.4, 29.7, 11.4.

HRMS (ESI): m/z $[M+Na]^+$ calculated for $C_{32}H_{28}N_2NaS_2$: 527.1586 found: 527.1586.

DAP-OTf 3-37: In a Schlenk flask, 0.27 g of DAP-Br **3-36** (0.44 mmol, 1.0 equiv.) was dissolved in 5 mL of dichloromethane followed by the addition of 0.08 mL of TMSOTf and stirred for 1 h. Then dichloromethane was removed in vacuo and the crude compound was purified with ether trituration (3 × 10 mL). Resulting in DAP-OTf **3-37** as an orange powder that was collected by filtration.

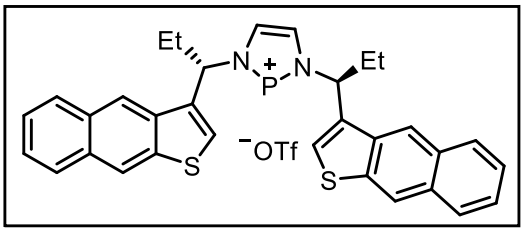

^{1}H NMR (500 MHz, $CDCl_3$): δ 8.36 (s, 2H), 8.32 (s, 2H), 8.14 (s, 2H), 7.85 (ap. d, J = 8.2 Hz, 2H), 7.79 (ap. d, J = 8.7 Hz, 2H), 7.73 (s, 2H), 7.48 (ap. t, J = 7.7 Hz, 2H), 7.37 (ap. t, J = 7.7 Hz, 2H), 5.93 (br. s, 2H), 2.44 (br. s, 4H), 0.98 (br. s, 6H).

^{31}P NMR (202 MHz, $CDCl_3$): 209.1.

Chapter 4 Substituted Backbone Diazaphospholenes

4.1 Research Overview and Contribution Report

The author wishes to clarify her contributions to the research described in Chapter 4 of this Thesis document. The work in this Chapter details the synthesis of a DAP variant **4-13** that contains a methyl substituted backbone and the enhanced enantioselectivity for acyclic and exocyclic amines. MSc student Adam Beckett obtained preliminary results for the synthesis of **4-14a** and **4-14b** that was the starting point of this work. Dr. Alex Speed synthesized the original diimines with methyl and ethyl substituents in backbone (**4-10a** and **4-10b**).

I carried out the synthesis and collected characterization data of all other compounds disclosed in this Chapter. Xiao Feng carried out mass spectroscopy analysis of all compounds. In addition, I optimized the catalytic conditions for reactions involving **4-13** to complete a substrate scope.

4.2 Introduction

Chapters 2 and 3 highlight the successes and failures of synthesizing DAP variants with alternative aryl and alkyl chains. The synthesis of alternate side chains from non-commercial amines requires multi-step synthesis with sometimes challenging purification steps to generate an enantiopure amine that then undergoes a three-step synthesis to be converted to the DAP-OTf. If the DAP-OTf is successfully generated, then it is used to catalyze the hydroboration of imines to determine the reactivity and enantioselectivity. Up to this point, no variation has competed with the DAP-OTf **1-28** that was synthesized from commercially available starting materials. Additionally, catalyst **1-28** only requires a three-step synthesis to generate the DAP-OTf with simple purification steps.

Considering this and wanting to synthesize a DAP that could compete with the current best DAP-OTf, brought me back to the generic structure of a diazaphospholene and the substituents surrounding the current best DAP-OTf (Figure 4-1). The other structural feature within the DAP scaffold that can be altered is the backbone (R^1). The goal is to synthesize a DAP with comparable ease to the current best DAP but incorporating a substituted backbone. Reflecting on the DAPs with a substituted backbone already reported, there are benzo-fused backbones but accessing the diimines of these variants already increases the complexity of the synthesis. Mono-halogenated backbones would result in a chiral phosphorus centre and increase the complexity of the DAP. Having a pair of alkyl substituent in the backbone would be ideal to explore the effect of backbone substitution but has yet to be reported for alkyl diimines.

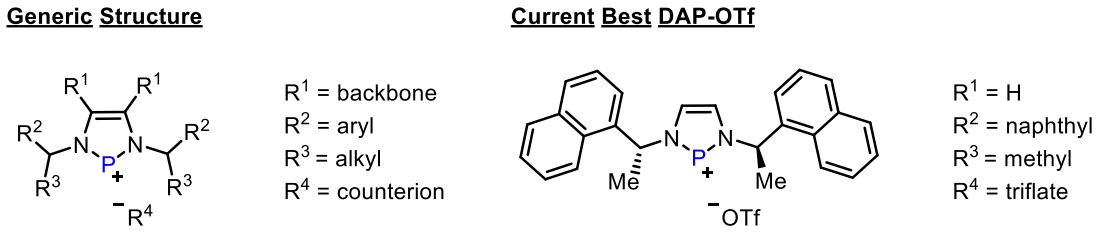

Figure 4-1. Generic structure of cationic DAP (left) and current best cationic DAP (right).

Altering the backbone substituents from protons to a more sterically demanding substituent such as a methyl or ethyl was hypothesized to increase the rigidity of the DAP by decreasing the free-rotation of exocyclic C-N bond due to allylic or $A^{1,3}$ strain (Figure 4-2). Allylic strain describes the strain between a substituent on an alkene and the substituents that are on a stereogenic centre in the allylic position, that is cis to the substituent on the alkene. When the substituent on the alkene is a proton, there will be relatively free rotation of the substituents on the stereogenic centre as the substituents will only ever eclipse a proton. As shown by structures **A**, **B**, and **C**, the only difference between

the structures is the position of the substituents around the stereogenic centre. Since a proton is the smallest substituent possible, each conformation is easily adopted as there is not much of an energy barrier to go from one conformation to another. When the substituent on the alkene is a larger R group, such as a methyl or ethyl, this will introduce steric clash for certain conformations as shown by structures **E** and **F**. One conformation minimizes the strain, as exemplified by structure **D**, where R is eclipsing an H in the stereogenic centre. As the substituents rotate around the stereogenic centre, the larger R group will eclipse bigger substituents, represented generically as R^2 and R^3 groups, as exemplified by structures **E** and **F**. This means the structure will preferentially remain in conformation **D** to minimize steric clash and it will require more energy to adopt conformation **E** or **F**. We extended this hypothesis to the DAP catalyst structure.

Applying $A^{1,3}$ strain to the diazaphospholene structure, a very similar relationship emerges, with the substituent on the backbone and the stereogenic centre in an allylic relationship. When the backbone has a proton as the substituent there will be relatively free rotation of the substituents around the stereogenic centre and multiple conformations may be adopted as they will have similar energies. When the backbone substituent is bigger, such as methyl, there will be steric clash and fewer confirmations will be adopted. This will increase the rigidity of the diazaphospholene and ideally increase the selectivity of the catalyst.

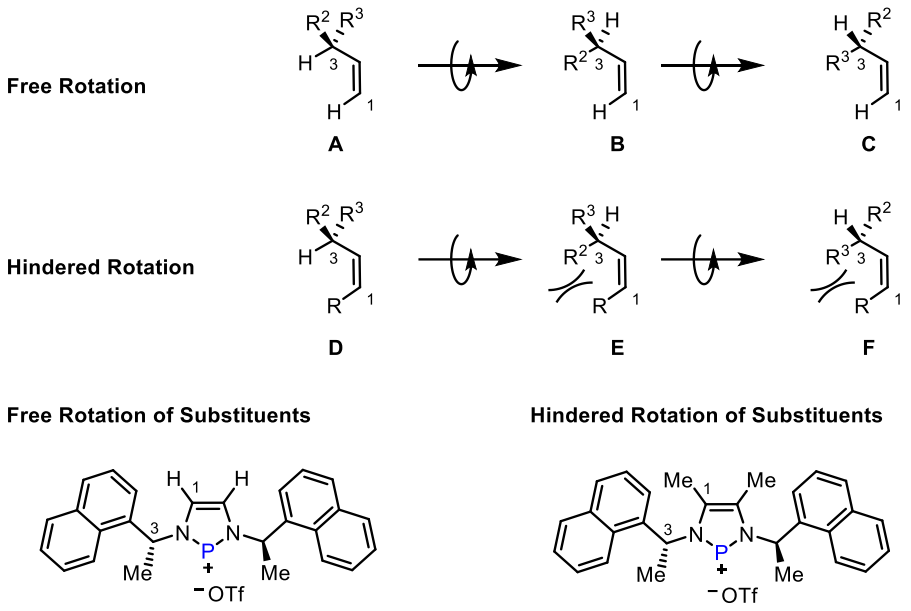

Figure 4-2. Generic A[1,3] strain (top) and applying theory to the DAP structure (bottom).

As mentioned in the introduction, the synthesis of DAPs containing an alkyl substituted backbone and alkyl side chains have not been reported, yet this is an attractive motif to explore since it may generate a more restricted, and possibly selective catalyst. It was already known that the typical methods of cyclization method with PBr_3/cyclohexene and a diimine that has enolizable protons in the backbone leads to decomposition. Specifically, applying the predominant cyclization method of PBr_3 and cyclohexene to diimine, lead to a complex mixture with some evidence of adduct **4-1**. Analysis of the proton NMR spectrum revealed the product mixture contained only one intact backbone methyl signal and the naphthylethyl groups were in different environments, which implied enamine formation of one of the imines had occurred (Scheme 4-1). This is possible by first a coordination of one nitrogen of the diimine to PBr_3, then the other nitrogen could deprotonate one of the methyls in the backbone. This decomposition was observed independently by former MSc student Matt Adams, and Dr. Alex Speed.

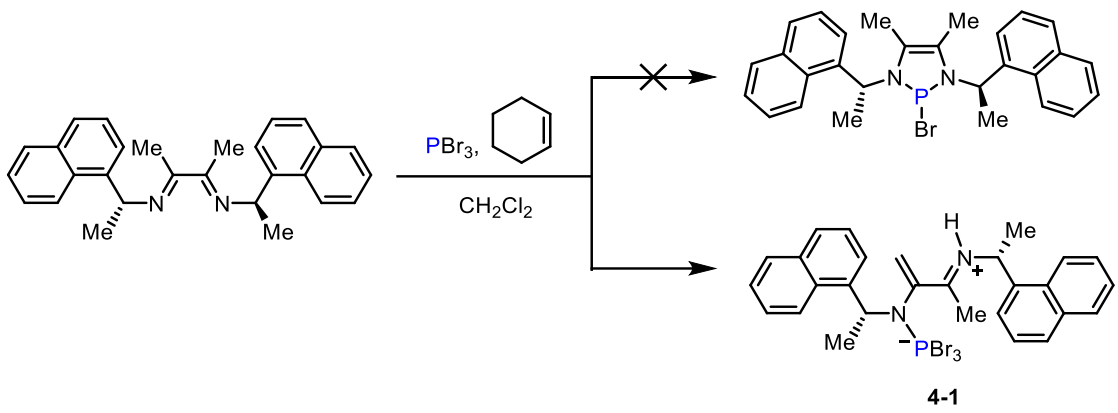

Scheme 4-1. Attempt at cyclization of diimine with methyl substituents in the backbone with PBr_3/cyclohexene.

To successfully cyclize the diimine involved investigation of alternative phosphorus reagents, namely bis(dialkylamino)chlorophosphines and dialkylaminodichlorophosphines, to introduce the phosphorus centre. These reagents cyclizing with diimines were originally reported by Mazieres and co-workers in 1987.[75] They demonstrated preliminary reactivity of these amino-phosphines with TMSOTf and $AlCl_3$ to generate the corresponding phospheniums that were further reacted with silyl cyanides and azides. In 1991 they demonstrated the bis(diethylamino)chlorophosphine **4-2a** being treated with TMSOTf to generate phosphenium **4-3a** with a triflate counterion which could cyclize with diimines **4-4a** and **4-4b** to genereate phosphoniums **4-5a** and **4-5b** (Scheme 4-2A). Furthermore, they demonstrated diisopropylaminodichlorophosphines **4-6a** being activated with $AlCl_3$ to phosphenium **4-7a** with an aluminate counterion that cyclized diimine **4-8** to generate phosphonium **4-9**.[76]

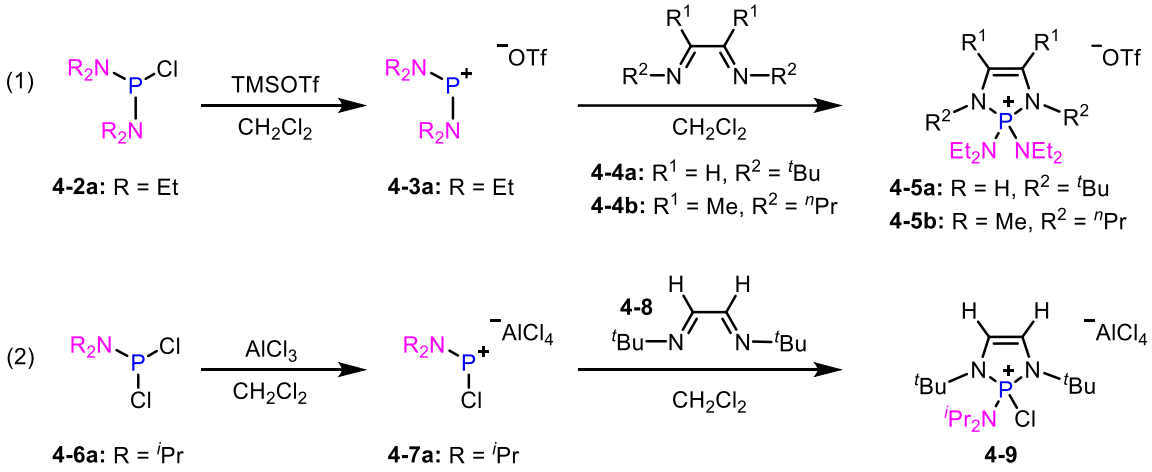

Scheme 4-2. (A) Synthesis of phosphoniums **4-5a** and **4-5b** from bis(diethylamino)chlorophosphine with TMSOTf. (B) Synthesis of phosphonium **4-9** from diisopropylaminodichlorophosphine with $AlCl_3$.

Mazieres work inspired us to try using these phospheniums as an alternative reagent to PBr_3/cyclohexene for the cyclization of diimines with chiral side chains and a methyl substituted backbone. In this Chapter, I report the synthesis of SPO **4-13** from diisopropylaminodichlorophosphine **4-6a** (Scheme 4-3A). As Mazieres reported, the first step requires the activation of the phosphine **4-6a** to phosphenium, **4-7a** with aluminate counterion, as $AlCl_3$ was the best chloride abstractor. The phosphenium **4-7a** successfully cyclized with diimine **4-10a** to generate a phosphorus (V) phosphonium cation **4-11a**. The phosphonium was reduced to a phosphorus (III) phosphine **4-12a** with Mg dust. The phosphine was treated with water in THF to form the secondary phosphine oxide (SPO) **4-13**. This pre-catalyst was successful for the reduction of acyclic imines with low catalyst loadings and high enantioselectivites (Scheme 4-3B).

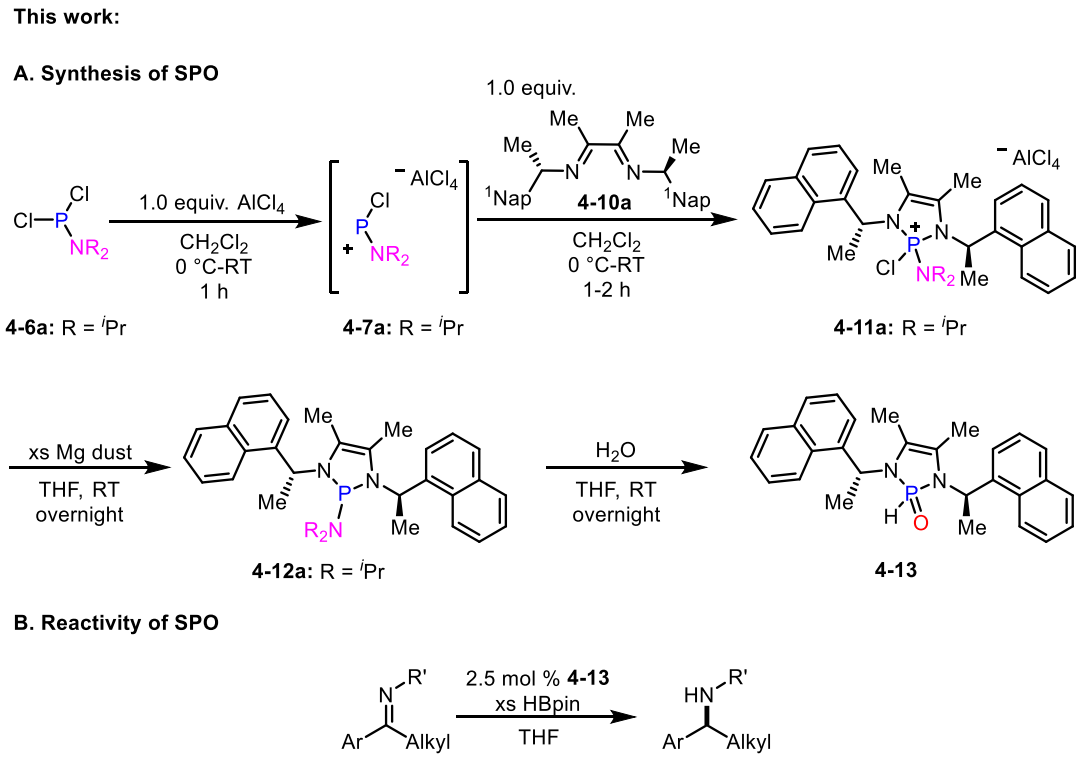

Scheme 4-3. (A) Synthesis of SPO with alkyl substituents in the backbone. (B) Reactivity of SPO with alkyl substituents in the backbone.

4.3 Results and Discussion

4.3.1 Synthesis of Substituted Backbone Diazaphospholene

Prior to the work reported in this Chapter, Adam Beckett (a previous MSc student in the Speed group) obtained preliminary results that were used as a starting point. Adam explored the use of various bis(dialkylamino)chlorophosphine reagents to cyclize the diimines with various substituted backbones. The syntheses of the diimines with a methyl and ethyl substituted backbone was previously done by Dr. Alex Speed that I later repeated. Analogous to the non-substituted backbone synthesis, the commercially available amine, (*R*)-1-(1-naphthyl)ethylamine, undergoes an acid catalyzed condensation reaction with the appropriate ketone diacetyl (in place of glyoxal), in the presence of 3 Å molecular sieves (a stronger drying reagent than Na_2SO_4) for a week to generate diimines **4-10a** and **4-10b**

(Scheme 4-4). The diimine with a methyl substituted backbone **4-10a** was the original variant Adam tested with the alternative phosphorus reagents.

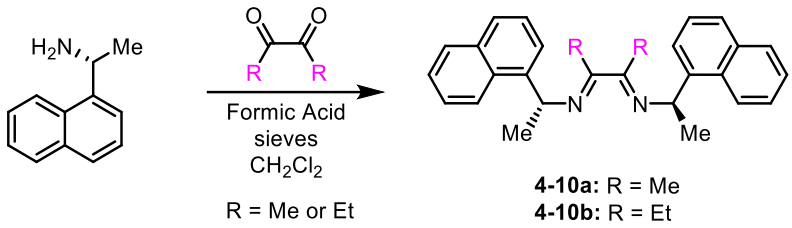

Scheme 4-4. Synthesis of diimines with alkyl substituents in the backbone.

Adam began using three variants of bis(dialkylamino)chlorophosphine ($ClP(N(R_2)_2$) **4-2a**, **4-2b**, and **4-2c**, to introduce the phosphorus centre to diimine **4-10a** (Scheme 4-5). The phosphine reagents were initially converted to the corresponding phosphenium, **4-3a** to **4-3c** with TMSOTf. The diimine **4-10a** cleanly cyclized to the phosphonium **4-14a** and **4-14b** from phospheniums **4-3a** and **4-3b**, respectively. The isopropyl phosphenium **4-3c** appeared to be too sterically demanding, and no cyclization was observed. The final key point Adam discovered was that the synthesis of phosphoniums could be done in a one-pot reaction. Starting with the bis(dialkylamino)chlorophosphine, undergoing a halide abstraction, then without isolating the phosphenium intermediate, the diimine was added to the same reaction flask which successfully generated the desired phosphonium. Followed by a simple purification lead to the successful isolation of the phosphonium.

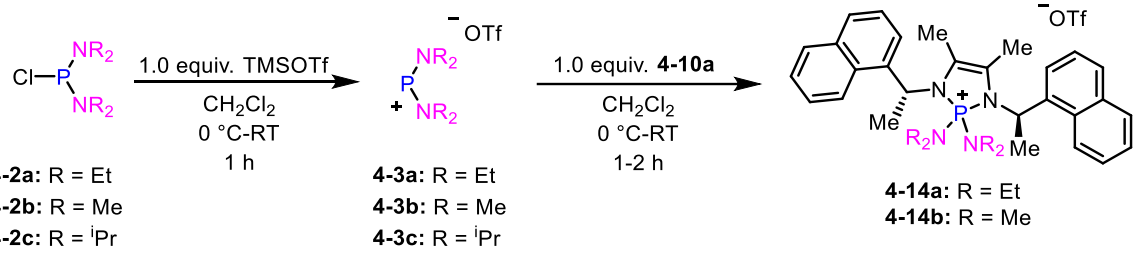

Scheme 4-5. Synthesis of phosphoniums with methyl substituted backbone.

Starting with the one-pot synthesis, I focused on the synthesis of the DAP that combined the methyl substituted backbone diimine **4-10a** and bis(diethylamino)chlorophosphine **4-2a**, as these reagents were in abundance within the laboratory already. I successfully repeated the synthesis as reported by Adam and I was able to follow up with a simple benchtop extraction purification as the phosphonium **4-14a** was found to be air and moisture stable. An aqueous extraction in a separatory funnel was sufficient to remove any impurities and not destroy the phosphonium. Unfortunately, **4-14a** proved resistant to reduction to a diazaphospholene, in the presence of HBpin, $PhSiH_3$, or Mg dust. It would not be a viable pre-catalyst without the conversion to a DAP-H.

We hypothesized a phosphonium bearing a phosphorus-halogen bond would be more susceptible to reduction. Looking at an ethyl containing phosphine again, diethylaminodichlorophosphine **4-7b** was treated with TMSOTf to abstract a chlorine creating phosphenium **4-15** *in situ*, then the solution of diimine **4-10a** was added to cyclize to the phosphonium **4-16** (Scheme 4-6). This yielded multiple products, as the halide abstraction from the starting phosphine is not favoured with TMSOTf. This is distinct from the bis(diethylamino)chlorophosphine, which undergoes complete halide abstraction. Mazieres reported glyoxal-derived diimines could undergo cyclization using equilibrating mixtures of phosphine/TMSOTf and phosphenium, but there was rapid decomposition with methyl-substituted diimine **4-10a** due to rapid independent reaction of the diacetyl-derived diimine with TMSOTf. A stronger chloride abstracter was required, to irreversibly generate the phosphenium *before* the diimine was added.

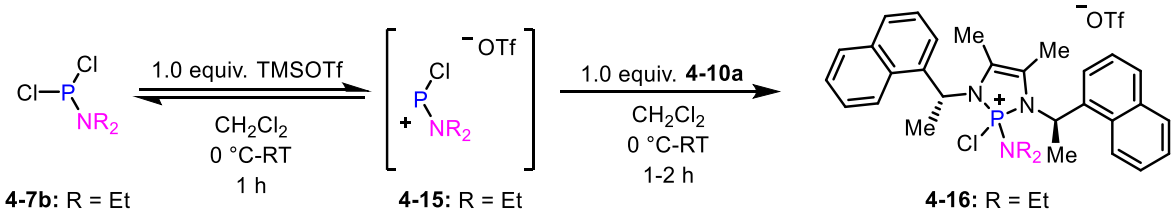

Scheme 4-6. Synthesis of phosphonium bearing a P-Cl bond to be reduced.

Reviewing Mazieres's work, they reported the generation of phospheniums with aluminum trichloride for the cyclization of a diimine with a methyl substituted backbone. Following this, I generated **4-7a** and **4-7b,** from the combination of the corresponding aminodichlorophosphines **4-6a** and **4-6b** with $AlCl_3$. Without isolation, a solution of the diimine **4-10a** was added to the reaction and underwent smooth cyclization and generated phosphoniums **4-11a** and **4-11b** (Scheme 4-7). Fortunately, **4-11a** could be reduced to phosphine **4-12a** with magnesium dust or turnings. Reduction of **4-11b** with Mg dust gave **4-12b** and a second product, hypothesized to be a P-P dimer, but formation of this compound could be suppressed by addition of LiCl to the reduction.

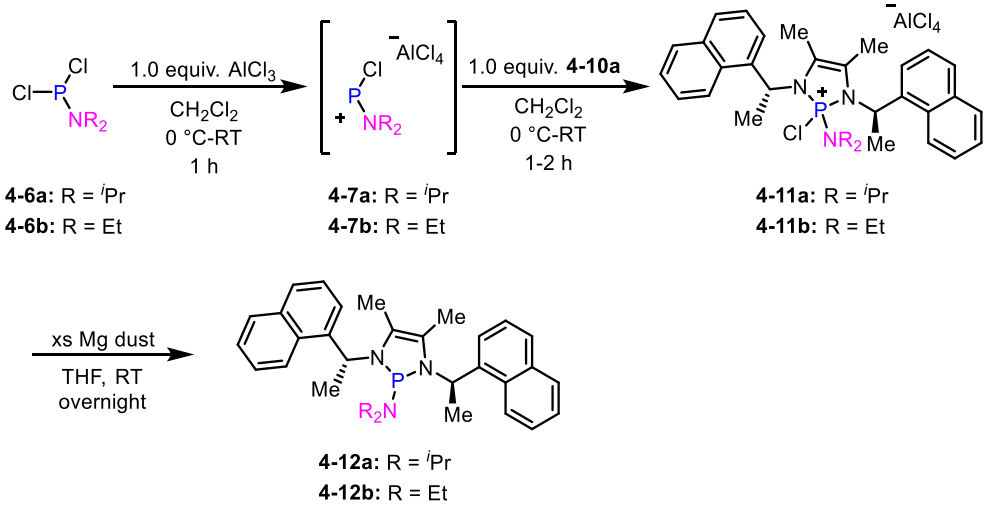

Scheme 4-7. Synthesis of phosphines with methyl substituted backbone.

The reduction of phosphoniums **4-11a** and **4-11b** required a trial-and-error process which is summarized in Table 4-1. Entries 1–5 correspond to when R = Et and entries 6–

10 correspond to when R = ^{i}Pr. As shown by reductions **4-11b**, Mg dust in either THF (Entry 1), or CH_3CN (Entry 2) resulted in two products shown in each of the ^{31}P NMR spectra, one peak at 93 ppm and one peak at 89 ppm. Replacing Mg dust with Mg turnings in THF was not fruitful and resulted in many products shown in the ^{31}P NMR spectrum (Entry 3). The addition of LiCl with Mg dust in THF resulted in one peak at 89 ppm in the ^{31}P NMR spectrum (Entry 4). Replacing Mg dust with Mn dust combined with LiCl in THF resulted in the one peak at 93 ppm in the ^{31}P NMR spectrum (Entry 5). With prior knowledge of neutral diazaphospholenes and DAP-dimers,[8][77] we determined one of these peaks must correspond to the phosphine, **4-12b**, and the other peak must correspond to the dimer. Additional testing would be required to assign each of the peaks. Fortunately, the reduction of **4-11a** resulted in only one peak at 83 ppm in the ^{31}P NMR spectrum. Regardless of reductant combination or solvent choice, Mg dust in THF (Entry 1), Mg dust in CH_3CN (Entry 2), Mg turnings in THF (Entry 3), Mg dust and LiCl in THF (Entry 4) or Mn dust in THF (Entry 5) all resulted in one product. Without additional testing, this peak could be assigned to the phosphine **4-12a**, as the value of the peak is not identical to either of the peaks found from the reduction of **4-11b**. If it was in fact the dimer, this would result in the same product as one of the products being produced from the reduction of **4-11b** and the peaks would be identical, since the exocyclic amine is absent in the dimer.

Table 4-1. Summary of phosphonium reduced to phosphine results.

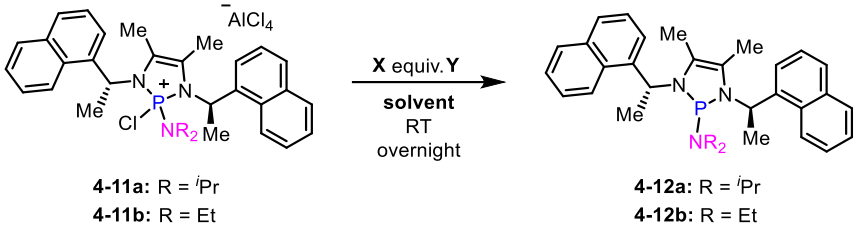

4-11a: R = ^{i}Pr
4-11b: R = Et

4-12a: R = ^{i}Pr
4-12b: R = Et

R = Et (4-11b)

Entry	**X** Equivalents	Reductant (**Y**)	Solvent	^{31}P NMR δ (ppm)
1	5	Mg dust	THF	93 & 89 (~1:1)
2	5	Mg dust	CH_3CN	93 (m) & 89 (M)
3	5	Mg turnings	THF	210, 93, 49 & 36
4	10/10	Mg dust/LiCl	THF	89
5	10/10	Mn dust/LiCl	THF	93

R = ^{i}Pr (4-11a)

Entry	**X** Equivalents	Reductant (**Y**)	Solvent	^{31}P NMR δ (ppm)
6	5	Mg dust	THF	83
7	5	Mg dust	CH_3CN	83
8	10	Mg turnings	THF	83
9	10/10	Mg dust/LiCl	THF	83
10	10/10	Mn dust	THF	83

Contemporaneously, phosphoniums derived from the cyclizations of a diimine bearing ethyl substituents in the backbone **4-10b** and diimines containing alternative side chains, **4-17** and **4-18** derived from commercially available enantiopure amines were being investigated (Scheme 4-8). Diimine **4-10b** was cyclized with phosphenium **4-7b** which generated phosphonium **4-19** with a complex mixture of products (Scheme 4-8A). Despite efforts to purify the phosphonium, there was no success. Unpurified **4-19** was carried forward with the possibility of being able to purify the following product to obtain a clean DAP. The phosphonium **4-19** was treated with Mg dust in an attempt to generate the

corresponding phosphine. However, the only isolable compound from the reaction was the starting material, diethylaminodichlorophosphine **4-6b**. No further attempts were made to optimize the synthesis of **4-19** as there was more progress with the methyl substituted backbone containing an identical side chain. It should be noted that it would be worth attempting the cyclization of diimine **4-10b** with phosphenium **4-7a** generated from diisopropylaminodichlorophosphine **4-6a**. Starting with the phosphine **4-6a** has resulted in generating a phosphonium with better user handling properties.

Two other diimines, one derived from (*R*)-(+)-1-(2-naphthyl)ethylamine **4-17** and the other derived from (*S*)-(+)-1-aminotetraline **4-18**, were cyclized with phosphenium **4-7a** to form phosphoniums **4-20** and **4-21**, respectively (Scheme 4-8B and 4-8C). Initially, the cyclizations appeared to work smoothly, but purification had been quite difficult despite multiple washes to remove impurities. Despite the impurities, the phosphoniums **4-20** and **4-21** were reduced with Mg dust to respective clean phosphines. Unfortunately, the resulting phosphines were not readily activated to the corresponding DAP-H with HBpin. Since there was a lot of promise with phosphonium **4-11a** there were no attempts to optimize these alternate scaffolds further. There could be more efforts made for the syntheses of phosphoniums **4-19**, **4-20** and **4-21** to isolate a clean product. Multiple factors could be varied, namely reaction time, temperature, and reagents. Different aminoalkylphosphines could be explored for the cyclization or cooling further may help remove impurities. Furthermore, alternative reagents for the reduction to the corresponding phosphine could lead to different outcomes and potentially a product that could be activated to the active catalyst species.

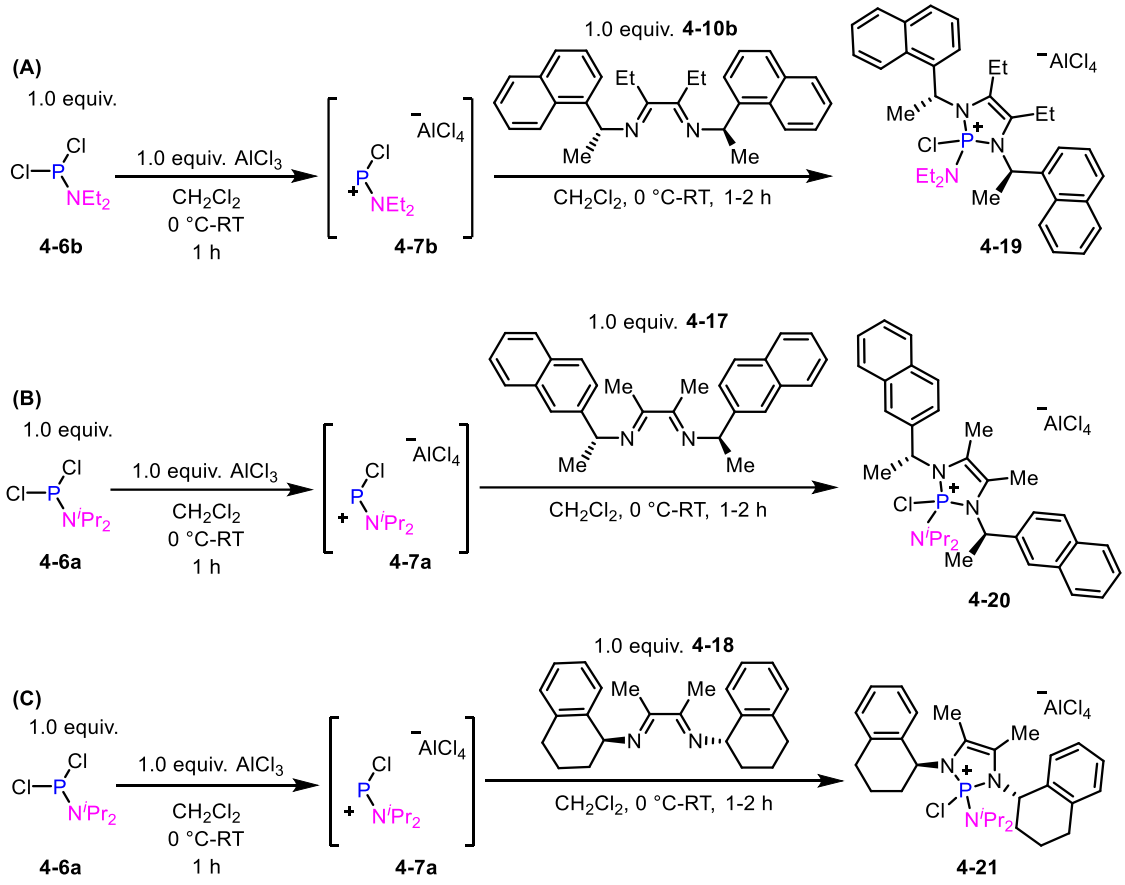

Scheme 4-8. Cyclizations of (A) diimine **4-10b** with phosphine **4-6b** (B) diimine **4-17** with phosphine **4-6a** (C) diimine **4-18** with phosphine **4-6a**.

Since the phosphine **4-12a** had the most reliable and robust synthesis, this was chosen as the focus for the remainder of this project. Phosphine **4-12a** was very hydrolytically sensitive and was deliberately hydrolyzed to **4-13** by addition of water to a THF solution (Scheme 4-9). Secondary phosphine oxide **4-13** is stable to air and moisture, and a crystal suitable for X-ray analysis was obtained from slow evaporation of a THF solution. Secondary phosphine oxide **4-13** and phosphine **4-12a** were both reactive with HBpin to generate the corresponding DAP-H, showing their suitability as diazaphospholene pre-catalysts. The catalyst also had an improved stability. As previously reported by the Speed group, **1-28** gradually decomposed to phosphine PH_3 in the presence of excess HBpin in

THF,[9] in contrast **4-13** was stable in the presence of a 10-fold excess of HBpin in THF for days, which likely an advantage in slow reduction reactions. With a route secured to a DAP-H from pre-catalyst **4-13**, exploration of reactivity and selectivity began.

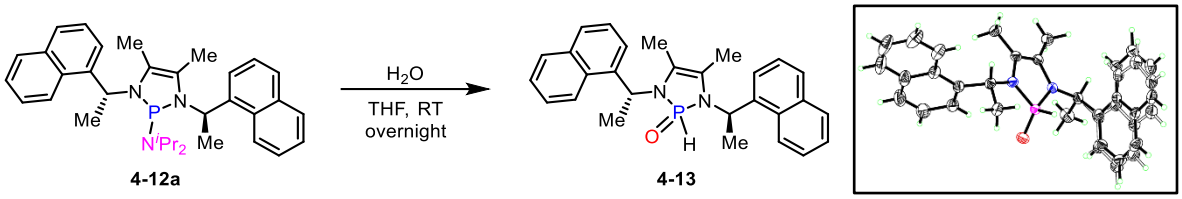

Scheme 4-9. Synthesis of SPO bearing methyl substituents in the backbone.

4.3.2 Reactivity of Substituted Backbone Diazaphospholene

The optimization began with the cyclic benchmark substrate **2-17a**. The reduction of cyclic imine **2-17a** with SPO **4-13** was tested at room temperature and at –35 °C. (Scheme 4-10). The reduction of **2-17a** with SPO **4-13** proceeded at room temperature to give amine **2-17b** with a 95:5 enantiomeric ratio, which is better than the performance of the current best DAP catalyst for this substrate at room temperature. No reaction was observed at –35 °C. Due to the advantages of the SPO: air, and moisture stability, and high selectivity at room temperature, the SPO was used for future reductions. Mixture of TMSOTf with the SPO to attempt to synthesize the DAP-OTf variant has shown promise and would be a future goal to reproducibly isolate this variant to compare the reactivity to the SPO variant, however this work focused on the SPO due to the above-mentioned advantages. The DAP-OTf variant would have the potential of complementary reactivity to the SPO variant. As noted, SPO **4-13** does not react at cooler temperatures while the DAP-OTf variant could and may produce high enantioselectivity for substrates that did not work well with SPO **4-13**.

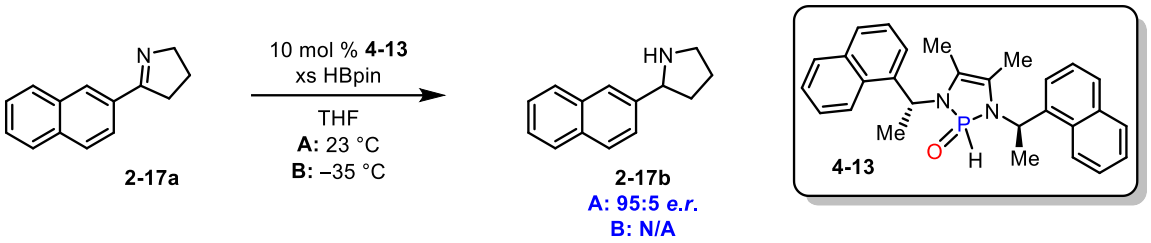

Scheme 4-10. Reduction of benchmark substrate with SPO **4-13**.

The good enantioselectivity of cyclic imines at room temperature was a promising start, but was anticipated to have limited impact as there was already a published DAP catalyst from our group that could reduce cyclic imines with high enantioselectivity. Therefore, the preliminary scope was expanded to acyclic imines that were already available within the laboratory. Acyclic imine substrates have been a limitation with previous DAP catalytic system with the highest enantiomeric ratio reported of 88:12, meaning there was room for improvement. The results from the preliminary scope of acyclic imines have been summarized in Table 4-3. The initial success with an acyclic imine was a fendiline precursor with an enantiomeric ratio of 95:5 for fendiline **4-23a** (Entry 1). The next acyclic imine that was successful with an enantiomeric ratio of 9:91 for amine **4-23b** which contained a benzylamine motif (Entry 2). An inferior substrate contained a phenyl group off the nitrogen with only an enantiomeric ratio of 76:24 for **4-23c** (Entry 3). The other two substrates were exocyclic amines **4-23d** and **4-23e** with enantiomeric ratios around 95:5 (Entries 4 and 5). Amine **4-23e** is rasagiline, a drug used to treat Parkinson's disease, which bears a propargyl group off the nitrogen and remains intact during the reduction reaction. This highlights the complementary reactivity between a main group catalyst compared to a transition metal-based catalyst as this propargyl group would likely be reduced with a metal centered catalyst. These results already showed a marked improvement over the existing DAP catalysts and guided the focus of the synthetic plan of the substrate scope.

Table 4-2. Preliminary results for acyclic and exocyclic imines.

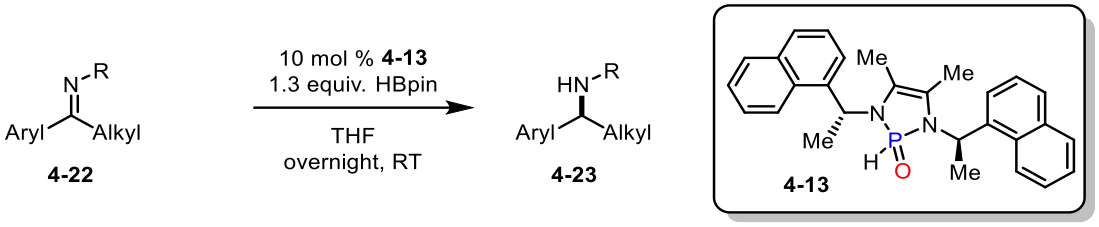

Entry	Reduced Substrate	Enantiomeric Ratio
1	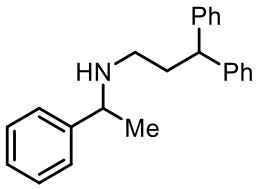 **4-23a**	95:5
2	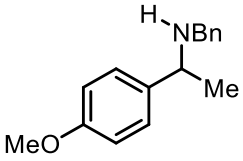 **4-23b**	9:91
3	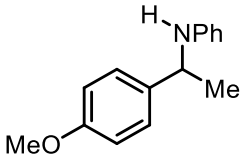 **4-23c**	76:24
4	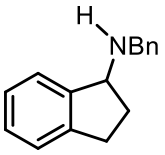 **4-23d**	95:5
5	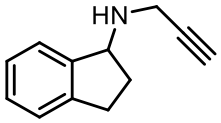 **4-23e**	96:4

The imines that were initially successful in the preliminary scope guided the substrate synthesis. The imines for the substrate scope were prepared through a condensation reaction between the corresponding ketone and amine in the presence of titanium ethoxide ($Ti(OEt)_4$) (Scheme 4-11). The substrate synthesis required minimal purification of the imines prior to catalysis, minor impurities or the presence of the starting ketone did not

interfere with the reduction. Removal of ethanol was essential, since ethanol promotes an uncatalyzed reduction of imines with pinacolborane, which lowers enantioselectivity.[77]

Structural features from the preliminary acyclic substrate scope were considered for the majority of the synthesized substrates. One important feature was maintaining the 3,3-diphenylpropylamine moiety as shown by substrates **4-24a** to **4-24t** highlighted in red. Other substrates, **4-24u** to **4-24y**, contained a benzylamine moiety highlighted in pink. One feature going beyond the original results was synthesizing imines containing 1,1-diphenylmethylamine moiety, as seen in substrates **4-24z** to **4-24ac** highlighted in blue. The inspiration to include this moiety was to eventually access 1° amines in high enantioselectivities, as the resulting 2° amine from the reduction could be treated with acid at high temperature to remove the diphenylmethane moiety.[78] The other class of substrates that appeared promising in the preliminary results were exocyclic imines, so substrates **4-24ad** to **4-24aj** highlighted in purple, were derived from indanone with varying alkyl side chains. Each class of substrates tried to incorporate both electron poor and electron rich rings determine a pattern or limitations of the SPO **4-13** as a catalyst.

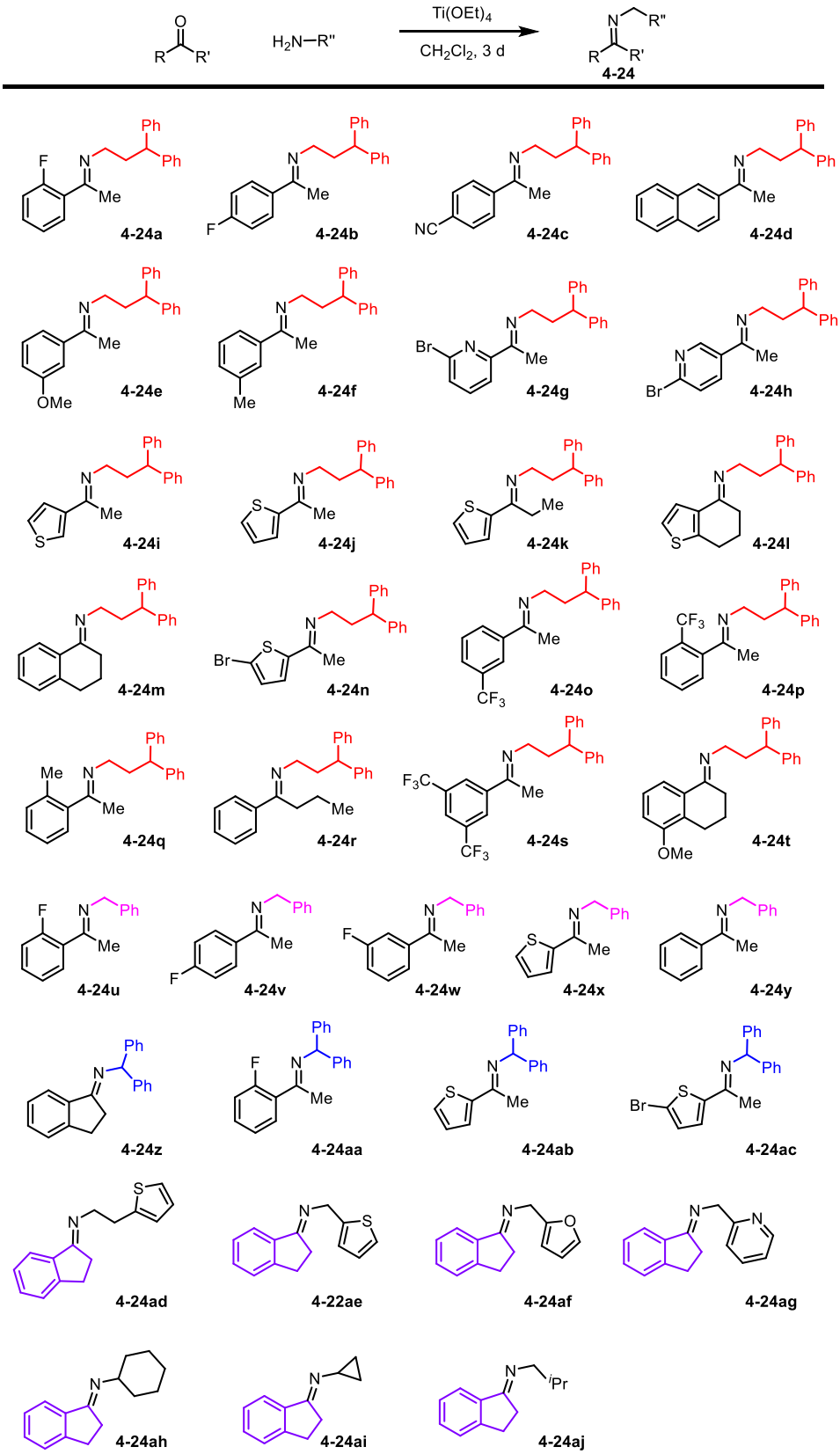

Scheme 4-11. Imine substrates that were synthesized.

With a library of substrates in hand the pre-catalyst was put to the test to determine the limitations (Scheme 4-12). Initially, the catalyst loading of **4-13** began at 10 mol % but loadings as low as 2.5 mol % were tolerated and maintained high enantioselectivity. The absolute configuration of the enantiomer SPO **4-13** is selective for has yet to be definitively determined and therefore enantiomeric ratios are reported based on order of elution off the HPLC. There have been some overall conclusions thus far. Fendiline precursor was effectively reduced to **4-23a** with a 2.5 mol % catalyst loading. A variety of arene substitution patterns with the diphenylpropylamino side chain gave high selectivities as shown by **4-25b**, **4-25c**, and **4-25f** with an *e.r.* of 90:10, and **4-23f** with an *e.r.* of 7:93. A naphthalene containing substrate was reduced generating **4-25d** with an *e.r.* of 87:13 and *m*-methoxy containing substrate was reduced to **4-25e** with an *e.r.* of 12:88. Pyridine containing substrates were a limitation of this catalyst system as shown by amines **4-25g** and **4-25h** with lower enantioselectivities of approximately 75:25. We observed a background reaction between these imines and HBpin, potentially promoted by the Lewis-basic pyridine. Imines derived from thienyl ketones were tolerated with high enantioselectivities, **4-25i** to **4-25k**, all with *e.r.* above 90:10. Substrates leading to products **4-25g** to **4-25k** were reduced at 2.5 mol % catalyst loading and a 24 h reaction time. Imine precursor to amine **4-25k** was reduced at 2.5 mol % catalyst loading and a 48 h reaction time. Tetralone-derived imines were reduced in 24 h with a 2.5 mol % catalyst loading resulting in **4-25l** with a high *e.r.* of 93:7 and **4-25m** with a poor *e.r.* of 67:37.

The benzylamino containing amines gave slightly lower selectivity relative to diphenylpropylamino containing amines. Substrates containing a fluoro-substituent in varying positions on the arene were reduced at 2.5 mol % catalyst loading and a 24 h

reaction time to give amines, **4-25u** (*e.r.* 11:89), **4-25v** (*e.r.* 15:85) and **4-25w** (*e.r.* 15:85) were reduced at a 2.5 mol % catalyst loading and 24 h reaction time. Reduction of a thiophene containing imine required a reaction time of 72 h at 2.5 mol % catalyst loading to generate amine **4-25x** (*e.r.* 15:85). Benzylamines **4-23g** to **4-23j** had poor to good enantioselectivities at 10 mol % catalyst loading and 24 h reaction time. Benzylamines for **4-23b** (*e.r.* 9:91 at 10 mol % catalyst loading) and **4-23d** (*e.r.* 95:5 at 2.5 mol % catalyst loading) had high enantioselectivities with a 24 h reaction time.

Reduction of the precursor to rasagiline to amine **4-23e** (95:5 *e.r.* at 10 mol % and 24 h) was highly effective, showing that exocyclic imines are good substrates. Indanone derived imine with branching on the side chain was reduced effectively to amine **4-25z** (5:95 *e.r.* at 2.5 mol % and 24 h). However, indanone derived imines with heterocyclic side chains were a limitation with catalyst, amines **25ad** (83:17 *e.r.* and 24 h), **4-25ae** (*e.r.* 88:12 and 48 h) and **4-25af** (*e.r.* 70:30 and 48 h) had poor to good enantioselectivities at 2.5 mol % catalyst loading and varying reaction times.

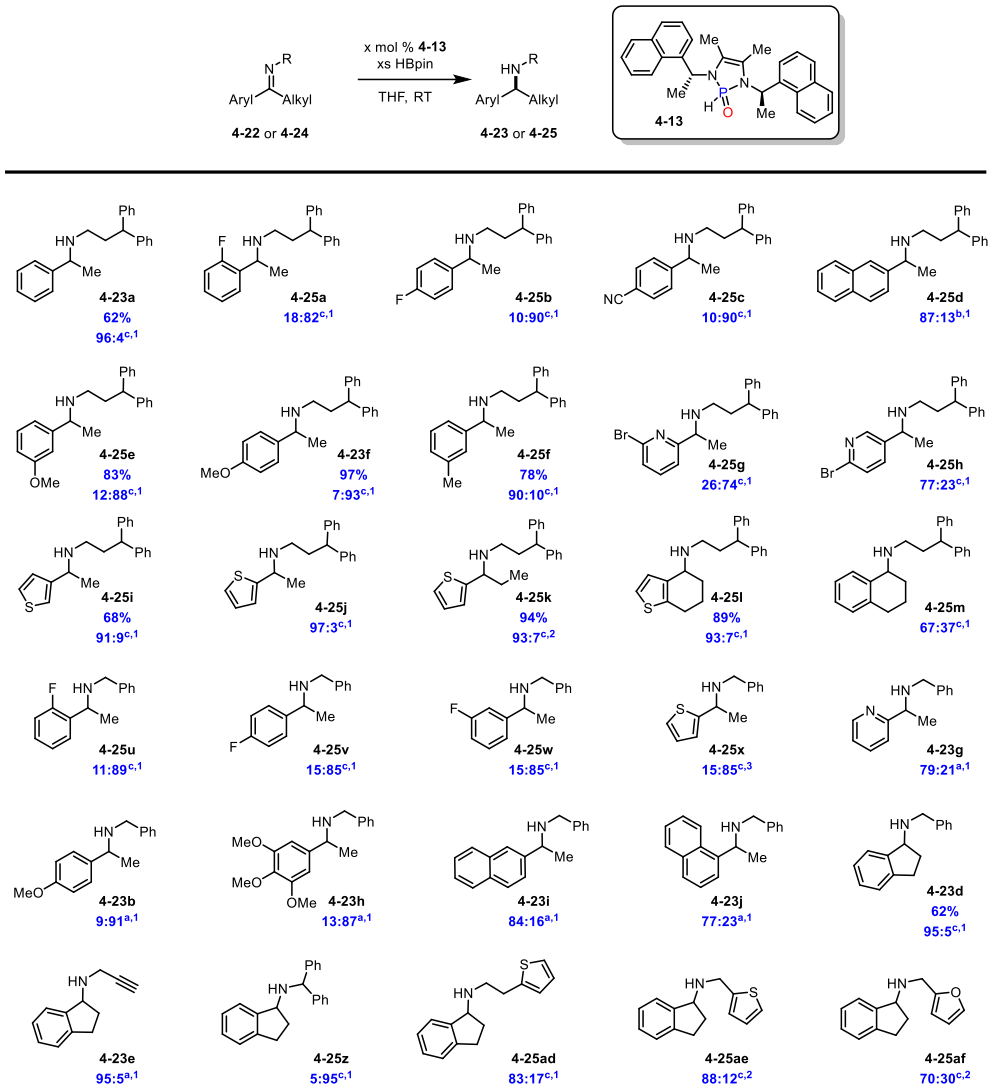

[a] = 10 mol % [b] = 5 mol % [c] = 2.5 mol % [1] = 24 h [2] = 48 h [3] = 72 h

Scheme 4-12. Reduction results of acyclic imines with SPO **4-13**.

Originally, reduction reactions were naively assumed to be complete after one day, but it was determined that for some sterically encumbered substrates, longer reaction times were required. Prior to determining that, some substrates, **4-25aa** and **4-25ab**, were preemptively quenched therefore did not go to completion (DNC). This resulted in the hydrolysis of the imine back to the ketone and amine. Additionally, if hydrolysis does not occur and imine is still present upon work-up, water is known to facilitate the

hydroboration of imines and would erode the enantioselectivity of the desired amine[77] and therefore the enantioselectivity of the amine could not be determined. From then on, analysis of reaction aliquots was obtained via NMR spectroscopy prior to quenching to confirm the reaction had gone to completion. Additionally, some substrates have been difficult to separate on the HPLC with the standard conditions and columns available to us, and so I have not been able to determine the enantioselectivity. Certain substrates containing the diphenylpropylamino side chain **4-25n** to **4-25r** and a benzylamine substrate **4-25y** did not separate (DNS). Additionally, indanone derived substrates **4-25ag** with a pyridyl side chain and **4-25ah** to **4-25aj** with various alkyl side chains DNS. These results are summarized in Scheme 4-13.

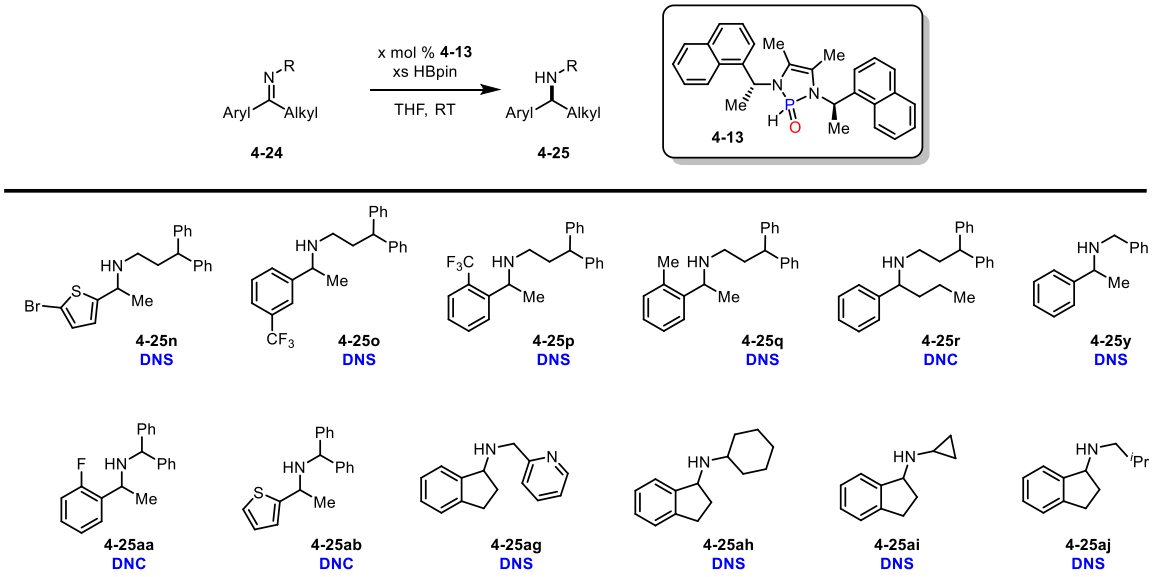

DNS = did not separate DNC = did not go to completion.

Scheme 4-13. Difficult substrates to determine the enantiomeric ratio.

4.4 Summary

In conclusion, a four-step synthetic route to access a chiral diazaphospholene bearing methyl substituents in the backbone was developed. Previously reported diazaphospholene synthesis reactions did not allow access to backbone methyl-substituted

diazaphospholenes. A couple of different synthetic routes to cyclize the diimine were attempted prior to a successful pre-catalyst isolation (Scheme 4-14). Amino-phosphine reagents were used that required activation to a phosphenium in order to be reactive with the diimine. The first attempt was using bis(diethylamino)chlorophosphine **4-2a** that resulted in an air and moisture stable phosphonium **4-14a** that was unreactive to conversion to an active catalyst (Scheme 4-14A). A successful route was developed which involved replacing an amino group on the starting phosphine with an additional halogen with the hypothesis that the resulting halo-phosphonium **4-16** would be more susceptible to reduction (Scheme 4-14B). Unfortunately, this resulted in some decomposition during cyclization, due to the incomplete activation of the phosphine to the phosphenium **4-15**. The phosphenium **4-15** and starting chlorophosphine were in equilibrium, and the diimine bearing methyl substituents in the backbone is known to react with the TMSOTf leading to a complex mixture of products. Fortunately, replacing TMSOTf with a stronger chloride abstractor, $AlCl_3$, to completely form phosphenium **4-7a** prior to cyclization solved this problem and formed a phosphonium **4-11a** that was susceptible to reduction to phosphine **4-12a**. This phosphine was successfully converted to the SPO **4-13** and was used as a pre-catalyst (Scheme 4-14C). This new system has advantages in selectivity over previously reported diazaphospholene catalyzed imine reduction.

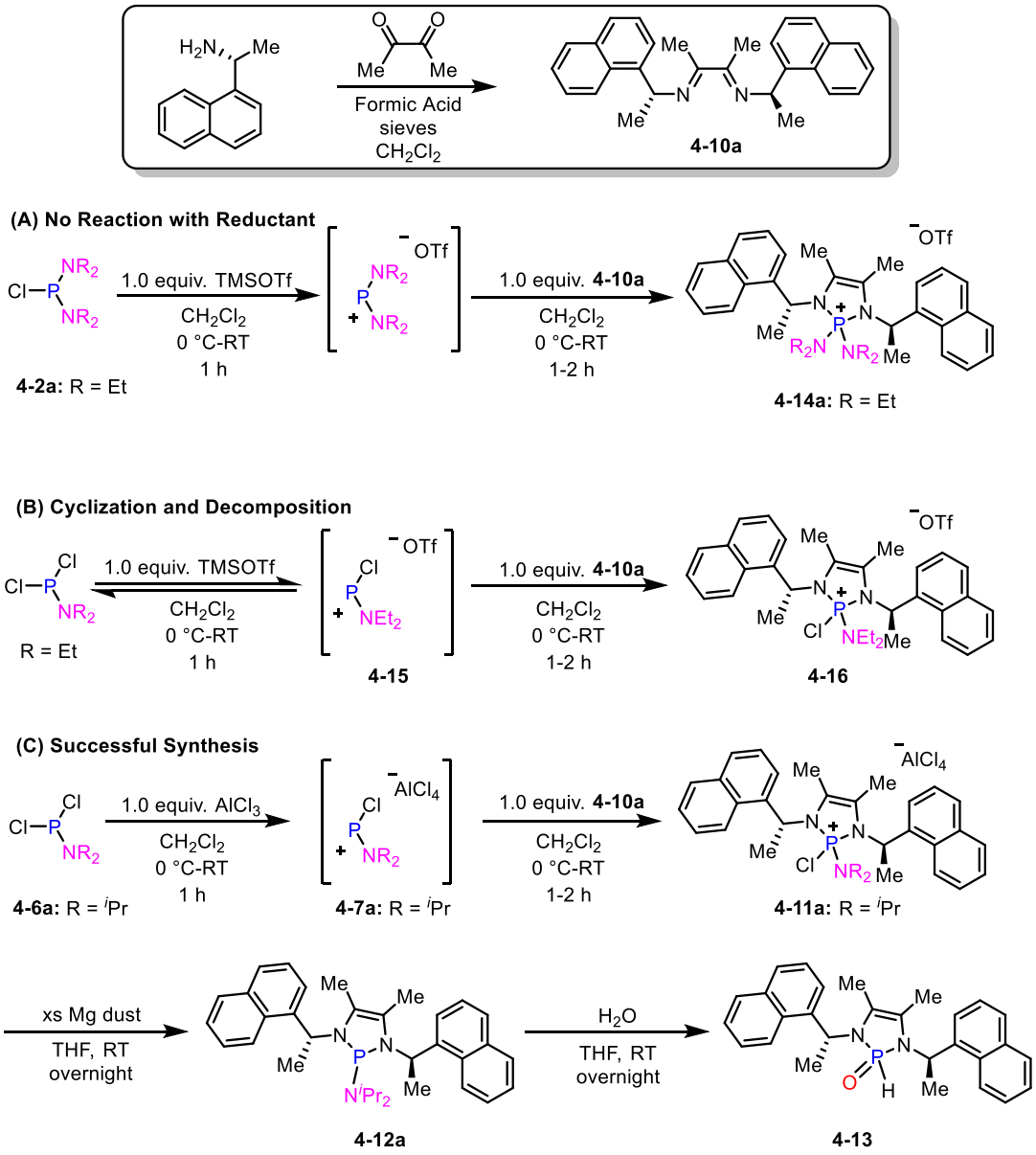

Scheme 4-14. Summary of attempted cyclizations of a diimine with a methyl substituted backbone. (A) Starting from bisamino(dialkyl)phosphine and TMSOTf. (B) Starting from diethylaminodichlorophosphine and TMSOTf. (C) Starting from dialkylaminodichlorophosphine and $AlCl_3$.

Reductions of acyclic and exocyclic imines were catalyzed by SPO **4-13** with high enantioselectivity at room temperature with low loadings, providing best-in-class selectivity for several classes of imine hydroboration (Scheme 4-15). The reduction reactions can be conducted without the need for a glovebox. The active catalyst is also

resistant to decomposition in the presence of excess HB(pin). Other applications of this new class of diazaphospholene catalyst are under investigation and will be reported in due course.

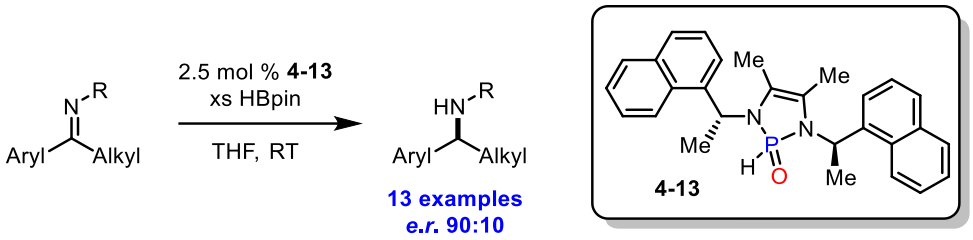

Scheme 4-15. Summary of reduction results of SPO with methyl substituted backbone.

4.5 Experimental

4.5.1 General Considerations

Reactions were run under nitrogen, using oven-dried glassware unless otherwise specified. ^{1}H, ^{13}C, and ^{11}B NMR data were collected at 300K on a Bruker AV-500 or Neo-400 NMR spectrometer. ^{1}H NMR spectra are referenced to residual non-deuterated NMR solvent ($CHCl_3$ = 7.26 ppm or CH_3CN = 1.94 ppm). ^{13}C NMR spectra are referenced to the central $CDCl_3$ peak (77.16 ppm) or CD_3CN (1.32 ppm). Mass spectrometric data were acquired by Mr. Xiao Feng (Mass Spectrometry Laboratory, Dalhousie University). Optical rotations were obtained in the solvents stated, using a DigiPol 781 Automatic Polarimeter from Rudolph Instruments. Concentrations for optical rotation are given in g/100 mL.

Solvents

Diethyl ether was purchased as anhydrous ACS reagent grade, >99.0% stabilized by BHT in 1 L metal cans from Aldrich.

Dichloromethane (ACS grade) was purchased from Fisher. Dichloromethane for reactions was distilled from calcium hydride immediately before use, while no purification was carried out on dichloromethane used for extractive work-ups.

Pentane for reactions was deoxygenated and dried by sparging with nitrogen gas then stored over activated 3 Å molecular sieves in the glovebox.

Tetrahydrofuran was purchased from Aldrich in a Sure/seal® bottle (anhydrous, >99.9%, inhibitor free, catalogue number 401757). Tetrahydrofuran was used directly from this bottle for Grignard reactions and lithiations.

Reagents

Amines was purchased from Aldrich Chemical and used as received.

Chlorophosphines, **aluminum trichloride** and **magnesium dust** were purchased from Aldrich Chemical, stored at ambient temperature in the glovebox, and used as received,

Ketones were purchased from Aldrich Chemical or Oakwood Chemical and used as received.

Pinacolborane was purchased from Oakwood Chemical, stored at refrigerated in the glovebox, and otherwise used as received.

Titanium ethoxide was purchased from Oakwood Chemical and used as received.

Trimethylsilyl triflate was purchased from Oakwood Chemical and distilled at 10 torr before use.

4.5.2 Experimental Procedures and Tabulated Data for the Synthesis of Substituted Backbone Diazaphospholenes

Diimine 4-10a: On the bench top, (*R*)-(+)-1-(1-naphthyl)ethylamine (17.0 g, 102 mmol, 1.0 equiv.) was weighed into a 250 mL round bottom flask equipped with a stir bar. The amine was dissolved in dichloromethane (150 mL) then reagents were added in the following order: 3 Å molecular sieves (15 g), formic acid (1 drop) and 1,2-butadione (4.6 mL, 51 mmol, 0.5 equiv.). The flask was enclosed with a yellow cap and sealed with electrical tape and allowed to stir. After 7 d, the reaction was filtered to remove sieves then washed exhaustively with diethyl ether (150 mL tot.). The filtrate was concentrated then suspended in diethyl ether and stirred for 0.5 h to allow the diimine powder out and the impurities remain in solution. The solid was collected via filtration and washed with ether (2 × 25 mL). The diimine **4-10a** was collected as a pale-yellow powder in a 57% yield (11.7 g, 30 mmol).

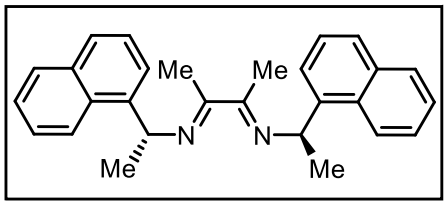

^{1}H NMR (500 MHz, $CDCl_3$): δ 8.34 (ap. d, *J* = 8.4 Hz, 2H), 7.89 (ap. d, *J* = 8.0 Hz, 2H), 7.81 (ap. d, *J* = 7.1 Hz, 2H), 7.76 (ap. d, *J* = 8.0 Hz, 2H), 7.57–7.45 (m, 6H), 5.60 (q, *J* = 6.4 Hz, 2H), 2.33 (s, 6H), 1.71 (ap. d, *J* = 6.4 Hz, 6H).

^{13}C{^{1}H} NMR (125 MHz, $CDCl_3$): δ 167.1, 142.1, 134.2, 130.8, 129.1, 127.2, 125.8, 125.8, 125.4, 124.2, 123.4, 57.4, 24.4, 13.3.

HRMS (ESI): *m/z* $[M+H]^+$ calculated for $C_{28}H_{29}N_2$: 393.2325 found: 393.2321.

Phosphonium 4-11a: In the glovebox, aluminum trichloride (0.33 g, 2.5 mmol, 1.0 equiv.) was weighed into a Schlenk flask equipped with a stir bar then placed on the Schlenk line. The $AlCl_3$ was suspended in dichloromethane (5 mL) then cooled to 0 °C. A solution of the diisopropylaminodichlorophosphine **4-6a** (0.46 mL, 2.5 mmol, 1.0 equiv.) in 3 mL of dichloromethane was transferred to the cooled $AlCl_3$ and the flask containing the phosphine was rinsed with additional 2 mL of dichloromethane to complete the transfer. After the transfer, the cooling bath was removed and stirred at room temperature for 1 h to form the phosphenium **4-7a** *in situ*. The phosphenium was re-cooled to 0 °C and a solution of the diimine **4-10a** (0.97 g, 2.5 mmol, 1.0 equiv.) in 7 mL of dichloromethane was transferred to the cooled phosphenium solution followed by an additional 3 mL of dichloromethane was used to complete the transfer of the diimine solution. The reaction stirred for 3 h and the cooling bath decayed naturally. After the cyclization was complete, the solvent was removed in vacuo on the line and the crude solid was taken into the glovebox for purification. The crude product was triturated with pentane to precipitate out a yellow powder that was collected via filtration as the phosphonium **4-11a** with an 85% yield.

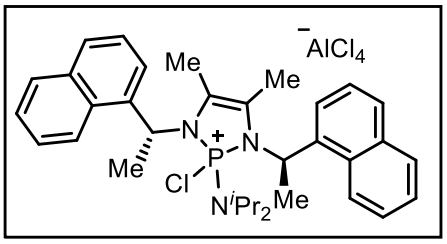

^{1}H NMR (500 MHz, CD_3CN): δ 8.07 (t, *J* = 8.4 Hz, 2H), 8.01–7.91 (m, 4H), 7.68–7.65 (m, 2H), 7.61–7.58 (m, 4H), 7.54 (t, *J* = 8.0 Hz, 1H), 7.46 (d, *J* = 7.2 Hz, 1H), 5.93–5.85 (m, 1H), 5.83–5.76 (m, 1H), 3.99–3.88 (m, 2H), 2.28 (s, 3H), 2.04 (d, *J* = 7.2 Hz, 3H), 2.00–1.97 (m, 6H), 1.36 (d, *J* = 6.8 Hz, 6H), 1.12–1.11 (m, 6H).

^{13}C{^{1}H} NMR (125 MHz, CD_3CN): δ 137.7 ($^3J_{PC}$ = 3.6 Hz), 137.6, 135.1 (d, $^3J_{PC}$ = 5.9 Hz), 130.5, 130.4, 130.3, 130.2, 130.1, 139.8, 129.8, 128.1, 128.1, 127.3, 127.3, 126.6, 126.5, 124.3, 124.1, 123.6, 123.4, 121.9 ($^3J_{PC}$ = 16 Hz), 121.3 ($^3J_{PC}$ = 17 Hz), 53.7 ($^2J_{PC}$ = 3.3 Hz), 52.1 ($^3J_{PC}$ = 6.3 Hz), 22.8 (J_{PC} = 7.7 Hz), 22.7, 22.2, 21.8 (J_{PC} = 3.7 Hz), 14.7 ($^3J_{PC}$ = 8.5 Hz), 12.8 ($^3J_{PC}$ = 7.5 Hz).

^{31}P NMR (202 MHz, $CDCl_3$): δ 29.7 (br. s).

HRMS (ESI): *m/z* $[M+H]^+$ calculated for $C_{34}H_{42}ClN_3P$: 558.2799 found: 558.2795.

Phosphonium 4-11b: In the glovebox, aluminum trichloride (0.19 g, 1.4 mmol, 1.0 equiv.) was weighed into a Schlenk flask equipped with a stir bar. The flask was placed on the Schlenk line then the $AlCl_3$ was suspended in 10 mL of dichloromethane. The solution was cooled to 0 °C followed by the addition of (diethylamino)dichlorophosphine **4-6b** (0.21 mL, 1.4 mmol, 1.0 equiv.) that stirred for 1 h and naturally warmed to room temperature to generate **4-7b** *in situ*. After 1 h, the solution was cooled back to 0 °C then a solution of the diimine **4-10a** (0.56 g, 1.4 mmol, 1.0 equiv.) in 5 mL of dichloromethane was added to the cooled reaction flask. An additional 3 mL of dichloromethane was used to complete the

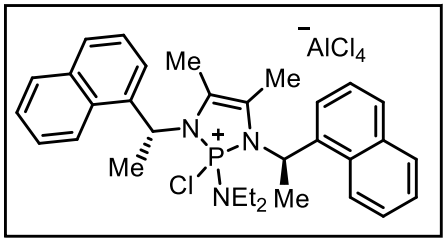

transfer of the diimine. After the addition, the ice bath was removed, and the reaction stirred for 3 h. The solvent was removed in vacuo leaving a tacky solid that was taken into the glovebox. The crude product was triturated with pentane then filtered to collect the purified phosphonium **4-11b** as an orange powder in a 93% yield.

^{1}H NMR (500 MHz, $CDCl_3$): δ 7.95–7.92 (m, 2H), 7.89–7.87 (m, 2H), 7.83–7.81 (m, 1H), 7.78–7.74 (m, 2H), 7.59 (m, 3H), 7.54–7.51 (m, 3H), 7.36 (ap. d, J = 7.0 Hz, 1H), 5.83–5.72 (m, 2H), 3.01 (m, 2H), 2.41 (s, 3H), 2.03 (ap. d, J = 6.7 Hz, 3H), 1.98 (s, 3H), 1.85 (ap. d, J = 6.8 Hz, 3H), 1.44 (m, 3H), 0.54 (br. s, 5H).

^{13}C{^{1}H} NMR (125 MHz, $CDCl_3$): δ 135.7 (ap. d, $^3J_{PC}$ = 3.0 Hz), 134.1 (ap. d, $^3J_{PC}$ = 3.3 Hz), 131.6, 131.3, 130.8, 129.6, 129.6, 129.5, 129.4, 128.6, 127.7, 127.2, 126.5, 126.0, 125.8, 125.6, 125.5, 122.9, 122.8, 122.0, 120.5 (ap. d, $^2J_{PC}$ = 17 Hz), 120.2 (ap. d, $^2J_{PC}$ = 14 Hz), 52.9 (ap. d, $^2J_{PC}$ = 2.9 Hz), 51.2 ($^2J_{PC}$ = 3.3 Hz), 42.4, 21.0 (ap. d, $^3J_{PC}$ = 3.4 Hz), 19.6 (br. s), 13.8 (br. s), 12.6 (d, $^3J_{PC}$ = 7.6 Hz), 12.1 ($^3J_{PC}$ = 7.0 Hz), 11.4.

^{31}P NMR (202 MHz, $CDCl_3$): δ 32.4–32.1 (m).

HRMS (ESI): *m/z* $[M+H]^+$ calculated for $C_{32}H_{38}ClN_3P$: 530.2486 found: 530.2486.

Phosphine 4-12a: Phosphonium **4-11a** (1.14 g, 1.48 mmol, 1.0 equiv.) was weighed into a 50 mL round bottom flask equipped with a stir bar. Then magnesium dust (0.18 g, 7.42 mmol, 5.0 equiv.) was added followed by tetrahydrofuran (20 mL) and the reaction stirred for 18 h. The stirring was stopped, then after the Mg dust settled to the bottom the solution was decanted into a clean round bottom flask. The Mg dust was washed with excess tetrahydrofuran (3 × 5 mL) to complete the transfer. The solution was concentrated, and the phosphine was extracted into pentane (3 × 15 mL) and vigorously triturated to precipitate out all the Mg and Al salts. The salts were removed via filtration and pentane was removed to isolate phosphine **4-12a** as a yellow powder in a 75% yield.

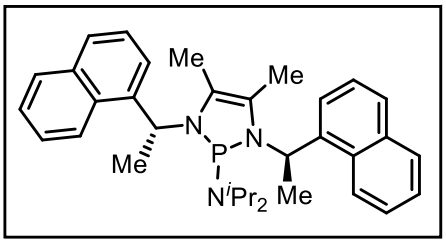

^{1}H NMR (500 MHz, $CDCl_3$): δ 8.43 (d, J = 8.5 Hz, 1H), 8.11 (d, J = 8.4 Hz, 1H), 7.89–7.86 (m, 3H), 7.79 (d, J = 8.2 Hz, 1H), 7.71 (d, J = 8.0 Hz, 1H), 7.55–7.48 (m, 5H), 7.37 (ap. t, J = 7.8 Hz, 1H), 7.23 (ap. d, J = 7.2 Hz, 1H), 5.61–5.58 (m, 1H), 5.54–5.49 (m, 1H), 3.16–3.06 (m, 2H), 2.02 (s, 3H), 1.86 (d, J = 7.1 Hz, 3H), 1.76 (d, J = 6.8 Hz, 3H), 1.55 (s, 3H), 0.95 (d, J = 6.8 Hz, 6H), 0.58 (ap. d, J = 5.1 Hz, 6H).

^{13}C{^{1}H} NMR (125 MHz, $CDCl_3$): δ 142.3 (ap. d, $^3J_{PC}$ = 3.7 Hz), 140.0 (ap. d, $^3J_{PC}$ = 5.0 Hz), 134.2, 134.1, 132.6, 130.4, 129.1, 128.7, 127.8, 127.2, 126.8, 125.9, 125.8, 125.7, 125.3, 125.2, 125.1, 124.6, 123.8, 123.7, 122.6, 120.6 (ap. d, $^2J_{PC}$ = 6.9 Hz), 117.9 (ap. d, $^2J_{PC}$ = 7.0 Hz), 52.1 (d, $^2J_{PC}$ = 21 Hz), 50.8 (d, $^2J_{PC}$ = 35 Hz), 45.8, 45.7, 24.5 (br. s), 24.1 (br. s), 23.3, 23.2, 20.9, 20.9, 12.2, 11.8.

^{31}P NMR (202 MHz, $CDCl_3$): δ 82.2.

Secondary Phosphine Oxide 4-13: In a receiving flask, the phosphine **4-12a** (0.57 g, 1.1 mmol, 1.0 equiv.) was dissolved in 5 mL of tetrahydrofuran containing 2.0 equiv. of water that stirred for 18 h. The secondary phosphine oxide precipitated out and the solution was decanted then the residue was dried in vacuo on the line. The secondary phosphine oxide **4-13** was isolated as a light-yellow powder.

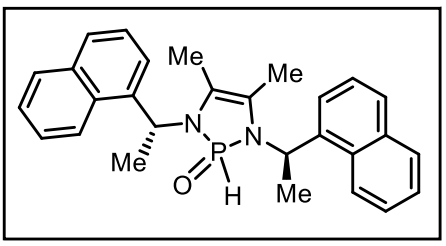

^{1}H NMR (500 MHz, $CDCl_3$): δ 8.89 (s, 0.5 H), 8.07 (d, *J* = 7.2 Hz, 1H), 7.99 (d, *J* = 8.4 Hz, 2H), 7.92–7.88 (m, 2H), 7.83 (d, *J* = 8.0 Hz, 1H), 7.75 (d, *J* = 8.1 Hz, 1H), 7.60–7.46 (m, 7.5 H), 5.62–5.58 (m, 2H), 2.02 (d, *J* = 6.8 Hz, 3H), 1.84 (s, 3H), 1.78 (d, *J* = 6.9 Hz, 3H), 1.47 (s, 3H).

^{13}C{^{1}H} NMR (125 MHz, $CDCl_3$): δ 140.1, 136.8 (ap. d, $^{3}J_{PC}$ = Hz), 134.2, 133.9, 130.9, 129.8, 129.4, 129.3, 128.6, 127.6, 126.7, 126.5, 126.3, 125.8, 125.7, 125.4, 124.7, 124.5, 122.7, 121.8, 116.9 (d, $^{2}J_{PC}$ = 9.4 Hz), 115.7 (d, $^{2}J_{PC}$ = 8.6 Hz), 50.8 (d, $^{2}J_{PC}$ = 5.0 Hz), 49.5 (d, $^{2}J_{PC}$ = 6.4 Hz), 22.6 (d, $^{3}J_{PC}$ = 3.1 Hz), 21.0 (d, $^{3}J_{PC}$ = 6.9 Hz), 10.7 (d, $^{3}J_{PC}$ = 4.2 Hz), 10.7 (d, $^{2}J_{PC}$ = 4.1 Hz).

^{31}P NMR (202 MHz, $CDCl_3$): δ 4.73 (dt, *J* = 646, 16 Hz).

HRMS (ESI): *m/z* $[M+Na]^+$ calculated for $C_{28}H_{29}N_2NaOP$: 463.1910 found: 463.1910.

Phosphonium 4-14a: Bis(diethylamino)chlorophosphine **4-2a** (0.5 mL, 2.4 mmol, 1.0 equiv.) was dispensed into a Schlenk flask equipped with a stir bar in the glovebox. The flask was then placed on the Schlenk line, and the phosphine was dissolved in 5 mL of dichloromethane. Followed by the addition of TMSOTf (0.4 mL, 2.4 mmol, 1.0 equiv.) and stirred for 1 h to for the phosphenium **4-3a** *in situ*. In a separate flask, diimine **4-10a** (0.93 g, 2.4 mmol, 1.0 equiv.) was dissolved in dichloromethane (3 mL) then transferred to the phosphenium reaction flask then an additional 2 mL of dichloromethane was used to rinse the flask containing the diimine and complete the transfer. The reaction stirred for 1 h then the solvent was removed in vacuo which leaves a tacky yellow solid. The crude product was re-dissolved in dichloromethane on the benchtop then washed with water (3 × 25 mL). The organic layer was collected and concentrated which resulted in 1.4 g (84% yield) of phosphonium **4-14a** as a yellow powder.

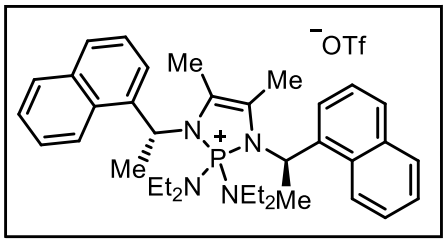

^{1}H NMR (500 MHz, $CDCl_3$): δ 7.99 (d, *J* = 8.7 Hz, 2H), 7.91 (d, *J* = 8.1 Hz, 2H), 7.85 (d, *J* = 8.2 Hz, 2H), 7.66 (ap. t, *J* = 7.4 Hz, 2H), 7.57–7.50 (m, 4H), 7.42 (ap. d, *J* = 7.1 Hz,

2H), 5.61–5.55 (m, 2H), 3.11–3.04 (m, 4H), 2.99–2.92 (m, 4H), 2.20 (s, 6H), 1.96 (d, J = 7.2 Hz, 6H), 0.89 (t, J = 7.0 Hz, 12H).

^{13}C{^{1}H} NMR (125 MHz, CDCl$_3$): δ 138.3, 134.1, 129.6, 129.4, 129.0, 127.6, 126.5, 127.6, 126.5, 125.2, 122.7, 122.4, 118.4, 118.3, 51.4 (d, $^{2}J_{PC}$ = 4.9 Hz), 40.6 ($^{2}J_{PC}$ = 3.5 Hz), 32.0, 29.8, 29.1, 22.8, 14.2, 14.1 (d, $^{3}J_{PC}$ = 6.9 Hz), 13.1 (d, $^{3}J_{PC}$ = 3.8 Hz).

^{31}P NMR (202 MHz, CDCl$_3$): δ 41.5.

^{19}F NMR (470 MHz, CDCl$_3$): δ −78.0.

HRMS (ESI): *m/z* [M+H]$^+$ calculated for $C_{36}H_{48}N_4P$: 567.3611 found: 567.3621.

Diimine 4-17: On the bench top, (*R*)-(+)-1-(2-naphthyl)ethylamine (9.7 g, 57 mmol, 1.0 equiv.) was weighed into a 250 mL round bottom flask equipped with a stir bar. The amine was dissolved in dichloromethane (60 mL) then reagents were added in the following order: 3 Å sieves (8.5 g), formic acid (1 drop) and 1,2-butadione (2.5 mL, 28 mmol, 0.5 equiv.). The flask was enclosed with a yellow cap and sealed with electrical tape and allowed to stir. After 7 d, the reaction was filtered to remove sieves then washed excessively with diethyl ether (150 mL tot.). The filtrate was concentrated then suspended in diethyl ether and stirred for 0.5 h to allow the diimine powder out and the impurities remain in solution. The solid was collected via filtration and washed with ether (2 × 25 mL). The diimine **4-17** was collected as a white powder in an 86% yield (9.6 g, 24 mmol).

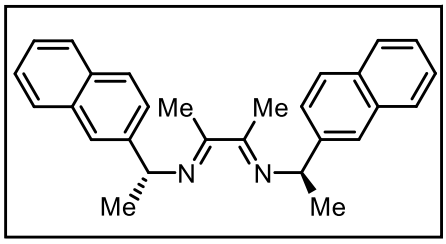

^{1}H NMR (500 MHz, CDCl$_3$): δ 7.81–7.78 (m, 8H), 7.60–7.58 (m, 2H), 7.45–7.39 (m, 4H), 4.98 (q, J = 6.5 Hz, 2H), 2.27 (s, 6H), 1.56 (d, J = 6.6 Hz, 6H).

^{13}C{^{1}H} NMR (125 MHz, CDCl$_3$): δ 166.8, 143.6, 133.6, 132.7, 128.2, 127.9, 127.7, 126.0, 125.6, 125.5, 124.9, 60.6, 24.8, 13.1.

HRMS (ESI): *m/z* [M+H]$^+$ calculated for $C_{28}H_{29}N_2$: 393.2325 found: 393.2316.

Diimine 4-18: On the bench top, (*S*)-(+)-1-aminotetraline (9.9 mL, 68 mmol, 1.0 equiv.) was dispensed into a 250 mL round bottom flask equipped with a stir bar. The amine was dissolved in dichloromethane (70 mL) then reagents were added in the following order: 3 Å sieves (10 g), formic acid (1 drop) and 1,2-butadione (3.0 mL, 34 mmol, 0.5 equiv.). The flask was enclosed with a yellow cap and sealed with electrical tape and allowed to stir. After 7 d, the reaction was filtered to remove sieves then washed excessively with diethyl ether (150 mL tot.). The filtrate was concentrated then suspended in diethyl ether and stirred for 0.5 h to allow the diimine powder out and the impurities remain in solution. The solid was collected via filtration and

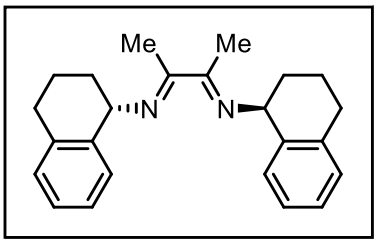

washed with ether (2 × 25 mL). The diimine **4-18** was collected as a light orange powder in a 71% yield (8.3 g, 24 mmol).

^{1}H NMR (500 MHz, $CDCl_3$): δ 7.17–7.13 (m, 6H), 7.00–6.98 (m, 2H), 4.85–4.82 (m, 2H), 2.95–2.92 (m, 2H), 2.89–2.84 (m, 2H), 2.25 (s, 6H), 2.14–2.10 (m, 2H), 1.97–1.79 (m, 6H).

^{13}C{^{1}H} NMR (125 MHz, $CDCl_3$): δ 167.7, 139.0, 137.0, 129.2, 128.1, 126.7, 125.9, 59.7, 30.4, 29.6, 21.0, 13.3.

HRMS (ESI): *m/z* $[M+H]^+$ calculated for $C_{24}H_{29}N_2$: 345.2325 found: 345.2328.

4.5.3 Experimental Procedures and Selected Tabulated Data for Synthesis of Substrates

General Synthesis: The appropriate ketone (1.0 equiv.) was placed in a 250 mL round bottom flask equipped with a stir bar and dissolved in dichloromethane (0.2 M). The appropriate amine (1.0 equiv.) was added to the solution followed by titanium ethoxide (1.5 equiv.). The flask was sealed with a yellow cap and secured with electrical tape and stirred for 72 hours. The reaction was quenched with 4 M KOH (2.0 equiv.) then continuously agitated for 1 min as a sludge began to form. This was filtered through a frit and into a round bottom flask containing sodium sulfate. The solid was washed with excess dichloromethane. The filtrate was filtered to remove the sodium sulfate then concentrated to isolate the imine. The product was used without further purification.

Imine 4-24a: 2-fluoroacetophenone (1.8 mL, 15 mmol) and 3,3-diphenylpropylamine (3.1 g, 15 mmol) produced 3.3 g of crude imine **4-24a** as a pale-yellow solid.

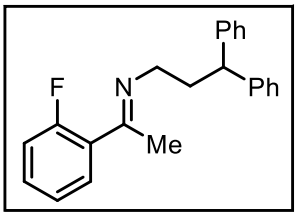

^{1}H NMR (400 MHz, $CDCl_3$): δ 7.52 (td, J = 7.6, 1.8 Hz, 1H), 7.29–7.28 (m, 8H), 7.20–7.12 (m, 3H), 7.07–7.01 (m, 1H), 4.15 (t, J = 7.9 Hz, 1H), 3.38 (t, J = 7.0 Hz, 2H), 2.53 (q, J = 7.5 Hz, 2H), 2.04 (ap. d, J = 2.9 Hz, 3H).

^{13}C{^{1}H} NMR (100 MHz, $CDCl_3$): δ 164.7, 160.5 (d, $^1J_{FC}$ = 249 Hz), 144.9, 130.6 ($^3J_{FC}$ = 8.4 Hz), 129.8 (d, $^3J_{FC}$ = 3.5 Hz), 128.6, 128.2 (d, $^2J_{FC}$ = 49 Hz), 126.3, 126.1, 124.4 (d, $^4J_{FC}$ = 3.2 Hz), 116.0 (d, $^2J_{FC}$ = 22.1 Hz), 50.2, 49.0, 36.4, 19.1 (d, $^4J_{FC}$ = 5.2 Hz).

^{19}F NMR (376 MHz, $CDCl_3$): δ −114.9 (m), −115.3 (m).

HRMS (ESI): *m/z* $[M+H]^+$ calculated for $C_{23}H_{23}FN$: 332.1809 found: 332.1816.

Imine 4-24b: 4-Fluoroacetophenone (5.0 g, 36 mmol) and 3,3-diphenylpropylamine (7.7 g, 36 mmol) produced the crude imine **4-24b** as an orange oil.

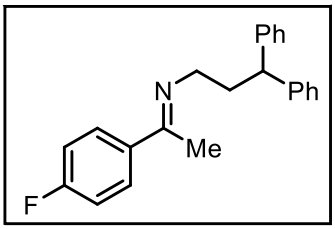

^{1}H NMR (400 MHz, CDCl$_3$): δ 7.78–7.74 (m, 2H), 7.28–7.27 (m, 8H), 7.19–7.15 (m, 2H), 7.05 (ap. t, *J* = 8.6 Hz, 2H), 4.16 (t, *J* = 7.8 Hz, 1H), 3.38 (t, *J* = 7.0 Hz, 2H), 2.51 (q, *J* = 7.3 Hz, 2H), 2.03 (s, 3H).

^{13}C{^{1}H} NMR (100 MHz, CDCl$_3$): δ 164.1, 163.8 (d, $^{1}J_{FC}$ = 249 Hz), 145.0, 137.5 ($^{4}J_{FC}$ = 2.8 Hz), 128.6, 128.1, 127.9 (d, $^{3}J_{FC}$ = 2.9 Hz), 126.3, 115.2 (d, $^{2}J_{FC}$ = 22 Hz), 50.3, 49.0, 36.7, 31.1, 15.5.

^{19}F NMR (376 MHz, CDCl$_3$): δ −112.4 (m).

HRMS (ESI): *m/z* $[M+H]^+$ calculated for $C_{23}H_{23}FN$: 332.1809 found: 332.1814.

Imine 4-24c: 4-Cyanoacetophenone (2.0 g, 14 mmol) and 3,3-diphenylpropylamine (2.9 mL, 14 mmol) produced 4.4 g of crude imine **4- 24c** as a pale orange solid.

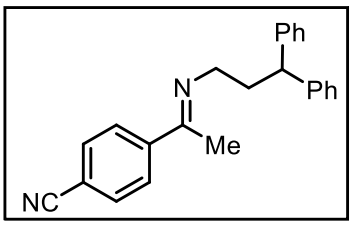

^{1}H NMR (400 MHz, CDCl$_3$): δ 7.86 (d, *J* = 8.7 Hz, 2H), 7.67 (d, *J* = 8.3 Hz, 2H), 7.29–7.27 (m, 8H), 7.20–7.16 (m, 2H), 4.16 (t, *J* = 7.8 Hz, 1H), 3.43 (t, *J* = 7.0 Hz, 2H), 2.53 (q, *J* = 7.2 Hz, 2H), 2.06 (s, 3H).

^{13}C{^{1}H} NMR (100 MHz, CDCl$_3$): δ 163.7, 145.1, 144.8, 132.2, 128.6, 128.1, 127.3, 126.4, 118.9, 113.0, 50.8, 49.0, 36.5, 15.5.

HRMS (ESI): *m/z* $[M+H]^+$ calculated for $C_{24}H_{23}N_2$: 339.1856 found: 339.1855.

Imine 4-24d: 2-Acetylnaphthalene (4.0 g, 24 mmol) and 3,3-diphenylpropylamine (5.0 g, 24 mmol) produced 7.9 g of crude imine **4-24d** as a yellow solid.

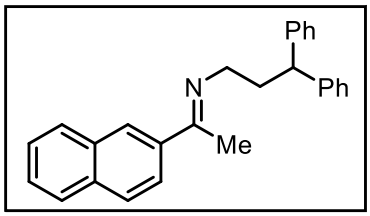

^{1}H NMR (400 MHz, CDCl$_3$): δ 8.13 (s, 1H), 8.07–8.05 (m, 1H), 7.90–7.88 (m, 1H), 7.84 (ap. d, *J* = 8.2 Hz, 2H), 7.50–7.48 (m, 2H), 7.31–7.29 (m, 8H), 7.20–7.14 (m, 2H), 4.23 (t, *J* = 7.7 Hz, 1H), 3.47 (t, *J* = 7.0 Hz, 2H), 2.58 (q, *J* = 7.5 Hz, 2H), 2.18 (s, 3H).

^{13}C{^{1}H} NMR (100 MHz, CDCl$_3$): δ 165.1, 145.1, 138.7, 134.1, 133.2, 128.9, 128.6, 128.2, 128.0, 127.8, 126.7, 126.5, 126.3, 124.4, 50.6, 49.1, 36.8, 15.6.

HRMS (ESI): *m/z* $[M+Na]^+$ calculated for $C_{27}H_{25}NNa$: 386.1879 found: 386.1884.

Imine 4-24e: 3-Methoxyacetophenone (1.8 mL, 13 mmol) and 3,3-diphenylpropylamine (2.8 g, 13 mmol) produced 4.5 g of crude imine **4-24e** as a yellow solid.

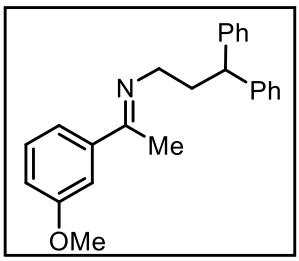

^{1}H NMR (400 MHz, $CDCl_3$): δ 7.37–7.36 (m, 1H), 7.31–7.27 (m, 9H), 7.19–7.16 (m 2H), 6.94–6.92 (m, 1H), 4.18 (t, *J* = 7.8 Hz, 1H), 3.85 (s, 3H), 3.39 (t, *J* = 7.1 Hz, 2H), 2.52 (q, *J* = 7.4 Hz, 2H), 2.04 (s, 3H).

^{13}C{^{1}H} NMR (100 MHz, $CDCl_3$): δ 165.2, 159.7, 145.0, 143.0, 129.3, 128.6, 128.2, 126.3, 119.3, 115.4, 111.9, 55.5, 50.4, 49.0, 36.7, 15.8.

HRMS (ESI): *m/z* $[M+H]^+$ calculated for $C_{24}H_{26}NO$: 344.2009 found: 344.2011.

Imine 4-24f: 3-Methylacetophenone (2.0 mL, 15 mmol) and 3,3-diphenylpropylamine (3.2 g, 15 mmol) produced 4.7 g of crude imine **4-24f** as a yellow solid.

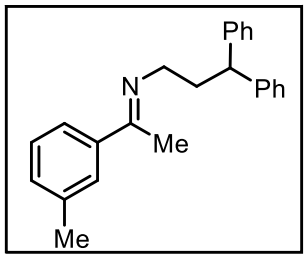

^{1}H NMR (400 MHz, $CDCl_3$): δ 7.59 (s, 1H), 7.53 (d, *J* = 7.7 Hz, 1H), 7.29–7.24 (m, 9H), 7.19–7.16 (m, 3H), 4.17 (t, *J* = 7.8 Hz, 1H), 3.39 (t, *J* = 7.2 Hz, 2H), 2.53 (q, *J* = 7.4 Hz, 2H), 2.38 (s, 3H), 2.04 (s, 3H).

^{13}C{^{1}H} NMR (100 MHz, $CDCl_3$): δ 207.1, 165.7, 145.1, 141.5, 138.0, 130.3, 128.6, 128.2, 127.3, 126.2, 123.9, 50.4, 49.1, 36.7, 31.1, 21.6, 15.8.

Imine 4-24g: 2-Acetyl-5-bromopyridine (2.0 g, 10 mmol) and 3,3-diphenylpropylamine (2.1 g, 10 mmol) produced 3.2 g of crude imine **4-24g** as a pale orange solid.

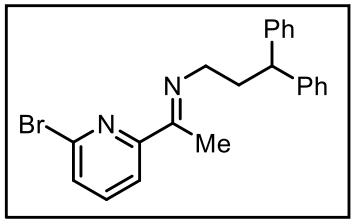

^{1}H NMR (400 MHz, $CDCl_3$): δ 8.05 (ap. d, *J* = 7.7 Hz, 1H), 7.58 (t, *J* = 7.7 Hz, 1H), 7.47 (d, *J* = 7.8 Hz, 1H), 7.31–7.27 (m, 8H), 7.21–7.16 (m, 2H), 4.16 (t, *J* = 7.8 Hz, 1H), 3.45 (t, *J* = 7.0 Hz, 2H), 2.51 (q, *J* = 7.1 Hz, 2H), 2.17 (s, 3H).

^{13}C{^{1}H} NMR (100 MHz, $CDCl_3$): δ 165.7, 159.0, 144.9, 140.7, 138.7, 128.6, 128.5, 128.1, 126.3, 119.7, 50.8, 49.1, 36.5, 14.1.

HRMS (ESI): *m/z* $[M+Na]^+$ calculated for $C_{22}H_{21}BrN_2Na$: 415.0780 found: 415.0788.

Imine 4-24h: 3-Acetyl-5-bromopyridine (2.0 g, 10 mmol) and 3,3-diphenylpropylamine (2.1 g, 10 mmol) produced 3.2 g of crude imine **4-24h** as a pale orange solid.

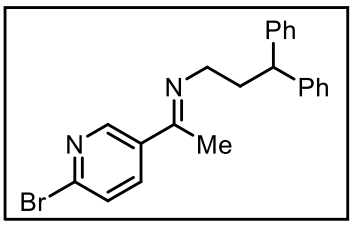

^{1}H NMR (400 MHz, CDCl$_3$): δ 8.67 (ap. d, *J* = 2.4 Hz, 1H), 7.99 (ap. dd, *J* = 8.4, 2.3 Hz, 1H), 7.49 (d, *J* = 8.4 Hz, 1H), 7.29–7.27 (m, 8H), 7.20–7.16 (m, 2H), 4.15 (t, *J* = 7.9 Hz, 1H), 3.41 (t, *J* = 6.9 Hz, 2H), 2.51 (q, *J* = 7.0 Hz, 2H), 2.05 (s, 3H).

^{13}C{^{1}H} NMR (100 MHz, CDCl$_3$): δ 161.8, 148.6, 144.8, 143.2, 136.7, 135.7, 128.6, 128.1, 127.8, 126.4, 50.5, 49.0, 36.5, 15.3.

HRMS (ESI): *m/z* $[M+Na]^+$ calculated for $C_{22}H_{21}BrN_2Na$: 415.0780 found: 415.0786.

Imine 4-24i: 3-Acetylthiophene (2.5 g, 20 mmol) and 3,3-diphenylpropylamine (4.2 g, 20 mmol) produced 5.7 g of crude imine **4-24i** as an orange solid.

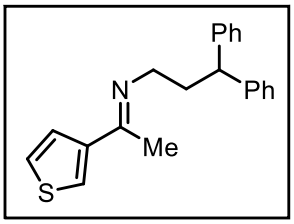

^{1}H NMR (400 MHz, CDCl$_3$): δ 7.58 (d, *J* = 5.1 Hz, 1H), 7.55–7.54 (m, 1H), 7.28–7.27 (m, 8H), 7.19–7.16 (m, 2H), 4.16 (t, *J* = 7.8 Hz, 1H), 3.37 (t, *J* = 7.0 Hz, 2H), 2.48 (q, *J* = 7.5 Hz, 2H), 2.03 (s, 3H).

^{13}C{^{1}H} NMR (100 MHz, CDCl$_3$): δ 161.0, 145.1, 128.6, 128.2, 126.7, 126.2, 125.6, 124.7, 49.9, 49.0, 36.7, 16.1.

HRMS (ESI): *m/z* $[M+H]^+$ calculated for $C_{21}H_{22}NS$: 320.1467 found: 320.1467.

Imine 4-24j: 2-Acetylthiophene (1.7 mL, 16 mmol) and 3,3-diphenylpropylamine (3.4 g, 16 mmol) produced 4.3 g of crude imine **4-24j** as an off white solid.

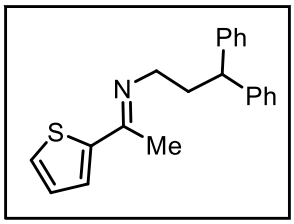

^{1}H NMR (400 MHz, CDCl$_3$): δ 7.33 (d, *J* = 5.0 Hz, 1H), 7.28–7.27 (m, 9H), 7.20–7.14 (m, 2H), 7.03–7.01 (m, 1H), 4.15 (t, *J* = 7.8 Hz, 1H), 3.37 (t, *J* = 7.0 Hz, 2H), 2.46 (q, *J* = 7.6 Hz, 2H), 2.04 (s, 3H).

^{13}C{^{1}H} NMR (100 MHz, CDCl$_3$): δ 207.1, 160.0, 148.2, 145.0, 128.6, 128.2, 127.3, 126.4, 126.2, 49.8, 48.9, 36.5, 31.1, 15.4.

HRMS (ESI): *m/z* $[M+H]^+$ calculated for $C_{21}H_{22}NS$: 320.1467 found: 320.1472.

Imine 4-24k: 2-Propionylthiophene (1.8 mL, 14 mmol) and 3,3-diphenylpropylamine (3.0 g, 14 mmol) produced 4.0 g of crude imine **4-24k** as a yellow solid.

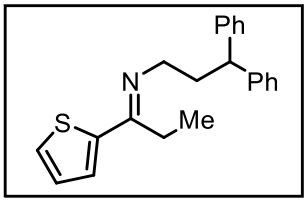

^{1}H NMR (400 MHz, $CDCl_3$): δ 7.32 (d, *J* = 4.9 Hz, 1H), 7.28–7.24 (m, 9H), 7.18–7.14 (m, 2H), 7.03–7.01 (m 1H), 4.18 (t, *J* = 7.8 Hz, 1H), 3.40 (t, *J* = 7.1 Hz, 2H), 2.51–2.43 (m, 4H), 1.01 (t, *J* = 7.8 Hz, 3H).

^{13}C{^{1}H} NMR (100 MHz, $CDCl_3$): δ 165.0, 147.2, 145.0, 128.5, 128.2, 127.3, 126.2, 126.1, 48.9, 48.8, 36.8, 22.6, 11.9.

HRMS (ESI): *m/z* $[M+H]^+$ calculated for $C_{22}H_{24}NS$: 334.1624 found: 334.1622.

Imine 4-24l: 6,7-Dihydrobenzo[b]thiophen-4(5H)-one (2.0 g, 13 mmol) and 3,3-diphenylpropylamine (2.8 g, 13 mmol) produced 4.3 g of crude imine **4-24l** as a brown solid.

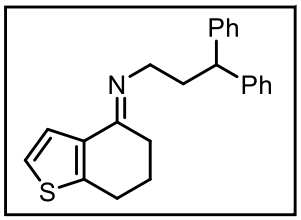

^{1}H NMR (400 MHz, $CDCl_3$): δ 7.49 (d, *J* = 5.2 Hz, 1H), 7.27–7.25 (m, 8H), 7.19–7.14 (m, 2H), 7.02 (d, *J* = 5.3 Hz, 1H), 4.14 (t, *J* = 7.7 Hz, 1H), 3.35 (t, *J* = 7.2 Hz, 2H), 2.85 (t, *J* = 6.0 Hz, 2H), 2.46 (q, *J* = 7.6 Hz, 2H), 2.28 (t, *J* = 6.5 Hz, 2H), 1.98–1.92 (m, 2H).

^{13}C{^{1}H} NMR (100 MHz, $CDCl_3$): δ 162.0, 145.1, 144.8, 137.7, 128.5, 128.2, 126.2, 125.1, 122.2, 49.0, 48.8, 36.8, 36.2, 26.2, 25.1, 23.9.

HRMS (ESI): *m/z* $[M+H]^+$ calculated for $C_{23}H_{24}NS$: 346.1624 found: 346.1624.

Imine 4-24m: 1-Tetralone (1.8 mL, 14 mmol) and 3,3-diphenylpropylamine (2.9 g, 14 mmol) produced 4.3 g of crude imine **4-24m** as a brown solid.

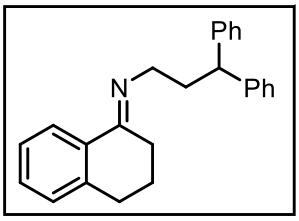

^{1}H NMR (500 MHz, $CDCl_3$): δ 8.21 (d, *J* = 7.8 Hz, 1H), 7.28–7.27 (m, 9H), 7.24–7.22 (m, 1H), 7.18–7.15 (m, 2H), 7.12 (d, *J* = 8.0 Hz, 1H), 4.21 (t, *J* = 8.0 Hz, 1H), 3.36 (t, *J* = 6.7 Hz, 2H), 2.77 (t, *J* = 6.1 Hz, 2H), 2.77 (t, *J* = 6.1 Hz, 2H), 2.52 (q, *J* = 7.1 Hz, 2H), 2.35 (t, *J* = 6.7 Hz, 2H), 1.86 (p, *J* = 6.3 Hz, 2H).

^{13}C{^{1}H} NMR (125 MHz, $CDCl_3$): δ 164.1, 160.8, 145.2, 142.2, 128.5, 128.2, 127.6, 126.2, 112.9, 112.5, 55.4, 49.0, 48.9, 37.0, 31.1, 30.3, 27.8, 22.7.

HRMS (ESI): *m/z* $[M+H]^+$ calculated for $C_{25}H_{26}N$: 340.2060 found: 340.2057.

Imine 4-24n: 2-Acetyl-5-bromothiophene (2.0 g, 9.8 mmol) and 3,3-diphenylpropylamine (2.1 g, 9.8 mmol) produced 3.8 g of crude imine **4-24n** as an orange solid.

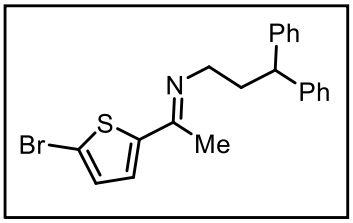

^{1}H NMR (400 MHz, CDCl$_3$): δ 7.28–7.27 (m, 8H), 7.20–7.16 (m, 2H), 7.0 (s, 2H), 4.16 (t, *J* = 8.1 Hz, 1H), 3.33 (t, *J* = 7.0 Hz, 2H), 2.44 (q, *J* = 7.0 Hz, 2H), 1.97 (s, 3H).

^{13}C{^{1}H} NMR (100 MHz, CDCl$_3$): δ 159.3, 149.8, 144.9, 130.2, 128.6, 128.2, 126.3, 116.5, 49.6, 48.8, 36.4, 14.6.

HRMS (ESI): *m/z* $[M+H]^+$ calculated for $C_{21}H_{21}BrNS$: 398.0573 found: 398.0574.

Imine 4-24r: Butyrophenone (2.0 mL, 14 mmol) and 3,3-diphenylpropylamine (2.9 g, 14 mmol) produced 3.7 g of crude imine **4-24r** as a yellow oil.

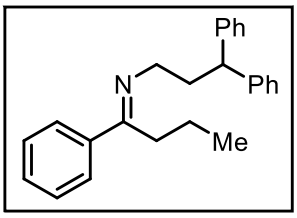

^{1}H NMR (400 MHz, CDCl$_3$): δ 7.74–7.72 (m, 2H), 7.38–7.36 (m, 3H), 7.29–7.28 (m, 8H), 7.21–7.16 (m, 4H), 4.19 (t, *J* = 7.9 Hz, 1H), 3.45 (t, *J* = 7.1 Hz, 2H), 2.53–2.46 (m, 4H), 1.39–1.33 (m, 2H), 0.82 (t, *J* = 7.1 Hz, 3H).

^{13}C{^{1}H} NMR (100 MHz, CDCl$_3$): δ 169.4, 145.0, 128.6, 128.5, 128.4, 128.2, 128.0, 127.0, 126.2, 49.8, 49.0, 37.0, 31.0, 20.5, 14.3.

HRMS (ESI): *m/z* $[M+H]^+$ calculated for $C_{25}H_{28}N$: 342.2216 found: 342.2212.

Imine 4-24t: 5-Methoxy tetralone (2.0 g, 11 mmol) and 3,3-diphenylpropylamine (2.4 g, 11 mmol) produced 3.9 g of crude imine **4-24t** as a brown powder.

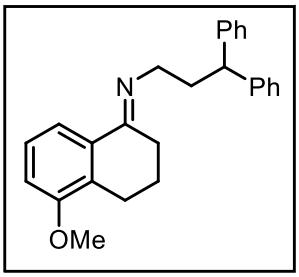

^{1}H NMR (400 MHz, CDCl$_3$): δ 8.16 (d, *J* = 8.8 Hz, 1H), 7.28–7.27 (m, 8H), 7.18–7.15 (m, 2H), 6.79 (ap. dd, *J* = 8.8, 2.6 Hz, 1H), 6.62 (ap. d, *J* = 2.4 Hz, 1H), 4.19 (t, *J* = 7.8 Hz, 1H), 3.82 (s, 3H), 3.33 (t, *J* = 7.0 Hz, 2H), 2.74 (t, *J* = 6.2 Hz, 2H), 2.50 (q, *J* = 7.4 Hz, 2H), 2.32 (t, *J* = 6.6 Hz, 2H), 1.85 (p, *J* = 6.2 Hz, 2H).

^{13}C{^{1}H} NMR (125 MHz, CDCl$_3$): δ 164.1, 160.8, 145.2, 142.2, 128.5, 128.2, 127.6, 126.2, 112.9, 112.5, 55.4, 49.0, 48.9, 37.0, 31.1, 30.3, 27.8, 22.7.

HRMS (ESI): *m/z* $[M+H]^+$ calculated for $C_{26}H_{28}NO$: 370.2165 found: 370.2163.

Imine 4-24u: 2-Fluoroacetophenone (4.4 mL, 36 mmol) and benzylamine (4.0 mL, 36 mmol) generated 7.1 g of crude imine **4-24u** as an orange liquid. The imine results in E/Z isomers leading to complex spectra.

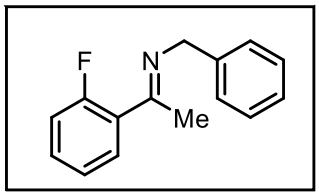

HRMS (ESI): *m/z* $[M+Na]^+$ calculated for $C_{15}H_{14}FNNa$: 250.1002 found: 250.1003.

Imine 4-24v: 4-Fluoroacetophenone (4.4 mL, 36 mmol) and benzylamine (4.0 mL, 36 mmol) generated 7.4 g of crude imine **4-24v** as an orange liquid.

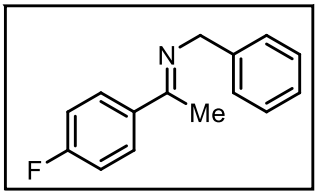

^{1}H NMR (400 MHz, $CDCl_3$): δ 7.91–7.87 (m, 2H), 7.44 (ap. d, J = 7.4 Hz, 2H), 7.37 (t, J = 7.8 Hz, 2H), 7.29–7.27 (m, 1H), 7.08 (ap. t, J = 8.8 Hz, 2H), 4.74 (s, 2H), 2.33 (s, 3H).

^{13}C{^{1}H} NMR (100 MHz, $CDCl_3$): δ 164.8, 163.9 ($^1J_{FC}$ = 249 Hz), 140.6, 137.3 (d, $^4J_{FC}$ = 3.0 Hz), 128.8 (d, ^3J = 8.7 Hz), 128.5, 127.8, 126.7, 115.2 (d, $^2J_{FC}$ = 22 Hz), 55.8, 15.8.

^{19}F NMR (376 MHz, $CDCl_3$): δ −112.0.

HRMS (ESI): *m/z* $[M+H]^+$ calculated for $C_{15}H_{15}FN$: 228.1183 found: 228.1191.

Imine 4-24w: 3-Fluoroacetophenone (4.4 mL, 36 mmol) and benzylamine (4.0 mL, 36 mmol) generated 7.2 g of crude imine **4-24w** as an orange liquid.

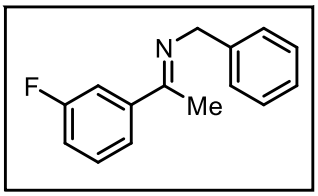

^{1}H NMR (400 MHz, $CDCl_3$): δ 7.65–7.62 (m, 2H), 7.44 (ap. d, J = 7.2 Hz, 2H), 7.39–7.35 (m, 3H), 7.28 (ap. t, J = 6.4 Hz, 1H), 4.75 (s, 2H), 2.33 (s, 3H).

^{13}C{^{1}H} NMR (100 MHz, $CDCl_3$): δ 164.7 (ap. d, $^4J_{FC}$ = 2.6 Hz), 163.0 (d, $^1J_{FC}$ = 246 Hz), 143.4 (d, $^3J_{FC}$ = 7.1 Hz), 140.4, 129.8 (d, $^3J_{FC}$ = 8.4 Hz), 128.6, 127.8, 126.8, 122.5 (d, $^4J_{FC}$ = 2.8 Hz), 116.6 (d, $^2J_{FC}$ = 22 Hz), 113.8 (d, $^2J_{FC}$ = 23 Hz), 55.9, 16.0.

^{19}F NMR (376 MHz, $CDCl_3$): δ −113.3.

HRMS (ESI): *m/z* $[M+Na]^+$ calculated for $C_{15}H_{14}FNNa$: 250.1002 found: 250.1003.

Imine 4-24x: 2-Acetylthiophene (1.7 mL, 16 mmol) and benzylamine (1.7 mL, 16 mmol) generated 4.7 g of crude imine **4-24x** as a yellow oil.

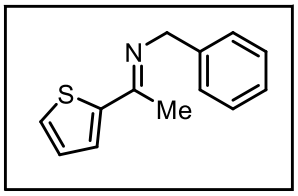

^{1}H NMR (400 MHz, $CDCl_3$): δ 7.39 (ap. d, J = Hz, 2H), 7.35–7.31 (m, 4H), 7.25–7.21 (m, 1H), 7.04–7.02 (m, 1H), 4.72 (s, 2H), 2.30 (s, 3H).

^{13}C{^{1}H} NMR (100 MHz, $CDCl_3$): δ 161.0, 148.0, 140.3, 128.9, 128.5, 127.6, 127.3, 126.9, 126.6, 55.1, 15.8.

HRMS (ESI): *m/z* $[M+H]^+$ calculated for $C_{13}H_{14}NS$: 216.0841 found: 216.0845.

Imine 4-24y: Acetophenone (5.4 mL, 47 mmol) and benzylamine (5.1 mL, 47 mmol) generated 7.8 g of crude imine **4-24y** as yellow liquid.

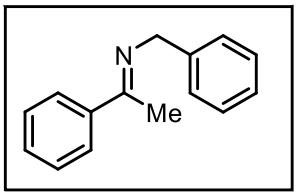

^{1}H NMR (400 MHz, CDCl$_3$): δ 7.88–7.85 (m, 2H), 7.44–7.33 (m, 8H), 4.74 (s, 2H), 2.33 (3H).

^{13}C{^{1}H} NMR (100 MHz, CDCl$_3$): δ 166.1, 140.7, 129.7, 128.5, 128.3, 127.8, 126.9, 126.7, 55.8, 16.0.

HRMS (ESI): *m/z* $[M+H]^+$ calculated for $C_{15}H_{16}N$: 210.1277 found: 210.1279.

Imine 4-24z: Indanone (2.0 g, 15 mmol) and 1,1-diphenylmethylamine (2.6 mL, 15 mmol) generated 3.9 g of crude imine **4-24z** as a dark red solid.

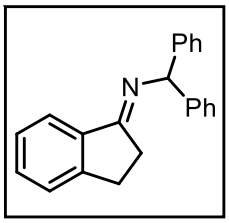

^{1}H NMR (400 MHz, CDCl$_3$): δ 8.00 (d, *J* = 7.5 Hz, 1H), 7.47–7.45 (m, 4H), 7.40–7.36 (m, 1H), 7.32–7.28 (m, 6H), 7.22–7.18 (m, 2H), 5.68 (s, 1H), 3.07–3.04 (m, 2H), 2.79–2.75 (m, 2H).

^{13}C{^{1}H} NMR (100 MHz, CDCl$_3$): δ 173.8, 149.7, 144.9, 131.3, 128.5, 127.8, 127.0, 126.8, 125.6, 123.0, 70.2, 28.6, 28.4.

HRMS (ESI): *m/z* $[M+H]^+$ calculated for $C_{22}H_{20}N$: 298.1590 found: 298.1589.

Imine 4-24ab: 2-Acetylthiophene (1.7 mL, 16 mmol) and 1,1-diphenylmethylamine (2.7 mL, 16 mmol) generated crude imine as **4-24ab** an off-white solid.

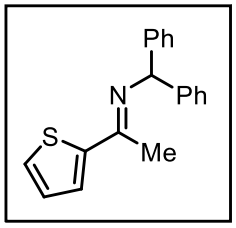

^{1}H NMR (400 MHz, CDCl$_3$): δ 7.46–7.44 (m, 4H), 7.35 (d, *J* = 5.1 Hz, 1H), 7.33–7.22 (m, 5H), 7.19 (ap. t, *J* = 7.3 Hz, 2H), 7.03–7.01 (m, 1H), 5.79 (s, 1H), 2.29 (s, 3H).

^{13}C{^{1}H} NMR (100 MHz, CDCl$_3$): δ 159.3, 144.9, 129.1, 128.6, 127.6, 127.3, 126.9, 67.9, 16.0.

HRMS (ESI): *m/z* $[M+Na]^+$ calculated for $C_{19}H_{17}NNaS$: 314.0978 found: 314.0974.

Imine 4-24ad: Indanone (2.0 g, 15 mmol) and 2-thiopheneethanamine (1.8 mL, 15 mmol) generated 3.4 g of crude imine **4-24ad** as a brown oil.

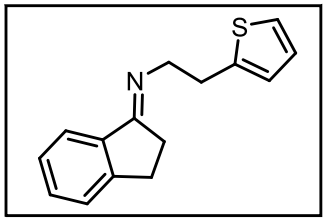

^{1}H NMR (400 MHz, CDCl$_3$): δ 7.84 (d, *J* = 7.6 Hz, 1H), 7.41–7.37 (m, 1H), 7.34–7.28 (m, 2H), 7.12–7.11 (m, 1H), 6.93–6.90 (m, 1H), 6.87 (m, 1H), 3.73 (t, *J* = 7.4 Hz, 2H), 3.29 (t, *J* = 7.4 Hz, 2H), 3.06–3.03 (m, 2H), 2.62–2.59 (m, 2H).

$^{13}C\{^1H\}$ NMR (100 MHz, $CDCl_3$): δ 174.8, 149.6, 143.1, 139.7, 131.1, 127.0, 126.6, 125.6, 124.9, 123.5, 122.3, 55.4, 31.5, 28.2.

HRMS (ESI): *m/z* $[M+H]^+$ calculated for $C_{15}H_{16}NS$: 242.0998 found: 242.0999.

Imine 4-24ae: Indanone (2.0 g, 15 mmol) and 2-thiophenemethylamine (1.6 mL, 15 mmol) generated 3.3 g of crude imine **4-24ae** as a red solid.

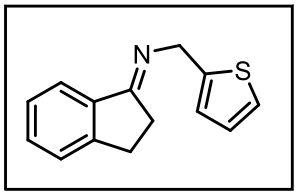

^1H NMR (400 MHz, $CDCl_3$): δ 7.89 (d, *J* = 7.7 Hz, 1H), 7.42–7.28 (m, 3H), 7.22–7.20 (m, 1H), 7.01–6.97 (m, 2H), 4.86 (s, 2H), 3.14–3.11 (m, 2H), 2.83–2.79 (m, 2H).

$^{13}C\{^1H\}$ NMR (100 MHz, $CDCl_3$): δ 175.7, 149.9, 143.8, 131.5, 127.1, 126.8, 125.7, 124.2, 124.2, 122.8, 52.6, 28.5, 28.3.

HRMS (ESI): *m/z* $[M+H]^+$ calculated for $C_{14}H_{14}NS$: 228.0841 found: 228.0843.

Imine 4-24af: Indanone (2.0 g, 15 mmol) and furfurylamine (1.3 mL, 15 mmol) generated 2.8 g of crude imine **4-24af** as a brown solid.

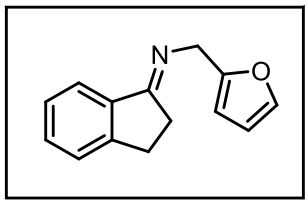

^1H NMR (400 MHz, $CDCl_3$): δ 7.86 (d, *J* = 7.7 Hz, 1H), 7.42–7.34 (m, 3H), 7.30–7.28 (1H), 6.34–6.33 (m, 1H), 6.28–6.27 (m, 1H), 4.66 (s, 2H), 3.14–3.11 (m, 2H), 2.86–2.83 (m, 2H).

$^{13}C\{^1H\}$ NMR (100 MHz, $CDCl_3$): δ 176.5, 153.6, 149.9, 141.9, 131.5, 127.1, 125.7, 122.8, 110.4, 106.8, 50.8, 28.4, 28.3.

HRMS (ESI): *m/z* $[M+H]^+$ calculated for $C_{14}H_{14}NS$: 212.1070 found: 212.1071.

Imine 4-24ag: Indanone (2.0 g, 15 mmol) and 2-picolylamine (1.6 mL, 15 mmol) generated 3.2 g of crude imine **4-24ag** as a brown solid.

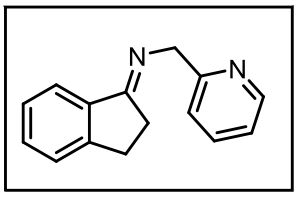

^1H NMR (400 MHz, $CDCl_3$): δ 8.56 (ap. d, *J* = 4.8 Hz, 1H), 7.91 (d, *J* = 7.5 Hz, 1H), 7.71–7.67 (m, 1H), 7.61 (ap. d, *J* = 7.8 Hz, 1H), 7.43–7.35 (m, 2H), 7.31 (ap. t, *J* = 7.3 Hz, 1H), 7.18–7.15 (m, 1H), 4.84 (s, 2H), 3.14–3.11 (m, 2H), 2.84–2.81 (m, 2H).

$^{13}C\{^1H\}$ NMR (100 MHz, $CDCl_3$): δ 176.2, 149.2, 136.8, 131.5, 127.1, 125.8, 122.7, 122.1, 121.9, 59.3, 28.8, 28.3.

HRMS (ESI): *m/z* $[M+H]^+$ calculated for $C_{15}H_{15}N_2$: 223.1230 found: 223.1234.

Imine 4-24ah: Indanone (2.0 g, 15 mmol) and cyclohexylamine (1.7 mL, 15 mmol) generated 2.5 g of crude imine **4-24ah** as a deep red oil.

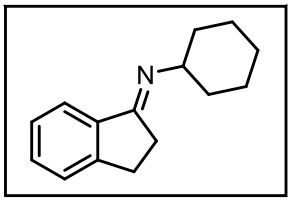

^{1}H NMR (400 MHz, $CDCl_3$): δ 7.84 (d, *J* = 7.7 Hz, 1H), 7.37–7.30 (m, 2H), 7.26 (ap. t, *J* = 6.0 Hz, 1H), 3.36–3.30 (m, 1H), 3.08–3.05 (m, 2H), 2.76–2.73 (m, 2H), 1.85–1.82 (m, 2H), 1.74–1.67 (m, 3H), 1.60–1.52 (m, 2H), 1.40–1.28 (m, 3H).

^{13}C{^{1}H} NMR (100 MHz, $CDCl_3$): δ 171.4, 149.4, 140.3, 130.9, 126.9, 125.6, 122.7, 62.3, 33.7, 28.3, 27.6, 25.9, 25.2.

HRMS (ESI): *m/z* $[M+H]^+$ calculated for $C_{15}H_{20}N$: 214.1590 found: 214.1594.

Imine 4-24ai: Indanone (2.0 g, 15 mmol) and cyclopropylamine (1.1 mL, 15 mmol) generated 2.5 g of crude imine **4-24ai** as a deep red solid.

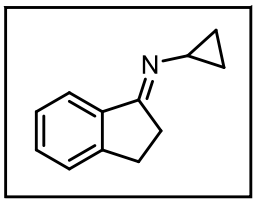

^{1}H NMR (400 MHz, $CDCl_3$): δ 7.74 (d, *J* = 7.6 Hz, 1H), 7.36–7.31 (m, 2H), 7.26–7.22 (m, 1H), 3.11–3.08 (m, 2H), 2.99–2.93 (m, 1H), 2.89–2.86 (m, 2H), 0.91 (d, *J* = 5.2 Hz, 4H).

^{13}C{^{1}H} NMR (100 MHz, $CDCl_3$): δ 173.0, 149.0, 140.0, 130.7, 126.9, 125.6, 122.2, 35.7, 28.6, 28.3, 8.7.

HRMS (ESI): *m/z* $[M+H]^+$ calculated for $C_{12}H_{14}N$: 172.1119 found: 172.1121.

Imine 4-24aj: Indanone (2.0 g, 15 mmol) and isobutylamine (1.5 mL, 15 mmol) generated 2.2 g of crude imine **4-24aj** as a brown oil.

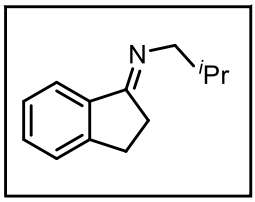

^{1}H NMR (400 MHz, $CDCl_3$): δ 7.82 (d, *J* = 7.6 Hz, 1H), 7.39–7.32 (m, 2H), 7.29–7.27 (m, 1H), 3.27 (d, *J* = 6.9 Hz, 2H), 3.09–3.05 (m, 2H), 2.70–2.67 (m, 2H), 2.12–2.02 (m, 1H), 1.00 (d, *J* = 6.7 Hz, 6H).

^{13}C{^{1}H} NMR (100 MHz, $CDCl_3$): δ 173.5, 149.5, 130.9, 127.0, 125.7, 122.4, 62.0, 30.1, 28.3, 21.1.

HRMS (ESI): *m/z* $[M+H]^+$ calculated for $C_{13}H_{18}N$: 188.1434 found: 188.1436.

4.5.4 Experimental Procedure and Tabulated Data for Selected Imine Reductions

General Reduction Conditions: Imine (0.64 mmol, 1.0 equiv.) was weighed into a 4-dram vial and secondary phosphine oxide (0.007g, 0.03 mmol, 0.025 equiv.) was weighed into a 1-dram vial on the benchtop and brought into the glovebox. The secondary phosphine oxide was dissolved in 2 mL of tetrahydrofuran and transferred to the vial containing the imine (the 1-dram vial was further rinsed with an additional 2 mL of tetrahydrofuran to

complete the transfer). Then HBpin (0.18 mL, 1.27 mmol, 2.0 equiv.) was dispensed into the reaction solution.

Amine 4-23a: Prepared according to the general procedure with imine **4-22a**. Purification by flash chromatography (Et_2O/Hex/NEt_3 10:89:1 v/v) provided **4-23a** (125 mg, 62% yield) as a yellow oil. Spectral data was in agreement with literature values.[9]

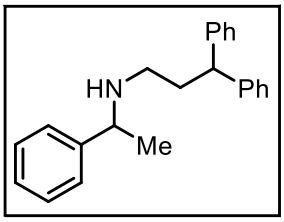

^{1}H NMR (500 MHz, $CDCl_3$): δ 7.34 (m, 14H), 4.02 (t, *J* = 7.8 Hz, 1H), 3.72 (q, *J* = 6.6 Hz, 1H), 2.56–2.43 (m, 2H), 2.31–2.19 (m, 2H), 1.33 (d, *J* = 6.6 Hz, 3H), 1.28 (br. s, 1H).

^{13}C{^{1}H} NMR (125 MHz, $CDCl_3$): δ 145.9, 145.1, 144.8, 128.5, 128.5, 128.0, 127.9, 126.9, 126.6, 126.2, 58.3, 49.1, 46.1, 36.2, 24.5.

The enantiomeric excess was determined by HPLC on a Chiralpak AD-H column with a 99.5:0.5 Hexane(1.0% $CyNH_2$):^{i}PrOH mobile phase at a 0.9 mL/min flow rate. t_{major}= 8.652 min, t_{min}= 9.355 min. Enantiomeric ratio= 96:4.

Amine 4-23d: Prepared according to the general procedure with imine **4-22d**. Purification by flash chromatography (Et_2O/Hex/NEt_3 10:89:1 v/v) provided **4-23d** (88 mg, 62% yield) as a yellow oil. Spectral data was in agreement with literature values.[8]

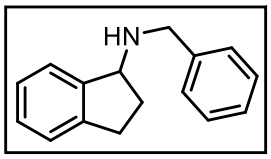

^{1}H NMR (500 MHz, $CDCl_3$): δ 7.43–7.40 (m, 3H), 7.37–7.34 (m, 2H), 7.29–7.22 (m, 4H), 4.33 (t, *J* = 6.7 Hz, 1H), 3.94 (ap. q, *J* = 10.2 Hz, 2H), 3.07–3.02 (m, 1H), 2.88–2.81 (m, 1H), 2.49–2.43 (m, 1H), 1.95–1.88 (m, 1H), 1.57 (br. s, 1H).

^{13}C{^{1}H} NMR (125 MHz, $CDCl_3$): δ 145.5, 143.8, 140.9, 128.5, 128.3, 127.5, 127.0, 126.4, 124.9, 124.3, 62.9, 51.6, 33.8, 30.6.

HRMS (ESI): *m/z* $[M+H]^+$ calculated for $C_{16}H_{18}N$: 224.1434 found: 224.1438.

The enantiomeric excess was determined by HPLC on a Chiralpak AD-H column with a 95:5 Hexane(0.1% $CyNH_2$):^{i}PrOH mobile phase at a 0.9 mL/min flow rate. t_{major}= 5.931 min, t_{min}= 6.719 min. Enantiomeric ratio= 95:5.

Amine 4-23f: Prepared according to the general procedure with imine **4-22f**. Purification by flash chromatography (Et_2O/Hex/NEt_3 20:79:1 v/v) provided **4-23f** (213 mg, 97% yield) as a yellow oil.

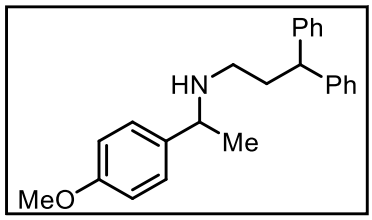

^{1}H NMR (500 MHz, $CDCl_3$): δ 7.25–7.13 (m, 12H), 6.82 (ap. d, *J* = 8.7 Hz, 2H), 3.97 (t, *J* = 7.9 Hz, 1H), 3.79 (s, 3H), 3.63 (q, *J* = 6.6 Hz, 1H), 2.49–2.39 (m, 2H), 2.27–2.13 (m, 2H), 1.27 (d, *J* = 6.6 Hz, 3H).

$^{13}C\{^1H\}$ NMR (125 MHz, $CDCl_3$): δ 158.6, 145.1, 144.9, 138.0, 128.5, 128.0, 127.9, 127.6, 126.2, 126.2, 113.8, 57.6, 55.4, 49.2, 46.1, 36.2, 24.5.

HRMS (ESI): *m/z* $[M+H]^+$ calculated for $C_{24}H_{28}NO$: 346.2165 found: 346.2167.

The enantiomeric excess was determined by HPLC on a Chiralpak AD-H column with a 95:5 Hexane(0.1% $CyNH_2$):^{i}PrOH mobile phase at a 0.9 mL/min flow rate. t_{major}= 9.584 min, t_{min}= 8.877 min. Enantiomeric ratio= 93:7.

Amine 4-25c: Prepared according to the general procedure with imine **4-24c**. Purification by flash chromatography (Et_2O/Hex/NEt_3 50:49:1 v/v) provided **4-25c** (151 mg, 70% yield) as a pale-yellow oil.

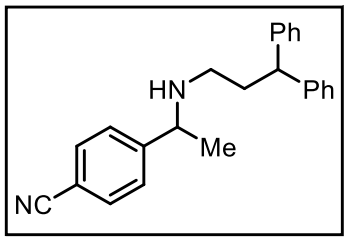

^1H NMR (500 MHz, $CDCl_3$): δ 7.54 (ap. d, *J* = 8.4 Hz, 2H), 7.33 (ap. d, *J* = 8.2 Hz, 2H), 7.27–7.18 (m, 10H), 4.00 (t, *J* = 7.9 Hz, 1H), 3.73 (q, *J* = 6.6 Hz, 1H), 2.50–2.44 (m, 1H), 2.37–2.32 (m, 1H), 2.26–2.14 (m, 2H), 1.27 (d, *J* = 6.6 Hz, 3H).

$^{13}C\{^1H\}$ NMR (125 MHz, $CDCl_3$): δ 144.9, 144.5, 132.4, 128.6, 128.0, 127.8, 127.5, 119.2, 110.6, 58.2, 49.0, 46.1, 36.1, 24.5.

HRMS (ESI): *m/z* $[M+H]^+$ calculated for $C_{24}H_{25}N_2$: 341.2012 found: 341.2011.

The enantiomeric excess was determined by HPLC on a Chiralpak AD-H column with a 95:5 Hexane(0.1% $CyNH_2$):^{i}PrOH mobile phase at a 0.9 mL/min flow rate. t_{major}= 16.810 min, t_{min}= 15.475 min. Enantiomeric ratio= 90:10.

Amine 4-25e: Prepared according to the general procedure with imine **4-24e**. Purification by flash chromatography (Et_2O/Hex/NEt_3 20:79:1 v/v) provided **4-25e** (182 mg, 83% yield) as a yellow oil.

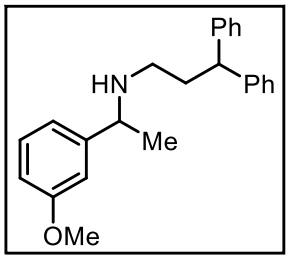

^1H NMR (500 MHz, $CDCl_3$): δ 7.25–7.13 (m, 11H), 6.82–6.80 (m, 2H), 6.77–6.74 (m, 1H), 3.97 (t, *J* = 7.8 Hz, 1H), 3.79 (s, 3H), 3.65 (q, *J* = 6.6 Hz, 1H), 2.49–2.43 (m, 2H), 2.26–2.17 (m, 2H), 1.28 (d, *J* = 6.6 Hz, 3H).

$^{13}C\{^1H\}$ NMR (125 MHz, $CDCl_3$): δ 159.9, 147.8, 145.1, 144.9, 129.5, 128.6, 128.0, 127.9, 126.3, 119.0, 112.2, 122.2, 58.3, 55.3, 49.2, 46.2, 36.3, 24.5.

HRMS (ESI): *m/z* $[M+H]^+$ calculated for $C_{24}H_{28}NO$: 346.2165 found: 346.2165.

The enantiomeric excess was determined by HPLC on a Chiralpak AD-H column with a 95:5 Hexane(0.1% $CyNH_2$):^{i}PrOH mobile phase at a 0.9 mL/min flow rate. t_{major}= 8.257 min, t_{min}= 7.567 min. Enantiomeric ratio= 88:12.

Amine 4-25f: Prepared according to the general procedure with imine **4-24f**. Purification by flash chromatography (Et_2O/Hex/NEt_3 20:79:1 v/v) provided **4-25f** (164 mg, 78% yield) as a yellow oil.

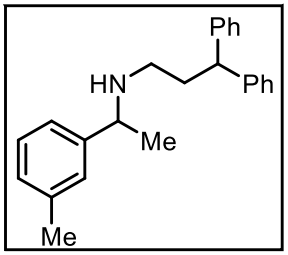

^{1}H NMR (500 MHz, $CDCl_3$): δ 7.26–7.14 (m, 11H), 7.05–7.03 (m, 3H), 3.98 (t, *J* = 7.8 Hz, 1H), 3.65 (q, *J* = 6.5 Hz, 1H), 2.50–2.41 (m, 2H), 2.33 (s, 3H), 2.27–2.19 (m, 2H), 1.29 (d, *J* = 6.6 Hz, 3H).

^{13}C{^{1}H} NMR (125 MHz, $CDCl_3$): δ 145.9, 145.2, 144.9, 138.0, 128.5, 128.4, 128.0, 127.9, 127.7, 127.3, 126.2, 126.2, 123.7, 58.2, 49.2, 46.2, 36.2, 24.5, 21.2.

HRMS (ESI): *m/z* $[M+H]^+$ calculated for $C_{24}H_{28}N$: 330.2216 found: 330.2214.

The enantiomeric excess was determined by HPLC on a Chiralpak AD-H column with a 93:7 Hexane(1.0% $CyNH_2$):^{i}PrOH mobile phase at a 0.9 mL/min flow rate. t_{major}= 5.616 min, t_{min}= 5.302 min. Enantiomeric ratio= 90:10.

Amine 4-25i: Prepared according to the general procedure with imine **4-24i**. Purification by flash chromatography (Et_2O/Hex/NEt_3 20:79:1 v/v) provided **4-25i** (132 mg, 65% yield) as a pale-yellow oil.

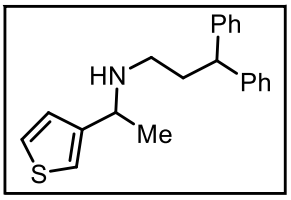

^{1}H NMR (500 MHz, $CDCl_3$): δ 7.27–7.16 (m, 11H), 6.99 (br. s, 2H), 3.99 (t, *J* = 7.8 Hz, 1H), 3.81 (q, *J* = 6.4 Hz, 1H), 2.52–2.48 (m, 2H), 2.25–2.17 (m, 2H), 1.31 (d, *J* = 6.5 Hz, 3H).

^{13}C{^{1}H} NMR (125 MHz, $CDCl_3$): δ 147.3, 145.1, 144.9, 128.6, 128.0, 127.9, 126.3, 126.2, 125.7, 120.2, 53.7, 49.2, 46.1, 36.2, 23.5.

HRMS (ESI): *m/z* $[M+H]^+$ calculated for $C_{21}H_{24}NS$: 322.1624 found: 322.1628.

The enantiomeric excess was determined by HPLC on a Chiralpak AD-H column with a 99:1 Hexane(0.1% $CyNH_2$):^{i}PrOH mobile phase at a 0.9 mL/min flow rate. t_{major}= 12.836 min, t_{min}= 14.049 min. Enantiomeric ratio= 91:9.

Amine 4-25k: Prepared according to the general procedure with imine **4-24k**. Purification by flash chromatography (Et_2O/Hex/NEt_3 10:89:1 v/v) provided **4-25k** (200 mg, 94% yield) as a pale-yellow oil.

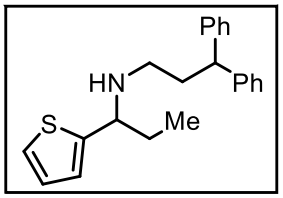

^{1}H NMR (500 MHz, $CDCl_3$): δ 7.28–7.14 (m, 11H), 6.91–6.89 (m, 1H), 6.81–6.80 (m, 1H), 3.99 (t, *J* = 7.9 Hz, 1H), 3.73–3.69 (m, 1H), 2.58–2.46 (m, 2H), 2.24–2.17 (m, 2H), 1.77–1.71 (m, 1H), 1.67–1.59 (m, 1H), 0.83 (t, *J* = 7.2 Hz, 3H).

^{13}C{^{1}H} NMR (125 MHz, $CDCl_3$): δ 149.5, 145.1, 145.0, 128.6, 128.0, 127.9, 126.3, 126.3, 124.3, 123.8, 60.5, 49.1, 45.9, 36.1, 31.7, 10.9.

HRMS (ESI): *m/z* $[M+H]^+$ calculated for $C_{22}H_{26}NS$: 336.1780 found: 336.1783.

The enantiomeric excess was determined by HPLC on a Chiralpak AD-H column with a 99:1 Hexane(0.1% $CyNH_2$):^{i}PrOH mobile phase at a 0.9 mL/min flow rate. t_{major}= 8.630 min, t_{min}= 9.400 min. Enantiomeric ratio= 93:7.

Amine 4-15l: Prepared according to the general procedure with imine **4-24l**. Purification by flash chromatography (Et_2O/Hex/NEt_3 20:79:1 v/v) provided **4-25l** (198 mg, 89% yield) as a colourless oil.

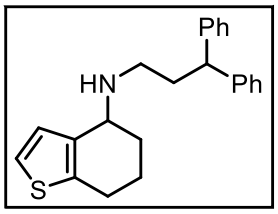

^{1}H NMR (500 MHz, $CDCl_3$): δ 7.30–7.25 (m, 8H), 7.20–7.16 (m, 2H), 7.04 (d, *J* = 5.2 Hz, 1H), 6.89 (d, *J* = 5.2 Hz, 1H), 4.10 (t, *J* = 8.1 Hz, 1H), 3.68 (ap. t, *J* = 5.4 Hz, 1H), 2.81–2.62 (m, 4H), 2.29–2.24 (m, 2H), 1.97–1.90 (m, 1H), 1.86–1.80 (m, 1H), 1.78–1.71 (m, 1H), 1.67–1.61 (m, 1H).

^{13}C{^{1}H} NMR (125 MHz, $CDCl_3$): δ 145.1, 145.0, 138.6, 137.6, 128.6, 128.0, 128.0, 127.0, 126.3, 122.0, 53.3, 49.1, 45.6, 36.5, 29.1, 25.2, 20.6.

HRMS (ESI): *m/z* $[M+H]^+$ calculated for $C_{23}H_{26}NS$: 348.1780 found: 348.1779.

The enantiomeric excess was determined by HPLC on a Chiralpak AD-H column with a 95:5 Hexane(0.1% $CyNH_2$):^{i}PrOH mobile phase at a 0.9 mL/min flow rate. t_{major}= 6.239 min, t_{min}= 7.598 min. Enantiomeric ratio= 93:7.

Chapter 5 Conclusion

5.1 Summary

In summary, this thesis has detailed the syntheses of many unsuccessful and successful attempts to generate a library of diazaphospholenes with variable structural differences. The goal was to synthesize a DAP that could outcompete or obtain complementary reactivity to the current best DAP catalyst **1-28**. The library of alternative DAPs contained varying substituents in the alkyl, aryl, and backbone positions. Originally, the hypothesis was that varying the substituents in the aryl and alkyl positions would be the most straightforward and have the biggest impact. That required the development of a robust synthetic route to obtain enantiopure chiral amines that were not commercially available. Due to ease of synthesis, heterocyclic analogues to replace the naphthyl group in the aryl position was the original goal.

Initially, this led to the successful synthesis of six enantiopure chiral amines, **2-21a** to **2-21f**, via Ellman chemistry (Scheme 5-1). Ellman chemistry provided a robust approach to chiral amines, via the formation of diastereomers, **2-20a** to **2-20f**, although often challenging all diastereomers were separable by column chromatography. The amines were generated from one of two synthetic routes, categorized as a lithiation (Scheme 5-1A) or a Grignard addition (Scheme 5-1B). For one variant in this cluster, the alkyl group was changed to a *tert*-butyl substituent in place of the typical methyl substituent in addition to the heterocyclic aryl group.

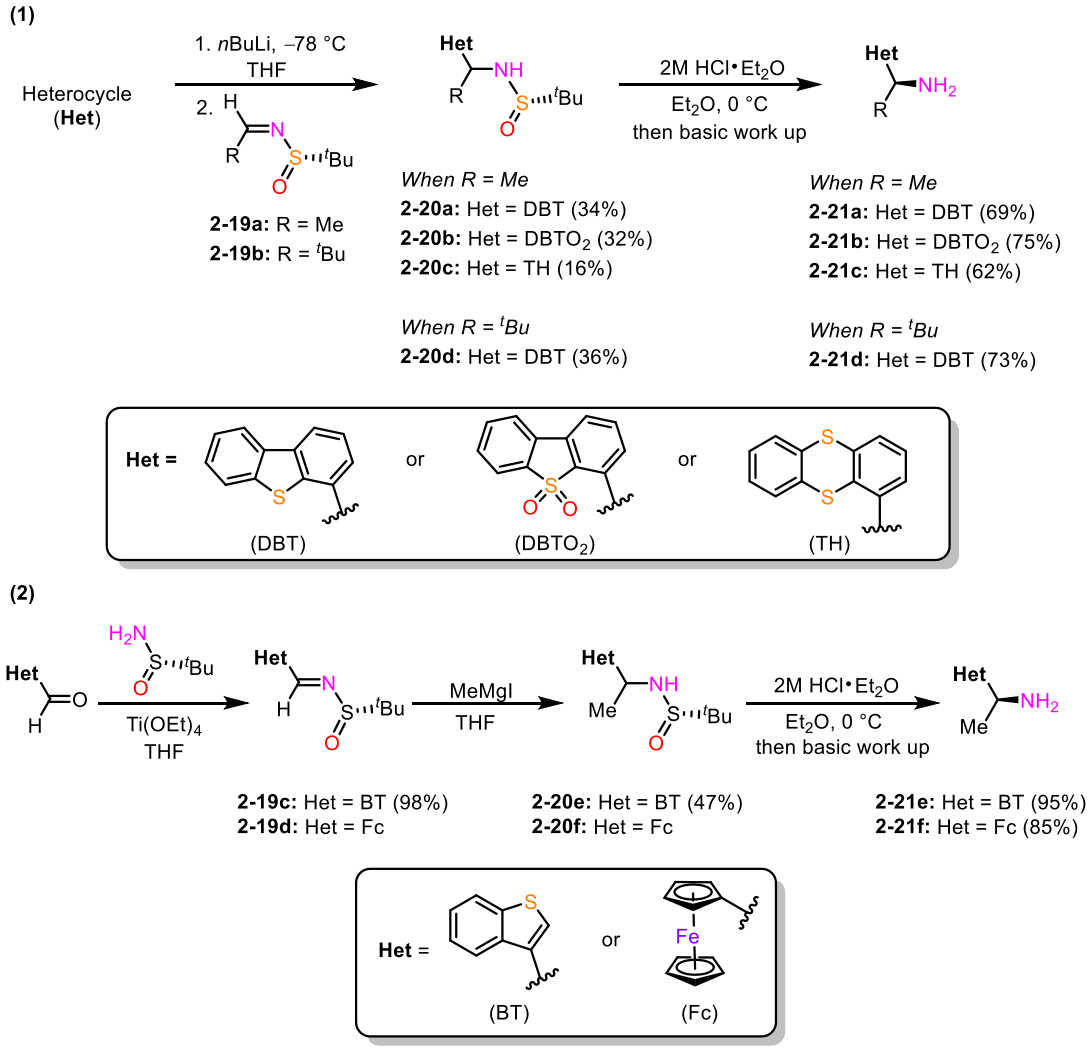

Scheme 5-1. Synthesis of heterocyclic containing chiral amines (1) via lithiation (2) via Grignard addition.

The results of the heterocyclic containing DAPs inspired the idea of accessing alternative substitution patterns for the DBT motif. Accessing the enantiopure amine in the 1-substituted position of DBT resulted in the development of an efficient synthetic route to obtain 1-substituted DBT derivatives. A one-pot cascade reaction starting with 2-fluorothiophenol was developed (Scheme 5-2). Thiophenol **3-1** reacted with a benzyne intermediate, generated from *n*BuLi and 1,2-dibromobenzene, to form **3-1Li**, that was quenched with DMF to obtain the desired aldehyde, **3-6**. The aldehyde was the starting

material that successfully converted to the desired amine **3-17** with the Ellman method via Grignard addition. In this case an ethyl Grignard was used which results in an ethyl substituent in the alkyl position of the corresponding DAP. Ethyl Grignard was used instead of the methyl Grignard because the resulting diastereomers **3-16a** and **3-16b** (not shown) were separable by column chromatography to generate one enantiopure amine **3-17**. When the methyl Grignard was used it resulted in inseparable diastereomers.

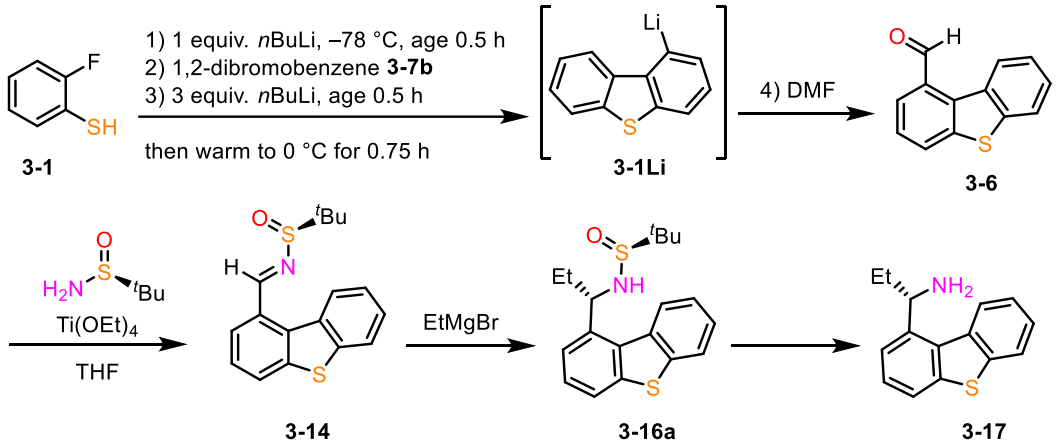

Scheme 5-2. Synthesis of enantiopure amine with 1-substituted DBT motif.

The other non-commercially available heterocyclic derivative of interest was a naphthothiophene (NTT) containing amine. The synthesis was done in collaboration with Emily Burke (MSc candidate). Emily developed a synthesis to access 3-bromonaphthothiophene, **3-31**, which I used as a starting material to synthesize the desired enantiopure amine **3-34**, once again using the Ellman chemistry (Scheme 5-3). The lithiation method was used to generate amine **3-34** from **3-31**. The end result was the same as the previously reported lithiation method, however there is a slight difference in reactivity of the starting heterocycle as there was a bromo-substituent. *n*BuLi undergoes a rapid halogen exchange when a bromine is present rather than the typical deprotonation. The lithiated intermediate **3-31Li** was quenched with Ellman imine **3-32** to generate the

diastereomers **3-33a** and **3-33b** then purified by column chromatography. The diastereomerically pure Ellman amine **3-33a** was treated with dilute acid followed by a base wash to isolate the desired enantiopure amine **3-34**.

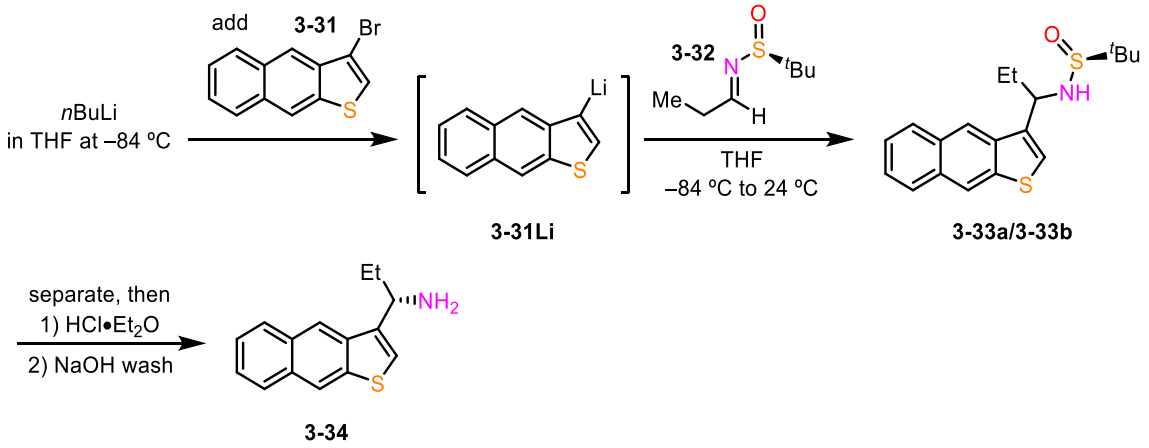

Scheme 5-3. Synthesis of enantiopure amine containing NTT motif.

In total, there were eight enantiopure amines with heterocyclic containing aryl groups with various alkyl side chains that were converted to the corresponding diimines then attempted to be cyclized with PBr_3 and cyclohexene. In the cases that were successful, the products were subsequently transformed to the corresponding cationic diazaphospholenes (Scheme 5-4). The formation of the diimines, **2-22a** to **2-22f**, **3-18**, and **3-35**, were all successful. The cyclization step with PBr_3/cyclohexene was not always successful as shown by DAP-Br **2-23a**, **2-23c**, **2-23e**, and **3-36**. There were four successfully synthesized DAP-OTfs as shown by **2-24a**, **2-24c**, **2-24e**, and **3-37**.

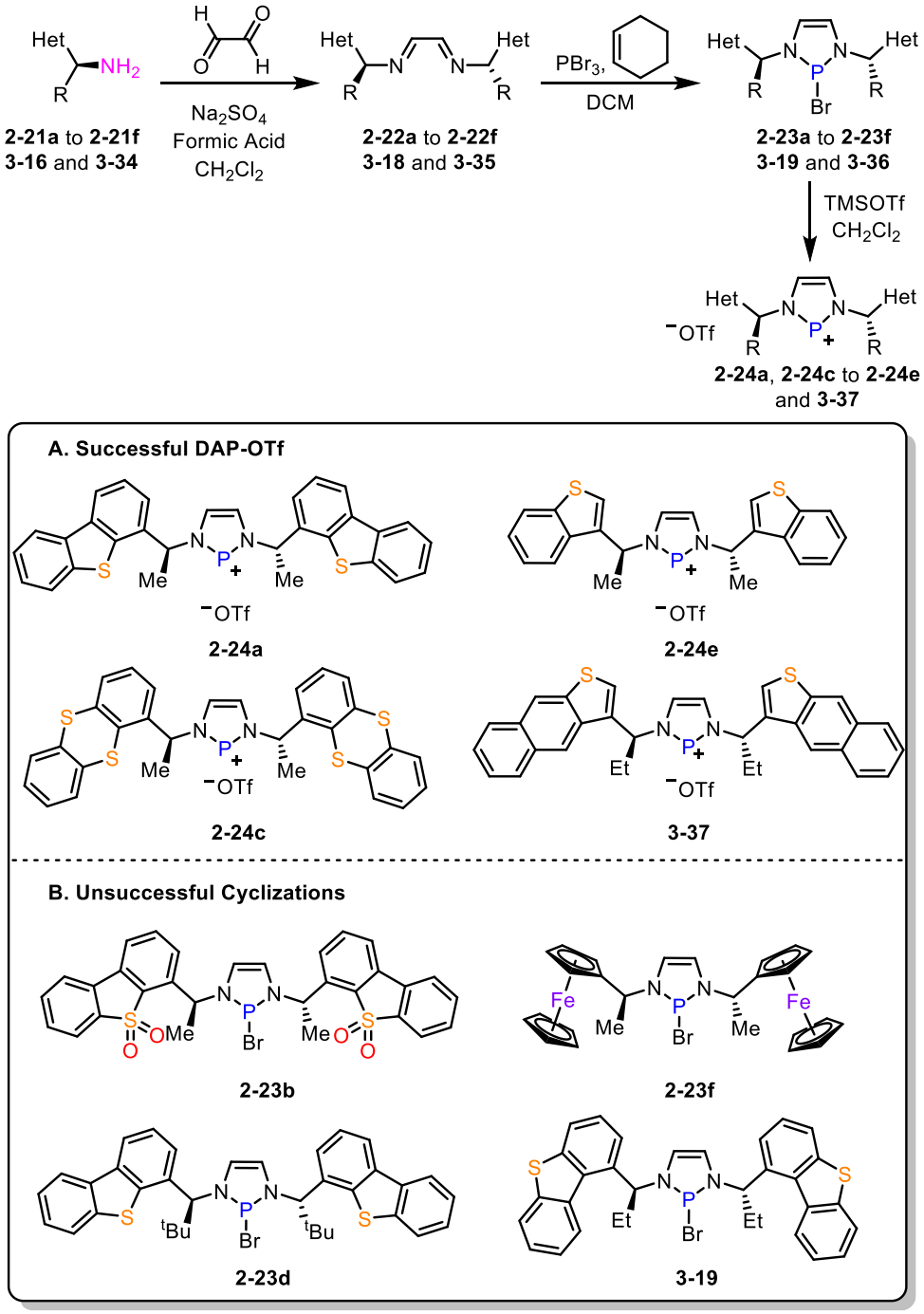

Scheme 5-4. Successful and unsuccessful syntheses of heterocyclic containing DAPs.

For the successful synthesis of heterocyclic containing DAP-OTfs, the reactivity and enantioselectivity was tested. Only one had comparable results to the current best diazaphospholene (Scheme 5-5). Using DAP-OTf **2-24e** as a catalyst, the *e.r.* of the

benchmark substrate was 91:9, leading to the synthesis and reactivity of DAP-OTf **2-24e** being published.

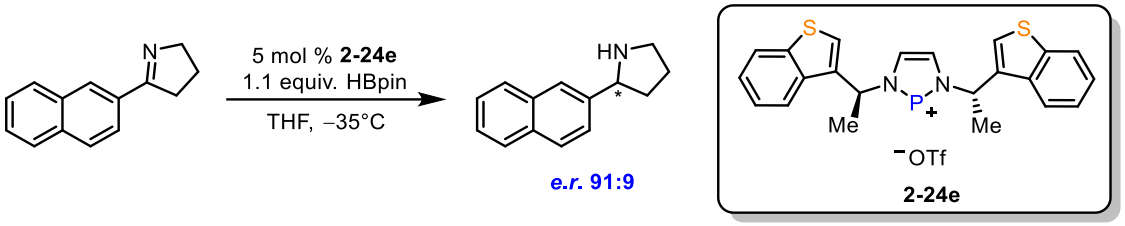

Scheme 5-5. Reduction of benchmark substrate with DAP **2-24e**.

It is evident alternate side chains require a lot of synthesis before the selectivity can be tested and often, the enantioinduction was worse than the current best diazaphospholene. Ultimately, there was minimal success with altering the side chain and even with switching the aryl groups to heterocyclic analogues for "ease of synthesis", and there were still many challenges encountered along the way. This work required developing more efficient synthesis for the heterocycles relative to what was reported in the literature to access certain motifs of interest. More interestingly, the most successful analogue, in terms of synthesis and reactivity, contained a methyl substituent in the backbone.

Synthesizing the DAP with a methyl substituted backbone requires only four steps (Scheme 5-6), which is just one additional step relative to the synthesis of the current best DAP. First the diimine was synthesized from the commercially available enantiopure amine and glyoxal to form **4-10a**. Then the diisopropylaminodichlorophosphine **4-6a** underwent halide abstraction to form the phosphenium **4-7a**, the diimine was added to the solution of the phosphenium to cyclize to the phosphonium **4-11a**, which was then reduced to the phosphine **4-12a** with Mg dust. The SPO **4-13** was successfully generated from **4-12a** being treated with water. The SPO **4-13** reduced acyclic and exocyclic imines at room

temperature with low catalyst loadings, high enantioinduction and good functional group tolerance.

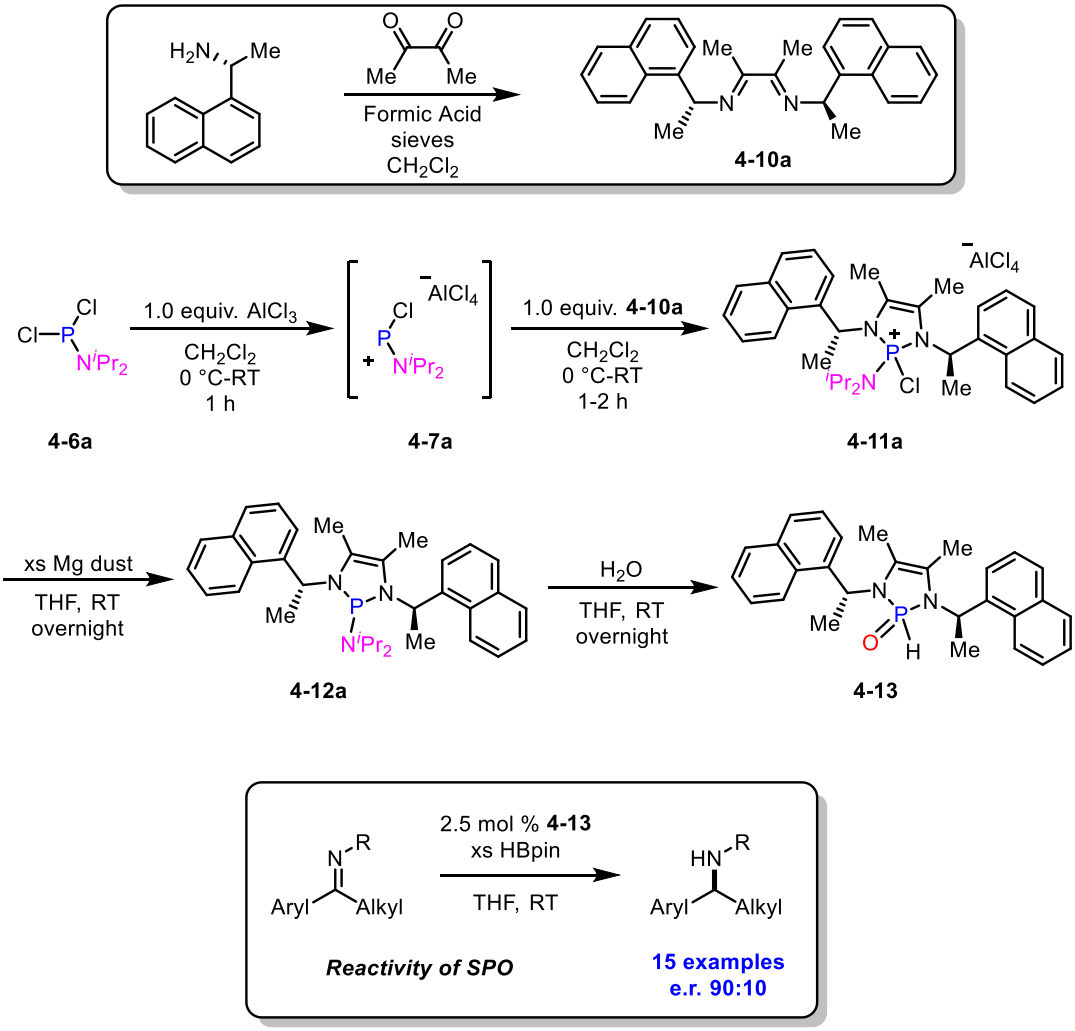

Scheme 5-6. Synthesis and reactivity of SPO **4-13**.

5.2 Future Work

The future direction of this work, my proposal would be to take the successful concepts from the work in Chapter 4 and apply it to the less successful and unsuccessful analogues reported in Chapters 2 and 3. The initial goal for synthesizing alternative DAPs, summarized in Chapters 2 and 3, was to generate the cationic variant, but from the findings described in Chapter 4, suggest the secondary phosphine oxide may show better

enantioselectivity in reduction, under neutral conditions. It would be worth revisiting these motifs and synthesizing the SPO versions of the heterocyclic containing analogues. For the variants that did cyclize with PBr_3, it would be easy to use the hydrolysis method that is already reported in the literature to synthesize the secondary phosphine oxide variants (Scheme 5-7A). In one-pot, the diimine, (**2-22a**, **2-22d**, **2-22f**, or **3-35**), can first react with PBr_3/cyclohexene to generate the corresponding DAP-Br followed by the addition of NEt_3 and water to form the secondary phosphine oxides **5-1a** to **5-1d**.

For the heterocyclic variants that did not cyclize with PBr_3/cyclohexene, the cyclization method starting where the dialkylaminodichlorophosphine is first activated to the phosphenium then cyclized with the diimine to generate the phosphonium could be used. If obtained, the resulting phosphonium salts can be reduced to the phosphine then converted to the secondary phosphine oxide variants (Scheme 5-7B). In one-pot, the chlorophosphine can be treated with $AlCl_3$ to form the intermediate phosphenium then the diimine (**2-22b**, **2-22d**, **2-22e**, or **3-18**) would be added to cyclize to the phosphonium (**5-2a** to **5-2d**) then the phosphonium would be reduced to the phosphine that could be treated with water to form the desired secondary phosphine oxides **5-3a** to **5-3d**. Once the SPO variants are isolated, the next step would be to test the reactivity and selectivity with acyclic imines, especially substrates that are not well tolerated with the current SPO. Alternatively, a different class of substrates all together could also be tested such as enamines.

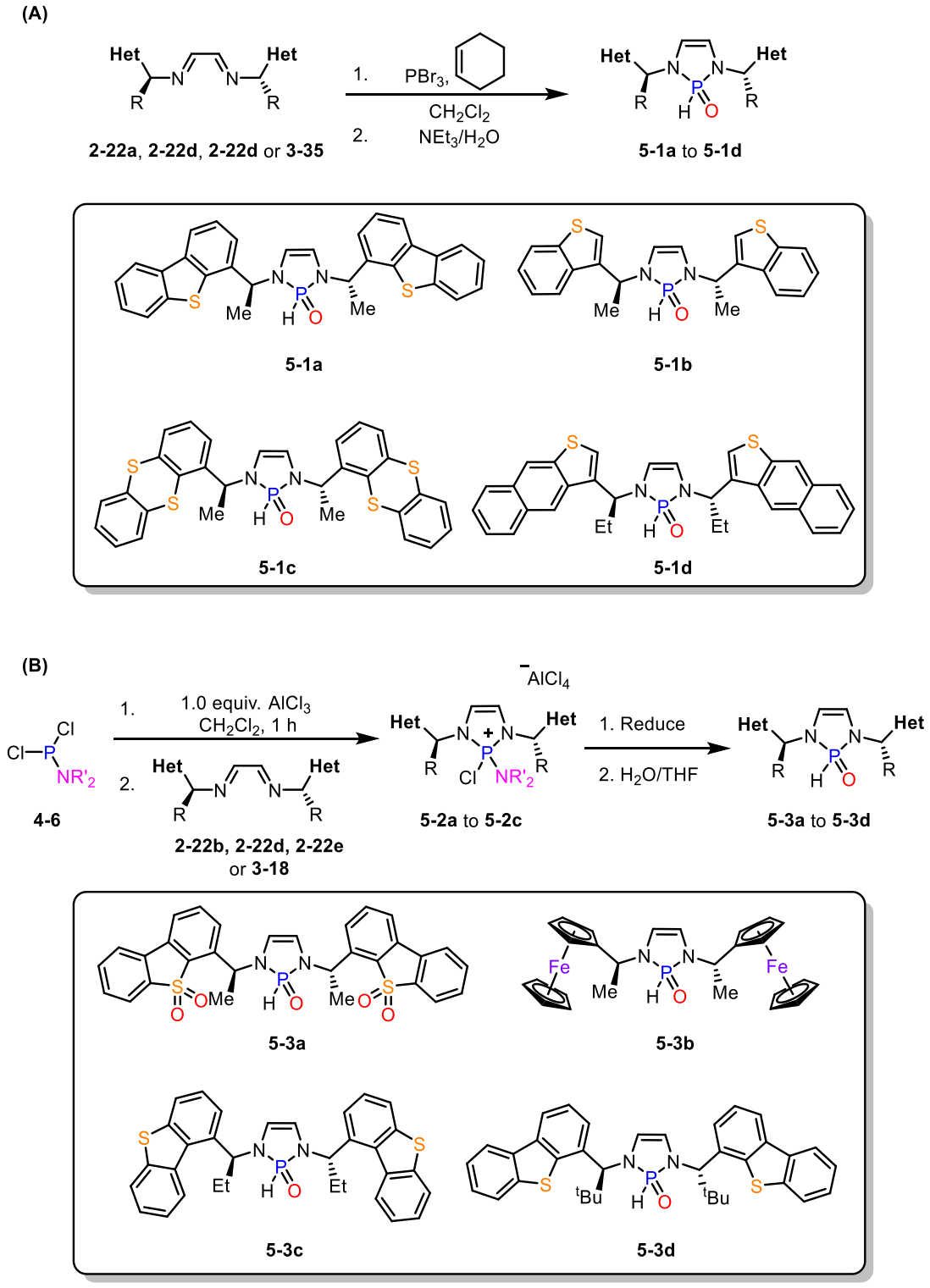

Scheme 5-7. Proposed synthesis of SPO variants of heterocyclic analogues (A) previous analogues that were successfully converted to the DAP-OTf. (B) Previous analogues that were unsuccessfully cyclized to the DAP-Br.

In addition to going back and expanding on the work reported in Chapters 2 and 3, the work in Chapter 4 could be expanded to other variants with a substituted backbone. As mentioned within the Chapter, the original attempts to synthesize variants with ethyl substituents in the backbone or altering the aryl group to a tetralone derivative or a 2-substituted naphthyl group combined with a methyl substituted backbone were deemphasized due to the ease of synthesis of the optimal catalyst, but could be revisited.

SPO **5-8** would be worth synthesizing and testing as it contains a naphthyl substituent in the aryl position combined with an ethyl substituent in the alkyl position and a methyl substituted backbone (Scheme 5-8). This would require the combination of the Ellman method to synthesize the enantiopure amine **5-5** (Scheme 5-8A) and the cyclization method described in Chapter 4 that will generate the SPO **5-8** (Scheme 5-8B). Overall, the synthesis would be relatively simple, beginning with 1-bromonaphthalene undergoing a lithium-halogen exchange which would be quenched with Ellman imine **3-32** to generate diastereomers **5-4a/b**. Under the assumption the diastereomers are separable, the diastereomerically pure Ellman-protected imine would be treated with dilute acid to followed by a basic work up to generate enantiopure amine **5-5**. The amine would undergo a condensation reaction with 2,3-butadione to generate the desired diimine **5-6** (Scheme 5-8A). From the diimine, the synthesis is analogues to SPO **4-13**. The starting phosphine **4-6** would be treated with $AlCl_3$ to generate phosphenium **4-7** *in situ*, followed by the addition of diimine **5-6** to cyclize to phosphonium **5-7**. Reduce the phosphonium followed by treating with water to generate SPO **5-8** (Scheme 5-8B).

This aryl (naphthlene) and alkyl (ethyl) side chain combination was chosen, because in the past a DAP-OTf variant with an unsubstituted backbone and a side chain containing a

naphthyl/ethyl combination showed promise to be better than the naphthyl/methyl combination for certain substrates. It would be worth testing the reactivity and enantioselectivity with cyclic, acyclic, and exocyclic imines that did not work well for the current best DAP-OTf and the SPO. It may also be worth taking the best heterocyclic analogue and combining it with methyl substituted backbone variant and testing the reactivity and selectivity of this variant.

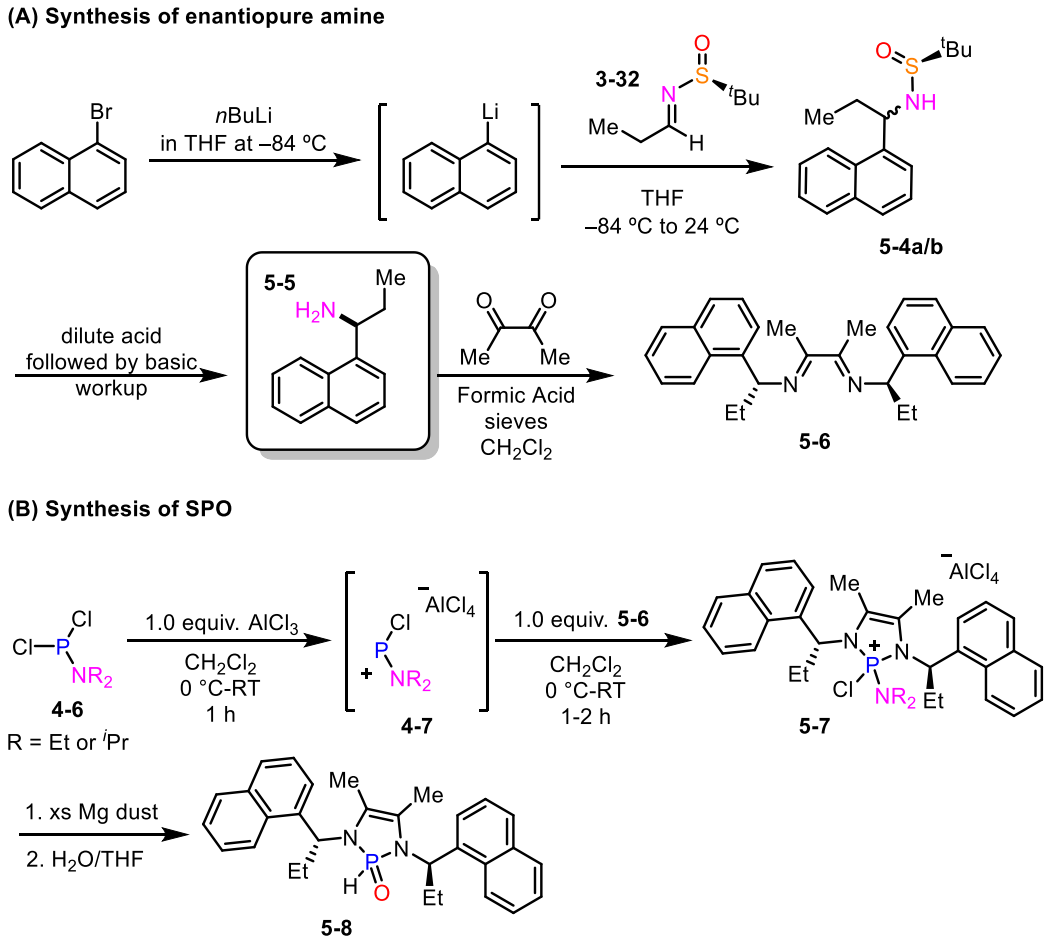

Scheme 5-8. Expansion of work in Chapter 4 (A) synthesis of enantiopure amine with ethyl substituent. (B) Synthesis of SPO starting from enantiopure amine.

References

[1] A. W. H. Speed, *Chem. Soc. Rev.* **2020**, *49*, 8335–8353.

[2] D. Gudat, A. Haghverdi, M. Nieger, *Angew. Chem., Int. Ed.* **2000**, *39*, 3084–3086.

[3] J. N. Li, L. Liu, Y. Fu, Q. X. Guo, *Tetrahedron* **2006**, *62*, 4453–4462.

[4] D. M. C. Ould, R. L. Melen, *Chem. Eur. J.* **2020**, *26*, 9835–9845.

[5] J. H. Reed, J. Klett, C. Steven, N. Cramer, *Org. Chem. Front.* **2020**, *7*, 3521–3529.

[6] T. Lundrigan, C. H. Tien, K. N. Robertson, A. W. H. Speed, *Chem. Commun.* **2020**, *56*, 8027–8030.

[7] M. R. Adams, C. H. Tien, B. S. N. Huchenski, M. J. Ferguson, A. W. H. Speed, *Angew. Chem., Int. Ed.* **2017**, *56*, 6268–6271.

[8] M. R. Adams, C. H. Tien, R. McDonald, A. W. H. Speed, *Angew. Chem., Int. Ed.* **2017**, *56*, 16660–16663.

[9] T. Lundrigan, E. N. Welsh, T. Hynes, C. H. Tien, M. R. Adams, K. R. Roy, K. N. Robertson, A. W. H. Speed, *J. Am. Chem. Soc.* **2019**, *141*, 14083–14088.

[10] B. Rao, C. C. Chong, R. Kinjo, *J. Am. Chem. Soc.* **2018**, *140*, 652–656.

[11] J. H. Reed, P. A. Donets, S. Miaskiewicz, N. Cramer, *Angew. Chem., Int. Ed.* **2019**, *58*, 8893–8897.

[12] S. Miaskiewicz, J. H. Reed, P. A. Donets, C. C. Oliveira, N. Cramer, *Angew. Chem., Int. Ed.* **2018**, *57*, 4039–4042.

[13] D. Gudat, *Acc. Chem. Res.* **2010**, *43*, 1307–1316.

[14] D. Gudat, A. Haghverdi, H. Hupfer, M. Nieger, *Chem. Eur. J.* **2000**, *6*, 3414–3425.

[15] B. W. Jennings, D. Randall, D. S. Worley, H. J. Hargis, *J.C.S. Perkin II* **1981**, *4*, 1411–1416.

[16] D. M. C. Ould, A. C. Rigby, L. C. Wilkins, S. J. Adams, J. A. Platts, S. J. A. Pope, E. Richards, R. L. Melen, *Organometallics* **2017**, *37*, 712–719.

[17] H. T. Dieck, J. Dietrich, *Chem. Ber.* **1984**, *117*, 694–701.

[18] I. A. Litvinov, V. A. Nuamov, T. V Gryaznova, A. N. Pudovik, A. M. Kibardin, *Dokl. Akad. Nauk SSSR* **1990**, *312*, 623.

[19] S. Burck, D. Gudat, M. Nieger, W. Du Mont, *J. Am. Chem. Soc.* **2006**, *128*, 3946–3955.

[20] J. W. Dube, G. J. Farrar, E. L. Norton, K. L. S. Szekely, B. F. T. Cooper, C. L. B. Macdonald, *Organometallics* **2009**, *28*, 4377–4384.

[21] D. Herrmannsdörfer, M. Kaaz, O. Puntigam, J. Bender, M. Nieger, D. Gudat, *Eur. J. Inorg. Chem.* **2015**, *2015*, 4819–4828.

[22] A. M. Kibardin, T. V Gryaznova, Y. B. Enikeev, A. N. Pudovik, *Izv. Akad. Nauk SSSR, Ser. Khim* **1987**, 1684.

[23] G. Reeske, C. R. Hoberg, N. J. Hill, A. H. Cowley, *J. Am. Chem. Soc.* **2006**, *128*, 2800–2801.

[24] Z. Benko, S. Burck, D. Gudat, M. Nieger, L. Nyulászi, N. Shore, *Dalt. Trans.* **2008**, 4937–4945.

[25] C. C. Chong, H. Hirao, R. Kinjo, *Angew. Chem., Int. Ed.* **2015**, *54*, 190–194.

[26] T. Hynes, E. N. Welsh, R. McDonald, M. J. Ferguson, A. W. H. Speed, *Organometallics* **2018**, *37*, 841–844.

[27] R. Noyori, *Adv. Synth. Catal.* **2003**, *345*, 15–32.

[28] W. S. Knowles, *Adv. Synth. Catal.* **2003**, *345*, 3–13.

[29] https://www.nobelprize.org/prizes/chemistry/2021/press-release/ accessed: 27 June 2023.

[30] S. K. Teo, W. A. Colburn, W. G. Tracewell, K. A. Kook, D. I. Stirling, M. S. Jaworsky, M. A. Scheffler, S. D. Thomas, O. L. Laskin, *Clin. Pharmacokinet.* **2004**, *43*, 311–327.

[31] A. Aumatell, R. J. Wells, *J. Chromatogr. Sci.* **1993**, *31*, 502–508.

[32] M. B. H. Youdim, A. Gross, J. P. M. Finberg, *Br. J. Pharmacol.* **2001**, *132*, 500–506.

[33] W. Schreibmayer, O. Tripathi, H. A. Tritthart, *Br. J. Pharmacol.* **1992**, *106*, 151–156.

[34] C. L. De Vane, H. L. Liston, J. S. Markowitz, *Clin. Pharmacokinet.* **2002**, *41*, 1247–1266.

[35] E. Salomó, A. Gallen, G. Sciortino, G. Ujaque, A. Grabulosa, A. Lledós, A. Riera, X. Verdaguer, *J. Am. Chem. Soc.* **2018**, *140*, 16967–16970.

[36] E. Salomó, P. Rojo, P. Hernández-Lladó, A. Riera, X. Verdaguer, *J. Org. Chem.* **2018**, *83*, 4618–4627.

[37] D. Gatineau, L. Giordano, G. Buono, *J. Am. Chem. Soc.* **2011**, *133*, 10728–10731.

[38] K. S. Egorova, V. P. Ananikov, *Angew. Chem., Int. Ed.* **2016**, *55*, 12150–12162.

[39] C. K. Blasius, N. F. Heinrich, V. Vasilenko, L. H. Gade, *Angew. Chem., Int. Ed.* **2020**, *59*, 15974–15977.

[40] J. Magano, J. R. Dunetz, *Org. Process Res. Dev.* **2012**, *16*, 1156–1184.

[41] A. Ault, *J. Chem. Educ.* **1965**, *42*, 269.

[42] C. J. Dunsmore, R. Carr, T. Fleming, N. J. Turner, *J. Am. Chem. Soc.* **2006**, *128*, 2224–2225.

[43] M. Nechab, N. Azzi, N. Vanthuyne, M. Bertrand, S. Gastaldi, G. Gil, *J. Org. Chem.* **2007**, *72*, 6918–6923.

[44] F. Iwasaki, O. Onomura, K. Mishima, T. Kanematsu, T. Maki, Y. Matsumura, *Tetrahedron Lett.* **2001**, *42*, 2525–2527.

[45] Y. Liu, H. Du, *J. Am. Chem. Soc.* **2013**, *135*, 6810–6813.

[46] J. A. Ellman, T. D. Owens, T. P. Tang, *Acc. Chem. Res.* **2002**, *35*, 984–995.

[47] M. R. Holmes, J. F. Manganaro, C. L. Barnes, B. W. Gung, *J. Organomet. Chem.* **2015**, *795*, 18–24.

[48] L. M. Klingensmith, K. A. Nadeau, G. A. Moniz, *Tetrahedron Lett.* **2007**, *48*, 4589–4593.

[49] R. Sanders, U. T. Mueller-Westerhoff, *J. Organomet. Chem.* **1996**, *512*, 219–224.

[50] L. X. Dai, T. Tu, S. L. You, W. P. Deng, X. L. Hou, *Acc. Chem. Res.* **2003**, *36*, 659–667.

[51] E. N. Welsh, K. N. Robertson, A. W. H. Speed, *Org. Biomol. Chem.* **2021**, *19*, 2000–2007.

[52] R. D. Riley, B. S. N. Huchenski, K. L. Bamford, A. W. H. Speed, *Angew. Chemie - Int. Ed.* **2022**, *61*, e2022040.

[53] B. S. N. Huchenski, K. N. Robertson, A. W. H. Speed, *Eur. J. Org. Chem.* **2020**, 5140–5144.

[54] E. N. Welsh, K. N. Robertson, A. W. H. Speed, *Can. J. Chem.* **2022**, *100*, 809–813.

[55] E. K. Burke, E. N. Welsh, K. N. Robertson, A. W. H. Speed, *Synthesis* **2023**, *55*, A-I.

[56] R. Sanz, Y. Fernández, M. P. Castroviejo, A. Pérez, F. J. Fañanás, *J. Org. Chem.* **2006**, *71*, 6291–6294.

[57] H. F. Bettinger, M. Filthaus, *J. Org. Chem.* **2007**, *72*, 9750–9752.

[58] J. W. Coe, M. C. Wirtz, C. G. Bashore, J. Candler, *Org. Lett.* **2004**, *6*, 1589–1592.

[59] W. F. Bailey, M. R. Luderer, K. P. Jordan, *J. Org. Chem.* **2006**, *71*, 2825–2828.

[60] J. F. Bunnett, *J. Chem. Educ.* **1961**, *38*, 278–285.

[61] C. Kuehm-Caubère, S. Adach-Becker, Y. Fort, P. Caubère, *Tetrahedron* **1996**, *52*, 9087–9092.

[62] B. S. N. Huchenski, A. W. H. Speed, *Chem. Commun.* **2021**, *57*, 7128–7131.

[63] D. Rombach, H. A. Wagenknecht, *Angew. Chem., Int. Ed.* **2020**, *59*, 300–303.

[64] K. Targos, O. P. Williams, Z. K. Wickens, *J. Am. Chem. Soc.* **2021**, *143*, 4125–4132.

[65] J. A. García-López, M. F. Greaney, *Chem. Soc. Rev.* **2016**, *45*, 6766–6798.

[66] S. Xiang, Z. Huang, S. Sun, X. Lv, L. Fan, S. Ye, H. Chen, R. Guo, L. Wang, *J. Mater. Chem. C* **2018**, *6*, 11436–11443.

[67] M. Hori, T. Kataoka, H. Shimizu, N. Ueda, *Tetrahedron Lett.* **1981**, *22*, 3071–3074.

[68] J. Nakayama, T. Fujita, M. Hoshino, *Chem. Lett.* **1982**, 1777–1780.

[69] G. M. Blackburn, W. D. Ollis, *Chem. Commun.* **1968**, 1261–1262.

[70] H. D. Xu, M. Q. Cai, W. J. He, W. H. Hu, M. H. Shen, *RSC Adv.* **2014**, *4*, 7623–7626.

[71] L. Li, G. N. Ndzeidze, M. G. Steinmetz, *Tetrahedron* **2019**, *75*, 70–83.

[72] D. Yue, R. C. Larock, *J. Org. Chem.* **2002**, *67*, 1905–1909.

[73] G. Liu, D. A. Cogan, J. A. Ellman, *J. Am. Chem. Soc.* **1997**, *119*, 9913–9914.

[74] T. Ishida, R. Kobayashi, T. Yamada, *Org. Lett.* **2014**, *16*, 2430–2433.

[75] M. R. Mazieres, C. Roques, M. Sanchez, J. P. Majoral, R. Wolf, *Tetrahedron* **1987**, *43*, 2109–2118.

[76] M.R. Mazieres, T. C. Kim, R. Wolf, M. Sanchez, *Phosphorus, Sulfur, and Silicon* **1991**, *55*, 147–158.

[77] B. S. N. Huchenski, A. W. H. Speed, *Org. Biomol. Chem.* **2019**, *17*, 1999–2004.

[78] E. J. Corey, M. J. Grogan, *Org. Lett.* **1999**, *1*, 157–160

Appendix A: Crystallographic Experimental Details

All of the data and information found in this appendix was provided directly by Dr. Kathy Robertson from Saint Mary's University.

X-ray Crystallography for Compound 3-9

The crystal chosen was attached to the tip of a MicroLoop with Paratone-N oil. Measurements were made on a Bruker D8 VENTURE diffractometer equipped with a PHOTON III CMOS detector using monochromated Mo Kα radiation (λ = 0.71073 Å) from an Incoatec micro-focus sealed tube at 100 K [1]. The initial orientation and unit cell were indexed using a least-squares analysis of the reflections collected from a complete 360° phi-scan, 1 second per frame. For data collection, a strategy was calculated to maximize data completeness and multiplicity, in a reasonable amount of time, and then implemented using the Bruker Apex 3 software suite [1]. The crystal to detector distance was set to 4 cm. Frame times were 5 seconds per frame. Cell refinement and data reduction were performed with the Bruker SAINT [2] software, which corrects for beam inhomogeneity, possible crystal decay, Lorentz and polarisation effects. A multi-scan absorption correction was applied (SADABS [3]). The structures were solved using SHELXT-2014 [4] and were refined using a full-matrix least-squares method on F^2 with SHELXL-2018 [4]. The non-hydrogen atoms were refined anisotropically. The hydrogen atoms bonded to carbon were included at geometrically idealized positions and were not refined. The isotropic thermal parameters of these hydrogen atoms were fixed at $1.2U_{eq}$ of the parent carbon atom or $1.5U_{eq}$ for methyl hydrogens.

In the final refinement, there were a number of reflections below $\sin\theta/\lambda = 0.600$ which were missing. These reflections, eight of them strong, were collected but must have saturated the detector during data collection or been partially obscured by the beam stop. They were removed from the data set during processing.

Table S1: Crystal data and structure refinement details for compound **3-9**.

Identification code	**3-9**
CCDC deposit number	1958921
Empirical formula	$C_{18}H_{19}BO_2S$
Formula weight	310.20
Crystal system	Monoclinic
Space group	$P2_1/c$
Unit cell dimensions (Å and º)	a = 11.4270(10)
	b = 10.2820(9)
	c = 13.6992(12)
	α = 90
	β = 99.468(3)
	γ = 90
Volume (Å^3)	1587.6(2)
Z	4
Density (calculated, Mg/m^3)	1.298
Absorption coefficient (mm^{-1})	0.207
F(000)	656
Crystal size (mm^3)	0.302x0.190x0.128
Theta range of data (º)	3.615 to 46.484
Index ranges (h, k, l)	-23/23, -20/20, -27/27
Reflections collected	135411
Independent reflections	14090
R(int)	0.0577
Completeness to 25.242º (%)	98.8
Max. and min. transmission	0.7493 and 0.6987
Data / restrains / parameters	14090 / 0 / 203
Goodness-of-fit on F^2	1.067
Final R indices [I>2sigma(I)]	R1 = 0.0414
	wR2 = 0.1119
R indices (all data)	R1 = 0.0600
	wR2 = 0.1297
Absolute structure parameter	n/a
Largest diff. peak and hole (e.Å^{-3})	0.908 and -0.617

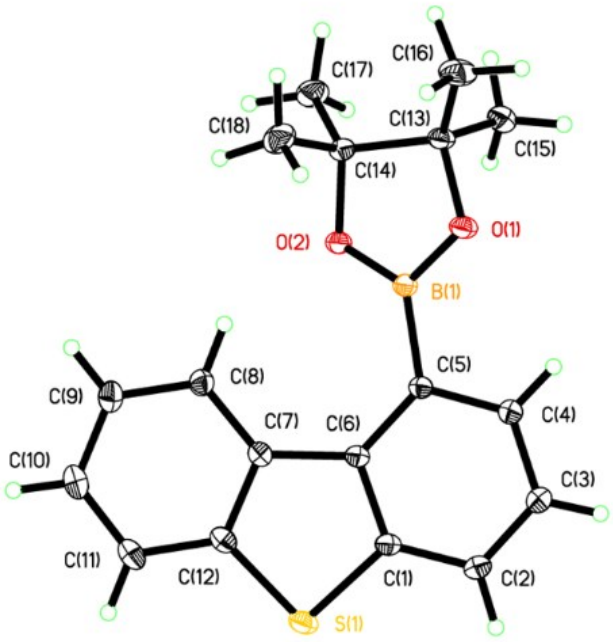

Figure S1. Structural diagram of compound **3-9**. Thermal ellipsoids have been drawn at the 50% probability level.

References

[1] APEX 3 (Bruker, 2018) Bruker AXS Inc., Madison, Wisconsin, USA.
[2] SAINT (Bruker, 2016) Bruker AXS Inc., Madison, Wisconsin, USA.
[3] SADABS (Bruker, 2016) Bruker AXS Inc., Madison, Wisconsin, USA.
[4] Sheldrick, G.M. (2015) *Acta Cryst*., A71, 3-8; Sheldrick, G.M. (2015) *Acta Cryst*., C71, 3-8.

X-ray Crystallography for Compound 3-16a

The crystal chosen was attached to the tip of a MicroLoop with Paratone-N oil. Measurements were made on a Bruker D8 VENTURE diffractometer equipped with a PHOTON III CMOS detector using monochromated Mo Kα radiation (λ = 0.71073 Å) from an Incoatec micro-focus sealed tube at 150 K [1]. The initial orientation and unit cell were indexed using a least-squares analysis of the reflections collected from a 180° phi-scan, 2 seconds per frame and 1° per frame. For data collection, a strategy was calculated to maximize data completeness and multiplicity, in a reasonable amount of time, and then implemented using the Bruker Apex 3 software suite [1]. The crystal to detector distance was set to 4.0 cm. Cell refinement and data reduction were performed with the Bruker SAINT [2] software, which corrects for beam inhomogeneity, possible crystal decay, Lorentz and polarisation effects. A multi-scan absorption correction was applied (SADABS [3]). The structure was solved using SHELXT-2014 [4] and was refined using a full-matrix least-squares method on F^2 with SHELXL-2018 [4]. The non-hydrogen atoms were refined anisotropically. The hydrogen atoms bonded to carbon were included at geometrically idealized positions and were not refined. The isotropic thermal parameters of these hydrogen atoms were fixed at $1.2U_{eq}$ of the parent carbon atom or $1.5U_{eq}$ for methyl hydrogens. The H(N) hydrogen atom was allowed to refine isotropically. It was not restrained in any way.

An error occurred during the data collection. The collection stopped after only 8 of 9 runs had been finished and it could not be restarted. However, there was enough data already collected that the structure could be refined and the final cif checked with no problems detected. Data was collected to maximum θ angle of 39.81° (0.56 Å resolution). However, the high angle data was very noisy above 0.65 Å (66.28°). The data was cut off at this value during refinement using a SHEL instruction. One reflection (3 3 0) was removed from the final refinement because of poor agreement between F_{obs}^2 and F_{calc}^2.

The structure was very disordered. One section of the molecule, involving O1 and the methyl groups of the t-butyl group, was modelled with a two part (50:50) disorder. The carbon atoms of the latter group were made equivalent using a SAME command to apply appropriate restraints. No other restraints were required. The other end of the molecule, beyond N1 and including C13, the ethyl group and a portion of the dibenzothiophene group, was also disordered. This included the 5-membered ring and the coordinated 6-membered ring of dibenzothiophene. This portion of the molecule was treated as one unit and was split over two sets of positions. The occupancy of each part was refined using a free variable to a total of one. A SAME instruction was used to set restraints to keep the geometries of the two parts similar. All of the carbon atoms in the two parts were restrained to have similar thermal parameters, as were (separately) S1A and S1B. Bond lengths of the same type between disordered and non-disordered regions of the molecule were restrained to be similar using SADI instructions during the refinement. Finally, enhanced rigid bond restraints were placed over the entire molecule using a RIGU command. The occupancies of the two parts refined to a final ratio of 86.7(3) and 13.3 %.

The molecule was found to crystallize in the chiral space group $P2_12_12_1$, with S chirality at C13 (A and B). The absolute structure of the molecule was reliably determined. Using the program Platon [5] the refined structure was calculated to have a Flack parameter of 0.019(15), a Parsons parameter of 0.024(16) and a Hooft parameter of 0.012(15). These values agree with the Parson's value calculated by the program SHELXL, 0.019(15) from 2398 selected quotients.

Table S2. Crystal data and structure refinement for **3-16a**.

Identification code	**3-16a**	
Empirical formula	$C_{19}H_{23}NOS_2$	
Formula weight	345.50	
Temperature	100(2) K	
Wavelength	0.71073 Å	
Crystal system	Orthorhombic	
Space group	$P2_12_12_1$	
Unit cell dimensions	a = 8.6260(5) Å	α= 90°
	b = 9.2018(5) Å	β = 90°
	c = 22.6467(11) Å	γ = 90°
Volume	1797.58(17) $Å^3$	
Z	4	
Density (calculated)	1.277 Mg/m^3	
Absorption coefficient	0.300 mm^{-1}	
F(000)	736	
Crystal size	0.265 x 0.089 x 0.068 mm^3	
Theta range for data collection	2.389 to 33.141°	
Index ranges	-13<=h<=13, -14<=k<=14, -34<=l<=34	
Reflections collected	75947	
Independent reflections	6840 [R(int) = 0.0537]	
Completeness to theta = 25.242°	99.9 %	
Absorption correction	Semi-empirical from equivalents	
Max. and min. transmission	0.7478 and 0.6501	
Refinement method	Full-matrix least-squares on F^2	
Data / restraints / parameters	6840 / 663 / 347	
Goodness-of-fit on F^2	1.056	
Final R indices [I>2sigma(I)]	R1 = 0.0392, wR2 = 0.0849	
R indices (all data)	R1 = 0.0475, wR2 = 0.0894	
Absolute structure parameter	0.019(15)	
Extinction coefficient	n/a	
Largest diff. peak and hole	0.422 and -0.471 e.$Å^{-3}$	

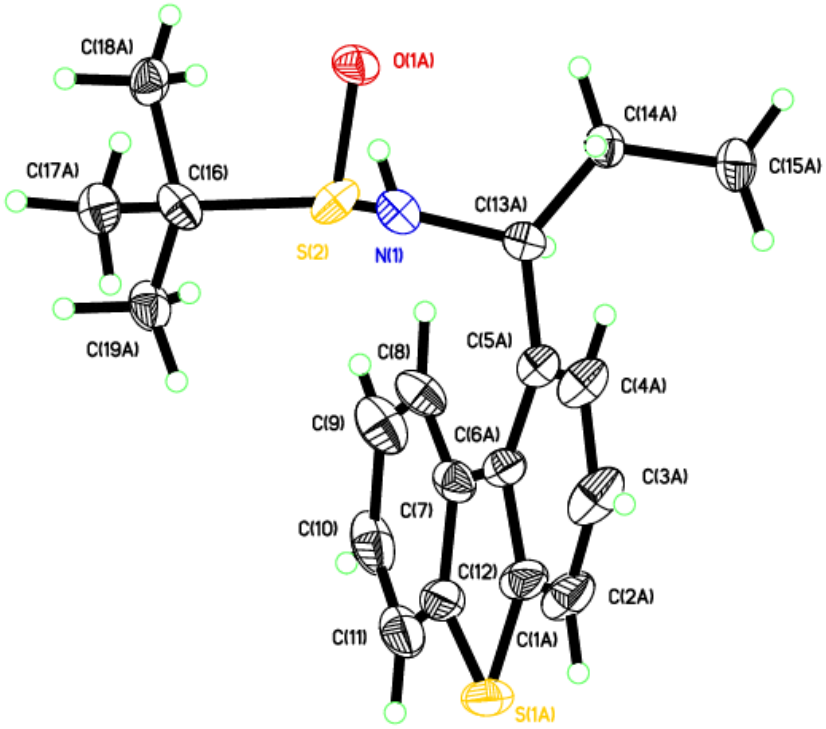

Figure S2. Structural diagram of compound **3-16a**. Thermal ellipsoids have been drawn at the 50% probability level.

References

[1] APEX 3 (Bruker, 2018) Bruker AXS Inc., Madison, Wisconsin, USA.
[2] SAINT (Bruker, 2016) Bruker AXS Inc., Madison, Wisconsin, USA.
[3] SADABS (Bruker, 2016) Bruker AXS Inc., Madison, Wisconsin, USA.
[4] Sheldrick, G.M. (2015) *Acta Cryst*., A71, 3-8; Sheldrick, G.M. (2015) *Acta Cryst*., C71, 3-8.
[5]Spek, A.L. (2009) *Acta Cryst*., D65, 148-155.

X-ray Crystallography for Compound 3-33a and 3-33b

The crystal chosen was attached to the tip of a MicroLoop with Paratone-N oil. Measurements were made on a Bruker D8 VENTURE diffractometer equipped with a PHOTON III CMOS detector using monochromated Mo Kα radiation (λ = 0.71073 Å) from an Incoatec micro-focus sealed tube at the temperature indicated, 100 to 150 K. The initial orientation and unit cell were indexed using a least-squares analysis of the reflections collected from a 180° phi-scan, 2 seconds per frame and 1° per frame. For data collection, a strategy was calculated to maximize data completeness and multiplicity, in a reasonable amount of time, and then implemented using the Bruker Apex 3 software suite.[1] The crystal to detector distance was set to 4 cm and 15 second frames were collected unless otherwise stated. Cell refinement and data reduction were performed with the Bruker SAINT software, which corrects for beam inhomogeneity, possible crystal decay, Lorentz and polarisation effects.[2] A multi-scan absorption correction was applied (SADABS).[3] The structure was solved using SHELXT-2014 and was refined using a full-matrix least-squares method on F^2 with SHELXL-2018.[4] The non-hydrogen atoms were refined either as part of a rigid group (see below) or anisotropically. The hydrogen atoms bonded to carbon were included at geometrically idealized positions and were not refined. The isotropic thermal parameters of these hydrogen atoms were fixed at $1.2U_{eq}$ of the parent carbon atom or $1.5U_{eq}$ for methyl hydrogens. All H(N) hydrogen atom positions were located in near final Fourier difference maps. They were allowed to refine isotropically and were not restrained in any way.

Compound **3-33a** (major product)

The crystal used for the data collection was not cut. When other crystals were cut, they shredded into long shards that were not suitable for data collection. To avoid this, a long needle/plate crystal was used without cutting it to fit it into the beam. However, this did result in a level C checkcif alert for the crystal being too long for the beam size. The other two dimensions were suitable.

The molecule was found to crystallize in the chiral space group $P2_1$, with an *S* configuration at C13. The absolute structure of the molecule was reliably determined. Using the program Platon[5] the refined structure was calculated to have a Flack parameter of –0.012(16), a Parsons parameter of –0.003(16) and a Hooft parameter of 0.012(15). These values agree with the Parson's value calculated by the program SHELXL, –0.012(16) from 3921 selected quotients.

Compound **3-33b** (minor product)

The molecule was found to crystallize in the chiral space group $P2_12_12_1$, with an R configuration at C13. The absolute structure of the molecule was reliably determined. Using the program Platon[5] the refined structure was calculated to have a Flack parameter of –0.002(8), a Parsons parameter of -0.001(7) and a Hooft parameter of –0.007(7). These values agree with the Parson's value calculated by the program SHELXL, –0.002(8) from 4386 selected quotients.

Table S3: Crystal data and structure refinement details for compounds **3-33a** and **3-33b**.

Identification code	**3-33a - major**	**3-33b - minor**
CCDC deposit number	1999812	1999815
Temperature (K)	125	125
Empirical formula	$C_{19}H_{23}NOS_2$	$C_{19}H_{23}NOS_2$
Formula weight	345.50	345.50
Crystal system	Monoclinic	Orthorhombic
Space group	$P2_1$	$P2_12_12_1$
Unit cell dimensions (Å and º)	a = 8.9768(4)	a = 8.9317(4)
	b = 9.4961(4)	b = 9.4815(4)
	c = 11.1085(5)	c = 21.8980(10)
	α = 90	α = 90
	β = 102.289(2)	β = 90
	γ = 90	γ = 90
Volume (Å^3)	925.24(7)	1854.45(14)
Z	2	4
Density (calculated, Mg/m^3)	1.240	1.237
Absorption coefficient (mm^{-1})	0.292	0.291
F(000)	368	736
Crystal size (mm^3)	0.651x0.103x0.032	0.374x0.152x0.098
Theta range of data (º)	2.657 to 39.384	2.341 to 39.380
Index ranges (h, k, l)	-15/15, -16/16, -19/19	-15/15, -16/16, -37/38
Reflections collected	41764	105907
Independent reflections	10545	10795
R(int)	0.0375	0.0335
Completeness to 25.242º (%)	99.3	98.1
Max. and min. transmission	0.7478 and 0.7004	0.7478 and 0.6954
Data / restrains / parameters	10545 / 1 / 216	10795 / 0 / 216
Goodness-of-fit on F^2	1.049	1.063
Final R indices [I>2sigma(I)]	R1 = 0.0342	R1 = 0.0276
	wR2 = 0.0774	wR2 = 0.0718
R indices (all data)	R1 = 0.0445	R1 = 0.0305
	wR2 = 0.0839	wR2 = 0.0736
Absolute structure parameter	-0.012(16)	-0.002(8)
Largest diff. peak and hole (e.Å^{-3})	0.370 and -0.376	0.318 and -0.269

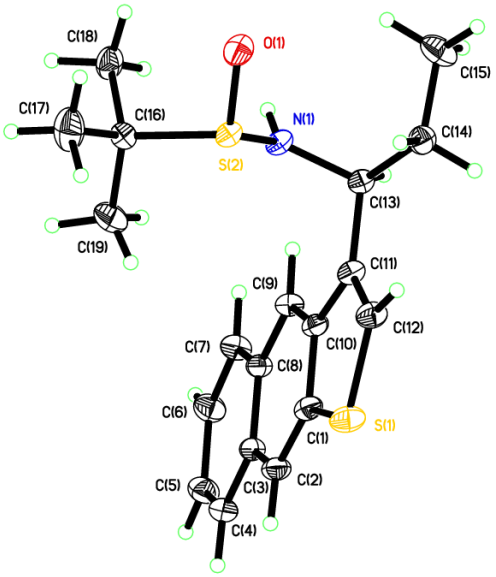

Figure S3. Structural diagram of compound compound **3-33a**. Thermal ellipsoids have been drawn at the 50% probability level. Hydrogen atoms have not been labelled.

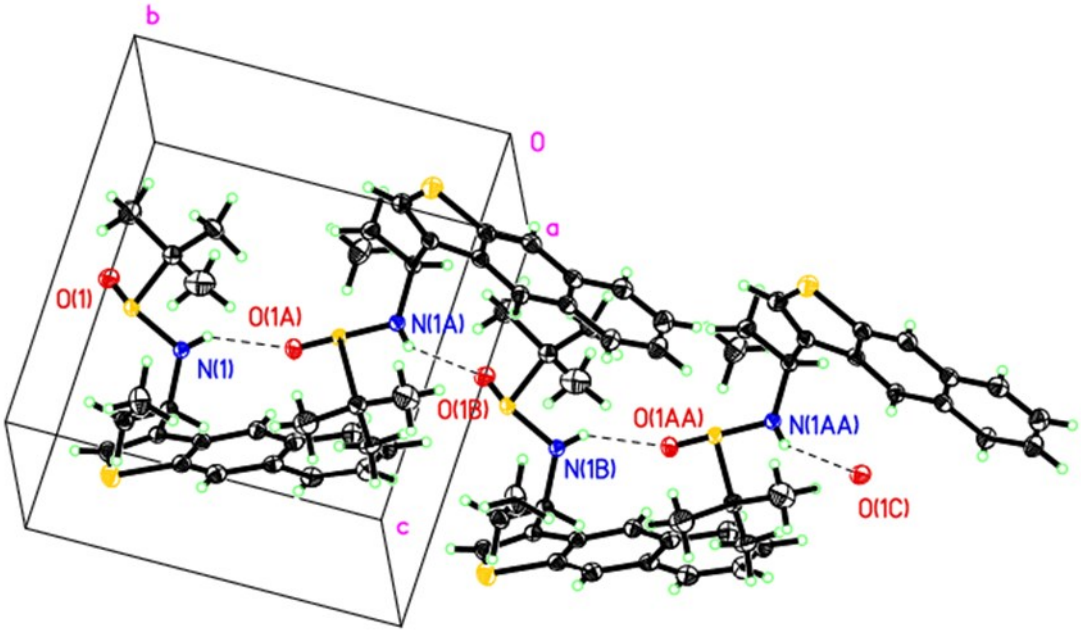

Figure S4. Structural diagram of the hydrogen bonded chain found in compound **3-33a**. Thermal ellipsoids have been drawn at the 50% probability level. Hydrogen atoms have not been labelled.

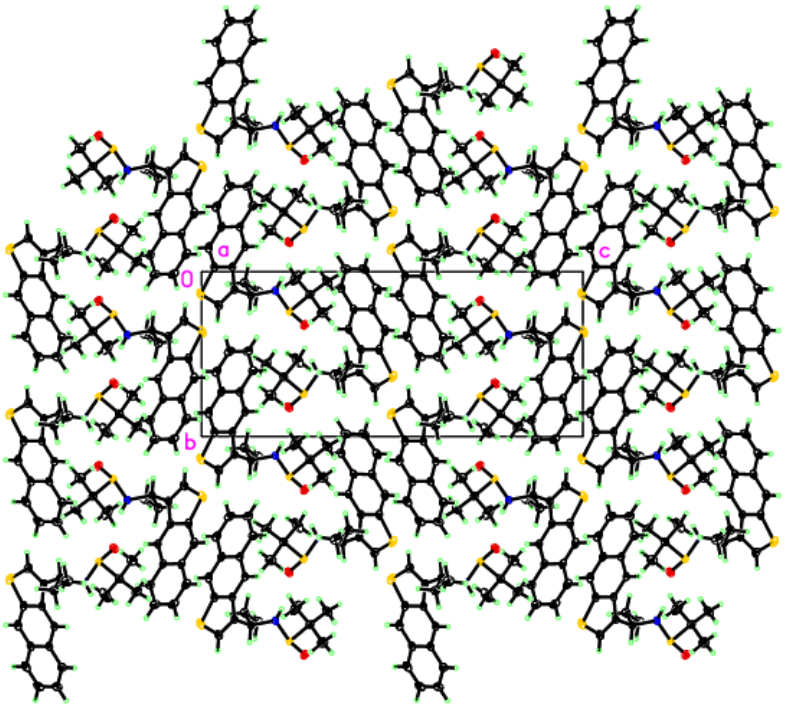

Figure S5. Packing diagram for compound **3-33a** viewed down the *X*-axis.

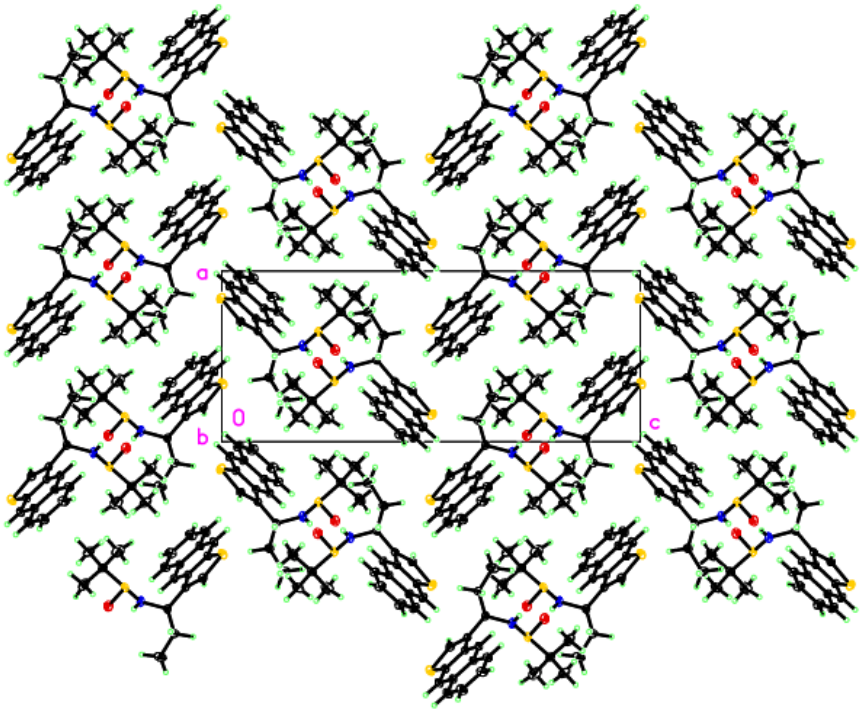

Figure S6. Packing diagram for compound **3-33a** viewed down the *Y*-axis.

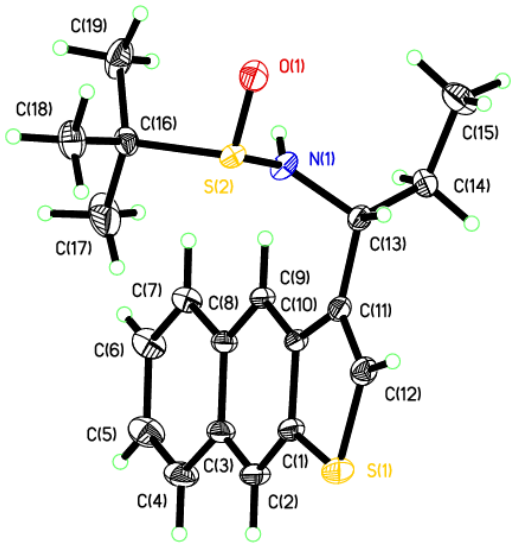

Figure S7. Structural diagram of compound compound **3-33b**. Thermal ellipsoids have been drawn at the 50% probability level. Hydrogen atoms have not been labelled.

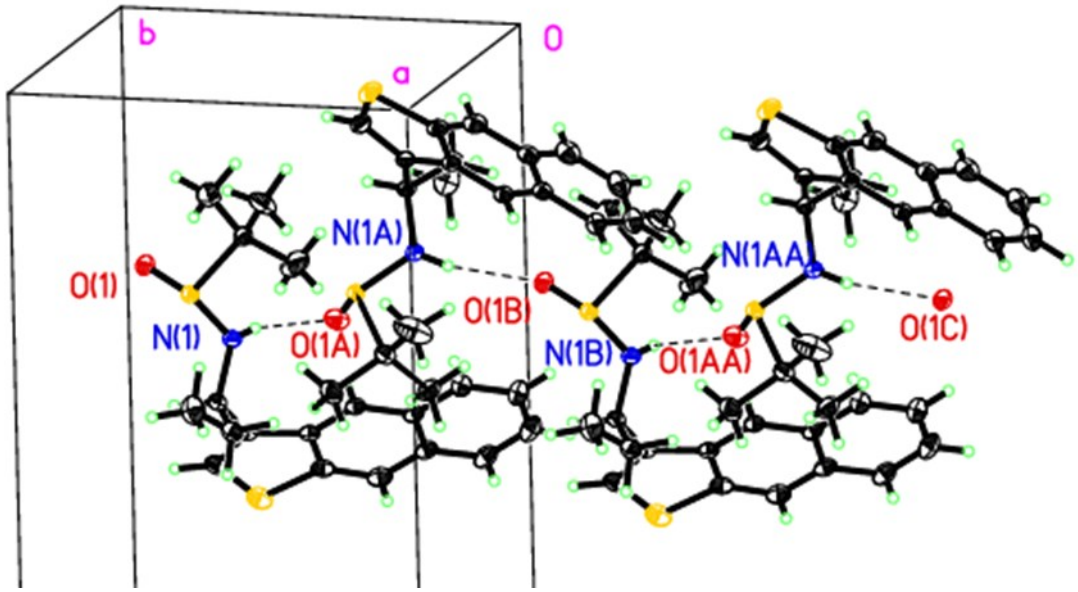

Figure S8. Structural diagram of the hydrogen bonded chains found in compound **3-33b**. Thermal ellipsoids have been drawn at the 50% probability level. Hydrogen atoms have not been labelled.

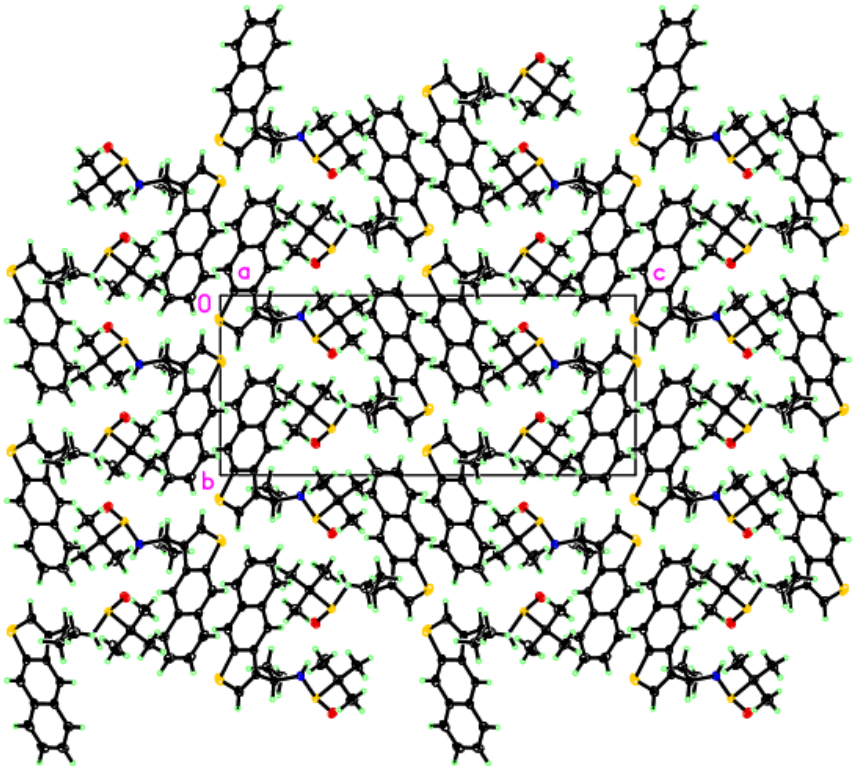

Figure S9. Packing diagram for compound **3-33b** viewed down the *X*-axis.

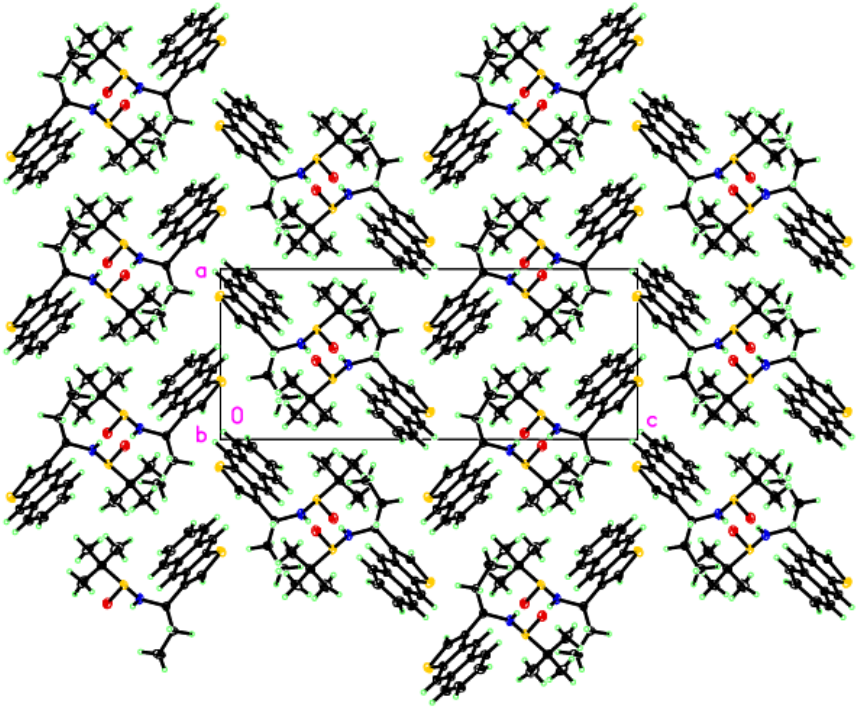

Figure S10. Packing diagram for compound **3-33b** viewed down the *Y*-axis.

References:

[1] APEX 3 (Bruker, 2018) Bruker AXS Inc., Madison, Wisconsin, USA.
[2] SAINT (Bruker, 2016) Bruker AXS Inc., Madison, Wisconsin, USA.
[3] SADABS (Bruker, 2016) Bruker AXS Inc., Madison, Wisconsin, USA.
[4] Sheldrick, G.M. (2015) *Acta Cryst*., A71, 3-8; Sheldrick, G.M. (2015) *Acta Cryst*., C71, 3-8.
[5]Spek, A.L. (2009) *Acta Cryst*., D65, 148-155.

X-ray Crystallography for Compound 4-13

The crystal chosen was attached to the tip of a MicroLoop with Paratone-N oil. Measurements were made on a Bruker D8 VENTURE diffractometer equipped with a PHOTON III CMOS detector using monochromated Cu Kα radiation (λ = 1.54178 Å) from an Incoatec micro-focus sealed tube at 125 K [1]. The initial orientation and unit cell were indexed using a least-squares analysis of the reflections collected from a 180° phi-scan, 3 seconds per frame and 1° per frame. For data collection, a strategy was calculated to maximize data completeness and multiplicity, in a reasonable amount of time, and then implemented using the Bruker Apex 4 software suite [1]. The crystal to detector distance was set to 4.0 cm and 30 sec frames were collected. Cell refinement and data reduction were performed with the Bruker SAINT [2] software, which corrects for beam inhomogeneity, possible crystal decay, Lorentz and polarisation effects. A multi-scan absorption correction was applied (SADABS [3]). The structure was solved using SHELXT-2014 [4] and was refined using a full-matrix least-squares method on F^2 with SHELXL-2018 [4]. The non-hydrogen atoms were refined anisotropically. The hydrogen atoms bonded to carbon were included at geometrically idealized positions and were not refined. The isotropic thermal parameters of these hydrogen atoms were fixed at $1.2U_{eq}$ of the parent carbon atom or $1.5U_{eq}$ for methyl hydrogens. The position of the hydrogen atom boned to phosphorus was located in a near final Fourier difference map. It was added to the atom list and allowed to refine isotropically without restraint.

The molecule crystallized in the chiral space group $P2_12_12_1$, with one molecule of the compound and one molecule of thf solvent in the asymmetric unit. The solvent was completely disordered; it was modelled over two parts which refined to have occupancies of 81.0(7) % and 19.0 %, respectively. The two parts were restrained to have similar geometries and their atoms to have similar anisotropic displacement parameters.

The structure was found to crystallize as a racemic twin, with a BASF value that refined to 0.18(2). The molecule crystallized predominantly with R chirality at C5 and C17. The structure itself was also disordered. One of the two naphthyl groups was disordered, with the naphthyl rings coordinated facing one way or the other relative to the rest of the molecule. This disorder was modelled with two parts and the occupancies refined to 87.8(8) % and 12.2 %, respectively. A SAME instruction was used to keep the geometries of the two parts similar. The carbon atoms of the disordered naphthyl rings were restrained to have similar anisotropic displacement parameters.

Table S4. Crystal data and structure refinement for **4-13**.

Identification code	**4-13**	
Empirical formula	$C_{32}H_{37}N_2O_2P$	
Formula weight	512.60	
Temperature	125(2) K	
Wavelength	1.54178 Å	
Crystal system	Orthorhombic	
Space group	$P2_12_12_1$	
Unit cell dimensions	a = 9.5173(4) Å	α = 90°
	b = 12.2696(5) Å	β = 90°
	c = 23.1662(10) Å	γ = 90°
Volume	2705.20(17) Å^3	
Z	4	
Density (calculated)	1.259 Mg/m^3	
Absorption coefficient	1.144 mm^{-1}	
F(000)	1096	
Crystal size	0.110 x 0.106 x 0.038 mm^3	
Theta range for data collection	3.816 to 79.757°	
Index ranges	-12<=h<=12, -15<=k<=15, -29<=l<=28	
Reflections collected	37777	
Independent reflections	5762 [R(int) = 0.0415]	
Completeness to theta = 67.679°	100.0 %	
Absorption correction	Semi-empirical from equivalents	
Max. and min. transmission	0.7542 and 0.6319	
Refinement method	Full-matrix least-squares on F^2	
Data / restraints / parameters	5762 / 523 / 480	
Goodness-of-fit on F^2	1.062	
Final R indices [I>2sigma(I)]	R1 = 0.0365, wR2 = 0.0897	
R indices (all data)	R1 = 0.0377, wR2 = 0.0909	
Absolute structure parameter	0.18(2)	
Extinction coefficient	n/a	
Largest diff. peak and hole	0.281 and -0.268 e.Å^{-3}	

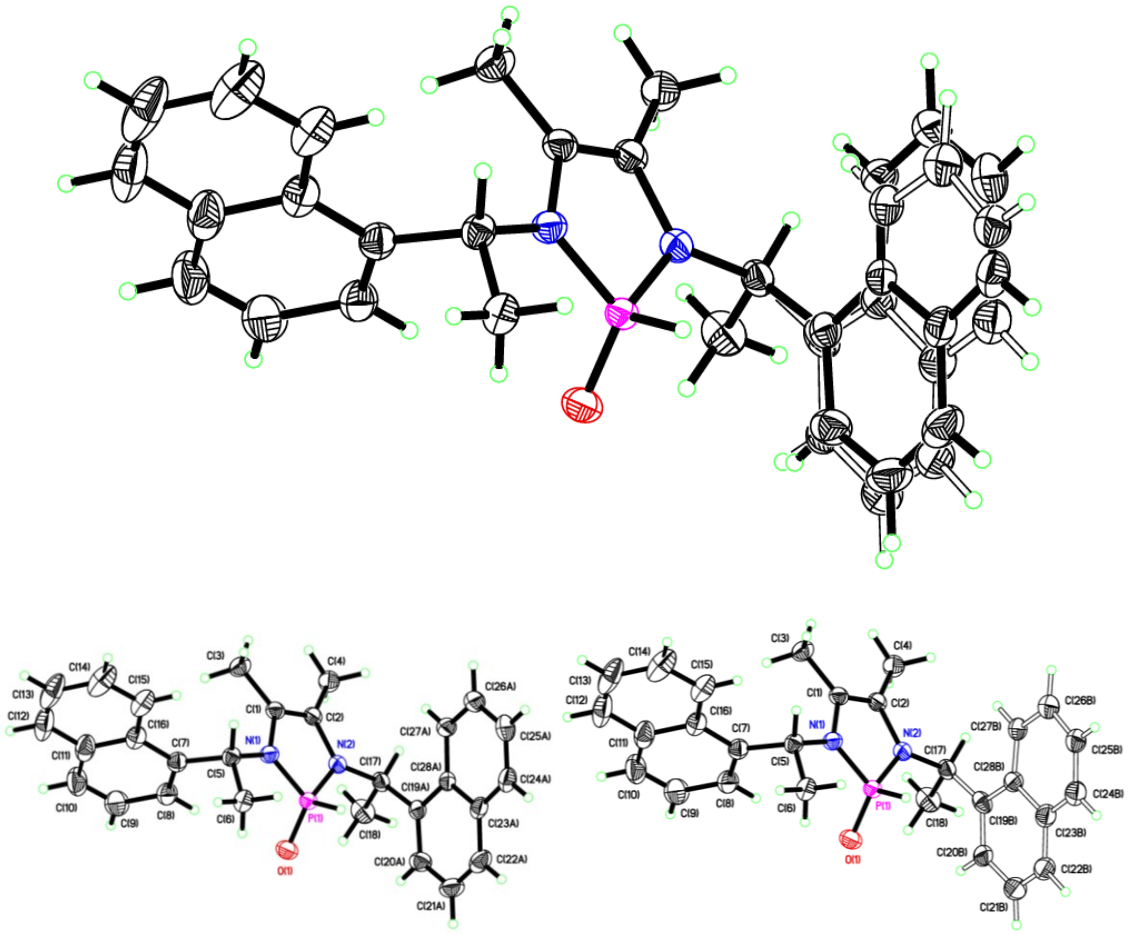

Figure S11. Structure of compound **4-13**, with the solvent removed for clarity. The two parts of the disordered model have been separated, Part A left and Part B right. Thermal ellipsoids are drawn at the 50 % probability level. Hydrogen atoms have not been labelled.

References

[1] APEX 4 (Bruker, 2021) Bruker AXS Inc., Madison, Wisconsin, USA.
[2] SAINT (Bruker, 2019) Bruker AXS Inc., Madison, Wisconsin, USA.
[3] SADABS (Bruker, 2016) Bruker AXS Inc., Madison, Wisconsin, USA.
[4] Sheldrick, G.M. (2015) *Acta Cryst*., A71, 3-8; Sheldrick, G.M. (2015) *Acta Cryst*., C71, 3-8.
[5] Spek, A.L. (2009) Acta Cryst., D65, 148-155.

Appendix B: Selected NMR Spectra

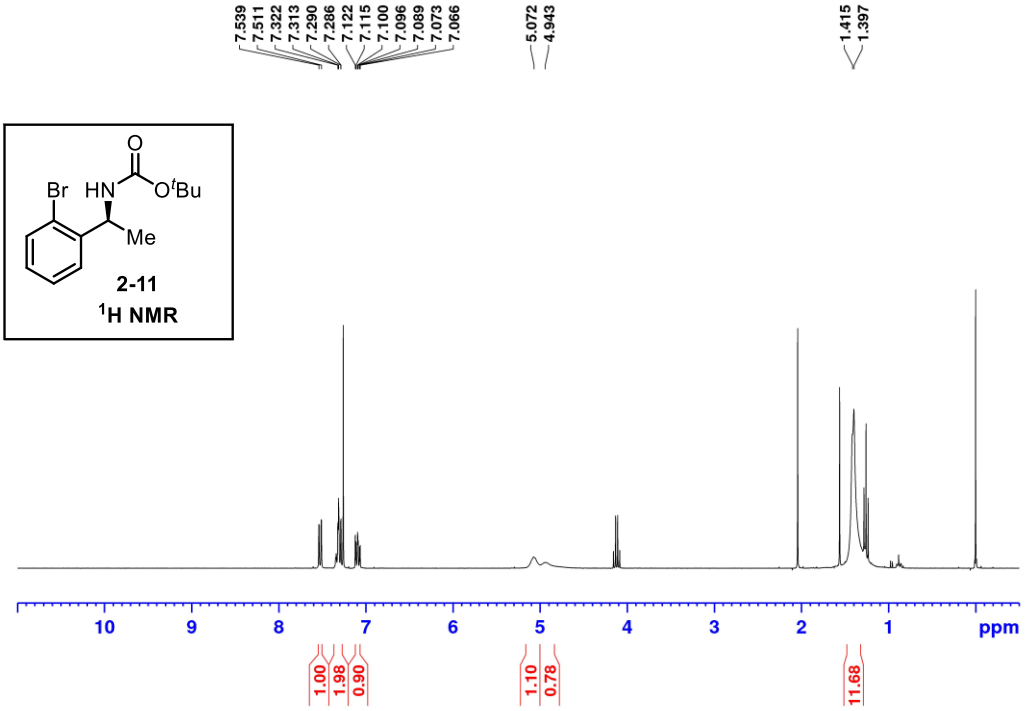

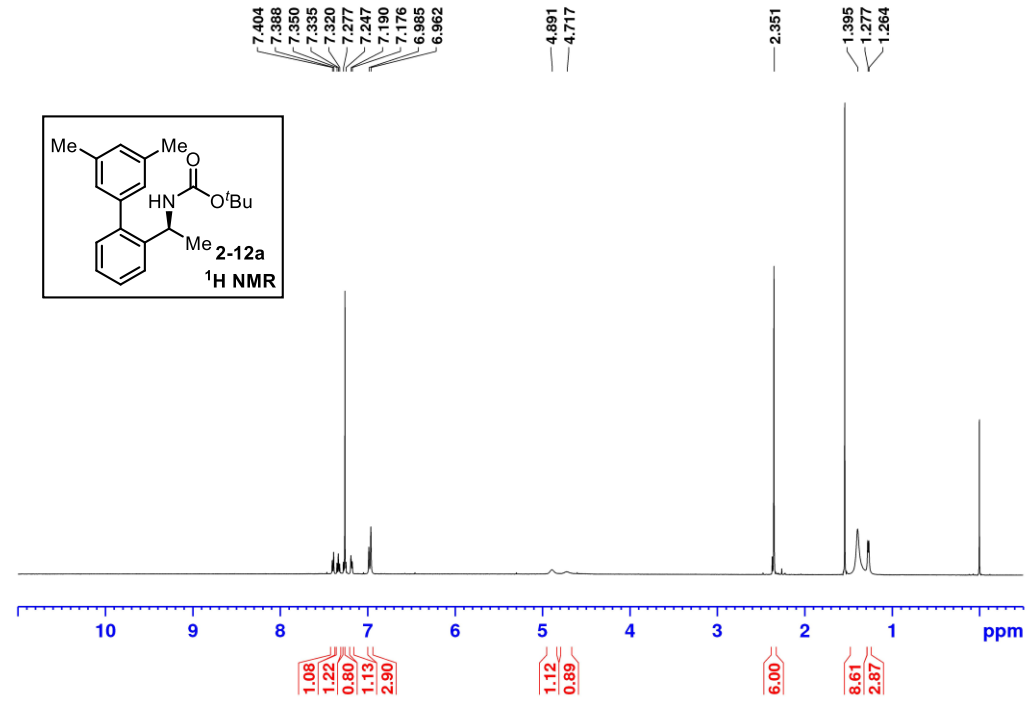

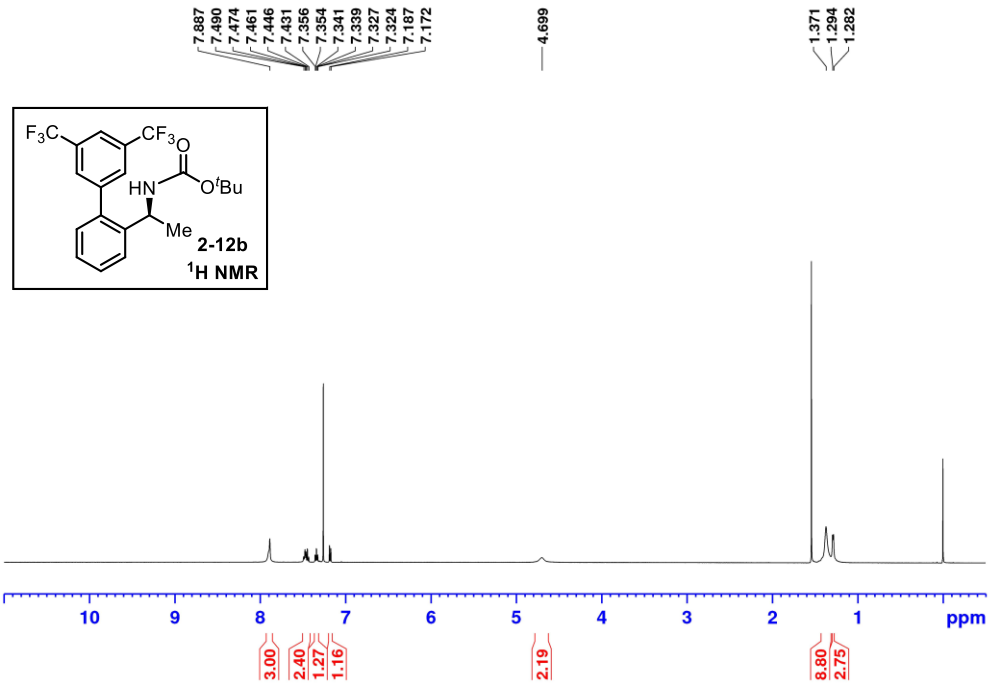
7.887
7.490
7.474
7.461
7.446
7.431
7.356
7.354
7.341
7.339
7.327
7.324
7.187
7.172
4.699
1.371
1.294
1.282
F3C
CF3
O
HN
O
tBu
Me
2-12b
1H NMR
10
9
8
7
6
5
4
3
2
1
ppm
3.00
2.40
1.27
1.16
2.19
8.80
2.75

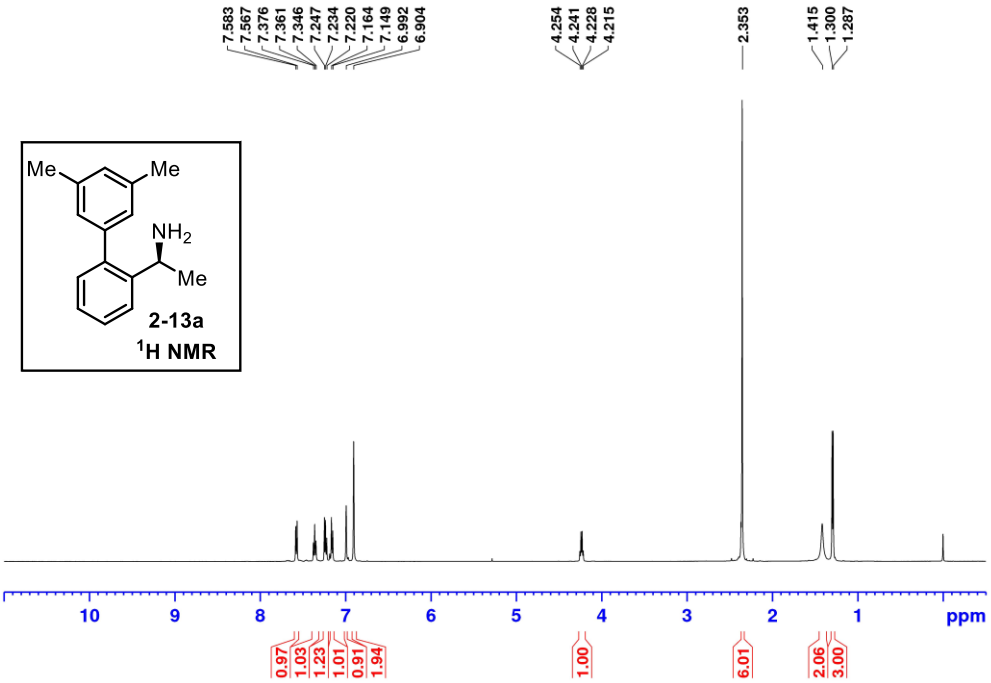
7.583
7.567
7.376
7.361
7.346
7.247
7.234
7.220
7.164
7.149
6.992
6.904
4.254
4.241
4.228
4.215
2.353
1.415
1.300
1.287
Me
Me
NH2
Me
2-13a
1H NMR
10
9
8
7
6
5
4
3
2
1
ppm
0.97
1.03
1.23
1.01
0.91
1.94
1.00
6.01
2.06
3.00

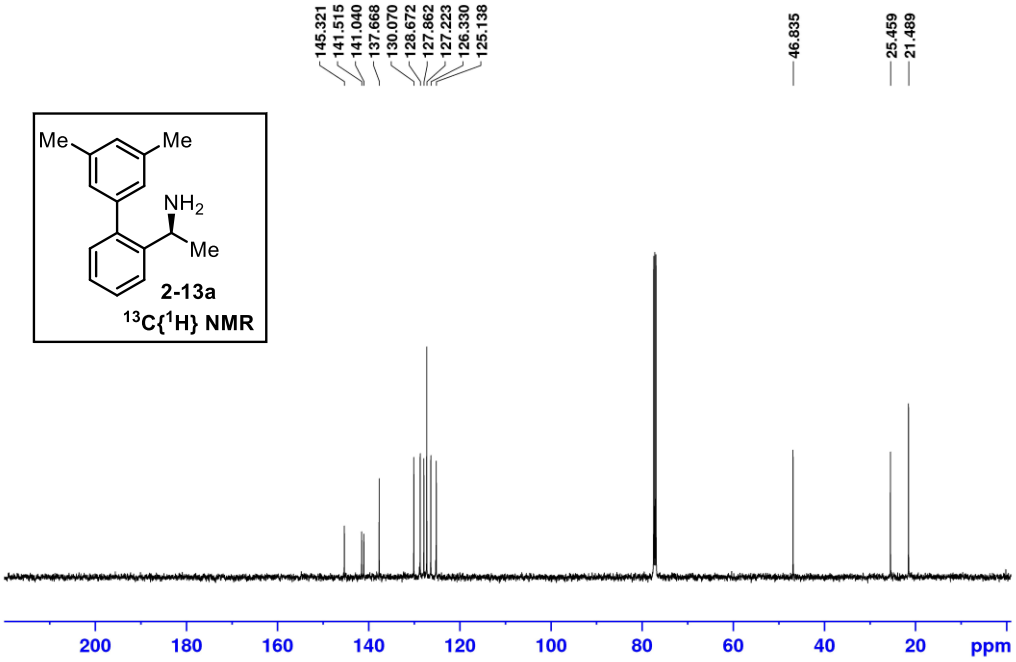
145.321
141.515
141.040
137.668
130.070
128.672
127.862
127.223
126.330
125.138
46.835
25.459
21.489
Me
Me
NH2
Me
2-13a
13C{1H} NMR
200
180
160
140
120
100
80
60
40
20
ppm

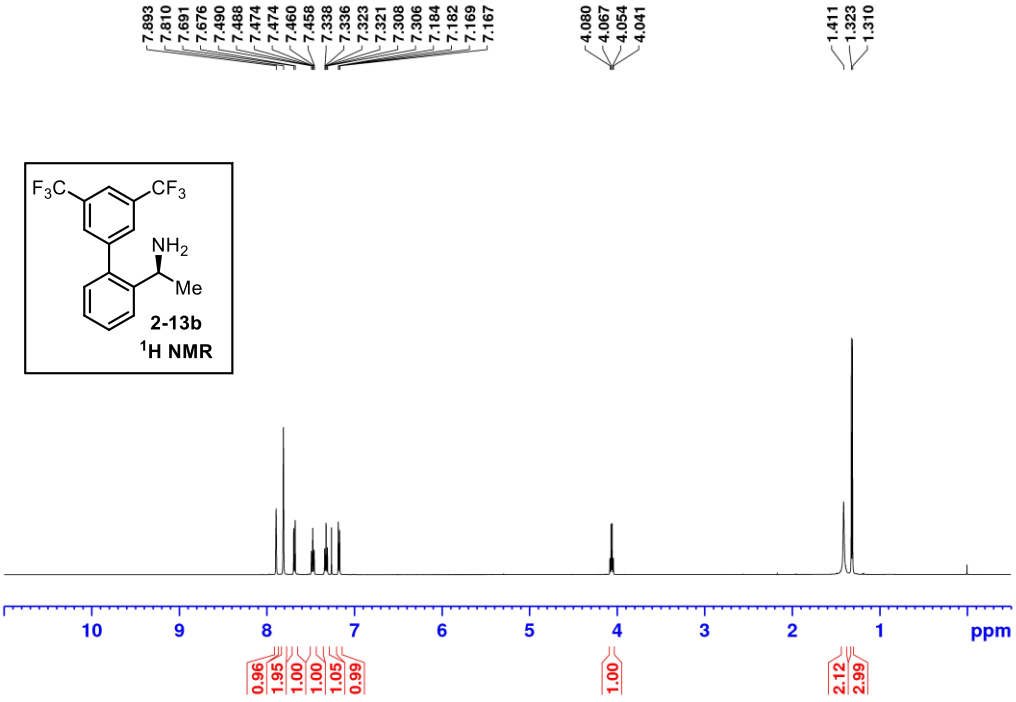
7.893
7.810
7.691
7.676
7.490
7.488
7.474
7.474
7.460
7.458
7.338
7.336
7.323
7.321
7.308
7.306
7.184
7.182
7.169
7.167
4.080
4.067
4.054
4.041
1.411
1.323
1.310
F3C
CF3
NH2
Me
2-13b
1H NMR
10
9
8
7
6
5
4
3
2
1
ppm
0.96
1.95
1.00
1.00
1.05
0.99
1.00
2.12
2.99

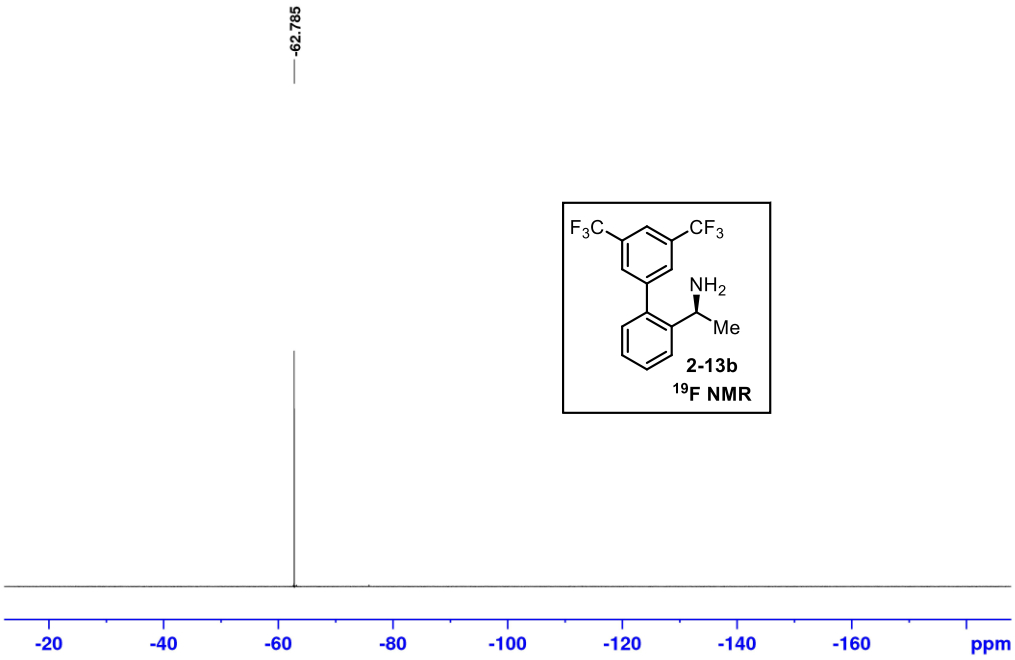
-62.785
F3C
CF3
NH2
Me
2-13b
19F NMR
-20
-40
-60
-80
-100
-120
-140
-160
ppm

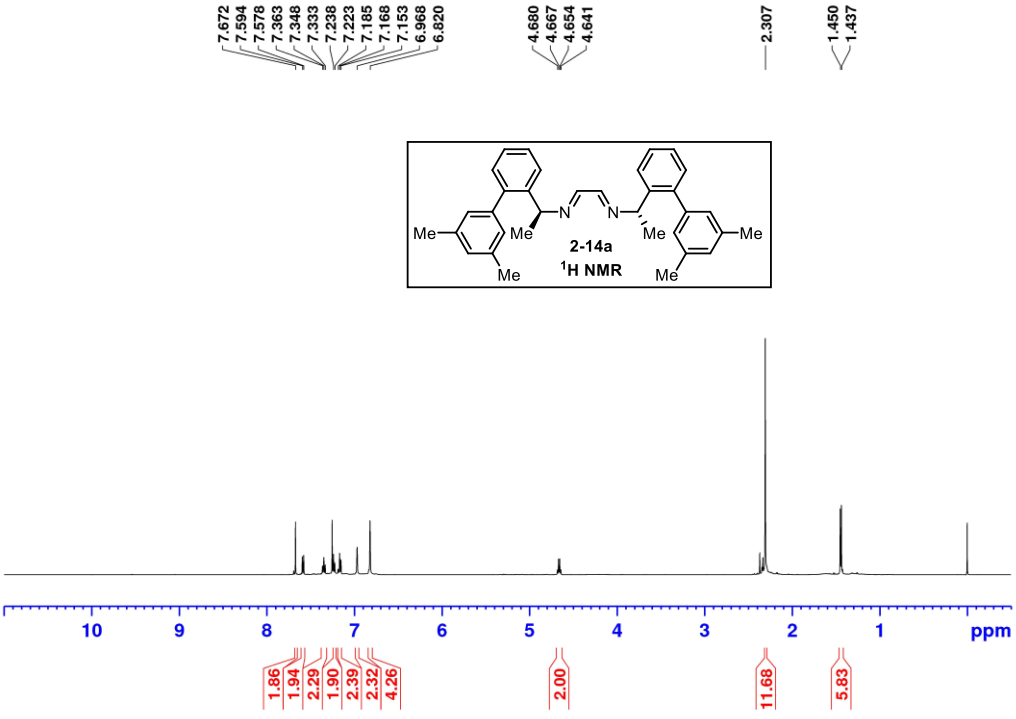
7.672
7.594
7.578
7.363
7.348
7.333
7.238
7.223
7.185
7.168
7.153
6.968
6.820
4.680
4.667
4.654
4.641
2.307
1.450
1.437
Me
Me
Me
Me
Me
Me
2-14a
1H NMR
10
9
8
7
6
5
4
3
2
1
ppm
1.86
1.94
2.29
1.90
2.39
2.32
4.26
2.00
11.68
5.83

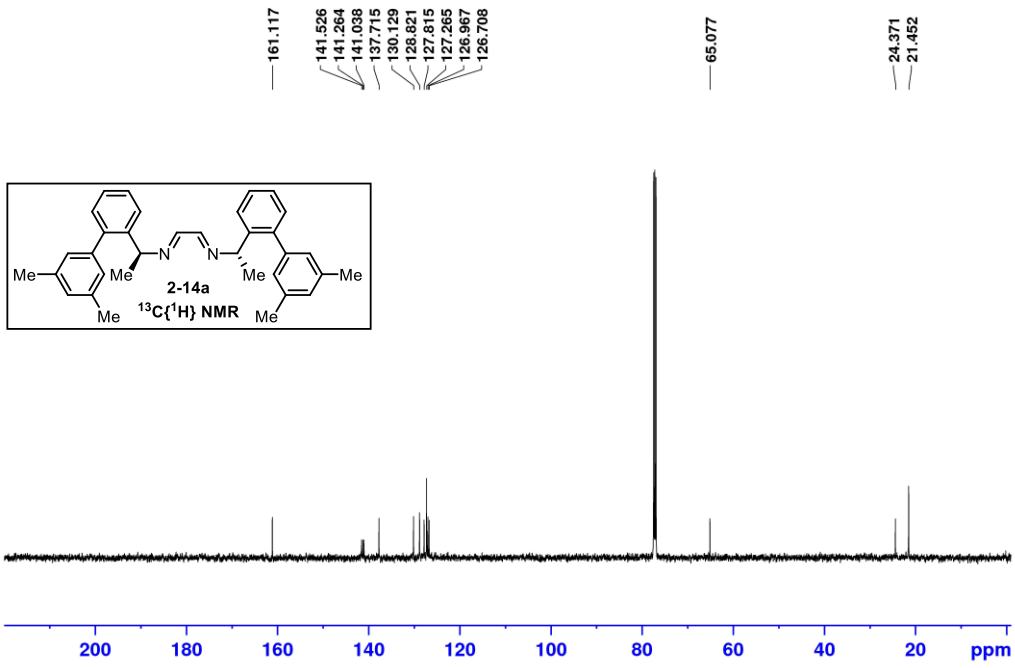
161.117
141.526
141.264
141.038
137.715
130.129
128.821
127.815
127.265
126.967
126.708
65.077
24.371
21.452
Me
Me
Me
Me
Me
Me
2-14a
13C{1H} NMR
200
180
160
140
120
100
80
60
40
20
ppm

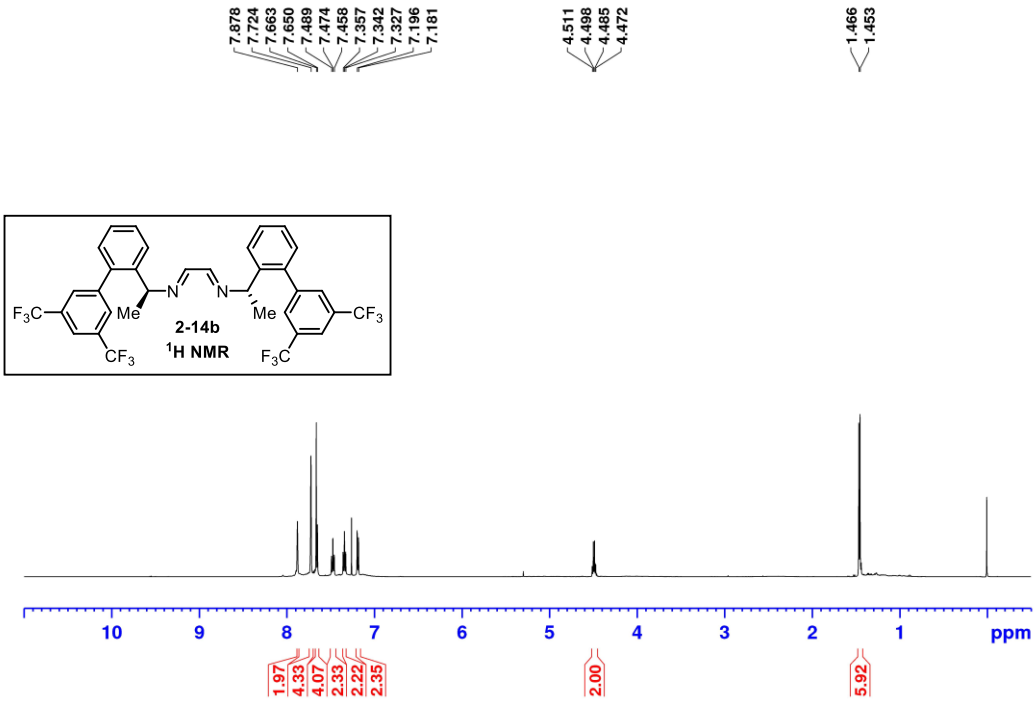
7.878
7.724
7.663
7.650
7.489
7.474
7.458
7.357
7.342
7.327
7.196
7.181
4.511
4.498
4.485
4.472
1.466
1.453
F3C
CF3
Me
Me
CF3
F3C
2-14b
1H NMR
10
9
8
7
6
5
4
3
2
1
ppm
1.97
4.33
4.07
2.33
2.22
2.35
2.00
5.92

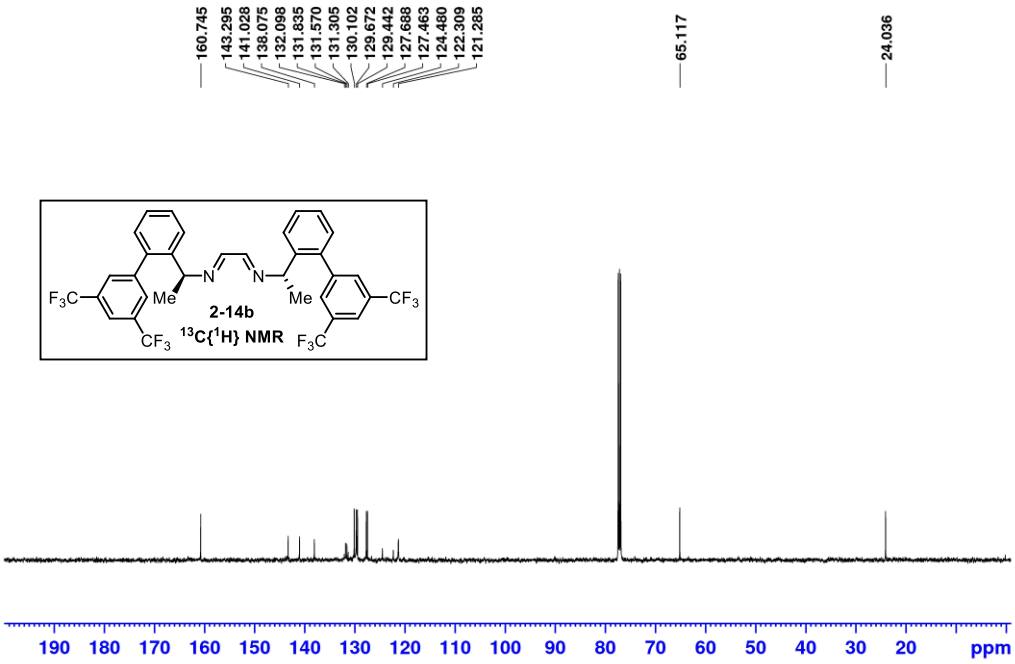
160.745
143.295
141.028
138.075
132.098
131.835
131.570
131.305
130.102
129.672
129.442
127.688
127.463
124.480
122.309
121.285
65.117
24.036
F3C
CF3
Me
N
N
Me
CF3
F3C
2-14b
13C{1H} NMR
190 180 170 160 150 140 130 120 110 100 90 80 70 60 50 40 30 20 ppm

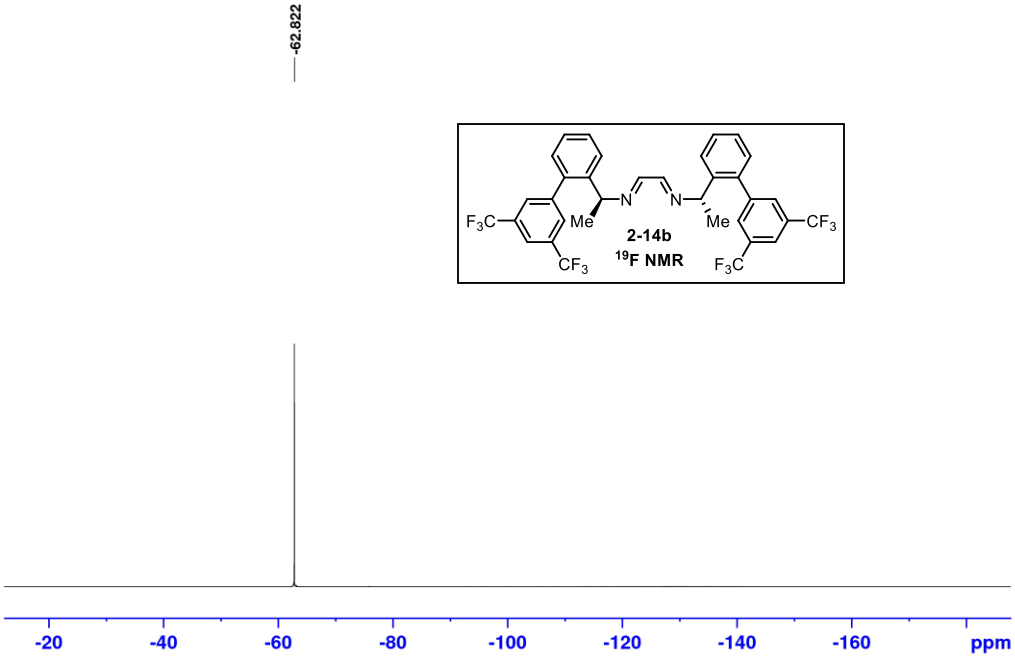
-62.822
F3C
CF3
Me
N
N
Me
CF3
F3C
2-14b
19F NMR
-20 -40 -60 -80 -100 -120 -140 -160 ppm

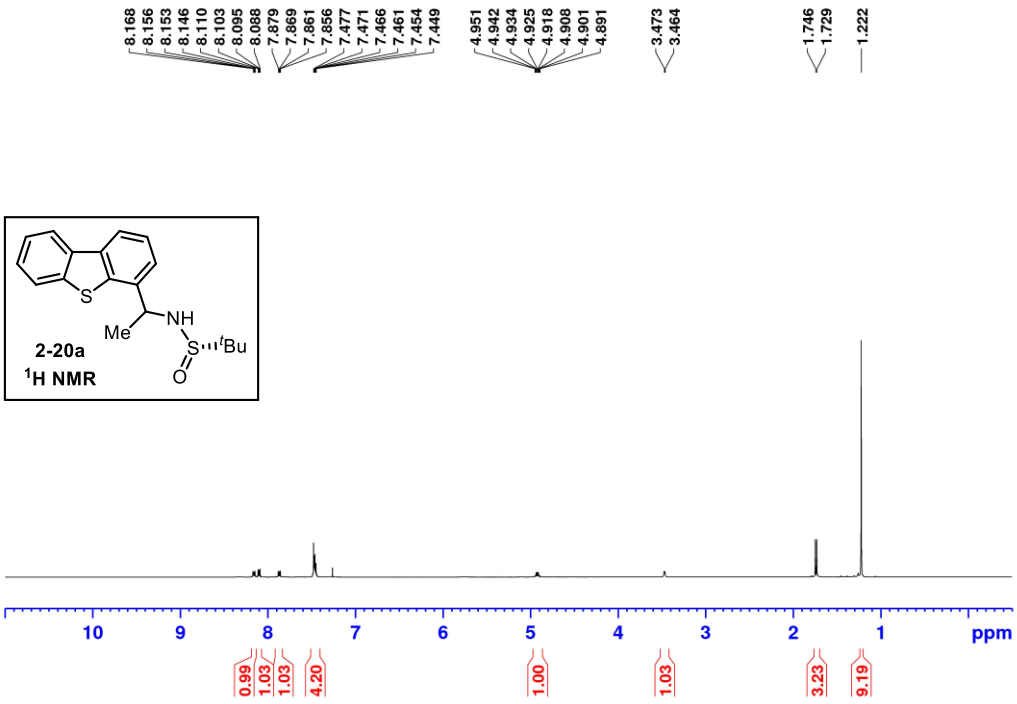
8.168
8.156
8.153
8.146
8.110
8.103
8.095
8.088
7.879
7.869
7.861
7.856
7.477
7.471
7.466
7.461
7.454
7.449
4.951
4.942
4.934
4.925
4.918
4.908
4.901
4.891
3.473
3.464
1.746
1.729
1.222
S
Me
NH
S
tBu
O
2-20a
1H NMR
10
9
8
7
6
5
4
3
2
1
ppm
0.99
1.03
1.03
4.20
1.00
1.03
3.23
9.19

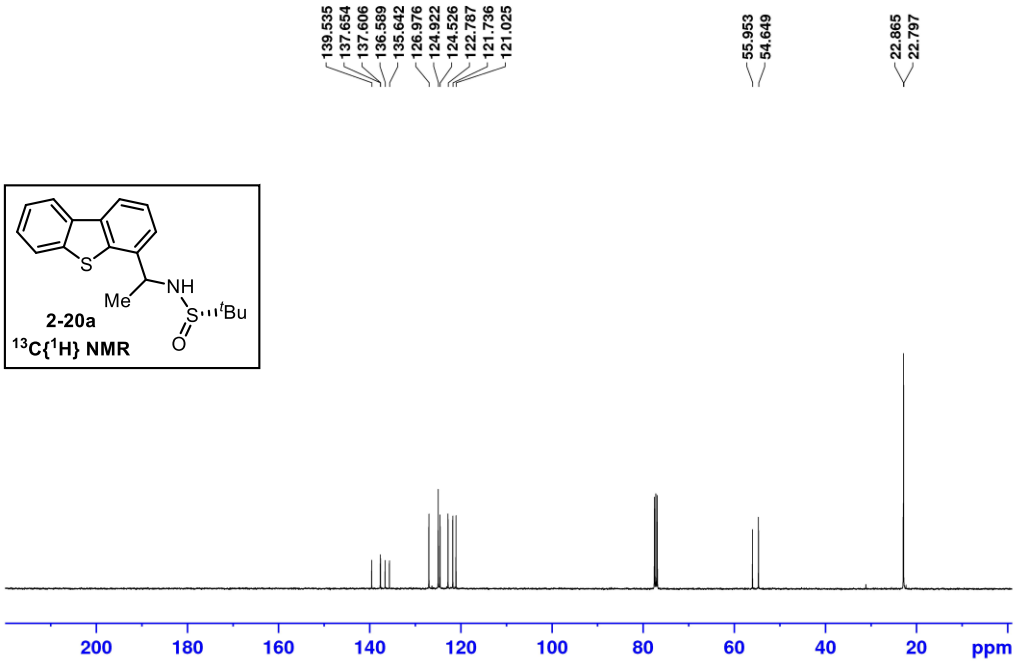
139.535
137.654
137.606
136.589
135.642
126.976
124.922
124.526
122.787
121.736
121.025
55.953
54.649
22.865
22.797
S
Me
NH
S
tBu
O
2-20a
13C{1H} NMR
200
180
160
140
120
100
80
60
40
20
ppm

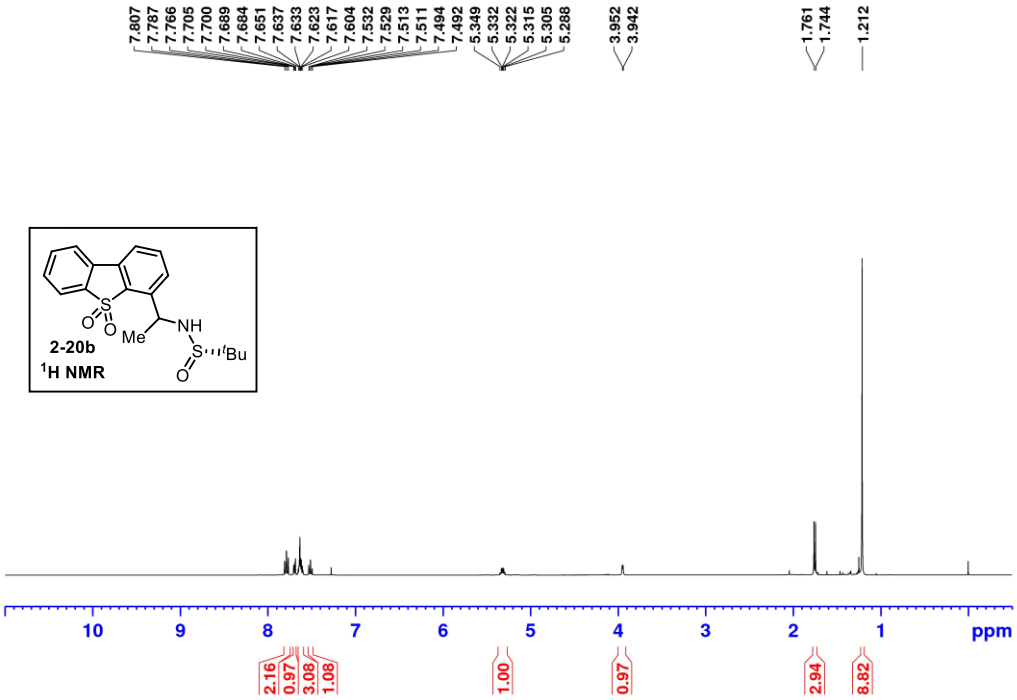
7.807
7.787
7.766
7.705
7.700
7.689
7.684
7.651
7.637
7.633
7.623
7.617
7.604
7.532
7.529
7.513
7.511
7.494
7.492
5.349
5.332
5.322
5.315
5.305
5.288
3.952
3.942
1.761
1.744
1.212
2-20b
1H NMR
10
9
8
7
6
5
4
3
2
1
ppm
2.16
0.97
3.08
1.08
1.00
0.97
2.94
8.82

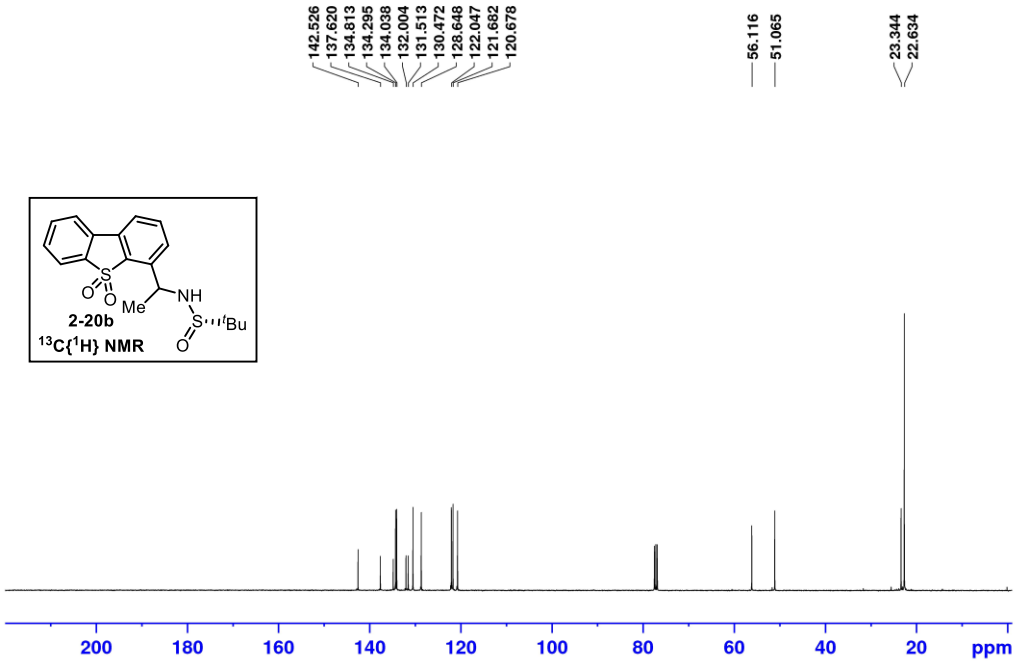
142.526
137.620
134.813
134.295
134.038
132.004
131.513
130.472
128.648
122.047
121.682
120.678
56.116
51.065
23.344
22.634
2-20b
13C{1H} NMR
200
180
160
140
120
100
80
60
40
20
ppm

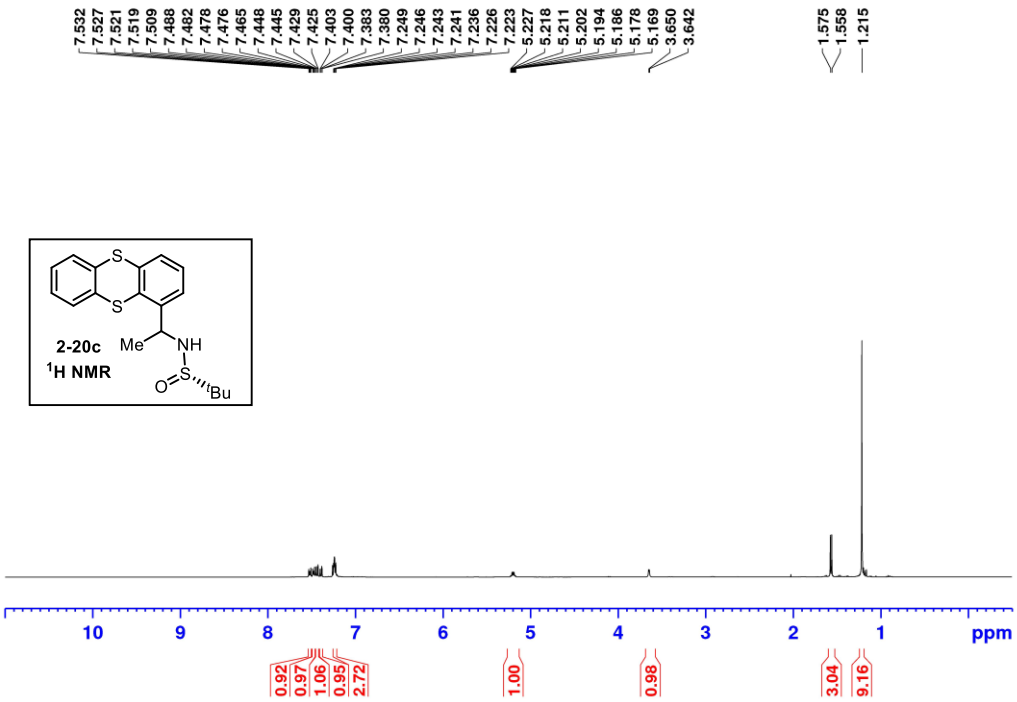
7.532
7.527
7.521
7.519
7.509
7.488
7.482
7.478
7.476
7.465
7.448
7.445
7.429
7.425
7.403
7.400
7.383
7.380
7.249
7.246
7.243
7.241
7.236
7.226
7.223
5.227
5.218
5.211
5.202
5.194
5.186
5.178
5.169
3.650
3.642
1.575
1.558
1.215
2-20c
1H NMR
Me
NH
tBu
10
9
8
7
6
5
4
3
2
1
ppm
0.92
0.97
1.06
0.95
2.72
1.00
0.98
3.04
9.16

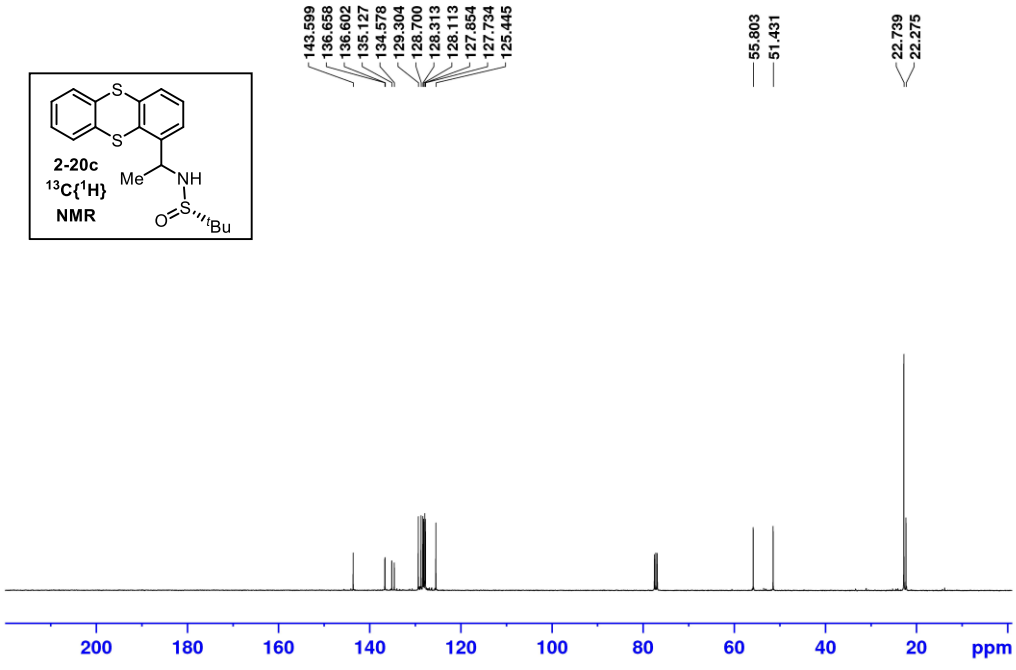
143.599
136.658
136.602
135.127
134.578
129.304
128.700
128.313
128.113
127.854
127.734
125.445
55.803
51.431
22.739
22.275
2-20c
13C{1H}
NMR
Me
NH
tBu
200
180
160
140
120
100
80
60
40
20
ppm

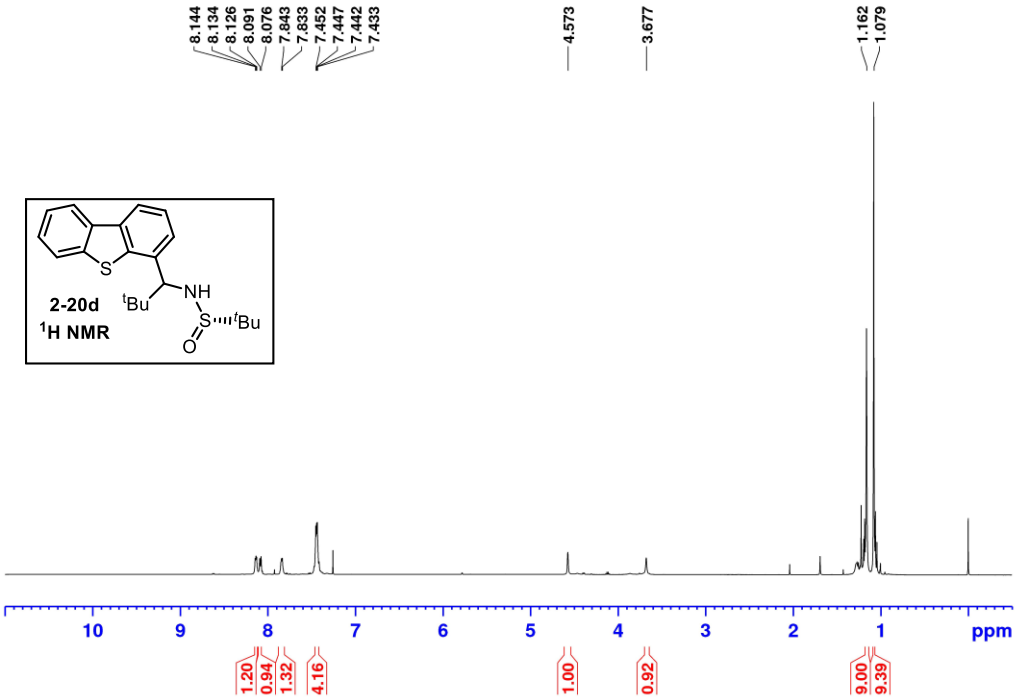
8.144
8.134
8.126
8.091
8.076
7.843
7.833
7.452
7.447
7.442
7.433
4.573
3.677
1.162
1.079
2-20d
^{1}H NMR
10
9
8
7
6
5
4
3
2
1
ppm
1.20
0.94
1.32
4.16
1.00
0.92
9.00
9.39

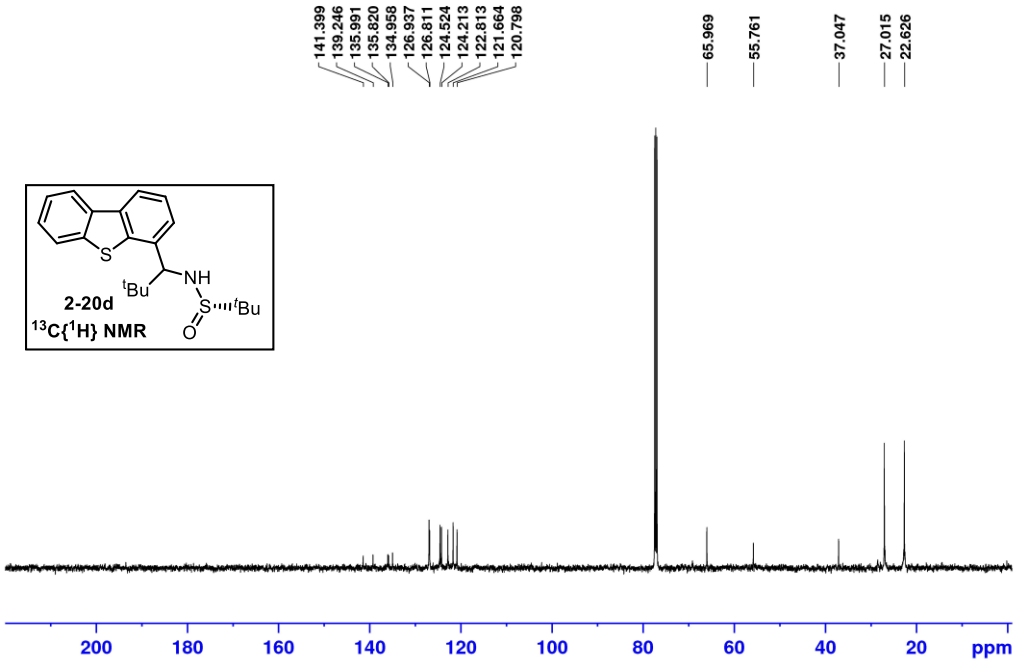
141.399
139.246
135.991
135.820
134.958
126.937
126.811
124.524
124.213
122.813
121.664
120.798
65.969
55.761
37.047
27.015
22.626
2-20d
^{13}C{^{1}H} NMR
200
180
160
140
120
100
80
60
40
20
ppm

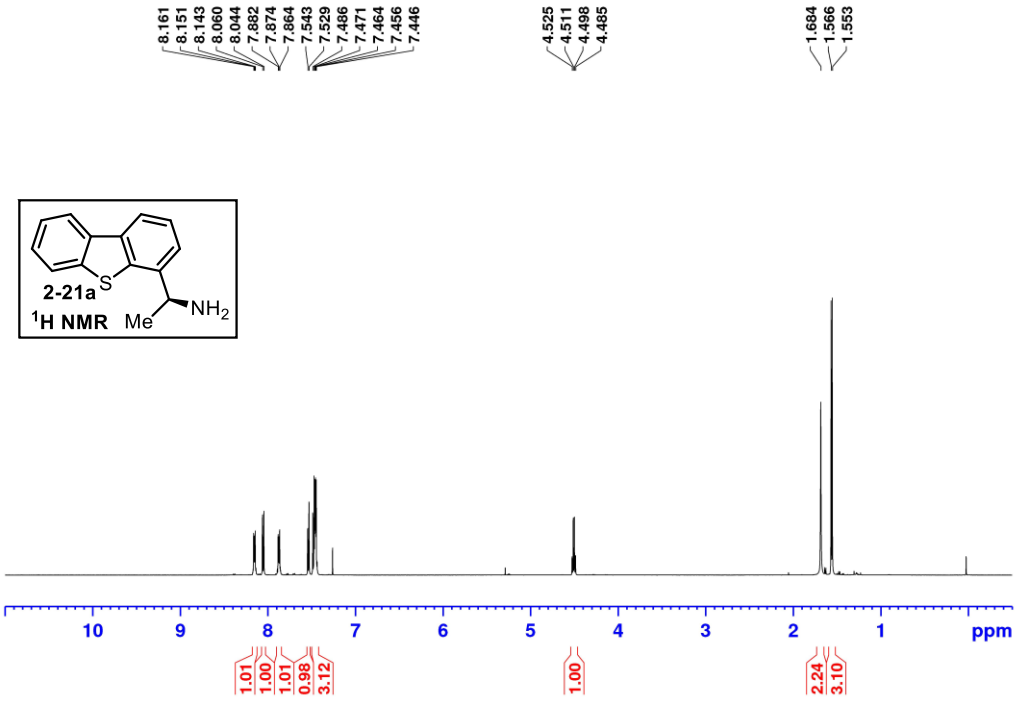
8.161
8.151
8.143
8.060
8.044
7.882
7.874
7.864
7.543
7.529
7.486
7.471
7.464
7.456
7.446
4.525
4.511
4.498
4.485
1.684
1.566
1.553
2-21a
1H NMR
Me
NH2
10
9
8
7
6
5
4
3
2
1
ppm
1.01
1.00
1.01
0.98
3.12
1.00
2.24
3.10

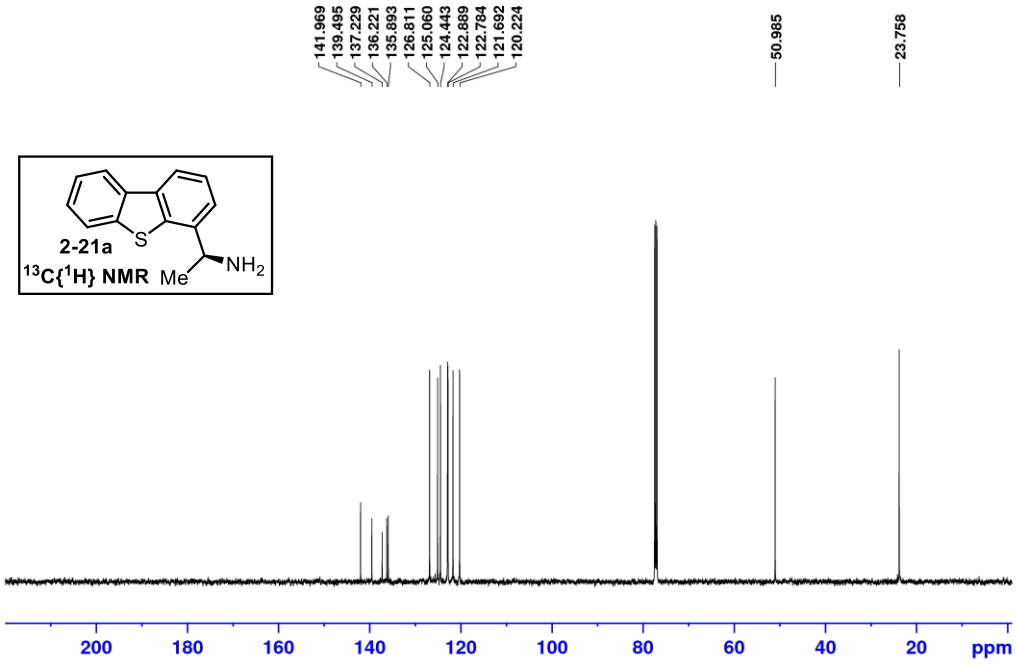
141.969
139.495
137.229
136.221
135.893
126.811
125.060
124.443
122.889
122.784
121.692
120.224
50.985
23.758
2-21a
13C{1H} NMR
Me
NH2
200
180
160
140
120
100
80
60
40
20
ppm

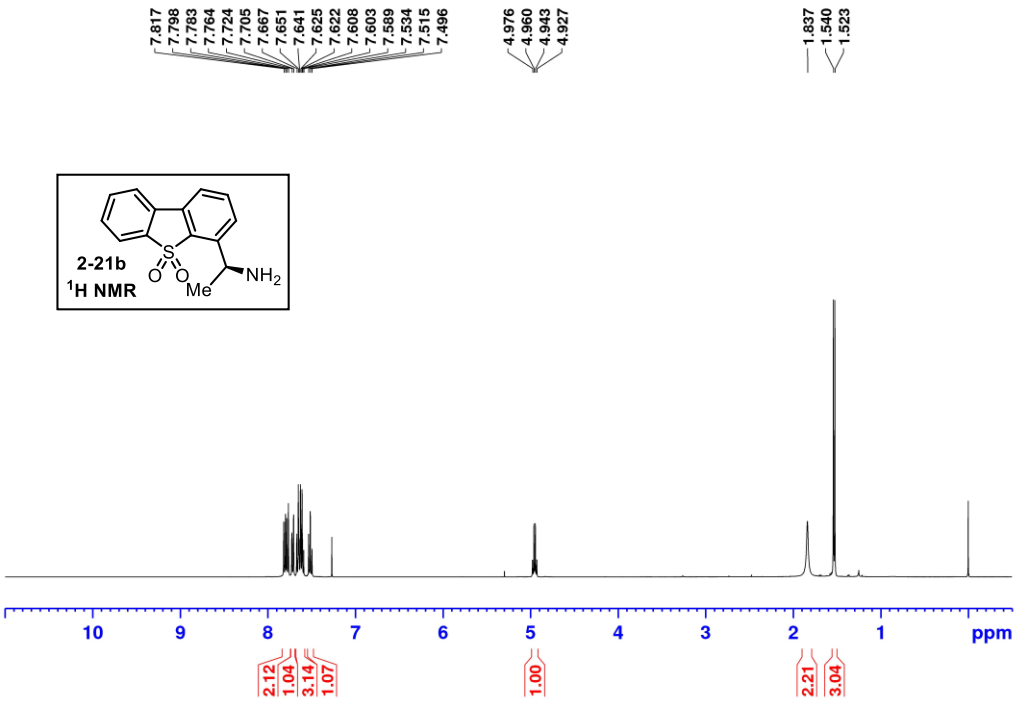
7.817
7.798
7.783
7.764
7.724
7.705
7.667
7.651
7.641
7.625
7.622
7.608
7.603
7.589
7.534
7.515
7.496
4.976
4.960
4.943
4.927
1.837
1.540
1.523
2-21b
1H NMR
NH2
Me
10
9
8
7
6
5
4
3
2
1
ppm
2.12
1.04
3.14
1.07
1.00
2.21
3.04

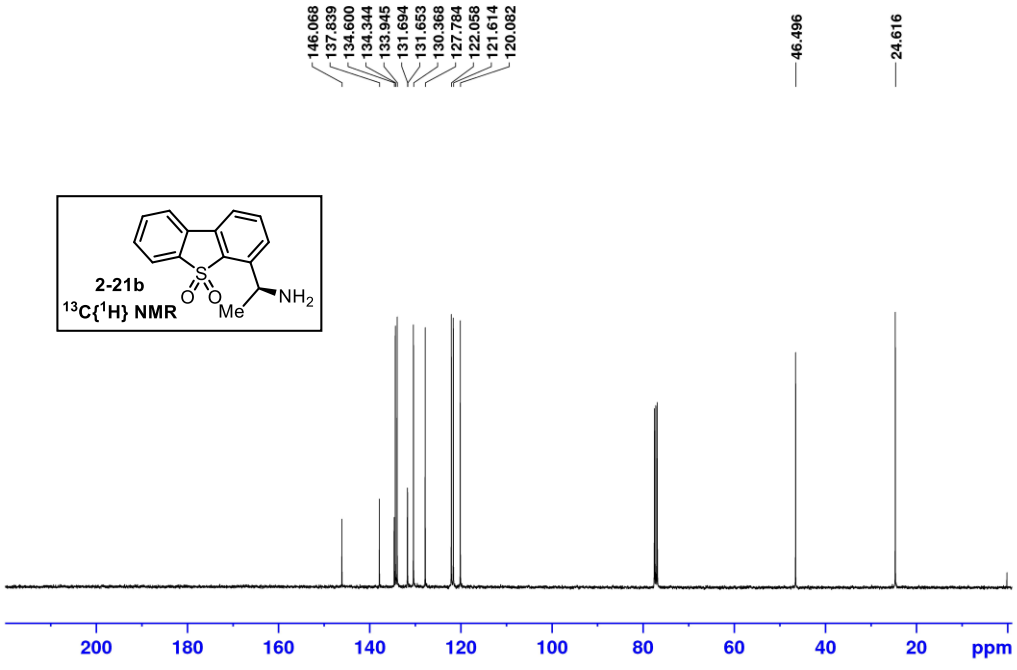
146.068
137.839
134.600
134.344
133.945
131.694
131.653
130.368
127.784
122.058
121.614
120.082
46.496
24.616
2-21b
13C{1H} NMR
NH2
Me
200
180
160
140
120
100
80
60
40
20
ppm

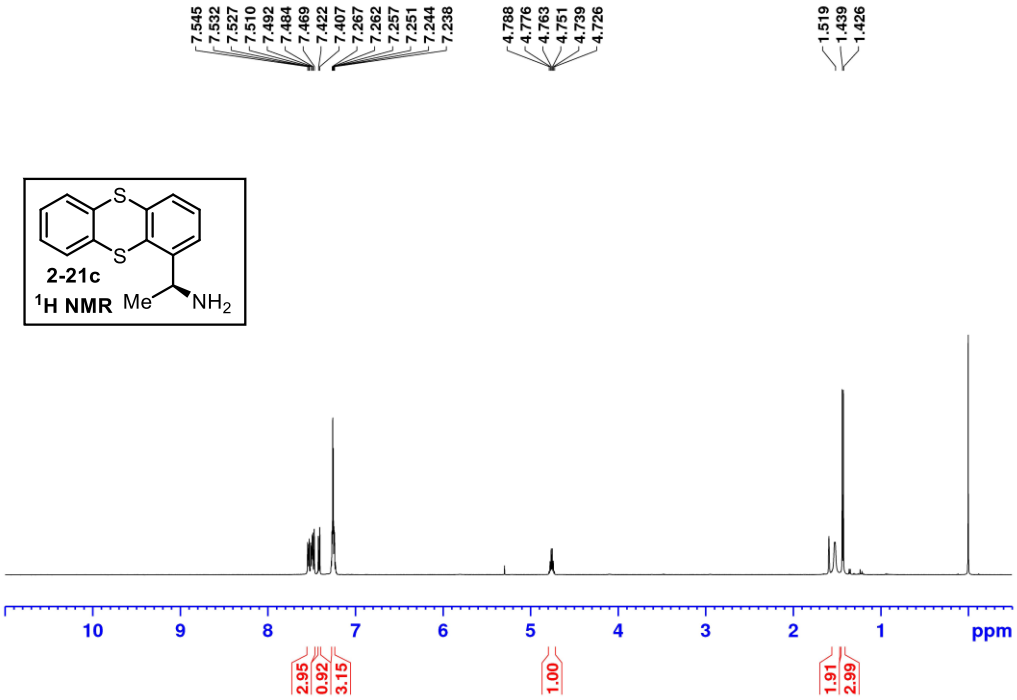
7.545
7.532
7.527
7.510
7.492
7.484
7.469
7.422
7.407
7.267
7.262
7.257
7.251
7.244
7.238
4.788
4.776
4.763
4.751
4.739
4.726
1.519
1.439
1.426
2-21c
1H NMR
Me
NH2
10
9
8
7
6
5
4
3
2
1
ppm
2.95
0.92
3.15
1.00
1.91
2.99

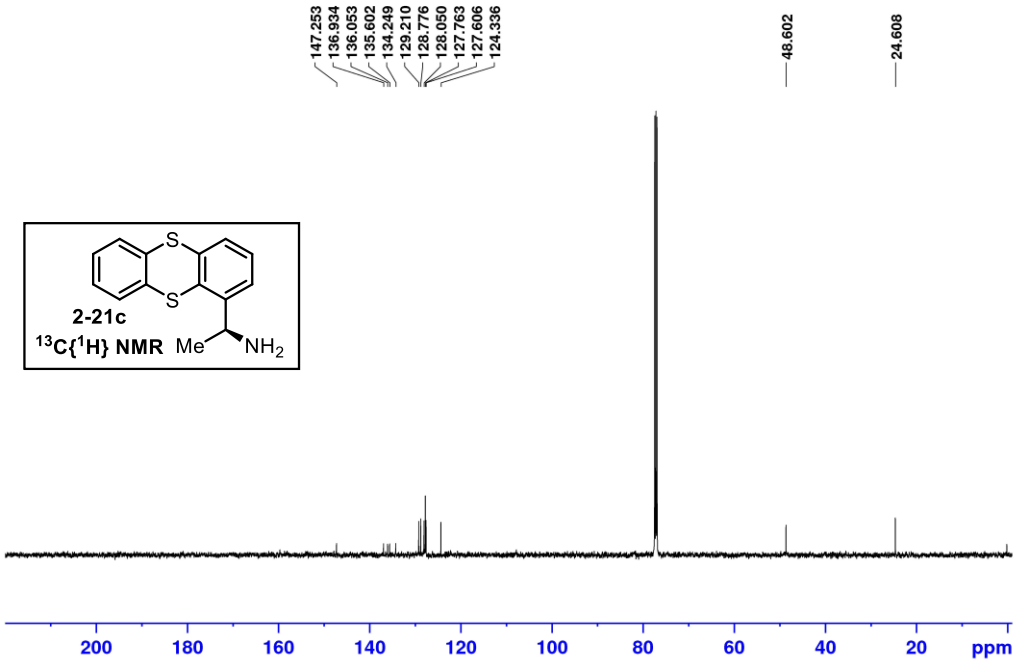
147.253
136.934
136.053
135.602
134.249
129.210
128.776
128.050
127.763
127.606
124.336
48.602
24.608
2-21c
13C{1H} NMR
Me
NH2
200
180
160
140
120
100
80
60
40
20
ppm

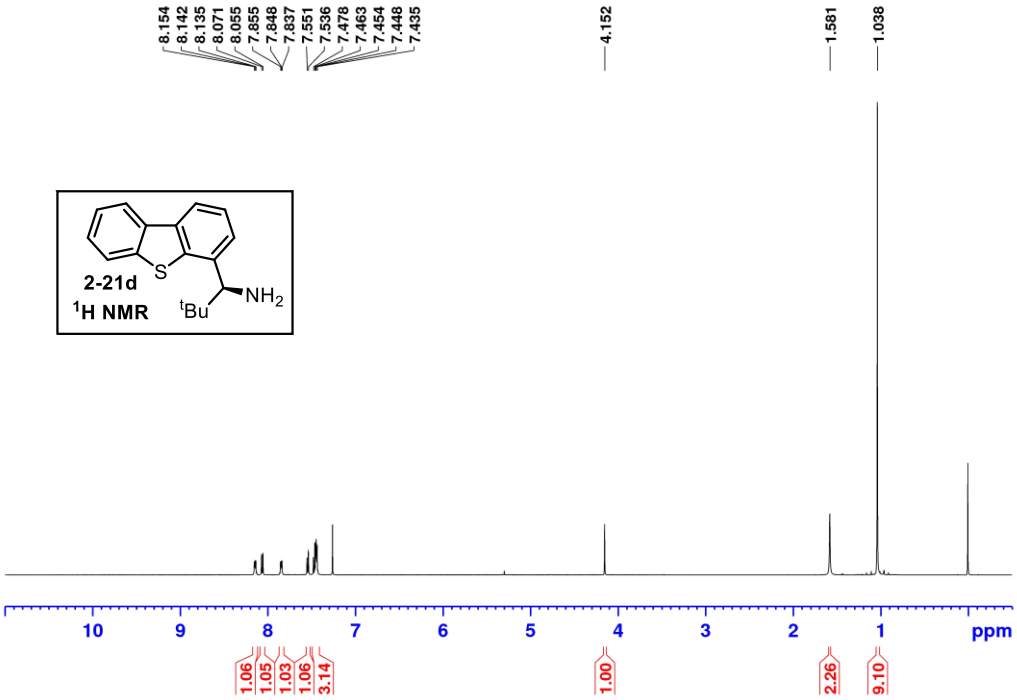
8.154
8.142
8.135
8.071
8.055
7.855
7.848
7.837
7.551
7.536
7.478
7.463
7.454
7.448
7.435
4.152
1.581
1.038
2-21d
1H NMR
tBu
NH2
10
9
8
7
6
5
4
3
2
1
ppm
1.06
1.05
1.03
1.06
3.14
1.00
2.26
9.10

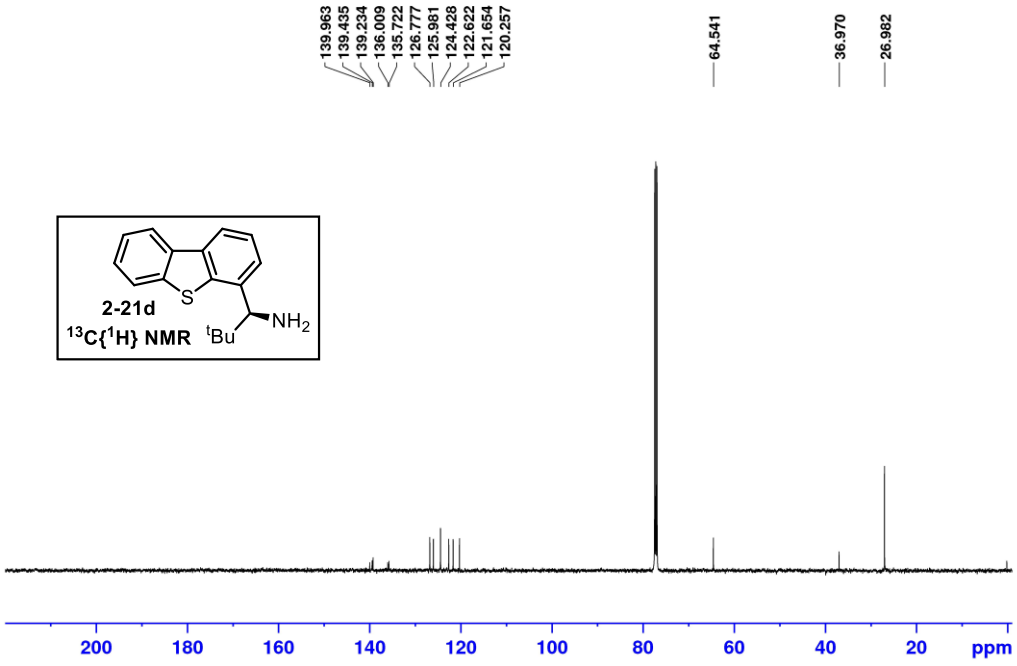
139.963
139.435
139.234
136.009
135.722
126.777
125.981
124.428
122.622
121.654
120.257
64.541
36.970
26.982
2-21d
13C{1H} NMR
tBu
NH2
200
180
160
140
120
100
80
60
40
20
ppm

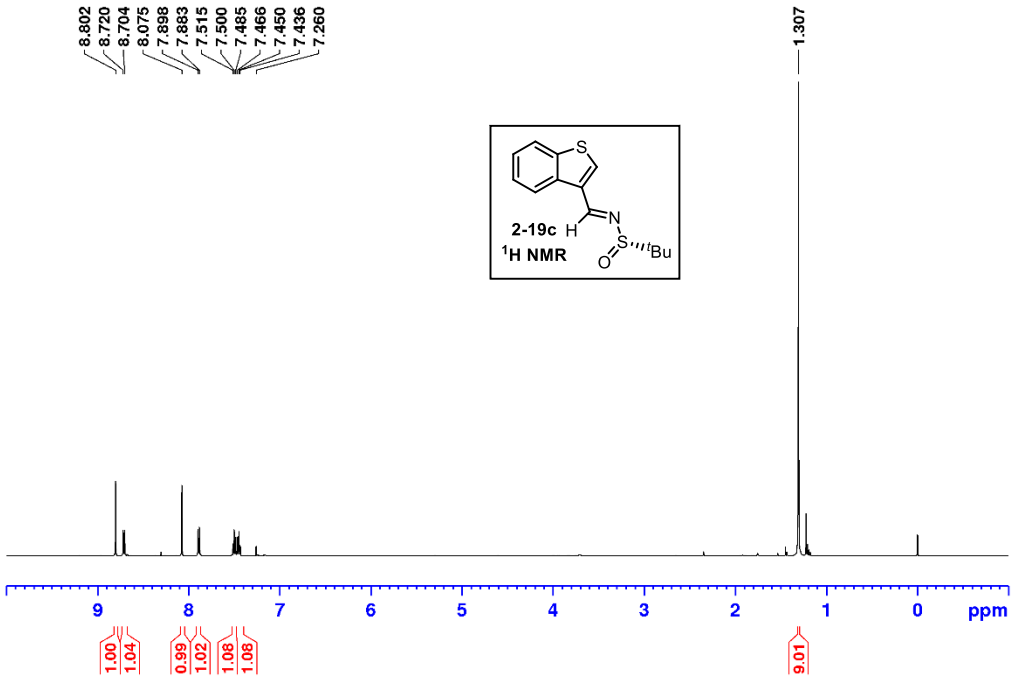
8.802
8.720
8.704
8.075
7.898
7.883
7.515
7.500
7.485
7.466
7.450
7.436
7.260
1.307
2-19c
^{1}H NMR
9
8
7
6
5
4
3
2
1
0
ppm
1.00
1.04
0.99
1.02
1.08
1.08
9.01

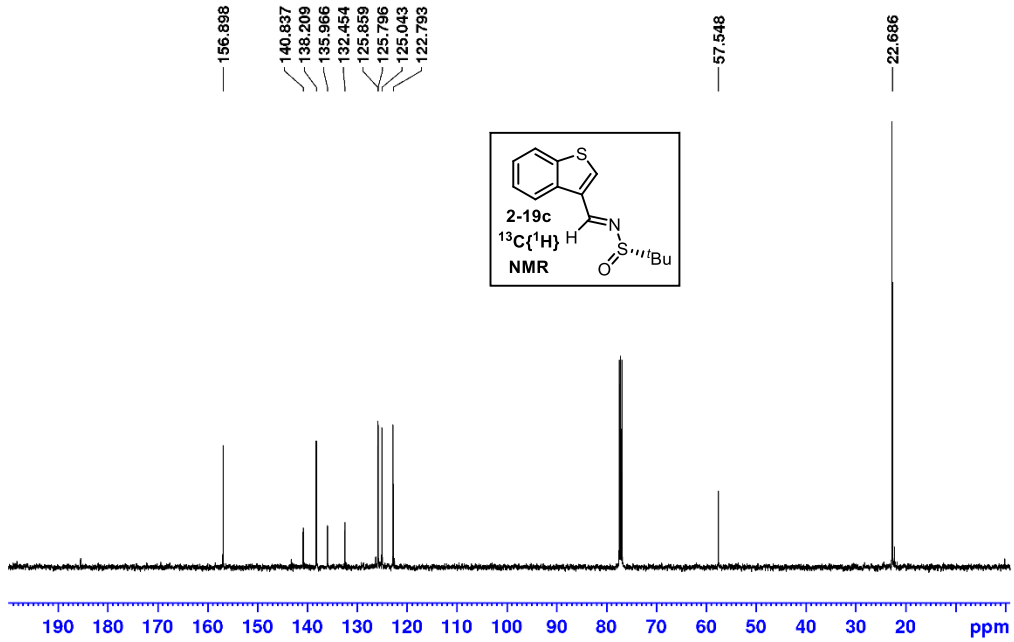
156.898
140.837
138.209
135.966
132.454
125.859
125.796
125.043
122.793
57.548
22.686
2-19c
^{13}C{^{1}H}
NMR
190
180
170
160
150
140
130
120
110
100
90
80
70
60
50
40
30
20
ppm

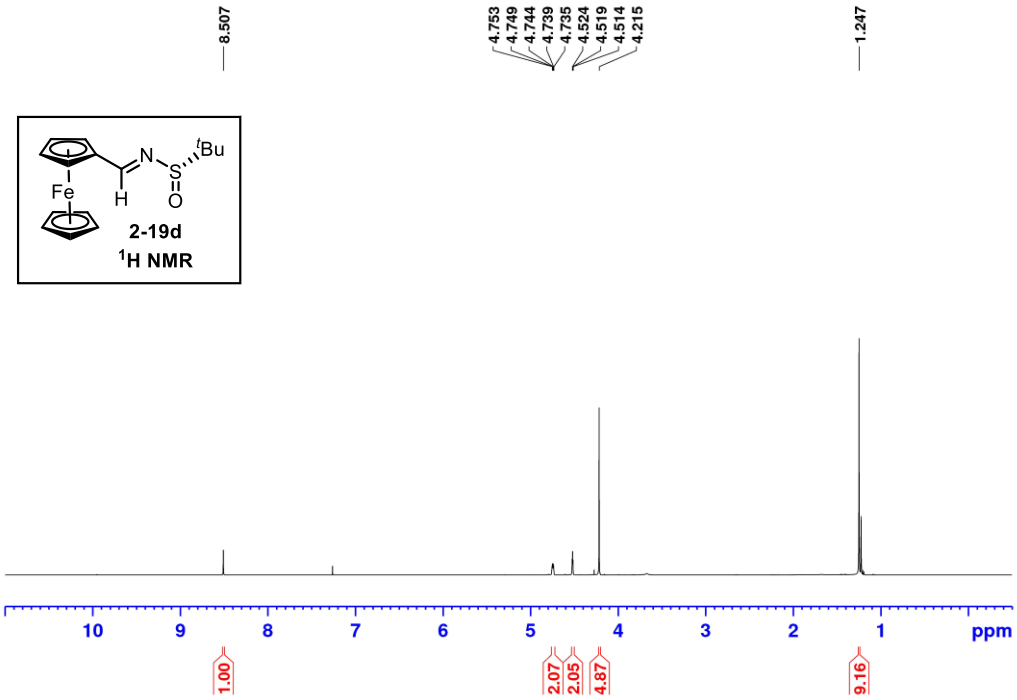
8.507
4.753
4.749
4.744
4.739
4.735
4.524
4.519
4.514
4.215
1.247
tBu
N
S
O
Fe
H
2-19d
1H NMR
10
9
8
7
6
5
4
3
2
1
ppm
1.00
2.07
2.05
4.87
9.16

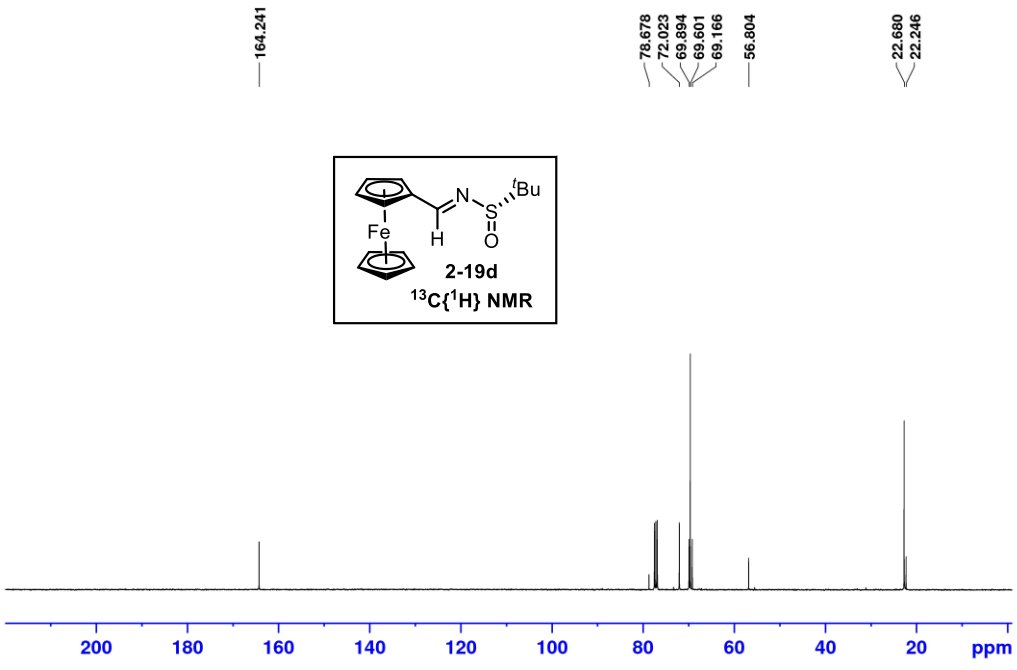
164.241
78.678
72.023
69.894
69.601
69.166
56.804
22.680
22.246
tBu
N
S
O
Fe
H
2-19d
13C{1H} NMR
200
180
160
140
120
100
80
60
40
20
ppm

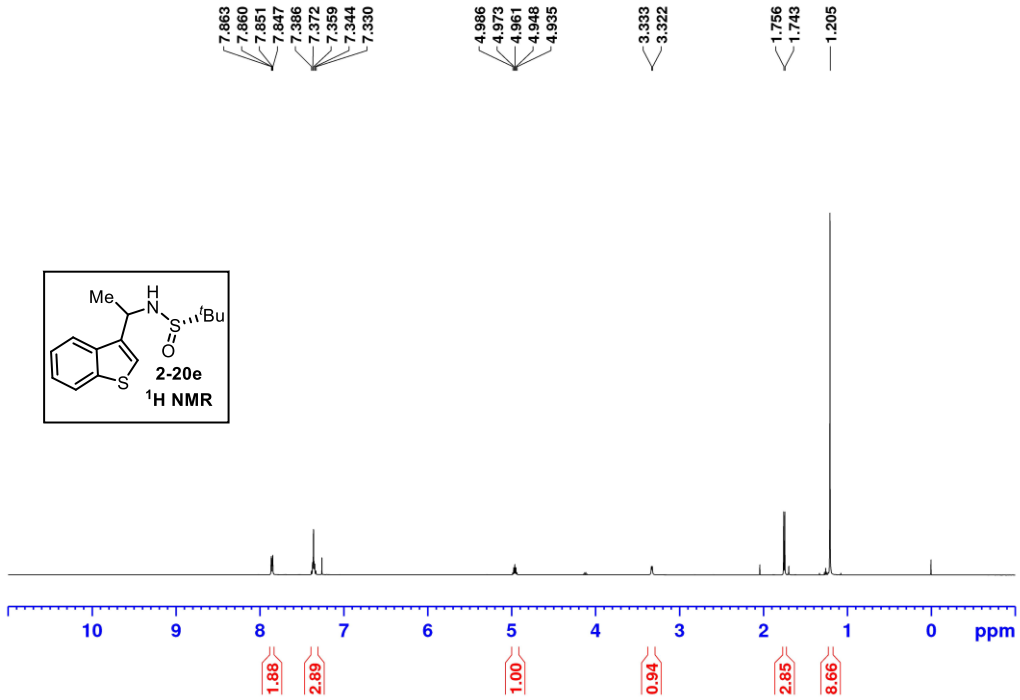
7.863
7.860
7.851
7.847
7.386
7.372
7.359
7.344
7.330
4.986
4.973
4.961
4.948
4.935
3.333
3.322
1.756
1.743
1.205
Me
H
N
S
O
tBu
S
2-20e
1H NMR
10
9
8
7
6
5
4
3
2
1
0
ppm
1.88
2.89
1.00
0.94
2.85
8.66

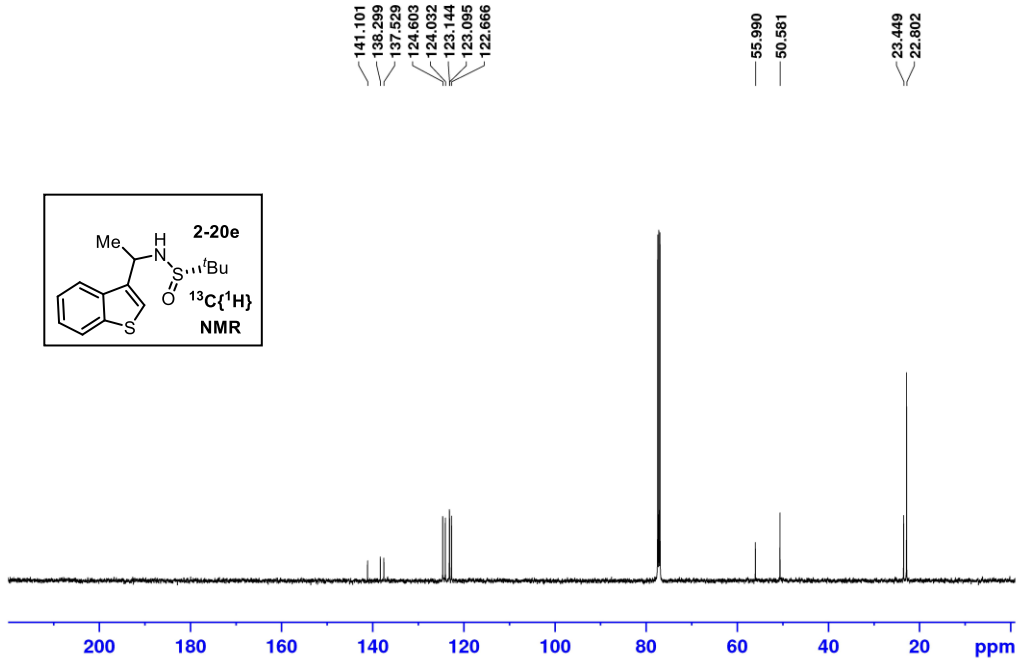
141.101
138.299
137.529
124.603
124.032
123.144
123.095
122.666
55.990
50.581
23.449
22.802
Me
H
N
S
O
tBu
S
2-20e
13C{1H}
NMR
200
180
160
140
120
100
80
60
40
20
ppm

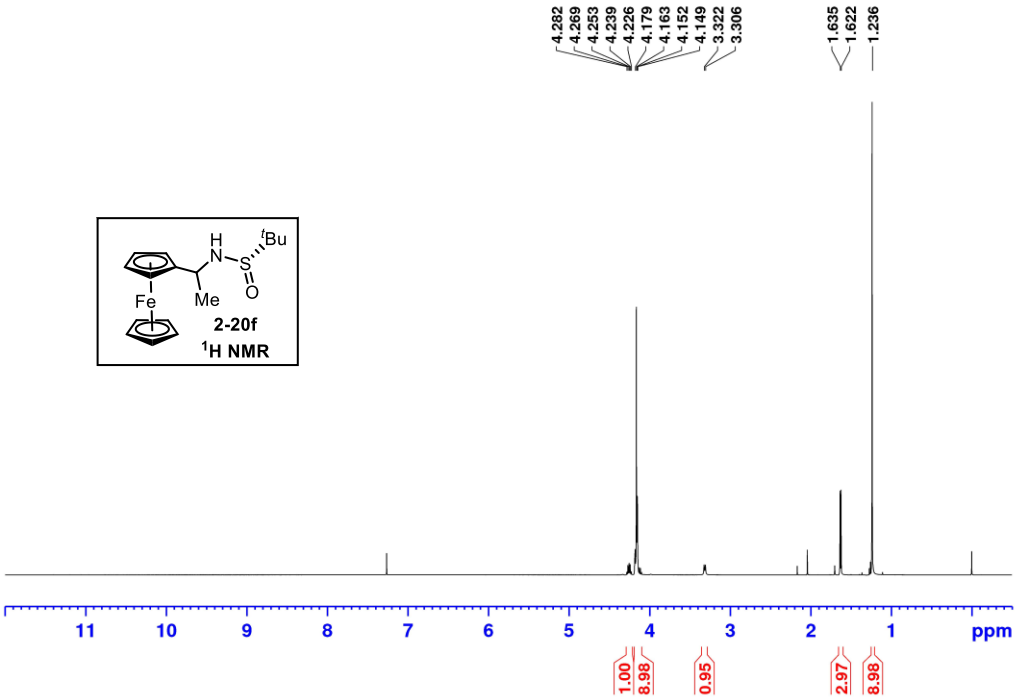
4.282
4.269
4.253
4.239
4.226
4.179
4.163
4.152
4.149
3.322
3.306
1.635
1.622
1.236
H
N
S
O
tBu
Fe
Me
2-20f
1H NMR
11
10
9
8
7
6
5
4
3
2
1
ppm
1.00
8.98
0.95
2.97
8.98

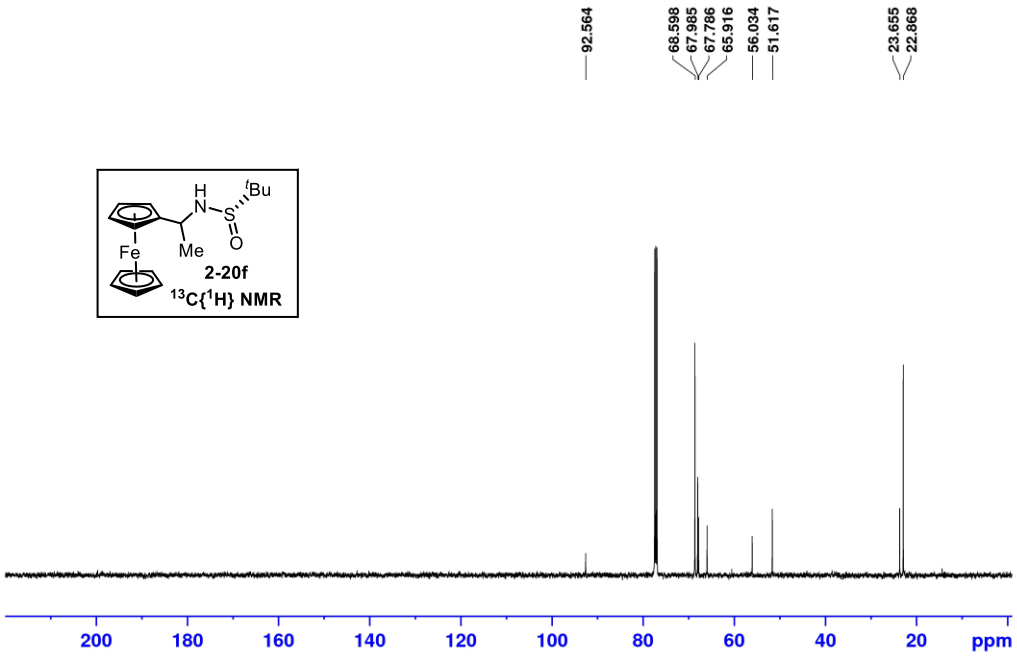
92.564
68.598
67.985
67.786
65.916
56.034
51.617
23.655
22.868
H
N
S
O
tBu
Fe
Me
2-20f
13C{1H} NMR
200
180
160
140
120
100
80
60
40
20
ppm

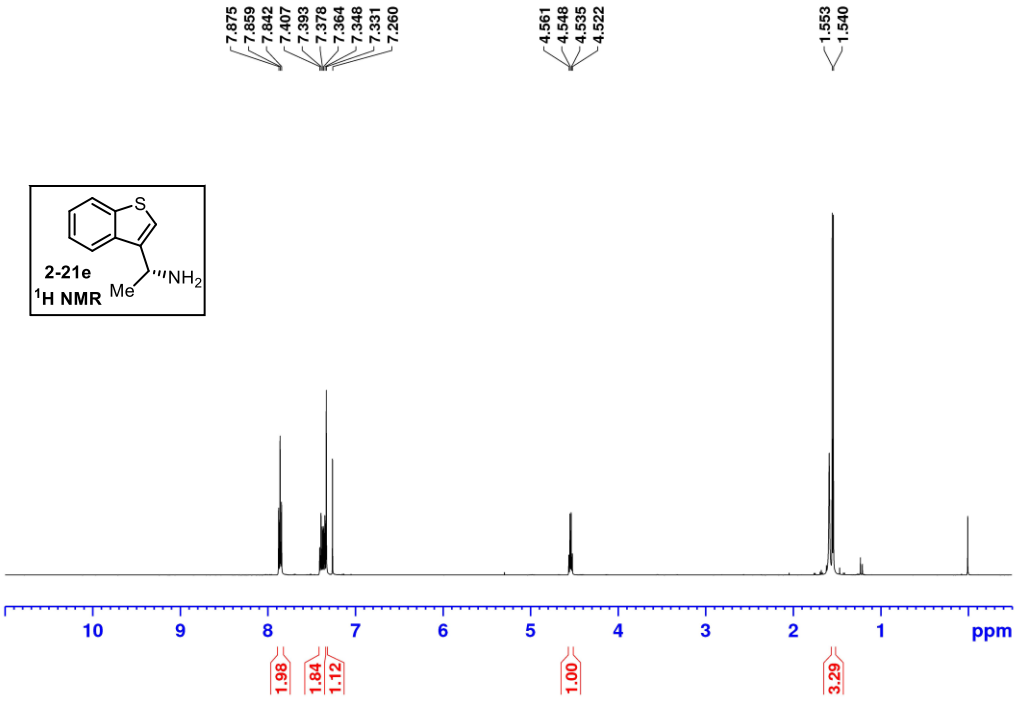
7.875
7.859
7.842
7.407
7.393
7.378
7.364
7.348
7.331
7.260
4.561
4.548
4.535
4.522
1.553
1.540
2-21e
1H NMR
Me
NH2
10
9
8
7
6
5
4
3
2
1
ppm
1.98
1.84
1.12
1.00
3.29

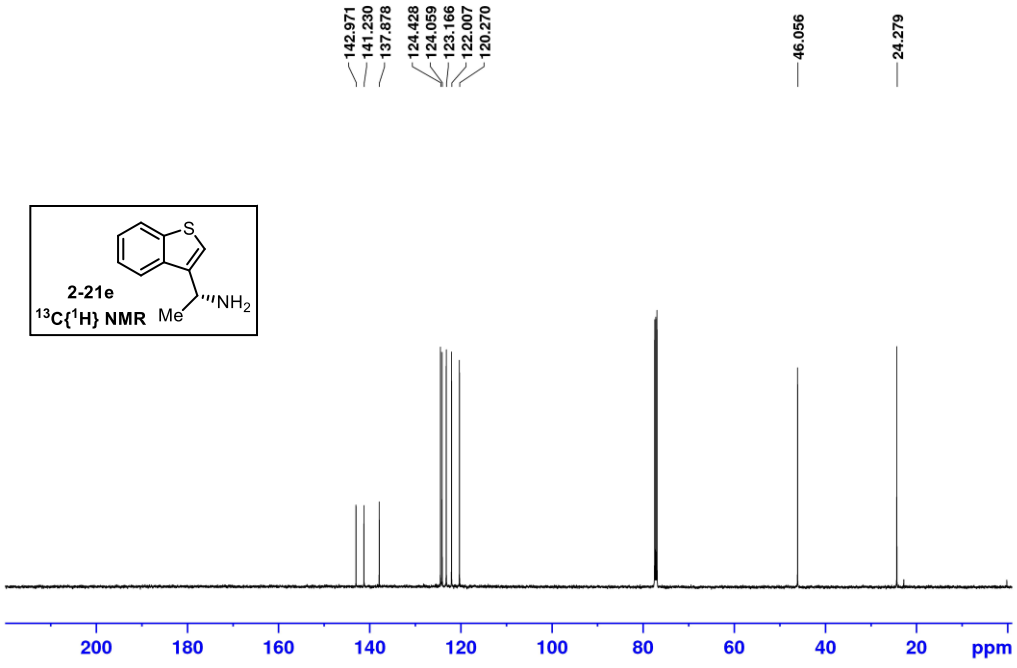
142.971
141.230
137.878
124.428
124.059
123.166
122.007
120.270
46.056
24.279
2-21e
13C{1H} NMR
Me
NH2
200
180
160
140
120
100
80
60
40
20
ppm

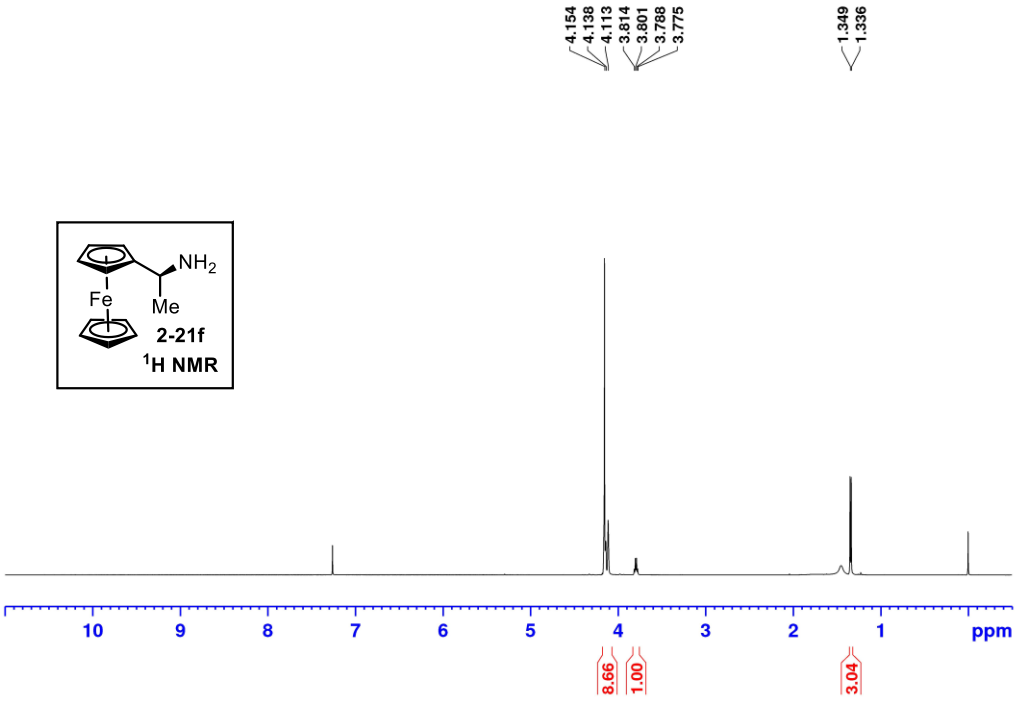
4.154
4.138
4.113
3.814
3.801
3.788
3.775
1.349
1.336
NH2
Fe
Me
2-21f
1H NMR
10
9
8
7
6
5
4
3
2
1
ppm
8.66
1.00
3.04

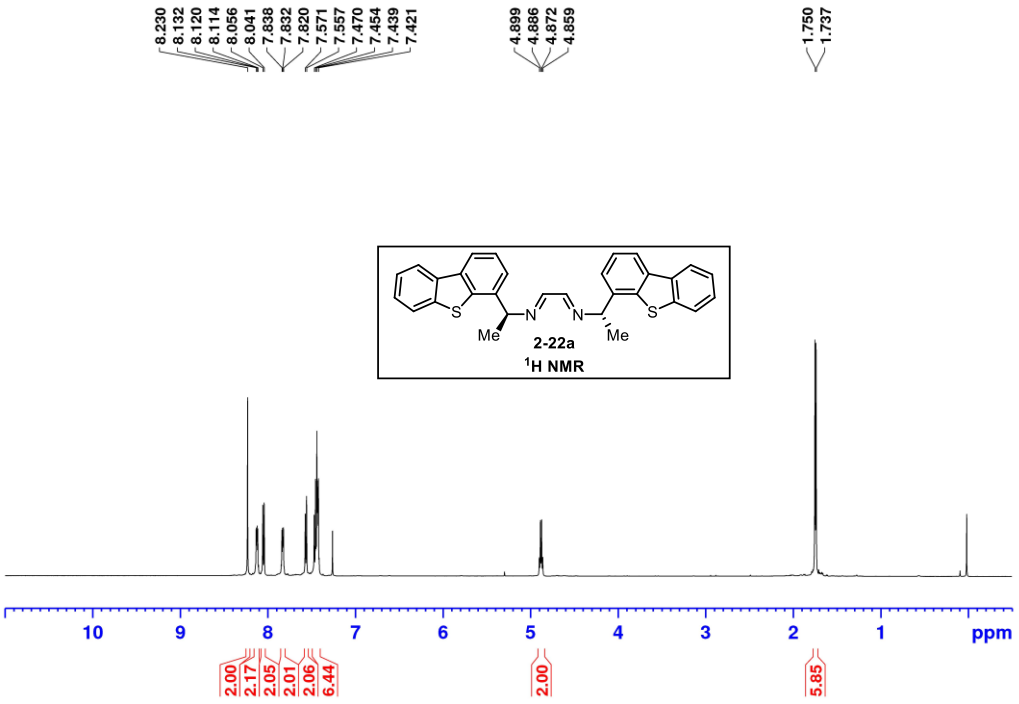
8.230
8.132
8.120
8.114
8.056
8.041
7.838
7.832
7.820
7.571
7.557
7.470
7.454
7.439
7.421
4.899
4.886
4.872
4.859
1.750
1.737
S
N
N
S
Me
Me
2-22a
1H NMR
10
9
8
7
6
5
4
3
2
1
ppm
2.00
2.17
2.05
2.01
2.06
6.44
2.00
5.85

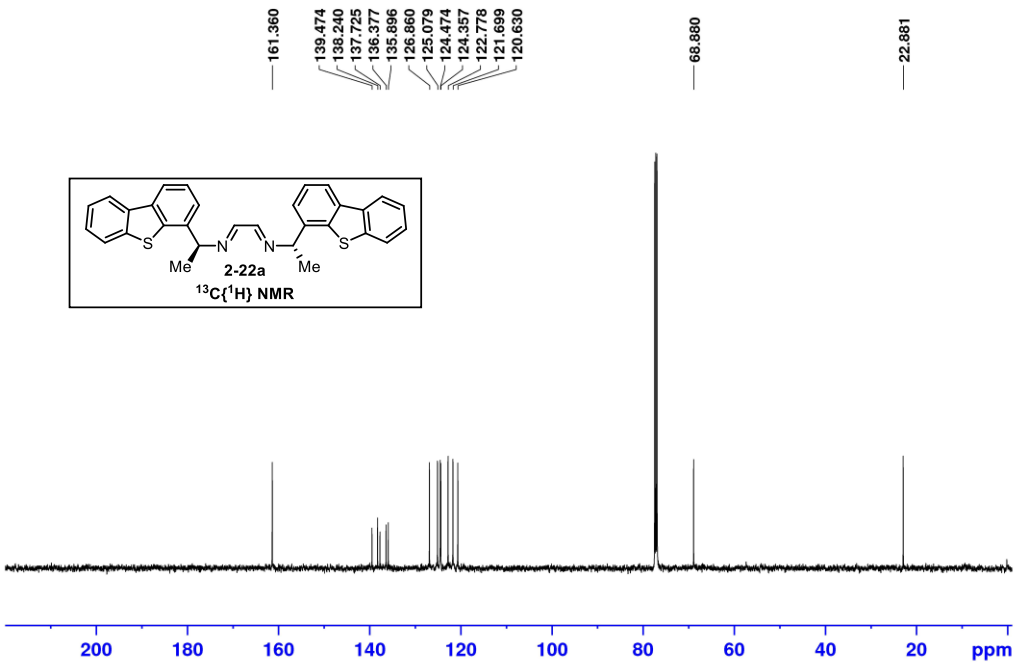
161.360
139.474
138.240
137.725
136.377
135.896
126.860
125.079
124.474
124.357
122.778
121.699
120.630
68.880
22.881
Me
2-22a
Me
$^{13}C\{^{1}H\}$ NMR
200
180
160
140
120
100
80
60
40
20
ppm

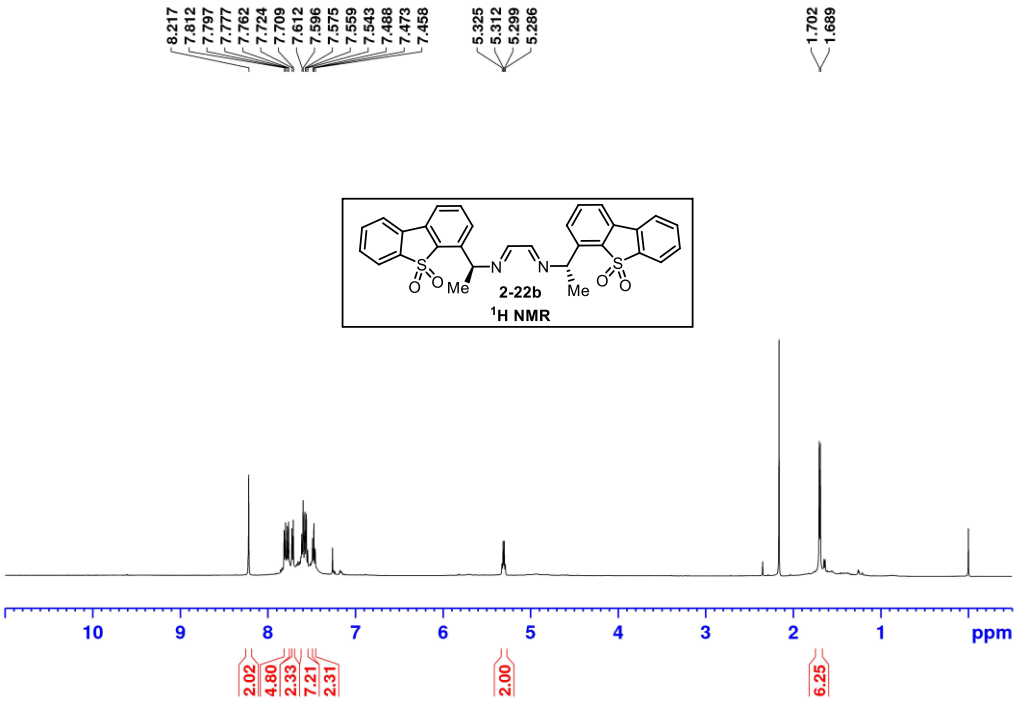
8.217
7.812
7.797
7.777
7.762
7.724
7.709
7.612
7.596
7.575
7.559
7.543
7.488
7.473
7.458
5.325
5.312
5.299
5.286
1.702
1.689
Me
2-22b
Me
^{1}H NMR
10
9
8
7
6
5
4
3
2
1
ppm
2.02
4.80
2.33
7.21
2.31
2.00
6.25

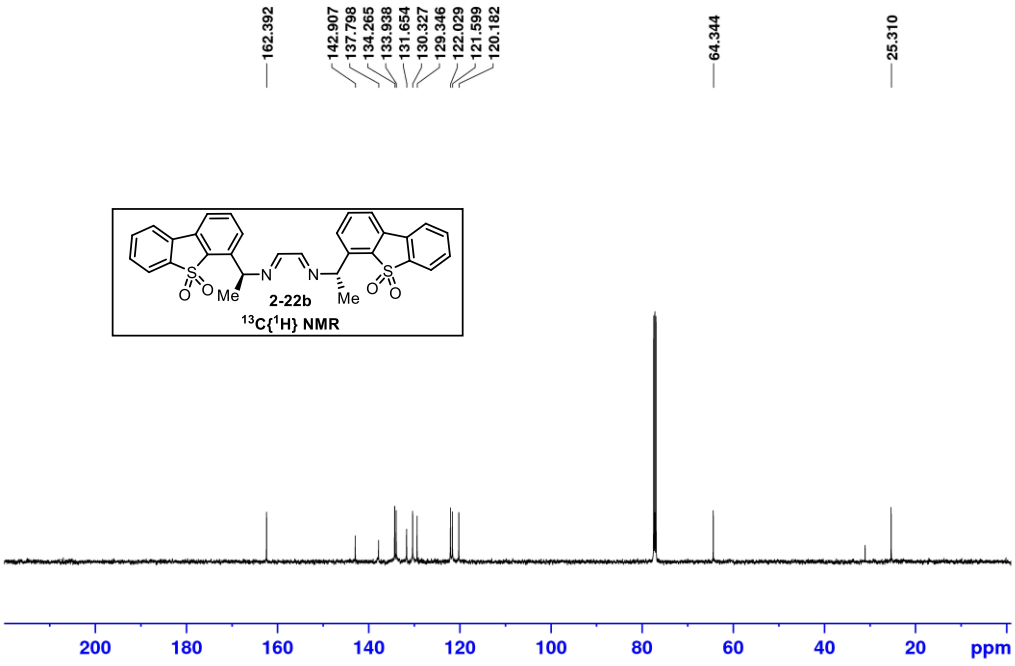
162.392
142.907
137.798
134.265
133.938
131.654
130.327
129.346
122.029
121.599
120.182
64.344
25.310
2-22b
$^{13}C\{^{1}H\}$ NMR
200
180
160
140
120
100
80
60
40
20
ppm

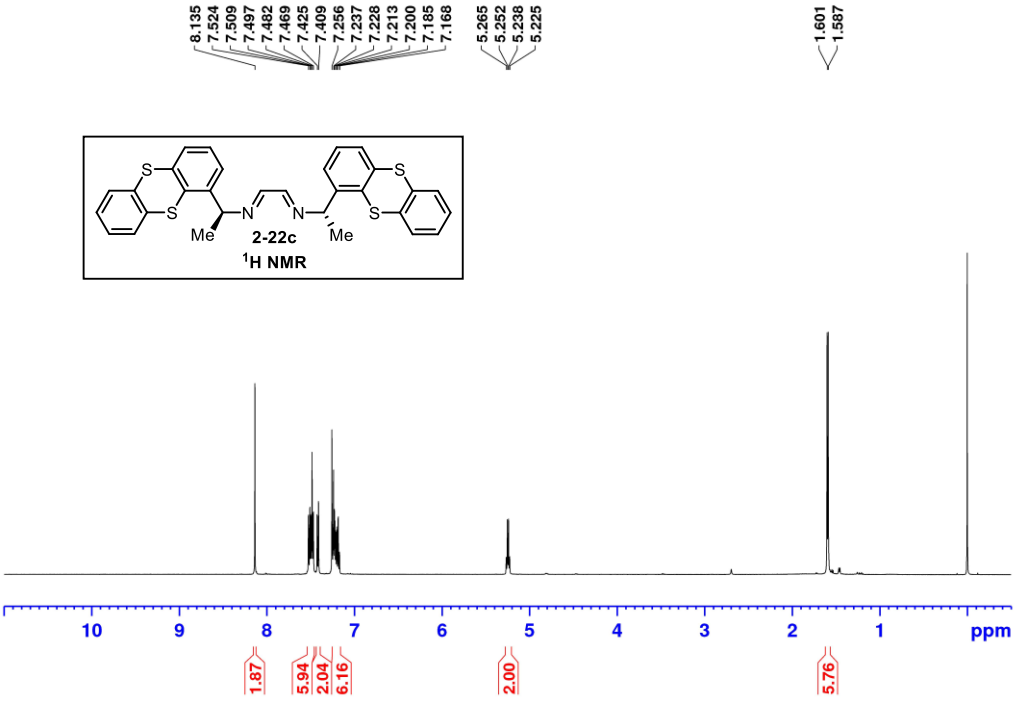
8.135
7.524
7.509
7.497
7.482
7.469
7.425
7.409
7.256
7.237
7.228
7.213
7.200
7.185
7.168
5.265
5.252
5.238
5.225
1.601
1.587
2-22c
^{1}H NMR
10
9
8
7
6
5
4
3
2
1
ppm
1.87
5.94
2.04
6.16
2.00
5.76

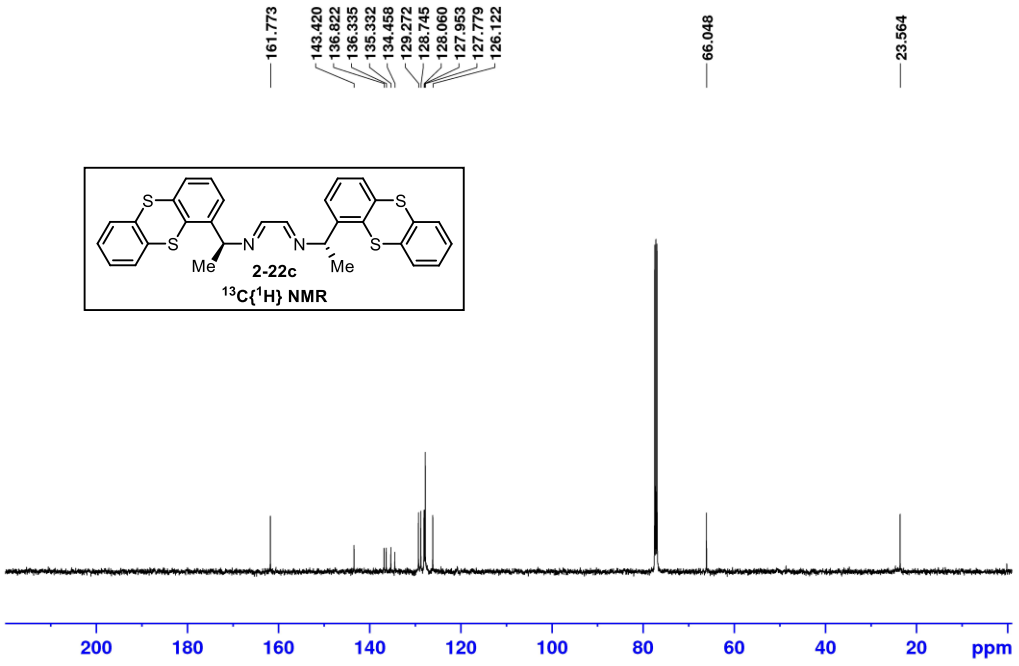
161.773
143.420
136.822
136.335
135.332
134.458
129.272
128.745
128.060
127.953
127.779
126.122
66.048
23.564
Me
2-22c
Me
$^{13}C\{^{1}H\}$ NMR
200
180
160
140
120
100
80
60
40
20
ppm

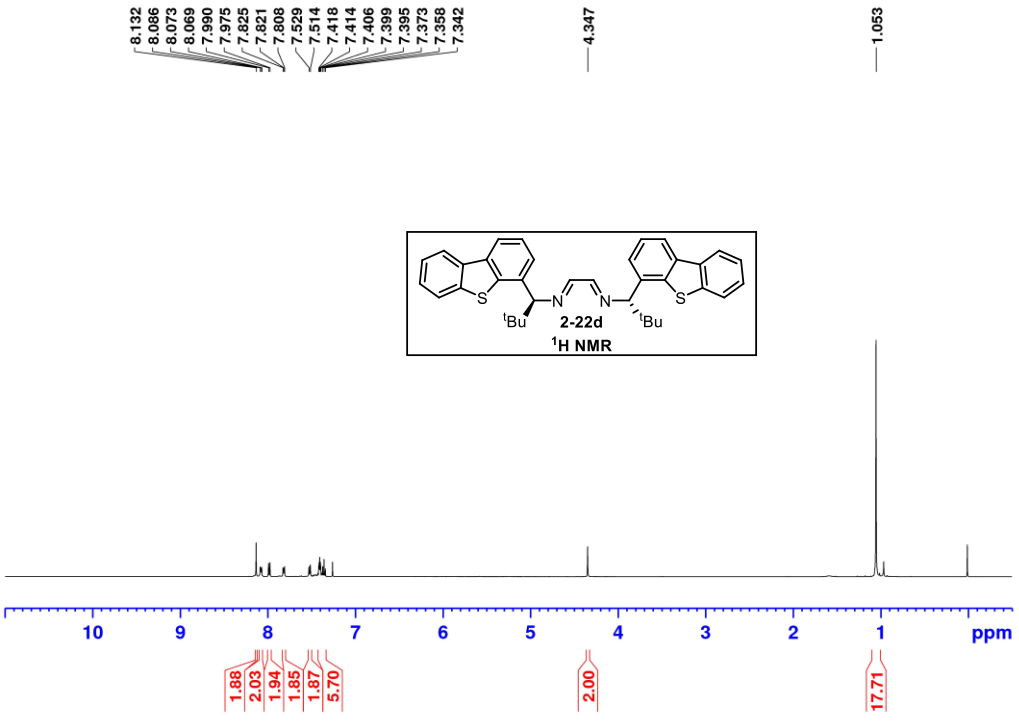
8.132
8.086
8.073
8.069
7.990
7.975
7.825
7.821
7.808
7.529
7.514
7.418
7.414
7.406
7.399
7.395
7.373
7.358
7.342
4.347
1.053
tBu
2-22d
tBu
^{1}H NMR
10
9
8
7
6
5
4
3
2
1
ppm
1.88
2.03
1.94
1.85
1.87
5.70
2.00
17.71

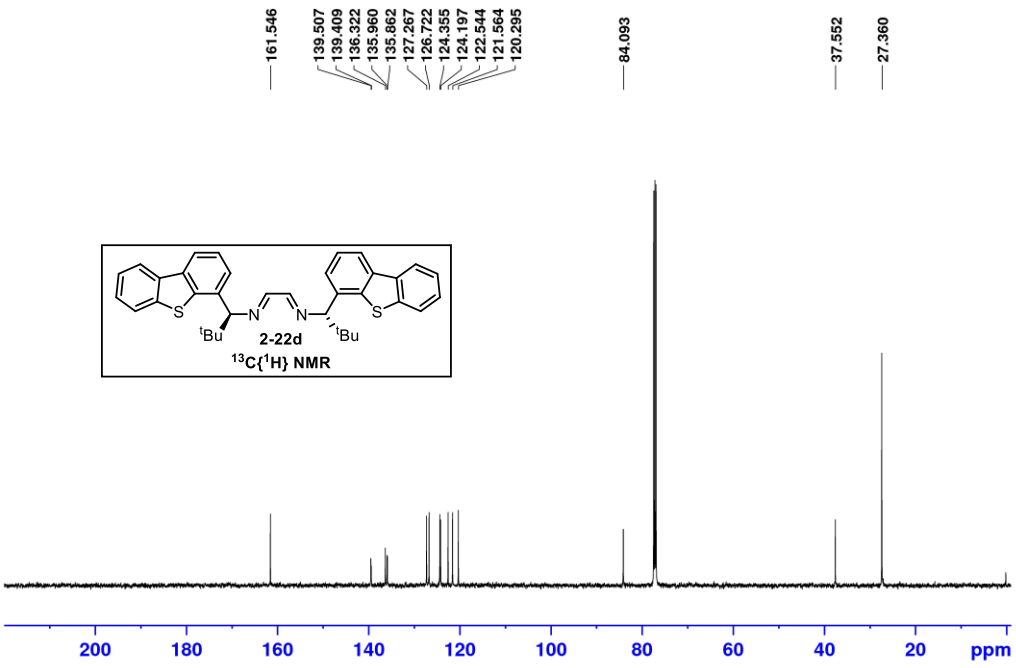
161.546
139.507
139.409
136.322
135.960
135.862
127.267
126.722
124.355
124.197
122.544
121.564
120.295
84.093
37.552
27.360
2-22d
13C{1H} NMR
200
180
160
140
120
100
80
60
40
20
ppm

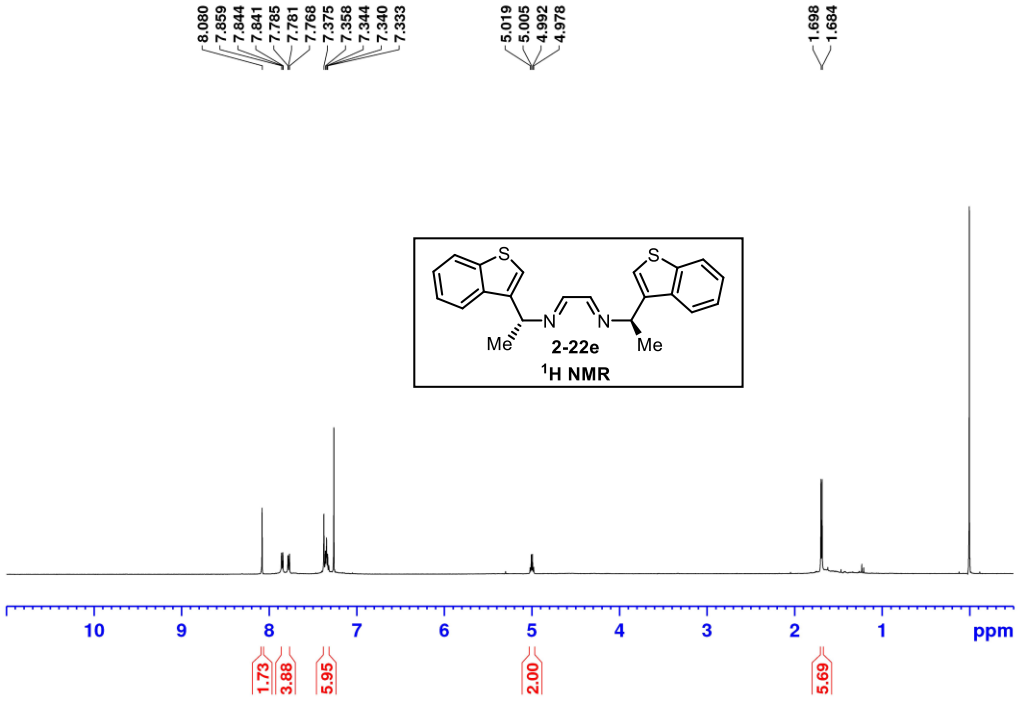
8.080
7.859
7.844
7.841
7.785
7.781
7.768
7.375
7.358
7.344
7.340
7.333
5.019
5.005
4.992
4.978
1.698
1.684
2-22e
1H NMR
10
9
8
7
6
5
4
3
2
1
ppm
1.73
3.88
5.95
2.00
5.69

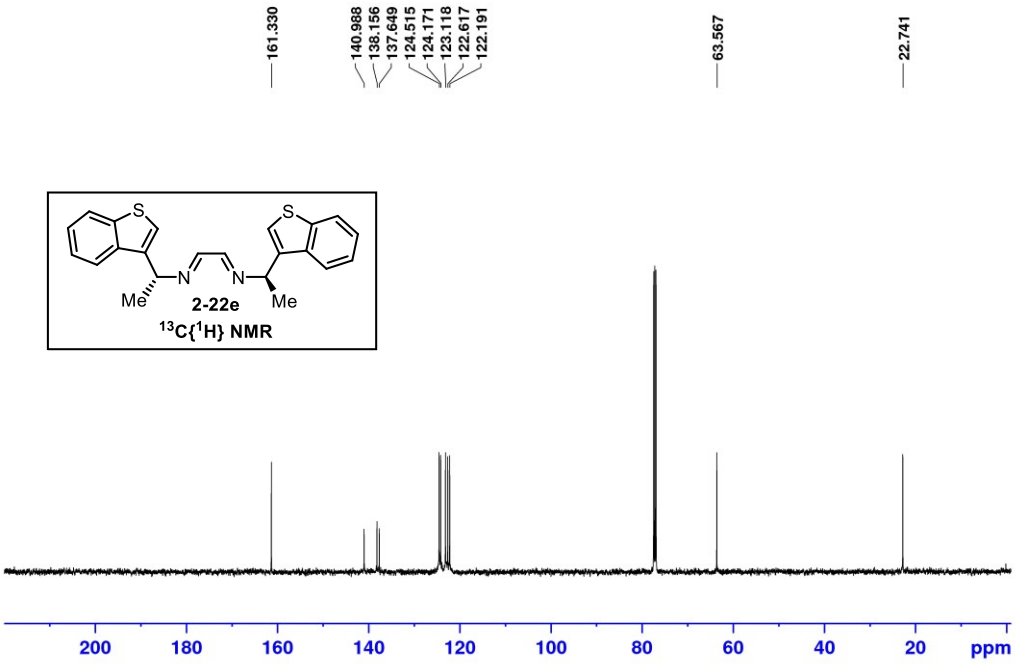
161.330
140.988
138.156
137.649
124.515
124.171
123.118
122.617
122.191
63.567
22.741
S
S
N
N
Me
Me
2-22e
$^{13}C\{^{1}H\}$ NMR
200
180
160
140
120
100
80
60
40
20
ppm

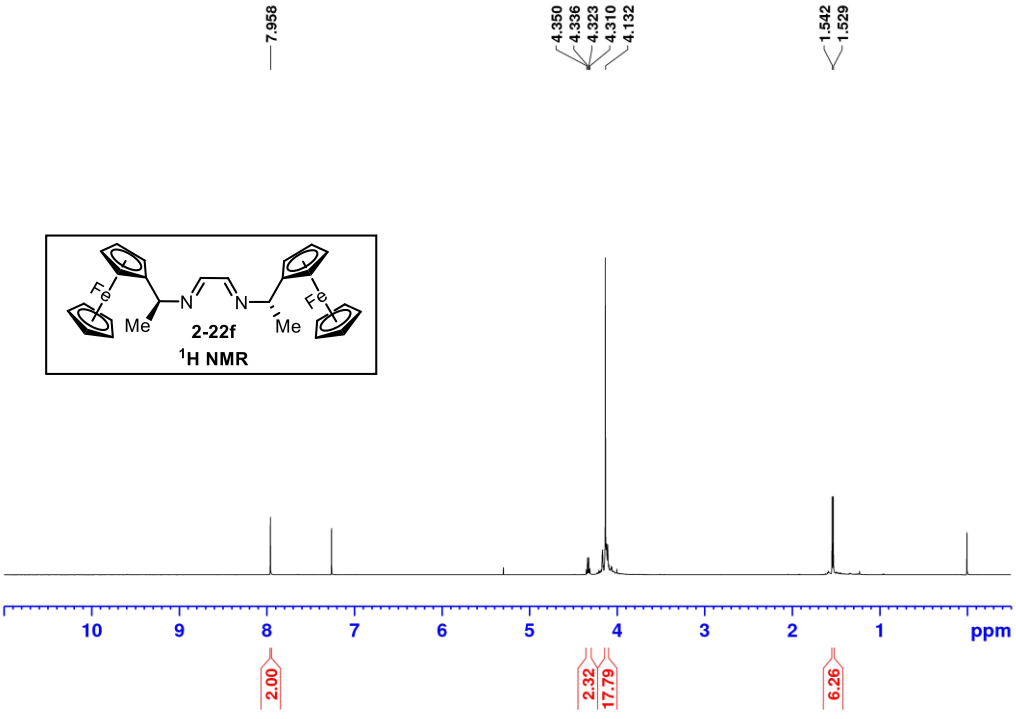
7.958
4.350
4.336
4.323
4.310
4.132
1.542
1.529
Fe
Fe
N
N
Me
Me
2-22f
^{1}H NMR
10
9
8
7
6
5
4
3
2
1
ppm
2.00
2.32
17.79
6.26

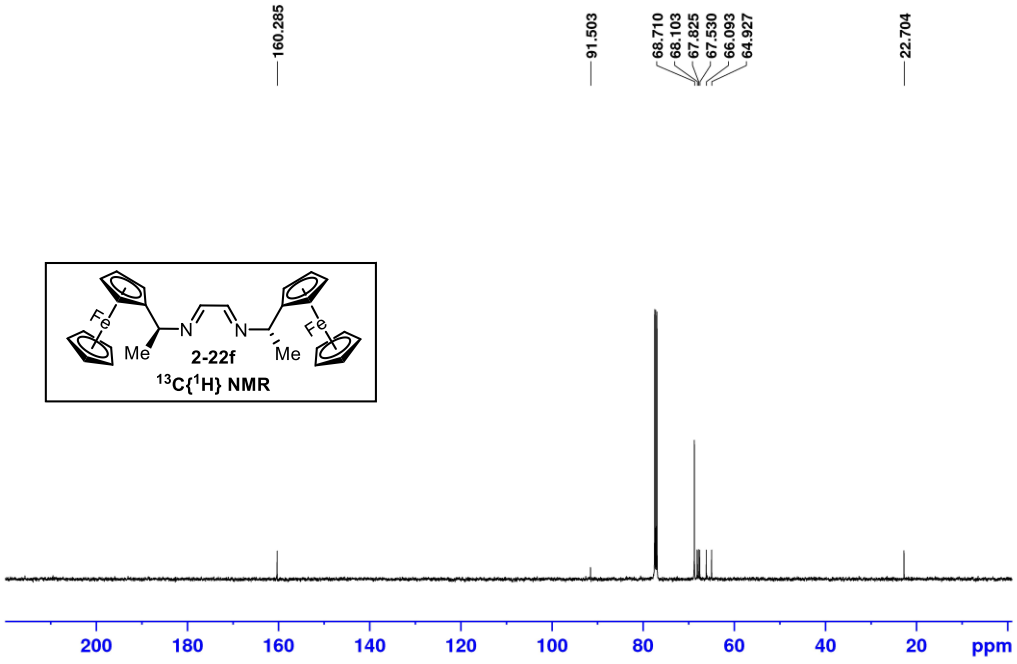
160.285
91.503
68.710
68.103
67.825
67.530
66.093
64.927
22.704
Me
2-22f
Me
$^{13}C\{^{1}H\}$ NMR
200
180
160
140
120
100
80
60
40
20
ppm

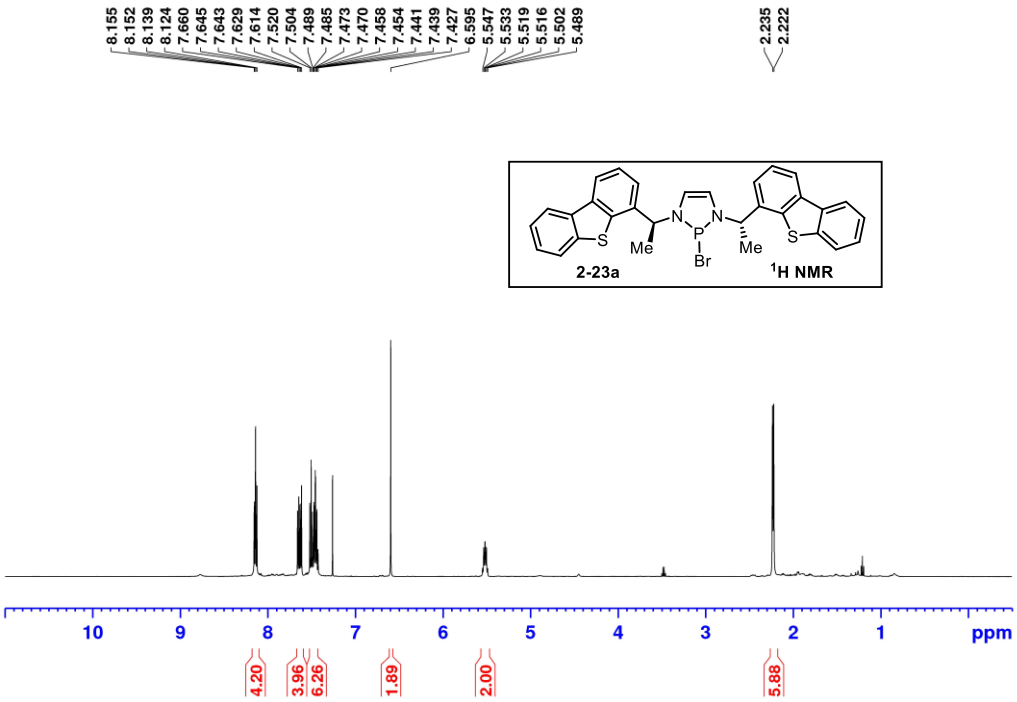
8.155
8.152
8.139
8.124
7.660
7.645
7.643
7.629
7.614
7.520
7.504
7.489
7.485
7.473
7.470
7.458
7.454
7.441
7.439
7.427
6.595
5.547
5.533
5.519
5.516
5.502
5.489
2.235
2.222
Me
Br
Me
2-23a
^{1}H NMR
10
9
8
7
6
5
4
3
2
1
ppm
4.20
3.96
6.26
1.89
2.00
5.88

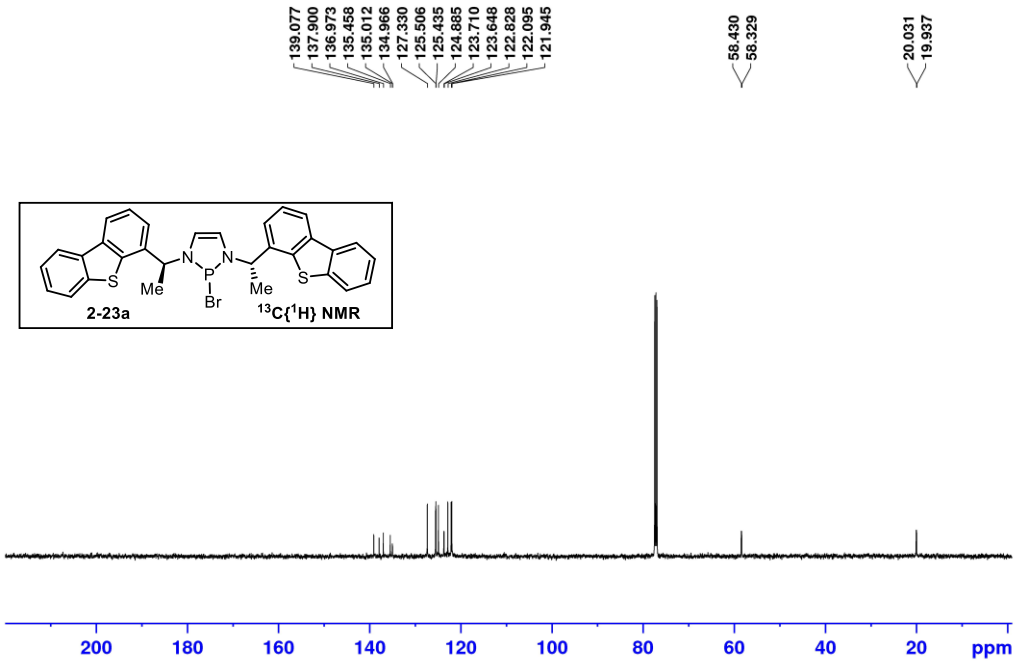
139.077
137.900
136.973
135.458
135.012
134.966
127.330
125.506
125.435
124.885
123.710
123.648
122.828
122.095
121.945
58.430
58.329
20.031
19.937
2-23a
$^{13}C\{^{1}H\}$ NMR
200
180
160
140
120
100
80
60
40
20
ppm

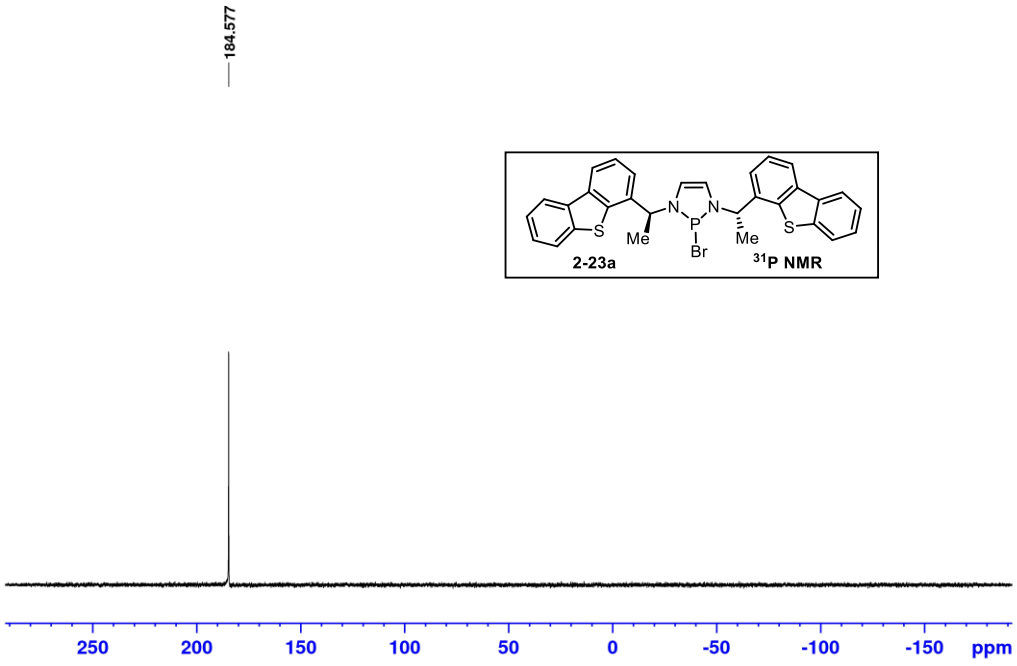
184.577
2-23a
^{31}P NMR
250
200
150
100
50
0
-50
-100
-150
ppm

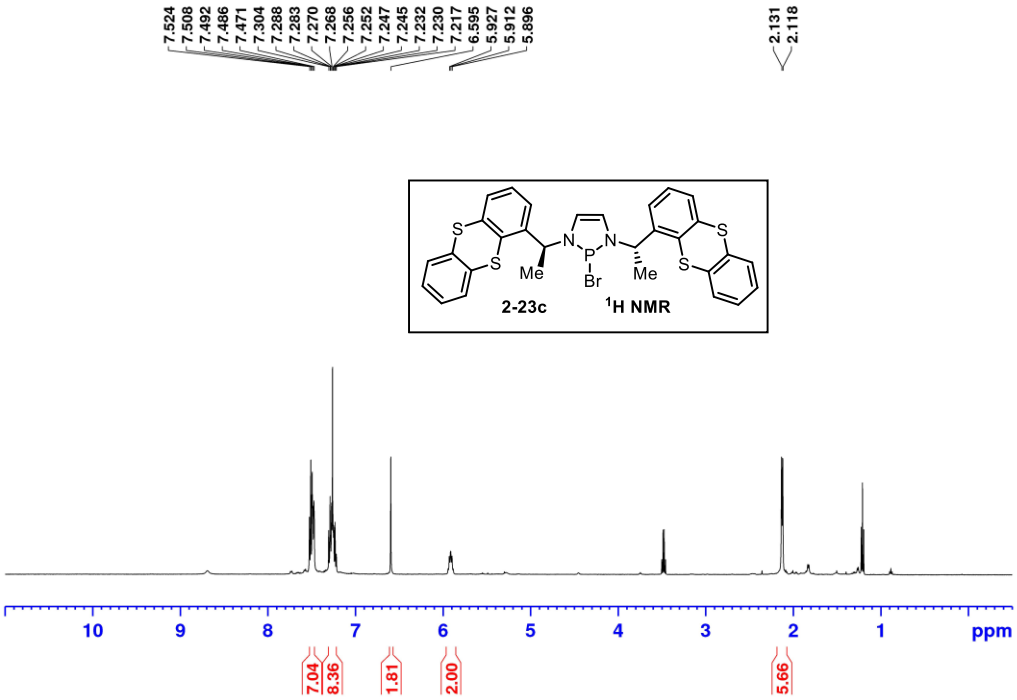
7.524
7.508
7.492
7.486
7.471
7.304
7.288
7.283
7.270
7.268
7.256
7.252
7.247
7.245
7.232
7.230
7.217
6.595
5.927
5.912
5.896
2.131
2.118
2-23c
1H NMR
10
9
8
7
6
5
4
3
2
1
ppm
7.04
8.36
1.81
2.00
5.66

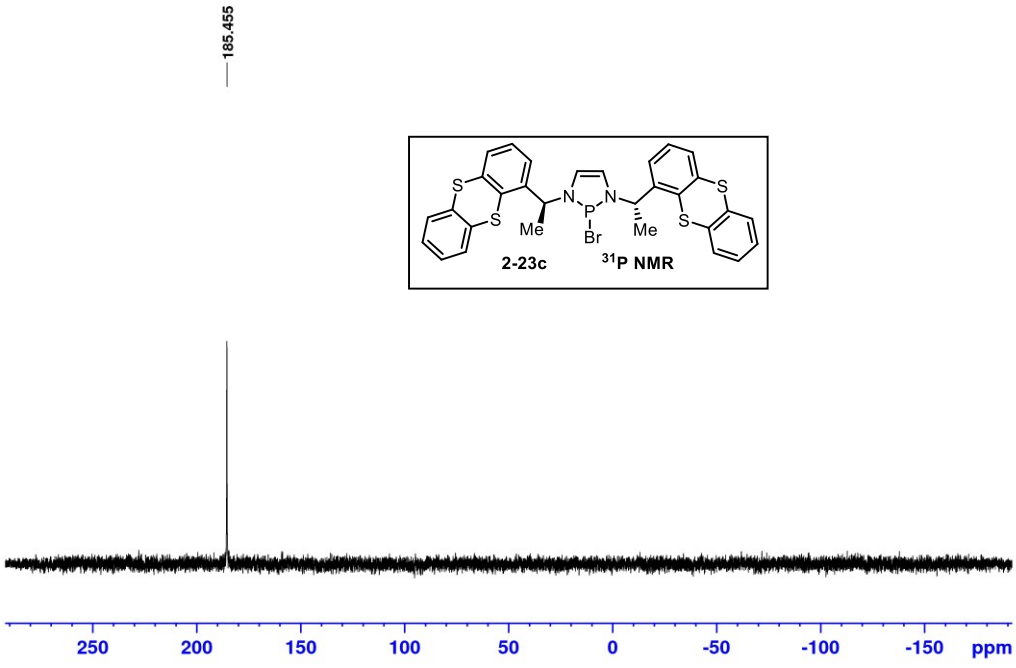
185.455
2-23c
31P NMR
250
200
150
100
50
0
-50
-100
-150
ppm

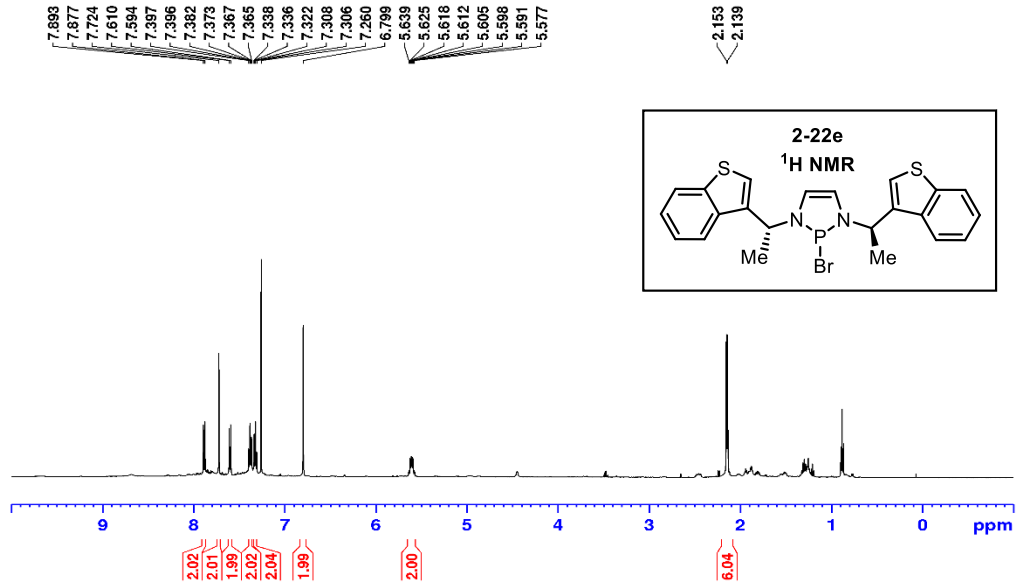
7.893
7.877
7.724
7.610
7.594
7.397
7.396
7.382
7.373
7.367
7.365
7.338
7.336
7.322
7.308
7.306
7.260
6.799
5.639
5.625
5.618
5.612
5.605
5.598
5.591
5.577
2.153
2.139
2-22e
1H NMR
S
S
N
P
N
Me
Br
Me
9
8
7
6
5
4
3
2
1
0
ppm
2.02
2.01
1.99
2.02
2.04
1.99
2.00
6.04

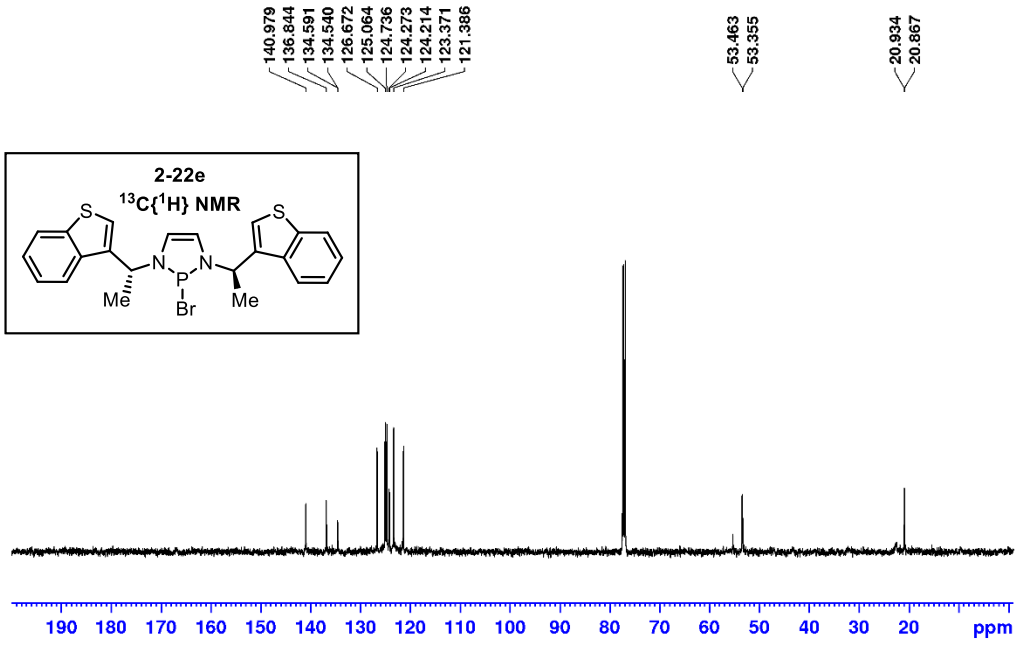
140.979
136.844
134.591
134.540
126.672
125.064
124.736
124.273
124.214
123.371
121.386
53.463
53.355
20.934
20.867
2-22e
13C{1H} NMR
S
S
N
P
N
Me
Br
Me
190
180
170
160
150
140
130
120
110
100
90
80
70
60
50
40
30
20
ppm

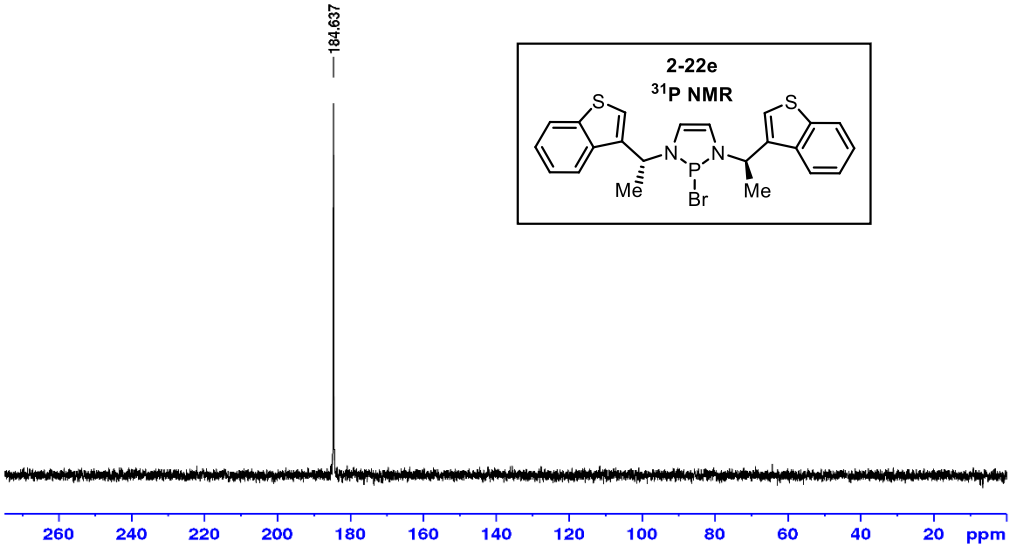
184.637
2-22e
31P NMR
S
N
P
N
S
Me
Br
Me
260
240
220
200
180
160
140
120
100
80
60
40
20
ppm

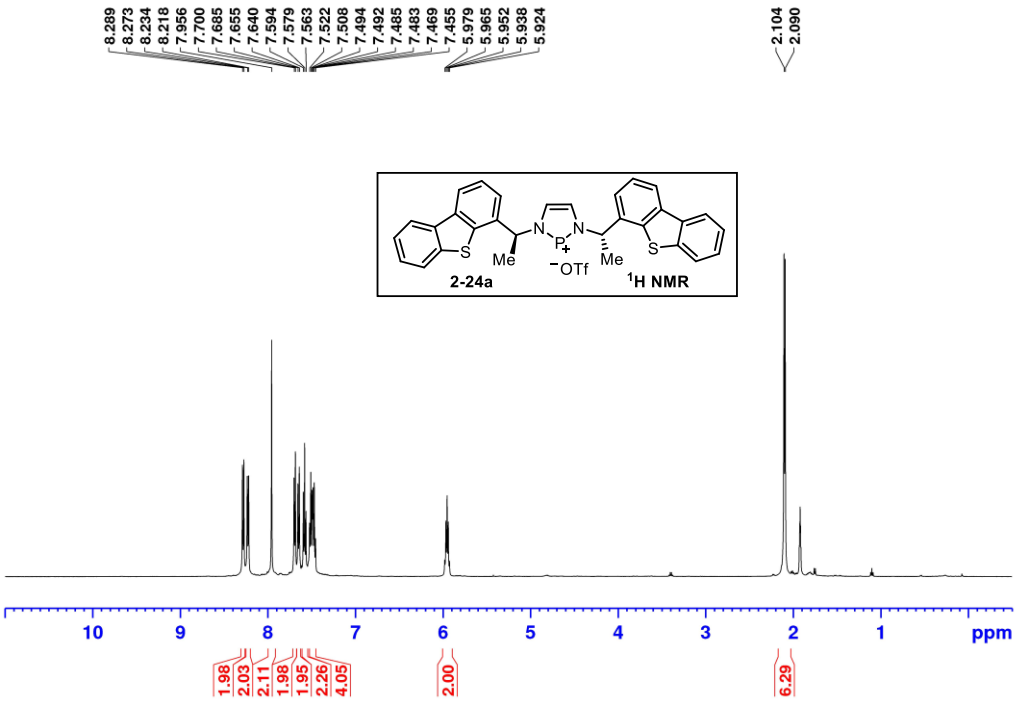
8.289
8.273
8.234
8.218
7.956
7.700
7.685
7.655
7.640
7.594
7.579
7.563
7.522
7.508
7.494
7.492
7.485
7.483
7.469
7.455
5.979
5.965
5.952
5.938
5.924
2.104
2.090
S
N
P
N
S
Me
−OTf
Me
2-24a
1H NMR
10
9
8
7
6
5
4
3
2
1
ppm
1.98
2.03
2.11
1.98
1.95
2.26
4.05
2.00
6.29

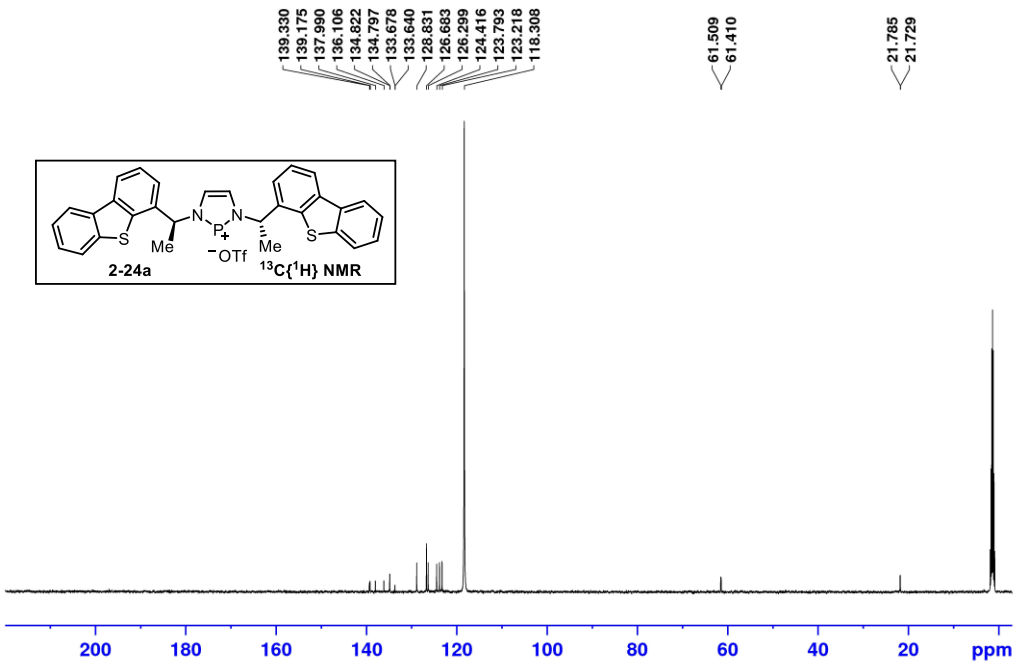
139.330
139.175
137.990
136.106
134.822
134.797
133.678
133.640
128.831
126.683
126.299
124.416
123.793
123.218
118.308
61.509
61.410
21.785
21.729
Me
Me
OTf
2-24a
13C{1H} NMR
200
180
160
140
120
100
80
60
40
20
ppm

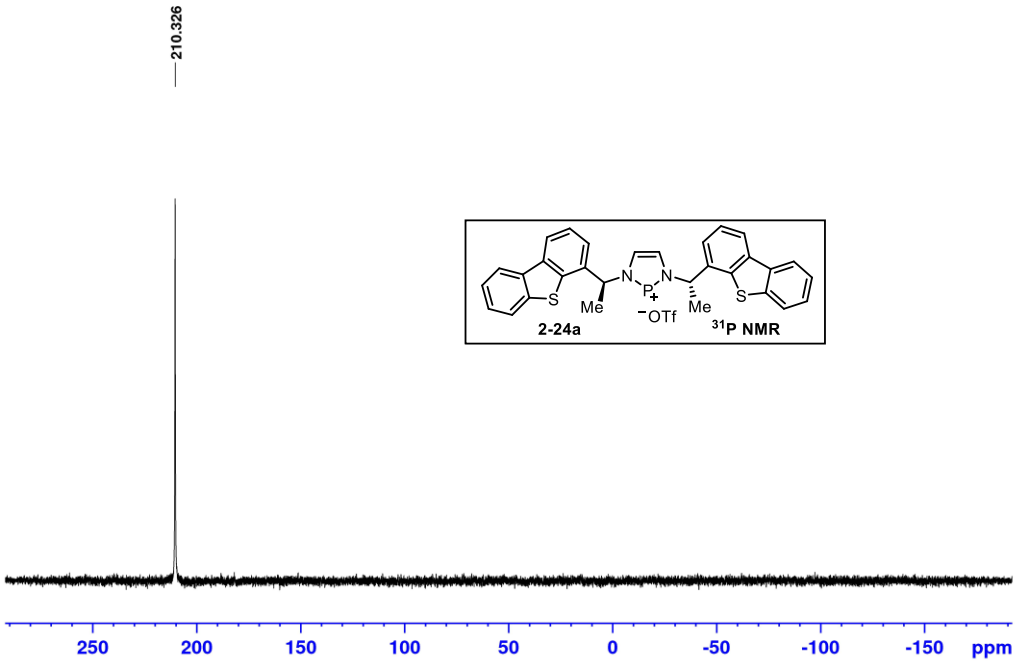
210.326
Me
Me
OTf
2-24a
31P NMR
250
200
150
100
50
0
-50
-100
-150
ppm

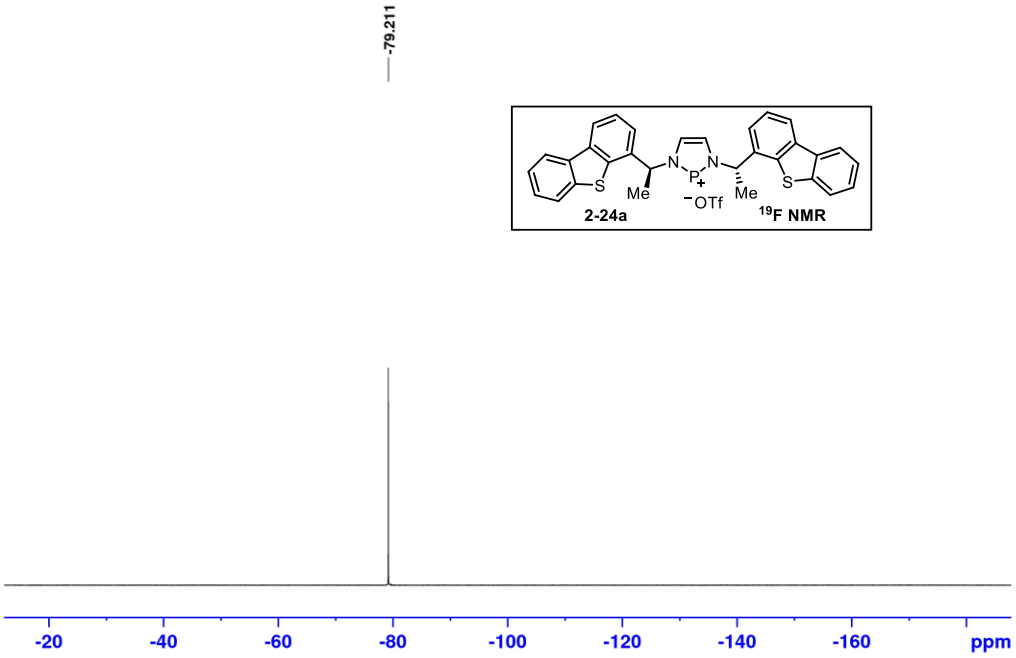
-79.211
2-24a
^{19}F NMR
-20
-40
-60
-80
-100
-120
-140
-160
ppm

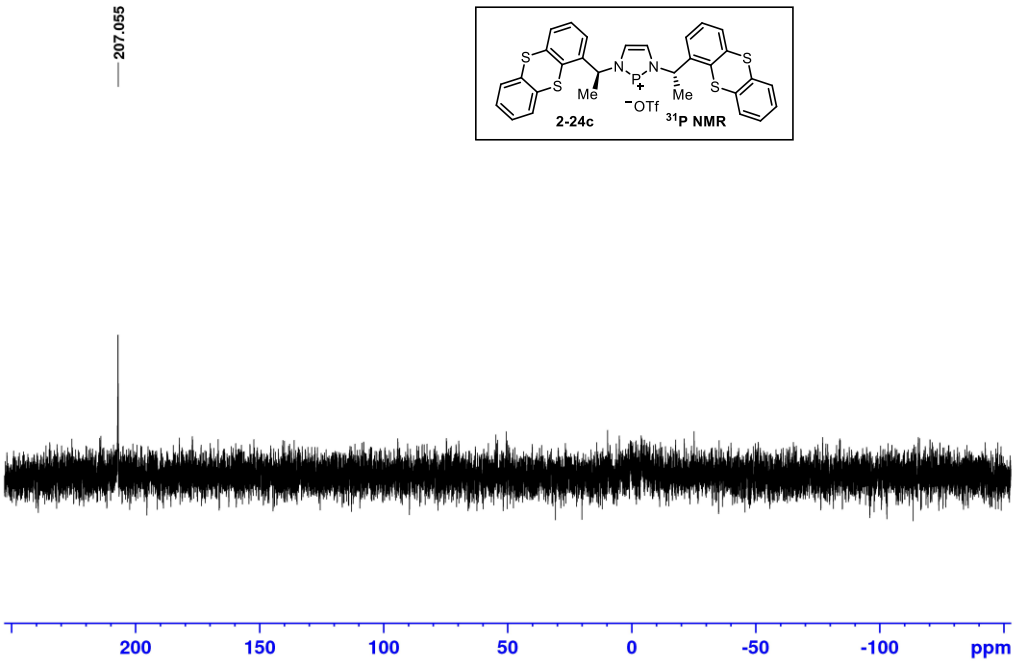
207.055
2-24c
^{31}P NMR
200
150
100
50
0
-50
-100
ppm

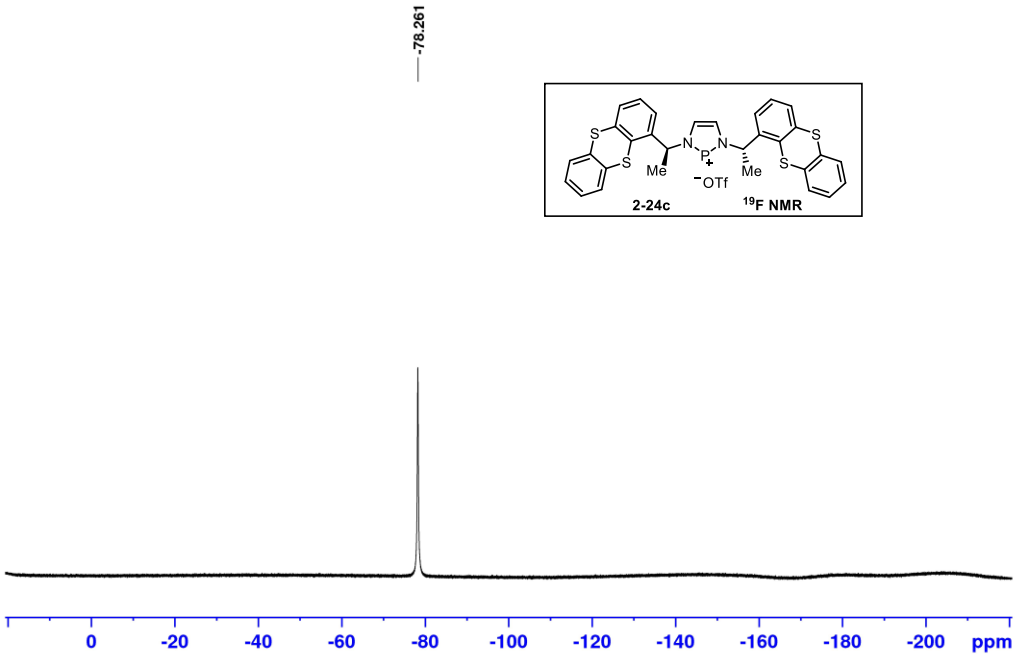
-78.261
2-24c
19F NMR
0
-20
-40
-60
-80
-100
-120
-140
-160
-180
-200
ppm

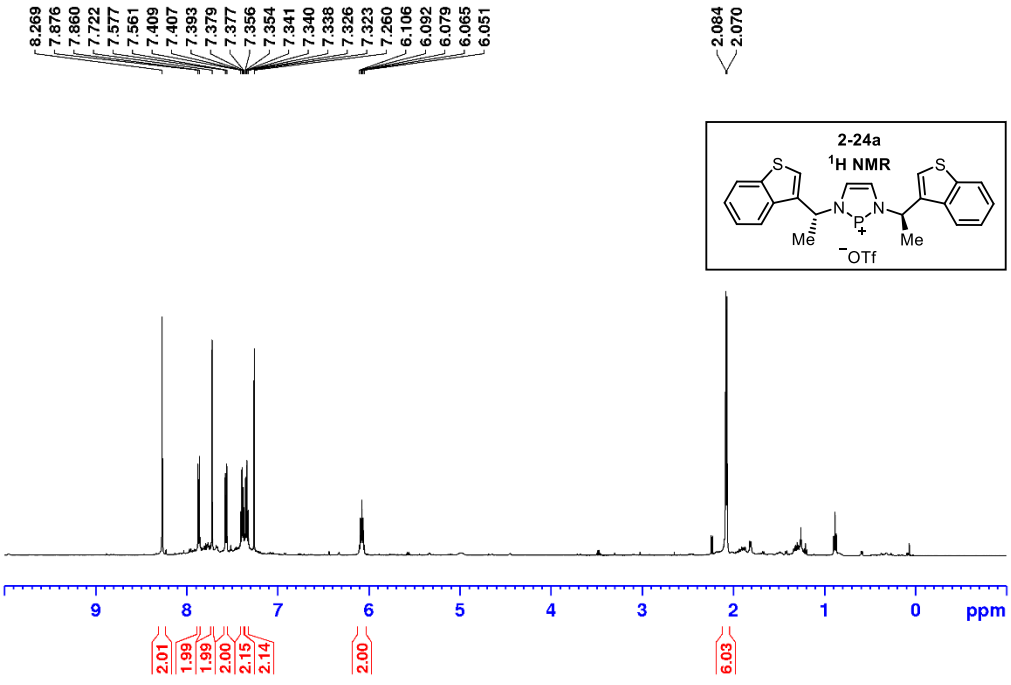
8.269
7.876
7.860
7.722
7.577
7.561
7.409
7.407
7.393
7.379
7.377
7.356
7.354
7.341
7.340
7.338
7.326
7.323
7.260
6.106
6.092
6.079
6.065
6.051
2.084
2.070
2-24a
1H NMR
Me
Me
OTf
9
8
7
6
5
4
3
2
1
0
ppm
2.01
1.99
1.99
2.00
2.15
2.14
2.00
6.03

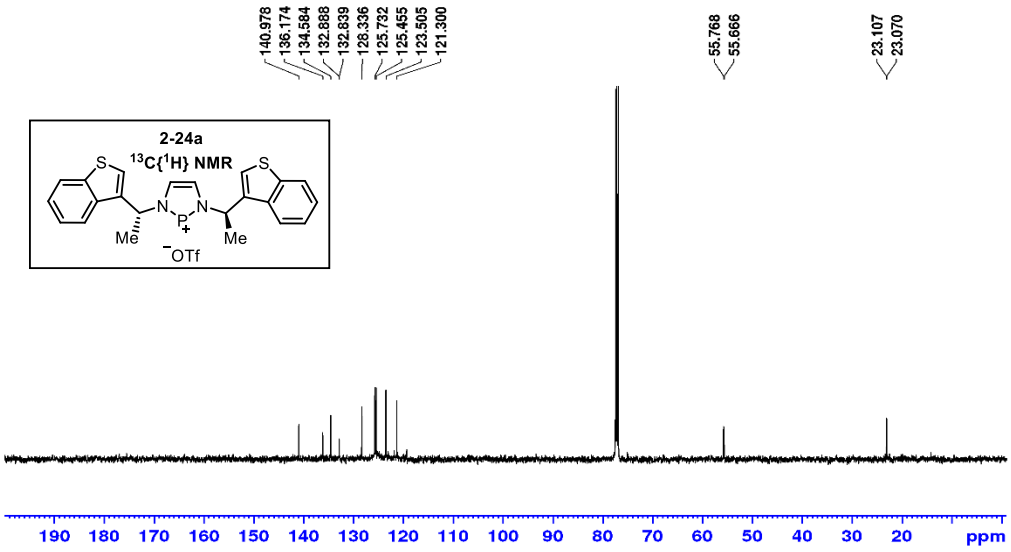
140.978
136.174
134.584
132.888
132.839
128.336
125.732
125.455
123.505
121.300
55.768
55.666
23.107
23.070
2-24a
$^{13}C\{^{1}H\}$ NMR
Me
Me
OTf
190 180 170 160 150 140 130 120 110 100 90 80 70 60 50 40 30 20 ppm

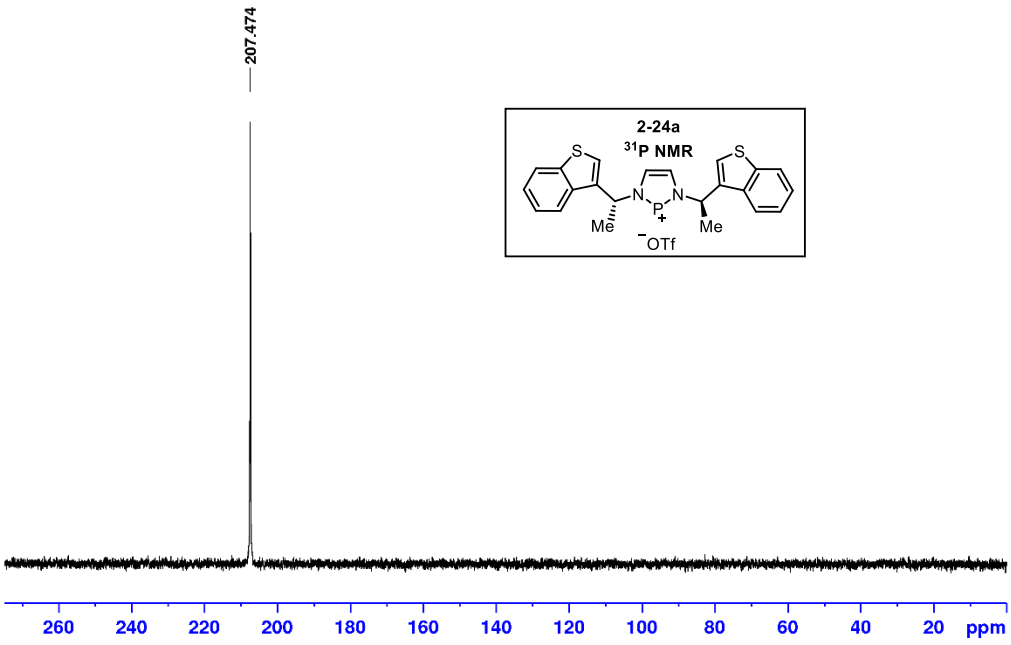
207.474
2-24a
^{31}P NMR
Me
Me
OTf
260 240 220 200 180 160 140 120 100 80 60 40 20 ppm

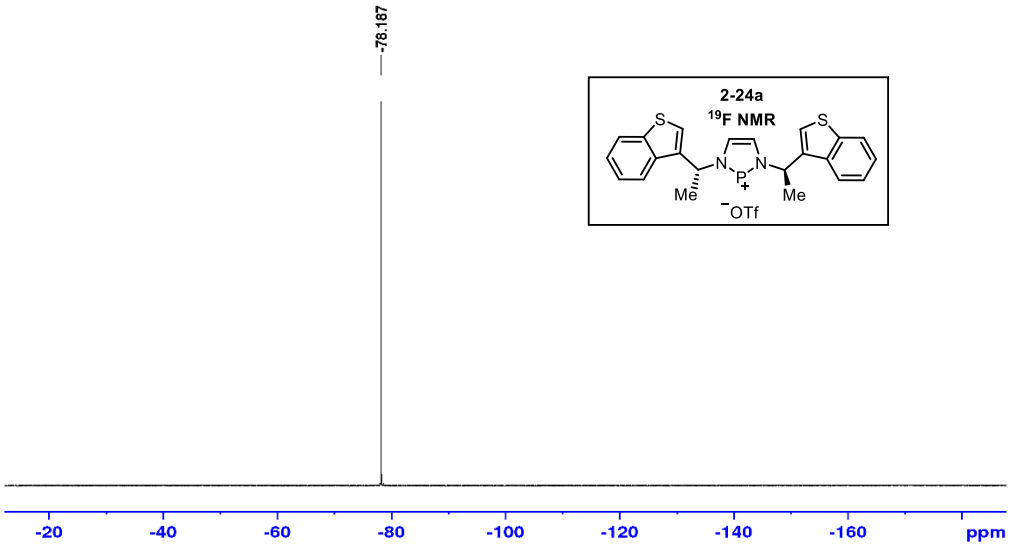
-78.167
2-24a
19F NMR
S
S
N
P
N
Me
Me
OTf
-20
-40
-60
-80
-100
-120
-140
-160
ppm

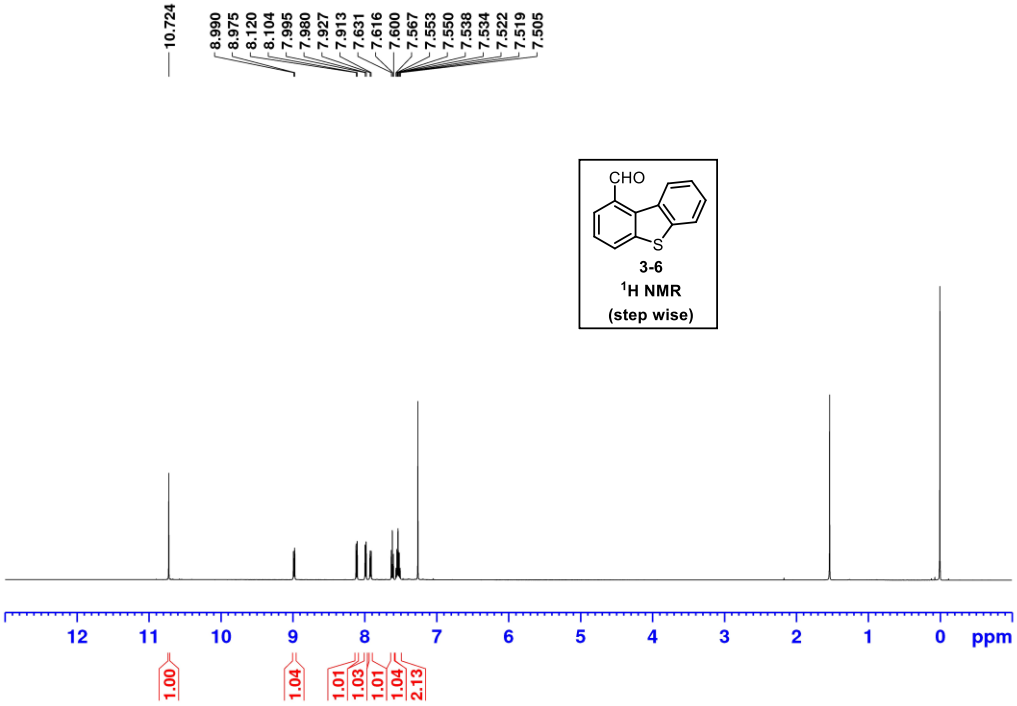
10.724
8.990
8.975
8.120
8.104
7.995
7.980
7.927
7.913
7.631
7.616
7.600
7.567
7.553
7.550
7.538
7.534
7.522
7.519
7.505
CHO
S
3-6
1H NMR
(step wise)
12
11
10
9
8
7
6
5
4
3
2
1
0
ppm
1.00
1.04
1.01
1.03
1.01
1.04
2.13

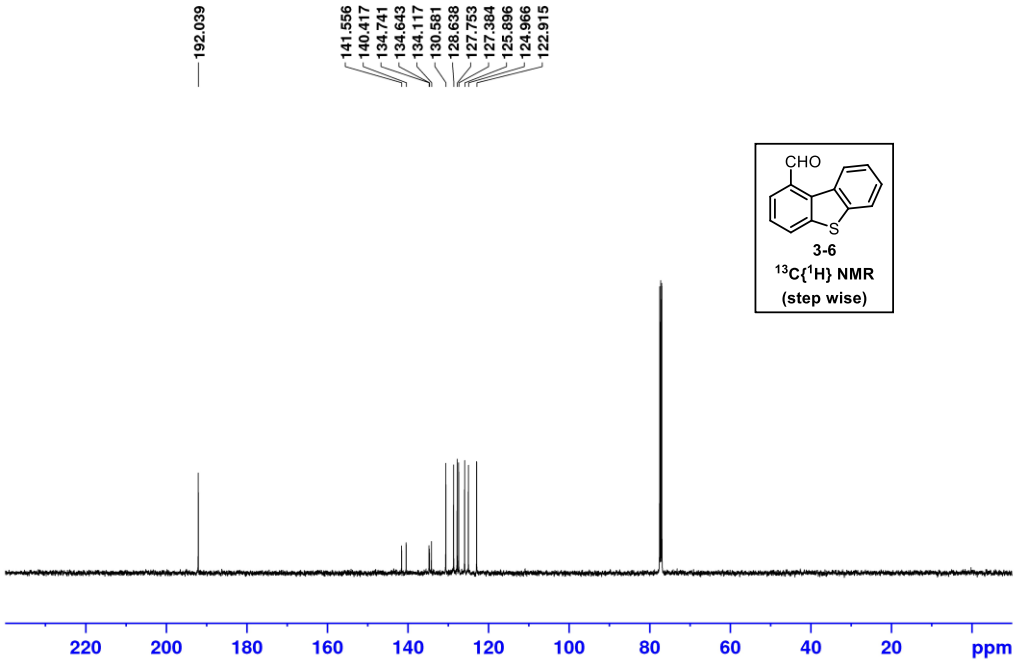
192.039
141.556
140.417
134.741
134.643
134.117
130.581
128.638
127.753
127.384
125.896
124.966
122.915
CHO
S
3-6
13C{1H} NMR
(step wise)
220
200
180
160
140
120
100
80
60
40
20
ppm

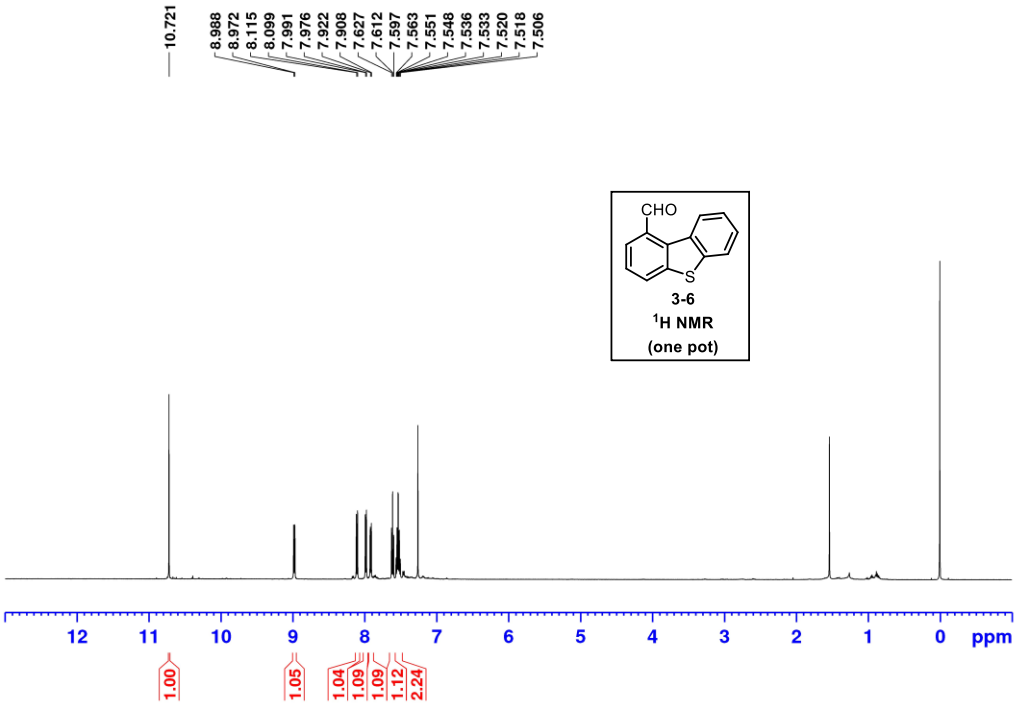
10.721
8.988
8.972
8.115
8.099
7.991
7.976
7.922
7.908
7.627
7.612
7.597
7.563
7.551
7.548
7.536
7.533
7.520
7.518
7.506
CHO
S
3-6
1H NMR
(one pot)
12
11
10
9
8
7
6
5
4
3
2
1
0
ppm
1.00
1.05
1.04
1.09
1.09
1.12
2.24

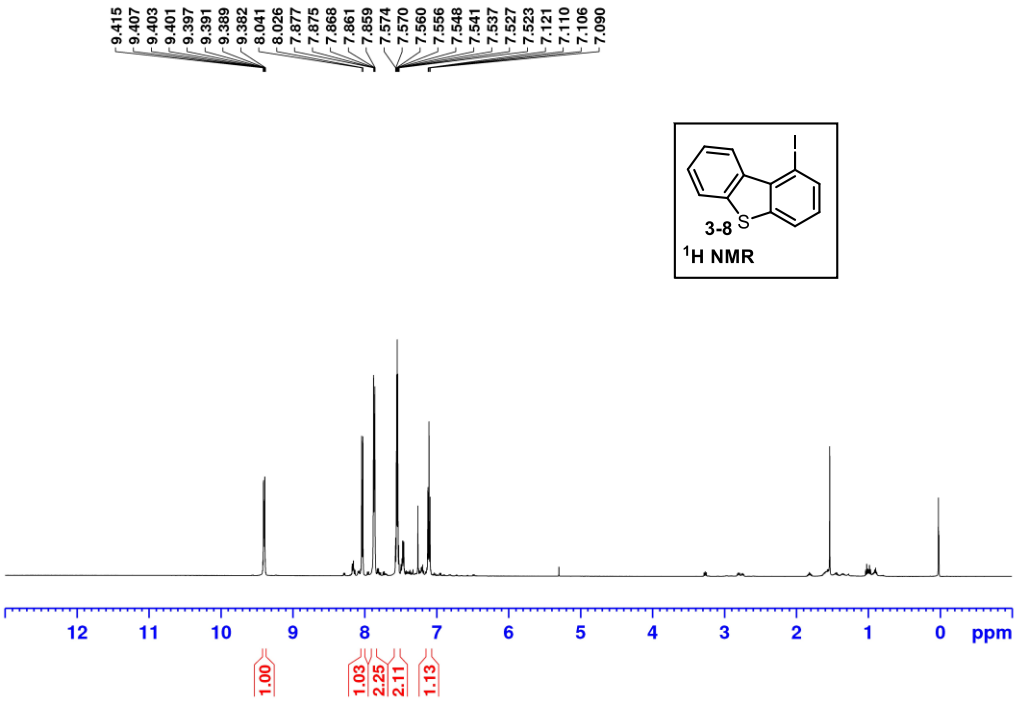
9.415
9.407
9.403
9.401
9.397
9.391
9.389
9.382
8.041
8.026
7.877
7.875
7.868
7.861
7.859
7.574
7.570
7.560
7.556
7.548
7.541
7.537
7.527
7.523
7.121
7.110
7.106
7.090
I
S
3-8
1H NMR
12
11
10
9
8
7
6
5
4
3
2
1
0
ppm
1.00
1.03
2.25
2.11
1.13

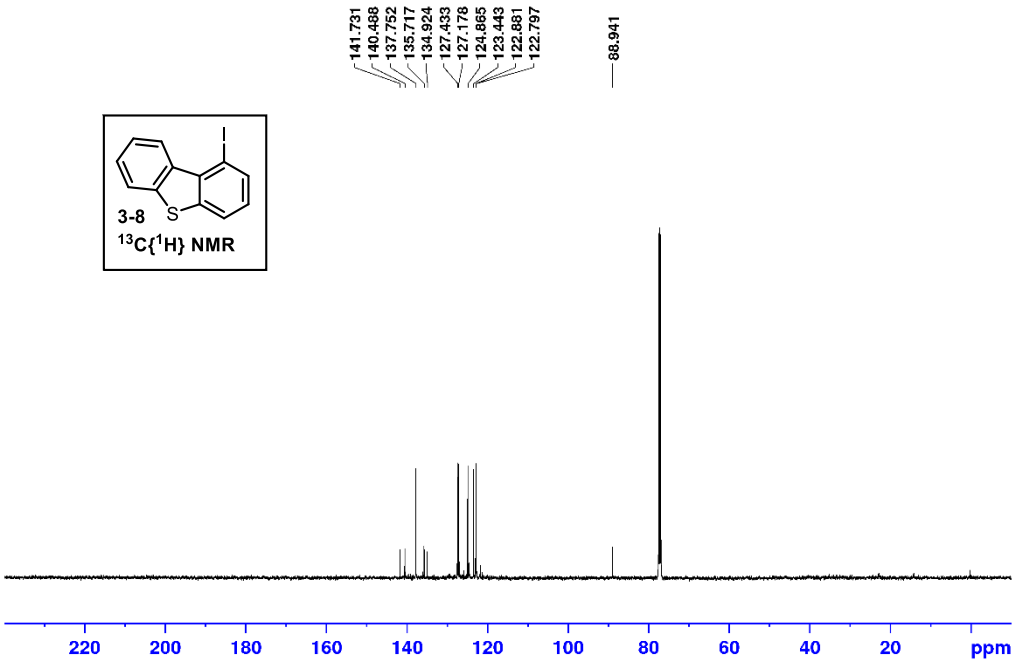
141.731
140.488
137.752
135.717
134.924
127.433
127.178
124.865
123.443
122.881
122.797
88.941
I
S
3-8
$^{13}C\{^{1}H\}$ NMR
220
200
180
160
140
120
100
80
60
40
20
ppm

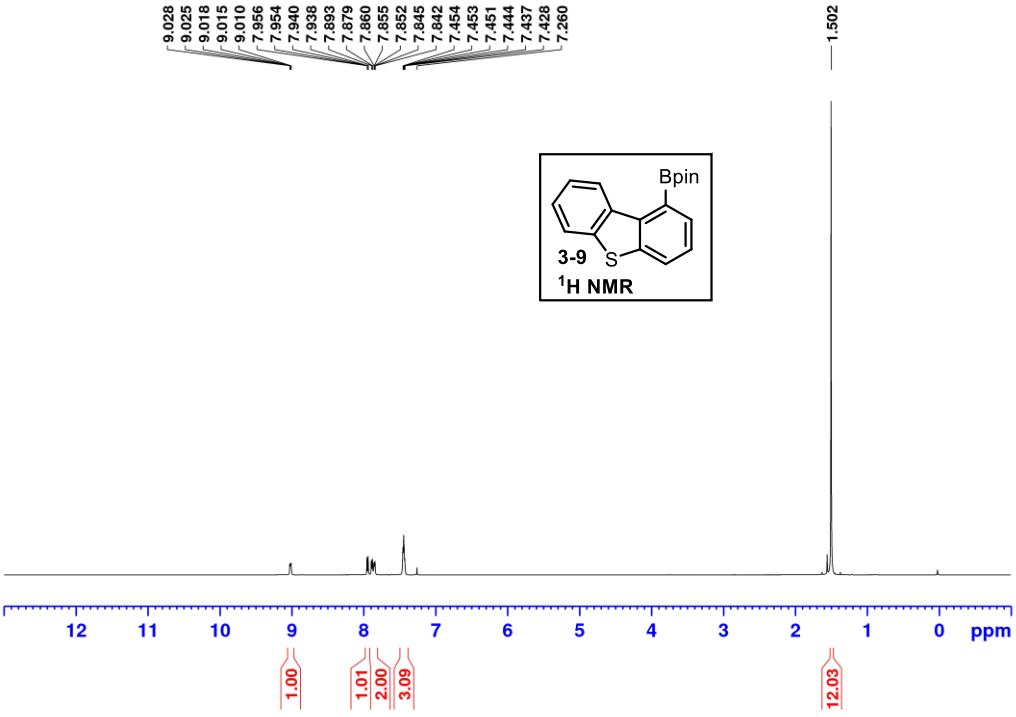
9.028
9.025
9.018
9.015
9.010
7.956
7.954
7.940
7.938
7.893
7.879
7.860
7.855
7.852
7.845
7.842
7.454
7.453
7.451
7.444
7.437
7.428
7.260
1.502
Bpin
S
3-9
^{1}H NMR
12
11
10
9
8
7
6
5
4
3
2
1
0
ppm
1.00
1.01
2.00
3.09
12.03

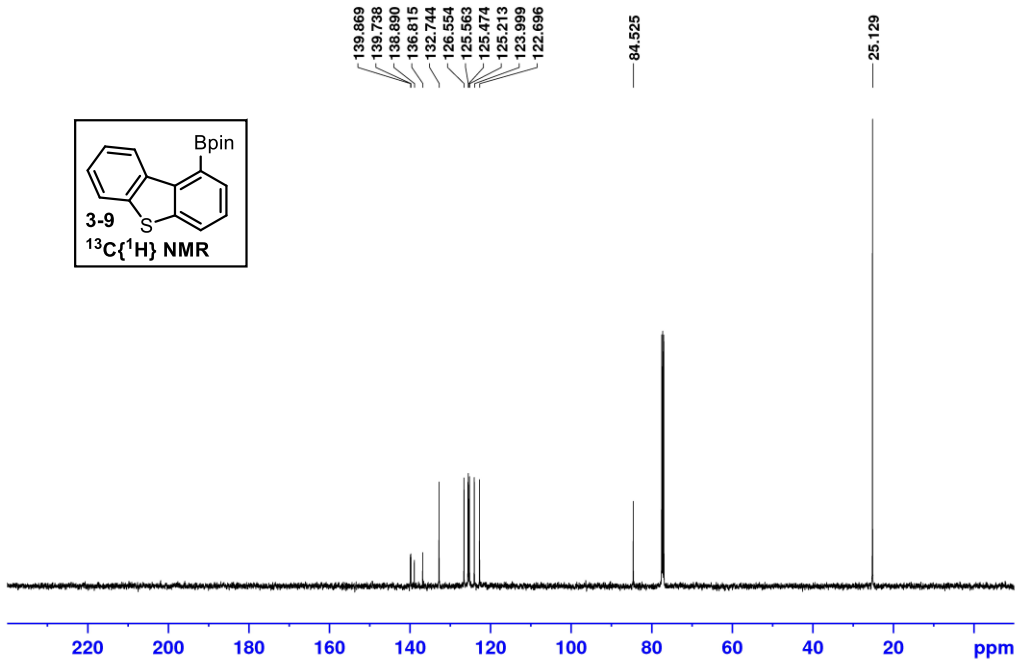
139.869
139.738
138.890
136.815
132.744
126.554
125.563
125.474
125.213
123.999
122.696
84.525
25.129
Bpin
3-9
$^{13}C\{^{1}H\}$ NMR
220
200
180
160
140
120
100
80
60
40
20
ppm

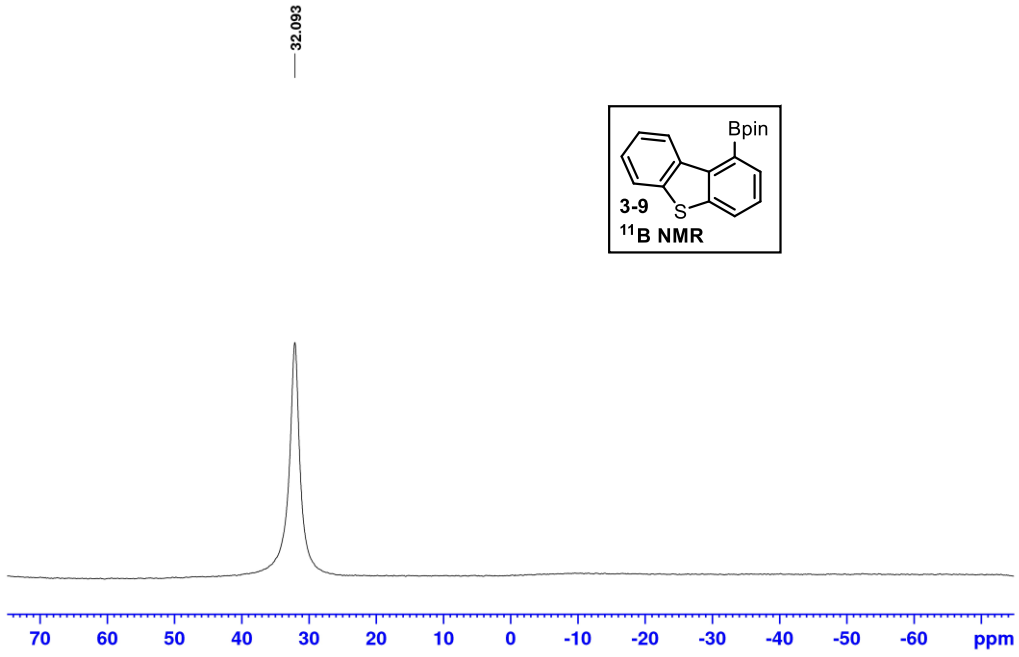
32.093
Bpin
3-9
^{11}B NMR
70
60
50
40
30
20
10
0
-10
-20
-30
-40
-50
-60
ppm

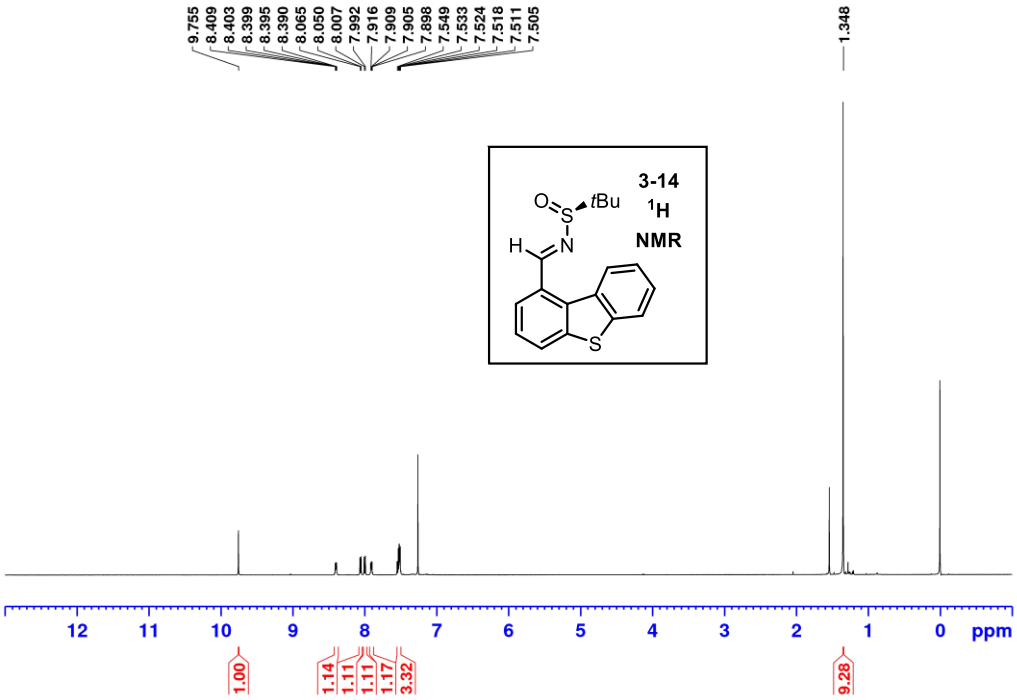
9.755
8.409
8.403
8.399
8.395
8.390
8.065
8.050
8.007
7.992
7.916
7.909
7.905
7.898
7.549
7.533
7.524
7.518
7.511
7.505
1.348
3-14
1H
NMR
tBu
O
S
N
H
S
12
11
10
9
8
7
6
5
4
3
2
1
0
ppm
1.00
1.14
1.11
1.11
1.17
3.32
9.28

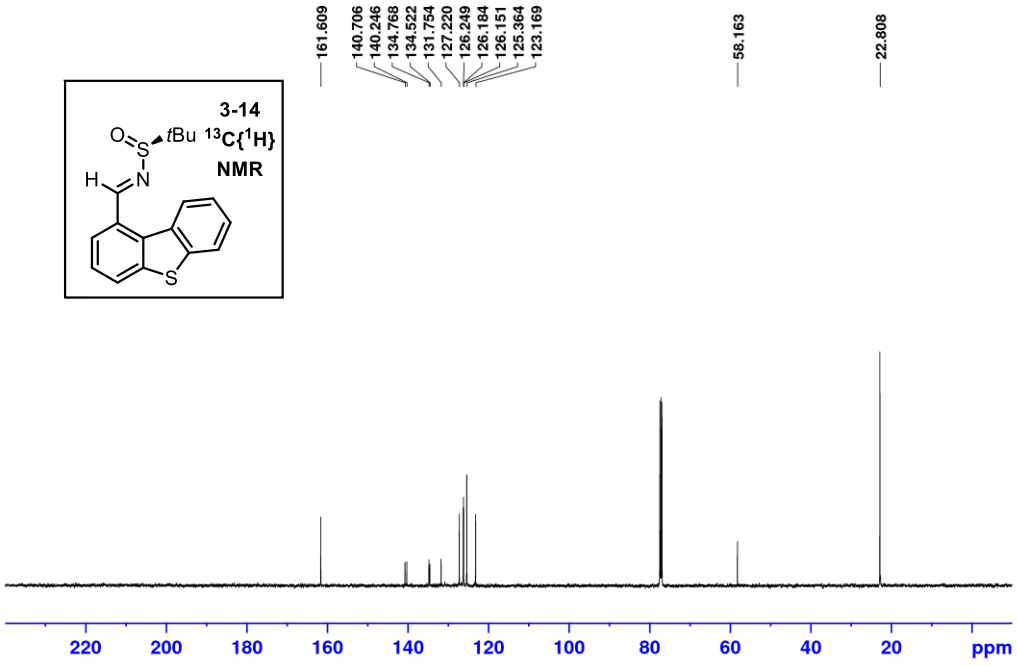
161.609
140.706
140.246
134.768
134.522
131.754
127.220
126.249
126.184
126.151
125.364
123.169
58.163
22.808
3-14
13C{1H}
NMR
tBu
O
S
N
H
S
220
200
180
160
140
120
100
80
60
40
20
ppm

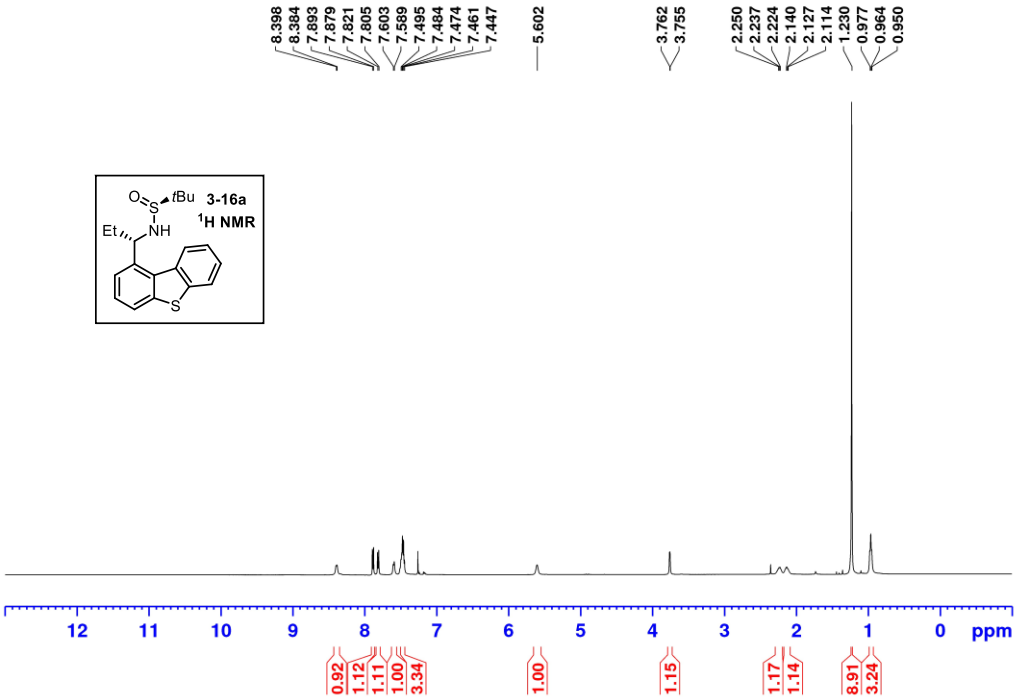
8.398
8.384
7.893
7.879
7.821
7.805
7.603
7.589
7.495
7.484
7.474
7.461
7.447
5.602
3.762
3.755
2.250
2.237
2.224
2.140
2.127
2.114
1.230
0.977
0.964
0.950
3-16a
1H NMR
Et
NH
tBu
12
11
10
9
8
7
6
5
4
3
2
1
0
ppm
0.92
1.12
1.11
1.00
3.34
1.00
1.15
1.17
1.14
8.91
3.24

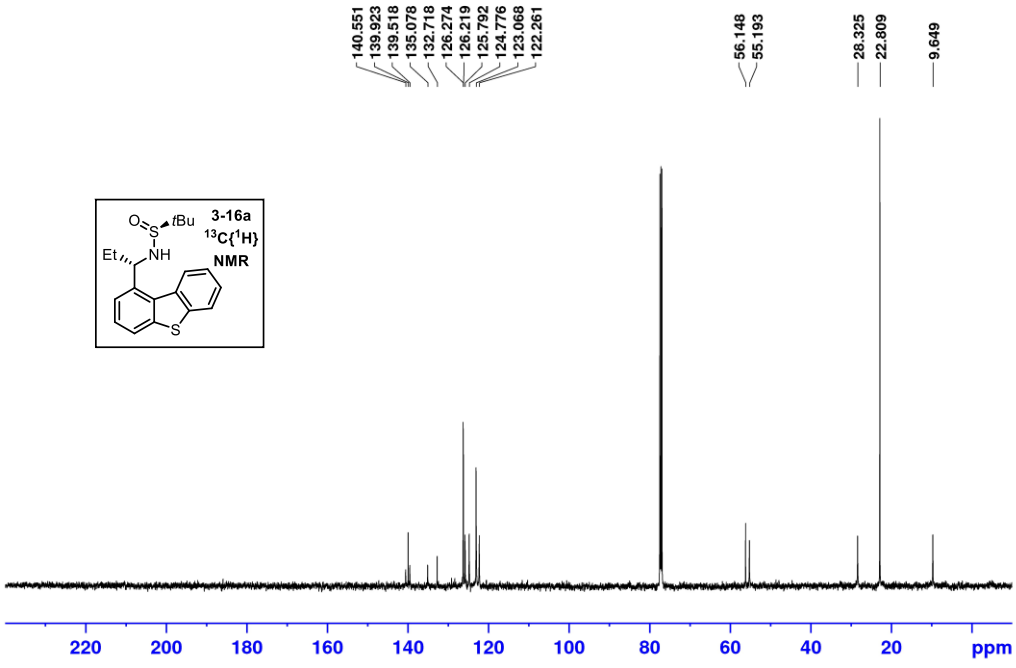
140.551
139.923
139.518
135.078
132.718
126.274
126.219
125.792
124.776
123.068
122.261
56.148
55.193
28.325
22.809
9.649
3-16a
13C{1H}
NMR
Et
NH
tBu
220
200
180
160
140
120
100
80
60
40
20
ppm

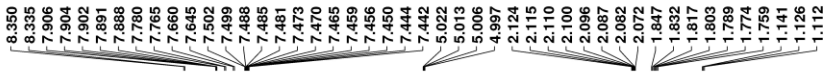
8.350
8.335
7.906
7.904
7.902
7.891
7.888
7.780
7.765
7.660
7.645
7.502
7.499
7.488
7.485
7.481
7.473
7.470
7.465
7.459
7.456
7.450
7.444
7.442
5.022
5.013
5.006
4.997
2.124
2.115
2.110
2.100
2.096
2.087
2.082
2.072
1.847
1.832
1.817
1.803
1.789
1.774
1.759
1.141
1.126
1.112

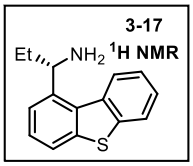
3-17
Et
NH2
1H NMR
S

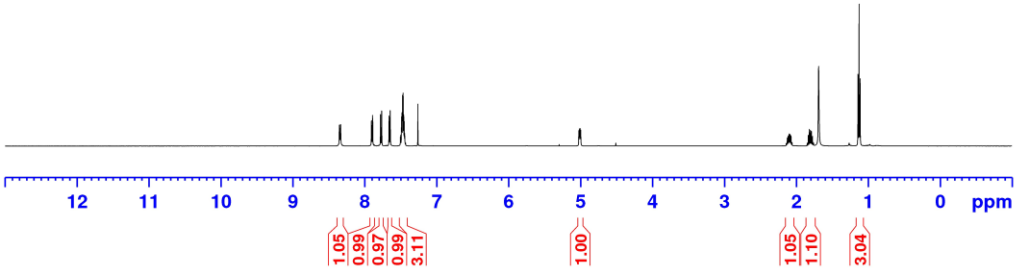
12
11
10
9
8
7
6
5
4
3
2
1
0
ppm
1.05
0.99
0.97
0.99
3.11
1.00
1.05
1.10
3.04


144.188
140.336
139.981
135.495
132.510
126.481
125.994
125.559
124.574
123.136
121.438
121.254
53.073
30.683
11.111

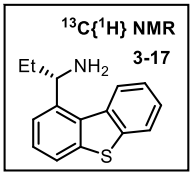
13C{1H} NMR
3-17
Et
NH2
S

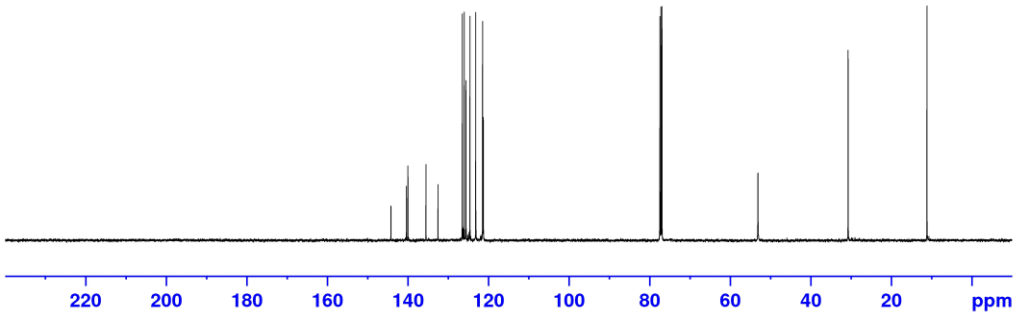
220
200
180
160
140
120
100
80
60
40
20
ppm

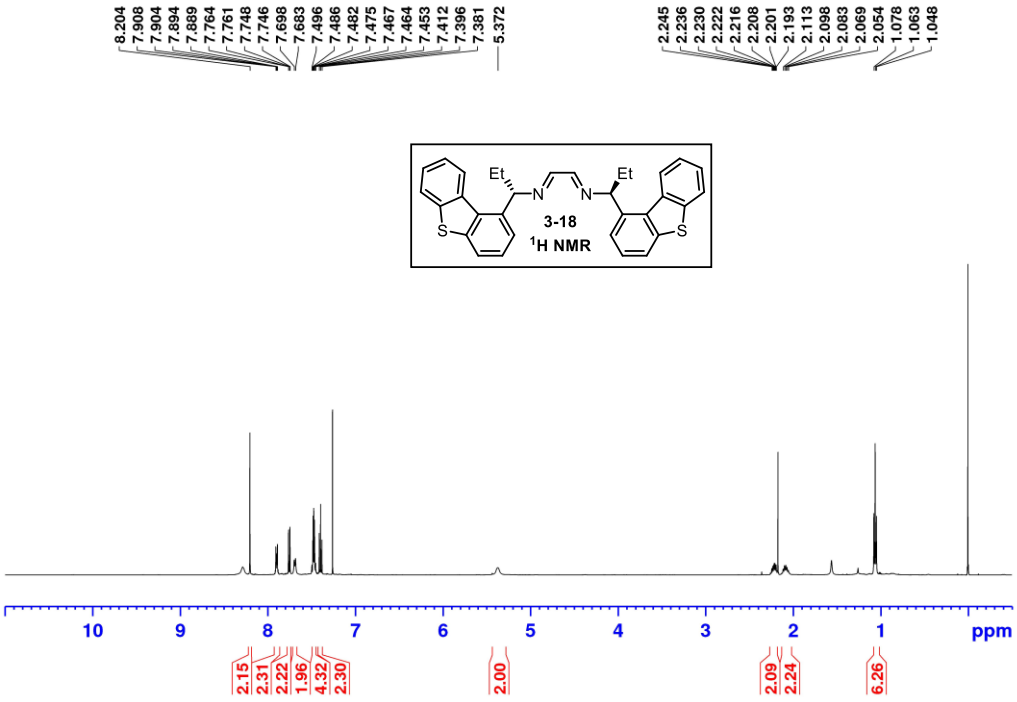
8.204
7.908
7.904
7.894
7.889
7.764
7.761
7.748
7.746
7.698
7.683
7.496
7.486
7.482
7.475
7.467
7.464
7.453
7.412
7.396
7.381
5.372
2.245
2.236
2.230
2.222
2.216
2.208
2.201
2.193
2.113
2.098
2.083
2.069
2.054
1.078
1.063
1.048
Et
N
N
Et
S
S
3-18
1H NMR
10
9
8
7
6
5
4
3
2
1
ppm
2.15
2.31
2.22
1.96
4.32
2.30
2.00
2.09
2.24
6.26

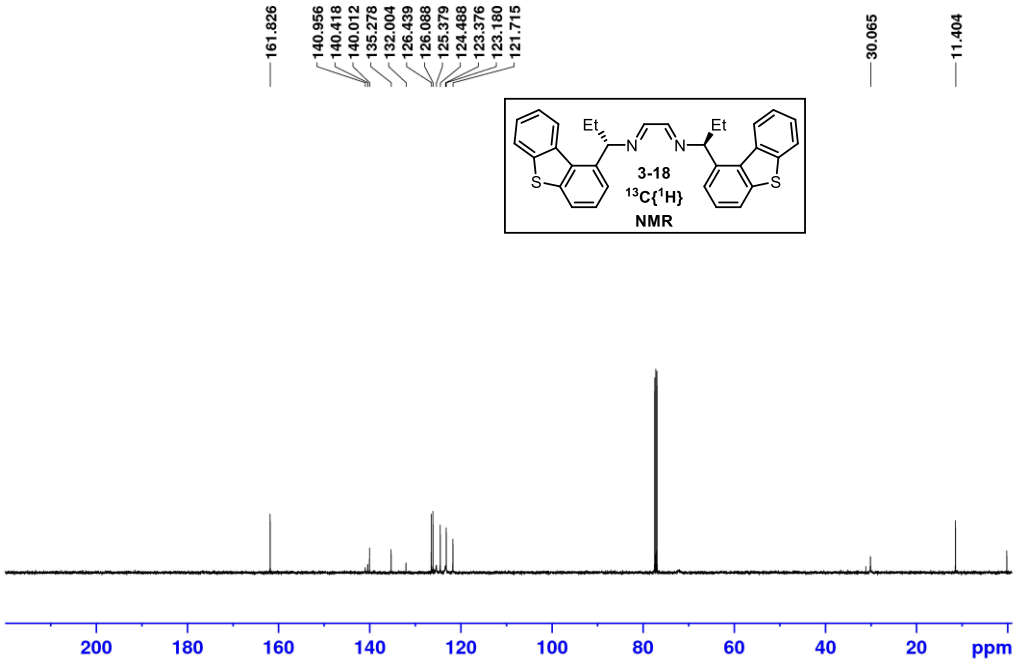
161.826
140.956
140.418
140.012
135.278
132.004
126.439
126.088
125.379
124.488
123.376
123.180
121.715
30.065
11.404
Et
N
N
Et
S
S
3-18
13C{1H}
NMR
200
180
160
140
120
100
80
60
40
20
ppm


7.678
7.662
7.647
7.550
7.535
7.520
7.417
7.400
7.082
7.078
7.067
7.063
6.937
6.923
6.906
6.870
6.867
6.855
6.852
6.840
6.838
6.172
6.155

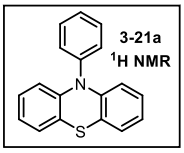
3-21a
1H NMR
N
S

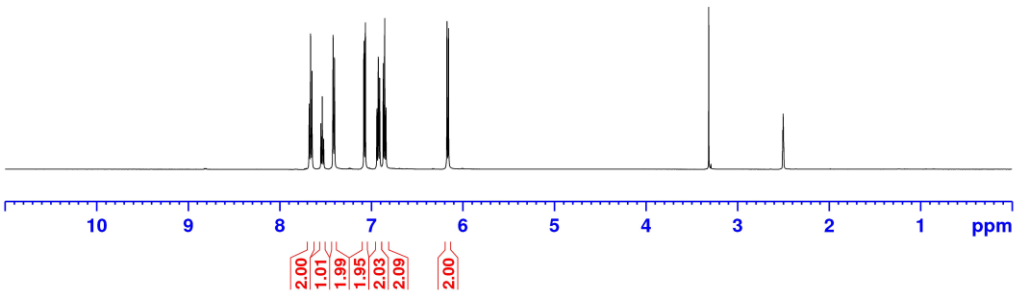
10
9
8
7
6
5
4
3
2
1
ppm
2.00
1.01
1.99
1.95
2.03
2.09
2.00


7.678
7.662
7.647
7.550
7.535
7.520
7.417
7.400
7.082
7.078
7.067
7.063
6.937
6.923
6.906
6.870
6.867
6.855
6.852
6.840
6.838
6.172
6.155

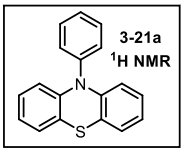
3-21a
1H NMR
N
S

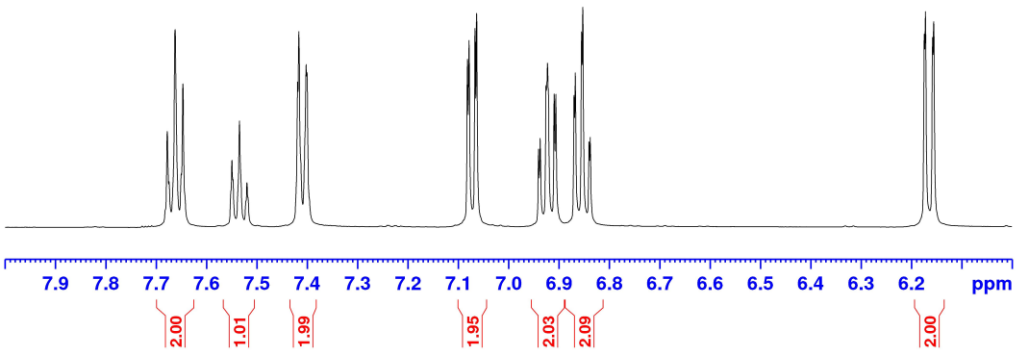
7.9
7.8
7.7
7.6
7.5
7.4
7.3
7.2
7.1
7.0
6.9
6.8
6.7
6.6
6.5
6.4
6.3
6.2
ppm
2.00
1.01
1.99
1.95
2.03
2.09
2.00

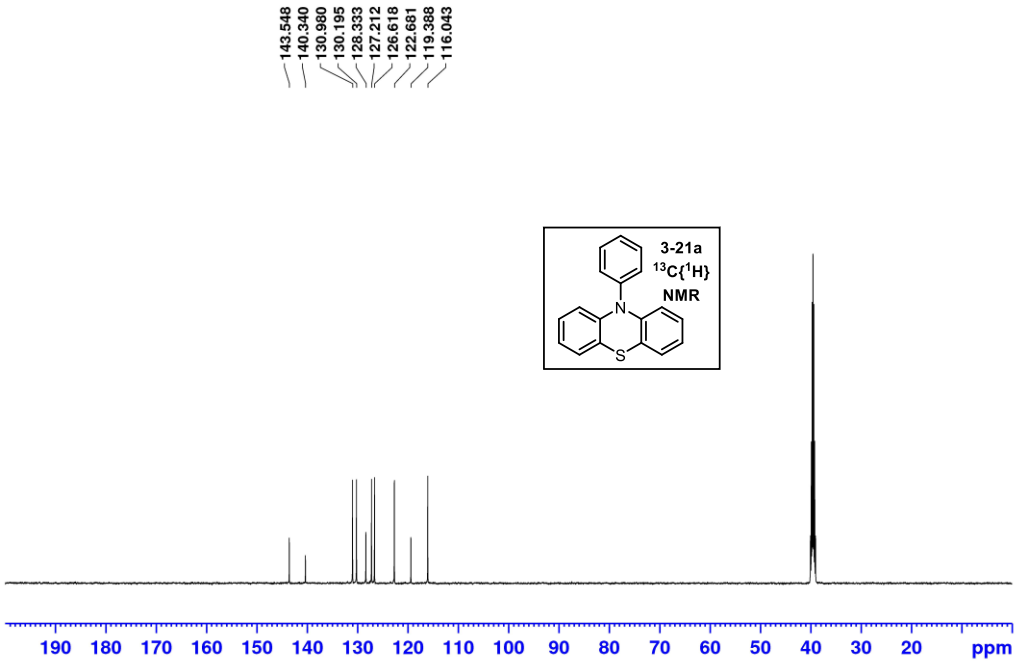
143.548
140.340
130.980
130.195
128.333
127.212
126.618
122.681
119.388
116.043
3-21a
$^{13}C\{^{1}H\}$
NMR
190 180 170 160 150 140 130 120 110 100 90 80 70 60 50 40 30 20 ppm

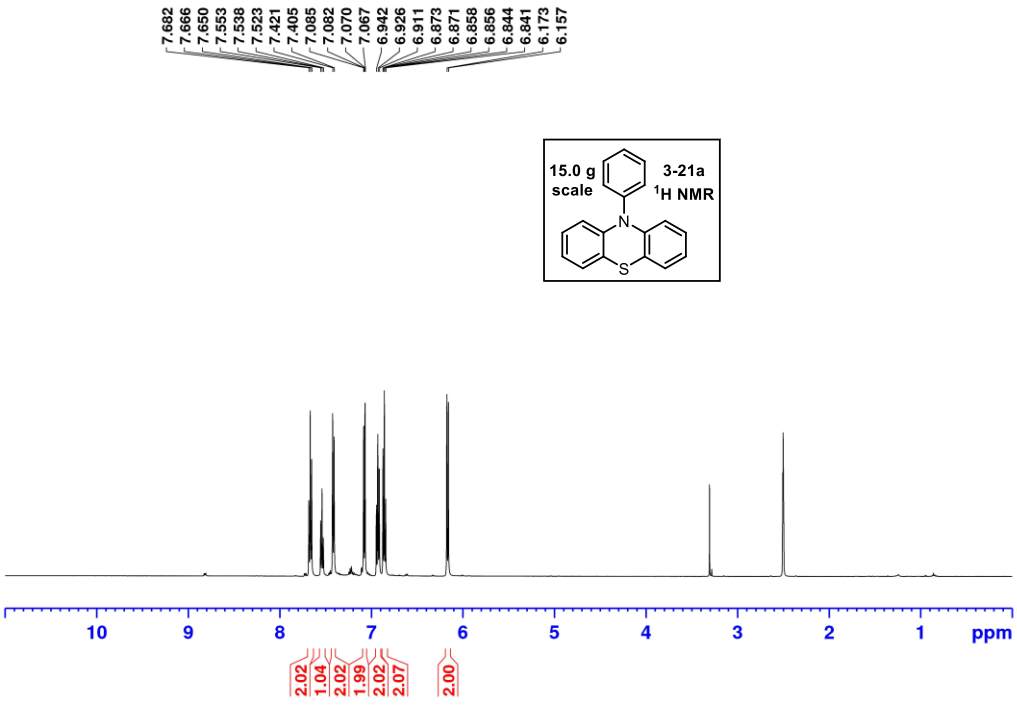
7.682
7.666
7.650
7.553
7.538
7.523
7.421
7.405
7.085
7.082
7.070
7.067
6.942
6.926
6.911
6.873
6.871
6.858
6.856
6.844
6.841
6.173
6.157
15.0 g
scale
3-21a
^{1}H NMR
10 9 8 7 6 5 4 3 2 1 ppm
2.02
1.04
2.02
1.99
2.02
2.07
2.00

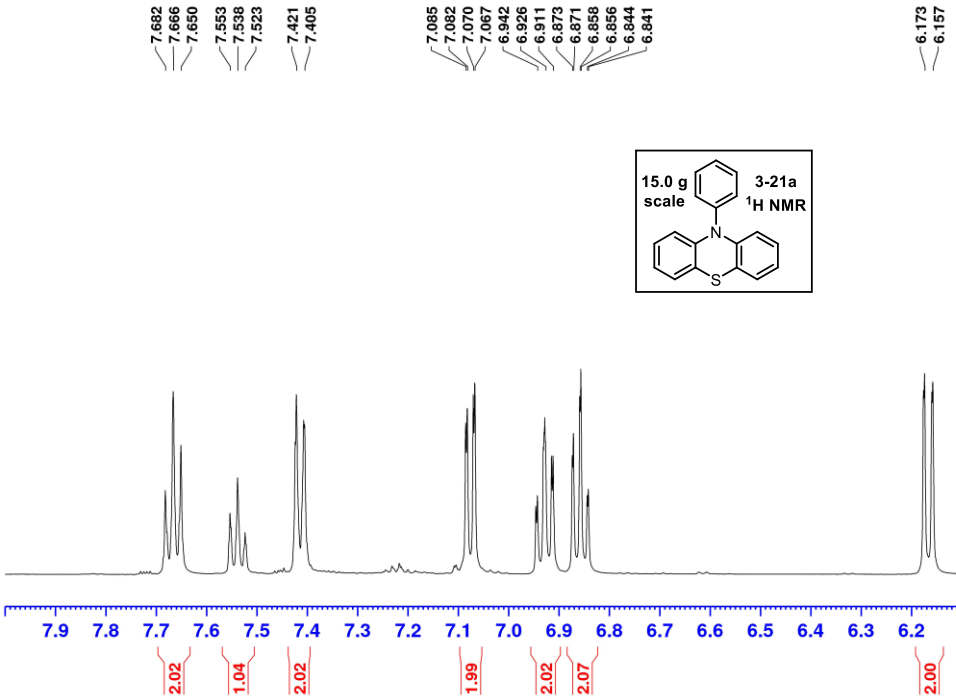
7.682
7.666
7.650
7.553
7.538
7.523
7.421
7.405
7.085
7.082
7.070
7.067
6.942
6.926
6.911
6.873
6.871
6.858
6.856
6.844
6.841
6.173
6.157
15.0 g scale
3-21a
1H NMR
N
S
7.9 7.8 7.7 7.6 7.5 7.4 7.3 7.2 7.1 7.0 6.9 6.8 6.7 6.6 6.5 6.4 6.3 6.2 ppm
2.02
1.04
2.02
1.99
2.02
2.07
2.00

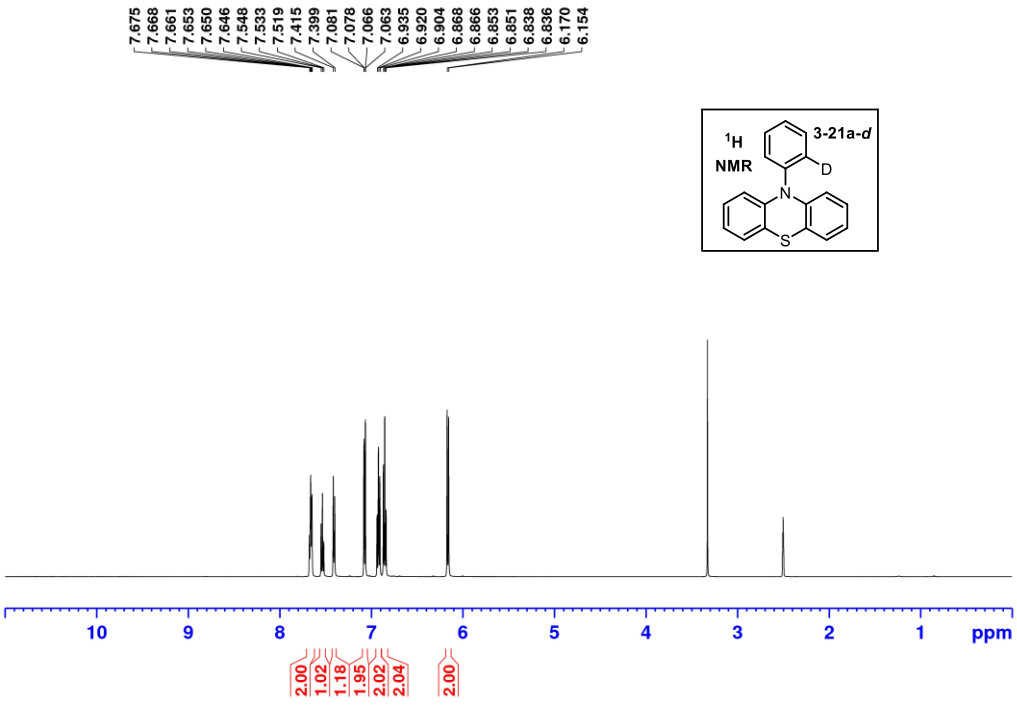
7.675
7.668
7.661
7.653
7.650
7.646
7.548
7.533
7.519
7.415
7.399
7.081
7.078
7.066
7.063
6.935
6.920
6.904
6.868
6.866
6.853
6.851
6.838
6.836
6.170
6.154
1H NMR
3-21a-d
D
N
S
10 9 8 7 6 5 4 3 2 1 ppm
2.00
1.02
1.18
1.95
2.02
2.04
2.00

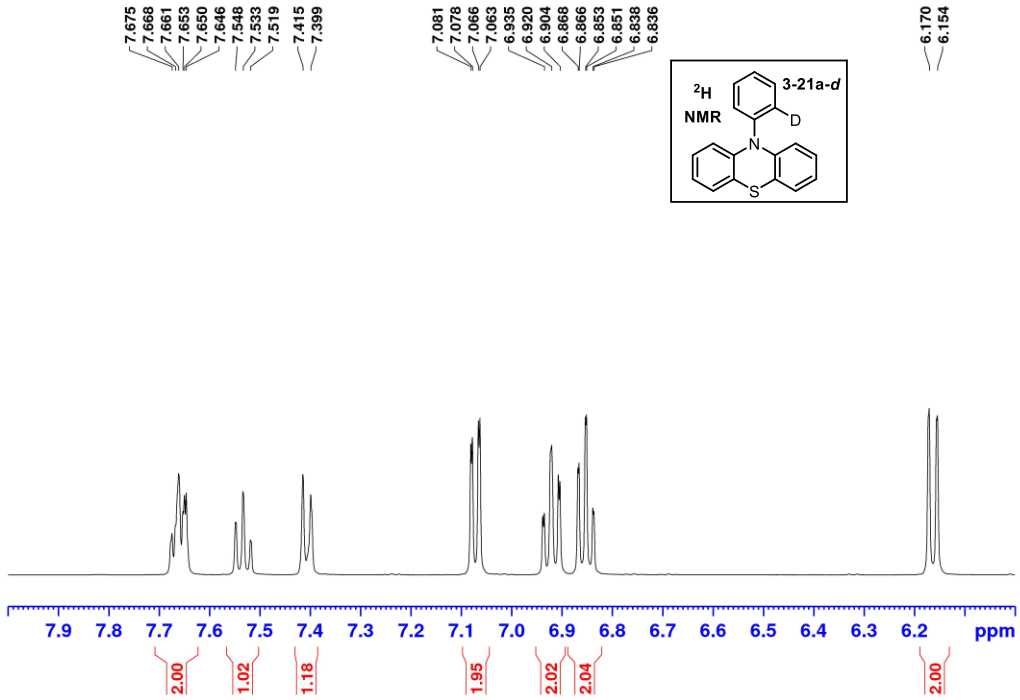
7.675
7.668
7.661
7.653
7.650
7.646
7.548
7.533
7.519
7.415
7.399
7.081
7.078
7.066
7.063
6.935
6.920
6.904
6.868
6.866
6.853
6.851
6.838
6.836
6.170
6.154
^{2}H NMR
3-21a-*d*
D
N
S
7.9 7.8 7.7 7.6 7.5 7.4 7.3 7.2 7.1 7.0 6.9 6.8 6.7 6.6 6.5 6.4 6.3 6.2 ppm
2.00
1.02
1.18
1.95
2.02
2.04
2.00

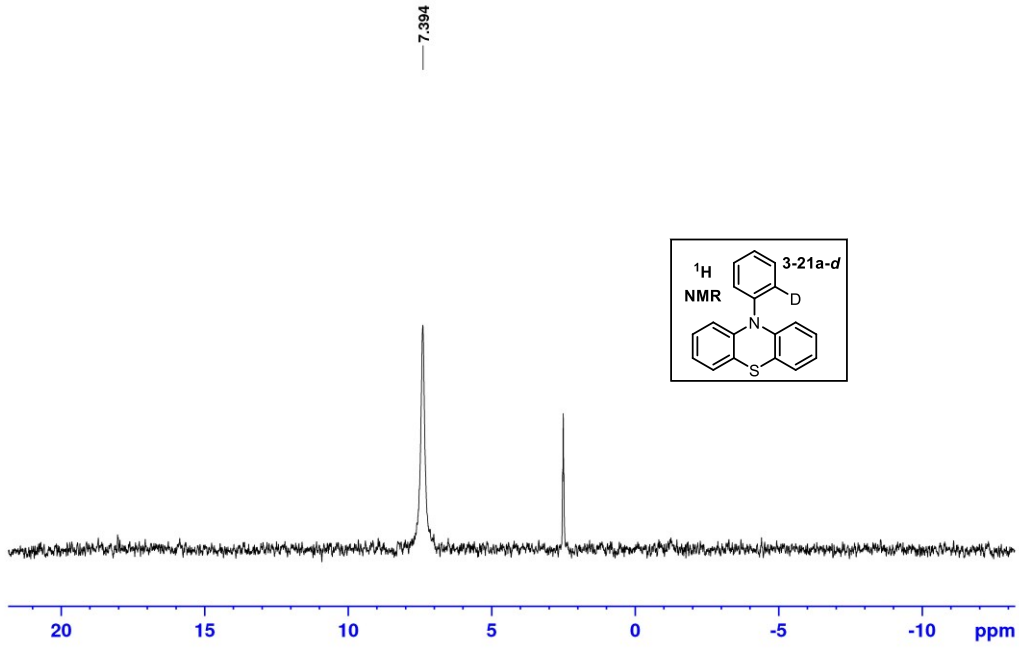
7.394
^{1}H NMR
3-21a-*d*
D
N
S
20 15 10 5 0 -5 -10 ppm

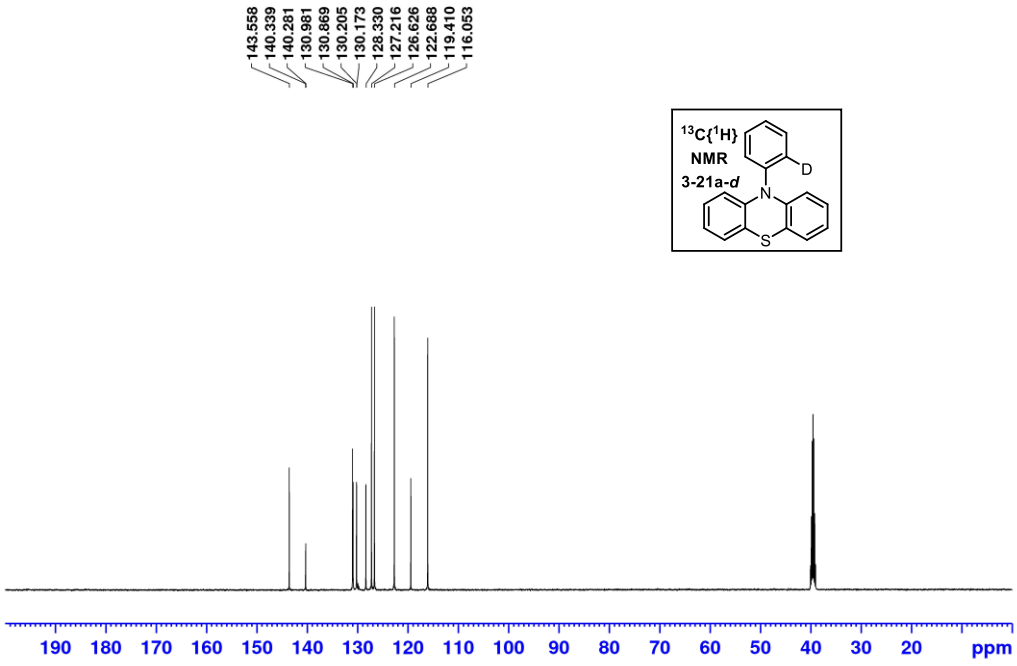
143.558
140.339
140.281
130.981
130.869
130.205
130.173
128.330
127.216
126.626
122.688
119.410
116.053
$^{13}C\{^{1}H\}$
NMR
3-21a-*d*
D
N
S
190 180 170 160 150 140 130 120 110 100 90 80 70 60 50 40 30 20 ppm

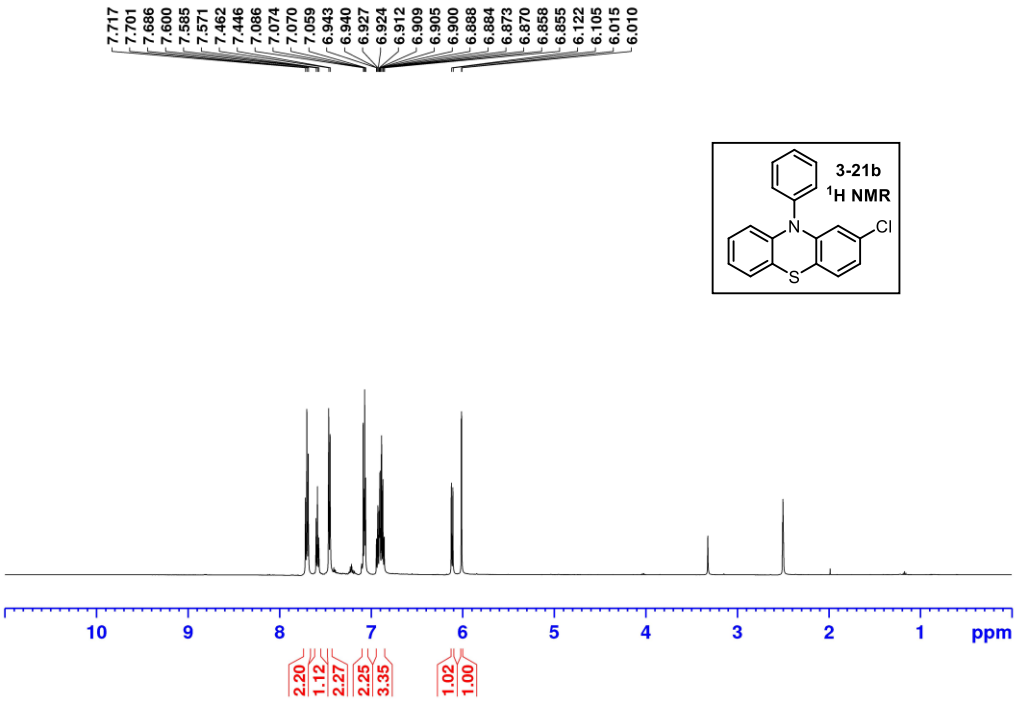
7.717
7.701
7.686
7.600
7.585
7.571
7.462
7.446
7.086
7.074
7.070
7.059
6.943
6.940
6.927
6.924
6.912
6.909
6.905
6.900
6.888
6.884
6.873
6.870
6.858
6.855
6.122
6.105
6.015
6.010
3-21b
^{1}H NMR
N
Cl
S
10 9 8 7 6 5 4 3 2 1 ppm
2.20
1.12
2.27
2.25
3.35
1.02
1.00

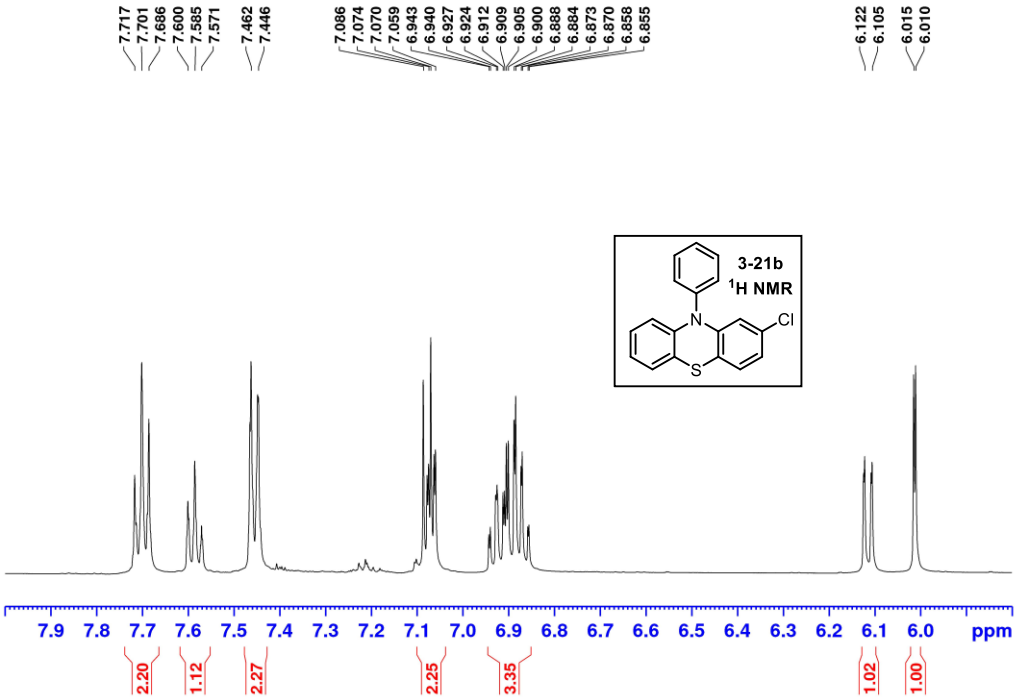
7.717
7.701
7.686
7.600
7.585
7.571
7.462
7.446
7.086
7.074
7.070
7.059
6.943
6.940
6.927
6.924
6.912
6.909
6.905
6.900
6.888
6.884
6.873
6.870
6.858
6.855
6.122
6.105
6.015
6.010
3-21b
1H NMR
N
Cl
S
7.9 7.8 7.7 7.6 7.5 7.4 7.3 7.2 7.1 7.0 6.9 6.8 6.7 6.6 6.5 6.4 6.3 6.2 6.1 6.0 ppm
2.20
1.12
2.27
2.25
3.35
1.02
1.00

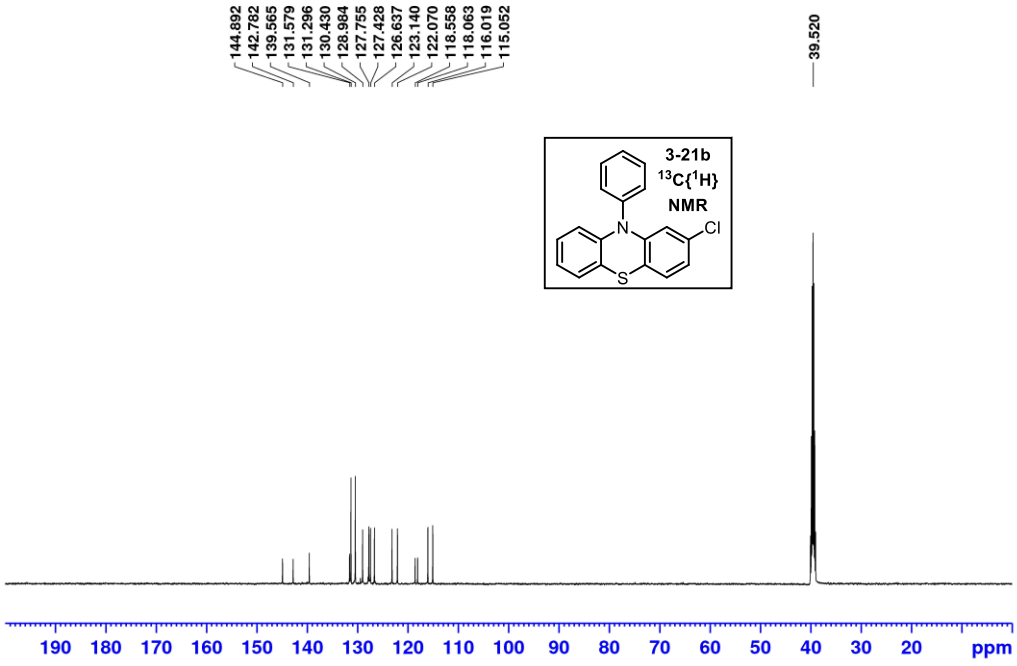
144.892
142.782
139.565
131.579
131.296
130.430
128.984
127.755
127.428
126.637
123.140
122.070
118.558
118.063
116.019
115.052
39.520
3-21b
13C{1H}
NMR
N
Cl
S
190 180 170 160 150 140 130 120 110 100 90 80 70 60 50 40 30 20 ppm

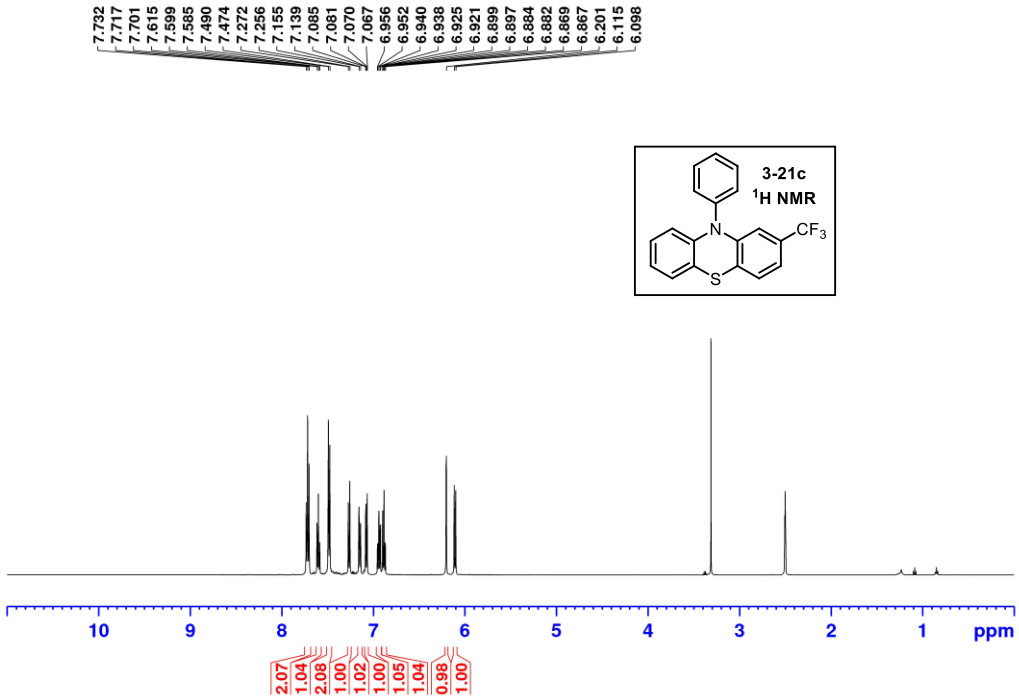
7.732
7.717
7.701
7.615
7.599
7.585
7.490
7.474
7.272
7.256
7.155
7.139
7.085
7.081
7.070
7.067
6.956
6.952
6.940
6.938
6.925
6.921
6.899
6.897
6.884
6.882
6.869
6.867
6.201
6.115
6.098
3-21c
1H NMR
CF3
N
S
10
9
8
7
6
5
4
3
2
1
ppm
2.07
1.04
2.08
1.00
1.02
1.00
1.05
1.04
0.98
1.00

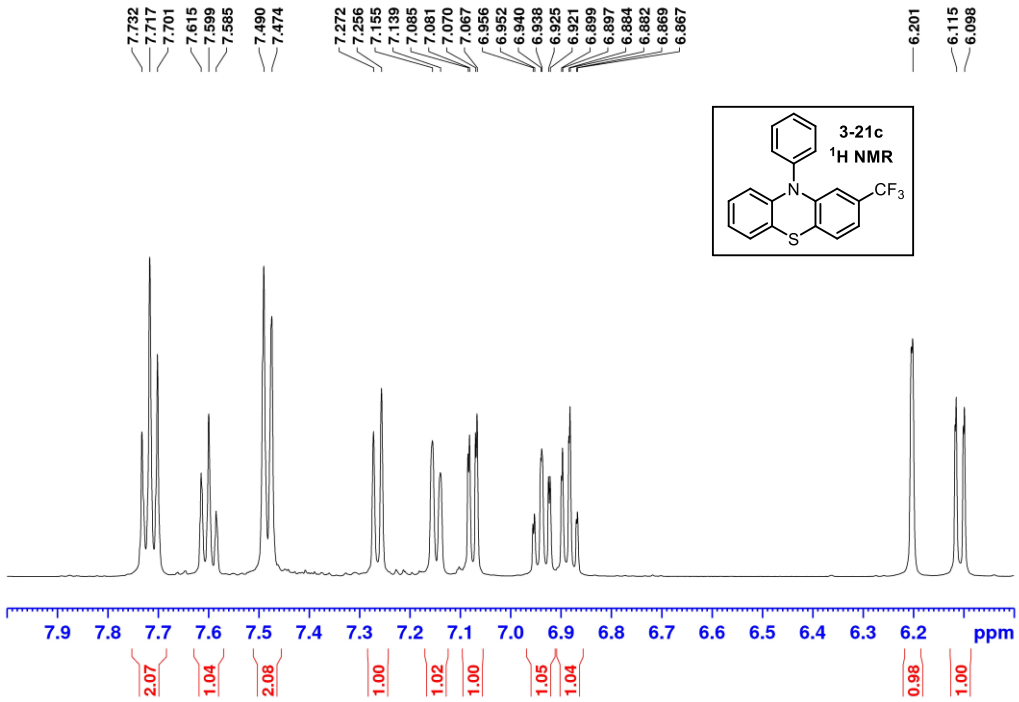
7.732
7.717
7.701
7.615
7.599
7.585
7.490
7.474
7.272
7.256
7.155
7.139
7.085
7.081
7.070
7.067
6.956
6.952
6.940
6.938
6.925
6.921
6.899
6.897
6.884
6.882
6.869
6.867
6.201
6.115
6.098
3-21c
1H NMR
CF3
N
S
7.9
7.8
7.7
7.6
7.5
7.4
7.3
7.2
7.1
7.0
6.9
6.8
6.7
6.6
6.5
6.4
6.3
6.2
ppm
2.07
1.04
2.08
1.00
1.02
1.00
1.05
1.04
0.98
1.00

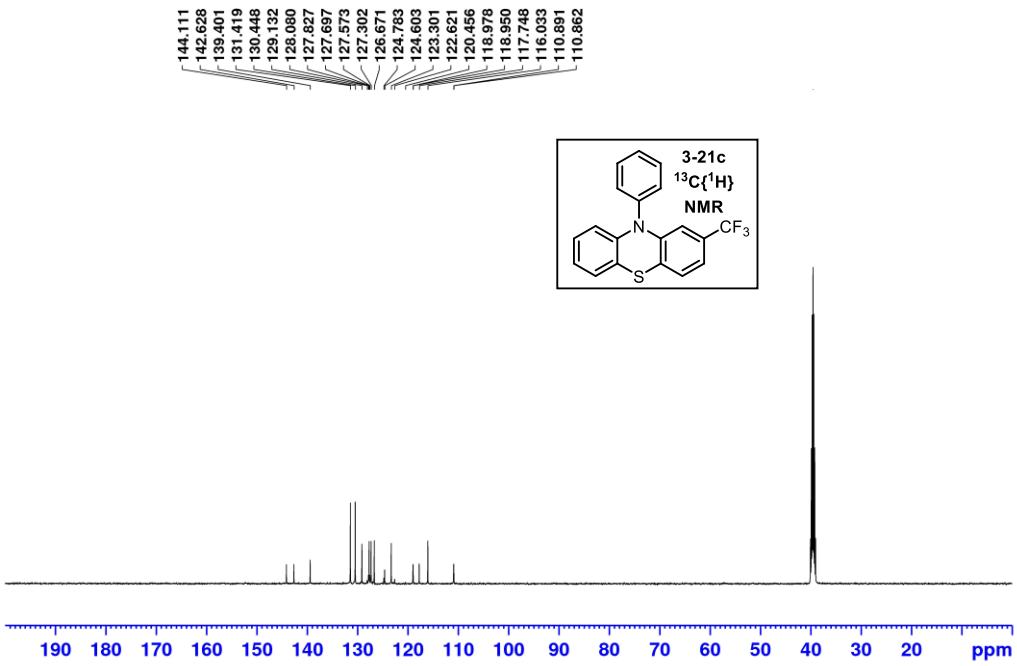
144.111
142.628
139.401
131.419
130.448
129.132
128.080
127.827
127.697
127.573
127.302
126.671
124.783
124.603
123.301
122.621
120.456
118.978
118.950
117.748
116.033
110.891
110.862
3-21c
$^{13}C\{^{1}H\}$
NMR
N
CF3
S
190 180 170 160 150 140 130 120 110 100 90 80 70 60 50 40 30 20 ppm

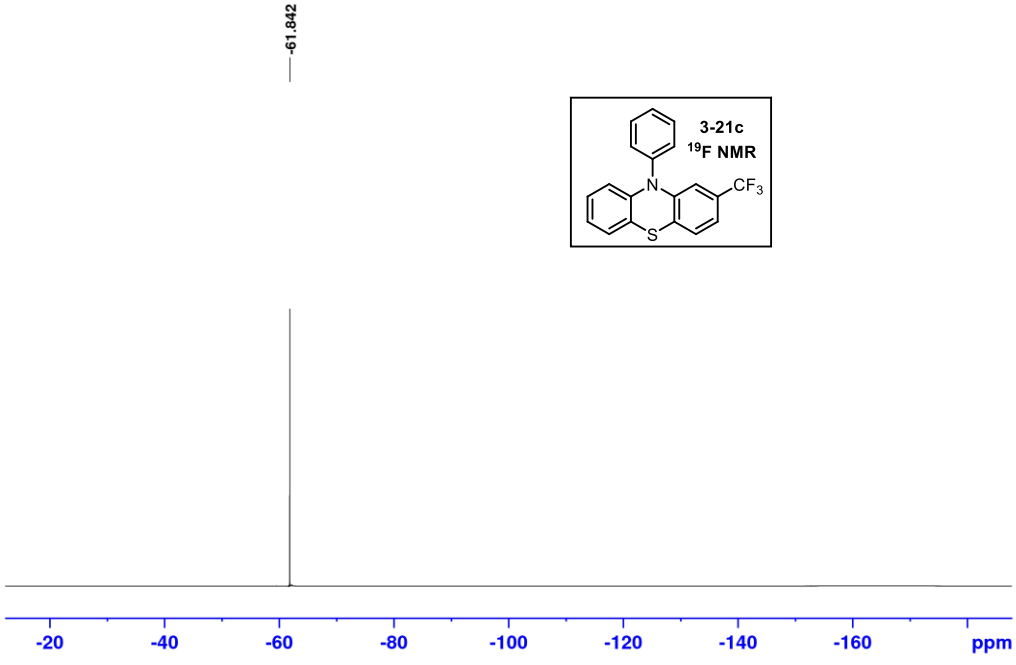
-61.842
3-21c
^{19}F NMR
N
CF3
S
-20 -40 -60 -80 -100 -120 -140 -160 ppm

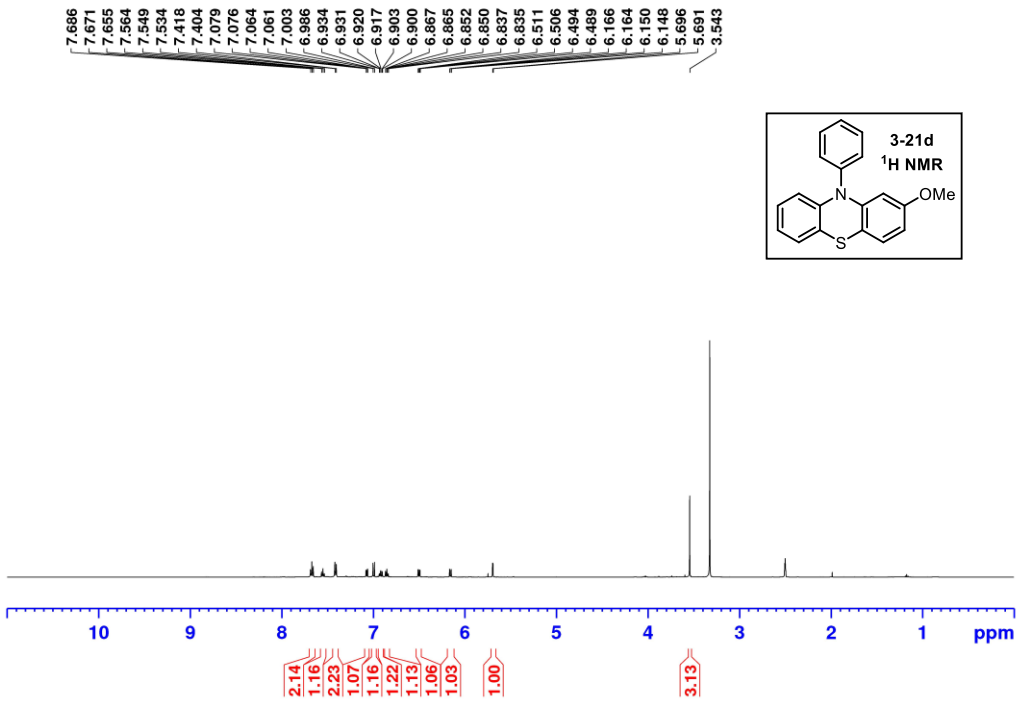
7.686
7.671
7.655
7.564
7.549
7.534
7.418
7.404
7.079
7.076
7.064
7.061
7.003
6.986
6.934
6.931
6.920
6.917
6.903
6.900
6.867
6.865
6.852
6.850
6.837
6.835
6.511
6.506
6.494
6.489
6.166
6.164
6.150
6.148
5.696
5.691
3.543
3-21d
1H NMR
N
OMe
S
10
9
8
7
6
5
4
3
2
1
ppm
2.14
1.16
2.23
1.07
1.16
1.22
1.13
1.06
1.03
1.00
3.13

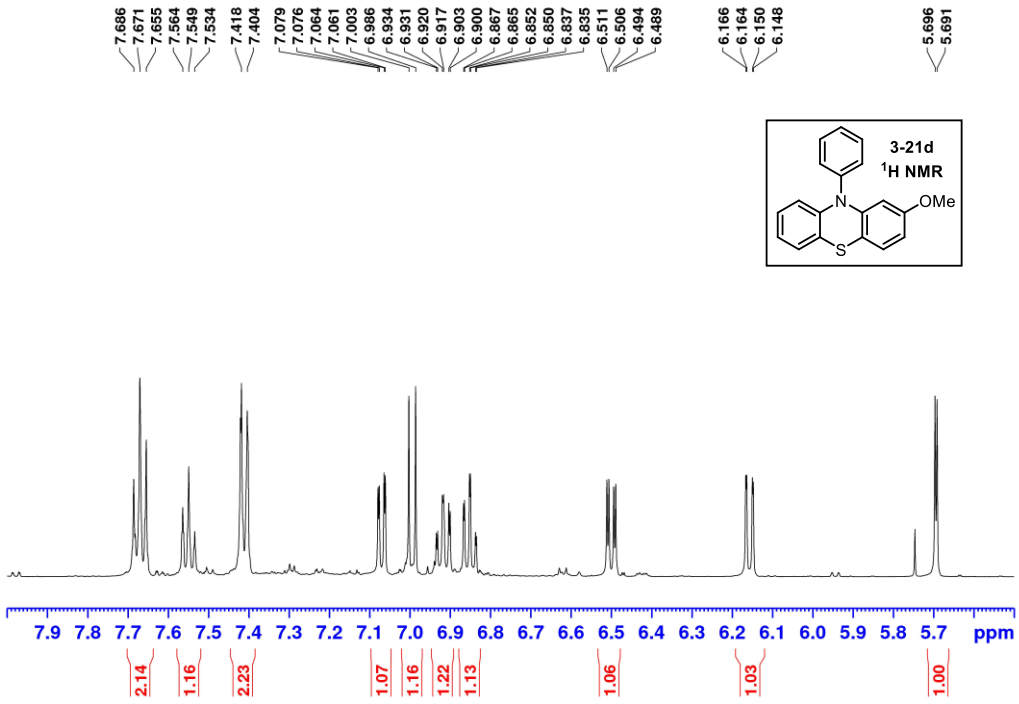
7.686
7.671
7.655
7.564
7.549
7.534
7.418
7.404
7.079
7.076
7.064
7.061
7.003
6.986
6.934
6.931
6.920
6.917
6.903
6.900
6.867
6.865
6.852
6.850
6.837
6.835
6.511
6.506
6.494
6.489
6.166
6.164
6.150
6.148
5.696
5.691
3-21d
1H NMR
N
OMe
S
7.9
7.8
7.7
7.6
7.5
7.4
7.3
7.2
7.1
7.0
6.9
6.8
6.7
6.6
6.5
6.4
6.3
6.2
6.1
6.0
5.9
5.8
5.7
ppm
2.14
1.16
2.23
1.07
1.16
1.22
1.13
1.06
1.03
1.00

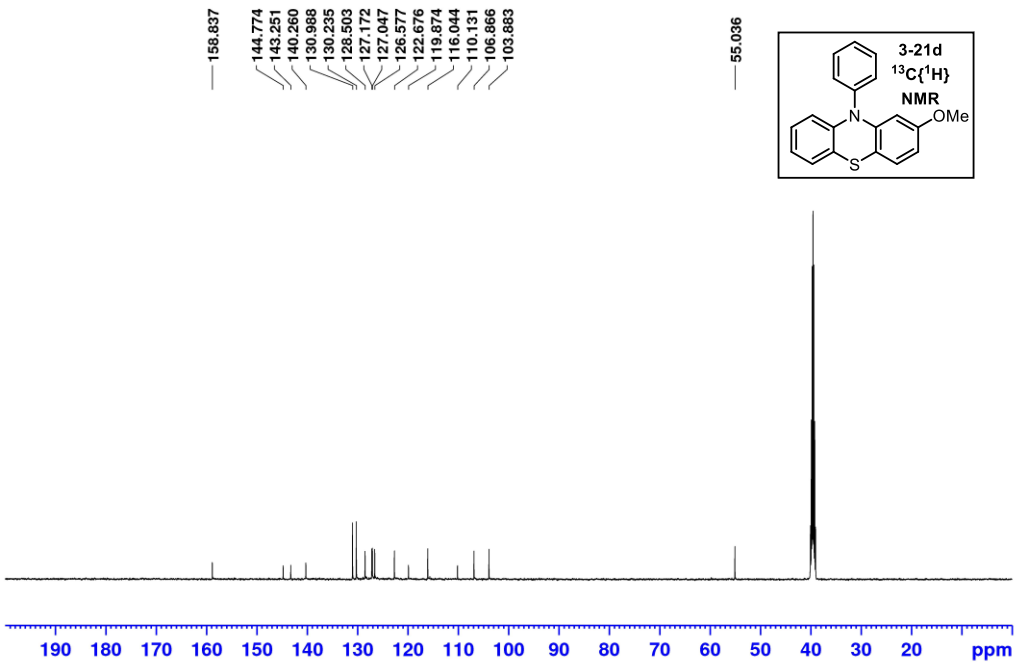
158.837
144.774
143.251
140.260
130.988
130.235
128.503
127.172
127.047
126.577
122.676
119.874
116.044
110.131
106.866
103.883
55.036
3-21d
$^{13}C\{^{1}H\}$
NMR
OMe
N
S
190 180 170 160 150 140 130 120 110 100 90 80 70 60 50 40 30 20 ppm

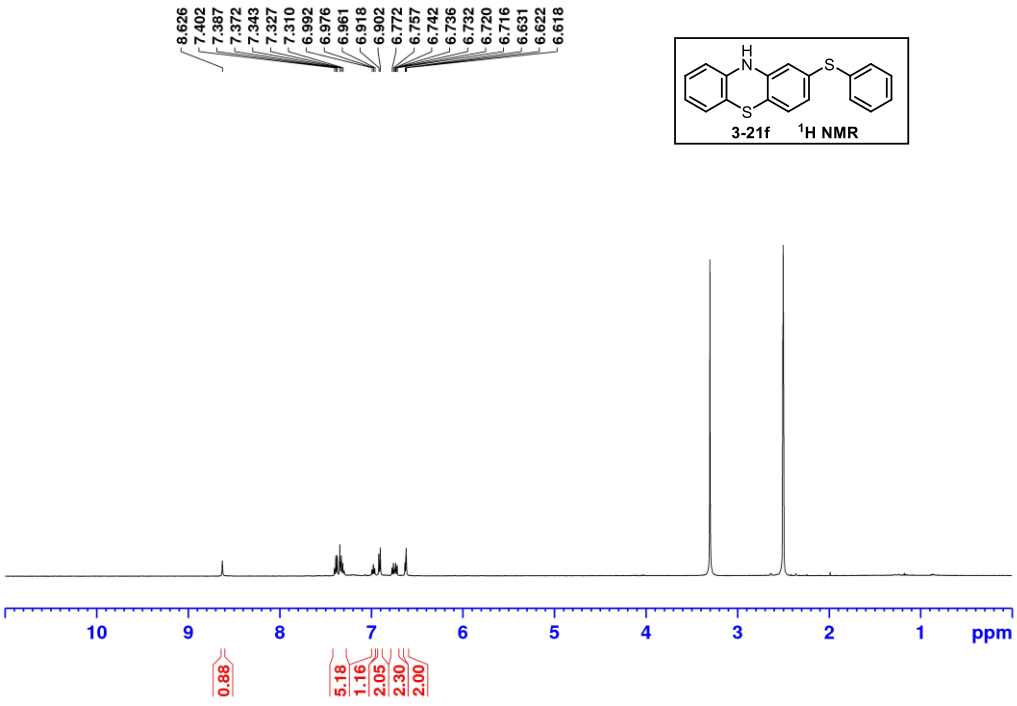
8.626
7.402
7.387
7.372
7.343
7.327
7.310
6.992
6.976
6.961
6.918
6.902
6.772
6.757
6.742
6.736
6.732
6.720
6.716
6.631
6.622
6.618
H
N
S
S
3-21f ^{1}H NMR
10 9 8 7 6 5 4 3 2 1 ppm
0.88
5.18
1.16
2.05
2.30
2.00

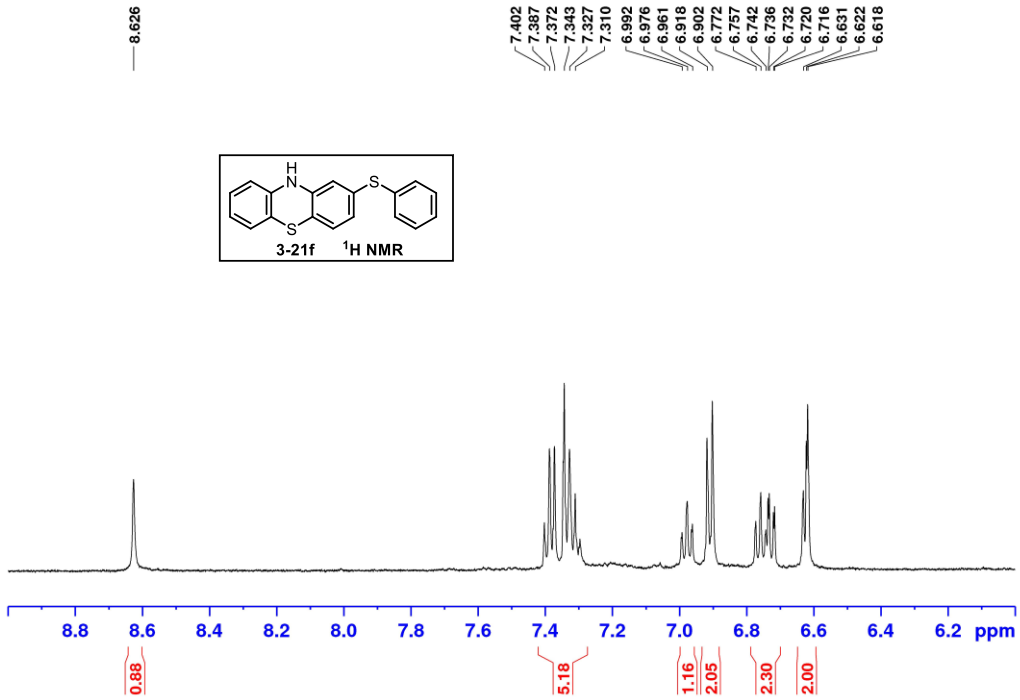
8.626
7.402
7.387
7.372
7.343
7.327
7.310
6.992
6.976
6.961
6.918
6.902
6.772
6.757
6.742
6.736
6.732
6.720
6.716
6.631
6.622
6.618
3-21f ¹H NMR
8.8
8.6
8.4
8.2
8.0
7.8
7.6
7.4
7.2
7.0
6.8
6.6
6.4
6.2
ppm
0.88
5.18
1.16
2.05
2.30
2.00

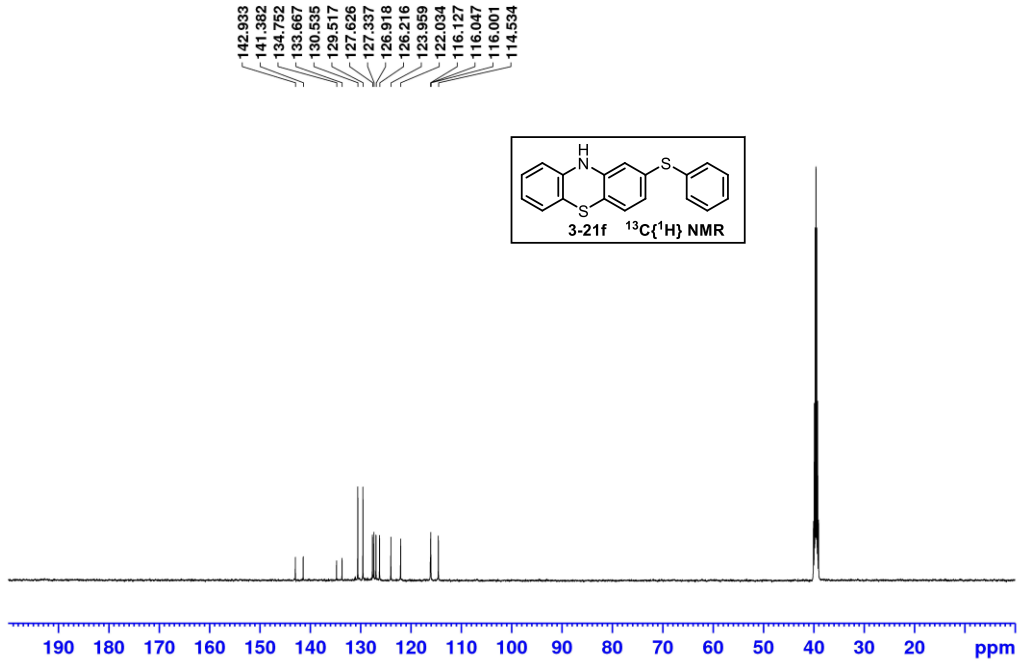
142.933
141.382
134.752
133.667
130.535
129.517
127.626
127.337
126.918
126.216
123.959
122.034
116.127
116.047
116.001
114.534
3-21f ¹³C{¹H} NMR
190
180
170
160
150
140
130
120
110
100
90
80
70
60
50
40
30
20
ppm

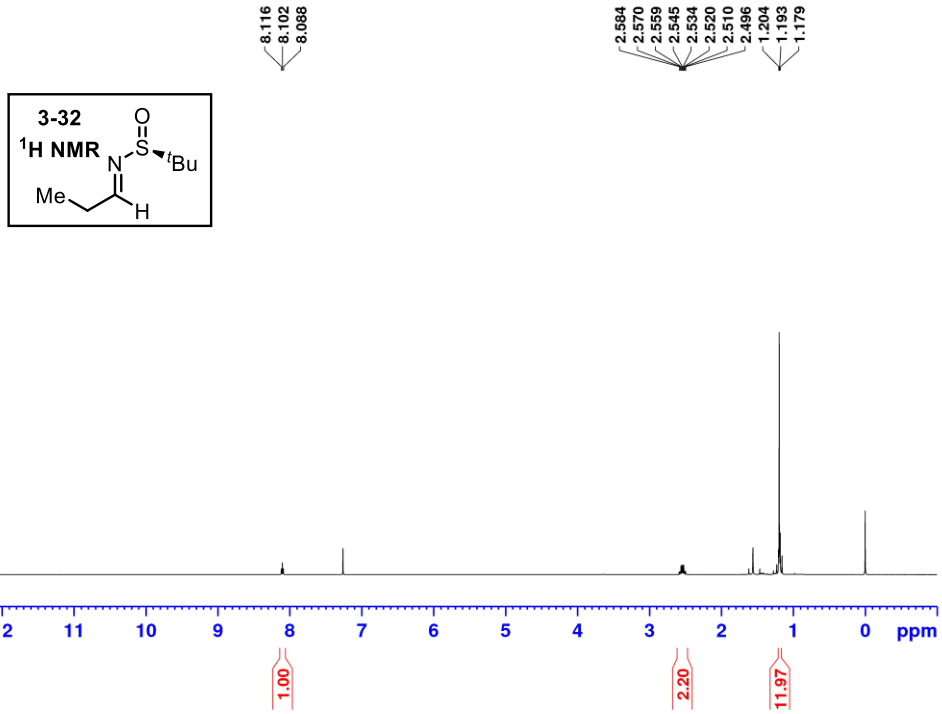
8.116
8.102
8.088
2.584
2.570
2.559
2.545
2.534
2.520
2.510
2.496
1.204
1.193
1.179
3-32
1H NMR
Me
H
tBu
12
11
10
9
8
7
6
5
4
3
2
1
0
ppm
1.00
2.20
11.97

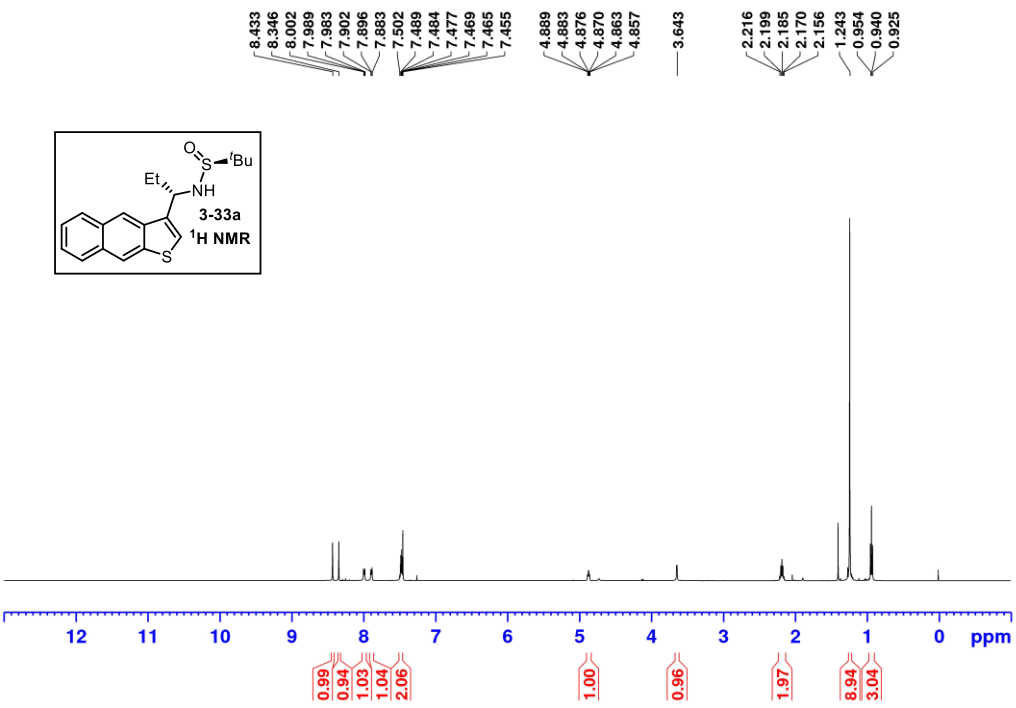
8.433
8.346
8.002
7.989
7.983
7.902
7.896
7.883
7.502
7.489
7.484
7.477
7.469
7.465
7.455
4.889
4.883
4.876
4.870
4.863
4.857
3.643
2.216
2.199
2.185
2.170
2.156
1.243
0.954
0.940
0.925
tBu
Et
NH
3-33a
1H NMR
12
11
10
9
8
7
6
5
4
3
2
1
0
ppm
0.99
0.94
1.03
1.04
2.06
1.00
0.96
1.97
8.94
3.04

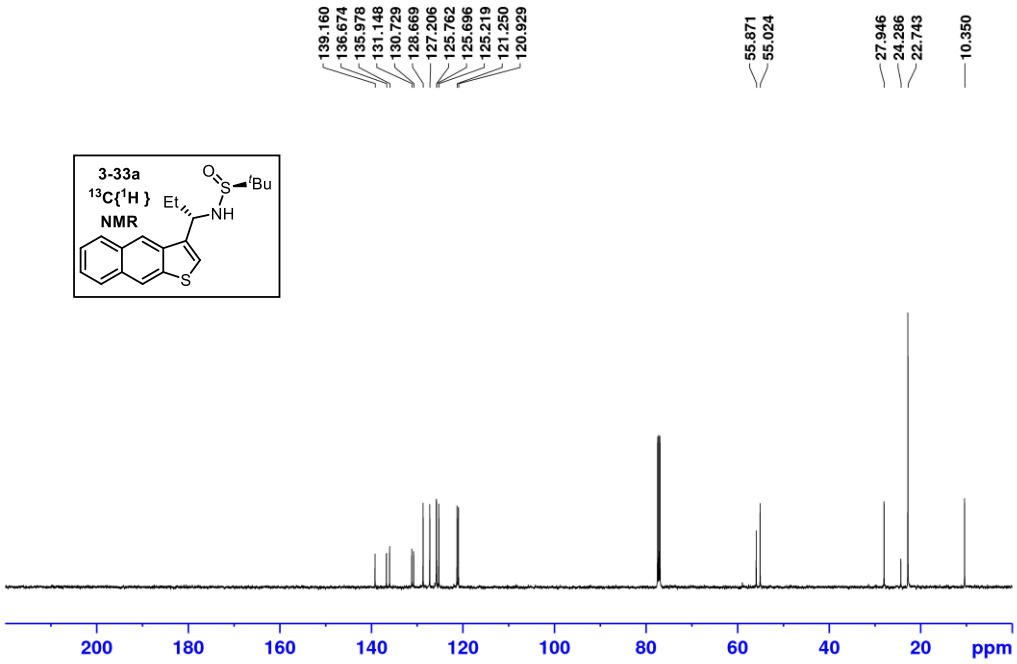
139.160
136.674
135.978
131.148
130.729
128.669
127.206
125.762
125.696
125.219
121.250
120.929
55.871
55.024
27.946
24.286
22.743
10.350
3-33a
$^{13}C\{^{1}H\}$ NMR
Et
NH
^{t}Bu
200
180
160
140
120
100
80
60
40
20
ppm

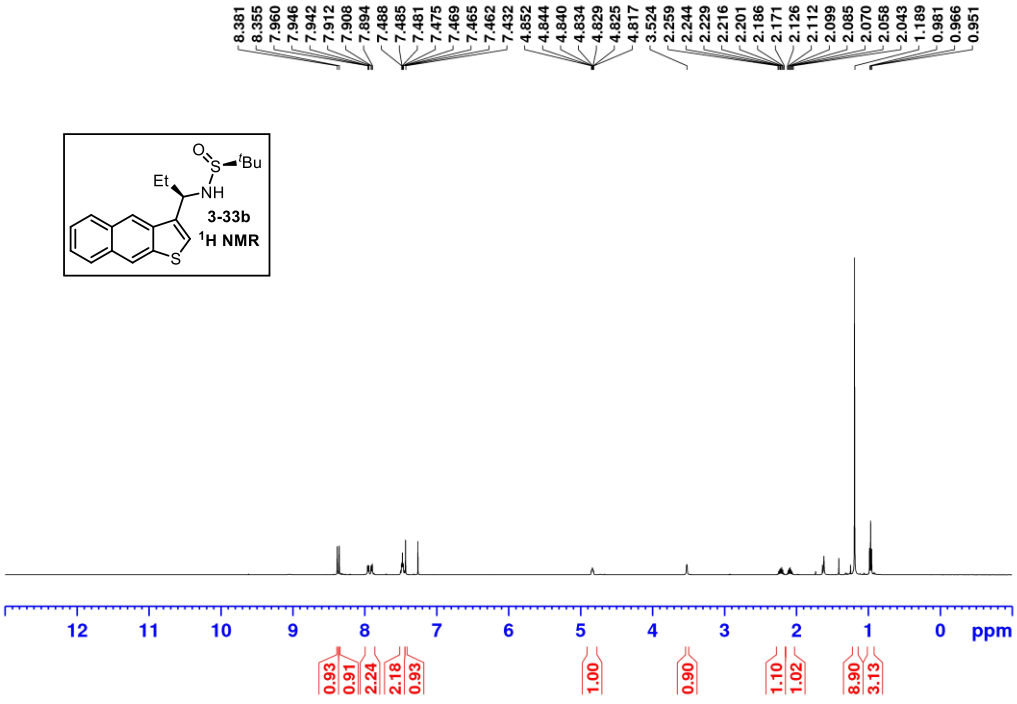
8.381
8.355
7.960
7.946
7.942
7.912
7.908
7.894
7.488
7.485
7.481
7.475
7.469
7.465
7.462
7.432
4.852
4.844
4.840
4.834
4.829
4.825
4.817
3.524
2.259
2.244
2.229
2.216
2.201
2.186
2.171
2.126
2.112
2.099
2.085
2.070
2.058
2.043
1.189
0.981
0.966
0.951
3-33b
^{1}H NMR
Et
NH
^{t}Bu
12
11
10
9
8
7
6
5
4
3
2
1
0
ppm
0.93
0.91
2.24
2.18
0.93
1.00
0.90
1.10
1.02
8.90
3.13

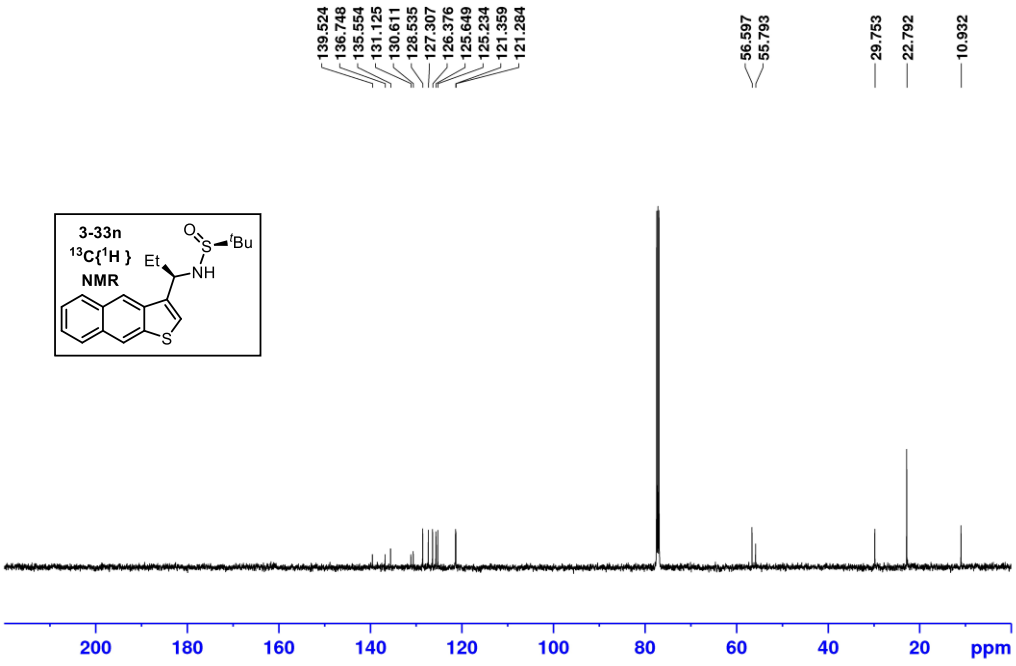
139.524
136.748
135.554
131.125
130.611
128.535
127.307
126.376
125.649
125.234
121.359
121.284
56.597
55.793
29.753
22.792
10.932
3-33n
$^{13}C\{^{1}H\}$ NMR
Et
NH
^{t}Bu
S
200
180
160
140
120
100
80
60
40
20
ppm

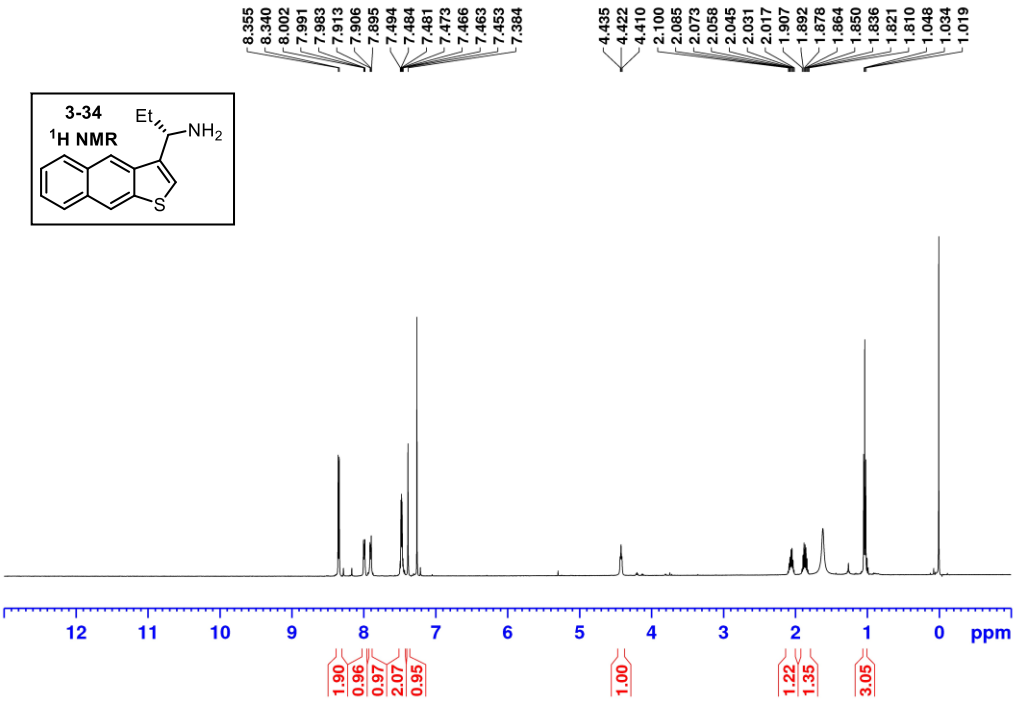
8.355
8.340
8.002
7.991
7.983
7.913
7.906
7.895
7.494
7.484
7.481
7.473
7.466
7.463
7.453
7.384
4.435
4.422
4.410
2.100
2.085
2.073
2.058
2.045
2.031
2.017
1.907
1.892
1.878
1.864
1.850
1.836
1.821
1.810
1.048
1.034
1.019
3-34
^{1}H NMR
Et
NH$_2$
S
12
11
10
9
8
7
6
5
4
3
2
1
0
ppm
1.90
0.96
0.97
2.07
0.95
1.00
1.22
1.35
3.05

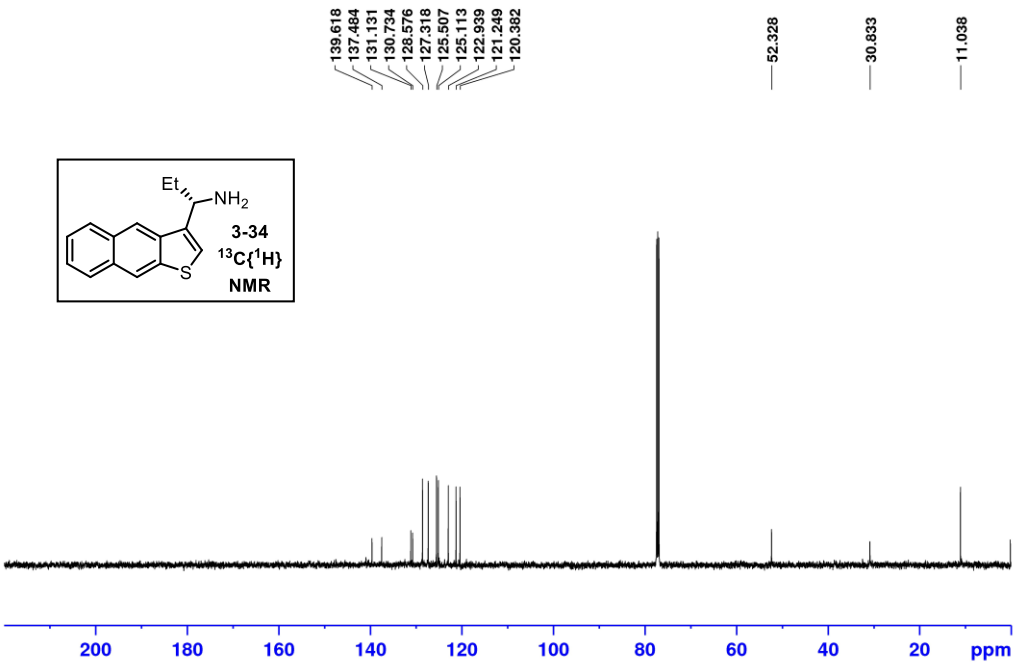
139.618
137.484
131.131
130.734
128.576
127.318
125.507
125.113
122.939
121.249
120.382
52.328
30.833
11.038
Et
NH2
3-34
13C{1H}
NMR
200
180
160
140
120
100
80
60
40
20
ppm

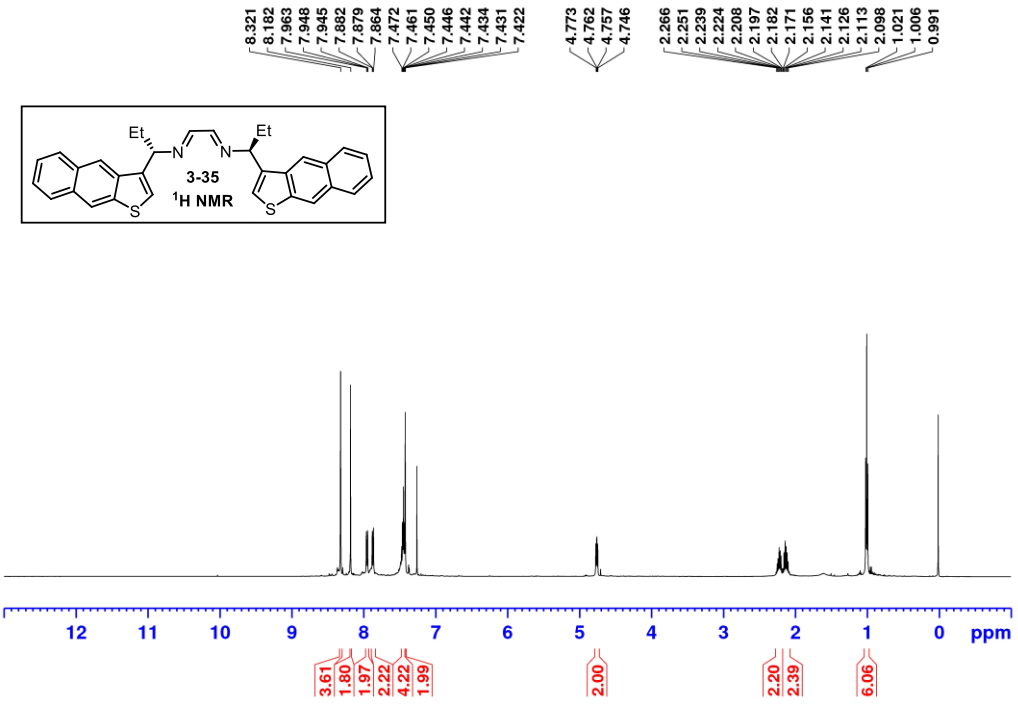
8.321
8.182
7.963
7.948
7.945
7.882
7.879
7.864
7.472
7.461
7.450
7.446
7.442
7.434
7.431
7.422
4.773
4.762
4.757
4.746
2.266
2.251
2.239
2.224
2.208
2.197
2.182
2.171
2.156
2.141
2.126
2.113
2.098
1.021
1.006
0.991
Et
N
N
Et
3-35
1H NMR
12
11
10
9
8
7
6
5
4
3
2
1
0
ppm
3.61
1.80
1.97
2.22
4.22
1.99
2.00
2.20
2.39
6.06

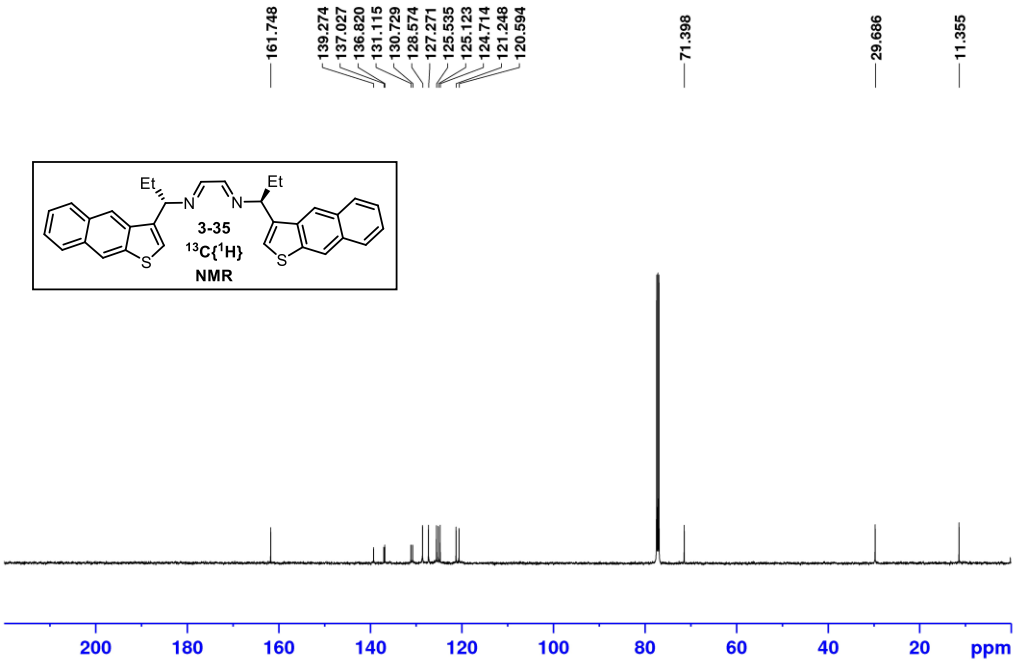
161.748
139.274
137.027
136.820
131.115
130.729
128.574
127.271
125.535
125.123
124.714
121.248
120.594
71.398
29.686
11.355
3-35
$^{13}C\{^{1}H\}$
NMR
200
180
160
140
120
100
80
60
40
20
ppm

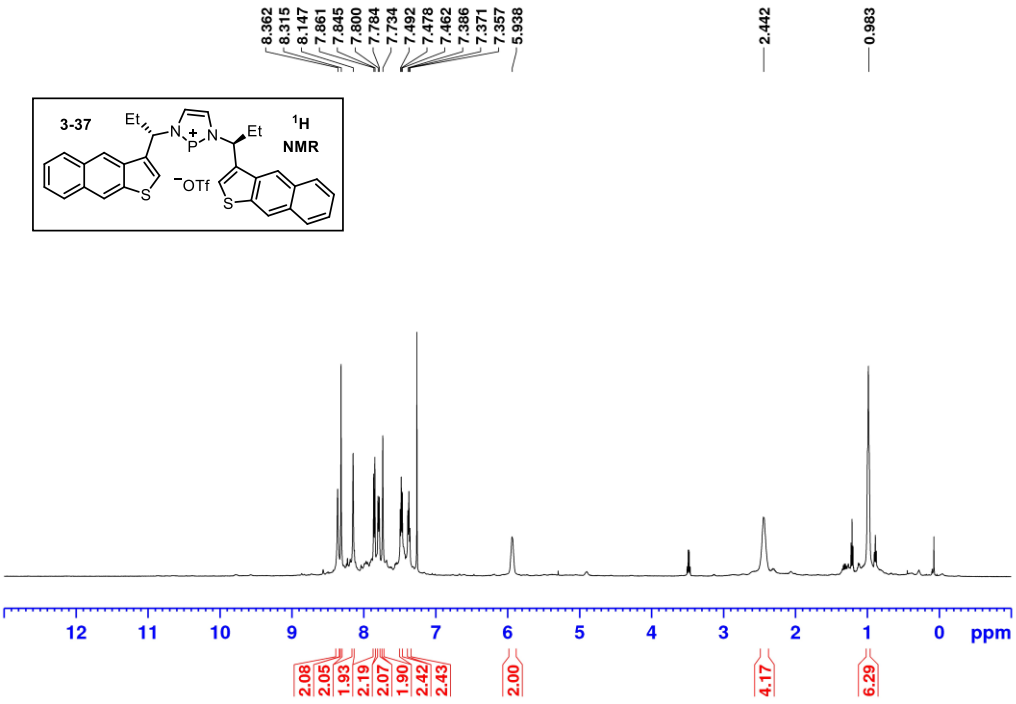
8.362
8.315
8.147
7.861
7.845
7.800
7.784
7.734
7.492
7.478
7.462
7.386
7.371
7.357
5.938
2.442
0.983
3-37
^{1}H
NMR
12
11
10
9
8
7
6
5
4
3
2
1
0
ppm
2.08
2.05
1.93
2.19
2.07
1.90
2.42
2.43
2.00
4.17
6.29

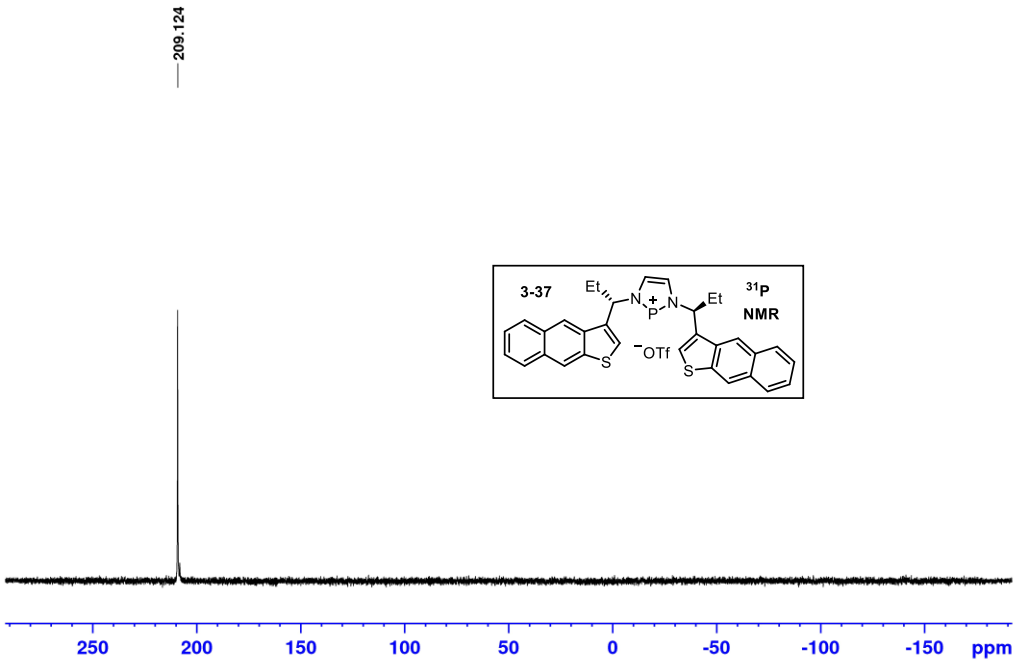
209.124
3-37
Et
N
P
N
Et
^{31}P
NMR
$^{-}$OTf
S
S
250
200
150
100
50
0
-50
-100
-150
ppm


8.353
8.336
7.902
7.886
7.819
7.805
7.766
7.750
7.570
7.556
7.540
7.518
7.502
7.487
7.480
7.465
7.450
5.617
5.605
5.591
5.579
2.331
1.721
1.708

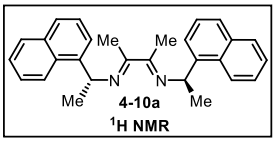
Me
Me
N
N
Me
Me
4-10a
^{1}H NMR

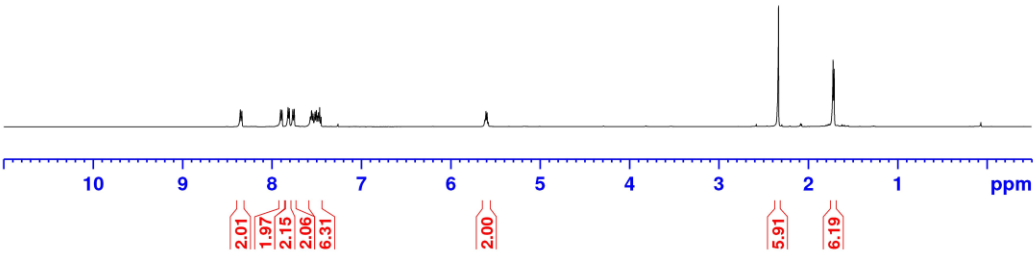
10
9
8
7
6
5
4
3
2
1
ppm
2.01
1.97
2.15
2.06
6.31
2.00
5.91
6.19


167.086
142.057
134.170
130.818
129.091
127.201
125.837
125.778
125.364
124.247
123.793
57.393
24.433
13.272

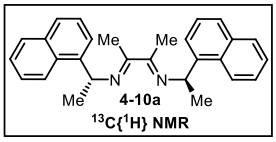
Me
Me
N
N
Me
Me
4-10a
^{13}C{^{1}H} NMR

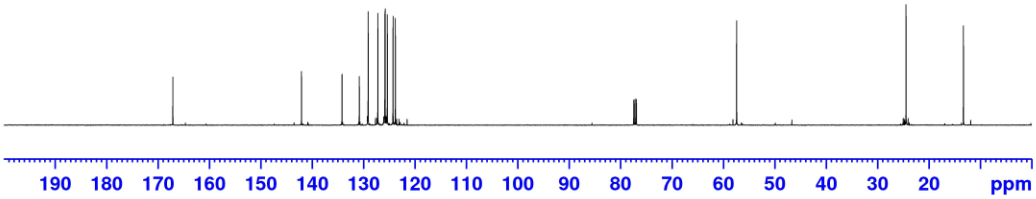
190
180
170
160
150
140
130
120
110
100
90
80
70
60
50
40
30
20
ppm

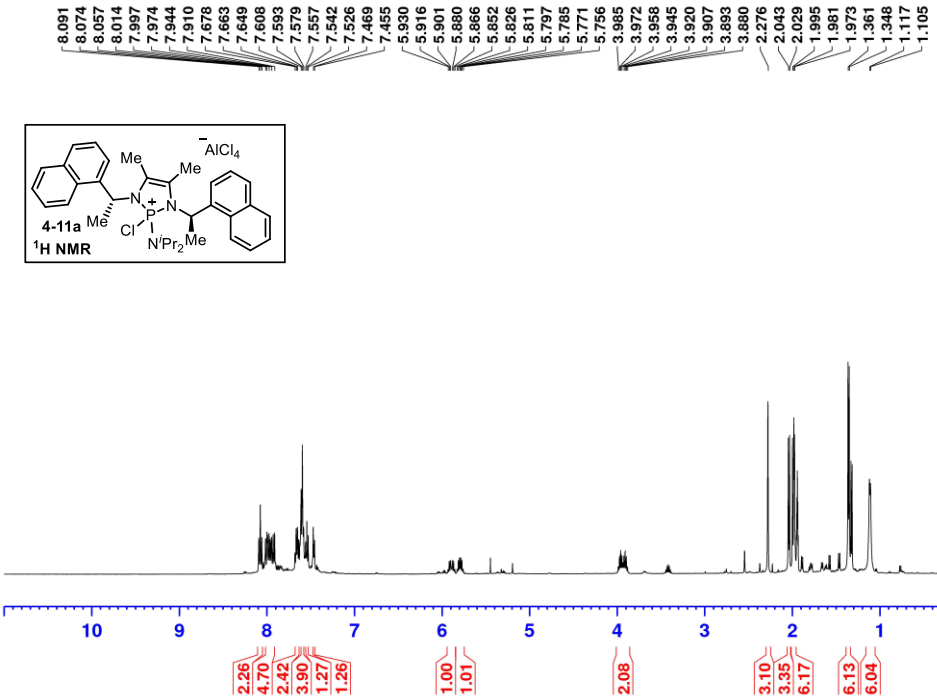
8.091
8.074
8.057
8.014
7.997
7.974
7.944
7.910
7.678
7.663
7.649
7.608
7.593
7.579
7.557
7.542
7.526
7.469
7.455
5.930
5.916
5.901
5.880
5.866
5.852
5.826
5.811
5.797
5.785
5.771
5.756
3.985
3.972
3.958
3.945
3.920
3.907
3.893
3.880
2.276
2.043
2.029
1.995
1.981
1.973
1.361
1.348
1.117
1.105
AlCl4
Me
Me
Me
Cl
N
P
N
N
iPr2Me
4-11a
1H NMR
10
9
8
7
6
5
4
3
2
1
ppm
2.26
4.70
2.42
3.90
1.27
1.26
1.00
1.01
2.08
3.10
3.35
6.17
6.13
6.04

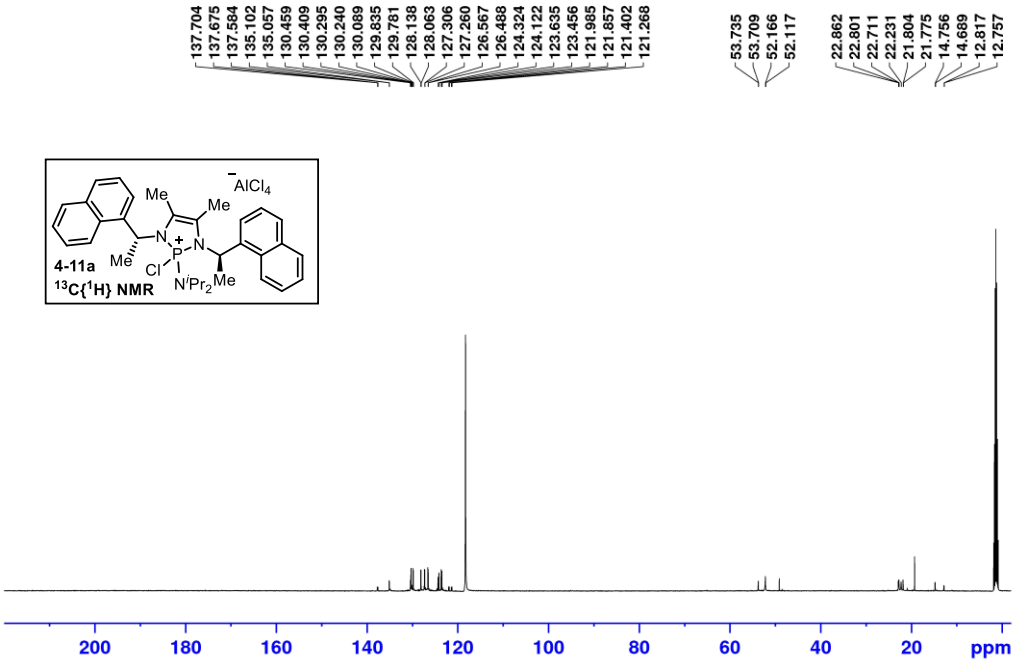
137.704
137.675
137.584
135.102
135.057
130.459
130.409
130.295
130.240
130.089
129.835
129.781
128.138
128.063
127.306
127.260
126.567
126.488
124.324
124.122
123.635
123.456
121.985
121.857
121.402
121.268
53.735
53.709
52.166
52.117
22.862
22.801
22.711
22.231
21.804
21.775
14.756
14.689
12.817
12.757
AlCl4
Me
Me
Me
Cl
N
P
N
N
iPr2Me
4-11a
13C{1H} NMR
200
180
160
140
120
100
80
60
40
20
ppm

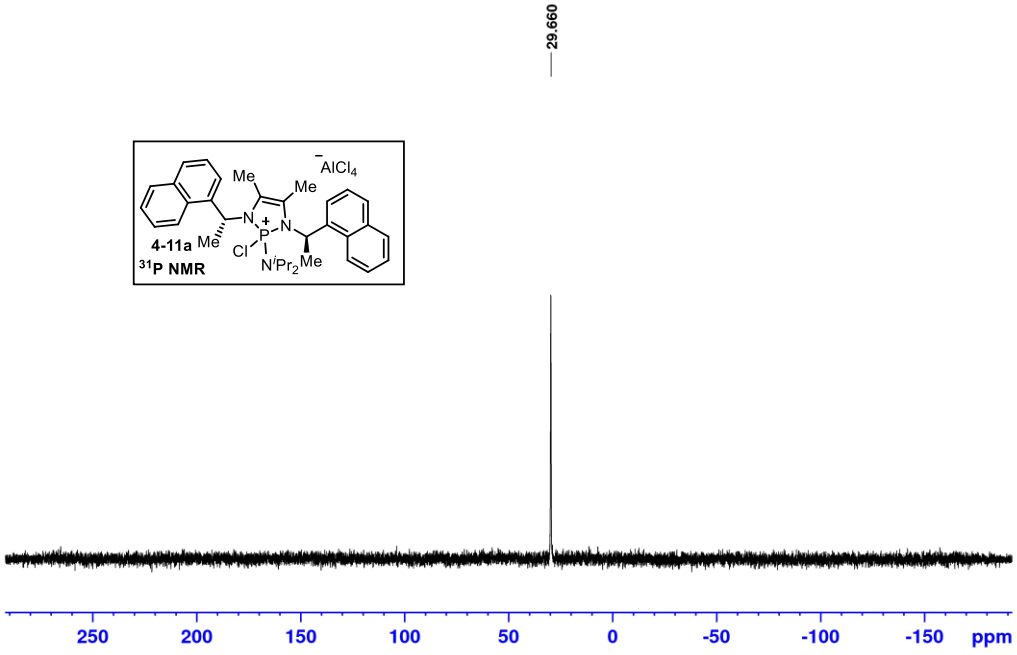
29.660
4-11a
31P NMR
AlCl4
Me
Me
Me
Cl
N/Pr2
Me
250
200
150
100
50
0
-50
-100
-150
ppm

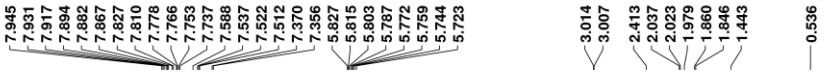
7.945
7.931
7.917
7.894
7.882
7.867
7.827
7.810
7.778
7.766
7.753
7.737
7.588
7.537
7.522
7.512
7.370
7.356
5.827
5.815
5.803
5.787
5.772
5.759
5.744
5.723
3.014
3.007
2.413
2.037
2.023
1.979
1.860
1.846
1.443
0.536

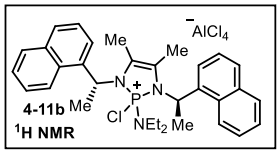
4-11b
1H NMR
AlCl4
Me
Me
Me
Cl
NEt2
Me

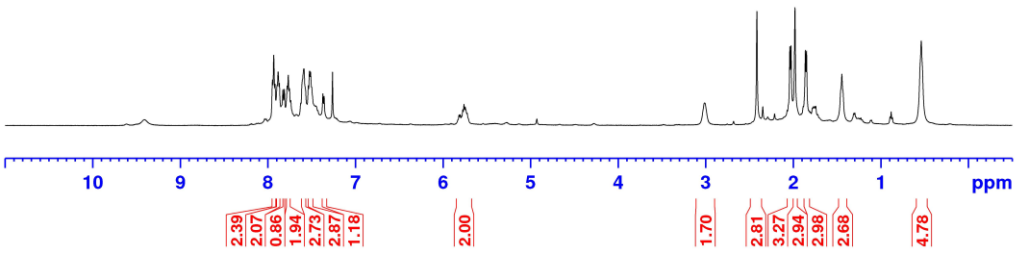
10
9
8
7
6
5
4
3
2
1
ppm
2.39
2.07
0.86
1.94
2.73
2.87
1.18
2.00
1.70
2.81
3.27
2.94
2.98
2.68
4.78

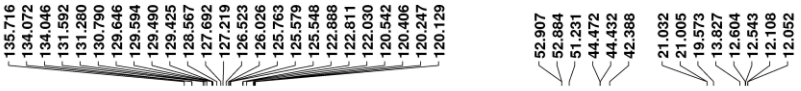
135.716
134.072
134.046
131.592
131.280
130.790
129.646
129.594
129.490
129.425
128.567
127.692
127.219
126.523
126.026
125.763
125.579
125.548
122.888
122.811
122.030
120.542
120.406
120.247
120.129
52.907
52.884
51.231
44.472
44.432
42.388
21.032
21.005
19.573
13.827
12.604
12.543
12.108
12.052

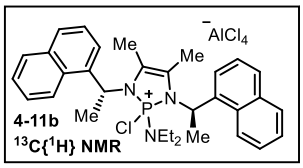
Me
Me
AlCl4
Me
N
P
N
Cl
NEt2
Me
4-11b
13C{1H} NMR

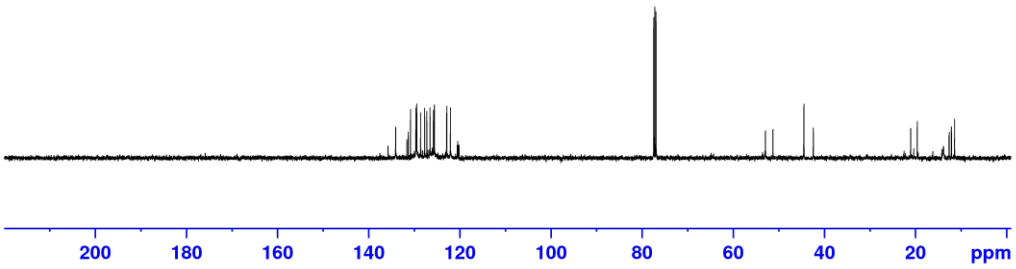
200
180
160
140
120
100
80
60
40
20
ppm


32.422
32.347
32.273
32.202
32.128
32.054

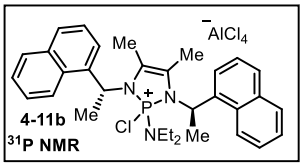
Me
Me
AlCl4
Me
N
P
N
Cl
NEt2
Me
4-11b
31P NMR

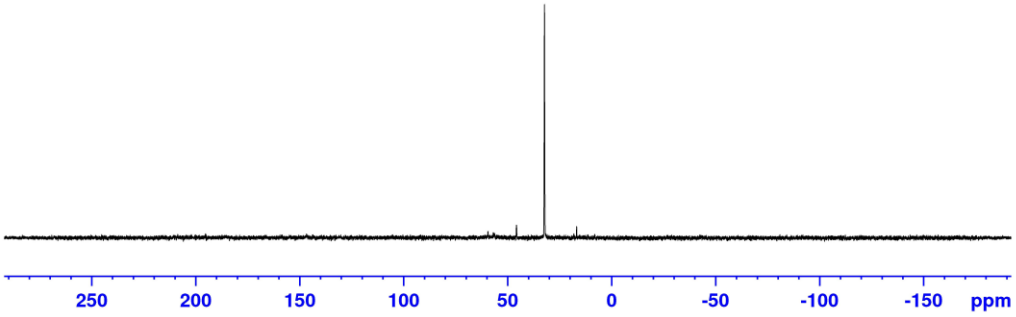
250
200
150
100
50
0
-50
-100
-150
ppm

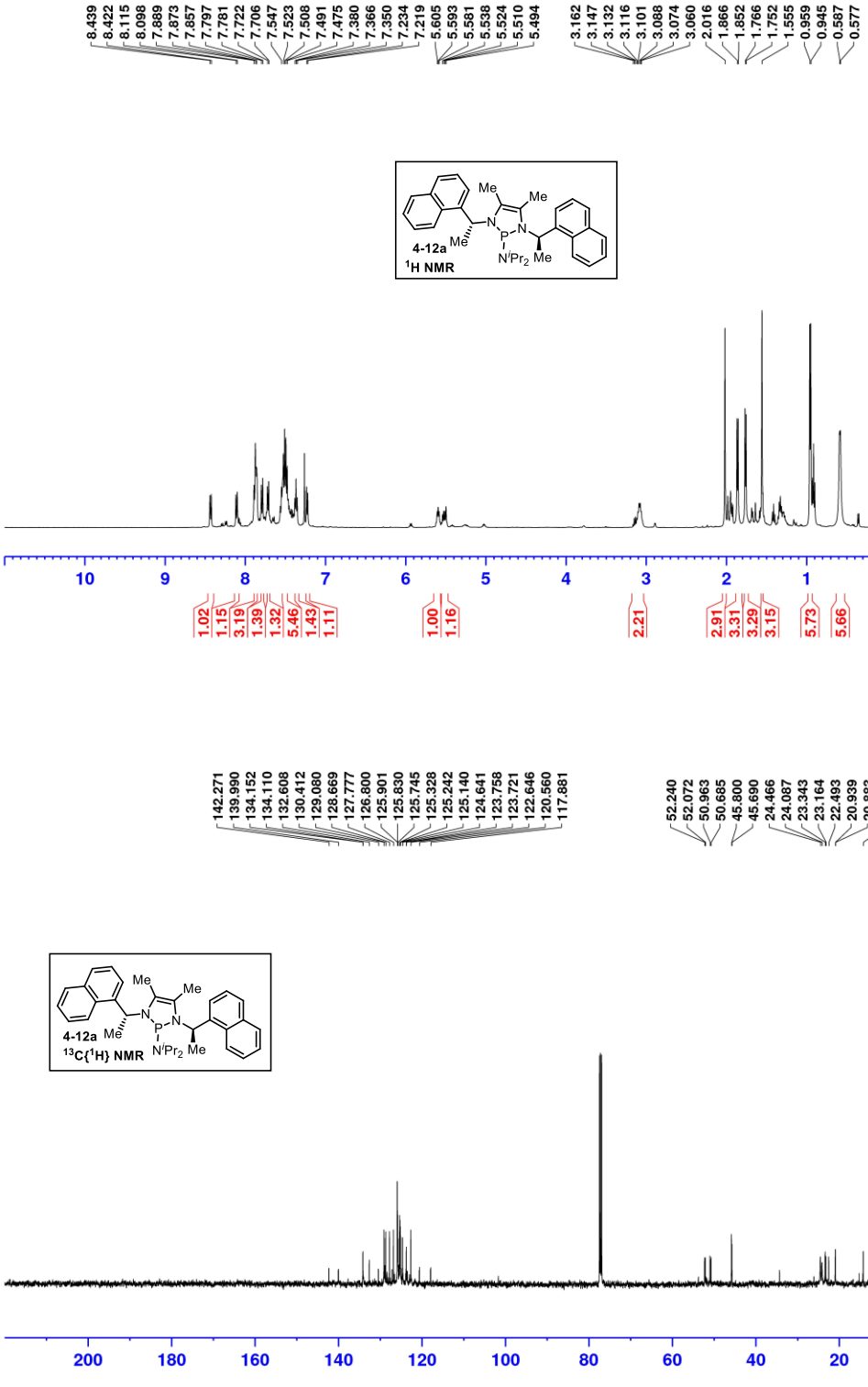
8.439
8.422
8.115
8.098
7.889
7.873
7.857
7.797
7.781
7.722
7.706
7.547
7.523
7.508
7.491
7.475
7.380
7.366
7.350
7.234
7.219
5.605
5.593
5.581
5.538
5.524
5.510
5.494
3.162
3.147
3.132
3.116
3.101
3.088
3.074
3.060
2.016
1.866
1.852
1.766
1.752
1.555
0.959
0.945
0.587
0.577
4-12a
1H NMR
Me
Me
Me
N
P
N
N^{i}Pr$_2$
Me
10
9
8
7
6
5
4
3
2
1
ppm
1.02
1.15
3.19
1.39
1.32
5.46
1.43
1.11
1.00
1.16
2.21
2.91
3.31
3.29
3.15
5.73
5.66
142.271
139.990
134.152
134.110
132.608
130.412
129.080
128.669
127.777
126.800
125.901
125.830
125.745
125.328
125.242
125.140
124.641
123.758
123.721
122.646
120.560
117.881
52.240
52.072
50.963
50.685
45.800
45.690
24.466
24.087
23.343
23.164
22.493
20.939
20.883
14.210
12.189
11.808
4-12a
13C{1H} NMR
200
180
160
140
120
100
80
60
40
20
ppm

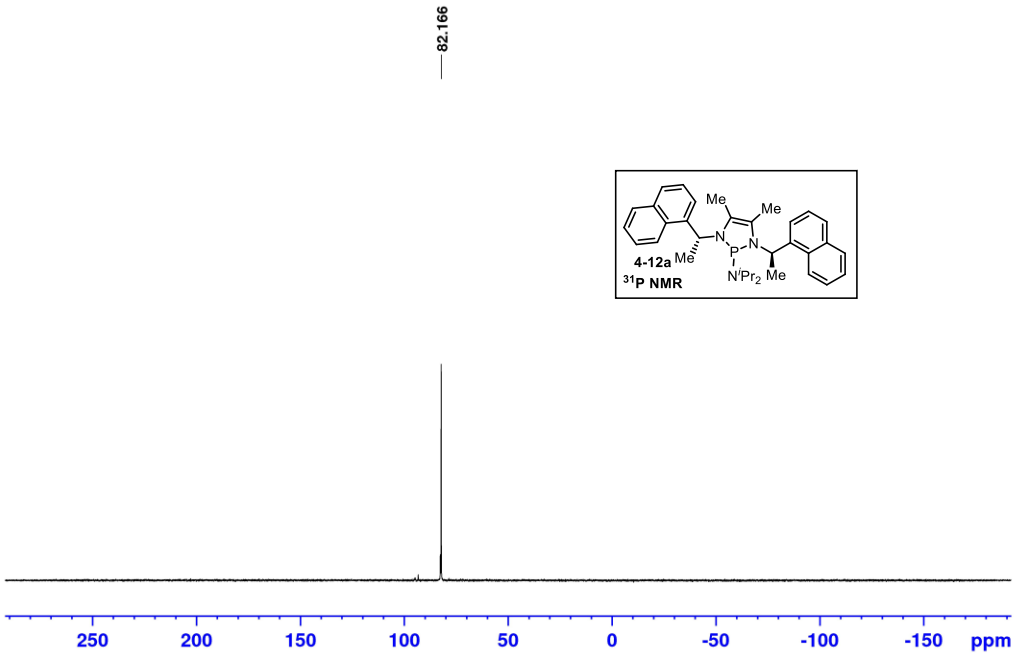
82.166
4-12a
31P NMR
250
200
150
100
50
0
-50
-100
-150
ppm

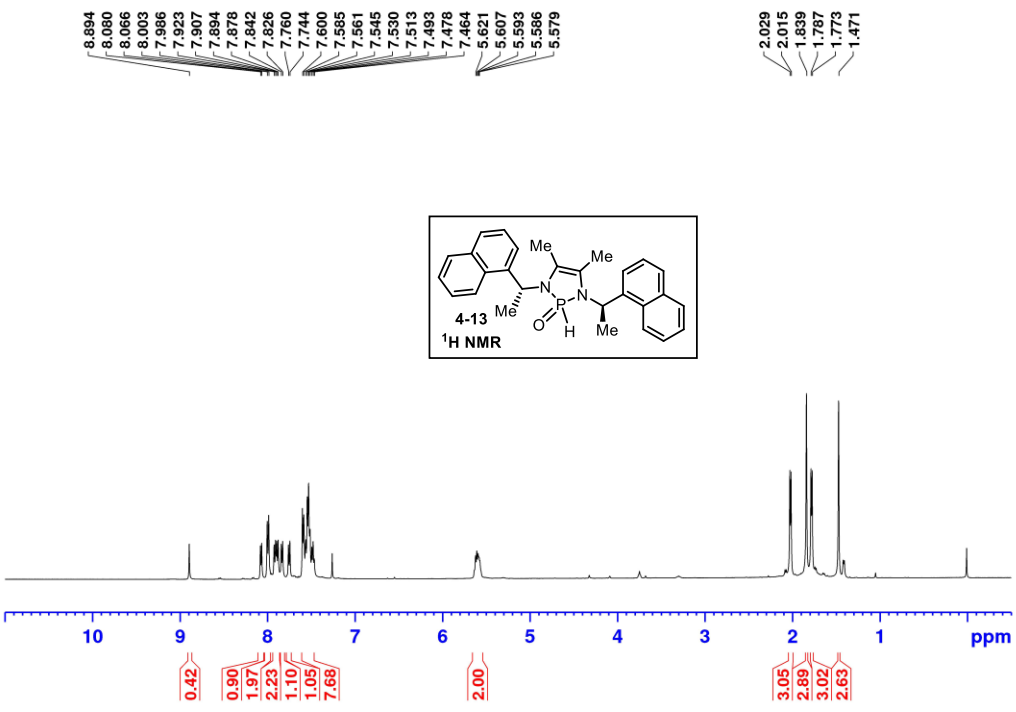
8.894
8.080
8.066
8.003
7.986
7.923
7.907
7.894
7.878
7.842
7.826
7.760
7.744
7.600
7.585
7.561
7.545
7.530
7.513
7.493
7.478
7.464
5.621
5.607
5.593
5.586
5.579
2.029
2.015
1.839
1.787
1.773
1.471
4-13
1H NMR
10
9
8
7
6
5
4
3
2
1
ppm
0.42
0.90
1.97
2.23
1.10
1.05
7.68
2.00
3.05
2.89
3.02
2.63

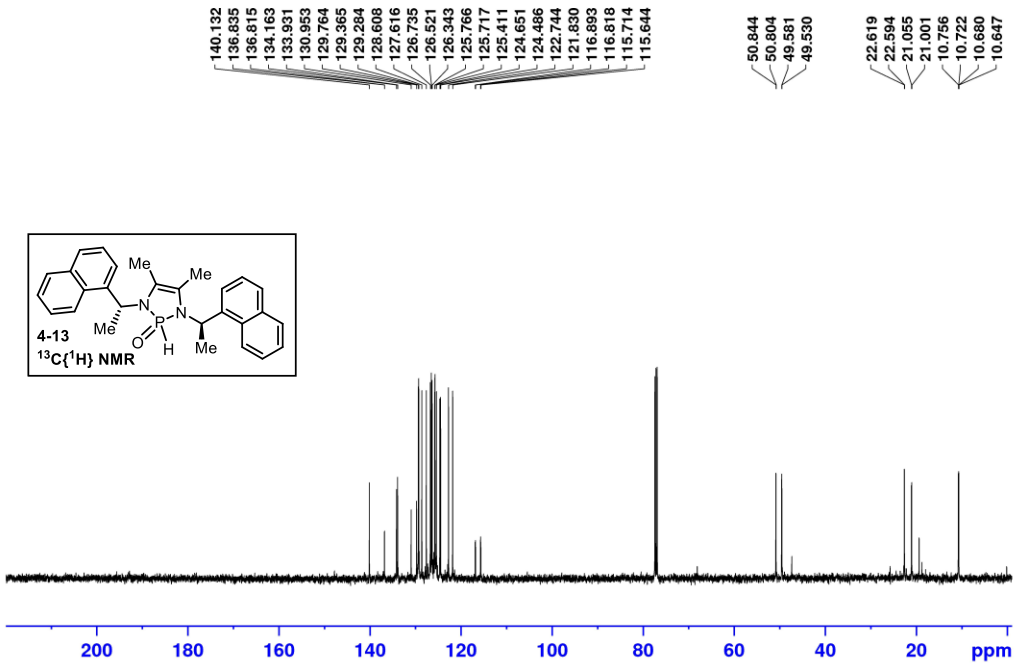
140.132
136.835
136.815
134.163
133.931
130.953
129.764
129.365
129.284
128.608
127.616
126.735
126.521
126.343
125.766
125.717
125.411
124.651
124.486
122.744
121.830
116.893
116.818
115.714
115.644
50.844
50.804
49.581
49.530
22.619
22.594
21.055
21.001
10.756
10.722
10.680
10.647
Me
Me
Me
Me
N
P
N
O
H
4-13
13C{1H} NMR
200
180
160
140
120
100
80
60
40
20
ppm

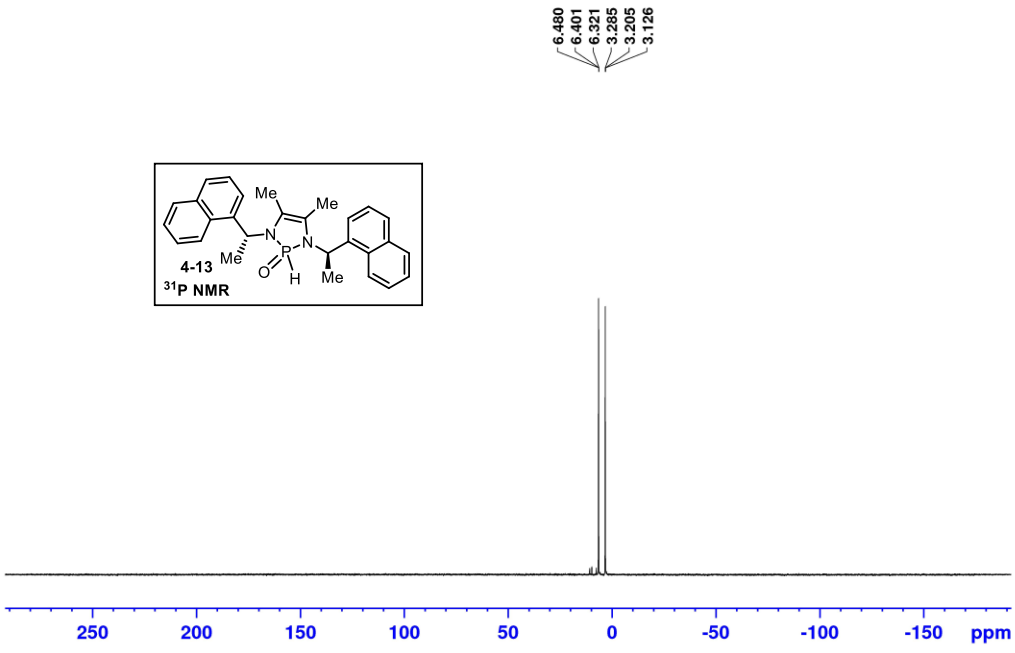
6.480
6.401
6.321
3.285
3.205
3.126
Me
Me
Me
Me
N
P
N
O
H
4-13
31P NMR
250
200
150
100
50
0
-50
-100
-150
ppm

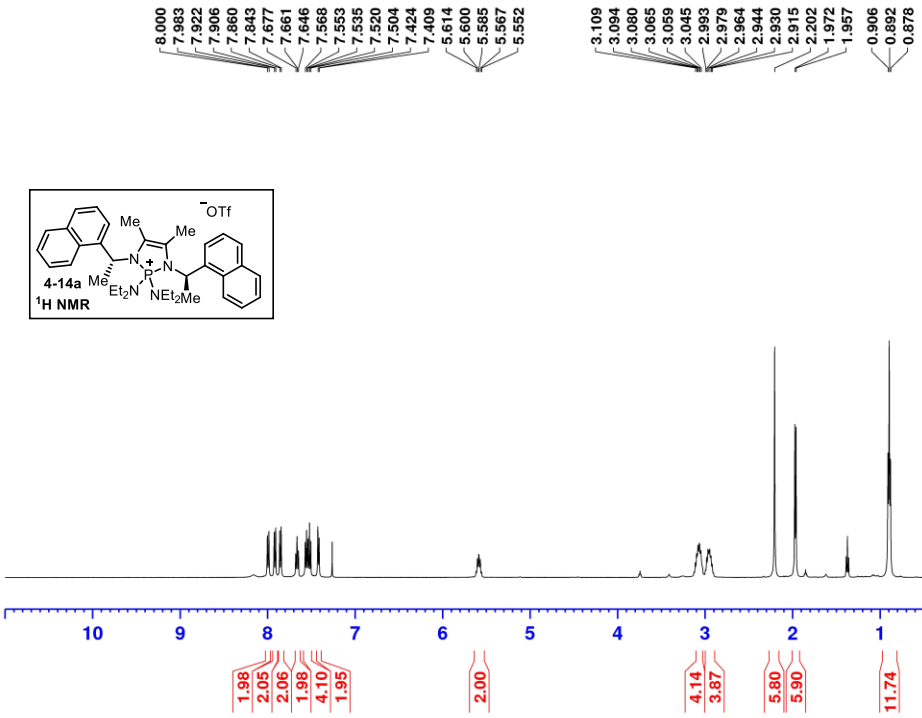
8.000
7.983
7.922
7.906
7.860
7.843
7.677
7.661
7.646
7.568
7.553
7.535
7.520
7.504
7.424
7.409
5.614
5.600
5.585
5.567
5.552
3.109
3.094
3.080
3.065
3.059
3.045
2.993
2.979
2.964
2.944
2.930
2.915
2.202
1.972
1.957
0.906
0.892
0.878
OTf
Me
Me
4-14a
Me
Et2N
NEt2Me
1H NMR
10
9
8
7
6
5
4
3
2
1
ppm
1.98
2.05
2.06
1.98
4.10
1.95
2.00
4.14
3.87
5.80
5.90
11.74

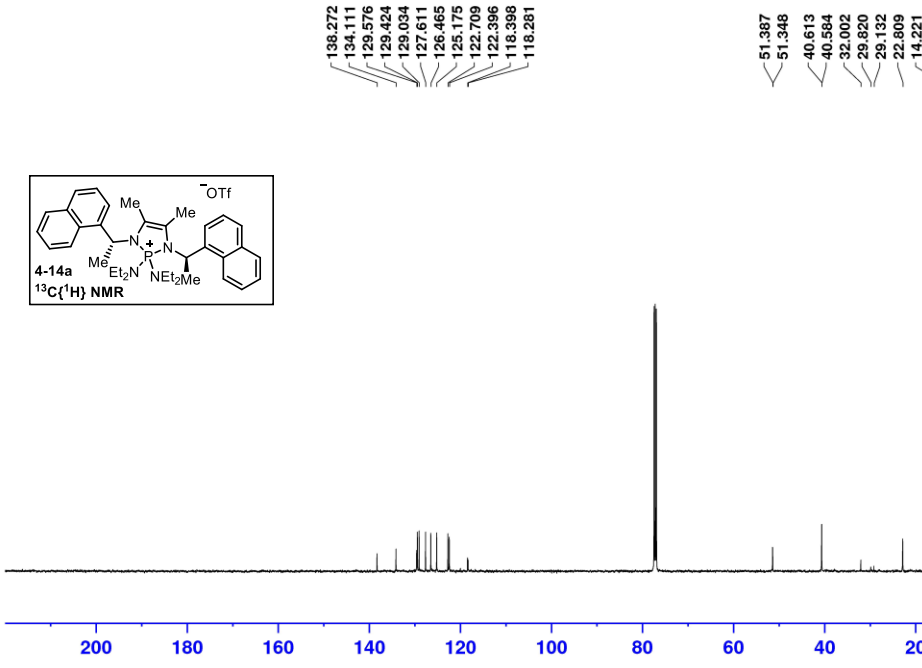
138.272
134.111
129.576
129.424
129.034
127.611
126.465
125.175
122.709
122.396
118.398
118.281
51.387
51.348
40.613
40.584
32.002
29.820
29.132
22.809
14.221
14.119
14.064
13.078
13.048
OTf
Me
Me
4-14a
Me
Et2N
NEt2Me
13C{1H} NMR
200
180
160
140
120
100
80
60
40
20
ppm

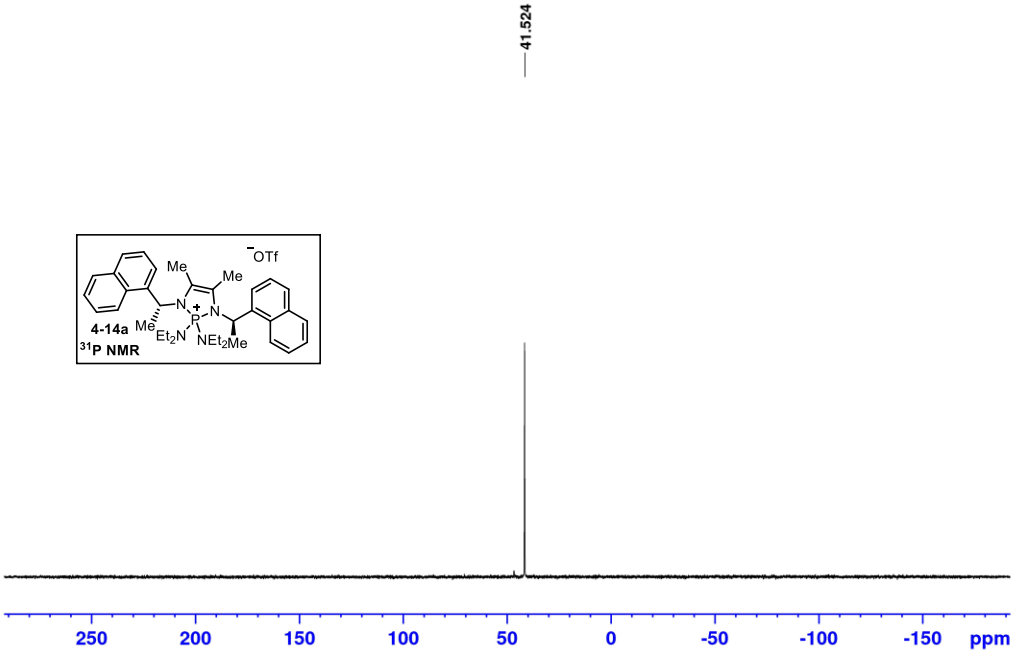
41.524
4-14a
31P NMR
OTf
Me
Me
Et2N
NEt2Me
250
200
150
100
50
0
-50
-100
-150
ppm

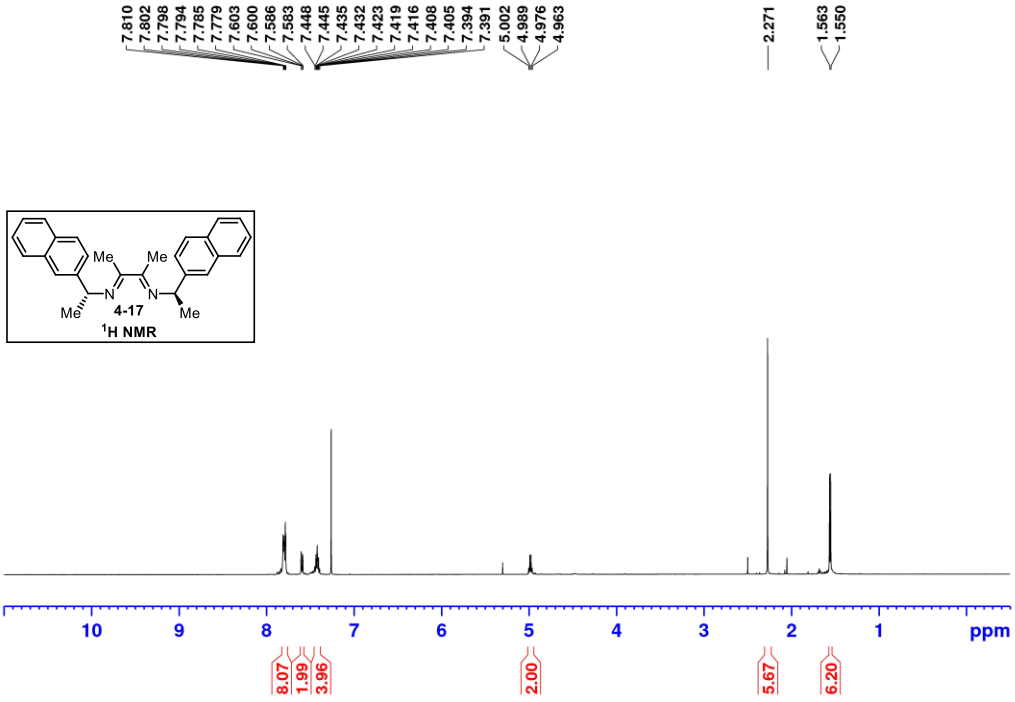
7.810
7.802
7.798
7.794
7.785
7.779
7.603
7.600
7.586
7.583
7.448
7.445
7.435
7.432
7.423
7.419
7.416
7.408
7.405
7.394
7.391
5.002
4.989
4.976
4.963
2.271
1.563
1.550
4-17
1H NMR
Me
Me
Me
Me
10
9
8
7
6
5
4
3
2
1
ppm
8.07
1.99
3.96
2.00
5.67
6.20

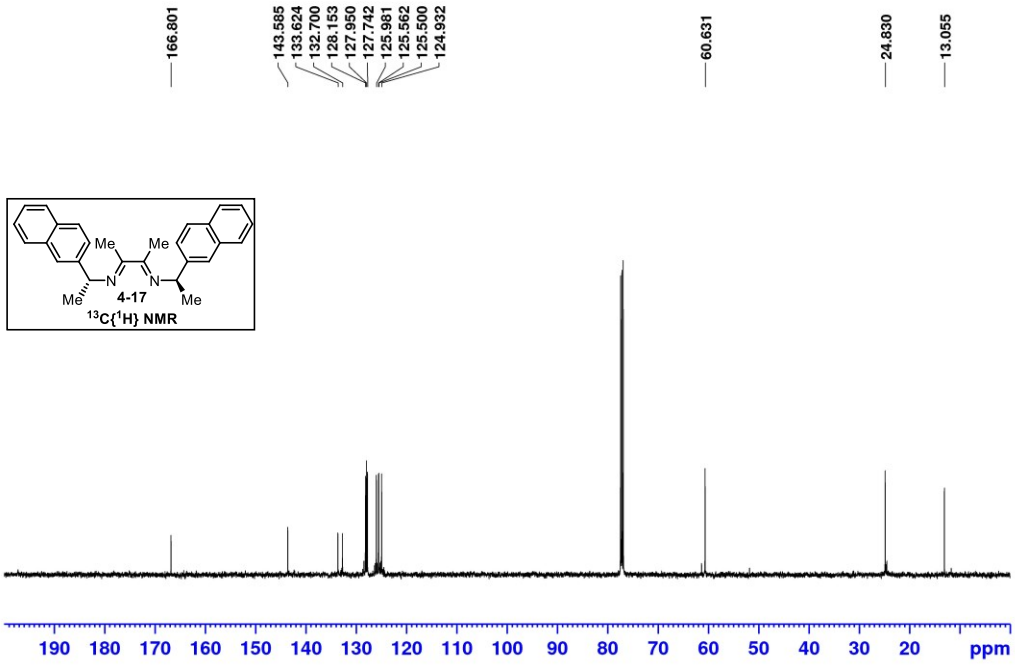
166.801
143.585
133.624
132.700
128.153
127.950
127.742
125.981
125.562
125.500
124.932
60.631
24.830
13.055
Me
Me
N
N
Me
Me
4-17
13C{1H} NMR
190 180 170 160 150 140 130 120 110 100 90 80 70 60 50 40 30 20 ppm

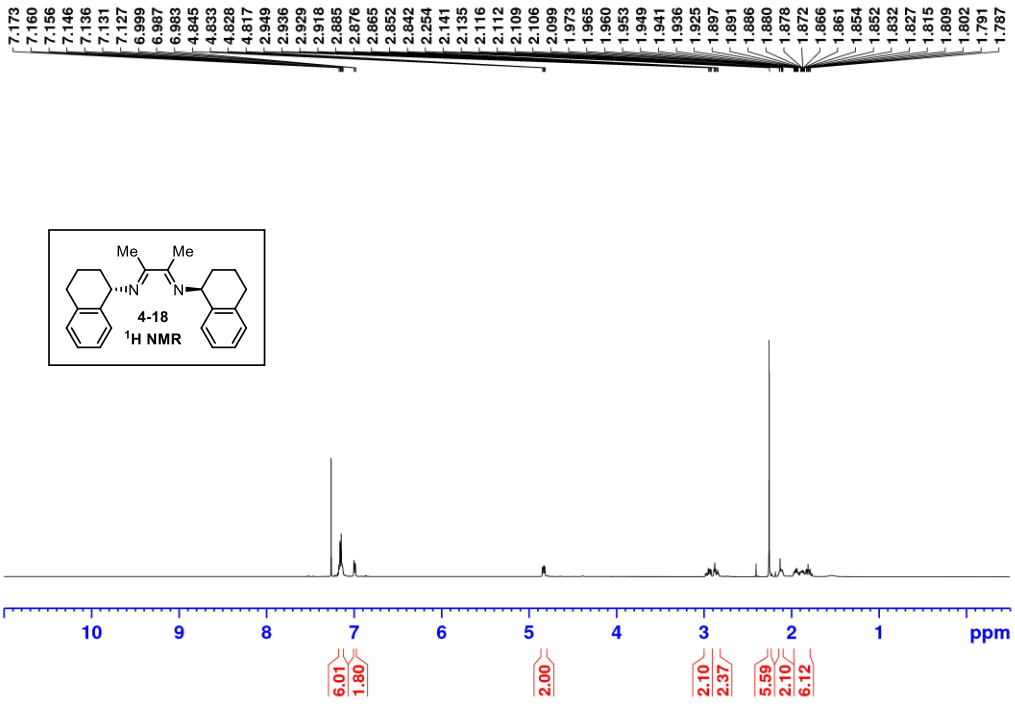
7.173
7.160
7.156
7.146
7.136
7.131
7.127
6.999
6.987
6.983
4.845
4.833
4.828
4.817
2.949
2.936
2.929
2.918
2.885
2.876
2.865
2.852
2.842
2.254
2.141
2.135
2.116
2.112
2.109
2.106
2.099
1.973
1.965
1.960
1.953
1.949
1.941
1.936
1.925
1.897
1.891
1.886
1.880
1.878
1.872
1.866
1.861
1.854
1.852
1.832
1.827
1.815
1.809
1.802
1.791
1.787
Me
Me
N
N
4-18
1H NMR
10 9 8 7 6 5 4 3 2 1 ppm
6.01
1.80
2.00
2.10
2.37
5.59
2.10
6.12

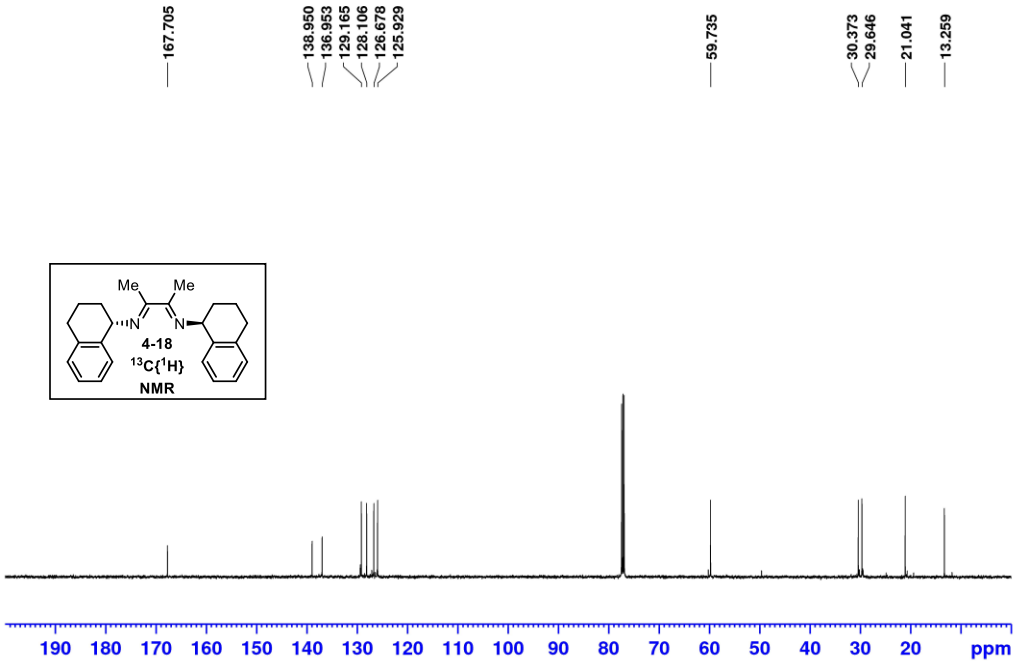
167.705
138.950
136.953
129.165
128.106
126.678
125.929
59.735
30.373
29.646
21.041
13.259
Me
Me
N
N
4-18
13C{1H}
NMR
190 180 170 160 150 140 130 120 110 100 90 80 70 60 50 40 30 20 ppm

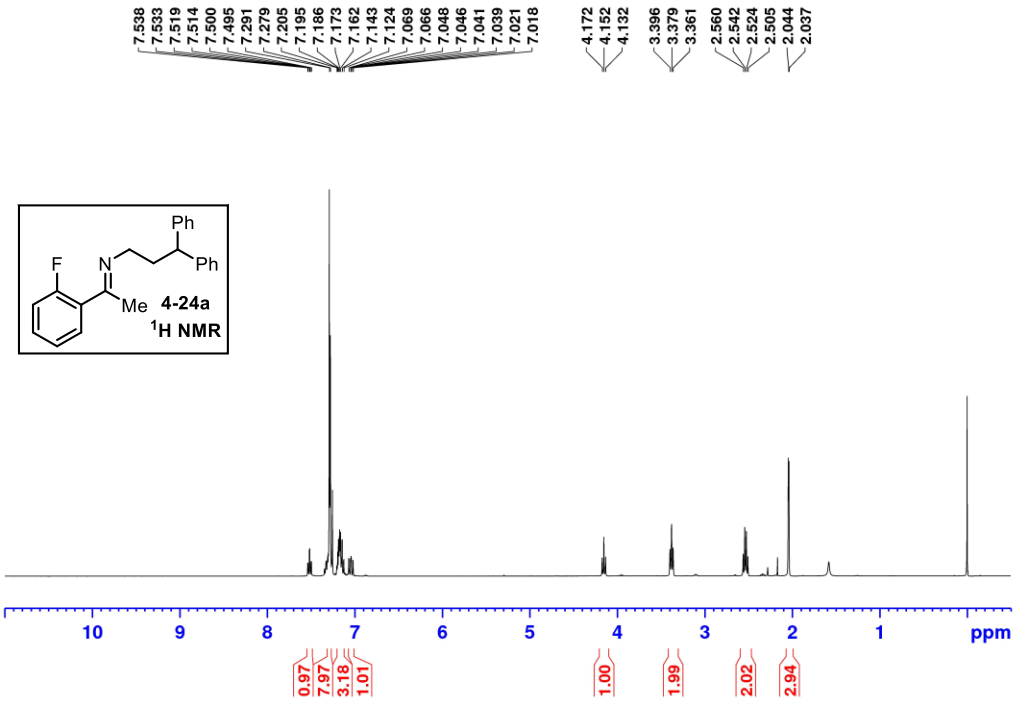
7.538
7.533
7.519
7.514
7.500
7.495
7.291
7.279
7.205
7.195
7.186
7.173
7.162
7.143
7.124
7.069
7.066
7.048
7.046
7.041
7.039
7.021
7.018
4.172
4.152
4.132
3.396
3.379
3.361
2.560
2.542
2.524
2.505
2.044
2.037
Ph
Ph
F
N
Me
4-24a
1H NMR
10 9 8 7 6 5 4 3 2 1 ppm
0.97
7.97
3.18
1.01
1.00
1.99
2.02
2.94

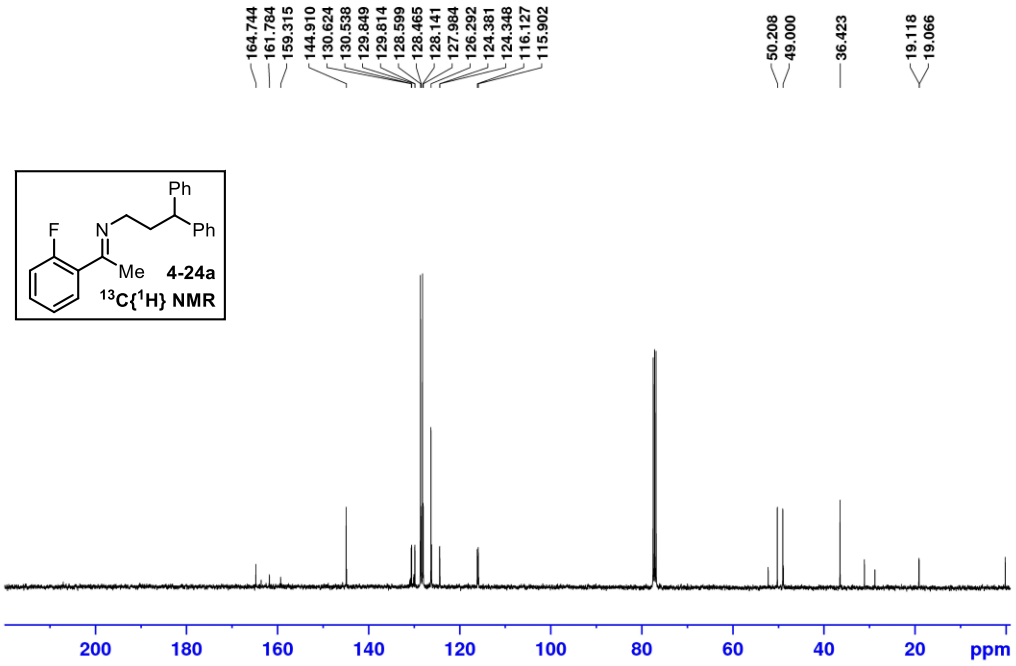
164.744
161.784
159.315
144.910
130.624
130.538
129.849
129.814
128.599
128.465
128.141
127.984
126.292
124.381
124.348
116.127
115.902
50.208
49.000
36.423
19.118
19.066
Ph
F
N
Ph
Me
4-24a
13C{1H} NMR
200
180
160
140
120
100
80
60
40
20
ppm

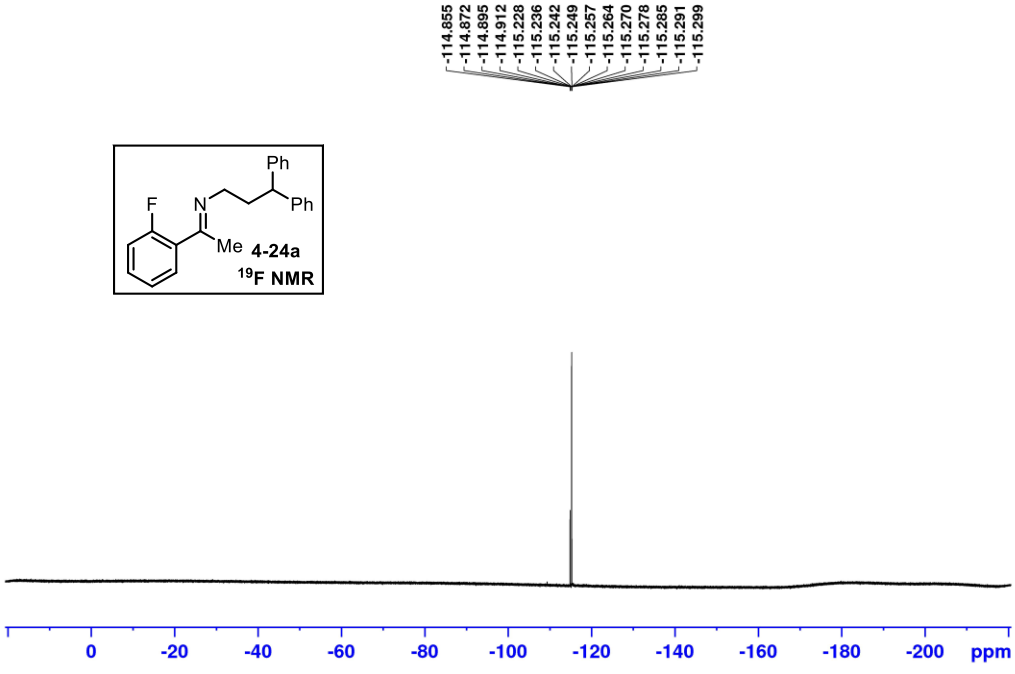
-114.855
-114.872
-114.895
-114.912
-115.228
-115.236
-115.242
-115.249
-115.257
-115.264
-115.270
-115.278
-115.285
-115.291
-115.299
Ph
F
N
Ph
Me
4-24a
19F NMR
0
-20
-40
-60
-80
-100
-120
-140
-160
-180
-200
ppm

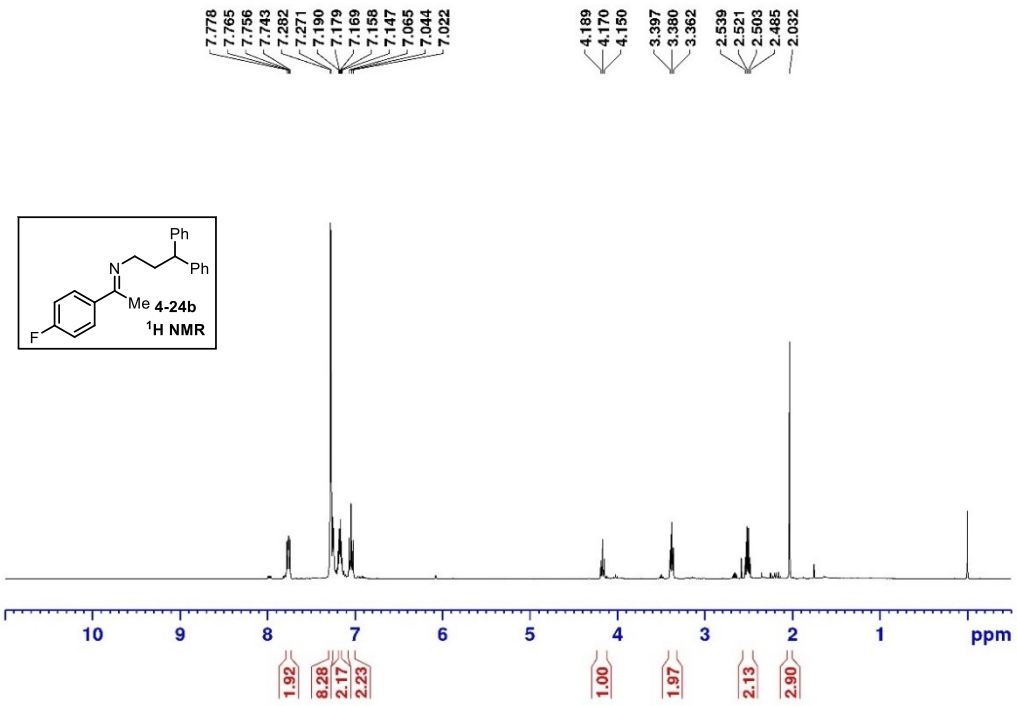
7.778
7.765
7.756
7.743
7.282
7.271
7.190
7.179
7.169
7.158
7.147
7.065
7.044
7.022
4.189
4.170
4.150
3.397
3.380
3.362
2.539
2.521
2.503
2.485
2.032
Ph
Ph
N
Me
F
4-24b
1H NMR
10
9
8
7
6
5
4
3
2
1
ppm
1.92
8.28
2.17
2.23
1.00
1.97
2.13
2.90

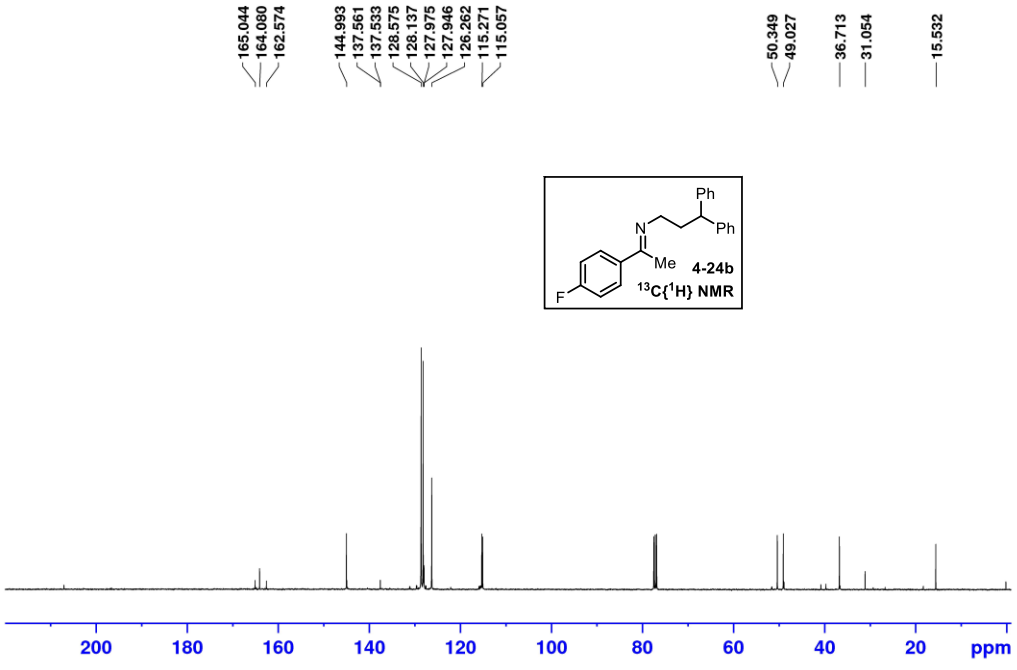
165.044
164.080
162.574
144.993
137.561
137.533
128.575
128.137
127.975
127.946
126.262
115.271
115.057
50.349
49.027
36.713
31.054
15.532
Ph
Ph
N
Me
F
4-24b
13C{1H} NMR
200
180
160
140
120
100
80
60
40
20
ppm

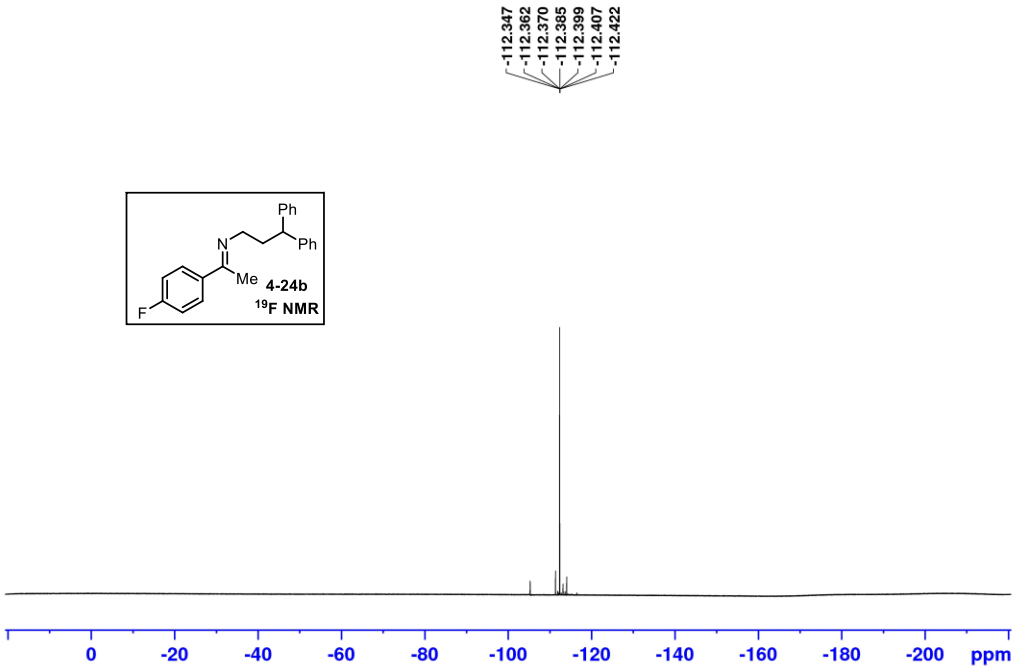
-112.347
-112.362
-112.370
-112.385
-112.399
-112.407
-112.422
Ph
N
Ph
Me
4-24b
19F NMR
F
0
-20
-40
-60
-80
-100
-120
-140
-160
-180
-200
ppm

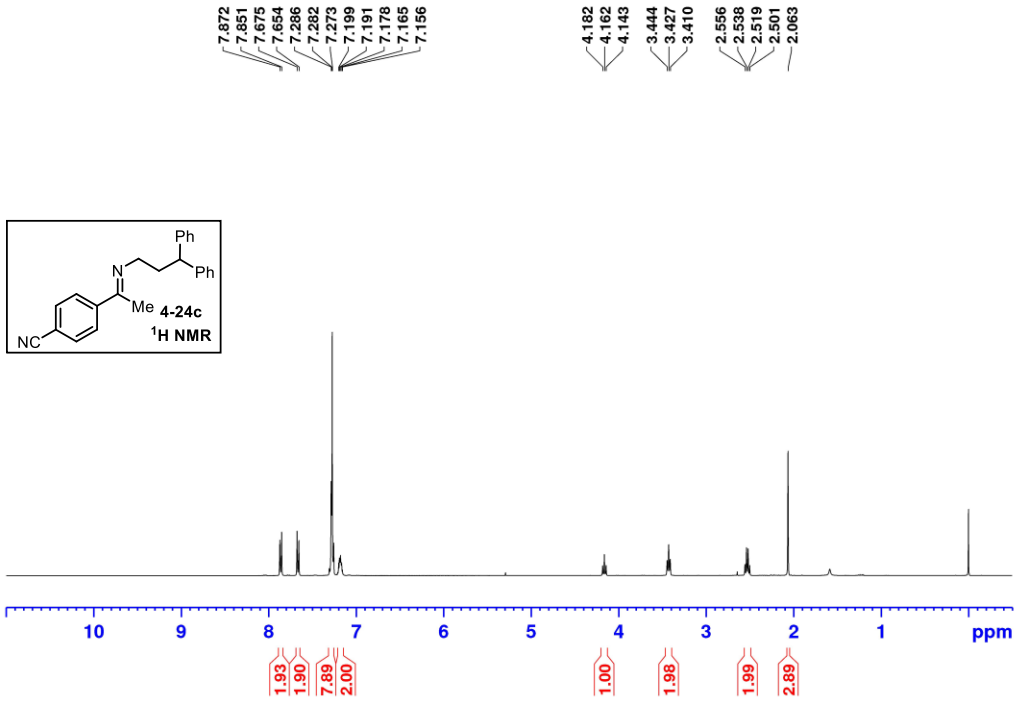
7.872
7.851
7.675
7.654
7.286
7.282
7.273
7.199
7.191
7.178
7.165
7.156
4.182
4.162
4.143
3.444
3.427
3.410
2.556
2.538
2.519
2.501
2.063
Ph
N
Ph
Me
4-24c
1H NMR
NC
10
9
8
7
6
5
4
3
2
1
ppm
1.93
1.90
7.89
2.00
1.00
1.98
1.99
2.89

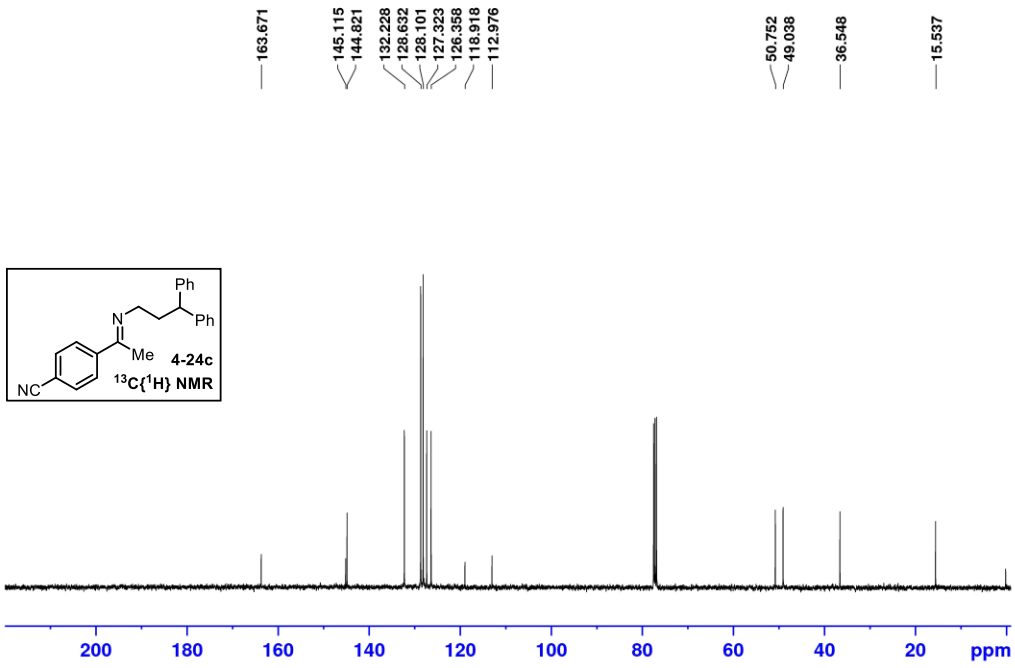
163.671
145.115
144.821
132.228
128.632
128.101
127.323
126.358
118.918
112.976
50.752
49.038
36.548
15.537
Ph
N
Ph
Me
NC
4-24c
13C{1H} NMR
200
180
160
140
120
100
80
60
40
20
ppm

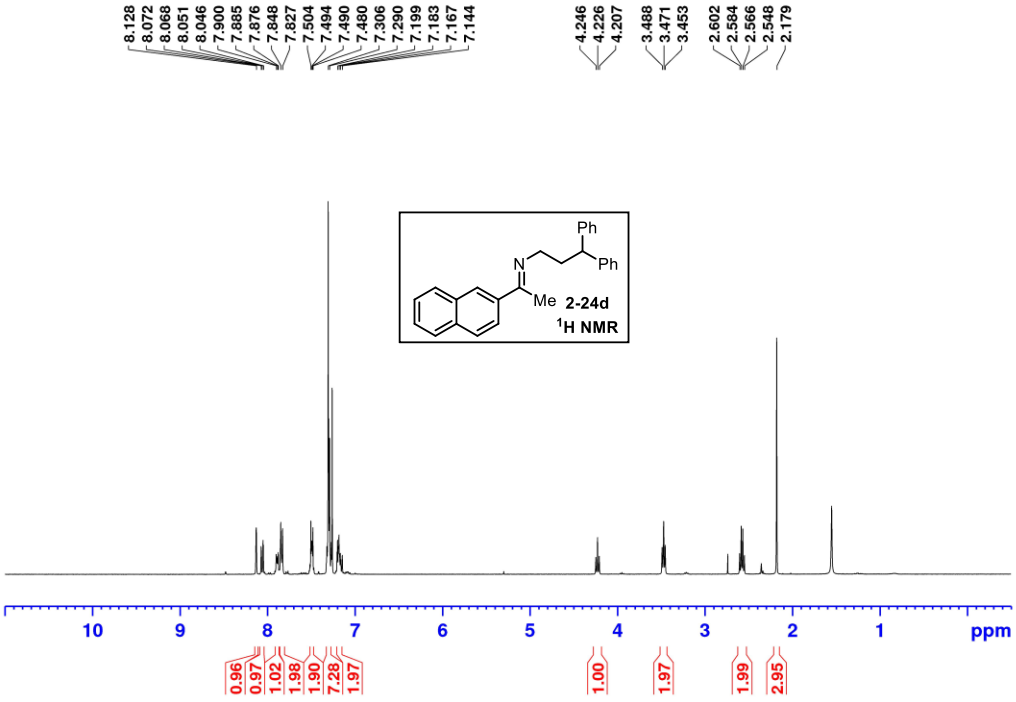
8.128
8.072
8.068
8.051
8.046
7.900
7.885
7.876
7.848
7.827
7.504
7.494
7.490
7.480
7.306
7.290
7.199
7.183
7.167
7.144
4.246
4.226
4.207
3.488
3.471
3.453
2.602
2.584
2.566
2.548
2.179
Ph
N
Ph
Me
2-24d
1H NMR
10
9
8
7
6
5
4
3
2
1
ppm
0.96
0.97
1.02
1.98
1.90
7.28
1.97
1.00
1.97
1.99
2.95

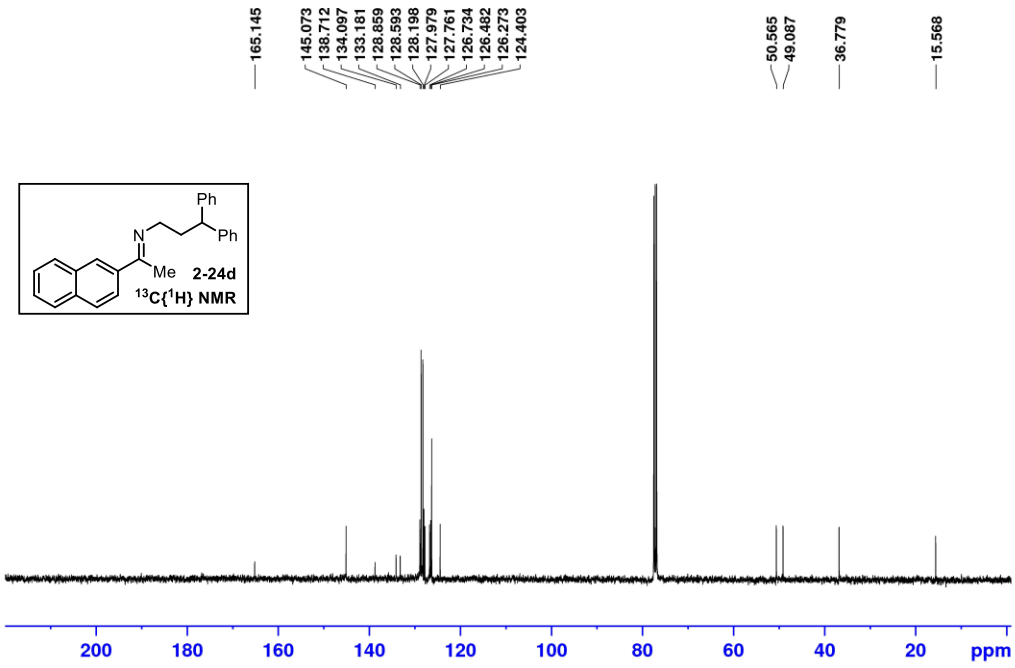
165.145
145.073
138.712
134.097
133.181
128.859
128.593
128.198
127.979
127.761
126.734
126.482
126.273
124.403
50.565
49.087
36.779
15.568
Ph
N
Ph
Me
2-24d
13C{1H} NMR
200
180
160
140
120
100
80
60
40
20
ppm

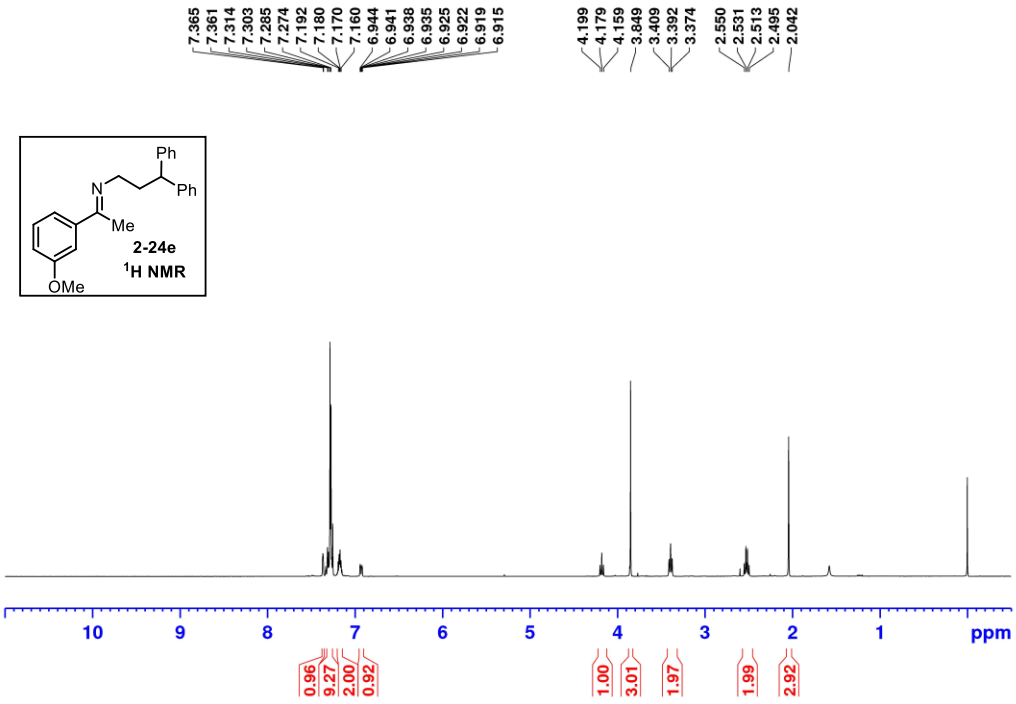
7.365
7.361
7.314
7.303
7.285
7.274
7.192
7.180
7.170
7.160
6.944
6.941
6.938
6.935
6.925
6.922
6.919
6.915
4.199
4.179
4.159
3.849
3.409
3.392
3.374
2.550
2.531
2.513
2.495
2.042
Ph
N
Ph
Me
OMe
2-24e
1H NMR
10
9
8
7
6
5
4
3
2
1
ppm
0.96
9.27
2.00
0.92
1.00
3.01
1.97
1.99
2.92

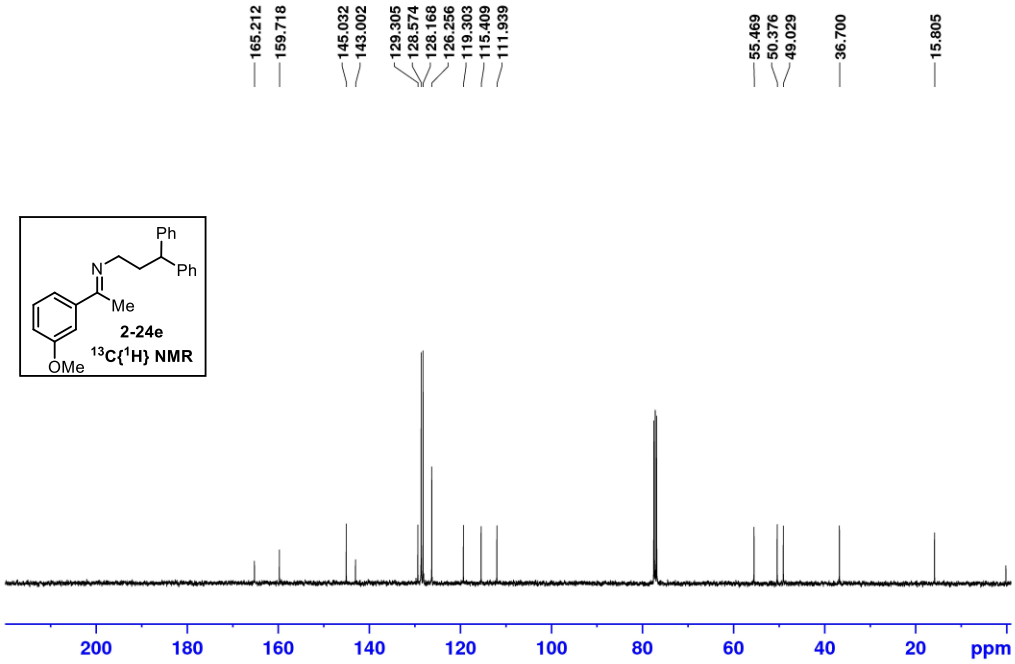
165.212
159.718
145.032
143.002
129.305
128.574
128.168
126.256
119.303
115.409
111.939
55.469
50.376
49.029
36.700
15.805
Ph
N
Ph
Me
OMe
2-24e
13C{1H} NMR
200
180
160
140
120
100
80
60
40
20
ppm

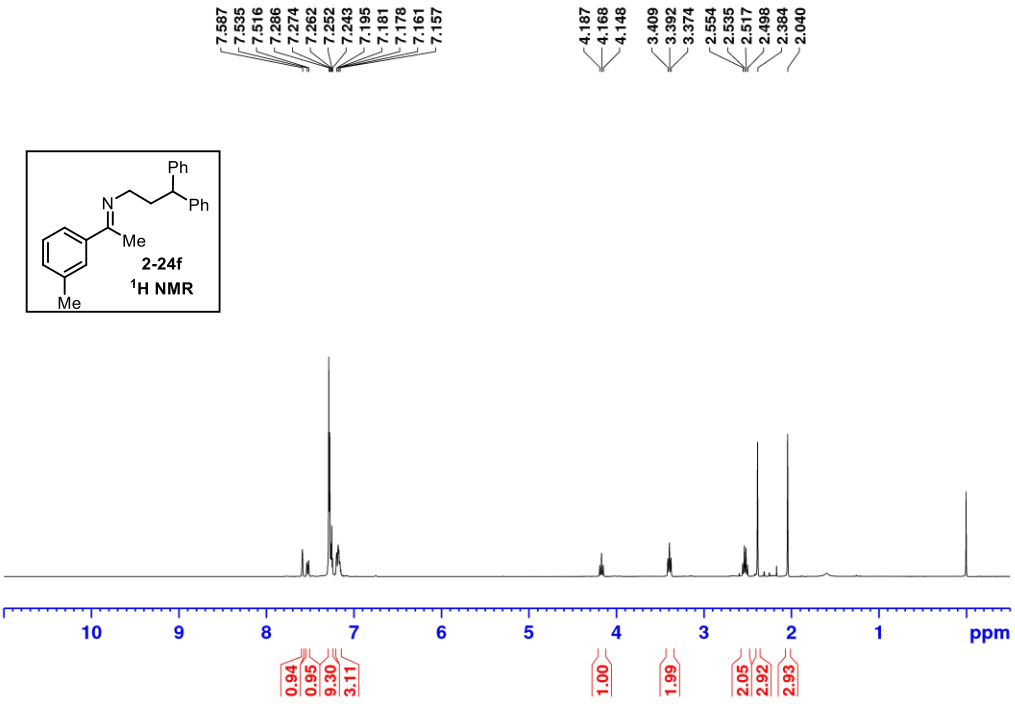
7.587
7.535
7.516
7.286
7.274
7.262
7.252
7.243
7.195
7.181
7.178
7.161
7.157
4.187
4.168
4.148
3.409
3.392
3.374
2.554
2.535
2.517
2.498
2.384
2.040
Ph
N
Ph
Me
Me
2-24f
1H NMR
10
9
8
7
6
5
4
3
2
1
ppm
0.94
0.95
9.30
3.11
1.00
1.99
2.05
2.92
2.93

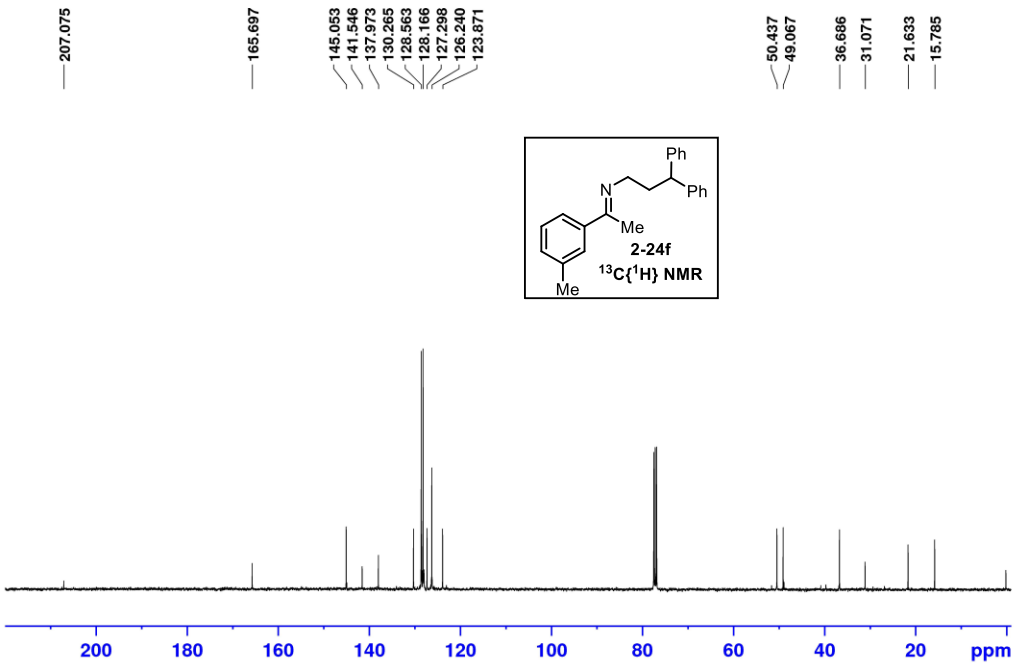
207.075
165.697
145.053
141.546
137.973
130.265
128.563
128.166
127.298
126.240
123.871
50.437
49.067
36.686
31.071
21.633
15.785
Ph
Ph
N
Me
Me
2-24f
13C{1H} NMR
200
180
160
140
120
100
80
60
40
20
ppm

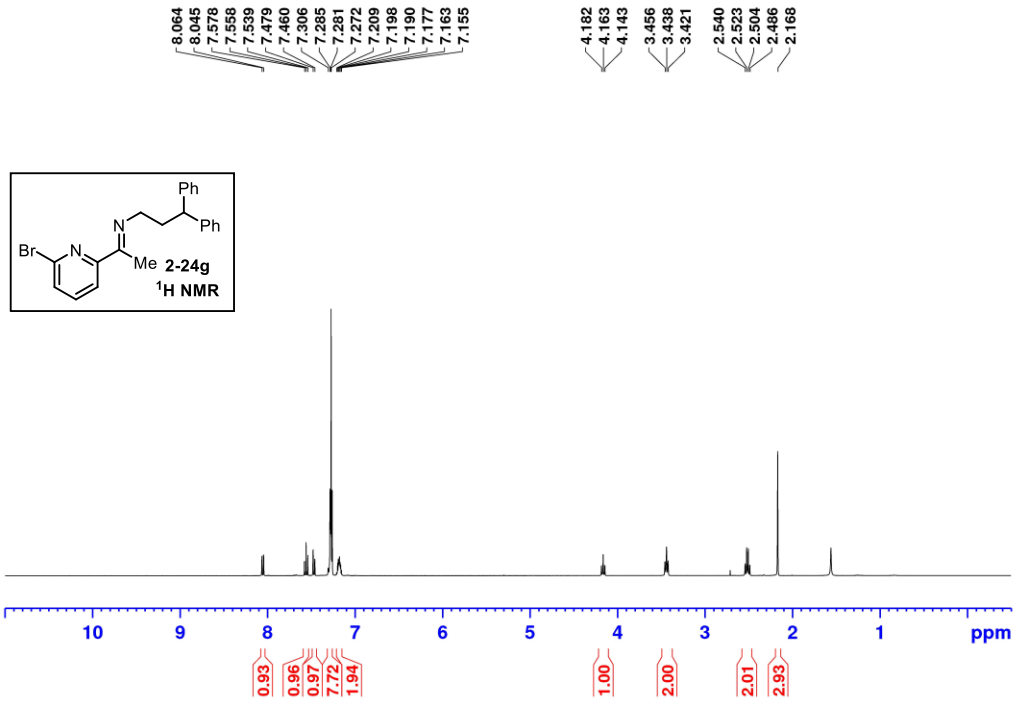
8.064
8.045
7.578
7.558
7.539
7.479
7.460
7.306
7.285
7.281
7.272
7.209
7.198
7.190
7.177
7.163
7.155
4.182
4.163
4.143
3.456
3.438
3.421
2.540
2.523
2.504
2.486
2.168
Ph
Ph
N
Br
N
Me
2-24g
1H NMR
10
9
8
7
6
5
4
3
2
1
ppm
0.93
0.96
0.97
7.72
1.94
1.00
2.00
2.01
2.93

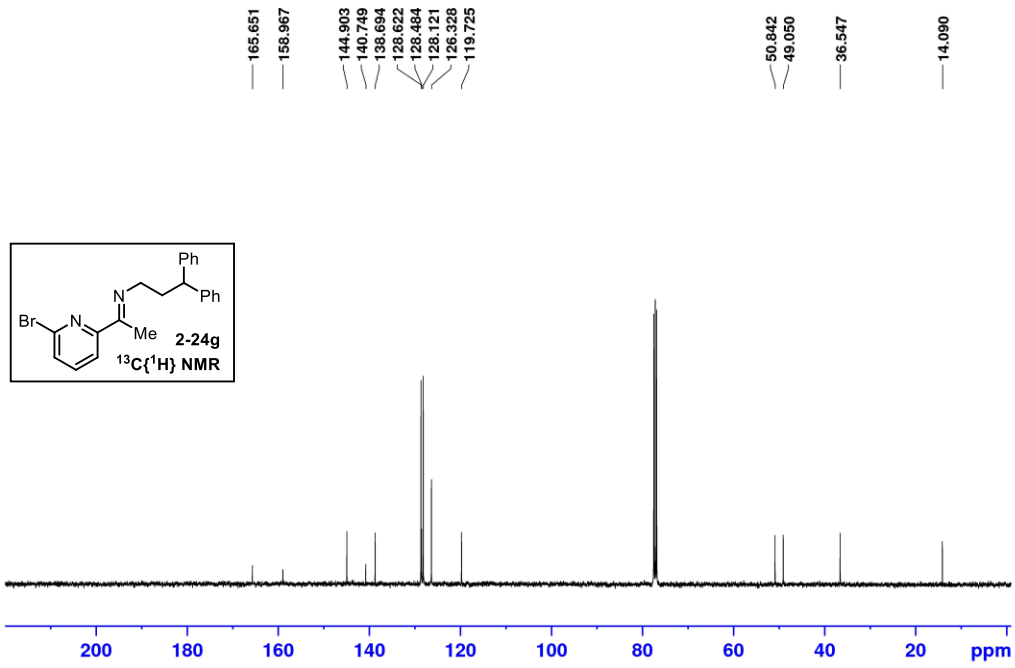
165.651
158.967
144.903
140.749
138.694
128.622
128.484
128.121
126.328
119.725
50.842
49.050
36.547
14.090
Ph
Ph
N
Br
N
Me
2-24g
13C{1H} NMR
200
180
160
140
120
100
80
60
40
20
ppm

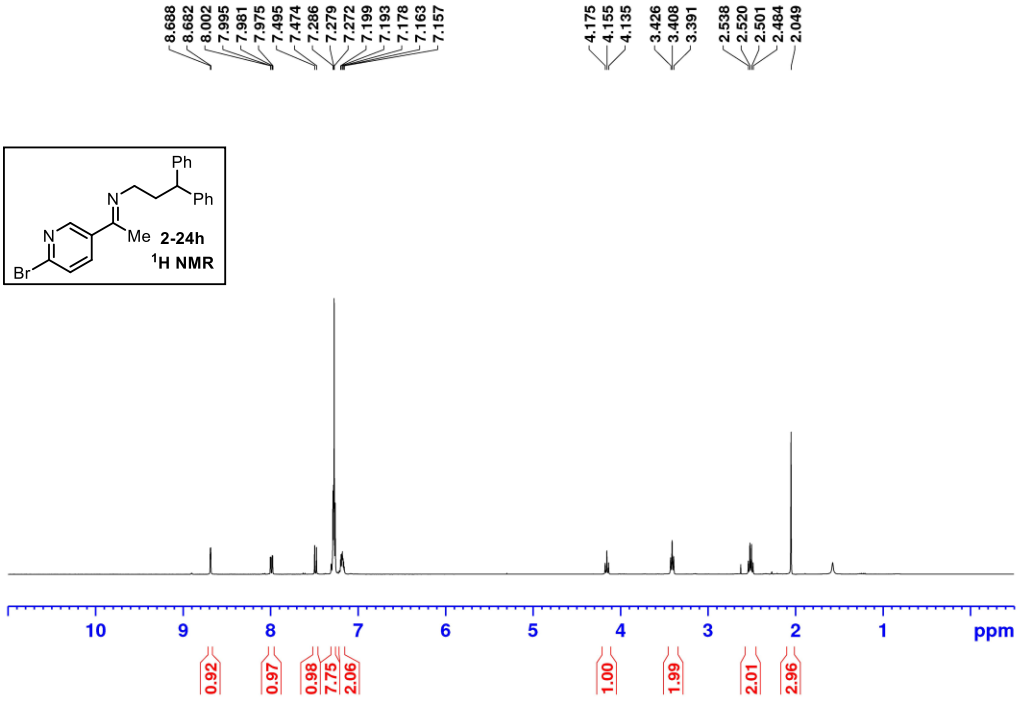
8.688
8.682
8.002
7.995
7.981
7.975
7.495
7.474
7.286
7.279
7.272
7.199
7.193
7.178
7.163
7.157
4.175
4.155
4.135
3.426
3.408
3.391
2.538
2.520
2.501
2.484
2.049
Ph
Ph
N
N
Me
2-24h
1H NMR
Br
10
9
8
7
6
5
4
3
2
1
ppm
0.92
0.97
0.98
7.75
2.06
1.00
1.99
2.01
2.96

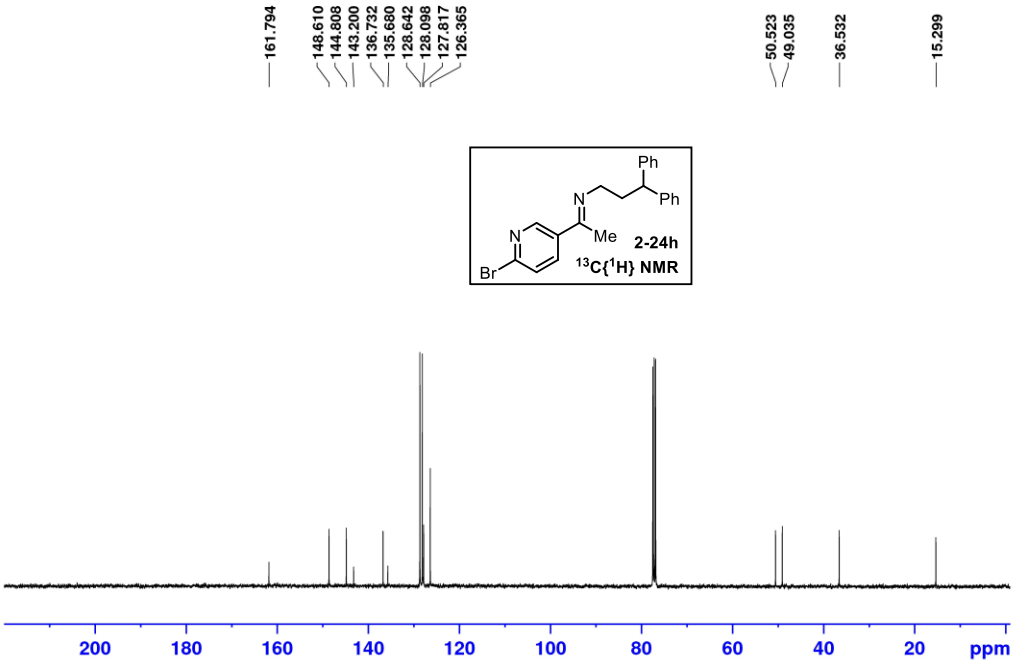
161.794
148.610
144.808
143.200
136.732
135.680
128.642
128.098
127.817
126.365
50.523
49.035
36.532
15.299
Ph
N
Ph
N
Me
2-24h
Br
13C{1H} NMR
200
180
160
140
120
100
80
60
40
20
ppm

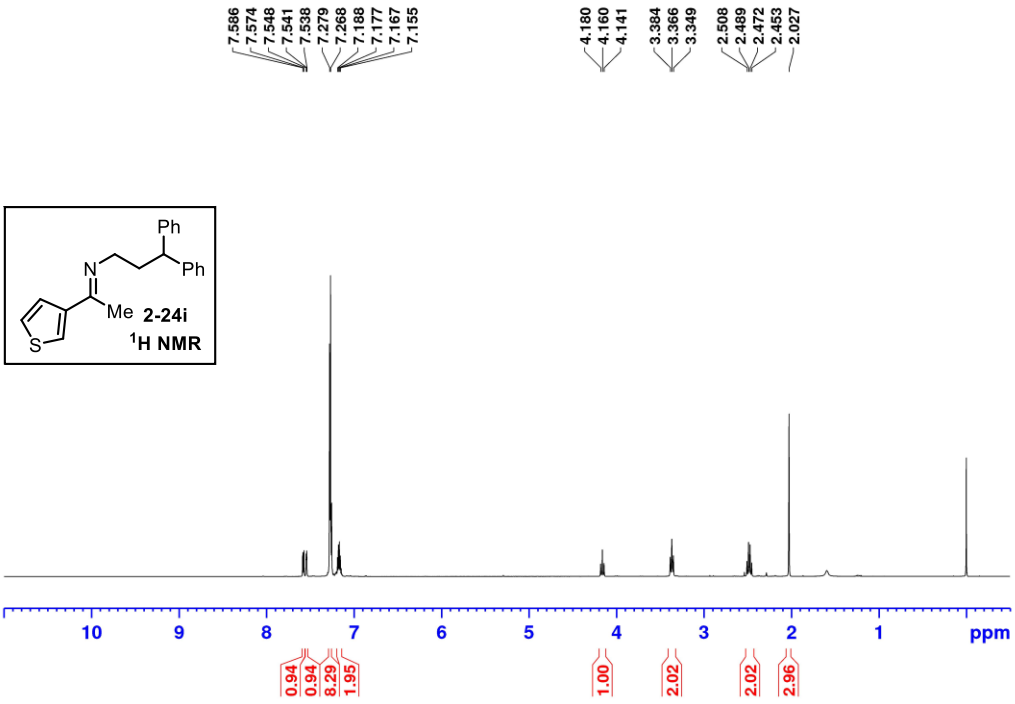
7.586
7.574
7.548
7.541
7.538
7.279
7.268
7.188
7.177
7.167
7.155
4.180
4.160
4.141
3.384
3.366
3.349
2.508
2.489
2.472
2.453
2.027
Ph
N
Ph
Me
2-24i
S
1H NMR
10
9
8
7
6
5
4
3
2
1
ppm
0.94
0.94
8.29
1.95
1.00
2.02
2.02
2.96

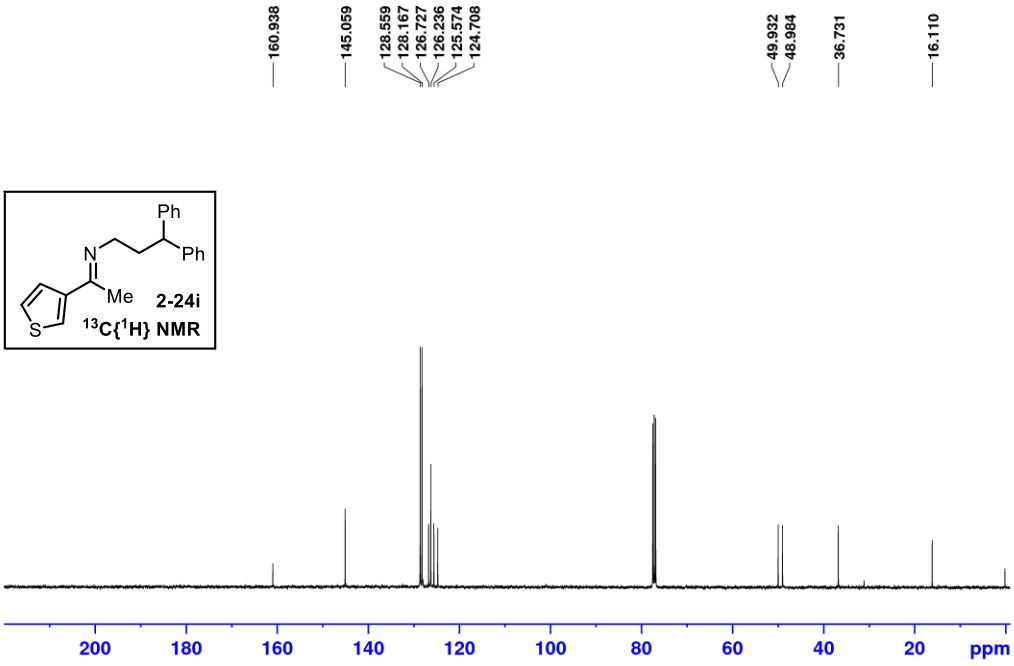
160.938
145.059
128.559
128.167
126.727
126.236
125.574
124.708
49.932
48.984
36.731
16.110
Ph
N
Ph
Me
S
2-24i
$^{13}C\{^{1}H\}$ NMR
200
180
160
140
120
100
80
60
40
20
ppm

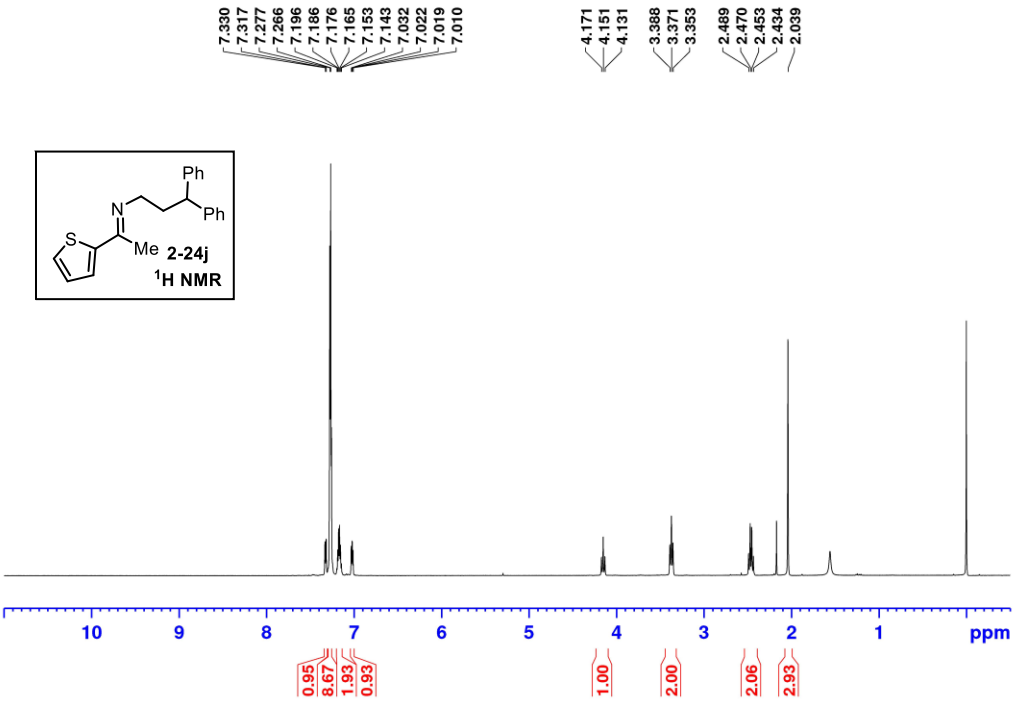
7.330
7.317
7.277
7.266
7.196
7.186
7.176
7.165
7.153
7.143
7.032
7.022
7.019
7.010
4.171
4.151
4.131
3.388
3.371
3.353
2.489
2.470
2.453
2.434
2.039
Ph
N
Ph
S
Me
2-24j
^{1}H NMR
10
9
8
7
6
5
4
3
2
1
ppm
0.95
8.67
1.93
0.93
1.00
2.00
2.06
2.93

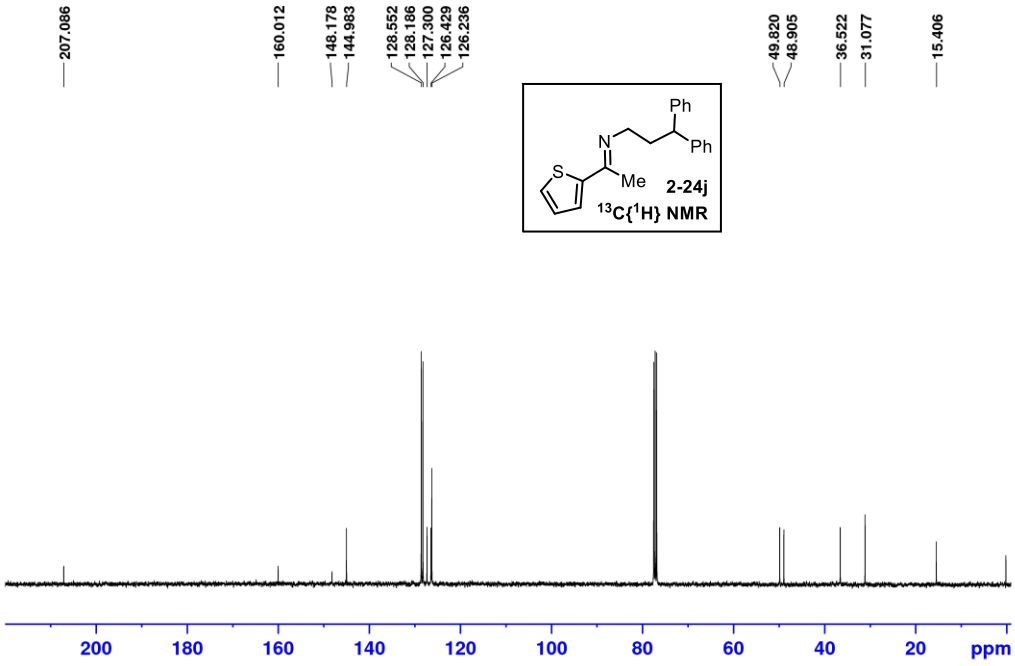
207.086
160.012
148.178
144.983
128.552
128.186
127.300
126.429
126.236
49.820
48.905
36.522
31.077
15.406
Ph
N
Ph
S
Me
2-24j
$^{13}C\{^{1}H\}$ NMR
200
180
160
140
120
100
80
60
40
20
ppm

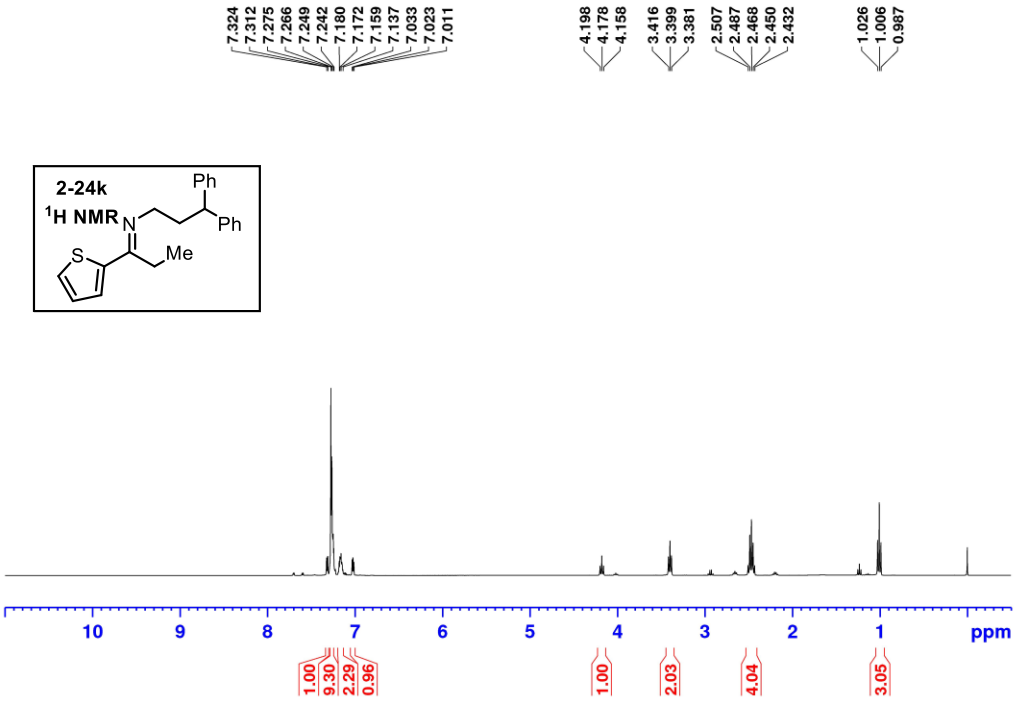
7.324
7.312
7.275
7.266
7.249
7.242
7.180
7.172
7.159
7.137
7.033
7.023
7.011
4.198
4.178
4.158
3.416
3.399
3.381
2.507
2.487
2.468
2.450
2.432
1.026
1.006
0.987
2-24k
^{1}H NMR
Ph
N
Ph
S
Me
10
9
8
7
6
5
4
3
2
1
ppm
1.00
9.30
2.29
0.96
1.00
2.03
4.04
3.05

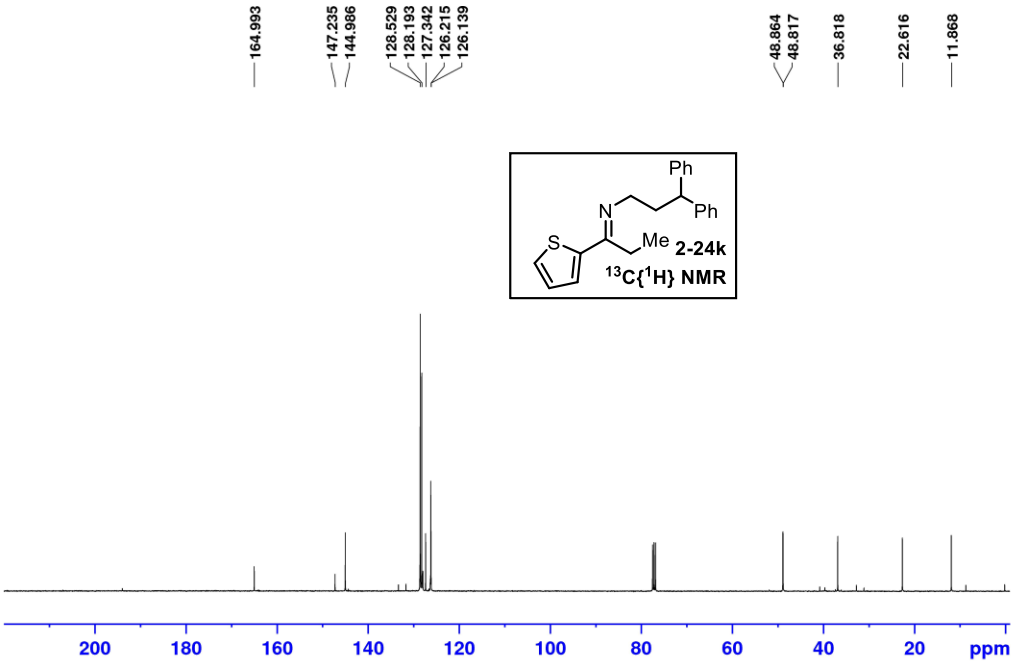
164.993
147.235
144.986
128.529
128.193
127.342
126.215
126.139
48.864
48.817
36.818
22.616
11.868
Ph
N
Ph
S
Me
2-24k
13C{1H} NMR
200
180
160
140
120
100
80
60
40
20
ppm

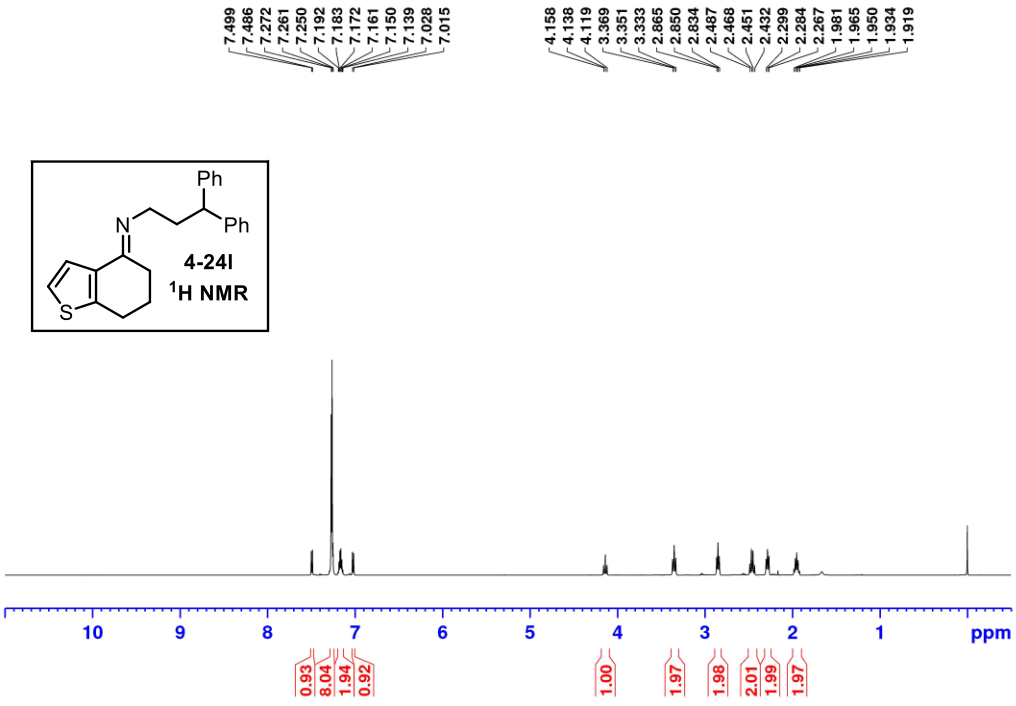
7.499
7.486
7.272
7.261
7.250
7.192
7.183
7.172
7.161
7.150
7.139
7.028
7.015
4.158
4.138
4.119
3.369
3.351
3.333
2.865
2.850
2.834
2.487
2.468
2.451
2.432
2.299
2.284
2.267
1.981
1.965
1.950
1.934
1.919
Ph
N
Ph
S
4-24l
1H NMR
10
9
8
7
6
5
4
3
2
1
ppm
0.93
8.04
1.94
0.92
1.00
1.97
1.98
2.01
1.99
1.97

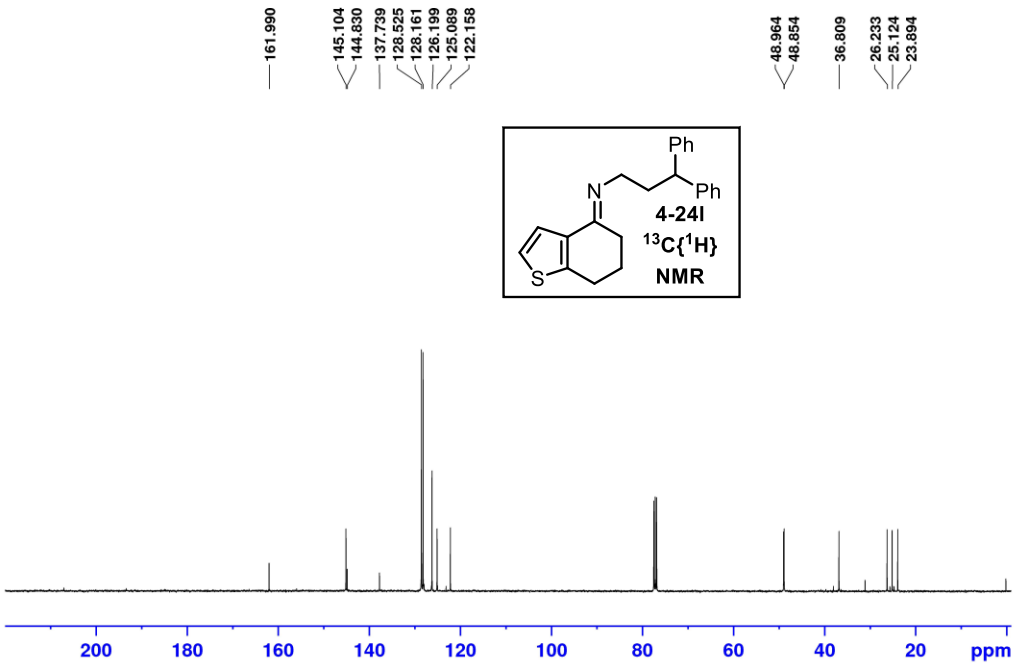
161.990
145.104
144.830
137.739
128.525
128.161
126.199
125.089
122.158
48.964
48.854
36.809
26.233
25.124
23.894
Ph
N
Ph
S
4-24l
13C{1H}
NMR
200
180
160
140
120
100
80
60
40
20
ppm

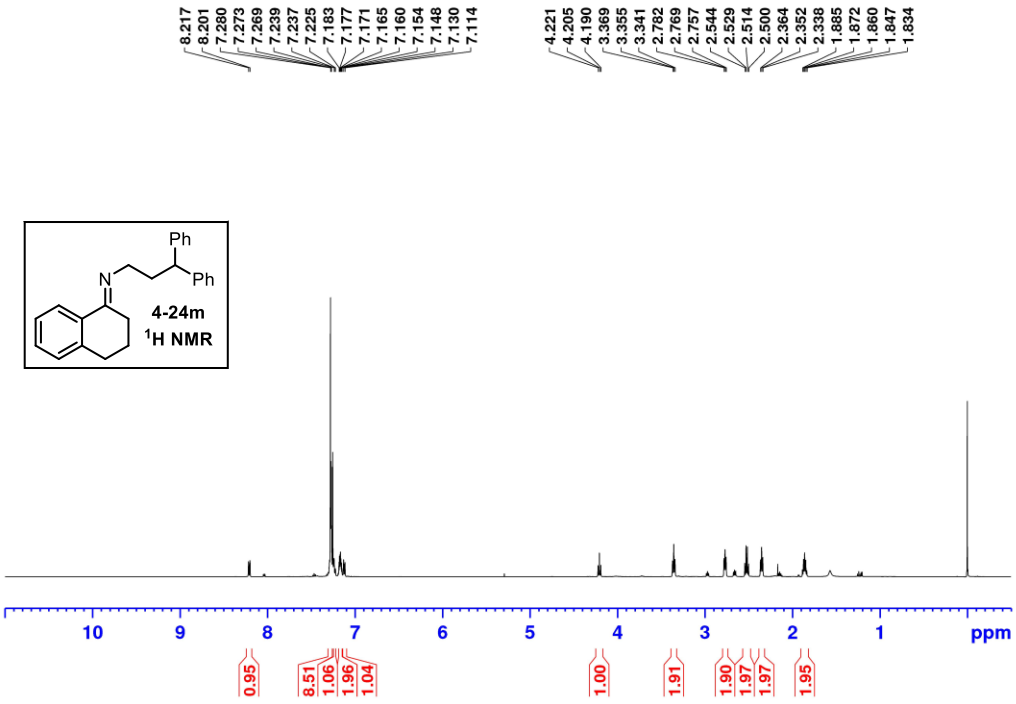
8.217
8.201
7.280
7.273
7.269
7.239
7.237
7.225
7.183
7.177
7.171
7.165
7.160
7.154
7.148
7.130
7.114
4.221
4.205
4.190
3.369
3.355
3.341
2.782
2.769
2.757
2.544
2.529
2.514
2.500
2.364
2.352
2.338
1.885
1.872
1.860
1.847
1.834
Ph
N
Ph
4-24m
1H NMR
10
9
8
7
6
5
4
3
2
1
ppm
0.95
8.51
1.06
1.96
1.04
1.00
1.91
1.90
1.97
1.97
1.95

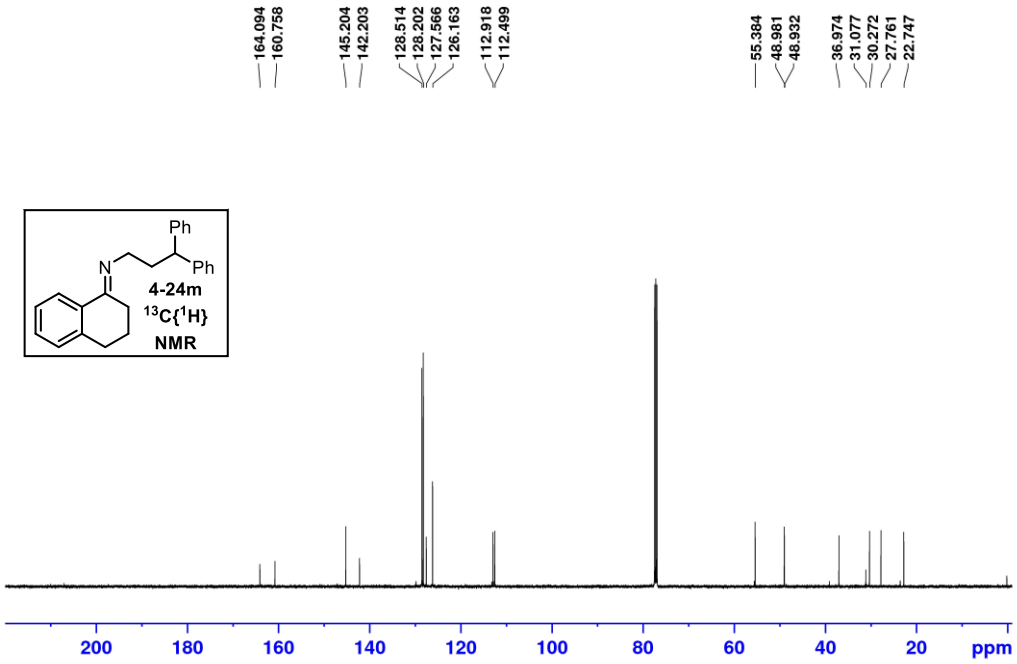
164.094
160.758
145.204
142.203
128.514
128.202
127.566
126.163
112.918
112.499
55.384
48.981
48.932
36.974
31.077
30.272
27.761
22.747
Ph
N
Ph
4-24m
13C{1H}
NMR
200
180
160
140
120
100
80
60
40
20
ppm

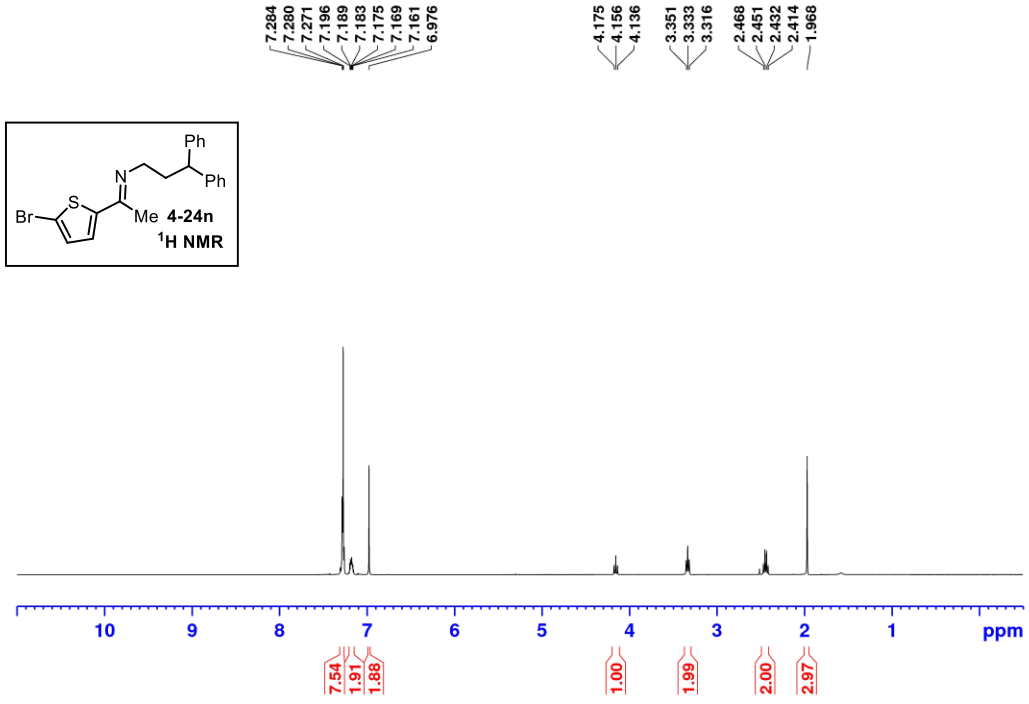
7.284
7.280
7.271
7.196
7.189
7.183
7.175
7.169
7.161
6.976
4.175
4.156
4.136
3.351
3.333
3.316
2.468
2.451
2.432
2.414
1.968
Ph
N
Ph
S
Br
Me
4-24n
1H NMR
10
9
8
7
6
5
4
3
2
1
ppm
7.54
1.91
1.88
1.00
1.99
2.00
2.97

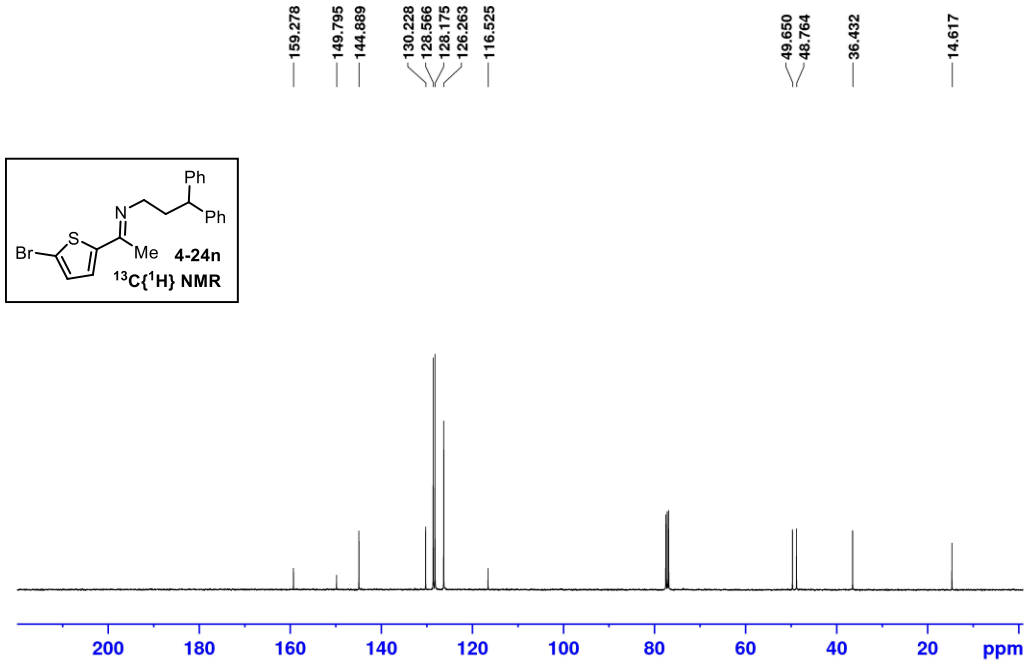
159.278
149.795
144.889
130.228
128.566
128.175
126.263
116.525
49.650
48.764
36.432
14.617
Ph
N
Ph
S
Br
Me
4-24n
$^{13}C\{^{1}H\}$ NMR
200
180
160
140
120
100
80
60
40
20
ppm

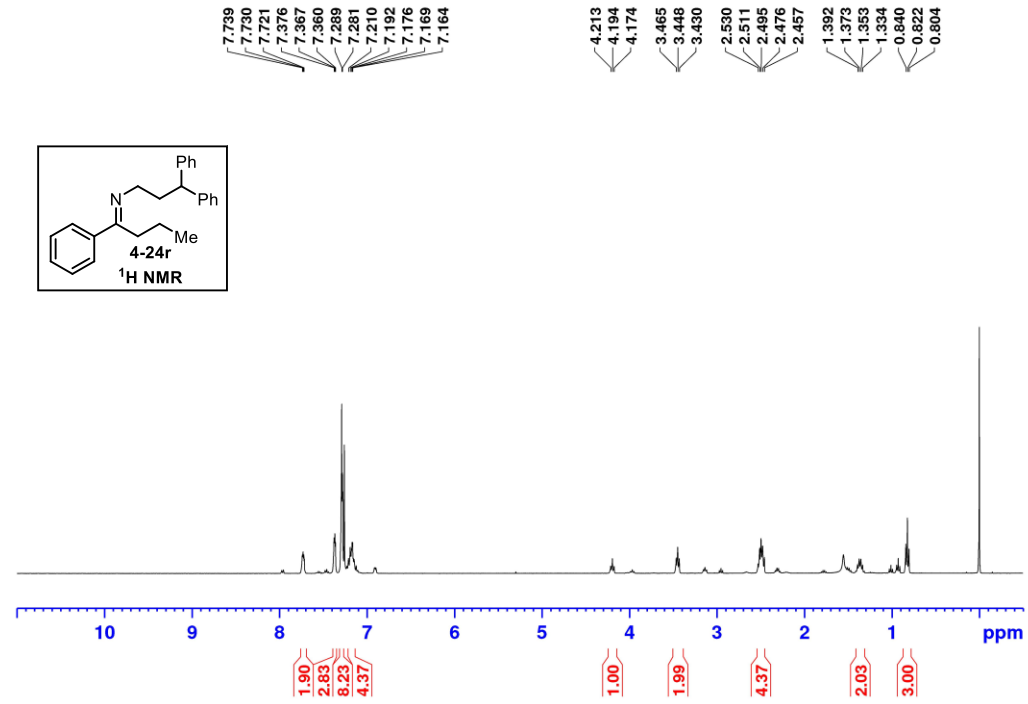
7.739
7.730
7.721
7.376
7.367
7.360
7.289
7.281
7.210
7.192
7.176
7.169
7.164
4.213
4.194
4.174
3.465
3.448
3.430
2.530
2.511
2.495
2.476
2.457
1.392
1.373
1.353
1.334
0.840
0.822
0.804
Ph
N
Ph
Me
4-24r
^{1}H NMR
10
9
8
7
6
5
4
3
2
1
ppm
1.90
2.83
8.23
4.37
1.00
1.99
4.37
2.03
3.00

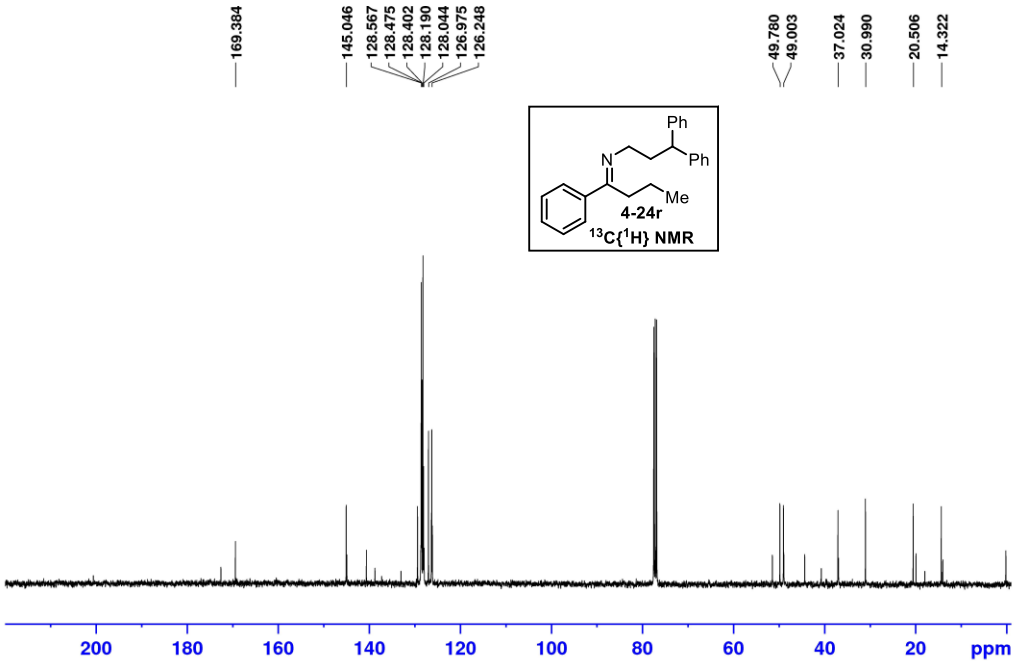
169.384
145.046
128.567
128.475
128.402
128.190
128.044
126.975
126.248
49.780
49.003
37.024
30.990
20.506
14.322
Ph
N
Ph
Me
4-24r
13C{1H} NMR
200
180
160
140
120
100
80
60
40
20
ppm

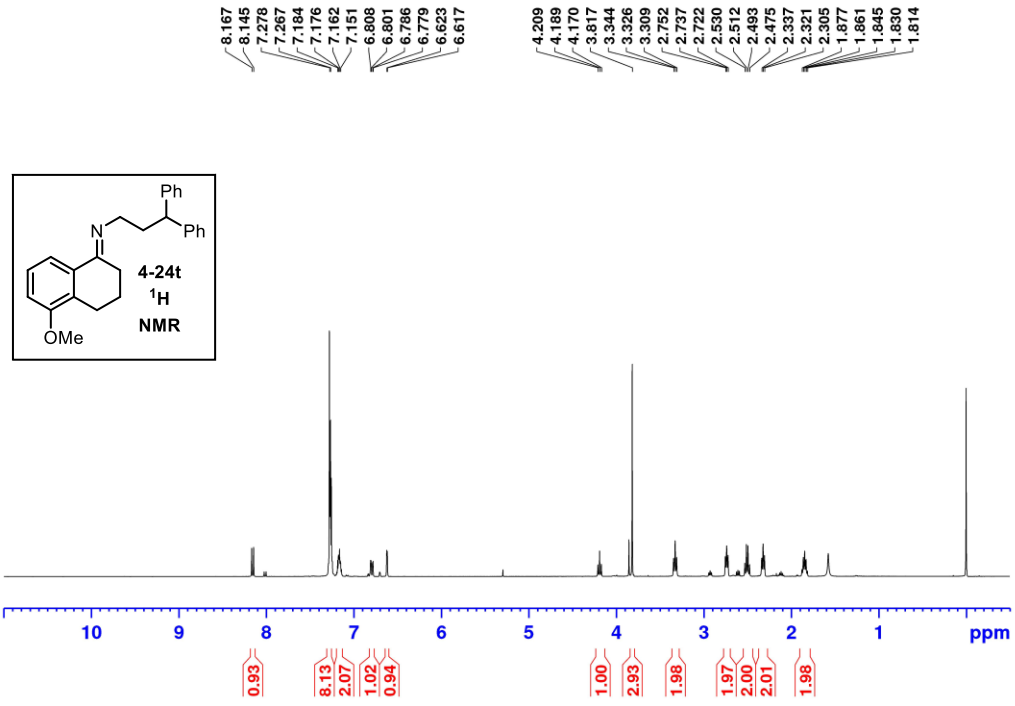
8.167
8.145
7.278
7.267
7.184
7.176
7.162
7.151
6.808
6.801
6.786
6.779
6.623
6.617
4.209
4.189
4.170
3.817
3.344
3.326
3.309
2.752
2.737
2.722
2.530
2.512
2.493
2.475
2.337
2.321
2.305
1.877
1.861
1.845
1.830
1.814
Ph
N
Ph
4-24t
1H
NMR
OMe
10
9
8
7
6
5
4
3
2
1
ppm
0.93
8.13
2.07
1.02
0.94
1.00
2.93
1.98
1.97
2.00
2.01
1.98

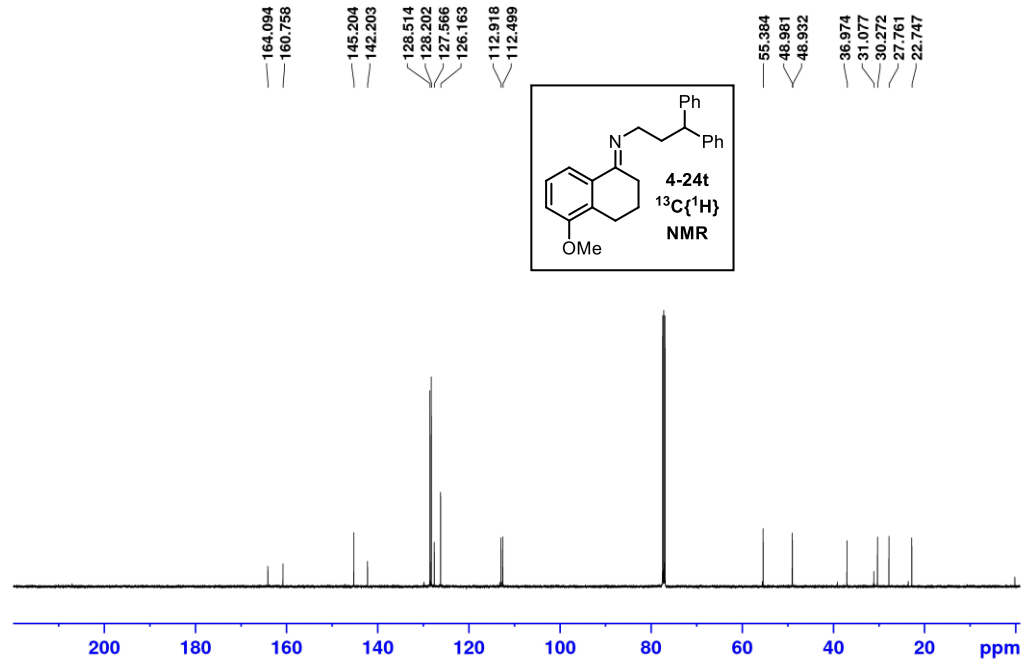
164.094
160.758
145.204
142.203
128.514
128.202
127.566
126.163
112.918
112.499
55.384
48.981
48.932
36.974
31.077
30.272
27.761
22.747
Ph
N
Ph
OMe
4-24t
13C{1H}
NMR
200
180
160
140
120
100
80
60
40
20
ppm

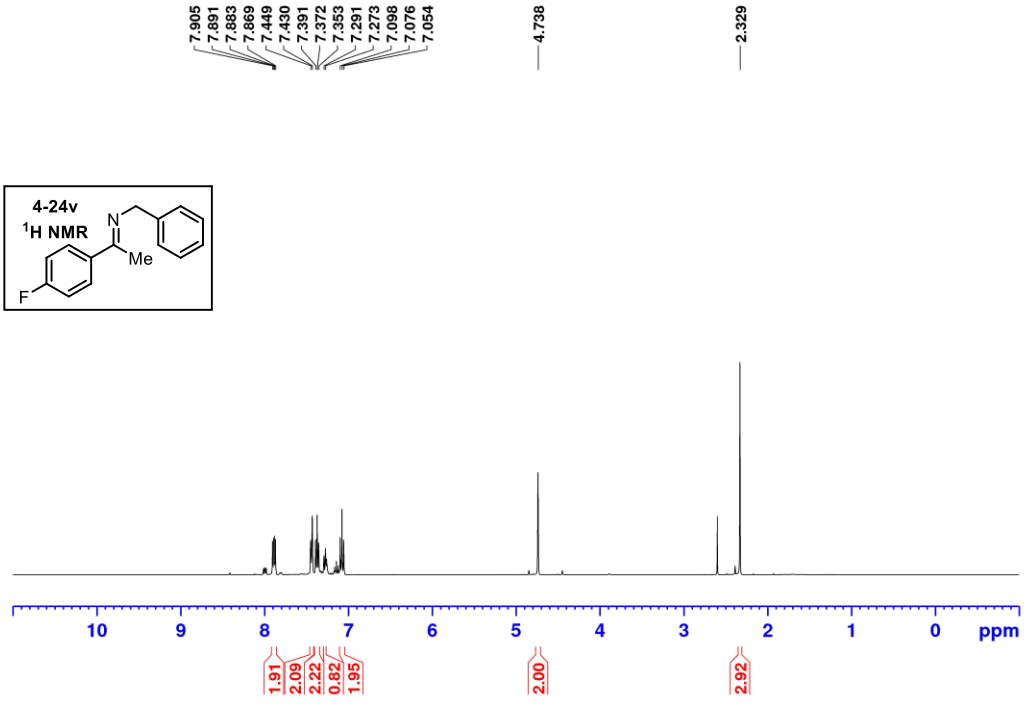
7.905
7.891
7.883
7.869
7.449
7.430
7.391
7.372
7.353
7.291
7.273
7.098
7.076
7.054
4.738
2.329
4-24v
1H NMR
N
Me
F
10
9
8
7
6
5
4
3
2
1
0
ppm
1.91
2.09
2.22
0.82
1.95
2.00
2.92

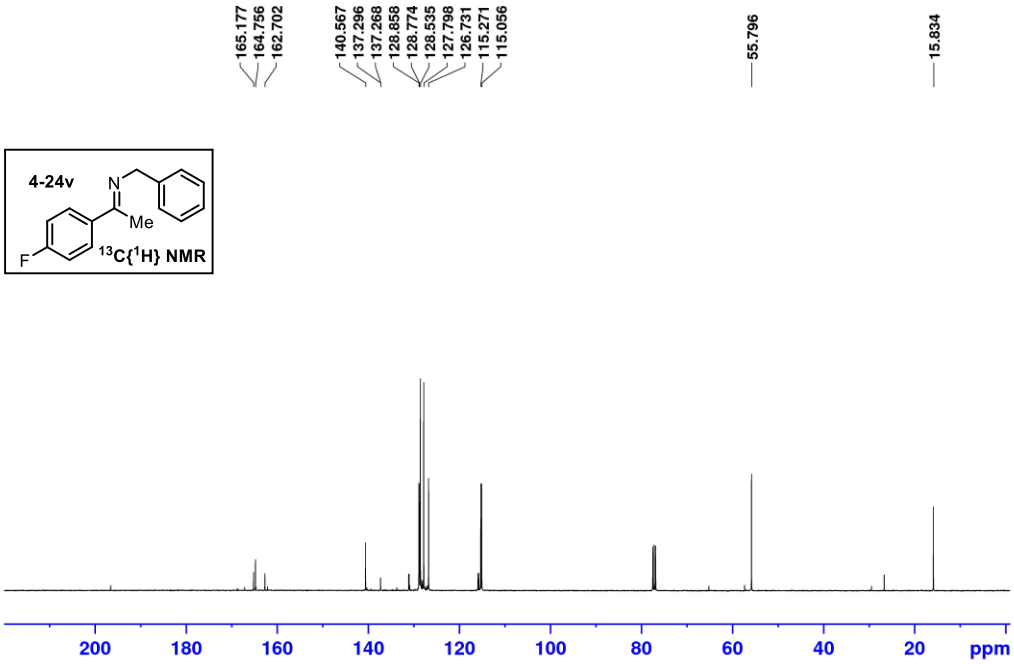
165.177
164.756
162.702
140.567
137.296
137.268
128.858
128.774
128.535
127.798
126.731
115.271
115.056
55.796
15.834
4-24v
N
Me
F
$^{13}C\{^{1}H\}$ NMR
200
180
160
140
120
100
80
60
40
20
ppm

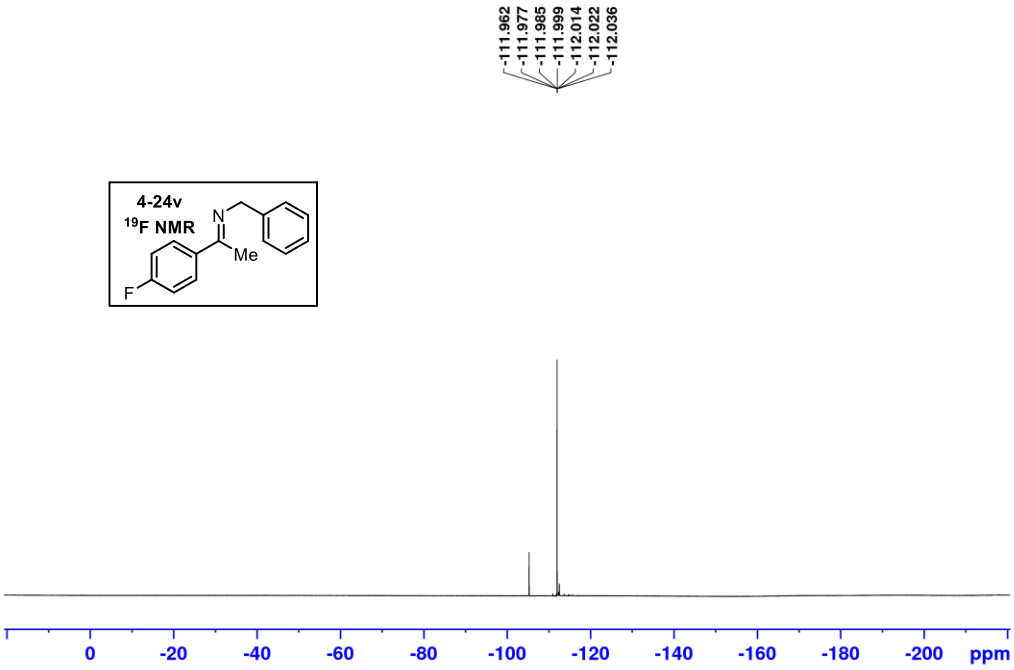
-111.962
-111.977
-111.985
-111.999
-112.014
-112.022
-112.036
4-24v
^{19}F NMR
N
Me
F
0
-20
-40
-60
-80
-100
-120
-140
-160
-180
-200
ppm


7.647
7.643
7.625
7.618
7.452
7.434
7.394
7.388
7.375
7.368
7.355
7.347
7.333
7.294
7.276
7.260
7.125
7.120
7.116
7.104
7.102
7.097
7.083
7.081
7.077
7.075
4.750
2.333

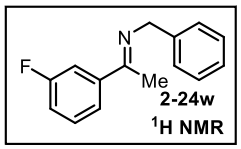
N
F
Me
2-24w
1H NMR

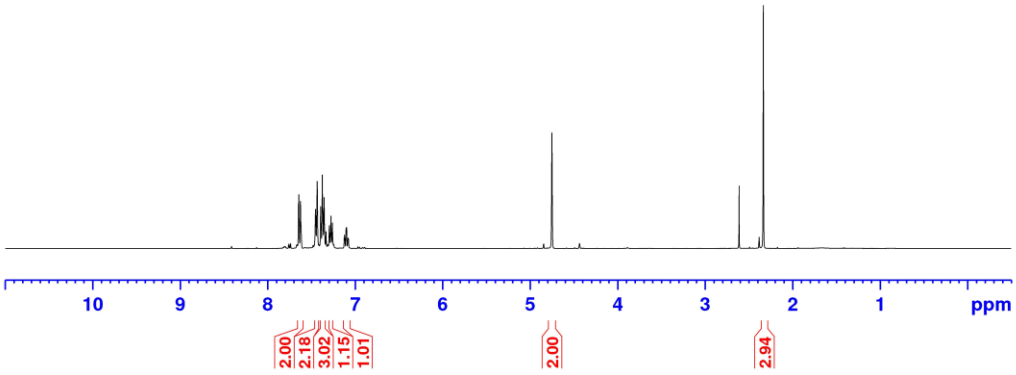
10
9
8
7
6
5
4
3
2
1
ppm
2.00
2.18
3.02
1.15
1.01
2.00
2.94


164.743
164.718
164.228
161.790
143.468
143.398
140.392
129.809
129.727
128.564
127.810
126.788
122.536
122.508
116.705
116.491
113.913
113.688
55.871
15.951

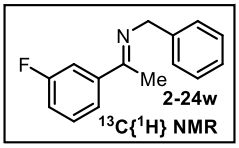
N
F
Me
2-24w
13C{1H} NMR

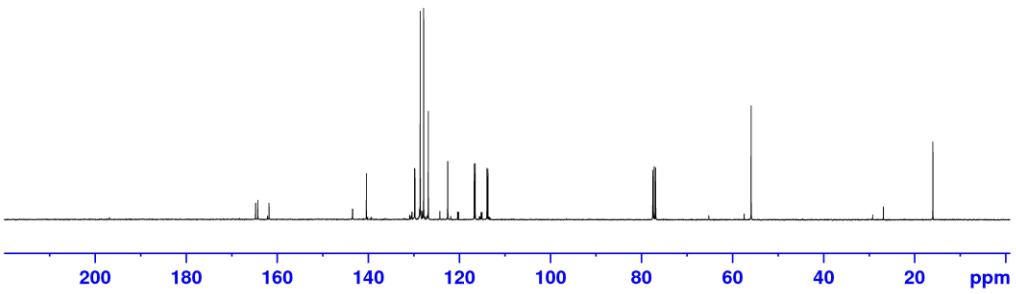
200
180
160
140
120
100
80
60
40
20
ppm

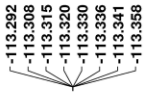
-113.292
-113.308
-113.315
-113.320
-113.330
-113.336
-113.341
-113.358

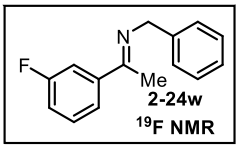
N
F
Me
2-24w
19F NMR

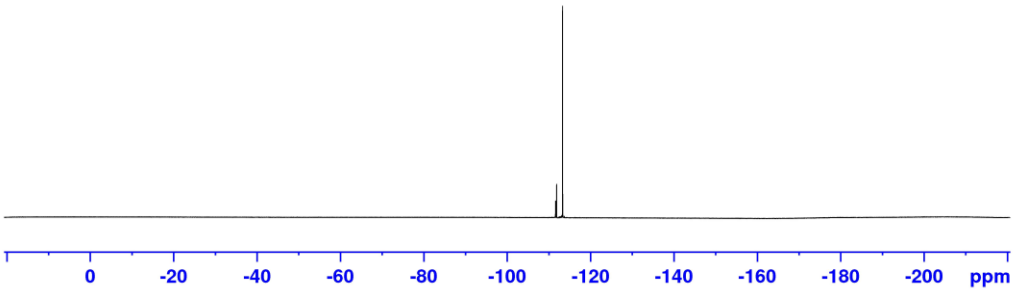
0
-20
-40
-60
-80
-100
-120
-140
-160
-180
-200
ppm


7.394
7.376
7.347
7.330
7.310
7.247
7.229
7.211
7.040
7.030
7.027
7.018
4.723
2.300

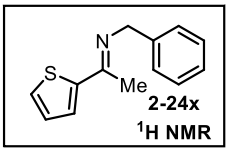
N
S
Me
2-24x
1H NMR

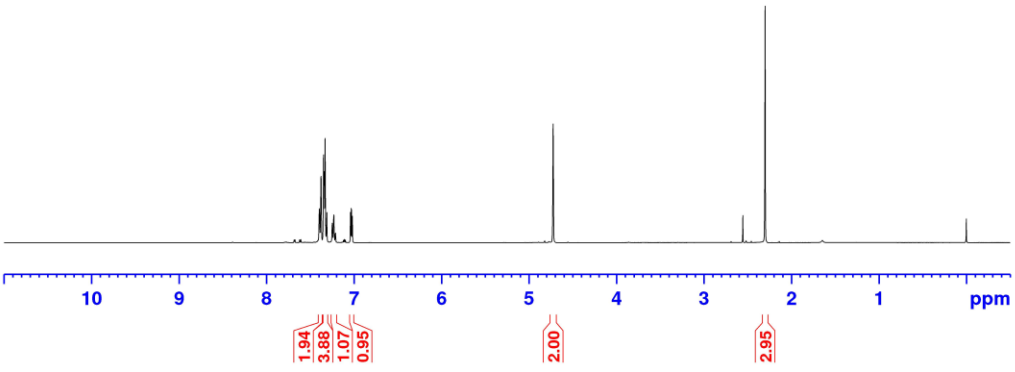
10
9
8
7
6
5
4
3
2
1
ppm
1.94
3.88
1.07
0.95
2.00
2.95

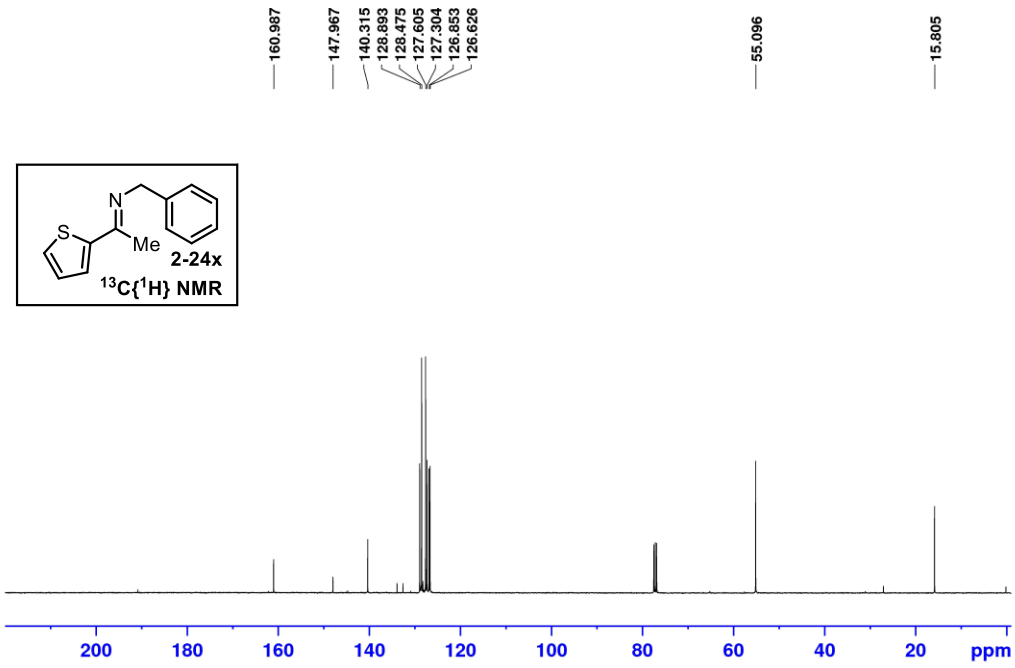
160.987
147.967
140.315
128.893
128.475
127.605
127.304
126.853
126.626
55.096
15.805
N
S
Me
2-24x
$^{13}C\{^{1}H\}$ NMR
200
180
160
140
120
100
80
60
40
20
ppm

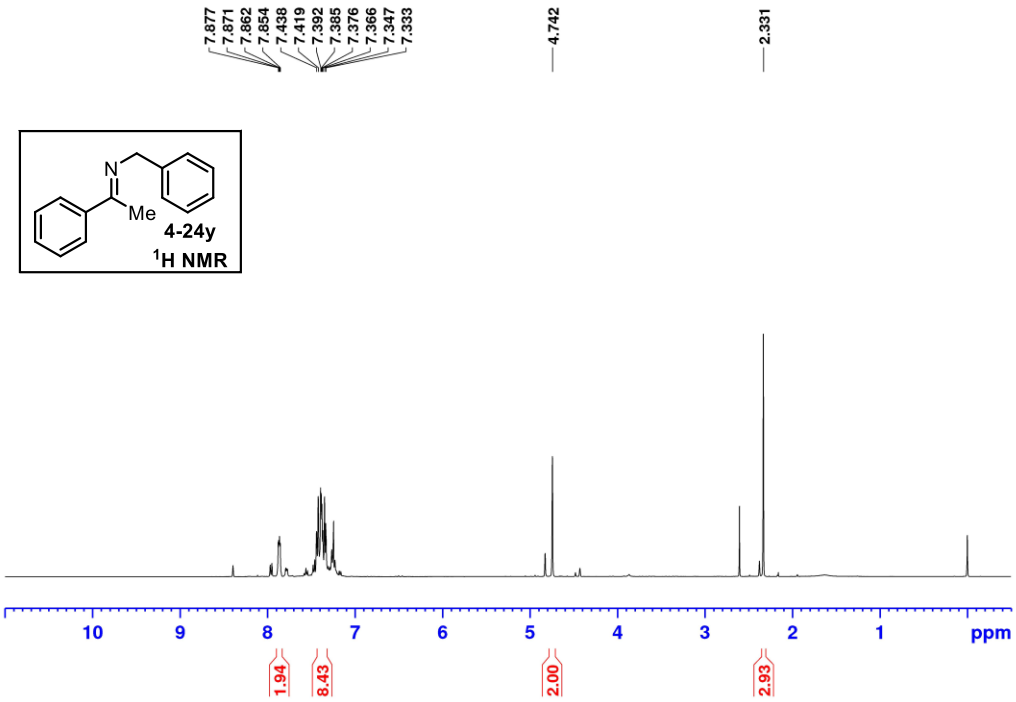
7.877
7.871
7.862
7.854
7.438
7.419
7.392
7.385
7.376
7.366
7.347
7.333
4.742
2.331
N
Me
4-24y
^{1}H NMR
10
9
8
7
6
5
4
3
2
1
ppm
1.94
8.43
2.00
2.93

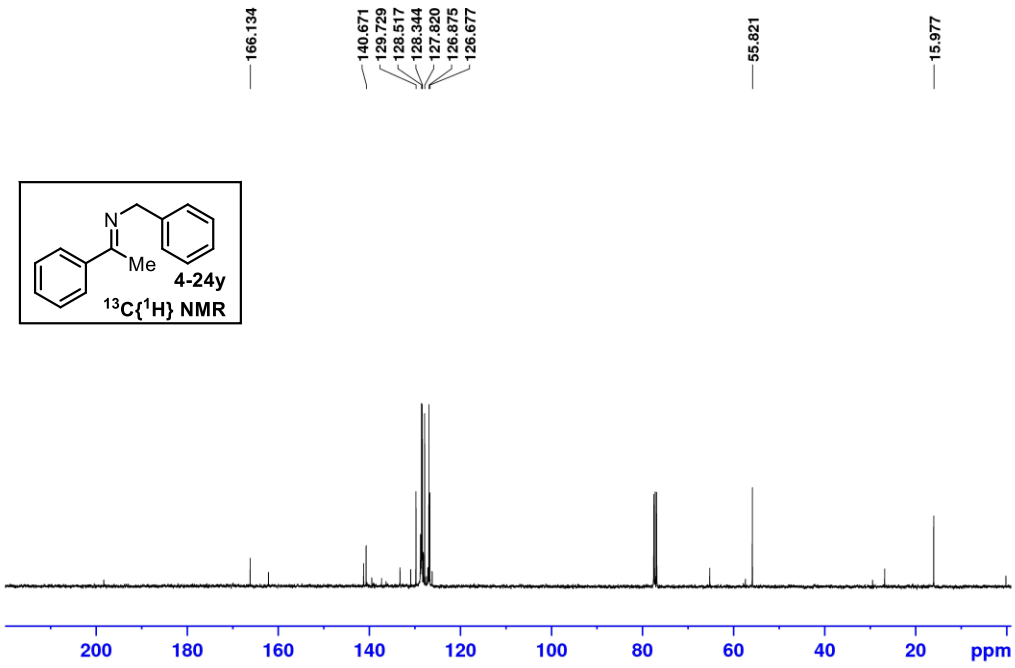
166.134
140.671
129.729
128.517
128.344
127.820
126.875
126.677
55.821
15.977
N
Me
4-24y
13C{1H} NMR
200
180
160
140
120
100
80
60
40
20
ppm

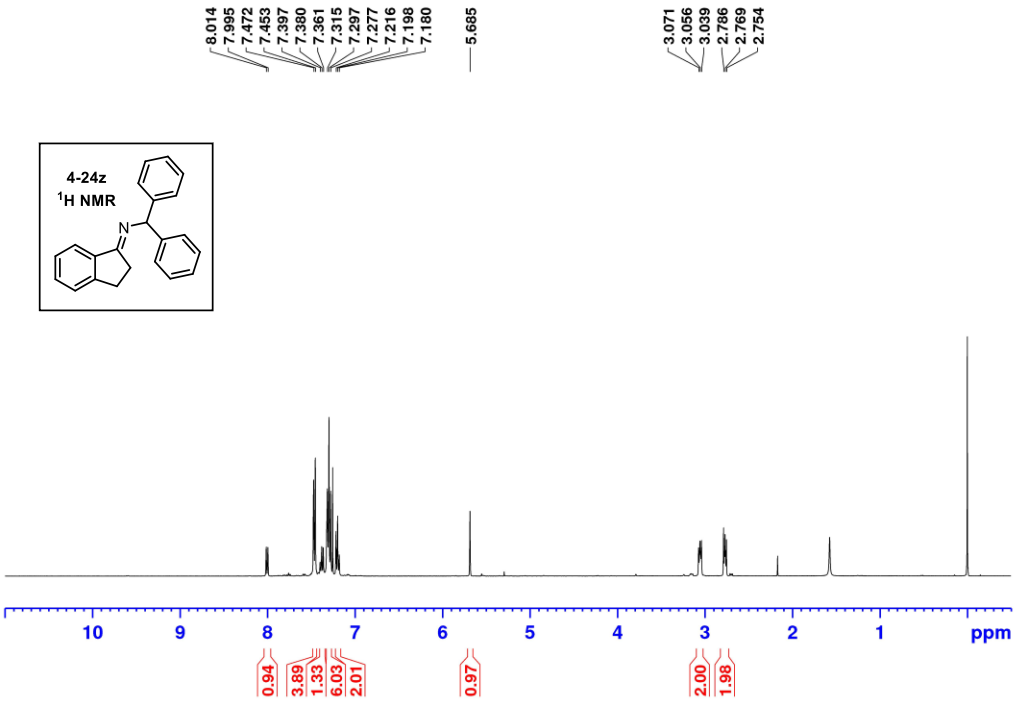
8.014
7.995
7.472
7.453
7.397
7.380
7.361
7.315
7.297
7.277
7.216
7.198
7.180
5.685
3.071
3.056
3.039
2.786
2.769
2.754
4-24z
1H NMR
N
10
9
8
7
6
5
4
3
2
1
ppm
0.94
3.89
1.33
6.03
2.01
0.97
2.00
1.98

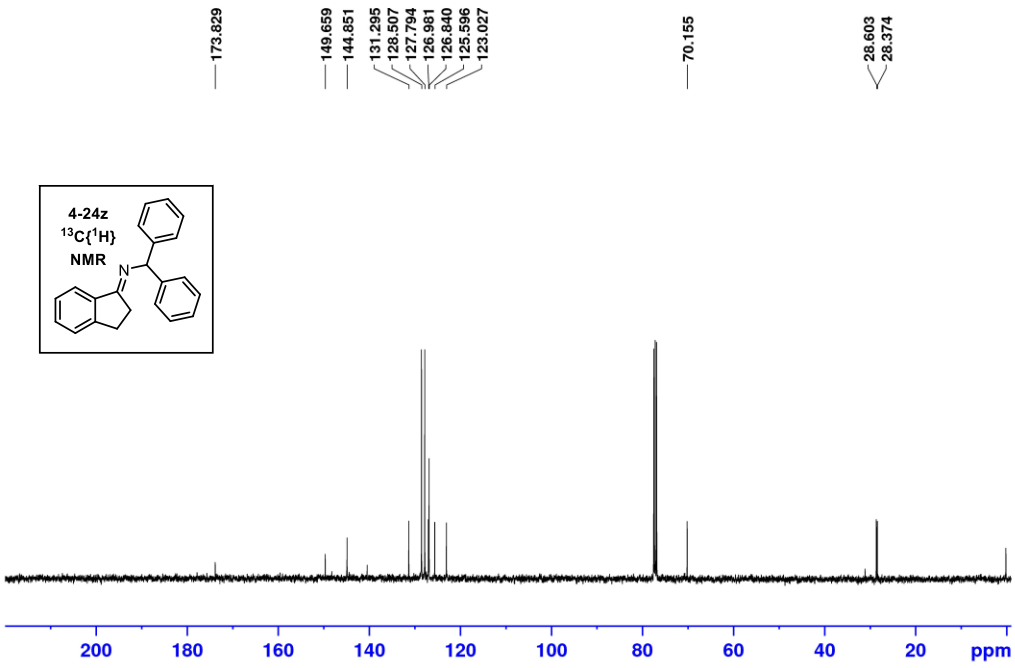
173.829
149.659
144.851
131.295
128.507
127.794
126.981
126.840
125.596
123.027
70.155
28.603
28.374
4-24z
$^{13}C\{^{1}H\}$
NMR
N
200
180
160
140
120
100
80
60
40
20
ppm

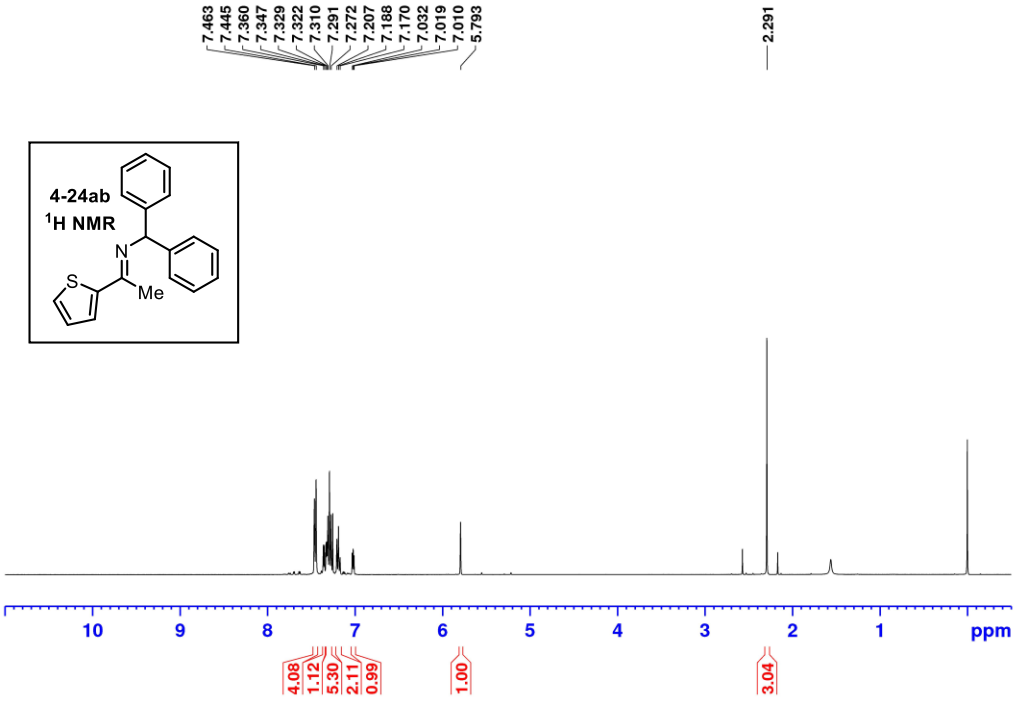
7.463
7.445
7.360
7.347
7.329
7.322
7.310
7.291
7.272
7.207
7.188
7.170
7.032
7.019
7.010
5.793
2.291
4-24ab
^{1}H NMR
N
S
Me
10
9
8
7
6
5
4
3
2
1
ppm
4.08
1.12
5.30
2.11
0.99
1.00
3.04

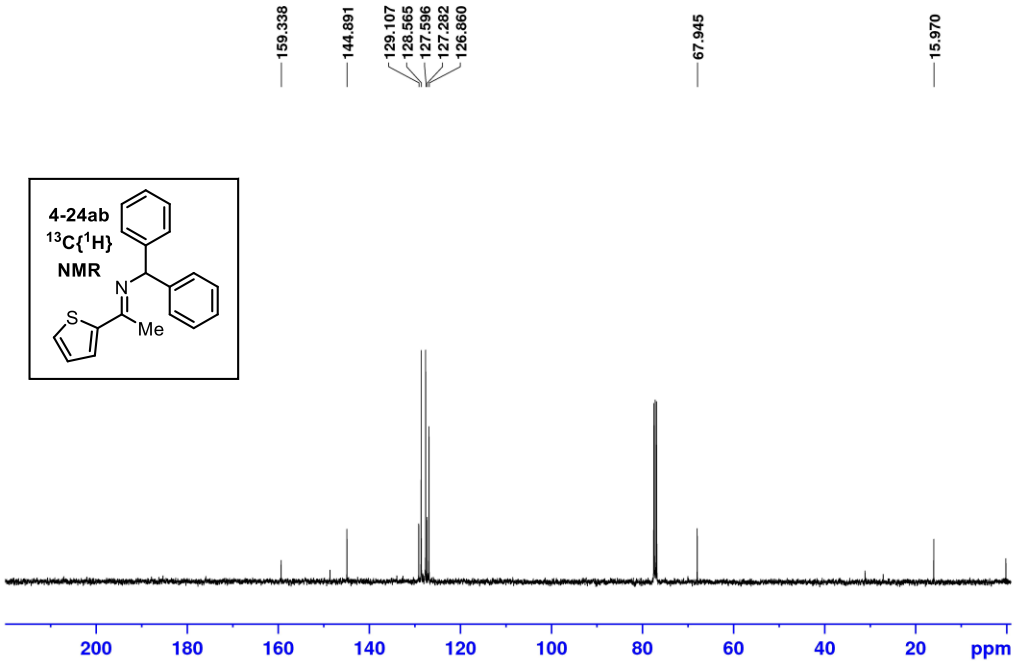
159.338
144.891
129.107
128.565
127.596
127.282
126.860
67.945
15.970
4-24ab
13C{1H}
NMR
N
S
Me
200
180
160
140
120
100
80
60
40
20
ppm

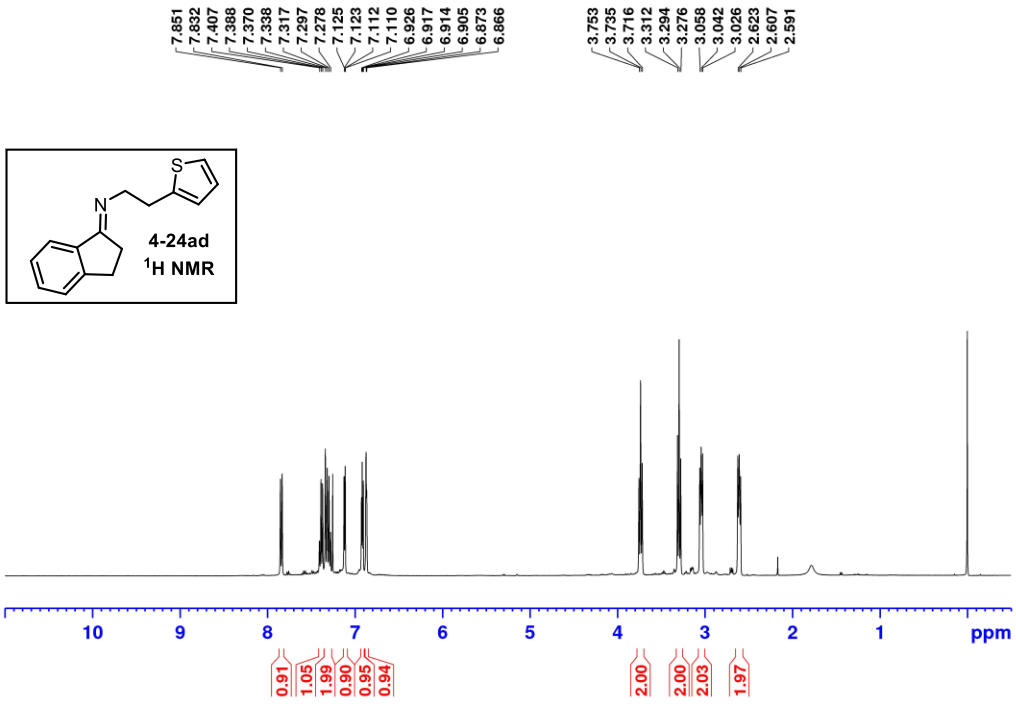
7.851
7.832
7.407
7.388
7.370
7.338
7.317
7.297
7.278
7.125
7.123
7.112
7.110
6.926
6.917
6.914
6.905
6.873
6.866
3.753
3.735
3.716
3.312
3.294
3.276
3.058
3.042
3.026
2.623
2.607
2.591
S
N
4-24ad
1H NMR
10
9
8
7
6
5
4
3
2
1
ppm
0.91
1.05
1.99
0.90
0.95
0.94
2.00
2.00
2.03
1.97

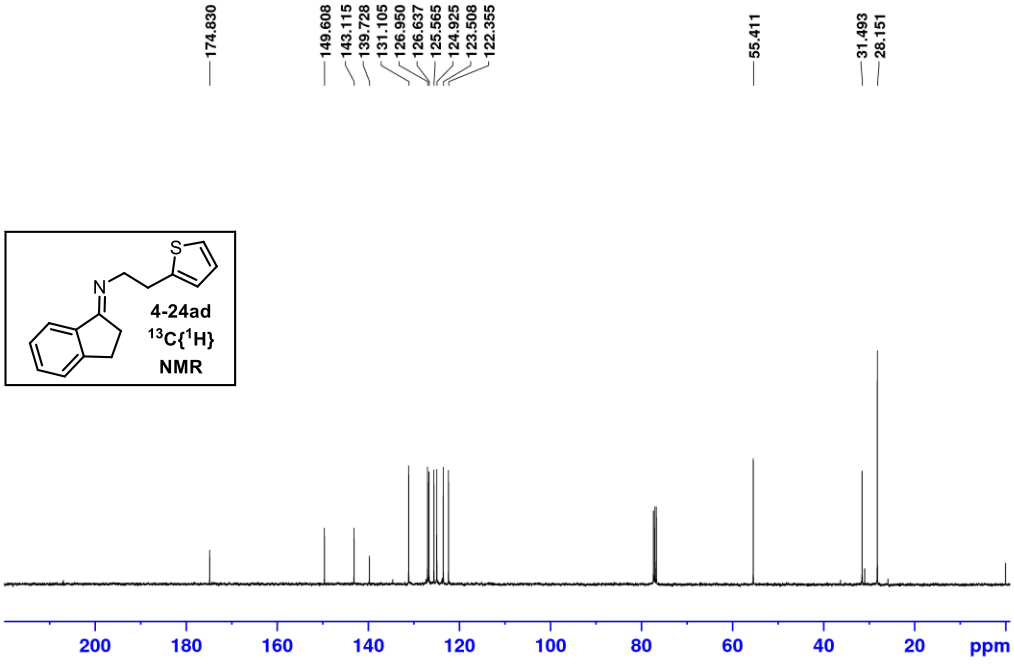
174.830
149.608
143.115
139.728
131.105
126.950
126.637
125.565
124.925
123.508
122.355
55.411
31.493
28.151
4-24ad
$^{13}C\{^{1}H\}$
NMR
200
180
160
140
120
100
80
60
40
20
ppm

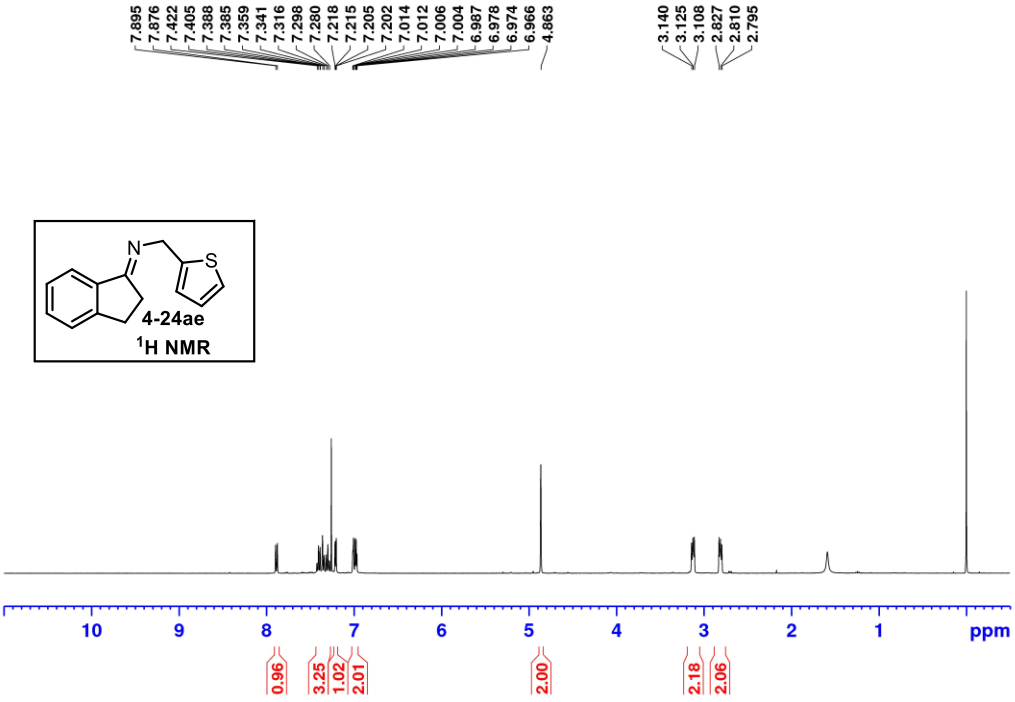
7.895
7.876
7.422
7.405
7.388
7.385
7.359
7.341
7.316
7.298
7.280
7.218
7.215
7.205
7.202
7.014
7.012
7.006
7.004
6.987
6.978
6.974
6.966
4.863
3.140
3.125
3.108
2.827
2.810
2.795
4-24ae
^{1}H NMR
10
9
8
7
6
5
4
3
2
1
ppm
0.96
3.25
1.02
2.01
2.00
2.18
2.06

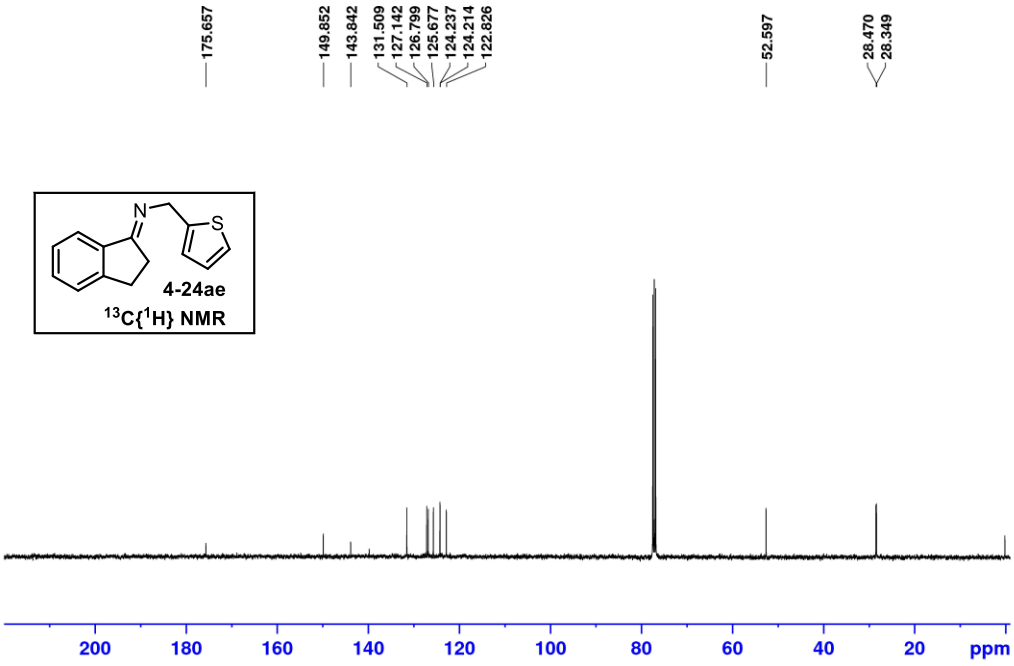
175.657
149.852
143.842
131.509
127.142
126.799
125.677
124.237
124.214
122.826
52.597
28.470
28.349
N
S
4-24ae
13C{1H} NMR
200
180
160
140
120
100
80
60
40
20
ppm

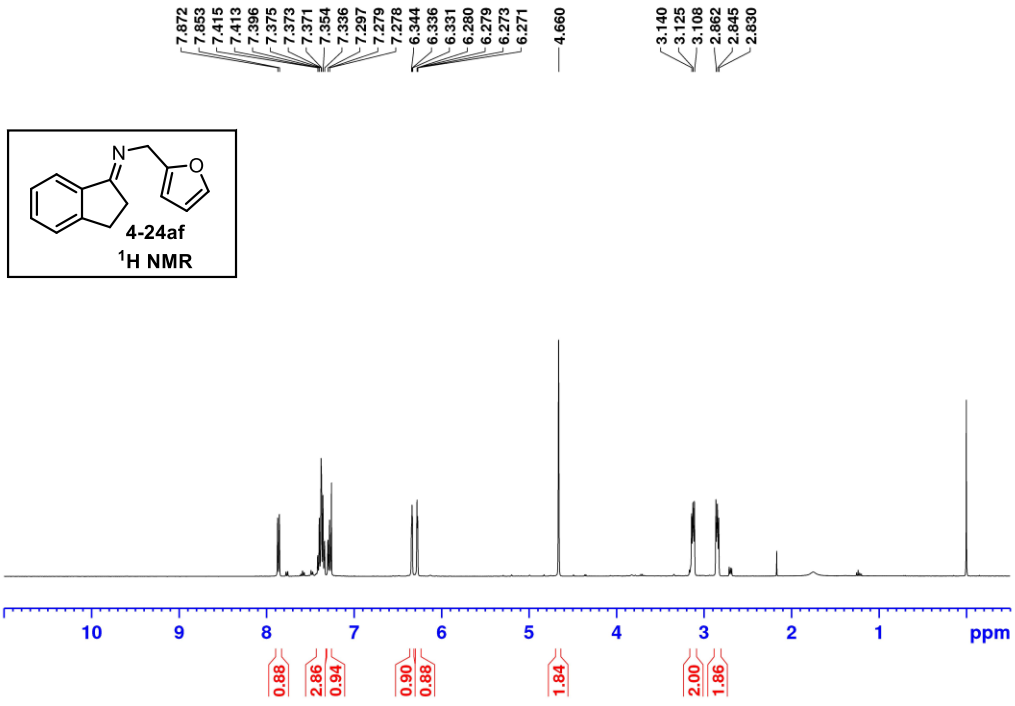
7.872
7.853
7.415
7.413
7.396
7.375
7.373
7.371
7.354
7.336
7.297
7.279
7.278
6.344
6.336
6.331
6.280
6.279
6.273
6.271
4.660
3.140
3.125
3.108
2.862
2.845
2.830
N
O
4-24af
1H NMR
10
9
8
7
6
5
4
3
2
1
ppm
0.88
2.86
0.94
0.90
0.88
1.84
2.00
1.86

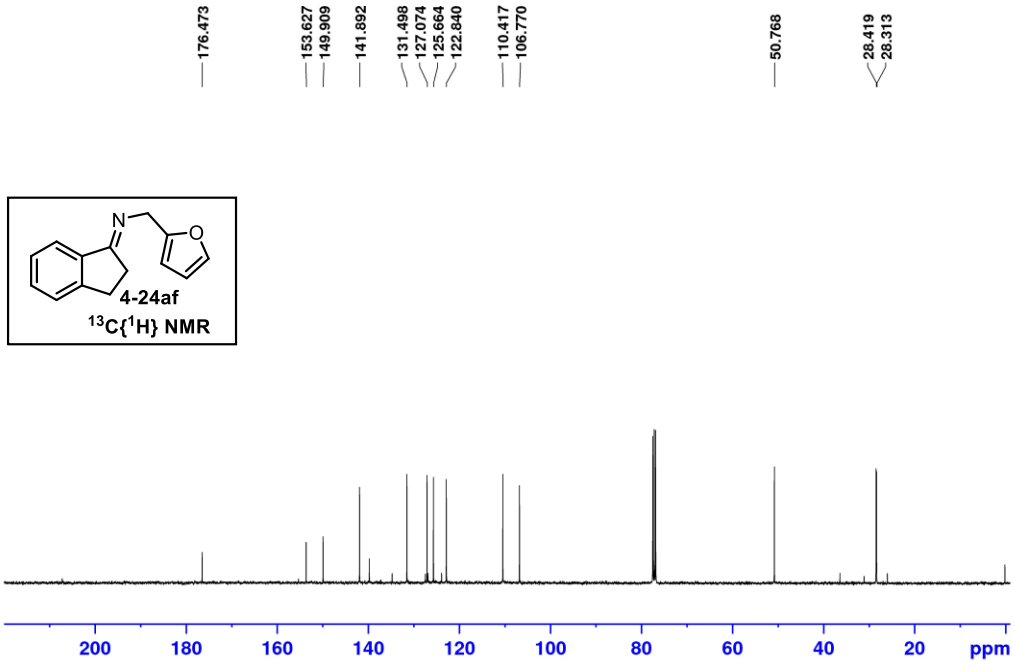
176.473
153.627
149.909
141.892
131.498
127.074
125.664
122.840
110.417
106.770
50.768
28.419
28.313
4-24af
13C{1H} NMR
200
180
160
140
120
100
80
60
40
20
ppm

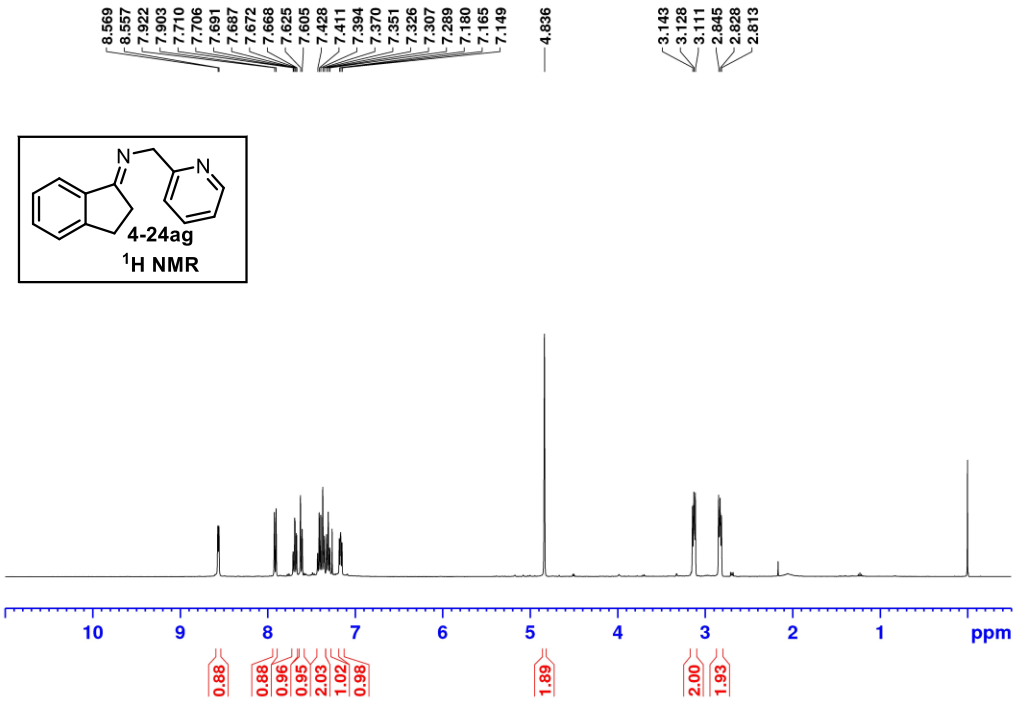
8.569
8.557
7.922
7.903
7.710
7.706
7.691
7.687
7.672
7.668
7.625
7.605
7.428
7.411
7.394
7.370
7.351
7.326
7.307
7.289
7.180
7.165
7.149
4.836
3.143
3.128
3.111
2.845
2.828
2.813
4-24ag
1H NMR
10
9
8
7
6
5
4
3
2
1
ppm
0.88
0.88
0.96
0.95
2.03
1.02
0.98
1.89
2.00
1.93

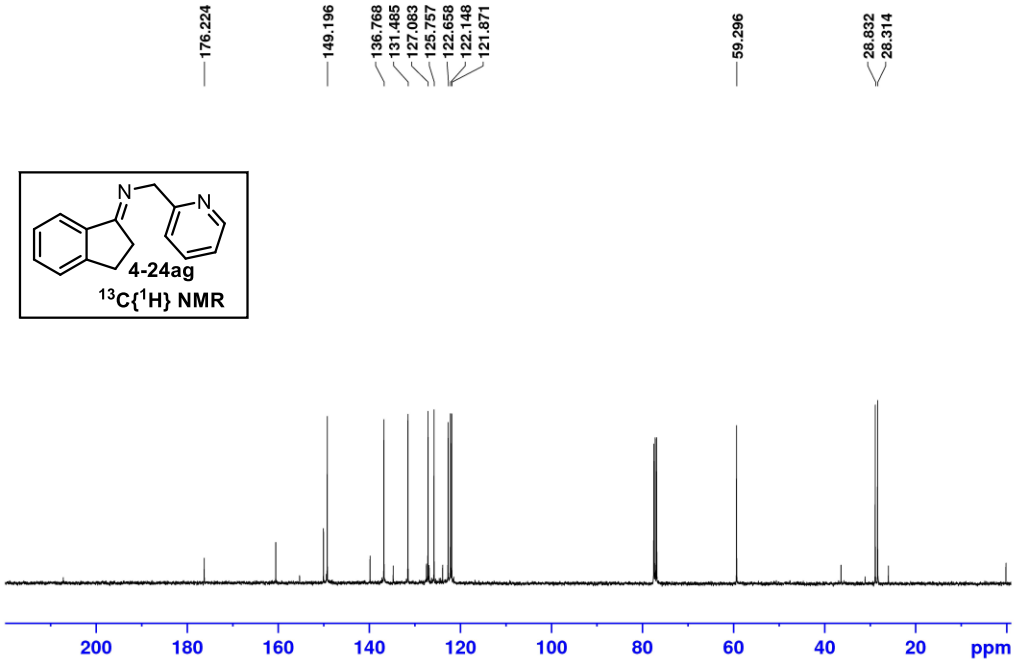
176.224
149.196
136.768
131.485
127.083
125.757
122.658
122.148
121.871
59.296
28.832
28.314
4-24ag
13C{1H} NMR
200
180
160
140
120
100
80
60
40
20
ppm

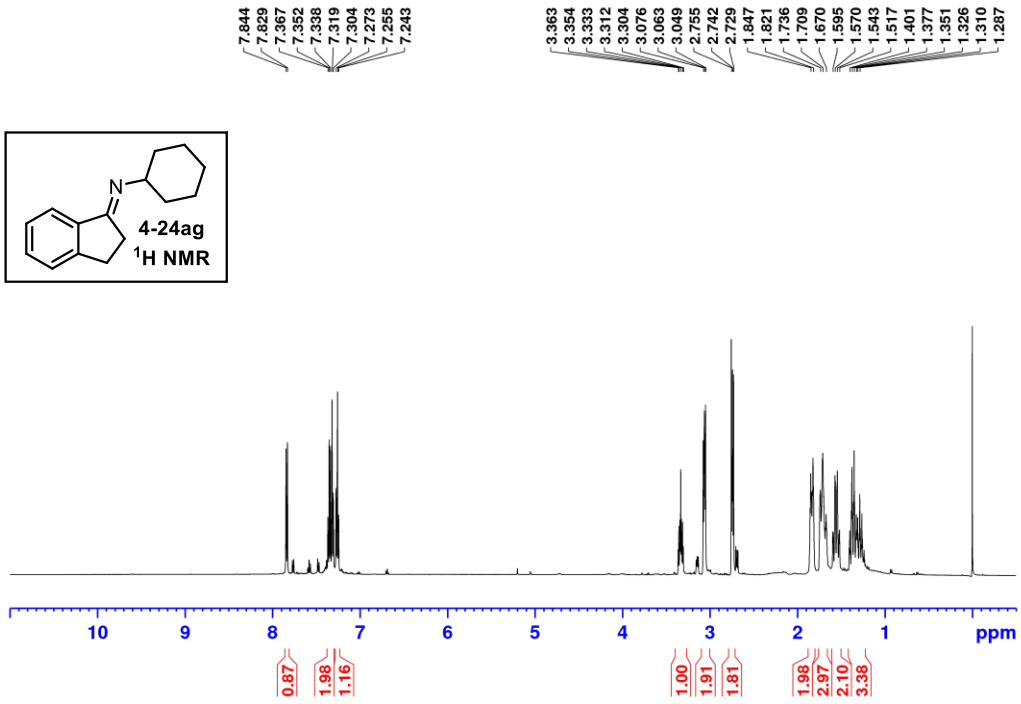
7.844
7.829
7.367
7.352
7.338
7.319
7.304
7.273
7.255
7.243
3.363
3.354
3.333
3.312
3.304
3.076
3.063
3.049
2.755
2.742
2.729
1.847
1.821
1.736
1.709
1.670
1.595
1.570
1.543
1.517
1.401
1.377
1.351
1.326
1.310
1.287
4-24ag
1H NMR
10
9
8
7
6
5
4
3
2
1
ppm
0.87
1.98
1.16
1.00
1.91
1.81
1.98
2.97
2.10
3.38

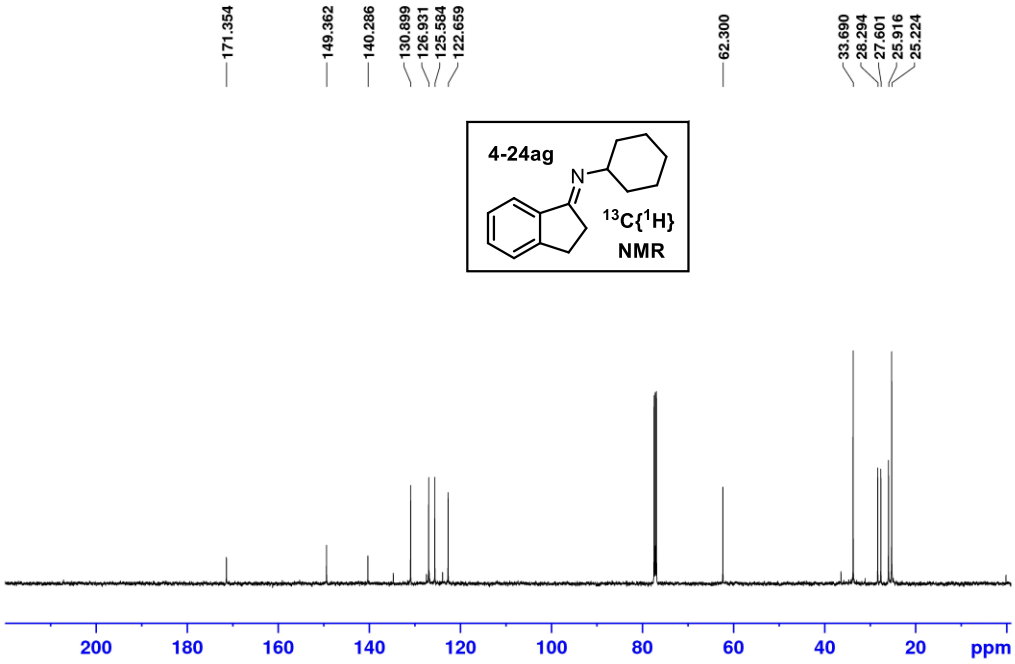
171.354
149.362
140.286
130.899
126.931
125.584
122.659
62.300
33.690
28.294
27.601
25.916
25.224
4-24ag
N
$^{13}C\{^{1}H\}$
NMR
200
180
160
140
120
100
80
60
40
20
ppm

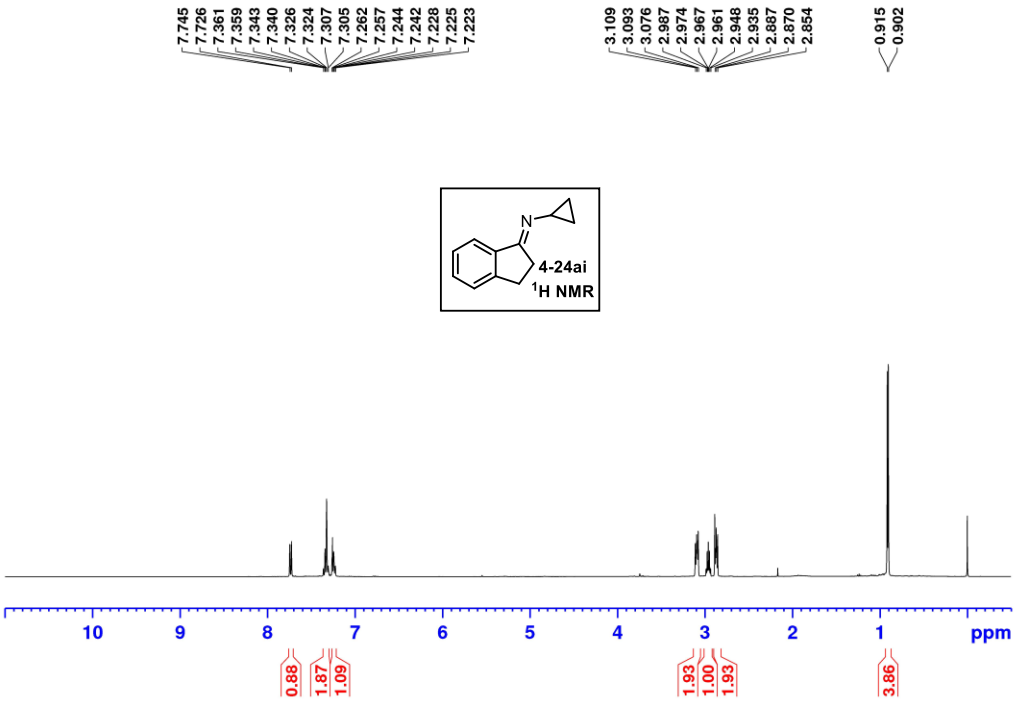
7.745
7.726
7.361
7.359
7.343
7.340
7.326
7.324
7.307
7.305
7.262
7.257
7.244
7.242
7.228
7.225
7.223
3.109
3.093
3.076
2.987
2.974
2.967
2.961
2.948
2.935
2.887
2.870
2.854
0.915
0.902
N
4-24ai
^{1}H NMR
10
9
8
7
6
5
4
3
2
1
ppm
0.88
1.87
1.09
1.93
1.00
1.93
3.86

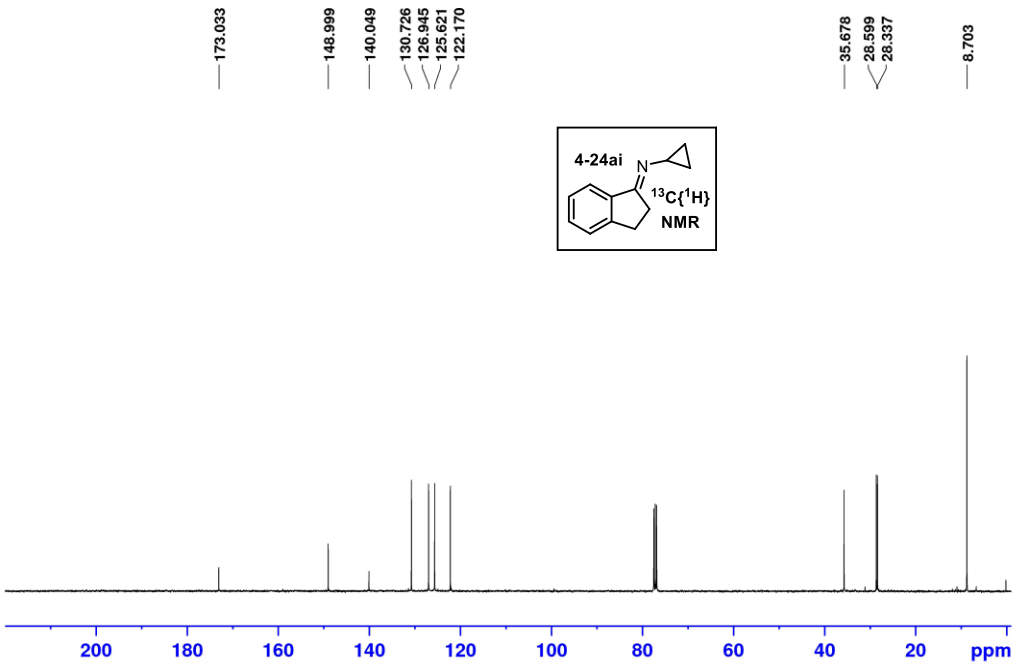
173.033
148.999
140.049
130.726
126.945
125.621
122.170
35.678
28.599
28.337
8.703
4-24ai
N
13C{1H}
NMR
200
180
160
140
120
100
80
60
40
20
ppm

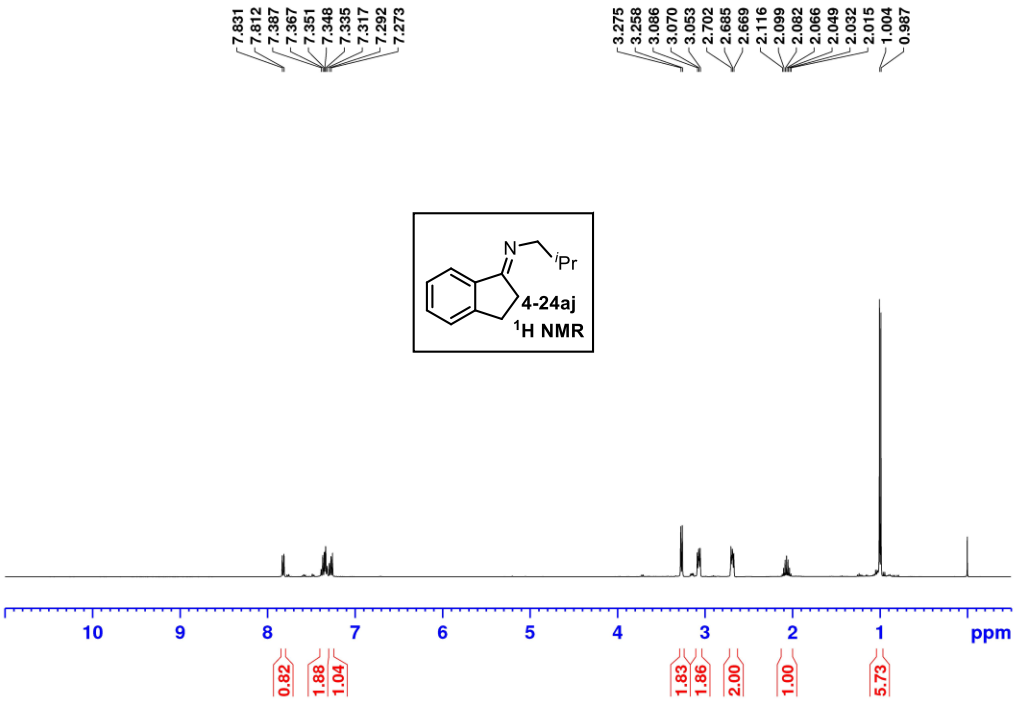
7.831
7.812
7.387
7.367
7.351
7.348
7.335
7.317
7.292
7.273
3.275
3.258
3.086
3.070
3.053
2.702
2.685
2.669
2.116
2.099
2.082
2.066
2.049
2.032
2.015
1.004
0.987
N
iPr
4-24aj
1H NMR
10
9
8
7
6
5
4
3
2
1
ppm
0.82
1.88
1.04
1.83
1.86
2.00
1.00
5.73

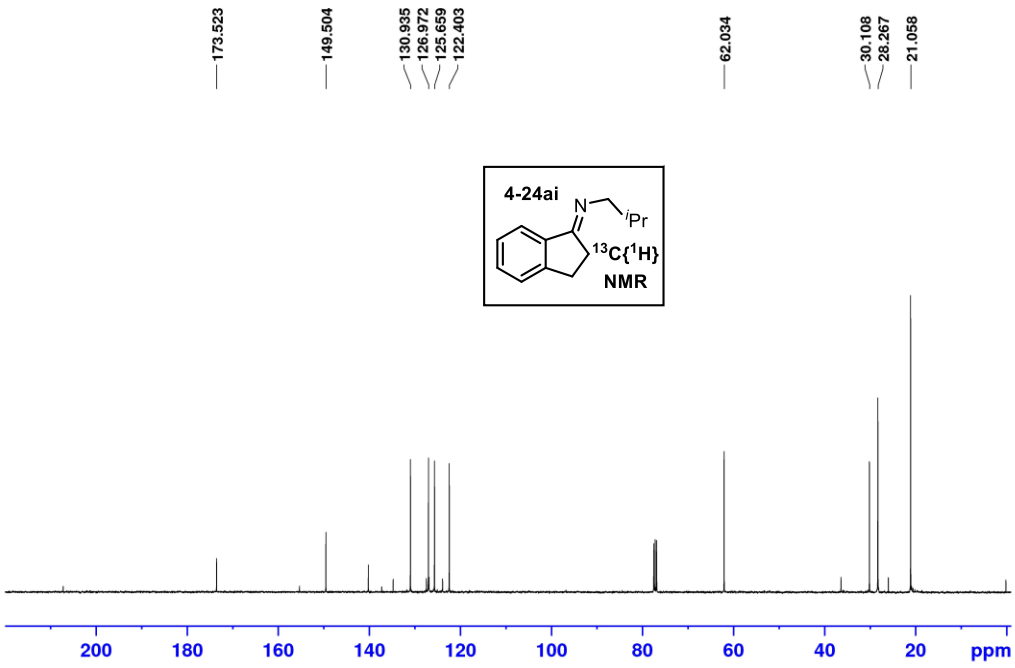
173.523
149.504
130.935
126.972
125.659
122.403
62.034
30.108
28.267
21.058
4-24ai
N
iPr
13C{1H}
NMR
200
180
160
140
120
100
80
60
40
20
ppm

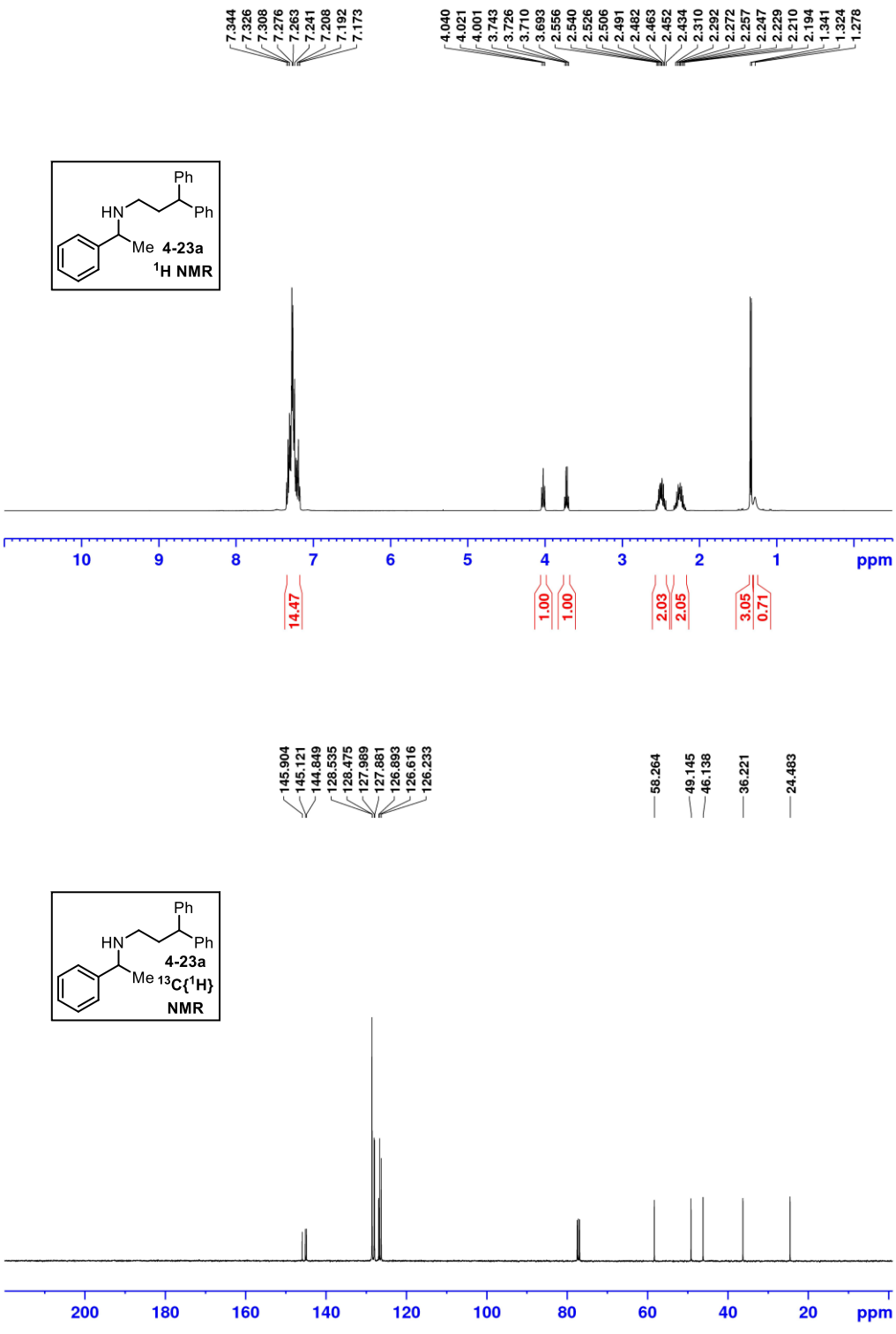
7.344
7.326
7.308
7.276
7.263
7.241
7.208
7.192
7.173
4.040
4.021
4.001
3.743
3.726
3.710
3.693
2.556
2.540
2.526
2.506
2.491
2.482
2.463
2.452
2.434
2.310
2.292
2.272
2.257
2.247
2.229
2.210
2.194
1.341
1.324
1.278
Ph
HN
Ph
Me
4-23a
1H NMR
10
9
8
7
6
5
4
3
2
1
ppm
14.47
1.00
1.00
2.03
2.05
3.05
0.71
145.904
145.121
144.849
128.535
128.475
127.989
127.881
126.893
126.616
126.233
58.264
49.145
46.138
36.221
24.483
Ph
HN
Ph
4-23a
Me
13C{1H}
NMR
200
180
160
140
120
100
80
60
40
20
ppm

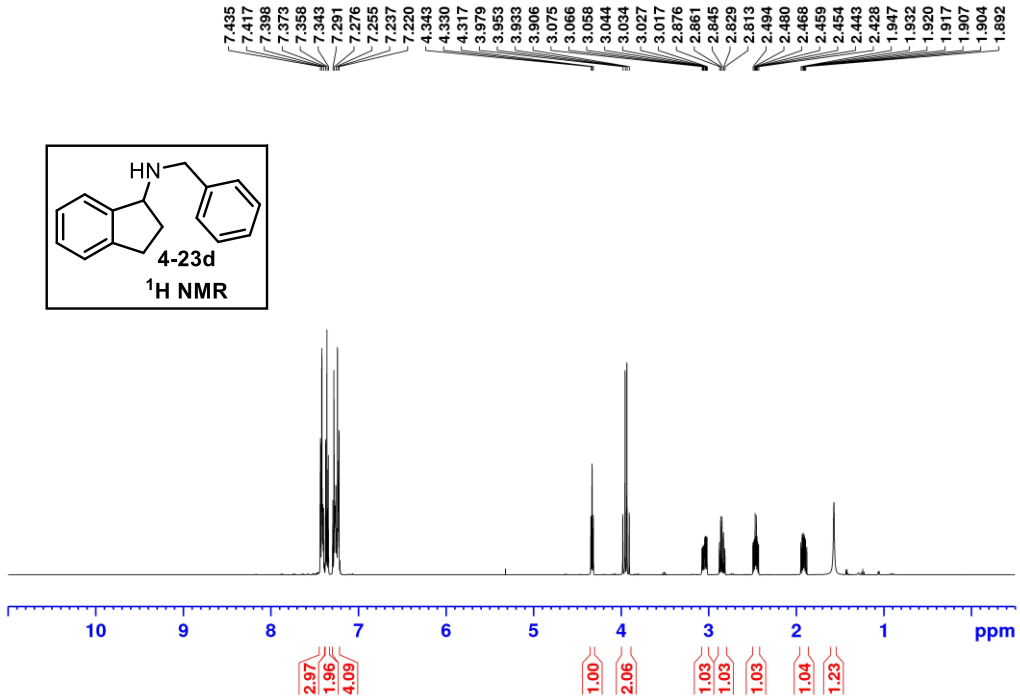
7.435
7.417
7.398
7.373
7.358
7.343
7.291
7.276
7.255
7.237
7.220
4.343
4.330
4.317
3.979
3.953
3.933
3.906
3.075
3.066
3.058
3.044
3.034
3.027
3.017
2.876
2.861
2.845
2.829
2.813
2.494
2.480
2.468
2.459
2.454
2.443
2.428
1.947
1.932
1.920
1.917
1.907
1.904
1.892
HN
4-23d
1H NMR
10
9
8
7
6
5
4
3
2
1
ppm
2.97
1.96
4.09
1.00
2.06
1.03
1.03
1.03
1.04
1.23

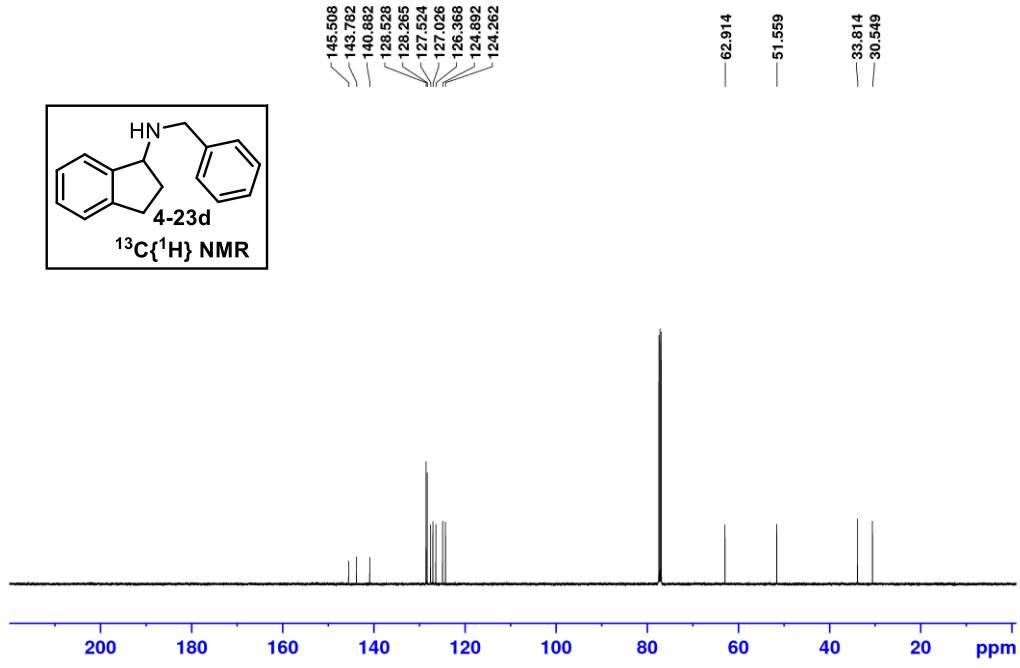
145.508
143.782
140.882
128.528
128.265
127.524
127.026
126.368
124.892
124.262
62.914
51.559
33.814
30.549
HN
4-23d
13C{1H} NMR
200
180
160
140
120
100
80
60
40
20
ppm

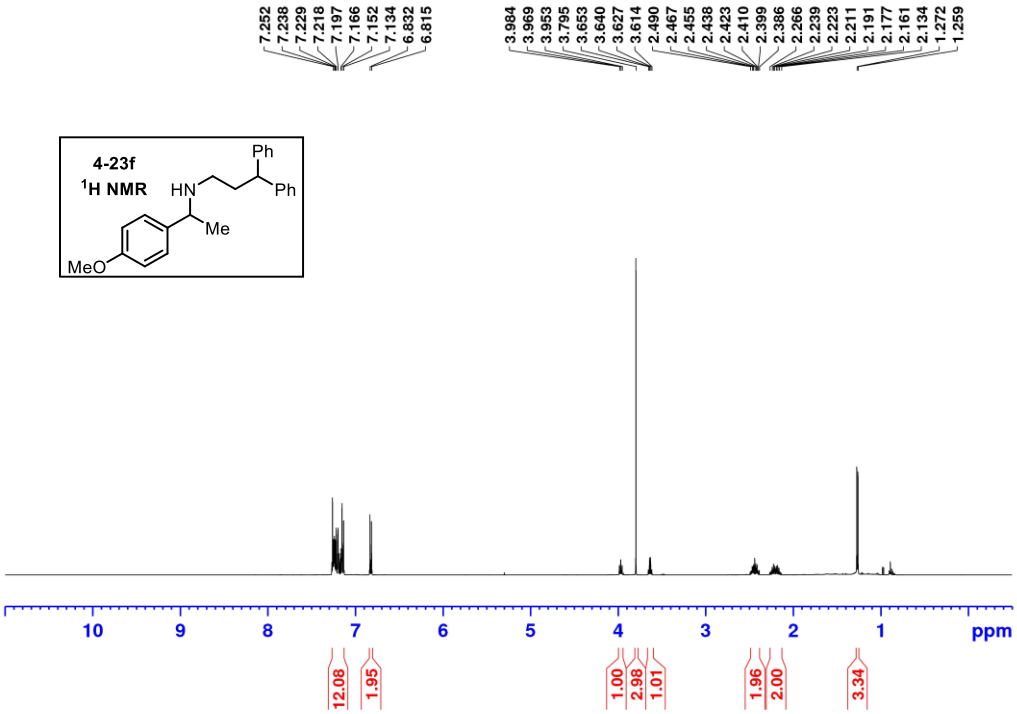
7.252
7.238
7.229
7.218
7.197
7.166
7.152
7.134
6.832
6.815
3.984
3.969
3.953
3.795
3.653
3.640
3.627
3.614
2.490
2.467
2.455
2.438
2.423
2.410
2.399
2.386
2.266
2.239
2.223
2.211
2.191
2.177
2.161
2.134
1.272
1.259
4-23f
1H NMR
HN
Ph
Ph
Me
MeO
10
9
8
7
6
5
4
3
2
1
ppm
12.08
1.95
1.00
2.98
1.01
1.96
2.00
3.34

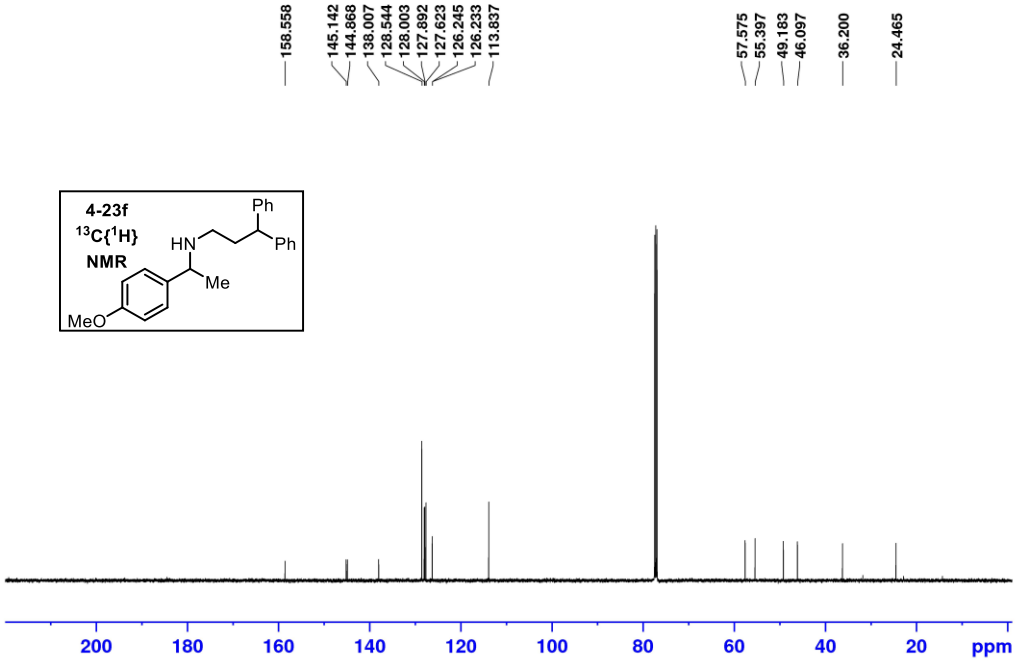
158.558
145.142
144.868
138.007
128.544
128.003
127.892
127.623
126.245
126.233
113.837
57.575
55.397
49.183
46.097
36.200
24.465
4-23f
13C{1H}
NMR
HN
Ph
Ph
Me
MeO
200
180
160
140
120
100
80
60
40
20
ppm

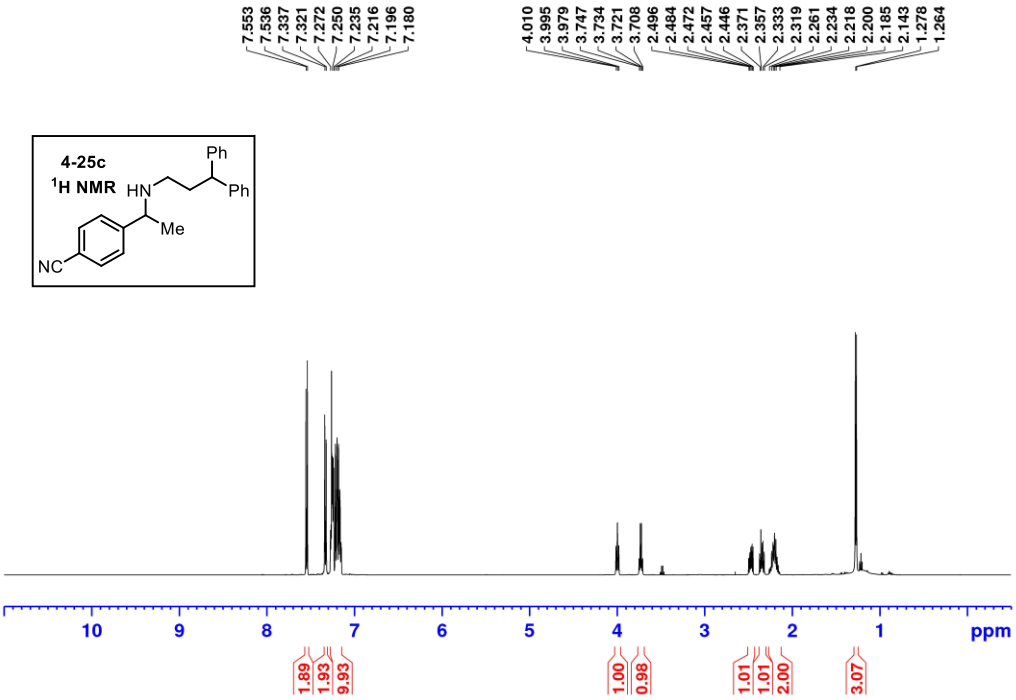
7.553
7.536
7.337
7.321
7.272
7.250
7.235
7.216
7.196
7.180
4.010
3.995
3.979
3.747
3.734
3.721
3.708
2.496
2.484
2.472
2.457
2.446
2.371
2.357
2.333
2.319
2.261
2.234
2.218
2.200
2.185
2.143
1.278
1.264
4-25c
1H NMR
HN
Ph
Ph
Me
NC
10
9
8
7
6
5
4
3
2
1
ppm
1.89
1.93
9.93
1.00
0.98
1.01
1.01
2.00
3.07

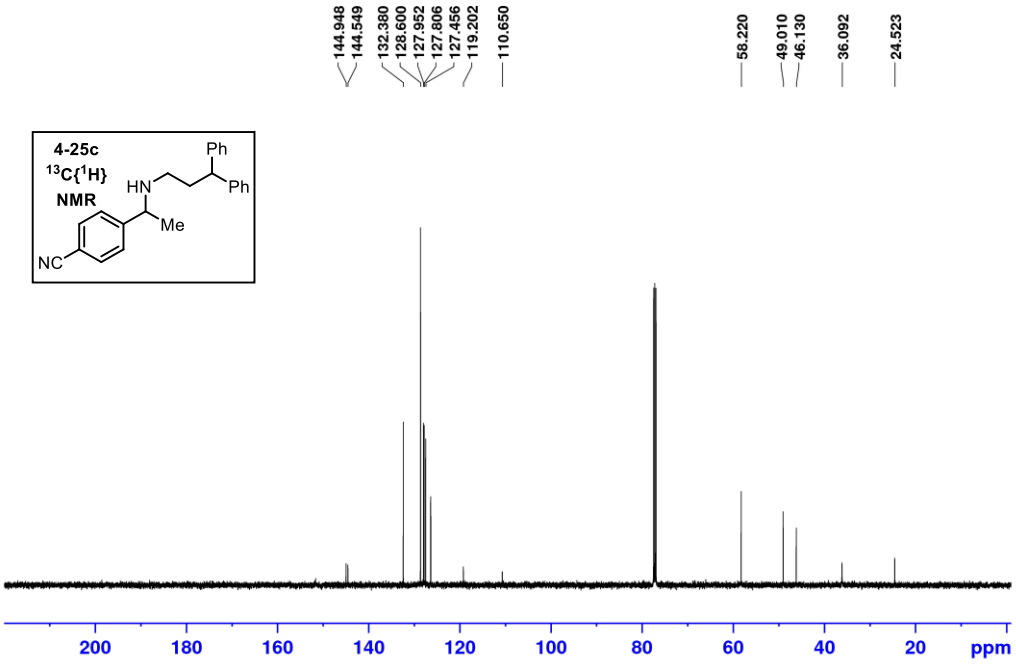
144.948
144.549
132.380
128.600
127.952
127.806
127.456
119.202
110.650
58.220
49.010
46.130
36.092
24.523
4-25c
13C{1H}
NMR
HN
Ph
Ph
Me
NC
200
180
160
140
120
100
80
60
40
20
ppm

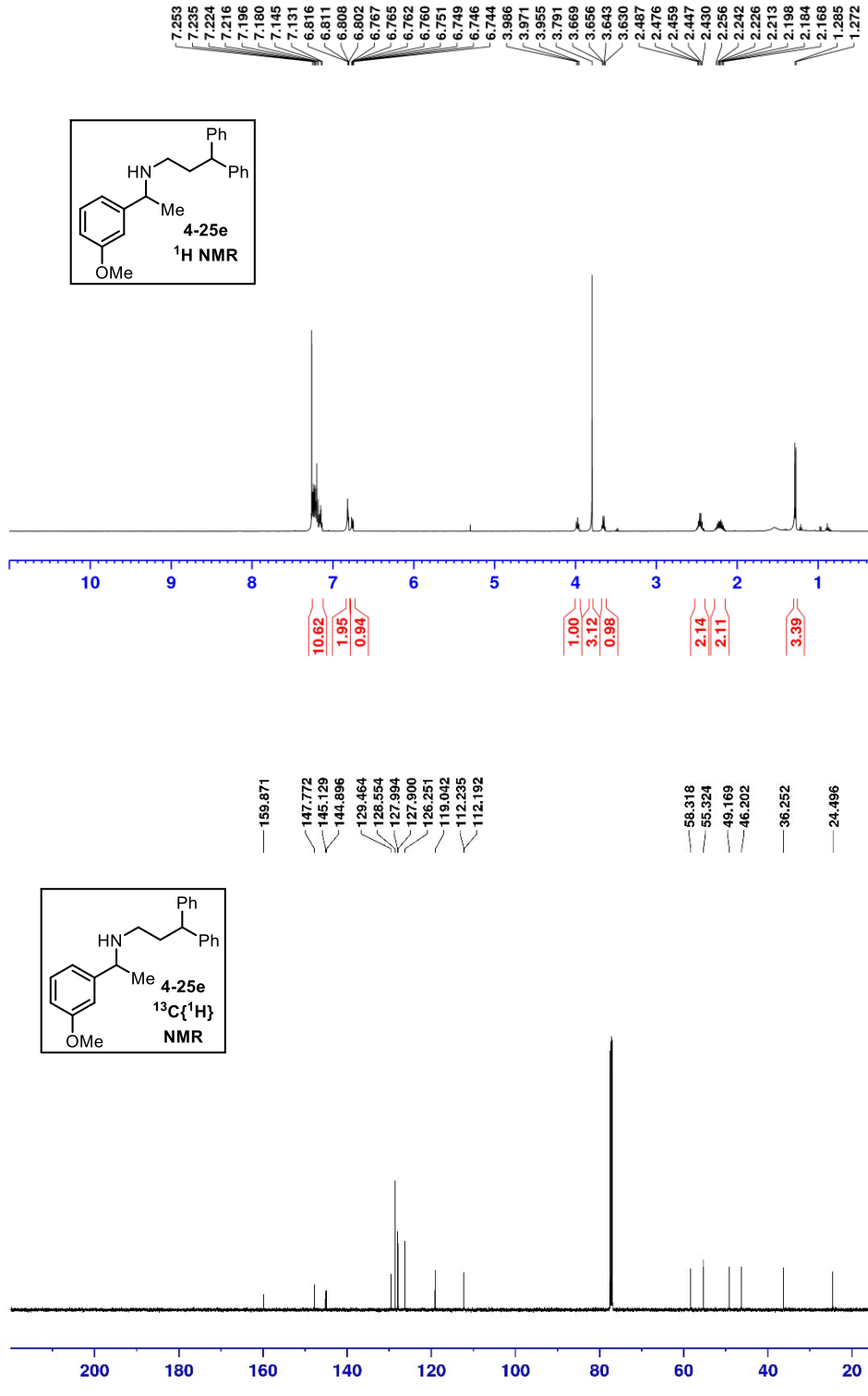
7.253
7.235
7.224
7.216
7.196
7.180
7.145
7.131
6.816
6.811
6.808
6.802
6.767
6.765
6.762
6.760
6.751
6.749
6.746
6.744
3.986
3.971
3.955
3.791
3.669
3.656
3.643
3.630
2.487
2.476
2.459
2.447
2.430
2.256
2.242
2.226
2.213
2.198
2.184
2.168
1.285
1.272
Ph
HN
Ph
Me
OMe
4-25e
1H NMR
10
9
8
7
6
5
4
3
2
1
ppm
10.62
1.95
0.94
1.00
3.12
0.98
2.14
2.11
3.39
159.871
147.772
145.129
144.896
129.464
128.554
127.994
127.900
126.251
119.042
112.235
112.192
58.318
55.324
49.169
46.202
36.252
24.496
Ph
HN
Ph
Me
OMe
4-25e
13C{1H}
NMR
200
180
160
140
120
100
80
60
40
20
ppm

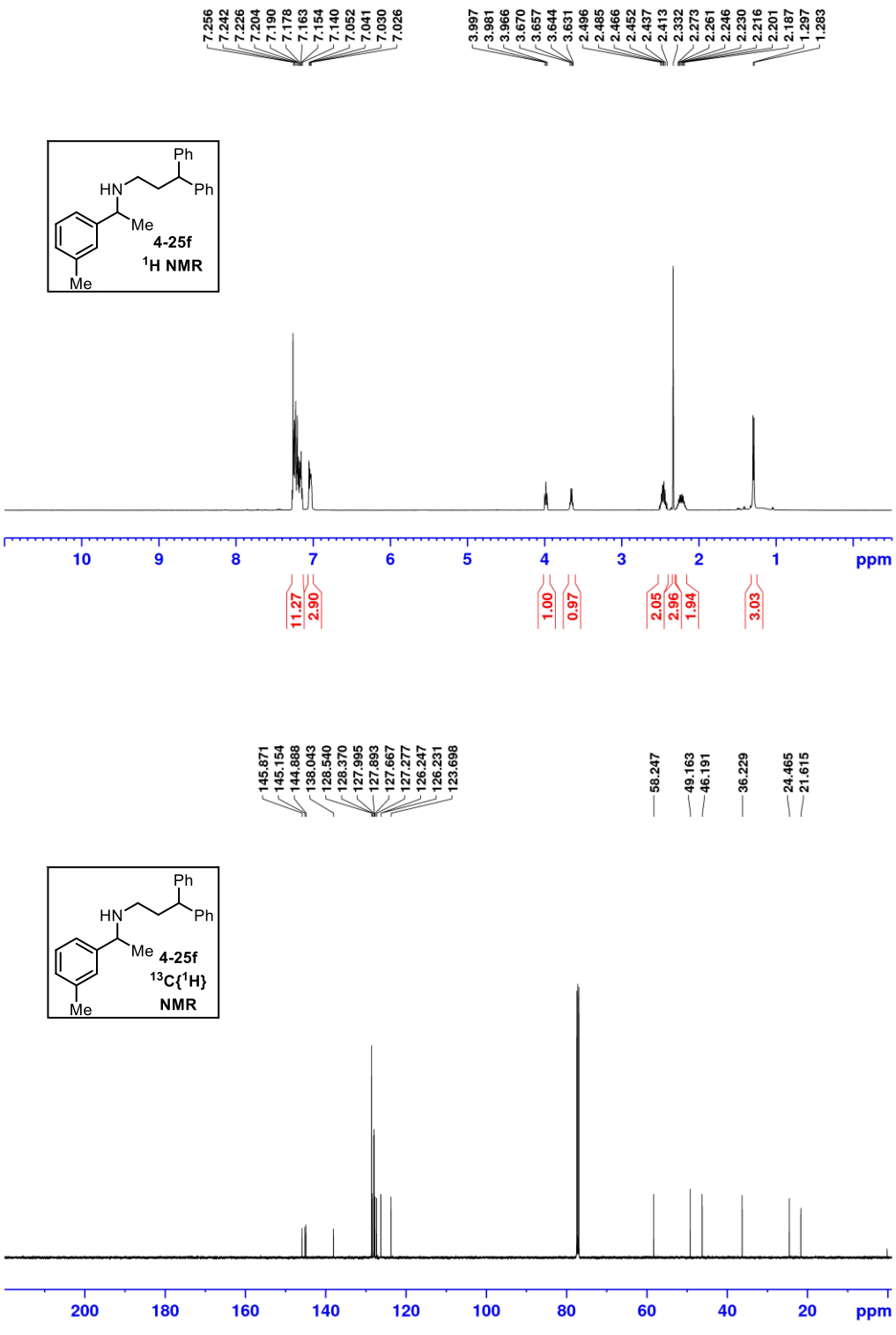
7.256
7.242
7.226
7.204
7.190
7.178
7.163
7.154
7.140
7.052
7.041
7.030
7.026
3.997
3.981
3.966
3.670
3.657
3.644
3.631
2.496
2.485
2.466
2.452
2.437
2.413
2.332
2.273
2.261
2.246
2.230
2.216
2.201
2.187
1.297
1.283
Ph
HN
Ph
Me
Me
4-25f
1H NMR
10
9
8
7
6
5
4
3
2
1
ppm
11.27
2.90
1.00
0.97
2.05
2.96
1.94
3.03
145.871
145.154
144.888
138.043
128.540
128.370
127.995
127.893
127.667
127.277
126.247
126.231
123.698
58.247
49.163
46.191
36.229
24.465
21.615
Ph
HN
Ph
Me
Me
4-25f
13C{1H}
NMR
200
180
160
140
120
100
80
60
40
20
ppm

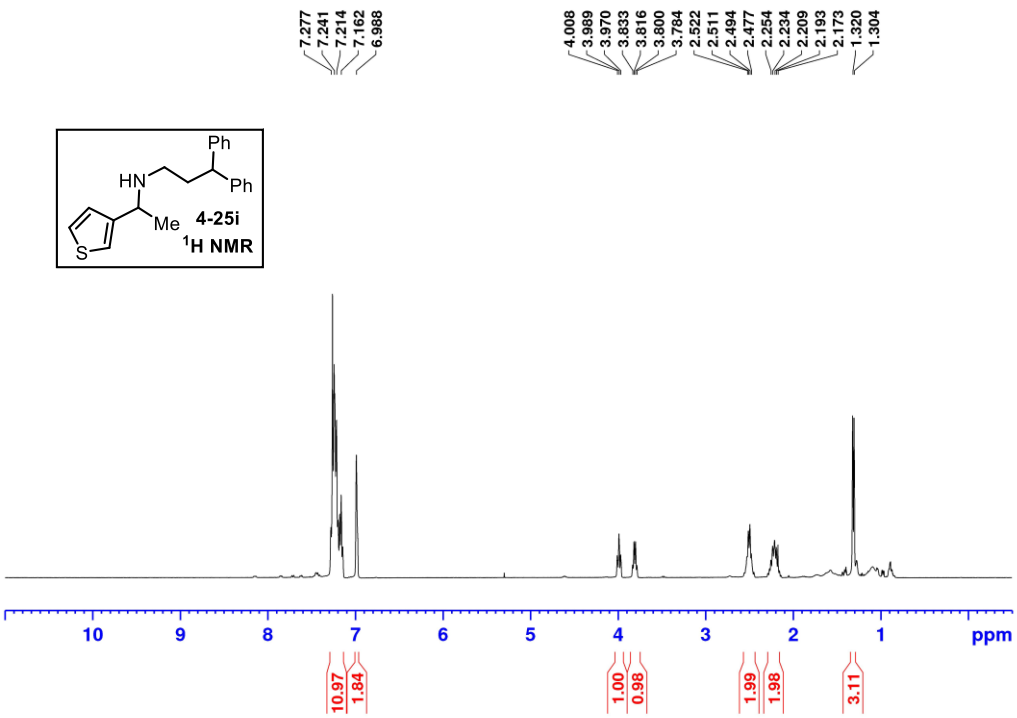
7.277
7.241
7.214
7.162
6.988
4.008
3.989
3.970
3.833
3.816
3.800
3.784
2.522
2.511
2.494
2.477
2.254
2.234
2.209
2.193
2.173
1.320
1.304
Ph
HN
Ph
Me
S
4-25i
1H NMR
10
9
8
7
6
5
4
3
2
1
ppm
10.97
1.84
1.00
0.98
1.99
1.98
3.11

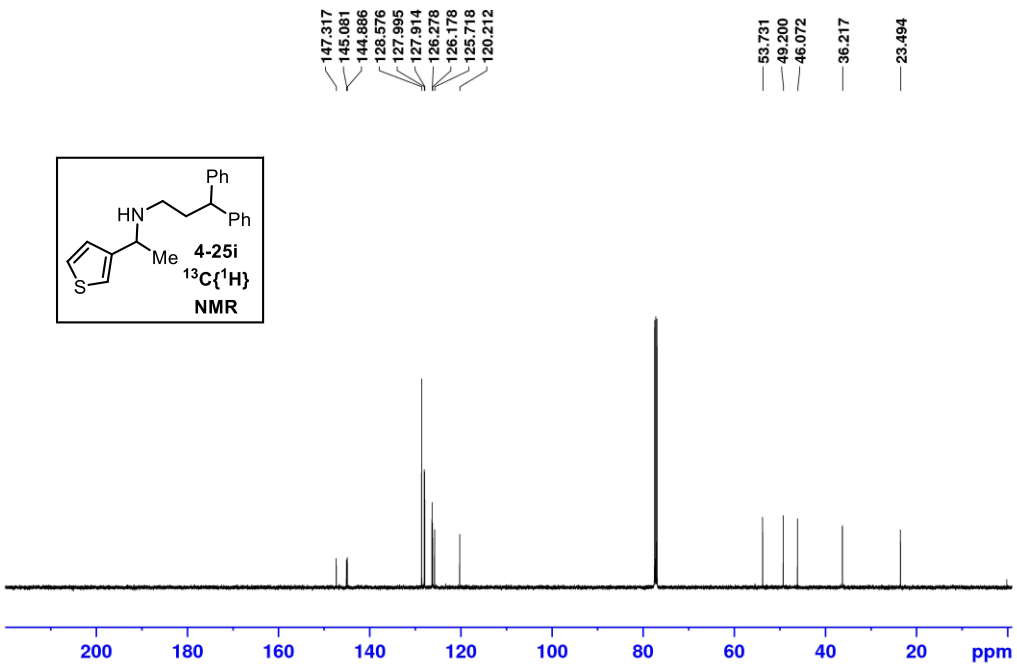
147.317
145.081
144.886
128.576
127.995
127.914
126.278
126.178
125.718
120.212
53.731
49.200
46.072
36.217
23.494
Ph
HN
Ph
Me
S
4-25i
13C{1H}
NMR
200
180
160
140
120
100
80
60
40
20
ppm

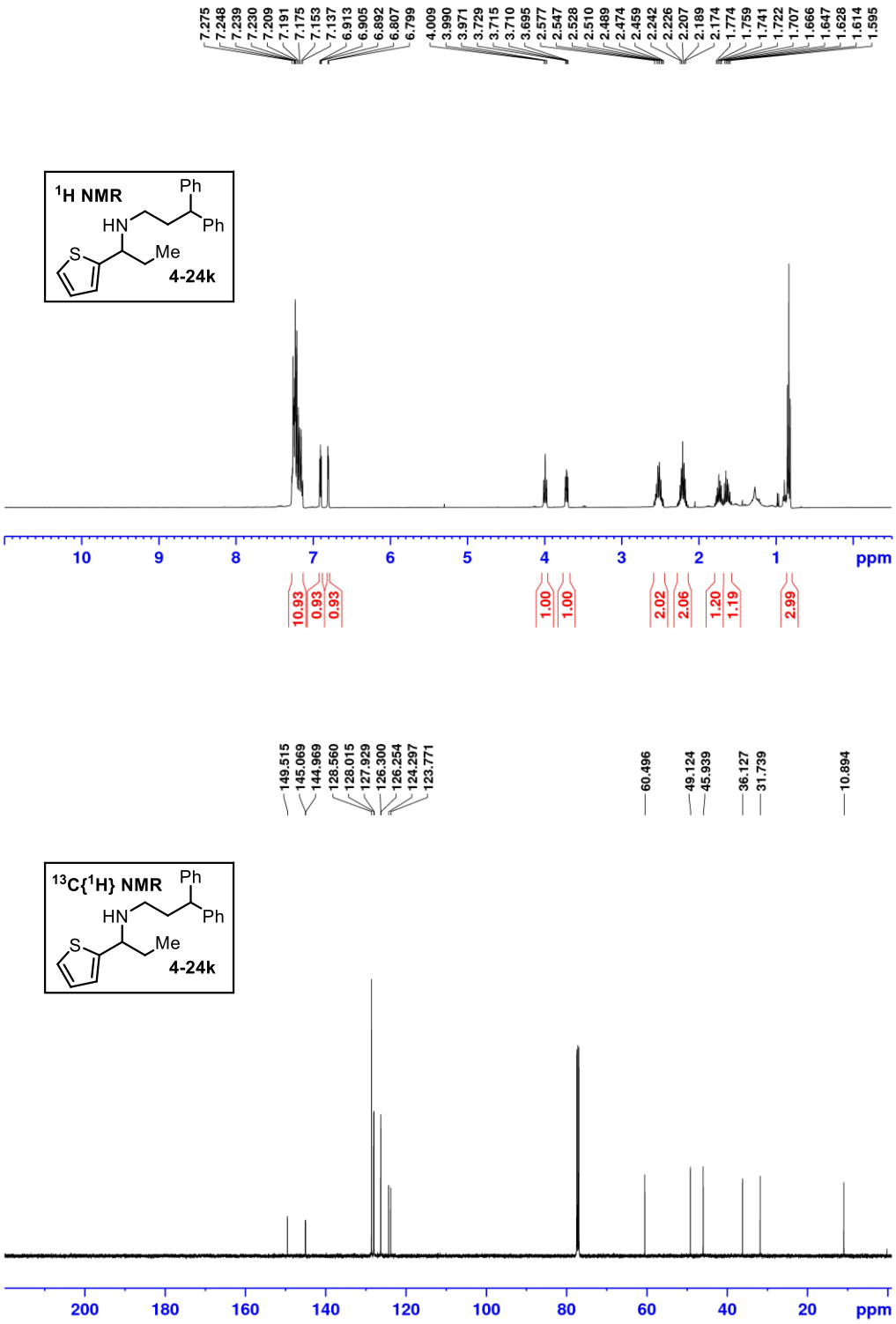
7.275
7.248
7.239
7.230
7.209
7.191
7.175
7.153
7.137
6.913
6.905
6.892
6.807
6.799
4.009
3.990
3.971
3.729
3.715
3.710
3.695
2.577
2.547
2.528
2.510
2.489
2.474
2.459
2.242
2.226
2.207
2.189
2.174
1.774
1.759
1.741
1.722
1.707
1.666
1.647
1.628
1.614
1.595
1H NMR
Ph
HN
Ph
S
Me
4-24k
10
9
8
7
6
5
4
3
2
1
ppm
10.93
0.93
0.93
1.00
1.00
2.02
2.06
1.20
1.19
2.99
149.515
145.069
144.969
128.560
128.015
127.929
126.300
126.254
124.297
123.771
60.496
49.124
45.939
36.127
31.739
10.894
13C{1H} NMR
Ph
HN
Ph
S
Me
4-24k
200
180
160
140
120
100
80
60
40
20
ppm

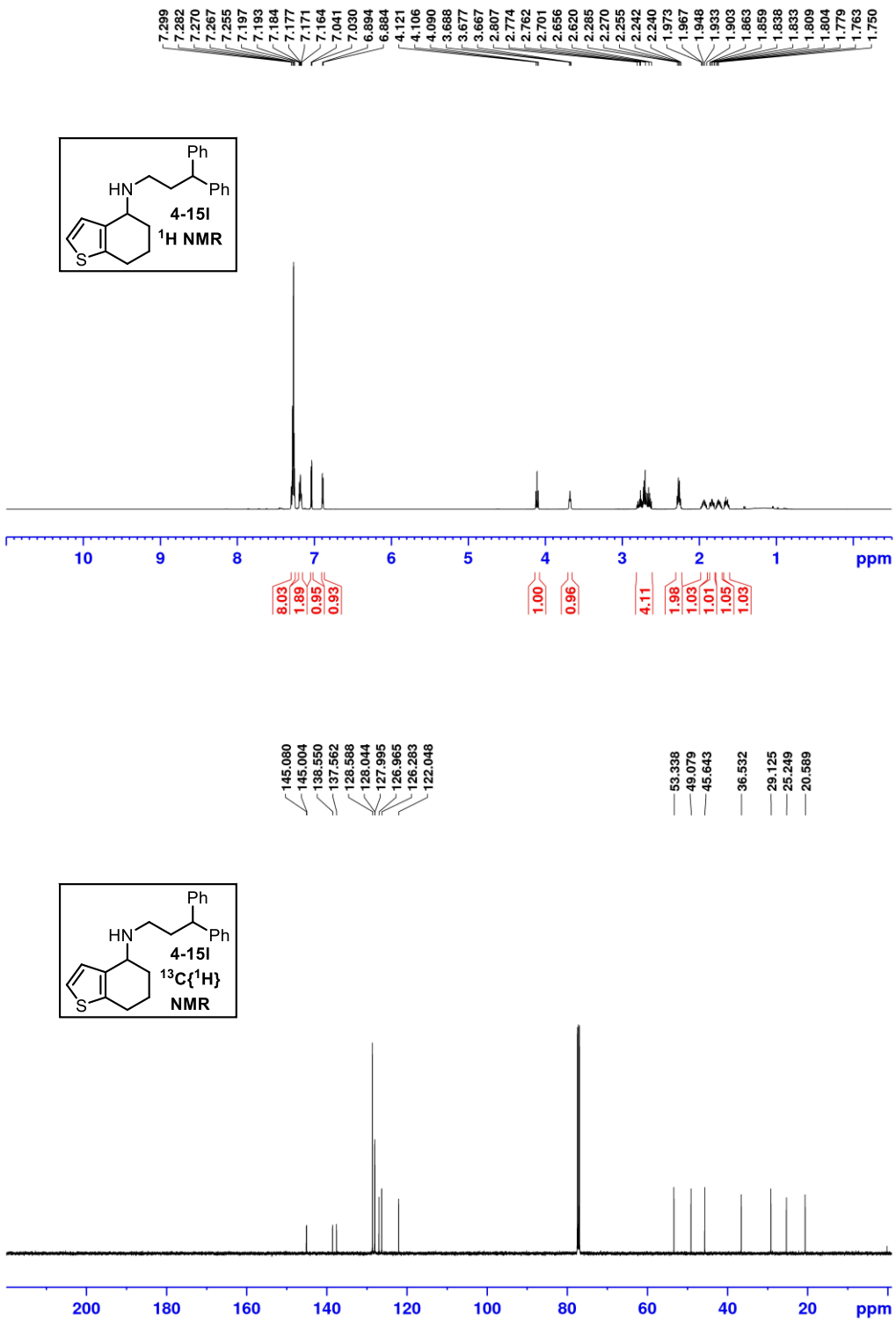
7.299
7.282
7.270
7.267
7.255
7.197
7.193
7.184
7.177
7.171
7.164
7.041
7.030
6.894
6.884
4.121
4.106
4.090
3.688
3.677
3.667
2.807
2.774
2.762
2.701
2.656
2.620
2.285
2.270
2.255
2.242
2.240
1.973
1.967
1.948
1.933
1.903
1.863
1.859
1.838
1.833
1.809
1.804
1.779
1.763
1.750
Ph
HN
Ph
4-15l
1H NMR
S
10
9
8
7
6
5
4
3
2
1
ppm
8.03
1.89
0.95
0.93
1.00
0.96
4.11
1.98
1.03
1.01
1.05
1.03
145.080
145.004
138.550
137.562
128.588
128.044
127.995
126.965
126.283
122.048
53.338
49.079
45.643
36.532
29.125
25.249
20.589
Ph
HN
Ph
4-15l
13C{1H}
NMR
S
200
180
160
140
120
100
80
60
40
20
ppm

Appendix C: Selected HPLC Traces

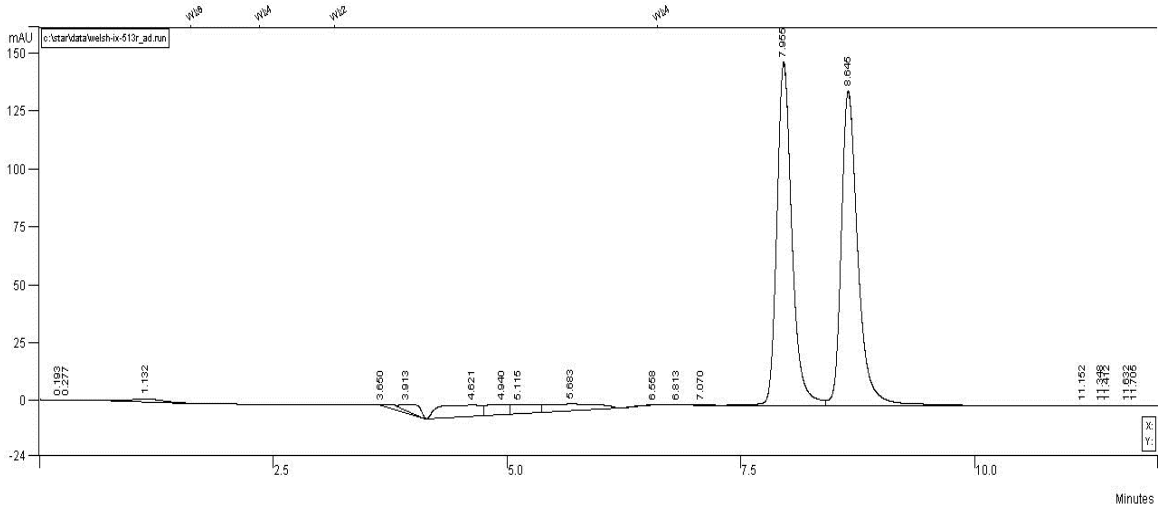

Peak Number	Retention Time	Area Number	Area Percent
1	7.955	16683010	49.6
2	8.645	16931830	50.4
Total			100

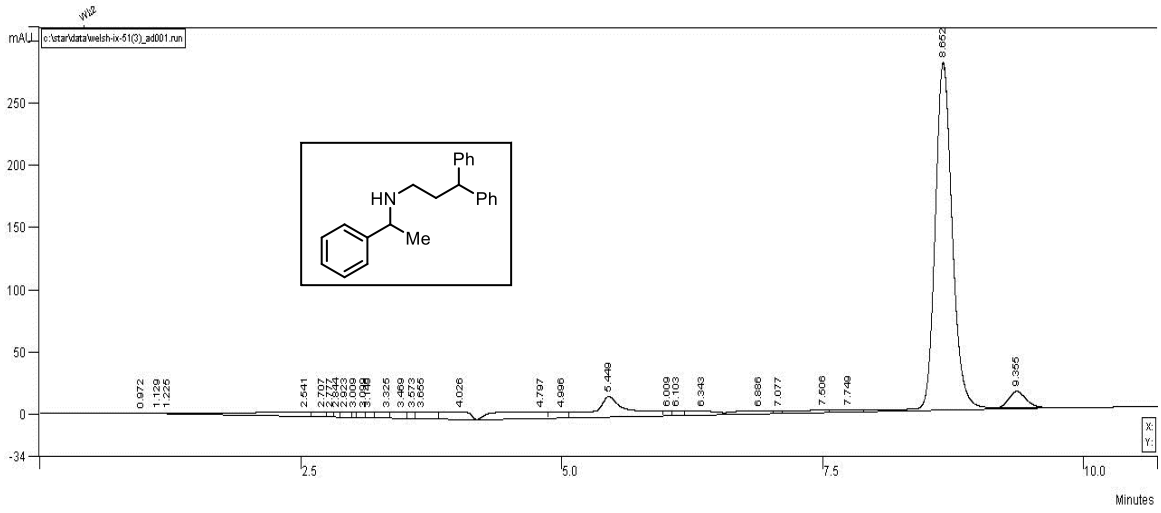

Peak Number	Retention Time	Area Number	Area Percent
1	8.652	32292378	95.5
2	9.355	1496801	4.5
Total			100

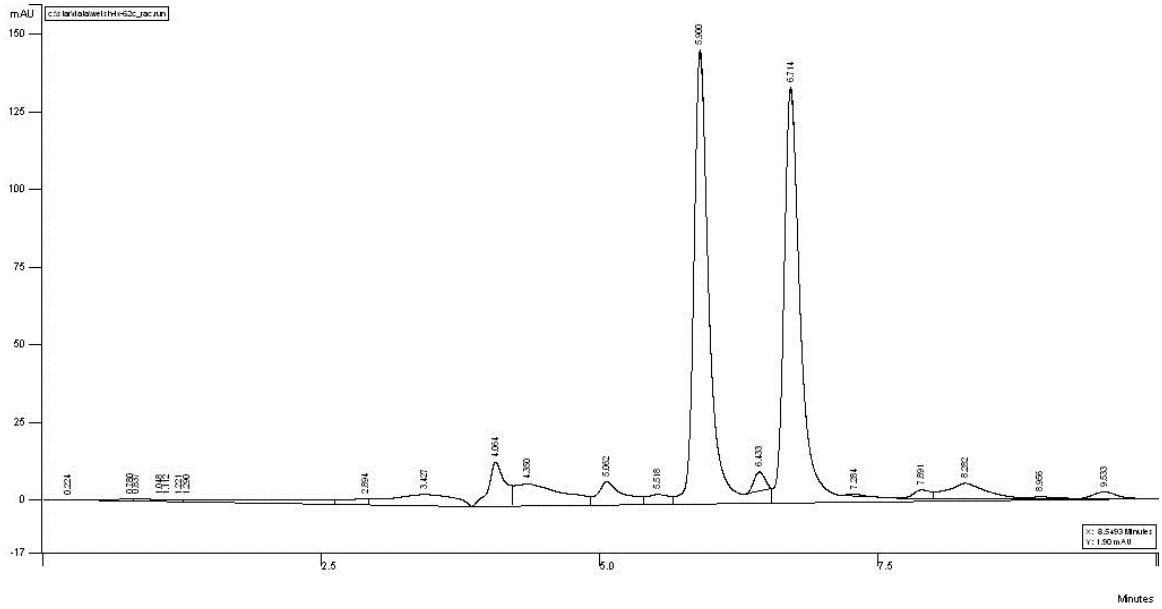

Peak Number	Retention Time	Area Number	Area Percent
1	5.900	14096581	48.9
2	6.714	14709535	51.1
Total			100

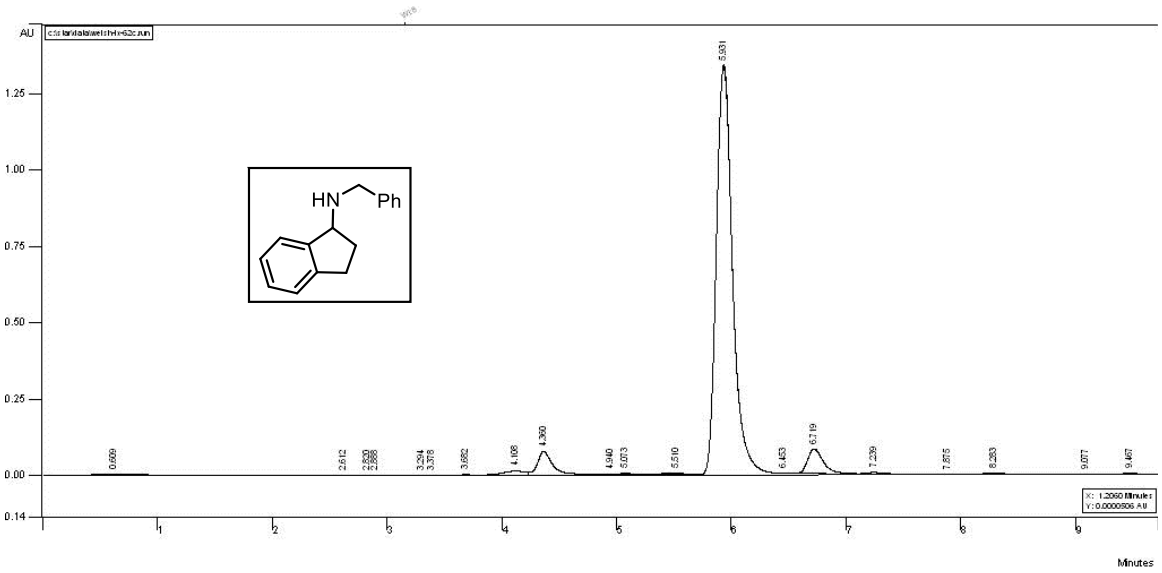

Peak Number	Retention Time	Area Number	Area Percent
1	5.931	135704016	94.7
2	6.719	7521807	5.3
Total			100

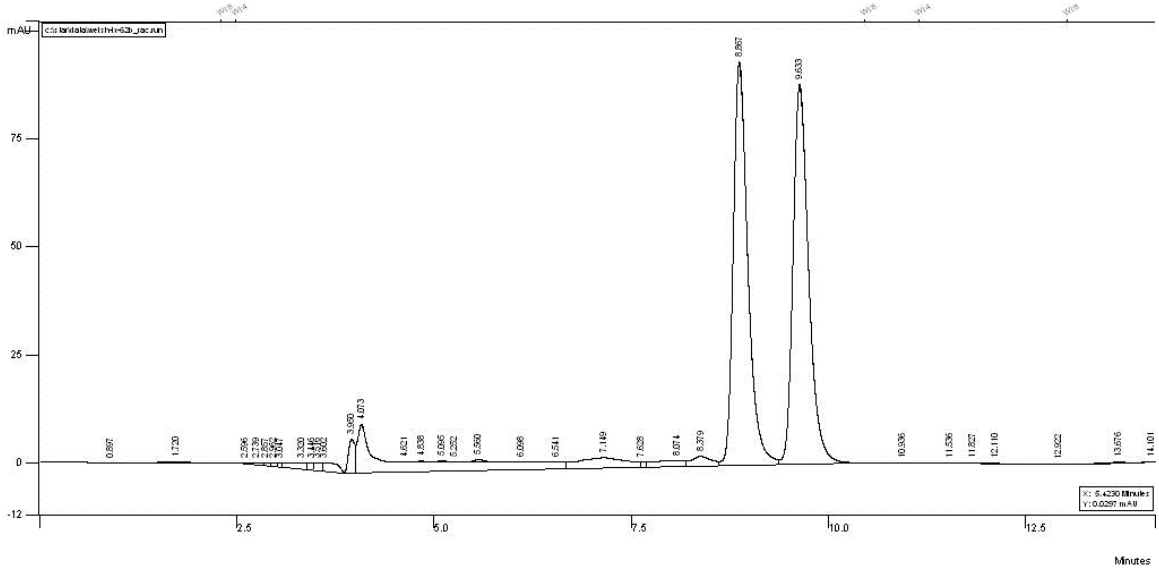

Peak Number	Retention Time	Area Number	Area Percent
1	8.867	12025104	49.9
2	9.633	12094943	50.1
Total			100

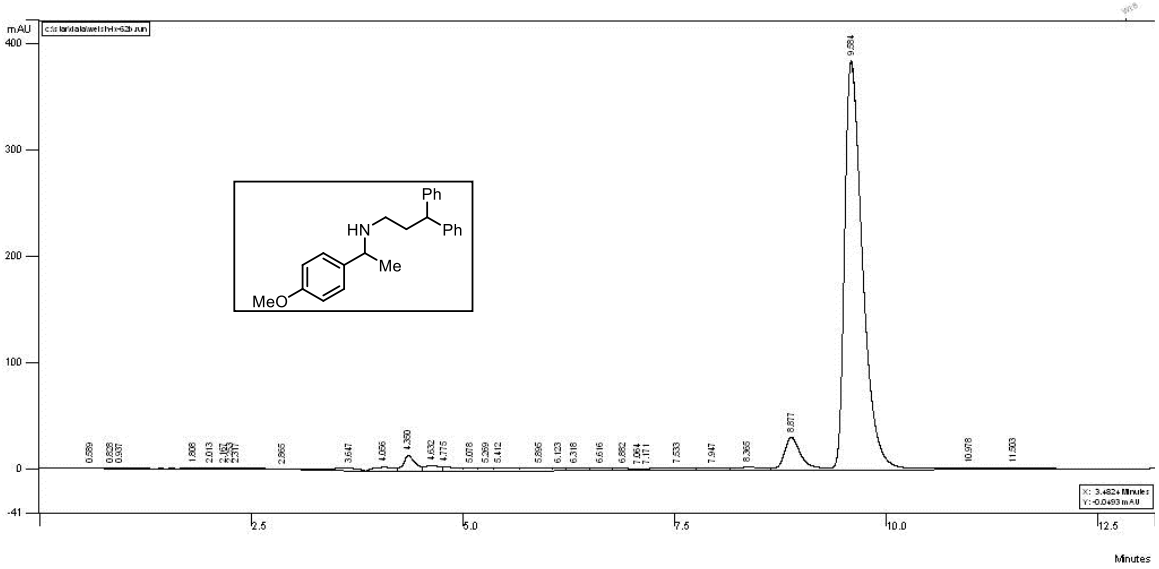

Peak Number	Retention Time	Area Number	Area Percent
1	8.877	4162346	6.8
2	9.584	56982996	93.2
Total			100

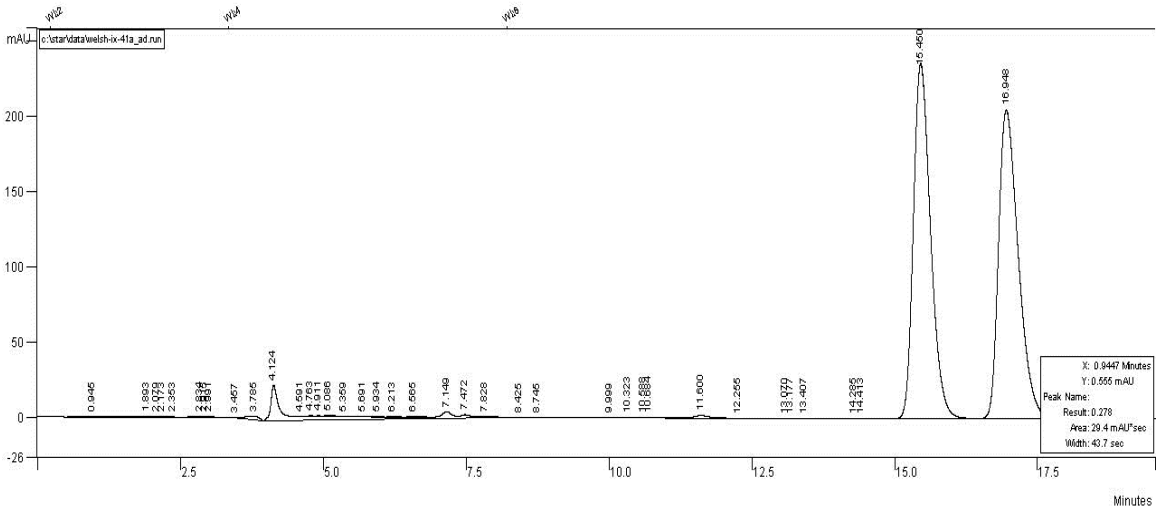

Peak Number	Retention Time	Area Number	Area Percent
1	15.450	49405112	50.0
2	16.948	49456972	50.0
Total			100

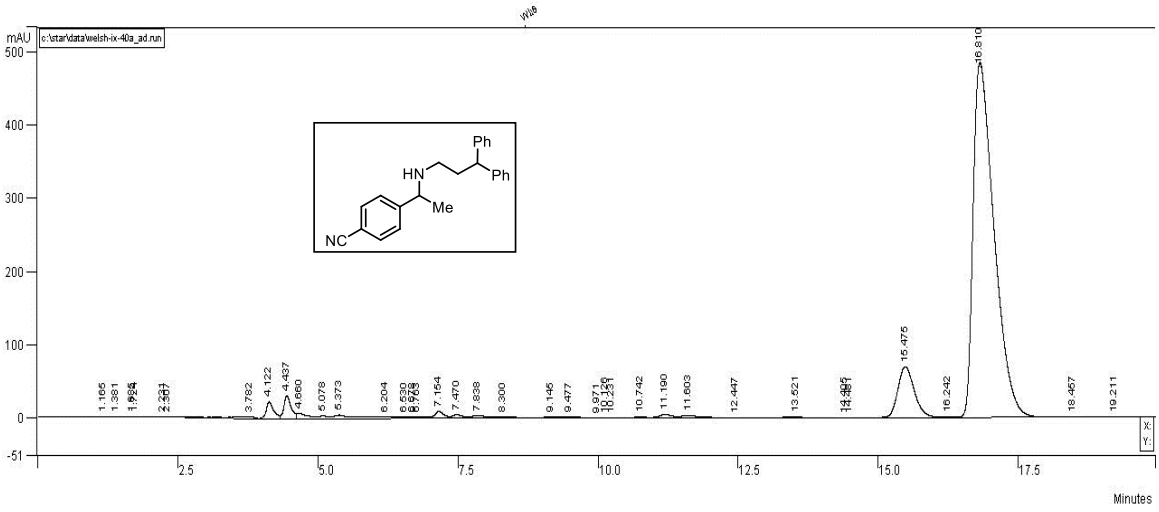

Peak Number	Retention Time	Area Number	Area Percent
1	15.475	14229690	10.1
2	16.810	126287720	89.9
Total			100

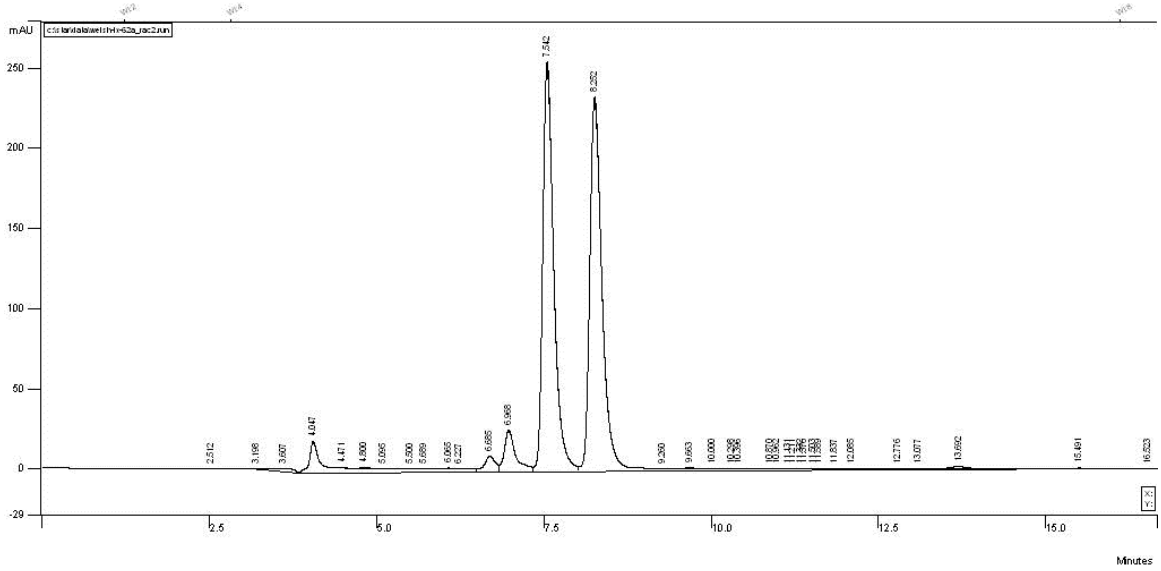

Peak Number	Retention Time	Area Number	Area Percent
1	7.542	29196514	47.1
2	8.252	32855860	52.9
Total			100

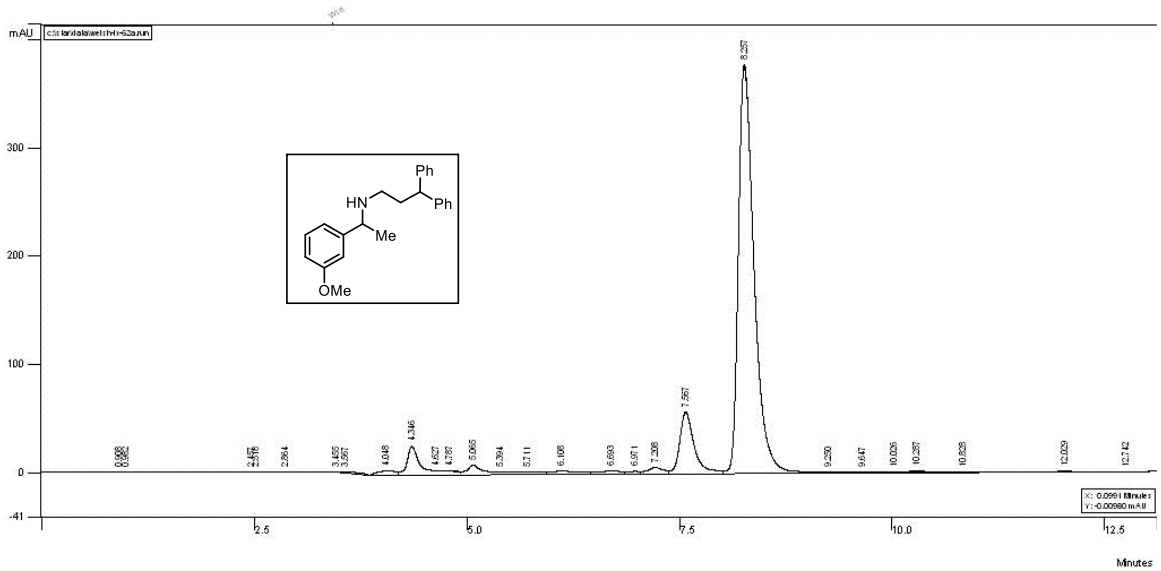

Peak Number	Retention Time	Area Number	Area Percent
1	7.567	6818366	12.0
2	8.257	49753240	88.0
Total			100

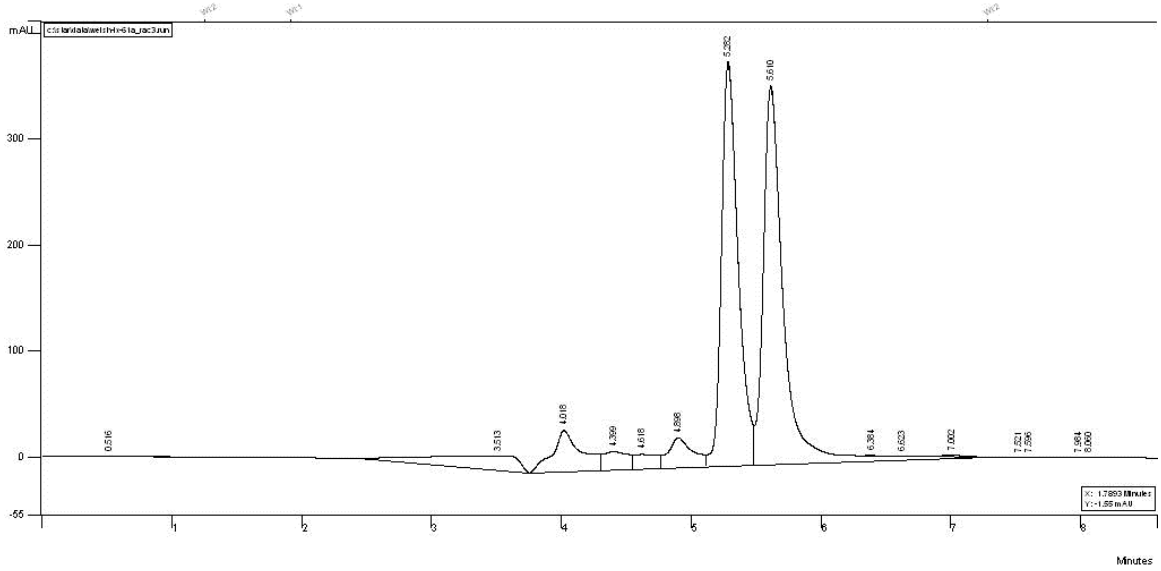

Peak Number	Retention Time	Area Number	Area Percent
1	5.282	34019056	46.5
2	5.610	39143352	53.5
Total			100

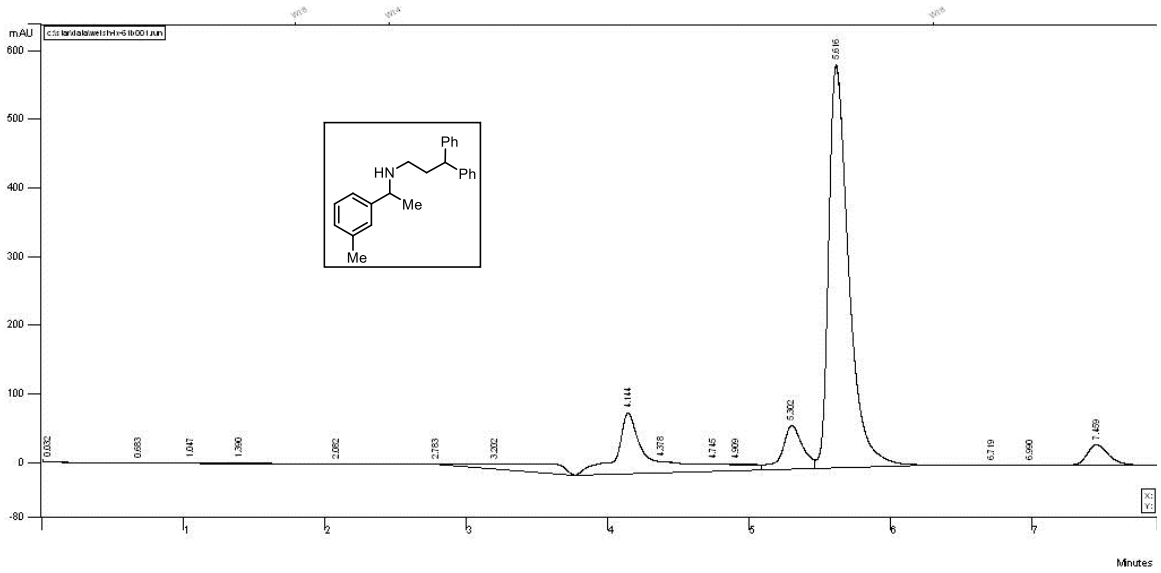

Peak Number	Retention Time	Area Number	Area Percent
1	5.302	6279669	9.8
2	5.616	57833320	90.2
Total			100

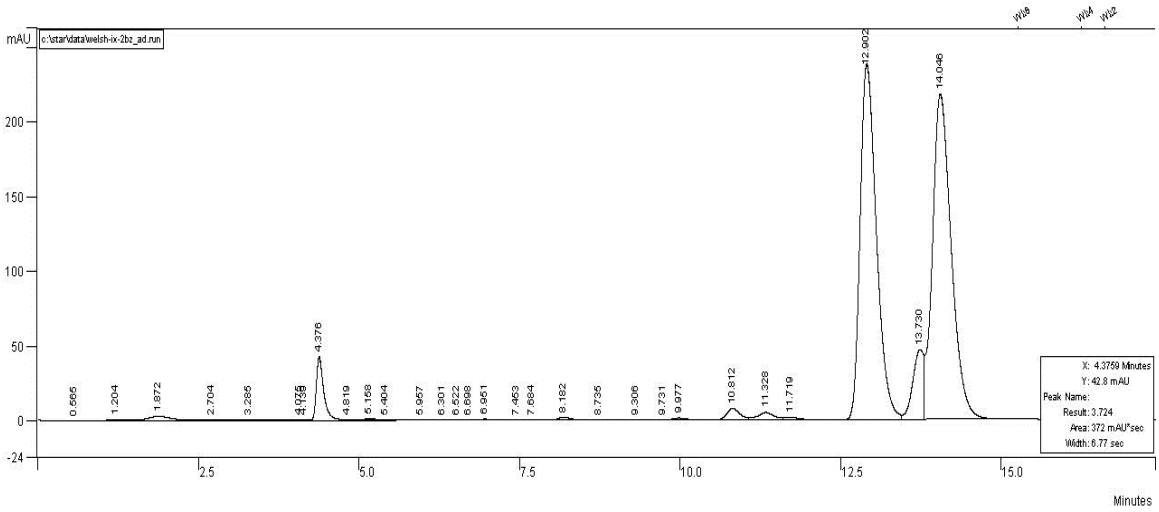

Peak Number	Retention Time	Area Number	Area Percent
1	12.902	41881568	48.6
2	14.046	44315508	51.4
Total			100

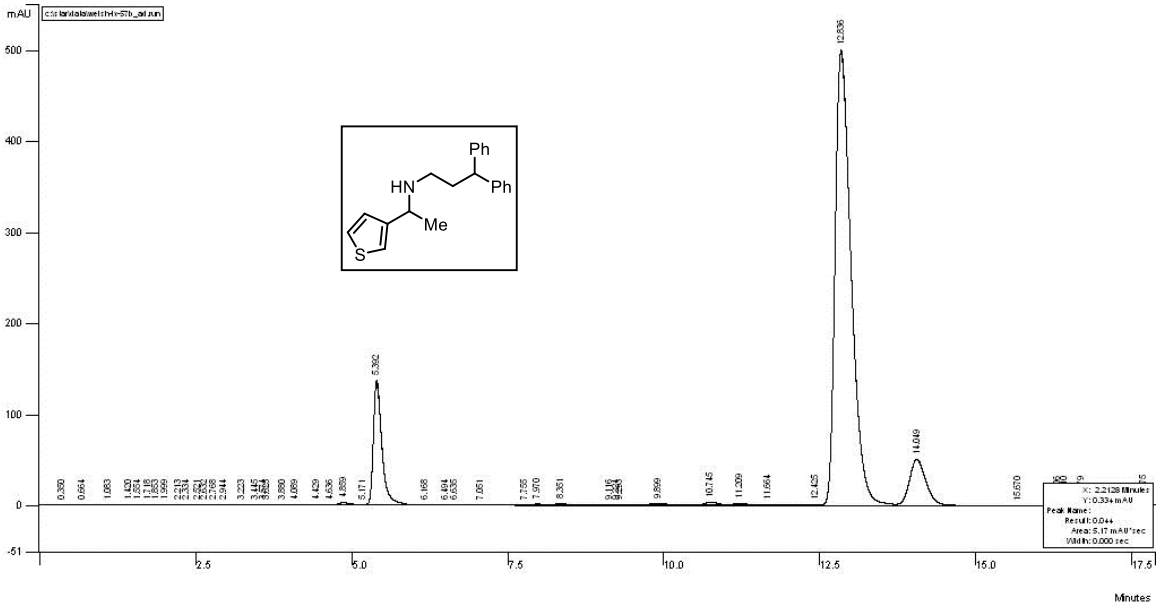

Peak Number	Retention Time	Area Number	Area Percent
1	12.836	89121424	90.5
2	14.049	9376846	9.5
Total			100

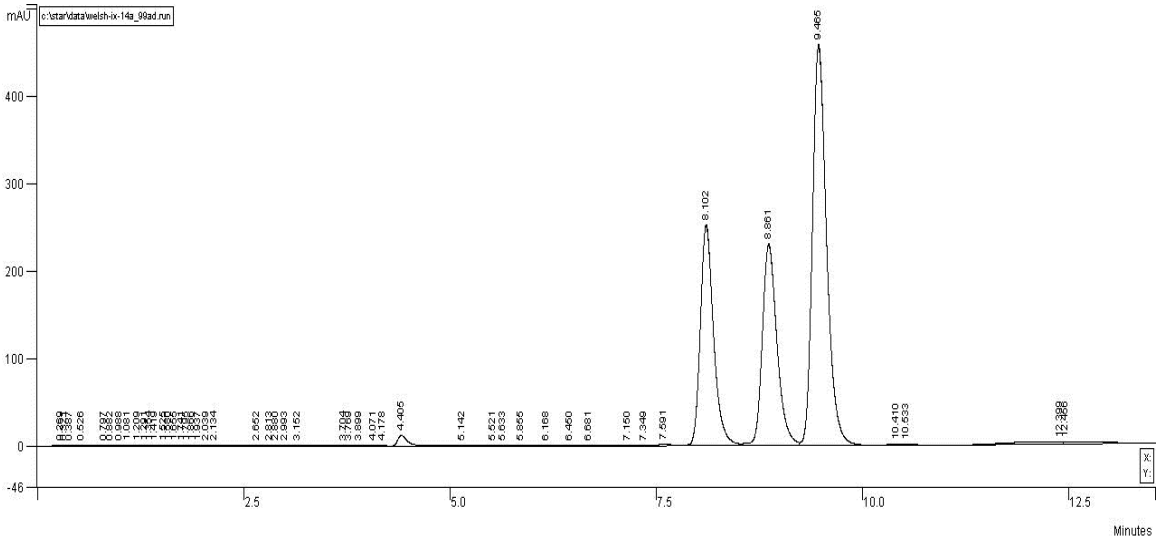

Peak Number	Retention Time	Area Number	Area Percent
1	8.102	28208076	49.7
2	8.861	28498524	50.3
Total			100

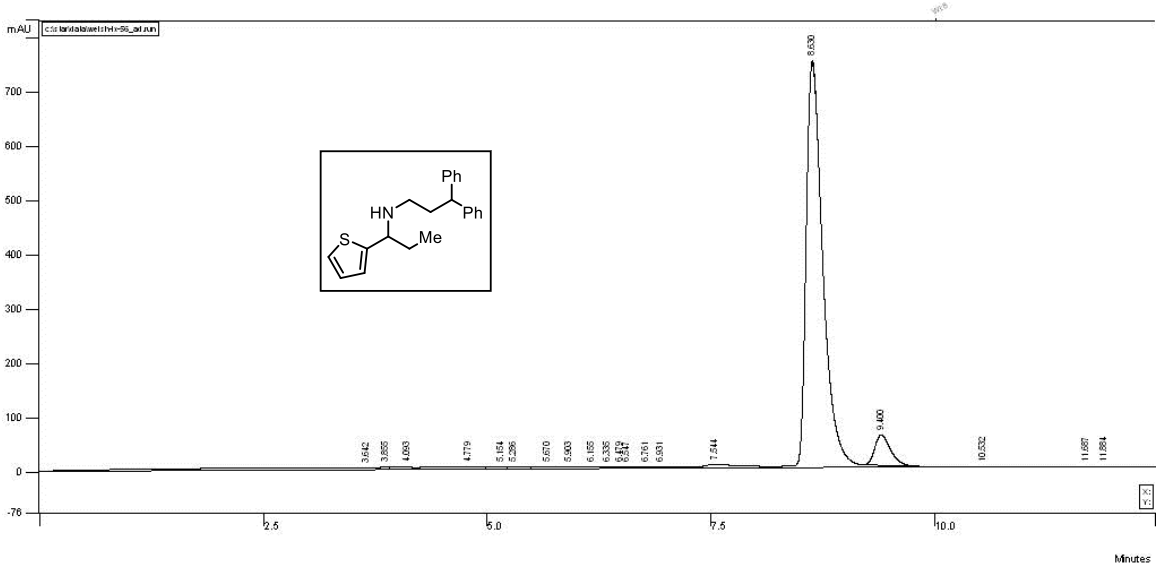

Peak Number	Retention Time	Area Number	Area Percent
1	8.630	97865184	93.3
2	9.400	6997855	6.7
Total			100

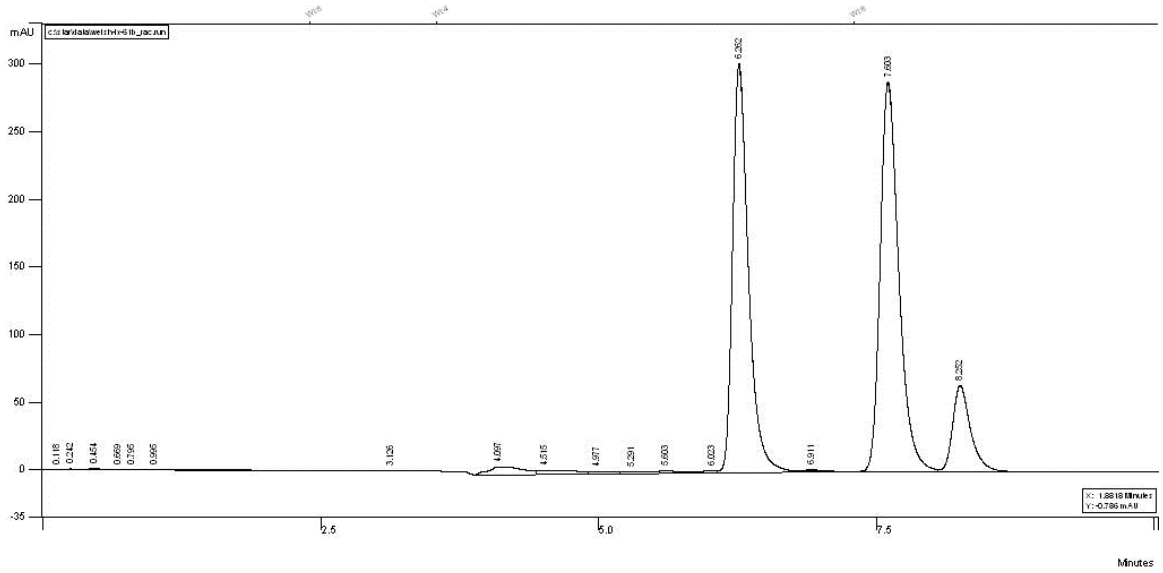

Peak Number	Retention Time	Area Number	Area Percent
1	6.262	30014778	47.2
2	7.603	33517720	52.8
Total			100

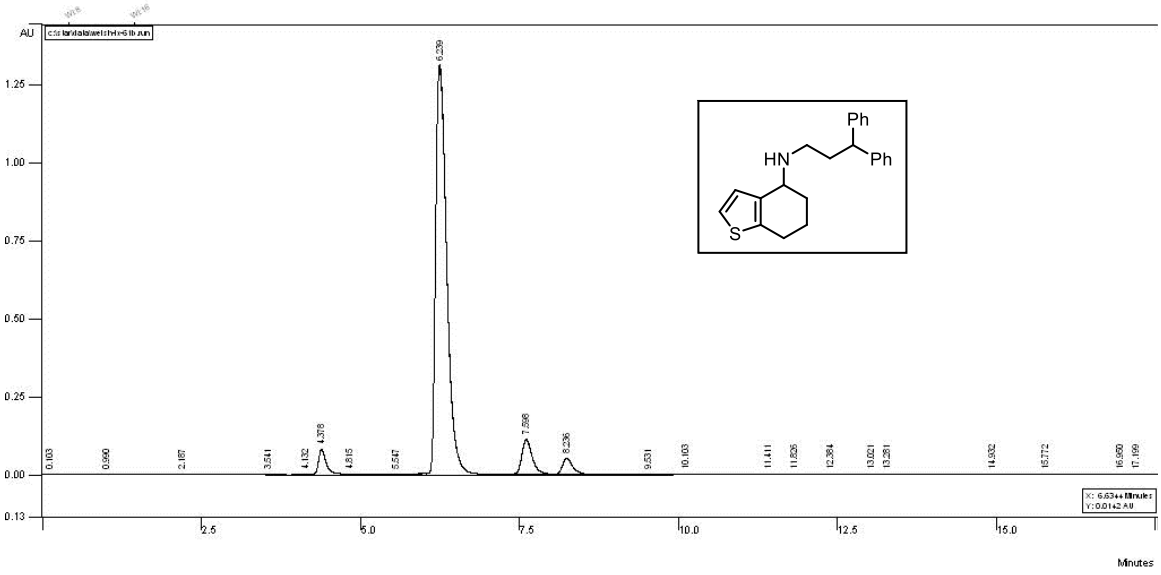

Peak Number	Retention Time	Area Number	Area Percent
1	6.239	164646160	92.9
2	7.598	12594102	7.1
Total			100